

**Synthesis and Characterization of Tetra- and Penta-dentate Schiff Base Complexes for  
Application in Actinide Sensing**

by

Emily Elizabeth Hardy

A dissertation submitted to the Graduate Faculty of  
Auburn University  
in partial fulfillment of the  
requirements for the Degree of  
Doctor of Philosophy

Auburn, Alabama  
August 4, 2018

Keywords: actinide, lanthanide, salen, Schiff base, coordination chemistry, uranyl chemosensor

Copyright 2018 by Emily Elizabeth Hardy

Approved by

Anne E. V. Gorden, Chair, Associate Professor, Dept. of Chemistry and Biochemistry  
David Stanbury, J. Milton Harris Professor, Dept. of Chemistry and Biochemistry  
German Mills, Professor, Dept. of Chemistry and Biochemistry  
Christopher J. Easley, Professor, Dept. of Chemistry and Biochemistry  
Virginia A. Davis, Alumni Professor, Dept. of Chemical Engineering

## Abstract

The advent of the nuclear power era has the potential to provide inexpensive, plentiful electricity with reduced carbon emissions, but these benefits are offset by concerns about the potential environmental effects of a waste spill or contamination event. Further exploration into the fundamental actinide and lanthanide coordination chemistry could provide knowledge that can be applied to nuclear waste detection and remediation. A fruitful method that has been employed to sequester and identify actinides, especially in selective sequestration even in the presence of lanthanides, has been to incorporate softer nitrogen donor atoms and pair them with phenolate donors. Here, the systematic characterization by X-ray crystallography and UV-visible spectroscopy of a salphenazine ligand ( $\text{H}_2\text{L}^{\text{I}}$ ), containing the O-N-N-O salen type bonding motif, and corresponding metal complexes revealed the extended  $\pi$ -conjugation of these ligands results in differentiation of a uranyl signal as compared to these transition metal contaminants. A series of new pentadentate binding ligands ( $\text{H}_2\text{L}^{\text{III}}\text{-H}_2\text{L}^{\text{VI}}$ ), which fully occupy the uranyl equatorial plane, removed the necessity of a coordinating solvent molecule or ligand rearrangement allowing to quickly and selectively bind uranyl in a one to one fashion. To further explore the *f*-element coordination chemistry with salen-type ligands, eleven lanthanide double decker sandwich complexes ( $\text{Ln}_2[\text{L}^{\text{VII}}]_3$ ) were synthesized and characterized and found to possess tunable solution and solid-state emission properties, with  $\text{Sm}_2[\text{L}^{\text{VII}}]_3$  emission at 556 nm to  $\text{Er}_2[\text{L}^{\text{VII}}]_3$  emission at 617 nm. Interestingly, lutetium exhibited a significant increase in fluorescent signal as compared to the other  $\text{Ln}_2[\text{L}^{\text{VII}}]_3$  complexes in the solid state, providing a

rare opportunity to differentiate one of the 14 lanthanides. Lastly, the double-decker thorium and cerium sandwich complexes, of the type  $M[L^{VII}]_2$  were synthesized; the thorium analogue was observed to possess unprecedented emission characteristics, and is the first example of this behavior reported in the literature. These observations about the preferential binding of uranyl and unexpected electronic properties from thorium provide insights into the fundamental coordination chemistry of the early actinides and may be useful for the future design of selective ligands for actinide and lanthanide detection and separations.

## **Acknowledgments**

I would like to begin by acknowledging that I will never be able to thank all who have helped me in my journey towards this dissertation. I will make a humble attempt to mention as many as I can.

First, I would like to thank Jennifer and Tripp for being the type of parents that encouraged me to try new things, question everything, and never give up. I appreciate every day that I was raised by a family that told me I could achieve whatever I wanted with enough hard work and dedication. I would like to thank my siblings, Will and Gillian (GG), for constantly listening to me talk about chemistry, reading my papers, and always acting interested. While I may not be excited about verb moods and GG may not be excited about a short bond length, I am glad that we can always share our excitement with each other. I would especially like to thank Graham Hindle, who bravely supported my moving 700 miles away for five years to pursue my education. I want to thank you for being my best friend, my partner, and my everything for the past ten years. I am excited to start a new chapter in our lives and would like you to know that without your unconditional support I may never have started or finished this work.

Many graduate students influenced my experiences at Auburn and I wish I had room to mention them all. I would like to thank my current and past lab-mates for becoming my family and support system at Auburn; my time here would have been entirely dull without them. I greatly appreciate the hours of conversation with Nick Klann and Julie Niklas about problematic results or new ideas that helped keep an often-overwhelming project in focus, as well as the time

Maddy Eddy and Kevin Wyss spent working with me as undergraduate researchers in the Gorden Lab. I would especially like to thank Charmaine Tutson and Maya West, both of whom have become great friends, ran to my side when I broke my leg and needed them, and were unconditionally supportive throughout my best and worst times at Auburn.

My years at Auburn have been filled with advisors who have helped me to grow. I would like to thank my research advisor Dr. Anne Gorden for providing opportunities that I could only have dreamed of before coming to Auburn; I will forever be grateful for my time in her lab. The advice and mentoring I received from Dr. Gorden has shaped me as a chemist, as well as helped me to grow as a person. I am indebted to Dr. John Gorden and Dr. Branson Maynard for the hours spent in the X-ray lab teaching me a new skill that I fell in love with. My path during graduate school was greatly affected by invaluable advice from Branson. I am also extremely fortunate to have met Bonnie Wilson and Mary Lou Ewald, both of whom provided me with guidance and opportunities that led me to discover my passion for science outreach. My involvement in outreach programs provided funding for my assistantship in the latter half of my time at Auburn, and I would like to thank Dr. Allen Landers, Dr. Virginia Davis, Dr. Paul Cobine, and Mary Lou Ewald for that experience. I would also like to take this time to thank the rest of my committee, Dr. David Stanbury, Dr. Jimmy Mills, Dr. Christopher Easley, and Dr. Virginia Davis.

I would like to acknowledge the funding sources that made this work possible. The research discussed here was funded by the Defense Threat Reduction Agency. I have had the opportunity to travel to conferences on many occasions to share my findings with the greater scientific community. I would like to acknowledge Dr. Gorden, the Auburn Local Section, the

Auburn Graduate School, the Auburn College of Science and Mathematics, and the Women in Science and Engineering Institute for providing funding for these opportunities.

Lastly, my decision to attend college, and eventually graduate school, was greatly influenced by my past teachers. One of these teachers was my undergraduate inorganic lab professor, Dr. Marie Melzer, who first showed me inorganic synthesis and helped me to discover coordination chemistry. Finally, I would like to give special thanks to Christine Dech, my late high-school chemistry teacher; I may never have found my love for chemistry if it were not for her class and passion for science. This manuscript is dedicated to her memory and to teachers like her, who inspire generations.

## Table of Contents

Abstract .....	ii
Acknowledgments.....	iv
List of Tables .....	x
List of Illustrations .....	xi
List of Abbreviations .....	xvi
Chapter 1: Introduction .....	1
Nuclear Power and Nuclear Waste .....	1
Why Fundamental <i>f</i> -element Coordination Chemistry? .....	4
Actinide Imine Coordination Compounds .....	5
Actinide Salen Compounds .....	7
Lanthanide Salen Compounds .....	11
References .....	18
Chapter 2: Solid State $\pi$ - $\pi$ Stacking and Higher Order Dimensional Crystal Packing, Reactivity, Microfluidic Detection and Electrochemical Behavior of Salphenazine Actinide and Transition Metal Complexes .....	30
Introduction.....	30
Results and Discussion .....	32
Synthesis .....	32
Crystallography.....	33
Spectroscopy .....	43

Electrochemistry .....	49
Microfluidic Detection .....	55
Conclusions .....	58
Experimental Details.....	59
References .....	66
<b>Chapter 3: An Unusual Example of Pyridine Donor Schiff Base Uranyl Complexes and Zinc Enhanced Ligand Emission.....</b>	
Introduction.....	74
Results and Discussion .....	76
Synthesis .....	76
Crystallography.....	78
Spectroscopy .....	81
Conclusions .....	90
Experimental Details .....	91
References .....	98
<b>Chapter 4: Unusual Thorium Fluorescence and Tunable Ligand Emission of Naphthylsalophen Uranyl(VI), Thorium(IV), and Lanthanide(III) Sandwich Complexes .....</b>	
Introduction.....	104
Results and Discussion .....	107
Synthesis .....	107
Crystallography.....	109
Uncharacteristic Th(IV) Emission .....	125
Tunable Ligand Emission of Ln <sub>2</sub> [L <sup>VII</sup> ] <sub>3</sub> .....	132
Conclusions .....	141



Experimental Details.....	143
References .....	153
Chapter 5: Conclusions and Future Work .....	166
Conclusions .....	166
Future Work .....	168
U(IV) Complexes with Redox Active Ligands.....	168
Increasing the Extinction Coefficient of $[H_2L^{III}]$ .....	170
Naphthylsalophen Derivatives .....	172
CAN oxidations and $Ce[L^{VII}]_2$ Derivatives.....	175
Macrocyclic Chemosensors .....	176
References .....	180
Appendix 1: Crystallographic Tables .....	183
References .....	406

## List of Tables

Table 2.1 Crystallographic data and details of data collection for $[\text{H}_2\text{L}^{\text{I}}]$ , $\text{UO}_2[\text{L}^{\text{I}}](\text{H}_2\text{O})$ , $\text{Cu}[\text{L}^{\text{I}}]$ , $\text{VO}[\text{L}^{\text{I}}]$ , $\text{Zn}[\text{L}^{\text{I}}](\text{CH}_3\text{OH})$ , and $\text{Fe}[\text{L}^{\text{I}}]\text{-O-Fe}[\text{L}^{\text{I}}]$ .....	35
Table 2.2 Selected bond distances (Å) and bond angles (deg) for $[\text{H}_2\text{L}^{\text{I}}]$ , $\text{UO}_2[\text{L}^{\text{I}}](\text{H}_2\text{O})$ , $\text{Cu}[\text{L}^{\text{I}}]$ , $\text{VO}[\text{L}^{\text{I}}]$ , $\text{Zn}[\text{L}^{\text{I}}](\text{CH}_3\text{OH})$ , and $\text{Fe}[\text{L}^{\text{I}}]\text{-O-Fe}[\text{L}^{\text{I}}]$ .....	36
Table 2.3 UV-Visible data for $\text{M}[\text{L}^{\text{I}}]$ complexes and free base $[\text{H}_2\text{L}^{\text{I}}]$ .....	43
Table 3.1 Crystallographic data for $\text{UO}_2[\text{L}^{\text{III}}]$ and $\text{UO}_2[\text{L}^{\text{IV}}]$ .....	79
Table 4.2 Crystallographic data for $[\text{H}_2\text{L}^{\text{VII}}]$ , $\text{Th}[\text{L}^{\text{VII}}]_2$ , and $\text{Ce}[\text{L}^{\text{VII}}]_2$ .....	111
Table 4.2 Crystallographic data for $\text{Nd}_2[\text{L}^{\text{VII}}]_3$ , $\text{Gd}_2[\text{L}^{\text{VII}}]_3$ , $\text{Ho}_2[\text{L}^{\text{VII}}]_3$ , and $\text{Yb}_2[\text{L}^{\text{VII}}]_3$ .....	114
Table 4.3 Crystallographic Data for $\text{Eu}_2[\text{L}^{\text{VII}}]_3$ , $\text{Tb}_2[\text{L}^{\text{VII}}]_3$ , $\text{Dy}_2[\text{L}^{\text{VII}}]_3$ , $\text{Er}_2[\text{L}^{\text{VII}}]_3$ , and $\text{Lu}_2[\text{L}^{\text{VII}}]_3$ complexes .....	120
Table 4.4 Selected bond angles of $\text{Ln}_2[\text{L}^{\text{VII}}]_3$ complexes.....	123
Table 4.5 Selected bond lengths of $\text{Ln}_2[\text{L}^{\text{VII}}]_3$ complexes .....	123
Table 4.6 Emission wavelength and quantum yield of $\text{Th}[\text{L}^{\text{VII}}]_2$ in various solvents .....	129
Table 4.7 Quantum yields of $\text{Ln}_2[\text{L}^{\text{VII}}]_3$ complexes in $\text{CHCl}_3$ solution .....	137
Table 4.8 Emission wavelengths of $\text{Ln}_2[\text{L}^{\text{VII}}]_3$ species in solid-state.....	141

## List of Illustrations

Figure 1.1 Ligand systems used for spent nuclear fuel remediation.....	3
Figure 1.2 1,2-HOPO ligand and projections of Th(1,2-HOPO) and Pu(1,2-HOPO).....	5
Figure 1.3 Projection of UO <sub>2</sub> (cyclo[1]furan[1]pyridine[4]pyrrole).....	6
Figure 1.4 Previously reported uranium complexes with salen and derivatives.....	8
Figure 1.5 Projections of UO <sub>2</sub> (salen) and co-crystallized CsF.....	9
Figure 1.6 Projection of a mixed U(VI)/U(V) salen species .....	11
Figure 1.7 Projections of U(II)(trisaryloxiarene), and Nd(II)(trisaryloxiarene) .....	12
Figure 1.8 Projection of Ishikawa's Tb SMM .....	14
Figure 1.9 Cartoon of the antenna effect .....	15
Figure 1.10 Schematic and of a 1,2-HOPO derivative and projection of the highly emissive 2:1 Eu complex .....	16
Scheme 2.1 Metal templated synthesis of salphenazine complexes M[LI] .....	33
Figure 2.1 Salphenazine [ <b>H<sub>2</sub>L<sup>I</sup></b> ] crystal structure .....	34
Figure 2.2 Projection of UO <sub>2</sub> [ <b>L<sup>I</sup></b> ] complex .....	37
Figure 2.3 Projection of Cu[ <b>L<sup>I</sup></b> ] complex.....	37
Figure 2.4 Projections of VO[ <b>L<sup>I</sup></b> ], Zn[ <b>L<sup>I</sup></b> ](CH <sub>3</sub> OH), and Fe[ <b>L<sup>I</sup></b> ]-O-Fe[ <b>L<sup>I</sup></b> ] complexes .....	39
Figure 2.5 Projections of M[ <b>L<sup>I</sup></b> ] series highlighting the pucker of the binding pocket .....	42
Figure 2.6 UV-Vis spectral changes of M[ <b>L<sup>I</sup></b> ] complexes .....	45
Figure 2.7 Vials with 20 μM solutions of <b>H<sub>2</sub>L<sup>I</sup></b> , Cu[ <b>L<sup>I</sup></b> ] and UO <sub>2</sub> [ <b>L<sup>I</sup></b> ] in pyridine.....	45
Figure 2.8 Cu <sup>2+</sup> titration of the ligand in pyridine indicates a 1:1 Cu <sup>2+</sup> to <b>H<sub>2</sub>L<sup>I</sup></b> .....	46

Figure 2.9 $\text{UO}_2^{2+}$ titration of the ligand in pyridine indicates a 1:1 $\text{UO}_2^{2+}$ to $\text{H}_2\text{L}^{\text{I}}$ .....	46
Figure 2.10 $\text{UO}_2^{2+}$ titration in pyridine indicates a 1:1 $\text{UO}_2^{2+}$ to $\text{H}_2\text{L}^{\text{I}}$ complex after 3 days ...	47
Figure 2.11 UV Vis spectrum of $[\text{H}_2\text{L}^{\text{I}}]$ solution with varying $\text{VO}(\text{acac})_2$ .....	47
Figure 2.12 UV Vis spectrum of $[\text{H}_2\text{L}^{\text{I}}]$ solution with varying $\text{Ni}(\text{acetate})_2$ .....	48
Figure 2.13 UV Vis spectrum of $[\text{H}_2\text{L}^{\text{I}}]$ solution with varying $\text{Co}(\text{acetate})_2$ .....	48
Scheme 2.2 Salqu $[\text{H}_2\text{L}^{\text{II}}]$ and Salqu complexes $\text{M}[\text{L}^{\text{II}}]$ .....	49
Figure 2.14 Cyclic voltammogram of $[\text{H}_2\text{L}^{\text{I}}]$ , $\text{UO}_2[\text{L}^{\text{I}}]$ , and $\text{Cu}[\text{L}^{\text{I}}]$ .....	50
Figure 2.15 Cyclic voltammogram of $[\text{H}_2\text{L}^{\text{II}}]$ , $\text{UO}_2[\text{L}^{\text{II}}]$ , and $\text{Cu}[\text{L}^{\text{II}}]$ .....	50
Figure 2.16 Cyclic voltammogram of $\text{UO}_2[\text{L}^{\text{I}}]$ .....	52
Figure 2.17 Cyclic voltammogram of Salphenazine $[\text{H}_2\text{L}^{\text{I}}]$ .....	52
Figure 2.18 Cyclic voltammogram of $\text{Cu}[\text{L}^{\text{II}}]$ .....	53
Figure 2.19 Cyclic voltammogram of $\text{UO}_2[\text{L}^{\text{II}}]$ .....	54
Figure 2.20 Cyclic voltammogram of Salqu $[\text{H}_2\text{L}^{\text{II}}]$ .....	54
Figure 2.21 Cyclic voltammogram of $\text{UO}_2[\text{L}^{\text{I}}]$ and $\text{UO}_2[\text{L}^{\text{II}}]$ .....	55
Figure 2.22 Microfluidic design, conditions, and CRAIC spectrum .....	56
Figure 2.23 CRAIC spectra of $\text{Cu}(\text{NO}_3)_2$ , $\text{UO}_2(\text{NO}_3)_2$ , $[\text{H}_2\text{L}^{\text{I}}]$ , $\text{Cu}[\text{L}^{\text{I}}]$ , and $\text{UO}_2[\text{L}^{\text{I}}]$ .....	57
Figure 2.24 Images of the microfluidic droplets and corresponding spectra .....	57
Scheme 3.1 Synthetic Scheme of $\text{UO}_2[\text{L}^{\text{III}}]$ and $\text{UO}_2[\text{L}^{\text{IV}}]$ .....	77
Scheme 3.2 Representations of ligands $[\text{H}_2\text{L}^{\text{III}}]$ , $[\text{H}_2\text{L}^{\text{IV}}]$ , $[\text{H}_2\text{L}^{\text{V}}]$ , and $[\text{H}_2\text{L}^{\text{VI}}]$ .....	77
Figure 3.1 Projection of $\text{UO}_2[\text{L}^{\text{III}}]$ .....	78
Figure 3.2 Projection of $\text{UO}_2[\text{L}^{\text{IV}}]$ .....	80
Figure 3.3 UV-Visible spectra of a serial titration of $[\text{H}_2\text{L}^{\text{III}}]$ with $\text{UO}_2^{2+}$ in DCM .....	81
Figure 3.4 UV-Visible spectra of a serial titration of $[\text{H}_2\text{L}^{\text{III}}]$ with $\text{UO}_2^{2+}$ in methanol .....	82

Figure 3.5 UV-Visible spectra of a serial titration of $[\text{H}_2\text{L}^{\text{III}}]$ with $\text{Cu}^{2+}$ in methanol .....	83
Figure 3.6 UV-Visible spectra of a serial titration of $[\text{H}_2\text{L}^{\text{III}}]$ with $\text{Co}^{2+}$ , $\text{Ni}^{2+}$ , $\text{Mn}^{2+}$ , and $\text{VO}^{2+}$ in methanol.....	84
Figure 3.7 UV-Visible spectra of a serial titration of $[\text{H}_2\text{L}^{\text{III}}]$ with $\text{Zn}^{2+}$ .....	84
Figure 3.8 Absorbance at 385 nm as a function of the ratio of $\text{Zn}^{2+}$ to $[\text{H}_2\text{L}^{\text{III}}]$ .....	85
Figure 3.9 Emission spectrum of a serial titration of $[\text{H}_2\text{L}^{\text{III}}]$ $\text{UO}_2^{2+}$ , $\text{Cu}^{2+}$ , $\text{Co}^{2+}$ , $\text{Ni}^{2+}$ in methanol after 365 nm excitation .....	86
Figure 3.10 Emission spectrum of a serial titration of $[\text{H}_2\text{L}^{\text{III}}]$ $\text{VO}^{2+}$ and $\text{Zn}^{2+}$ in methanol after 365 nm excitation.....	86
Figure 3.11 Solution fluorescence of a serial titration of $[\text{H}_2\text{L}^{\text{III}}]$ with metal salts.....	87
Figure 3.12 $\text{Zn}[\text{L}^{\text{III}}]$ fluorescence at 473 nm after 365 nm excitation vs. absorbance .....	88
Figure 3.13 Zinc emission in comparison with $[\text{H}_2\text{L}^{\text{III}}]$ and the metal titrations .....	89
Scheme 3.3 Potential zinc binding with $[\text{H}_2\text{L}^{\text{III}}]$ .....	89
Figure 3.13 Absorbance spectrum of $[\text{H}_2\text{L}^{\text{IV}}]$ .....	90
Scheme 4.1 Synthesis of $\text{H}_2[\text{L}^{\text{VII}}]$ .....	107
Scheme 4.2 Synthesis of $\text{Th}[\text{L}^{\text{VII}}]_2$ and $\text{Ce}[\text{L}^{\text{VII}}]_2$ .....	107
Figure 4.1 Solution phase absorbance of $[\text{H}_2\text{L}^{\text{VII}}]$ and spectrophotometric observation of the formation of $\text{Ce}[\text{L}^{\text{VII}}]_2$ .....	108
Scheme 4.3 Synthesis of $\text{Ln}_2[\text{L}^{\text{VII}}]_3$ complexes.....	109
Scheme 4.4 Synthesis of $\text{UO}_2[\text{L}^{\text{VII}}]$ complex .....	109
Figure 4.2 Projection of $[\text{H}_2\text{L}^{\text{VII}}]$ .....	110
Scheme 4.5 Tautomerization of $[\text{H}_2\text{L}^{\text{VII}}]$ observed in the solid-state and solution.....	111
Figure 4.3 Projection of $\text{Th}[\text{L}^{\text{VII}}]_2$ highlighting the 8-coordinate thorium(IV) .....	112
Figure 4.4 Projection of $\text{Ce}[\text{L}^{\text{VII}}]_2$ highlighting the 8-coordinate cerium (IV) .....	113
Figure 4.5 Projections of $\text{Nd}_2[\text{L}^{\text{VII}}]_3$ .....	116

Figure 4.6 Projections of $Gd_2[L^{VII}]_3$ .....	117
Figure 4.7 Projections of $Ho_2[L^{VII}]_3$ .....	118
Figure 4.8 Projections of $Yb_2[L^{VII}]_3$ .....	119
Figure 4.9 Projections of $Eu_2[L^{VII}]_3$ .....	120
Figure 4.10 Projections of $Tb_2[L^{VII}]_3$ .....	121
Figure 4.11 Projections of $Dy_2[L^{VII}]_3$ .....	121
Figure 4.12 Projections of $Er_2[L^{VII}]_3$ .....	121
Figure 4.13 Projections of $Lu_2[L^{VII}]_3$ .....	122
Figure 4.14 Projection of the asymmetric unit of $UO_2[L^{VII}]$ .....	124
Figure 4.15 Projections of the $UO_2[L^{VII}]$ complex highlighting the hydrogen bonded tetramers and pi-pi stacking interactions.....	125
Figure 4.16 Absorption and emission of $Th[L^{VII}]_2$ $CHCl_3$ solution and single crystals.....	126
Figure 4.17 Solid-state and solution absorbance and emission spectra of $Ce[L^{VII}]_2$ .....	126
Figure 4.18 Solid-state and solution absorbance and emission spectra of $Th[L^{VII}]_2$ .....	127
Figure 4.19 Solid-state and solution absorbance and emission spectra of $H_2[L^{VII}]_2$ .....	128
Figure 4.20 Normalized solution and solid-state emission of $Th[L^{VII}]_2$ .....	129
Figure 4.21 Ground state HOMO and LUMO of $Th[L^{VII}]_2$ and $Ce[L^{VII}]_2$ .....	130
Figure 4.22 Vertically excited electronic levels of $Th[L^{VII}]_2$ and $Ce[L^{VII}]_2$ .....	131
Figure 4.23 Absorption spectra of 15 $\mu M$ solutions of $Nd_2[L^{VII}]_3$ , $Gd_2[L^{VII}]_3$ , $Ho_2[L^{VII}]_3$ , $Yb_2[L^{VII}]_3$ and $[H_2L^{VII}]$ .....	132
Figure 4.24 Normalized emission spectra of 15 $\mu M$ solutions of $Nd_2[L^{VII}]_3$ , $Gd_2[L^{VII}]_3$ , $Ho_2[L^{VII}]_3$ , $Yb_2[L^{VII}]_3$ and $[H_2L^{VII}]$ .....	133
Figure 4.25 Solution phase absorbance and emission after 365 nm excitation of 15 $\mu M$ $CHCl_3$ solutions of $Pr_2[L^{VII}]_3$ , $Nd_2[L^{VII}]_3$ , $Sm_2[L^{VII}]_3$ , and $Eu_2[L^{VII}]_3$ .....	134
Figure 4.26 Solution phase absorbance and emission after 365 nm excitation of solutions of $Gd_2[L^{VII}]_3$ , $Tb_2[L^{VII}]_3$ , $Dy_2[L^{VII}]_3$ , $Ho_2[L^{VII}]_3$ , $Er_2[L^{VII}]_3$ , $Yb_2[L^{VII}]_3$ .....	135

Figure 4.27 Solution phase absorbance and emission after 365 nm excitation of $\text{Lu}_2[\text{L}^{\text{VII}}]_3$ ..	136
Figure 4.28 Quantum Yield Plot of $\text{Ln}_2[\text{L}^{\text{VII}}]_3$ complexes .....	137
Figure 4.29 Solid-state absorbance and emission of a single crystal of $\text{Lu}_2[\text{L}^{\text{VII}}]_3$ .....	138
Figure 4.30 Solid-state absorbance and emission of $\text{Pr}_2[\text{L}^{\text{VII}}]_3$ . and $\text{Nd}_2[\text{L}^{\text{VII}}]_3$ .....	138
Figure 4.31 Solid-state absorbance and emission of $\text{Sm}_2[\text{L}^{\text{VII}}]_3$ , $\text{Eu}_2[\text{L}^{\text{VII}}]_3$ , $\text{Gd}_2[\text{L}^{\text{VII}}]_3$ , $\text{Tb}_2[\text{L}^{\text{VII}}]_3$ , $\text{Dy}_2[\text{L}^{\text{VII}}]_3$ , and $\text{Ho}_2[\text{L}^{\text{VII}}]_3$ .....	139
Figure 4.32 Solid-state absorbance and emission of $\text{Er}_2[\text{L}^{\text{VII}}]_3$ . and $\text{Yb}_2[\text{L}^{\text{VII}}]_3$ .....	140
Figure 4.33 Solid-state emission spectra of the $\text{Ln}_2[\text{L}^{\text{VII}}]_3$ complexes.....	141
Figure 5.1 Projections of ligands described in this work.....	166
Scheme 5.1 General synthetic scheme for U(IV) salphenzaine complex, $\text{U}[\text{L}^{\text{I}}]_2$ .....	168
Scheme 5.2 General synthetic scheme for naphthylsalophen U(IV) complex, $\text{U}[\text{L}^{\text{VII}}]_2$ .....	169
Scheme 5.3 Synthesis reported to result in the formation of <b>1</b> .....	170
Scheme 5.4 Proposed synthesis for <b>2</b> .....	171
Scheme 5.5 Synthesis for formation of <b>3</b> , a derivative of $\text{H}_2[\text{L}^{\text{III}}]$ .....	172
Figure 5.2 Proposed naphthylsalophen derivatives .....	173
Scheme 5.7 Synthetic scheme for the formation of 1,2-diamino-4-methoxybenzene.....	173
Scheme 5.8 Proposed synthetic scheme for the formation of 1,2-diamino-4-sulfobenzene.....	174
Figure 5.3 Proposed salqu derivatized macrocyle, reported sensor for uranyl, and proposed benzene derivatized macrocycle .....	177
Scheme 5.9 Synthetic strategy to attain compound <b>7</b> .....	177
Scheme 5.10 Synthetic strategy to synthesize compounds <b>8</b> and <b>6</b> .....	178
Scheme 5.11 Proposed alternate synthetic strategy to form compound <b>8</b> .....	179

## List of Abbreviations

Ace	Acetone
Acac	Acetylacetonate
ACN	Acetonitrile
CAN	Ceric ammonium nitrate
CCDC	Cambridge Crystallographic Data Center
CIF	Crystallographic Information File
DCM	Dichloromethane
DDQ	2,3-Dichloro-5,6-dicyano-1,4-benzoquinone
DIAMEX	Diamide extraction
DFT	Density functional theory
DMF	Dimethylformamide
DMSO	Dimethylsulfoxide
En	Ethylenediamine
ESI	Electrospray ionization
Et <sub>2</sub> O	Ether
EtOH	Ethanol
GANEX	Group actinide extraction
HOMO	Highest occupied molecular orbital
LAH	Lithium aluminum hydride



LUMO	Lowest unoccupied molecular orbital
MeOH	Methanol
MOF	Metal organic framework
NEt <sub>3</sub>	Triethylamine
NIR	Near Infrared
OLED	Organic light emitting diodes
OAc	Acetate
PET	Positron emission topography
PUREX	Plutonium uranium recover by extraction
SMM	Single molecule magnet
t-bu	tert-butyl
TD-DFT	Time dependent density functional theory
TBP	Tributyl Phosphate
TFA	Trifluoroacetic Acid
TFAA	Trifluoroacetic Anhydride
THF	Tetrahydrofuran
TOF MS	Time of flight mass spectrometry
Tol	Toluene
TRUEX	Transuranium extraction process
UV	Ultraviolet
XRD	X-ray diffraction

## **Chapter 1: Introduction**

### **Main Objective**

The main goal of this work is to describe new Schiff base and salen ligands and explore fundamental *f*-block coordination chemistry. Herein, two new salen ligand derivatives containing extended conjugation or pyridyl coordination are synthesized and characterized in terms of their ability to sense actinide ions colorimetrically. The first new compound introduces a phenazine backbone into the salen-type ligand structure; the second includes a pyridine coordination moiety in addition to the salen coordination environment. A third salen ligand derivative, “naphthylsalophen”, was synthesized and became a conduit to further explore *f*-block coordination chemistry and unusual emission properties in the presences of both lanthanides and actinides. The theme of this text is to explore *f*-block coordination chemistry in solution and the solid-state through salen-type compounds which may bring forth properties that can be applied in the areas of sensing.

### **Nuclear Power and Nuclear Waste**

In the twentieth century, scientists discovered new ways to utilize the actinide elements, which prompted great advances in both energy and weaponry. The advent of the nuclear power era has the potential to provide inexpensive, plentiful electricity with reduced carbon emissions, but these benefits are offset by concerns about the potential environmental effects of a waste spill or contamination event. Release events have occurred in the past and introduced radioactive

isotopes into the environment that have long-lasting effects on the environment. These types of instances have tarnished the reputation of the actinides as well as raised awareness for more fundamental research into these elements. Currently, these elements are used to generate about 20% of the United States energy and about 11% of the world's electricity.<sup>1</sup> Of the 30 countries that use nuclear power as an energy source, 12 use these elements to generate at least 30% of their national electricity.<sup>1</sup> As there are 449 operational nuclear power plants around the world, and 56 more that are currently in planning or under construction, the problem of nuclear waste generation is once again on the minds of the general public, especially given the disastrous environmental effects observed after the recent Fukushima incident.<sup>2-4</sup>

While the nuclear-power-related release events that have occurred were from poor design, human error, or natural disasters, the possibility of nuclear waste release still remains at the forefront of public concern. Although the waste volumes generated through nuclear power production in comparison to the energy created is much smaller than fossil fuel energy sources, residual radioactive isotopes remain after the nuclear fuel cycle, which is a once-through process in the United States.<sup>5-7</sup> Unfortunately, high-level waste must be stored on-site in the United States, and oftentimes the storage methods and aging containers leave room to be improved.<sup>8</sup> There are two main ways of approaching this problem for the long term: remediation of waste and improved storage facilities.

Research into better storage methods that would prevent these radioactive isotopes from leaching into the environment is one way engineers can help with this issue.<sup>9-10</sup> Another long-term solution would be to reduce the need for on-site storage by removing the most harmful nuclei, thereby reducing the volume of high-level waste. The most commonly used process to separate uranium and plutonium in this waste is the Plutonium Uranium Recover by EXtraction

(PUREX) process, which uses a tributyl phosphate (TBP) ligand and hydrocarbon solvent.<sup>11-12</sup> Other processes such as the diamide extraction (DIAMEX) and the transuranium extraction process (TRUEX) are also used worldwide.<sup>11-12</sup> Group actinide extraction (GANEX) is a proposed process currently gaining popularity in Europe to replace the PUREX process.<sup>11</sup> Many of these ligands shown in **Figure 1.1** use a mix of hard oxygen donor atoms and softer phosphorous or nitrogen atoms. Softer donors have been found to improve selectivity for the actinides over the lanthanides due to the more ionic character of the 4f elements and the radial extension of the 5f orbitals.<sup>11</sup>

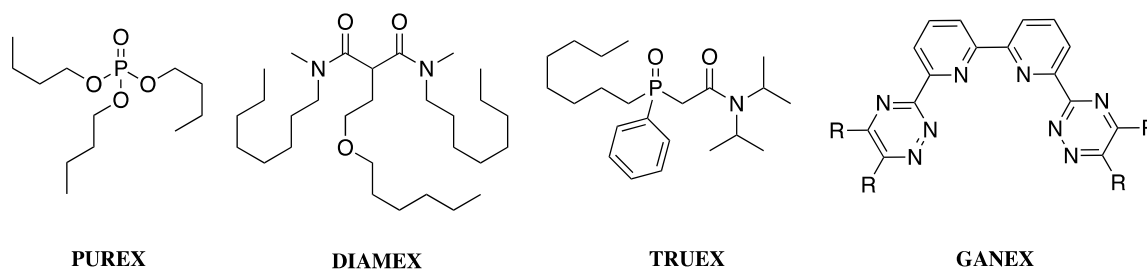


**Figure 1.1.** Ligand systems used during spent nuclear fuel remediation for each of the aforementioned separation techniques.<sup>11</sup>

In the immediate future, however, the need to identify when radioactive waste or material has been leaked into the environment is great. While methods to detect radioactive material are available, many of these methods cannot identify the isotope present or have high rates of misidentification.<sup>13-14</sup> Geiger counters are easy to use and identify radioactive material when  $\beta$ -particles send a charge through their wiring, but no identifying features other than the amount of  $\beta$ -particles present can be discerned.<sup>13</sup> Gamma detectors are available and can potentially identify the radioactive nuclide present, but require specialized equipment, are high cost, and need a specialist to glean any of the identifying information for a specific element.<sup>14</sup> A need exists for a reliable on-site sensor that can be operated by a non-specialist for these materials.

## Why Fundamental *f*-element Coordination Chemistry?

Long-term storage, as well as the more immediate need for environmental sensors, relies on our fundamental understanding of *f*-element chemistry. To illustrate the room for fundamental chemistry left in the *f*-block, currently, the number of metal containing structures deposited to the Cambridge Crystallographic Data Center (CCDC) is 551,204.<sup>15</sup> Of these, 41,947 of them contain any *f*-block metal; only 7,666, or 1.4 %, of these structures contain an actinide metal. Of the structure containing any of the fourteen actinides, 82 % (6,295) contain uranium and 55 % (3,440) of those contain uranyl ( $[\text{UO}_2]^{2+}$ ), the hexavalent and most stable oxidation state of uranium in an aqueous environment.<sup>15</sup> For comparison purposes, only 961 thorium, 215 neptunium, and 163 plutonium structures of any oxidation state can be found in the CCDC.<sup>15</sup> The prevalence of this particular oxidation state of uranium is due to its presence in nuclear waste as well as the robust linear dioxo uranyl unit, which provides predictable coordination geometry.

Neptunium and plutonium are also found in the *-yl* form in aqueous media ( $[\text{NpO}_2]^+$  and  $[\text{PuO}_2]$ ), meaning that the design and isolation of ligands designed and optimized for uranyl sensing may be useful for further study with the transactinides. Neptunium and plutonium are more difficult to work with and disproportionate at faster rates, meaning making stock solutions of a single oxidation state of these metals can be very difficult.<sup>16-17</sup> Highly radioactive alpha emitters also require specialized handling, which is why this text only discusses the sensing of uranyl.<sup>18</sup> Identifying on-site sensors that could distinguish uranyl from both transition metals and other actinides are synthetic targets of interest, with potential for further application and new knowledge about the coordination spheres of these actinide elements.

## Actinide Imine Coordination Compounds

Many methods have been employed to coordinate actinide ions, one of the first being synthesizing ligands that contain hard oxygen donors, which capitalizes on the strong Lewis acid character and oxophilic nature of the actinides.<sup>19</sup> Synthetic examples and computational analyses of extraction methods for actinide cations with crown ether type compounds are common in the literature.<sup>20-22</sup> Another example, reported by the Raymond research group, is the 1-Hydroxypyridin-2-one (1,2-HOPO) ligand system, and derivatives thereof, containing nitrogen and oxygen donor atoms. In this case, exclusively the oxygen donors were found to bind to the actinide metal centers Th(IV),  $\text{UO}_2^{2+}$  (VI), and Pu(IV) when characterized in the solid-state.<sup>23-26</sup>

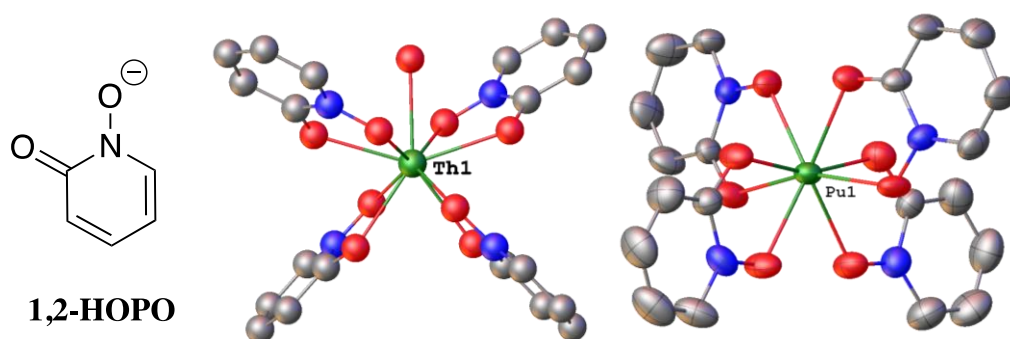


**Figure 1.2.** 1,2-HOPO ligand and projections of the 9-coordinate  $\text{Th}(1,2\text{-HOPO})_4\text{H}_2\text{O}$  and 8-coordinate  $\text{Pu}(1,2\text{-HOPO})_4$ . Carbon atoms are shown in grey, oxygen in red, nitrogen in blue and the metal center in green.<sup>23,26</sup>

Another fruitful method that has been employed to sequester and identify actinides, especially in selective sequestration of actinides even in the presence of lanthanides, has been to incorporate softer nitrogen donor atoms in the coordination sphere. This can be achieved through multidentate ligands, but there are also examples of successful macrocyclic systems, which can be designed to have high selectivity and large extinction coefficients. One family of macrocyclic chelators and their corresponding actinide complexes have been characterized using an expanded porphyrin framework. This area of actinide coordination chemistry has been heavily influenced

by the Sessler research group; their efforts have resulted in several unusually selective actinide coordination complexes.<sup>27-29</sup> One particularly interesting, recent example is a macrocyclic ligand proposed as a chemosensor that can detect uranyl in as low as parts per billion concentrations through the use of photoacoustic imaging.<sup>29</sup> This ligand has pyridine, pyrrole, and furan donors and is hexacoordinate; a projection of the uranyl complex of this ligand is shown below in **Figure 1.3.**<sup>30</sup>

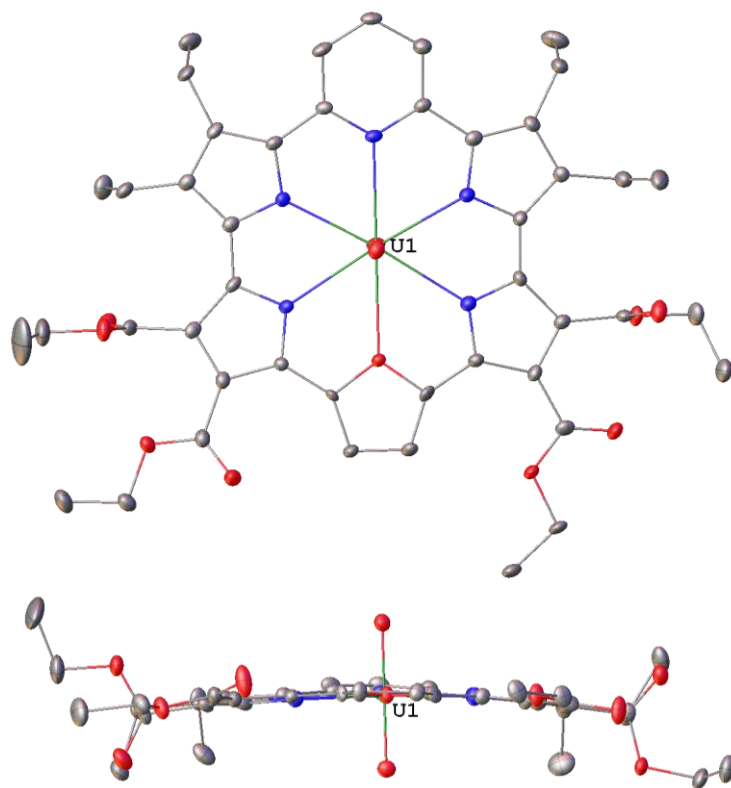


**Figure 1.3.** Projection of  $\text{UO}_2(\text{cyclo}[1]\text{furan}[1]\text{pyridine}[4]\text{pyrrole})$ . Carbon atoms are shown in gray, oxygen atoms shown in red, nitrogen in blue, and uranium in green.<sup>30</sup>

While there have been examples in the macrocyclic literature, these cryptand or porphyrin derived compounds are often quite synthetically challenging and may not scale well in mass production.<sup>26-28</sup> Additionally, these ligands can be difficult to manipulate as the pocket size is rigid, which both increases specificity for a particular ion and complicates synthetic efforts. An alternative sensing strategy that allows for easier modification, and perhaps decreases selectivity

of binding while broadening the capacity for use in real-time applications, is to use a non-macrocyclic ligand environment. Ligands used in this endeavor that contain N-donors such as pyridine, imine, or amine have been observed to have applications in catalysis and sensing.<sup>31</sup>

Specifically, salen ligand architectures, named for the salicylaldehyde and ethylenediamine starting materials, incorporate softer imine donors commonly found in the actinide sensing literature and pair them with the harder phenolate donors to yield a O-N-N-O binding pocket. These ligands have high affinities for many metals, but if differentiation can be attained in the UV-Vis signature or emission profile, more information about the contents of a waste solution can be attained. New information about the coordination chemistry of the actinides and lanthanides can be achieved through the study of these tunable compounds.

### **Actinide Salen Compounds**

The first examples of UO<sub>2</sub>-salen were synthesized by Pfeiffer and co-workers in 1937,<sup>32</sup> and the first single crystal x-ray characterization of these compounds was described in 1972 by Vigato and co-workers.<sup>33</sup> Since that time, actinide salen coordination chemistry has been of interest. Salen complexes of uranyl (VI), uranium (IV), thorium (IV) and neptunium (V) have been characterized in the literature.<sup>34-37</sup>

Salen derivatives have been applied in the development of chemosensors for uranyl. The addition of a phenolic donor in the presence of the soft imine donor, reminiscent of previously described Schiff base sensors, allows for better binding to the actinide center. A salen derivative, which includes an extended conjugated quinoxaline backbone presented in **Figure 1.4**, was synthesized in the Gorden lab and has shown promise.<sup>38-39</sup> The fluorescence observed from the quinoxaline and the ability to synthesize derivatives from common amino acid starting materials makes this complex unique in uranyl chemosensing.<sup>40</sup> The more simple salophen derivative



deposited into a film was reported in 2012 as a sensor for uranyl, although neither the solid-state characterization of the ligand nor the metal complex were reported.<sup>41</sup> Water soluble analogues of salen sensors have been shown to be selective in complexation of neptunyl and uranyl, with a preference for neptunyl and a very low affinity for lanthanides.<sup>42</sup> A few selected examples of uranyl salen complexes are shown in **Figure 1.4**.

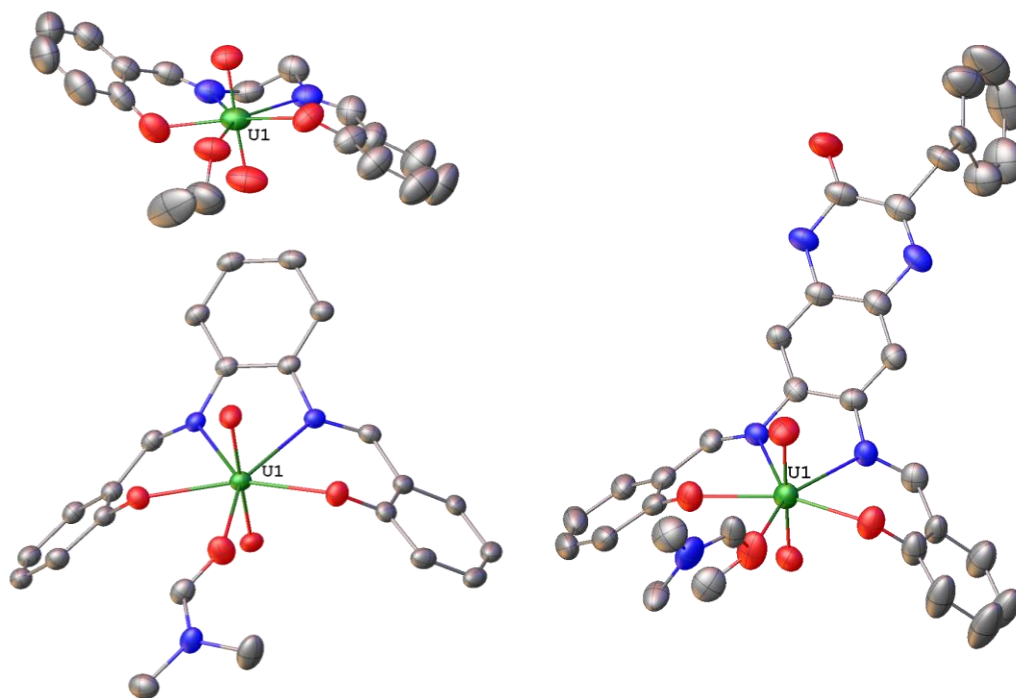


**Figure 1.4.** Projections of previously reported uranium complexes of salen, salophen, and quinoxaline salen ligands.<sup>39,44</sup>

Uranyl salen type species have also been used for anion recognition, capitalizing on the Lewis acidic nature of the uranyl moiety.<sup>42-47</sup> An early example by Reinhoudt and co-workers showed that urea and a uranyl salen complex could be co-crystallized, beginning a line of inquiry of these neutral uranyl salens applied to ion sensing.<sup>43</sup> Reinhoudt reported that functionalized uranyl salens were especially good receptors for phosphate ions,<sup>44-45</sup> and fluoride ions;<sup>46-47</sup> A projection of this co-crystallized complex can be found in **Figure 1.5**. Hosseini and co-workers have also shown selective recognition of the acetate anion in 2012.<sup>48</sup>

In addition to anion sensing, examples of cation recognition have also been observed. The Cametti and Rissanen research groups first observed recognition of quaternary ammonium halides in 2003,<sup>49</sup> and continued to publish many of the known examples of uranyl salens sensing quaternary ammonium salts, iminium salts, and lithium ions.<sup>50-52</sup> Another interesting example of uranyl salen complexes was observed in 2012 when the metal complex was bound to a chiral cavitand, and showed enantiodiscrimination of amino acid salts.<sup>53</sup>

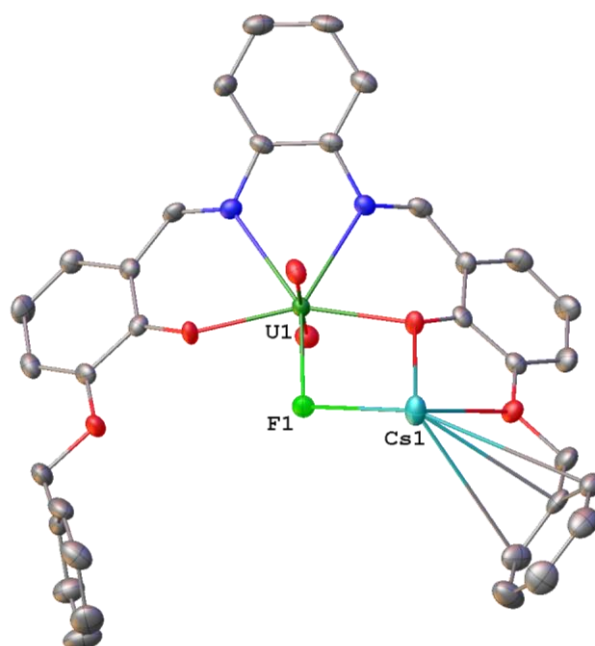


**Figure 1.5.** Projection of  $\text{UO}_2(\text{salen})$  derivative and co-crystallized  $\text{CsF}$ . Carbon atoms are shown in gray, oxygen in red, nitrogen in blue, fluoride in lime green, cesium in teal, and uranium in dark green.<sup>46</sup>

While there have been many examples of catalysis with organometallic and low valent uranium species,<sup>54</sup> many of these systems contain mixed oxo and aza donor coordination environments. Uranyl salen complexes, which contain similar mixed aza and oxo donor groups, have also been characterized for their potential use in catalysis. Uranyl salens have been employed as catalysts in 1,4-thiol additions.<sup>55-56</sup> Through the use of asymmetric salen moieties, a chiral uranyl salen catalyst has been prepared.<sup>57-58</sup> One example of an asymmetric uranyl salen

was used to catalyze a Diels Alder [4+2] cycloaddition. This catalyst functioned by stabilizing the transition state as described by Mandolini and co-workers.<sup>59-60</sup>

Salen type ligands have more recently been investigated for their ability to act as redox-active ligands and to store multiple electrons in the ligand scaffold for use in catalytic processes.<sup>54,61-62</sup> Actinide metal ions have many oxidation states readily available and they also provide opportunities for multiple electron transfer. Coupling actinide metals with redox-active ligands provides a route to synthesize new catalysts with the capability of transferring as many as 4 electrons, providing a possible pathway to complete transformations that are unattainable or extremely difficult with traditional transition metal catalysts.<sup>54</sup>

There are examples of this multielectron transfer and ligand non-innocence in uranium complexes with nitrogen-donating systems, although these are rare.<sup>61-63</sup> Salen ligands are a useful system to further explore this type of chemistry, and have been shown by Mazzanti and co-workers in 2009 to stabilize pentavalent uranyl complexes as well as polymetallic, mixed valent systems, one of which is highlighted below in **Figure 1.6**.<sup>64</sup> In a follow up study in 2010, salen complexes of both uranium(III) and uranium(IV) were used to promote C-C bond formation; these compounds could then release four electrons through oxidative cleavage of that same C-C bond.<sup>36</sup>

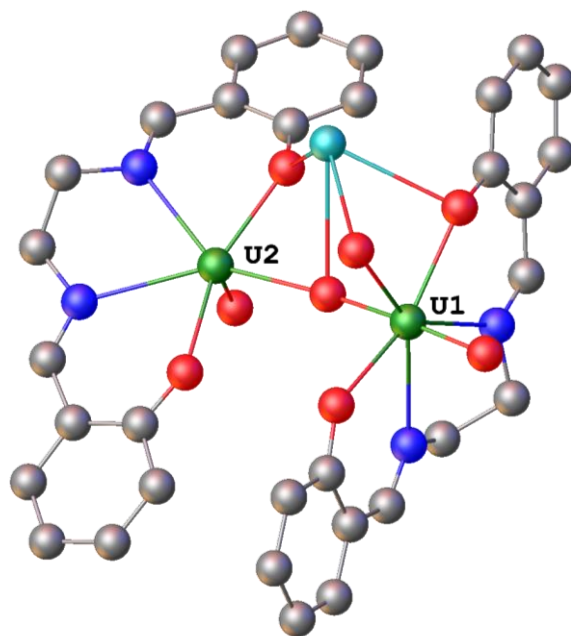


**Figure 1.6.** Projection of a mixed U(VI)/U(V) salen species, reported by Mazzanti and coworkers. Carbon atoms shown in grey, oxygen in red, nitrogen in blue, uranium in green, and potassium in teal. An interstitial pyridine, and crown ether sequestered potassium cation have been removed for clarity.<sup>64</sup>

### Lanthanide Salen Compounds

Lanthanide salen compounds are less common in the literature, as lanthanides tend to be purely ionic donors and only loosely bind to the imine nitrogen donors of salen. There are, however, examples of supramolecular aggregates of salen ligands and lanthanides proposed for use in catalysis, as single molecule magnets (SMMs), and to investigate their characteristic emission properties.

Salen *f*-block complexes have the potential to be very useful in catalysis because of their varying oxidation states and large coordination spheres. While the lanthanide metals do not have the multielectron or redox potential of the actinides, they do have large, flexible coordination spheres. This can be very useful for catalysis when coupled with a redox active ligand. The first example of such a redox active salen ligand with a lanthanide was reported by Mazzanti and coworkers in 2012.<sup>65</sup> Karsten Meyer recently showed in 2017 that nitrogen donors in a

tetraazacyclododecane ligand framework could stabilize an air-stable mixed valent U(IV) and U(V) system.<sup>66</sup> A similar aryloxide derivative, with a coordinating arene unit rather than a tetraazacyclododecane, has been shown to stabilize U(II) complexes as well as Nd(II) complexes (**Figure 1.7**).<sup>67-68</sup> This notable example involving reduction of Ln(III) to Ln(II) complexes, which can then be used as a catalyst, was observed and further developed by Evans, Meyer, and co-workers showing tunability of overpotential depending on the lanthanide present.<sup>68</sup>

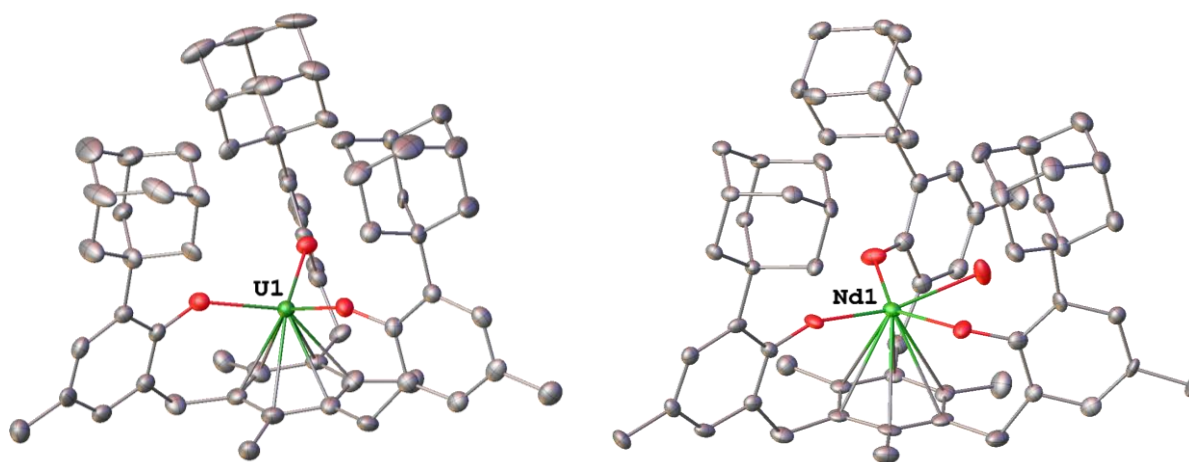


**Figure 1.7.** Projections of U(II)(arene) and Nd(II)(arene) ligands. Potassium counterions, coordinated in cryptand have been removed for clarity. Carbon atoms shown in grey, oxygen in red, nitrogen in blue, and metal ion in green.<sup>66-67</sup>

The tendency of the lanthanide ions is to remain trivalent may be somewhat limiting for catalysis purposes, but this stability in oxidation state with multiple unpaired *f*-electrons in these ions can be very useful in terms of synthesizing compounds with interesting magnetic properties.<sup>69</sup> The high number of unpaired *f*-electrons, seven in Gd(III), provides the potential of high magnetic moments. Multimetallic lanthanide species provide an opportunity to have multiple magnetic centers in a single complex and can be very useful for SMM applications.<sup>69</sup> Lanthanide chemistry varies drastically depending on the pH of solutions, the counter ions present, and equivalents used during synthesis, making multimetallic species difficult to reliably synthesize.<sup>70-71</sup>

In 2014, seven salophen lanthanide complexes were synthesized and characterized for potential SMM applications as the Pr, Nd, Gd, Sm, Eu, Tb, and Dy analogues.<sup>72</sup> Building on this work, Evangelisti and Milios reported 1-D lanthanide chains prepared from a salen derivative which demonstrated interesting magnetic cooling and relaxation of Dy and Gd analogues.<sup>73</sup> In 2017, Sanudo and co-workers applied the salen coordination geometry to breakthrough SMM compounds containing Tb or Dy with phthalocyanide ligands previously reported by Ishikawa (highlighted in **Figure 1.8**).<sup>74-75</sup> The recently reported salen multi-decker sandwich complexes of Yb and Er were described as SMMs with potential applications in quantum computing.<sup>75-78</sup> These compounds are also often observed to have interesting emission properties in the near infrared (NIR).<sup>75-76</sup>

A fair number of salen multimetallic lanthanide species have interesting emission properties lending to their use as white organic light emitting diodes (OLEDs).<sup>79-81</sup> One way to overcome the high cost barriers and difficulties synthesizing lanthanide coordination compounds is to use polymer-based OLEDs, as described in a recent report by Lu and coworkers.<sup>82</sup> Lu capitalized on the self-assembly of lanthanide salen compounds and designed metallopolymer LEDs consisting of Eu(III) or Zn(II)/Gd(III) that emitted white light.<sup>82</sup>

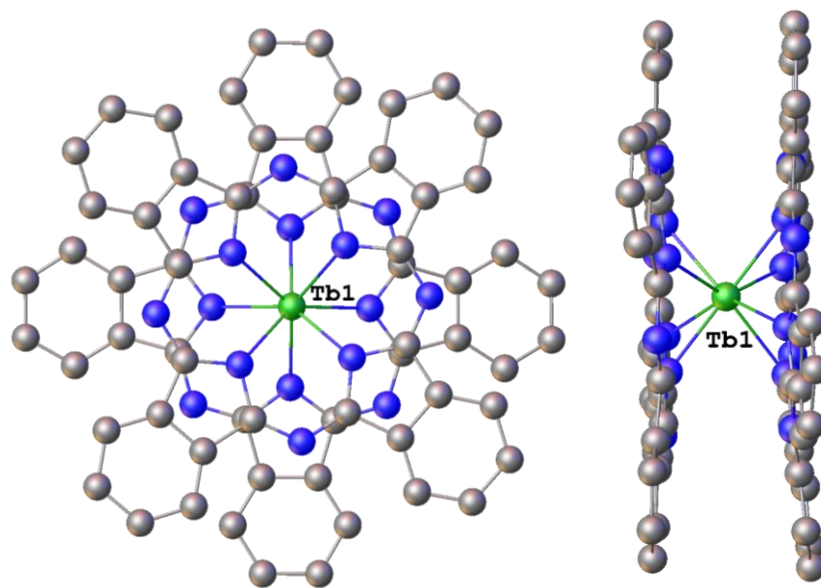


**Figure 1.8.** Projection of a Tb single molecule magnet

Finally, lanthanides have specific emission profiles and are of interest for non-invasive medical imaging. Of interest in this case, is emission in the NIR region.<sup>83</sup> While each lanthanide has a specific emission profile dependent on electronic transitions present in the metal center, these emissions are often low intensity as they are Laporte forbidden.<sup>84-85</sup> Therefore, strategies including the “antenna effect” have been employed to sensitize the lanthanide emission.<sup>81, 86</sup> The antenna effect (illustrated in **Figure 1.9**) couples a light-harvesting ligand species with a lanthanide metal center, and relies on ligand-to-metal electron transfer followed by emission to sensitize the lanthanide and increase the intensity of emission.<sup>87</sup> Salen ligands are one example of systems that have been employed as “antennas” to sensitize lanthanide emission.<sup>85,88</sup>

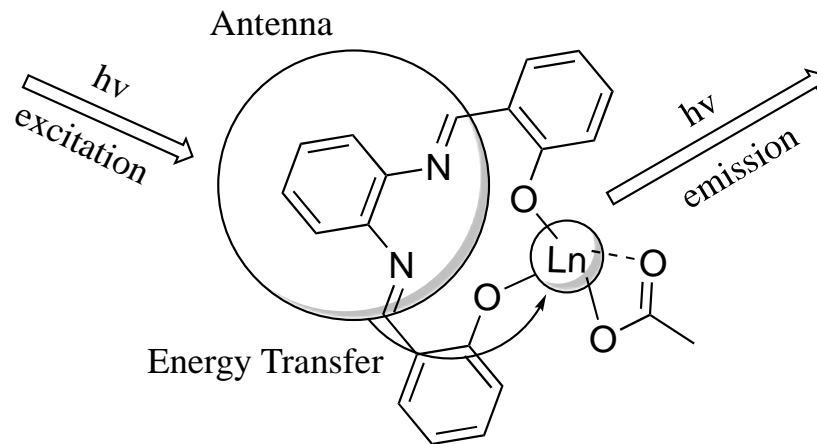


**Figure 1.9.** Cartoon of the antenna effect

One particularly useful example by Werner and co-workers incorporated a salen binding motif into a macrocyclic chelator and saw a “turn-on” emission from Eu(III) ions.<sup>89</sup> The tunability of these ligands and their affinity for electron absorption makes them a perfect candidate for this type of chemistry. These types of systems often consist of mixed d and f block metal complexes and multimetallic *f*-block metal complexes.<sup>90</sup> Examples of these light harvesting ligands contain oxygen and nitrogen donor systems, including work by De Bettencourt-Dias and Muller, which revolves around dipicolinic acid (2,6-pyridinedicarboxylic acid) derivatives.<sup>91-93</sup> The Raymond research group has studied water-stable lanthanide compounds with quantum yields as high as 60% and polarized emission from a 1,2-HOPO derivative ligand that contains aza and oxo donor atoms, shown in **Figure 1.10**.<sup>94-95</sup>



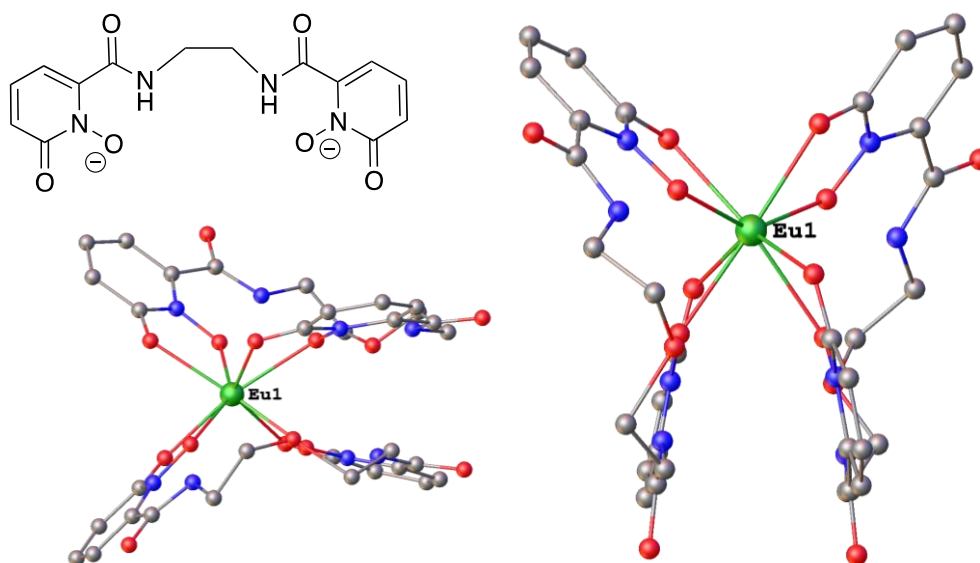


**Figure 1.10.** Schematic of a 1,2-HOPO derivative and projection of the highly emissive 2:1 Eu complex reported by Raymond in 2006. Carbon atoms shown in grey, oxygen in red, nitrogen in blue, and Eu in green. Hydrogen atoms have been removed for clarity.<sup>89</sup>

While salen complexes are abundant in the literature, much of the potential of these complexes with lanthanides and actinides remains unexplored. In this text, Schiff base and salen ligands are described for some of the uses described in this introduction. Two new salen ligand derivatives containing extended conjugation or pyridyl coordination are synthesized and characterized in terms of their ability to sense actinide ions colorimetrically. The first new compound is the next logical progression of the previously mentioned quinoxaline salen, introducing a phenazine backbone into the salen ligand structure; the second includes the addition of a pyridine coordination moiety, which is reminiscent of the aforementioned macrocyclic ligands, and retains the flexibility of a salen system. New insights into the binding kinetics and scaffold necessary for rapid, on-site sensing were gained from these studies.

A large portion of this text is devoted to the actinide and lanthanide naphthylsalophen complexes, which provide a conduit to further explore *f*-block coordination chemistry. Specifically, unexpected emission properties for thorium complexes, uncommon redox

stabilization of cerium complexes, and tunable ligand emission in self-assembled lanthanide triple-decker sandwich complexes is observed and explained herein. The overarching theme of this text is that exploring *f*-block coordination chemistry through the use of salen-type compounds may bring forth new knowledge and reveal unusual properties that can be applied in the areas of sensing, catalysis, and redox active complexes.

## References

1. Krikorian, S., International Atomic Energy Agency Releases Country Nuclear Power Profiles 2017. *IAEA News* March 15, 2018.
2. Hess, G., Spotlight on Nuclear Power. *CE&N Archive* **2011**, 89 (29), 10.
3. Buessler, K.; Aoyama, M.; Fukasawa, M., Impacts of the Fukushima Nuclear Power Plants on Marine Radioactivity. *Environ. Sci. Technol.* **2011**, 45 (23), 9931-9935.
4. Johnson, J., *Chem. Eng. News* **2014**, 92 (14), 11.
5. Peterson, P. F., Spent Nuclear Fuel is not the Problem [Point of View]. *Proc. IEEE* **2017**, 105 (3), 411-414.
6. Bruno, J.; Ewing, R. C., Spent Nuclear Fuel. *Elements* **2006**, 2 (6), 343-349.
7. Kleykamp, H., The chemical state of the fission products in oxide fuels. *J. Nucl. Mater.* **1985**, 131 (2), 221-246.
8. Slovic, P.; Layman, M.; Flynn, J. H., Risk Perception, Trust, and Nuclear Waste: Lessons from Yucca Mountain. *Environment: Science and Policy for Sustainable Development* **1991**, 33 (3), 6-30.
9. Ewing, R. C., Long-term storage of spent nuclear fuel. *Nature Materials* **2015**, 14, 252.
10. Lefort-Mary, F.; Clement, G.; Lamouroux, C.; Dumont, B. *An optimized cask technology for conditional transportation and long term interim storage of "End of Life" nuclear waste*; Nuclear Energy Agency of the OECD (NEA): NEA-Preceedings, 2016; pp 754-774.
11. Gorden, A. E.; DeVore, M. A., II; Maynard, B. A., Coordination chemistry with f-element complexes for an improved understanding of factors that contribute to extraction selectivity. *Inorg. Chem.* **2013**, 52 (7), 3445-58.

12. Paiva, A. P.; Malik, P., Recent advances on the chemistry of solvent extraction applied to the reprocessing of spent nuclear fuels and radioactive wastes. *J. Radioanal. Nucl. Chem.* **2004**, *261* (2), 485-496.
13. Montgomery, C. G.; Montgomery, D. D., The Discharge Mechanism of Geiger-Mueller Counters. *Phys. Rev.* **1940**, *57* (11), 1030-1040.
14. Minty, B. R. S., Fundamentals of airborne gamma-ray spectrometry. *J. Aus. Geo. Geophys.* **1997**, *17* (2), 39-50.
15. Allen, F. H., The Cambridge Structural Database: a quarter of a million crystal structures and rising. *Acta Cryst.* **2002**, *B58*, 380-388.
16. Sessler, J. L.; Gordon, A. E. V.; Seidel, D.; Hannah, S.; Lynch, V.; Gordon, P. L.; Donohoe, R. J.; Drew Tait, C.; Webster Keogh, D., Characterization of the interactions between neptunyl and plutonyl cations and expanded porphyrins. *Inorg. Chim. Acta* **2002**, *341*, 54-70.
17. Newton, T. W.; Hobart, D. E.; Palmer, P. D. *The Preparation and Stability of Pure Oxidation States of Neptunium, Plutonium and Americium*; Los Alamos National Laboratory: LA-UR-86-967, 1986.
18. Stout, E. L. *Safety Considerations for Handling Plutonium, Uranium, Thorium, the Alkali Metals, Zirconium, Titanium, Magnesium, and Calcium*; US Dept. of Energy Los Alamos Scientific Lab, LA-2147, 1957.
19. Diamond, R. M.; Street, K.; Seaborg, G. T., An Ion-exchange Study of Possible Hybridized 5f Bonding in the Actinides. *J. Am. Chem. Soc.* **1954**, *76* (6), 1461-1469.
20. Bombieri, G.; De Paoli, G.; Immirzi, A., Crown ether complexes of actinide elements an X-ray study of the conformational change of the crown ether within the  $\text{UO}_2(\text{NO}_3)_2(\text{H}_2\text{O})_2$  (18-crown-6) molecule. *J. Inorg. Nucl. Chem.* **1978**, *40* (5), 799-802.

21. Shamov, G. A.; Schreckenbach, G.; Martin, R. L.; Hay, P. J., Crown Ether Inclusion Complexes of the Early Actinide Elements,  $[\text{AnO}_2(18\text{-crown-}6)]^{n+}$ , An = U, Np, Pu and n = 1, 2: A Relativistic Density Functional Study. *Inorg. Chem.* **2008**, *47* (5), 1465-1475.
22. Clark, D. L.; Keogh, D. W.; Palmer, P. D.; Scott, B. L.; Tait, C. D., Synthesis and Structure of the First Transuranium Crown Ether Inclusion Complex:  $[\text{NpO}_2(18\text{-crown-}6)]\text{ClO}_4$ . *Angew. Chem. Int. Ed.* **1998**, *37* (1- 2), 164-166.
23. Riley, P. E.; Abu-Dari, K.; Raymond, K. N., Specific sequestering agents for the actinides. Synthesis of metal complexes of 1-hydroxy-2-pyridinone and the crystal structure of tetrakis(1-oxy-2-pyridinone)aquathorium(IV) dihydrate. *Inorg. Chem.* **1983**, *22* (26), 3940-3944.
24. Xu, J.; Raymond, K. N., Uranyl Sequestering Agents: Correlation of Properties and Efficacy with Structure for  $\text{UO}_2^{2+}$  Complexes of Linear Tetradentate 1-Methyl-3-hydroxy-2(1H)-pyridinone Ligands *Inorg. Chem.* **1999**, *38* (2), 308-315.
25. Xu, J.; Whisenhunt, D. W.; Veeck, A. C.; Uhlir, L. C.; Raymond, K. N., Thorium(IV) Complexes of Bidentate Hydroxypyridinonates. *Inorg. Chem.* **2003**, *42* (8), 2665-2674.
26. Gorden, A. E. V.; Xu, J.; Szigethy, G.; Oliver, A.; Shuh, D. K.; Raymond, K. N., Characterization of a Mixed Salt of 1-Hydroxypyridin-2-one Pu(IV) Complexes. *J. Am. Chem. Soc.* **2007**, *129* (21), 6674-6675.
27. Sessler, J. L.; Vivian, A. E.; Seidel, D.; Burrell, A. K.; Hoehner, M.; Mody, T. D.; Gebauer, A.; Weghorn, S. J.; Lynch, V., Actinide expanded porphyrin complexes. *Coord. Chem. Rev.* **2001**, *216-217*, 411-434.
28. Sessler, J. L.; Melfi, P. J.; Seidel, D.; Gorden, A. E. V.; Ford, D. K.; Palmer, P. D.; Tait, C. D., Hexaphyrin(1.0.1.0.0.0). A new colorimetric actinide sensor. *Tetrahedron* **2004**, *60*, 11089-11097.

29. Ho, I. T.; Sessler, J. L.; Gambhir, S. S.; Jokerst, J. V., Parts per billion detection of uranium with a porphyrinoid-containing nanoparticle and in vivo photoacoustic imaging. *Analyst* **2015**, *140* (11), 3731-3737.
30. Ho, I. T.; Zhang, Z.; Ishida, M.; Lynch, V. M.; Cha, W.-Y.; Sung, Y. M.; Kim, D.; Sessler, J. L., A Hybrid Macrocyclic with a Pyridine Subunit Displays Aromatic Character upon Uranyl Cation Complexation. *J. Am. Chem. Soc.* **2014**, *136* (11), 4281-4286.
31. Sessler, J. L.; Melfi, P. J.; Pantos, G. D., Uranium complexes of multidentate N-donor ligands. *Coord. Chem. Rev.* **2006**, *250* (7), 816-843.
32. Pfeiffer, P.; Hesse, T.; Pfitzner, H.; Scholl, W.; Thielert, H., Innere Komplexsalze der Aldimin- und Azoreihe. *Journal Praktische Chemie* **1937**, *149* (8- 10), 217-296.
33. Bandoli, G.; Clemente, D. A.; Croatto, U.; Vidali, M.; Vigato, P. A., Crystal and Molecular Structure of [NN'ethylene-bis(salicylideneiminato)UO<sub>2</sub>(MeOH)]. *Inorg. Nucl. Chem. Letters* **1972**, *8*, 961-964.
34. Hill, R. J.; Rickard, C. E. F.; White, H. E., The preparation of some complexes of Th(IV) and U(IV) with tetradentate Schiff bases The crystal structure of bis[N,N'-ethylenebis (3-methoxysalicylaldiminato)] thorium(IV) monopyridine. *J. Inorg. Nucl. Chem.* **1981**, *43* (4), 721-726.
35. Sessler, J.; Melfi, P.; Pantos, G., Uranium complexes of multidentate N-donor ligands. *Coordin. Chem. Rev.* **2006**, *250* (7-8), 816-843.
36. Camp, C.; Mougel, V.; Horeglad, P.; Pécaut, J.; Mazzanti, M., Multielectron Redox Reactions Involving C–C Coupling and Cleavage in Uranium Schiff Base Complexes. *J. Am. Chem. Soc.* **2010**, *132* (49), 17374-17377.

37. Copping, R.; Mougel, V.; Den Auwer, C.; Berthon, C.; Moisy, P.; Mazzanti, M., A tetrameric neptunyl(v) cluster supported by a Schiff base ligand. *Dalton Trans.* **2012**, 41 (36), 10900-10902.
38. Wu, X.; Gorden, A. E. V., *J. Comb. Chem.* **2007**, 9, 601.
39. Wu, X.; Bharara, M. S.; Bray, T. H.; Tate, B. K.; Gorden, A. E. V., Synthesis and characterization of 2-quinoxalinol Schiff-base metal complexes. *Inorg. Chim. Acta* **2009**, 362 (6), 1847-1854.
40. DeVore Li, M. A.; Kerns, S. A.; Gorden, A. E. V., Characterization of Quinoxolinol Salen Ligands as Selective Ligands for Chemosensors for Uranium. *Eur. J. Inorg. Chem.* **2015**, 2015 (34), 5708-5714.
41. Ghaedi, M.; Tashkhourian, J.; Montazerzohori, M.; Pebdani, A. A.; Khodadoust, S., Design of an efficient uranyl ion optical sensor based on 1'-2,2'-(1,2-phenylene)bis(ethene-2,1-diyl)dinaphthalen-2-ol. *Materials Science and Engineering: C* **2012**, 32 (7), 1888-1892.
42. Hawkins, C. A.; Bustillos, C. G.; May, I.; Copping, R.; Nilsson, M., Water-soluble Schiff base-actinyl complexes and their effect on the solvent extraction of f-elements. *Dalton Trans.* **2016**, 45 (39), 15415-15426.
43. Van Staveren, C. J.; Fenton, D. E.; Reinhoudt, D. N.; Van Eerden, J.; Harkema, S., Co-complexation of urea and  $\text{UO}_2^{2+}$  in a Schiff base macrocycle: a mimic of an enzyme binding site. *J. Am. Chem. Soc.* **1987**, 109 (11), 3456-3458.
44. Rudkevich, D. M.; Stauthamer, W. P. R. V.; Verboom, W.; Engbersen, J. F. J.; Harkema, S.; Reinhoudt, D. N., Uranyl  $\text{UO}_2$ -salenes: neutral receptors for anions with a high selectivity for dihydrogen phosphate. *J. Am. Chem. Soc.* **1992**, 114 (24), 9671-9673.

45. Rudkevich, D. M.; Verboom, W.; Brzozka, Z.; Palys, M. J.; Stauthamer, W. P. R. V.; van Hummel, G. J.; Franken, S. M.; Harkema, S.; Engbersen, J. F. J.; Reinhoudt, D. N., Functionalized UO<sub>2</sub> Salenes: Neutral Receptors for Anions. *J. Am. Chem. Soc.* **1994**, *116* (10), 4341-4351.
46. Cametti, M.; Rissanen, K., Recognition and sensing of fluoride anion. *Chem. Commun.* **2009**, (20), 2809-2829.
47. Bartocci, S.; Sabaté, F.; Bosque, R.; Keymeulen, F.; Bartik, K.; Rodríguez, L.; Dalla Cort, A., Colorimetric and fluorescence “turn-on” recognition of fluoride by a maleonitrile-based uranyl salen-complex. *Dyes and Pigments* **2016**, *135*, 94-101.
48. Hosseini, M.; Ganjali, M. R.; Veismohammadi, B.; Faridbod, F.; Abkenar, S. D.; Salavati-Niasari, M., Selective recognition of acetate ion based on fluorescence enhancement chemosensor. *Luminescence* **2012**, *27* (5), 341-345.
49. Cametti, M.; Nissinen, M.; Cort, A. D.; Mandolini, L.; Rissanen, K., Uranyl-salophen based ditopic receptors for the recognition of quaternary ammonium halides. *Chem. Commun.* **2003**, (19), 2420-2421.
50. Cametti, M.; Nissinen, M.; Dalla Cort, A.; Mandolini, L.; Rissanen, K., Recognition of Alkali Metal Halide Contact Ion Pairs by Uranyl-Salophen Receptors Bearing Aromatic Sidearms. The Role of Cation- $\pi$  Interactions. *J. Am. Chem. Soc.* **2005**, *127* (11), 3831-3837.
51. Cametti, M.; Nissinen, M.; Dalla Cort, A.; Mandolini, L.; Rissanen, K., Ion Pair Recognition of Quaternary Ammonium and Iminium Salts by Uranyl-Salophen Compounds in Solution and in the Solid State. *J. Am. Chem. Soc.* **2007**, *129* (12), 3641-3648.
52. Cametti, M.; Ilander, L.; Rissanen, K., Recognition of Li<sup>+</sup> by a Salophen-UO<sub>2</sub> Homodimeric Complex. *Inorg. Chem.* **2009**, *48* (17), 8632-8637.



53. Pappalardo, A.; Amato, M. E.; Ballistreri, F. P.; Tomaselli, G. A.; Toscano, R. M.; Trusso Sfrassetto, G., Pair of Diastereomeric Uranyl Salen Cavitands Displaying Opposite Enantiodiscrimination of  $\alpha$ -Amino Acid Ammonium Salts. *The Journal of Organic Chemistry* **2012**, *77* (17), 7684-7687.
54. Fox, A. R.; Bart, S. C.; Meyer, K.; Cummins, C. C., Towards uranium catalysts. *Nature* **2008**, *455* (7211), 341-349.
55. van Axel Castelli, V.; Cort, A. D.; Mandolini, L.; Reinhoudt, D. N., Supramolecular Catalysis of 1,4-Thiol Addition by Salophen–Uranyl Complexes. *J. Am. Chem. Soc.* **1998**, *120* (48), 12688-12689.
56. Castelli, V. v. A.; Cort, A. D.; Mandolini, L.; Reinhoudt, D. N.; Schiaffino, L., New Insight into the Mechanism of the Conjugate Addition of Benzenethiol to Cyclic and Acyclic Enones and of the Corresponding Uranyl–Salophen- Catalysed Version. *Eur. J. Org. Chem.* **2003**, *2003* (4), 627-633.
57. Cort, A. D.; Murua, J. I. M.; Pasquini, C.; Pons, M.; Schiaffino, L., Evaluation of Chiral Recognition Ability of a Novel Uranyl–Salophen- Based Receptor: An Easy and Rapid Testing Protocol. *Chem. Euro. J.* **2004**, *10* (13), 3301-3307.
58. Dalla Cort, A.; Mandolini, L.; Pasquini, C.; Schiaffino, L., Isolation and Epimerization Kinetics of the First Diastereoisomer of an Inherently Chiral Uranyl–Salophen Complex. *Org. Lett.* **2004**, *6* (11), 1697-1700.
59. Dalla Cort, A.; Mandolini, L.; Schiaffino, L., Exclusive transition state stabilization in the supramolecular catalysis of Diels-Alder reaction by a uranyl salophen complex. *Chem. Commun.* **2005**, (30), 3867-3869.

60. van Axel Castelli, V.; Dalla Cort, A.; Mandolini, L.; Pinto, V.; Schiaffino, L., A Kinetic Study of the Conjugate Addition of Benzenethiol to Cyclic Enones Catalyzed by a Nonsymmetrical Uranyl–Salophen Complex. *J. Org. Chem.* **2007**, *72* (14), 5383-5386.
61. Kraft, S. J.; Williams, U. J.; Daly, S. R.; J. Schelter, E.; Kozimor, S. A.; Boland, K. S.; Kikkawa, J. M.; Forrest, W. P.; Christensen, C. N.; Schwarz, D. E.; Fanwick, P. E.; Clark, D. L.; Conradson, S. D.; Bart, S. C., Synthesis, Characterization, and Multielectron Reduction Chemistry of Uranium Supported by Redox-Active  $\alpha$ -Diimine Ligands. *Inorg. Chem.* **2011**, *50* (20), 9838-9848.
62. Anderson, N. H.; Odoh, S. O.; Yao, Y.; Williams, U. J.; Schaefer, B. A.; Kiernicki, J. J.; Lewis, A. J.; Goshert, M. D.; Fanwick, P. E.; Schelter, E. J.; Walensky, J. R.; Gagliardi, L.; Bart, S. C., Harnessing redox activity for the formation of uranium tris(imido) compounds. *Nat. Chem.* **2014**, *6* (10), 919-926.
63. Broere, D. L. J.; Plessius, R.; van der Vlugt, J. I., New avenues for ligand-mediated processes - expanding metal reactivity by the use of redox-active catechol, o-aminophenol and o-phenylenediamine ligands. *Chem. Soc. Rev.* **2015**, *44* (19), 6886-6915.
64. Mougél, V.; Horeglad, P.; Nocton, G.; Pécaut, J.; Mazzanti, M., Stable Pentavalent Uranyl Species and Selective Assembly of a Polymetallic Mixed- Valent Uranyl Complex by Cation–Cation Interactions. *Angew. Chem.* **2009**, *121* (45), 8629-8632.
65. Camp, C.; Guidal, V.; Biswas, B.; Pecaut, J.; Dubois, L.; Mazzanti, M., Multielectron redox chemistry of lanthanide Schiff-base complexes. *Chem. Sci.* **2012**, *3* (8), 2433-2448.
66. Hümmer, J.; Heinemann, F. W.; Meyer, K., Uranium Tetrakis-Aryloxy Derivatives Supported by Tetraazacyclododecane: Synthesis of Air-Stable, Coordinatively-Unsaturated U(IV) and U(V) Complexes. *Inorg. Chem.* **2017**, *56* (6), 3201-3206.

67. Halter, D. P.; Heinemann, F. W.; Bachmann, J.; Meyer, K., Uranium-mediated electrocatalytic dihydrogen production from water. *Nature* **2016**, *530* (7590), 317-321.
68. Halter, D. P.; Palumbo, C. T.; Ziller, J. W.; Gembicky, M.; Rheingold, A. L.; Evans, W. J.; Meyer, K., Electrocatalytic H<sub>2</sub>O Reduction with f-Elements: Mechanistic Insight and Overpotential Tuning in a Series of Lanthanide Complexes. *J. Am. Chem. Soc.* **2018**, *140* (7), 2587-2594.
69. Sorace, L.; Benelli, C.; Gatteschi, D., Lanthanides in molecular magnetism: old tools in a new field. *Chem. Soc. Rev.* **2011**, *40* (6), 3092-3104.
70. Yang, X.; Jones, R. A.; Wong, W.-K., Anion dependant self-assembly and the first X-ray structure of a neutral homoleptic lanthanide salen complex Tb<sub>4</sub>(salen)<sub>6</sub>. *Chem. Commun.* **2008**, (28), 3266-3268.
71. Yang; Jones, R. A., Anion Dependent Self-Assembly of "Tetra-Decker" and "Triple-Decker" Luminescent Tb(III) Salen Complexes. *J. Am. Chem. Soc.* **2005**, *127* (21), 7686-7687.
72. Mikhalyova, E. A.; Yakovenko, A. V.; Zeller, M.; Gavrilenko, K. S.; Lofland, S. E.; Addison, A. W.; Pavlishchuk, V. V., Structure, magnetic and luminescence properties of the lanthanide complexes Ln<sub>2</sub>(Salphen)<sub>3</sub>·H<sub>2</sub>O (Ln = Pr, Nd, Sm, Eu, Gd, Tb, Dy; H<sub>2</sub>Salphen = N,N'-bis(salicylidene)-1,2-phenylenediamine). *Inorg. Chim. Acta* **2014**, *414*, 97-104.
73. Canaj, A. B.; Siczek, M.; Otreba, M.; Lis, T.; Lorusso, G.; Evangelisti, M.; Milios, C. J., Building 1D lanthanide chains and non-symmetrical [Ln<sub>2</sub>] "triple-decker" clusters using salen-type ligands: magnetic cooling and relaxation phenomena. *Dalton Trans.* **2016**, *45* (46), 18591-18602.

74. Ishikawa, N.; Sugita, M.; Ishikawa, T.; Koshihara, S.-y.; Kaizu, Y., Lanthanide Double-Decker Complexes Functioning as Magnets at the Single-Molecular Level. *J. Am. Chem. Soc.* **2003**, *125* (29), 8694-8695.
75. Dogahneh, S. G.; Khanmohammadi, H.; Sanudo, E. C., Double-decker luminescent ytterbium and erbium SMMs with symmetric and asymmetric Schiff base ligands. *New J. Chem.* **2017**, *41* (18), 10101-10111.
76. Liu, T.-Q.; Yan, P.-F.; Luan, F.; Li, Y.-X.; Sun, J.-W.; Chen, C.; Yang, F.; Chen, H.; Zou, X.-Y.; Li, G.-M., Near-IR Luminescence and Field-Induced Single Molecule Magnet of Four Salen-type Ytterbium Complexes. *Inorg. Chem.* **2015**, *54* (1), 221-228.
77. Ren, M.; Xu, Z.-L.; Bao, S.-S.; Wang, T.-T.; Zheng, Z.-H.; Ferreira, R. A. S.; Zheng, L.-M.; Carlos, L. D., Lanthanide salen-type complexes exhibiting single ion magnet and photoluminescent properties. *Dalton Trans.* **2016**, *45*, 2974-2982.
78. McAdams, S. G.; Ariciu, A.-M.; Kostopoulos, A. K.; Walsh, J. P. S.; Tuna, F., Molecular single-ion magnets based on lanthanides and actinides: Design considerations and new advances in the context of quantum technologies. *Coord. Chem. Rev.* **2017**, *346*, 216-239.
79. Utochnikova, V. V.; Kalyakina, A. S.; Bushmarinov, I. S.; Vashchenko, A. A.; Marciniak, L.; Kaczmarek, A. M.; Van Deun, R.; Brase, S.; Kuzmina, N. P., Lanthanide 9-anthracenate: solution processable emitters for efficient purely NIR emitting host-free OLEDs. *J. Mater. Chem. C* **2016**, *4* (41), 9848-9855.
80. Katkova, M. A.; Pushkarev, A. P.; Balashova, T. V.; Konev, A. N.; Fukin, G. K.; Ketkov, S. Y.; Bochkarev, M. N., Near-infrared electroluminescent lanthanide [Pr(III), Nd(III), Ho(III), Er(III), Tm(III), and Yb(III)] N,O-chelated complexes for organic light-emitting devices. *J. Mater. Chem.* **2011**, *21* (41), 16611-16620.

81. Armelao, L.; Quici, S.; Barigelletti, F.; Accorsi, G.; Bottaro, G.; Cavazzini, M.; Tondello, E., Design of luminescent lanthanide complexes: From molecules to highly efficient photo-emitting materials. *Coord. Chem. Rev.* **2010**, *254* (5), 487-505.
82. Liu, L.; Li, H.; Su, P.; Zhang, Z.; Fu, G.; Li, B.; Lu, X., Red to white polymer light-emitting diode (PLED) based on  $\text{Eu}^{3+}$ - $\text{Zn}^{2+}$ - $\text{Gd}^{3+}$ -containing metallopolymer. *J. Mater. Chem. C* **2017**, *5* (19), 4780-4787.
83. Martinić, I.; Eliseeva, S. V.; Petoud, S., Near-infrared emitting probes for biological imaging: Organic fluorophores, quantum dots, fluorescent proteins, lanthanide(III) complexes and nanomaterials. *J. Lumin.* **2017**, *189*, 19-43.
84. Bünzli, J.-C. G., Lanthanide Luminescence for Biomedical Analyses and Imaging. *Chem. Rev.* **2010**, *110* (5), 2729-2755.
85. Eliseeva, S. V.; Bunzli, J.-C. G., Lanthanide luminescence for functional materials and bio-sciences. *Chem. Soc. Rev.* **2010**, *39* (1), 189-227.
86. Bunzli, J.-C. G.; Piguet, C., Taking advantage of luminescent lanthanide ions. *Chem. Soc. Rev.* **2005**, *34* (12), 1048-1077.
87. Moore, E. G.; Samuel, A. P. S.; Raymond, K. N., From Antenna to Assay: Lessons Learned in Lanthanide Luminescence. *Acc. Chem. Res.* **2009**, *42* (4), 542-552.
88. Feng, W.-X.; Hui, Y.-N.; Shi, G.-X.; Zou, D.; Lü, X.-Q.; Song, J.-R.; Fan, D.-D.; Wong, W.-K.; Jones, R. A., Synthesis, structure and near-infrared (NIR) luminescence of series of  $\text{Zn}_2\text{Ln}$  (Ln=Nd, Yb or Er) complexes based on the Salen-type Schiff-base ligand with the flexible linker. *Inorg. Chem. Commun.* **2012**, *20*, 33-36.

89. Makhinson, B.; Duncan, A. K.; Elam, A. R.; de Bettencourt-Dias, A.; Medley, C. D.; Smith, J. E.; Werner, E. J., Turning on Lanthanide Luminescence via Nanoencapsulation. *Inorg. Chem.* **2013**, *52* (11), 6311-6318.
90. Yang, X.; Jones, R. A.; Huang, S., Luminescent 4f and d-4f polynuclear complexes and coordination polymers with flexible salen-type ligands. *Coord. Chem. Rev.* **2014**, *273-274*, 63-75.
91. Hua, K. T.; Xu, J.; Quiroz, E. E.; Lopez, S.; Ingram, A. J.; Johnson, V. A.; Tisch, A. R.; de Bettencourt-Dias, A.; Straus, D. A.; Muller, G., Structural and Photophysical Properties of Visible- and Near-IR-Emitting Tris Lanthanide(III) Complexes Formed with the Enantiomers of N,N'-Bis(1-phenylethyl)-2,6-pyridinedicarboxamide. *Inorg. Chem.* **2012**, *51* (1), 647-660.
92. Monteiro, J. H. S. K.; de Bettencourt-Dias, A.; Sigoli, F. A., Estimating the Donor–Acceptor Distance To Tune the Emission Efficiency of Luminescent Lanthanide Compounds. *Inorg. Chem.* **2017**, *56* (2), 709-712.
93. de Bettencourt-Dias, A.; Rossini, J. S. K., Ligand Design for Luminescent Lanthanide-Containing Metallopolymers. *Inorg. Chem.* **2016**, *55* (20), 9954-9963.
94. Petoud, S.; Cohen, S. M.; Bünzli, J.-C. G.; Raymond, K. N., Stable Lanthanide Luminescence Agents Highly Emissive in Aqueous Solution: Multidentate 2-Hydroxyisophthalamide Complexes of Sm<sup>3+</sup>, Eu<sup>3+</sup>, Tb<sup>3+</sup>, Dy<sup>3+</sup>. *J. Am. Chem. Soc.* **2003**, *125* (44), 13324-13325.
95. Petoud, S.; Muller, G.; Moore, E. G.; Xu, J.; Sokolnicki, J.; Riehl, J. P.; Le, U. N.; Cohen, S. M.; Raymond, K. N., Brilliant Sm, Eu, Tb, and Dy Chiral Lanthanide Complexes with Strong Circularly Polarized Luminescence. *J. Am. Chem. Soc.* **2007**, *129* (1), 77-83.

## **Chapter 2: Solid State $\pi$ - $\pi$ Stacking and Higher Order Dimensional Crystal Packing, Reactivity, Microfluidic Detection and Electrochemical Behavior of Salphenazine Actinide and Transition Metal Complexes**

Portions of this chapter are reproduced from Hardy, E. E.; Eddy, M. A.; Maynard, B. A.; Gorden, A. E. V., *Dalton Trans.* **2016**, *45*, 14243-14251 and Maynard, B. A.; Brooks, J. C.; Hardy, E. E.; Easley, C. J.; Gorden, A. E. V., *Dalton Trans.*, **2015**, *44*, 4428-4430 with permission from the Royal Society of Chemistry.

### **Introduction**

As the population rises, so does the need for power production. The environmental ramifications of high carbon emission energy sources are well documented, and production of energy that is renewable or carbon neutral is of great importance. The application of actinides in nuclear power production is one option for the reduction of greenhouse gas emissions.<sup>1-2</sup> The positive attributes of nuclear power production are counterbalanced by highly publicized radioactive material release events, which subsequently raise concerns about the potential for harmful environmental and health effects.<sup>3-5</sup>

One way to combat these widespread environmental concerns is to apply fundamental chemical knowledge about the actinides to the creation of sensor ligands that can allow for rapid, in-the-field detection if a contamination event occurs. The rational design of ligands for actinide

selective coordination is complicated by the much higher concentrations of first row transition metals that are naturally found in environmental systems.<sup>6-8</sup> In particular, the highly electropositive and earth abundant copper has been found to yield a false positive result in many ligand systems designed to selectively isolate or detect uranyl ( $\text{UO}_2^{2+}$ ), the most stable form of uranium in aqueous solution.<sup>9</sup>

The development of sensors that are able to selectively signal the presence of actinides in the environment is a key goal in immediate emergency response should release events occur *via* accident or incident, and such sensors could greatly improve the ease of remediation.<sup>10-12</sup> Schiff base-type ligands with an O-N-N-O coordination core have been investigated in numerous applications including: catalysis,<sup>13-16</sup> antimicrobial assays,<sup>17-18</sup> in organic light emitting diodes,<sup>19-21</sup> and as fluorescent or colorimetric sensors.<sup>22-25</sup> Salen metal complexes, in particular, are of interest in these and other applications due to the relative ease of introducing functionality.<sup>23</sup>

The O-N-N-O binding coordination pocket of salen-type ligands that can accommodate the equatorial binding geometry preferred by the uranyl dication coupled with the imine nitrogen soft donor, improves binding of actinides as compared to lanthanides, which are highly oxophilic and thus tend to form polymeric aggregates.<sup>26-29</sup> Our interest lies in the development of aromatic organic ligands that could be used in selective coordination of actinide ions.<sup>30-31</sup> It has been reported that the salen derived Salqu ligand [ $\text{H}_2\text{L}^{\text{II}}$ ] with an extended conjugated heterocycle (2-quinoxolinol) backbone can be selective for uranyl and act as a fluorescent sensor.<sup>25</sup> The salphenazine [ $\text{H}_2\text{L}^{\text{I}}$ ] ligand features the further extended phenazine backbone and a distinct hypsochromic shift with the coordination of uranyl dication ( $\text{UO}_2^{2+}$ ). This is very distinct from the bathochromic shift seen in the complexes with the dicationic transition metals copper, cobalt, zinc, nickel, and the tetravalent vanadyl ( $\text{VO}^{2+}$ ).<sup>32-33</sup>



Described here is the detailed characterization of salphenazine [ $\mathbf{H}_2\mathbf{L}^{\mathbf{I}}$ ],  $\mathbf{M}[\mathbf{L}^{\mathbf{I}}]$  complexes, where  $\mathbf{M} = \text{UO}_2(\text{VI})$ ,  $\text{Cu}(\text{II})$ ,  $\text{VO}(\text{IV})$ ,  $\text{Zn}(\text{II})$ ,  $\text{Co}(\text{II})$ , and  $\text{Ni}(\text{II})$  and comparable salqu [ $\mathbf{H}_2\mathbf{L}^{\mathbf{II}}$ ] metal complexes through x-ray crystallography, solution phase absorbance spectroscopy, and electrochemistry. A sterically constrained  $\mu$ -oxo  $\text{Fe}(\text{III})$  dimer complex was also characterized. Also described is a method of real-time microfluidic sensing *via* a microspectrophotometer on sub-nanoliter droplets. Droplet generating microfluidic devices retain many advantages of standard microfluidics, while allowing the formation of discrete, monodispersed droplets at rates up to 100 kHz.<sup>34-37</sup> These droplets are not strictly necessary for our proposed purposes, but they can be used to achieve statistically relevant sample sizes and provide a pathway to screen multiple ligands and metals in the same assay. A principle tenet of *5f* chemistry is reduction of waste generation, and using these microfluidic devices can be advantageous for the aforementioned ligand screening with minimal waste production.

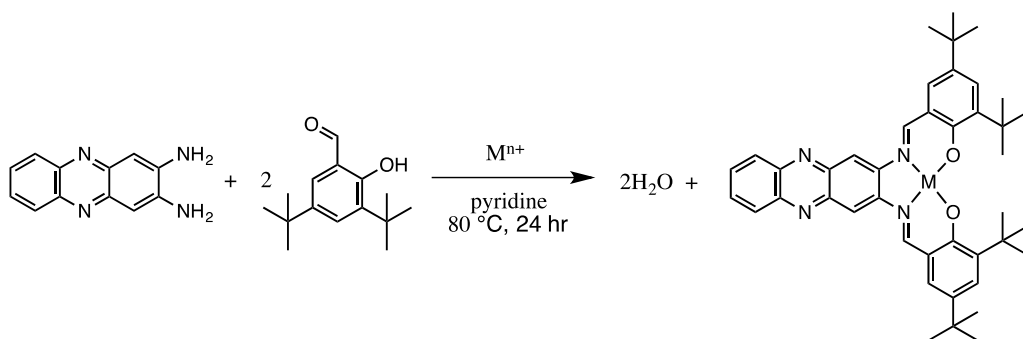
## Results and Discussion

### Synthesis

The condensation of 2,3-diaminophenazine with two equivalents of 3,5-ditertbutylsalicylaldehyde was employed to prepare a series of 1:1 metal:ligand complexes  $\mathbf{M}[\mathbf{L}^{\mathbf{I}}]$  in reasonable yields (20 - 36 %). The use of metal templation to prepare the metal complexes limits the formation of an imidazole 2-(1H-imidazo[4,5-b]phenazin-2-yl)phenol side product. This templation synthetic scheme (**Scheme 2.1**) was used to prepare the salphenazine  $\mathbf{M}[\mathbf{L}^{\mathbf{I}}]$  complexes where  $\mathbf{M} = \text{UO}_2(\text{VI})$ ,  $\text{Cu}(\text{II})$ ,  $\text{VO}(\text{IV})$ ,  $\text{Zn}(\text{II})$ ,  $\text{Fe}(\text{III})$ ,  $\text{Co}(\text{II})$ , and  $\text{Ni}(\text{II})$ . These compounds have been characterized in the solid state via single crystal X-ray diffraction and in

the liquid phase *via* nuclear magnetic resonance, mass spectrometry, UV spectroscopy, and electrochemistry.

The preparation of the free-base form of  $[\mathbf{H}_2\mathbf{L}^1]$  in quantity both large enough and pure enough for further studies required preparing the complex in the templation reaction followed by subsequent stripping of the coordinating metal from the complex using a nitric acid wash. The free-base was dissolved in chloroform, and washed with 1 M  $\text{HNO}_3$ . The organic phase was then washed three times with water, and then with a saturated brine solution, followed by evaporation under reduced pressure. Finally, the free-base was separated from the monosubstituted 2-(1H-imidazo[4,5-b]phenazin-2-yl)phenol product via column chromatography.



**Scheme 2.1.** Metal templated synthesis of salphenazine complexes  $\text{M}[\mathbf{L}^1]$ .

## X-Ray Crystallography

The structure of the free-base form of  $\mathbf{H}_2\mathbf{L}^1$  has been characterized by single crystal X-ray diffraction. Crystallographic details of ligand and metal series are listed in **Table 2.1**. The ligand  $[\mathbf{H}_2\mathbf{L}^1]$  crystallizes in the monoclinic space group  $\text{P}2_1/\text{n}$ . Structural representations of  $[\mathbf{H}_2\mathbf{L}^1]$  are shown in **Figure 2.1**. The  $\pi$ - $\pi$  distance between the P1-P3 rings, also depicted in **Figure 2.1**, is 3.471 Å. Of note is the non-planarity of the tetradentate binding pocket. This is counterintuitive from the highly conjugated system; however, the bond distances are such that repulsion of the

two oxygen atoms distorts the planarity of the extended  $\pi$ -conjugated network. One phenol oxygen atom is almost in plane with the phenazine backbone while the second distorts from planarity significantly, distances above the plane are O1-plane = 1.054(2) Å and O2-plane = 0.316(2) Å.

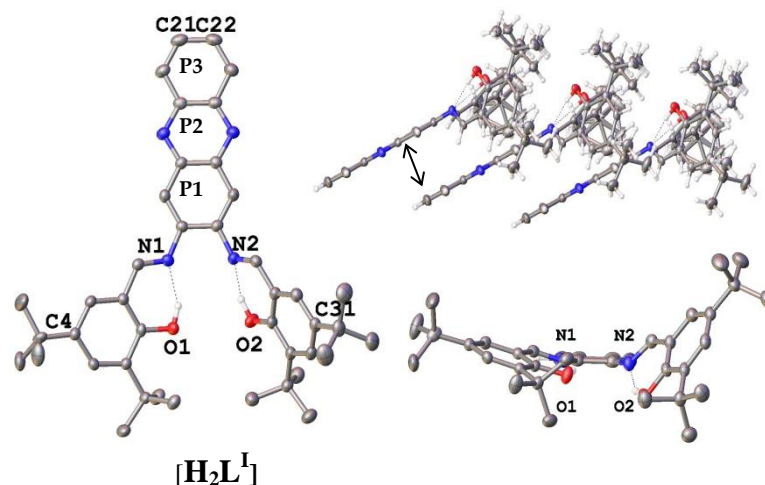


**Figure 2.1.** Salphenazine  $[\text{H}_2\text{L}^1]$  crystal structure. Carbon atoms shown in grey, nitrogen shown in blue, oxygen shown in red, hydrogen atoms and interstitial ethyl acetate removed for clarity. Solid-state  $\pi$ - $\pi$  interactions are highlighted in this projection.<sup>31</sup>

The binding of a metal to the binding pocket causes a significant change in  $\pi$ -overlap, which can be observed by the change in the electronic spectra of both ligands. In particular, the yellow solution of the free-base  $[\text{H}_2\text{L}^1]$  turns red in the presence of common first row transition metals while it turns an orange color in the presence of uranyl, the coordination of which more greatly disturbs the planarity of conjugation. When a metal is bound, the electronic repulsion of the phenol oxygen atoms is eliminated.

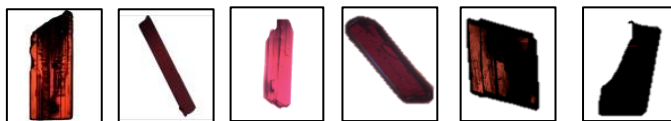
**Table 2.1.** Crystallographic data and details of data collection for  $[\text{H}_2\text{L}^{\text{I}}]$ ,  $\text{UO}_2[\text{L}^{\text{I}}](\text{H}_2\text{O})$ ,  $\text{Cu}[\text{L}^{\text{I}}]$ ,  $\text{VO}[\text{L}^{\text{I}}]$ ,  $\text{Zn}[\text{L}^{\text{I}}](\text{CH}_3\text{OH})$ , and  $\text{Fe}[\text{L}^{\text{I}}]\text{-O-Fe}[\text{L}^{\text{I}}]$ .<sup>31</sup>

	$[\text{H}_2\text{L}^{\text{I}}]\bullet 0.5\text{EtOAc}$	$\text{UO}_2[\text{L}^{\text{I}}](\text{H}_2\text{O})\bullet 2\text{H}_2\text{O}$	$\text{Cu}[\text{L}^{\text{I}}]$	$\text{VO}[\text{L}^{\text{I}}]$	$\text{Zn}[\text{L}^{\text{I}}](\text{CH}_3\text{OH})$	$\text{Fe}[\text{L}^{\text{I}}]\text{-O-Fe}[\text{L}^{\text{I}}]\bullet 1.5\text{THF}$
<b>Formula</b>	$\text{C}_{46}\text{H}_{58}\text{N}_4\text{O}_4$	$\text{C}_{42}\text{H}_{54}\text{N}_4\text{O}_7\text{U}$	$\text{C}_{42}\text{H}_{48}\text{N}_4\text{O}_2\text{Cu}$	$\text{C}_{42}\text{H}_{48}\text{N}_4\text{O}_3\text{V}$	$\text{C}_{48}\text{H}_{53}\text{N}_4\text{O}_3\text{Zn}$	$\text{C}_{90}\text{H}_{112}\text{Fe}_2\text{N}_8\text{O}_{6.5}$
<b>MM (g/mol)</b>	714.87	955.85	704.39	707.82	810.42	1529.56
<b>Crys. size (mm)</b>	0.8x0.15x0.02	0.1x0.4x0.2	0.4x0.09x0.05	0.6x0.08x0.08	0.2x0.1x0.1	0.1 x 0.3 x 0.6
<b>Crystal system</b>	monoclinic	monoclinic	triclinic	triclinic	triclinic	monoclinic
<b>space group</b>	$\text{P}2_1/\text{n}$	$\text{P}2_1/\text{n}$	$\text{P}\bar{1}$	$\text{P}\bar{1}$	$\text{P}\bar{1}$	$\text{C}_2/\text{c}$
<b>volume (<math>\text{\AA}^3</math>)</b>	3901.1(2)	5047.6(9)	1836.17(7)	2120.59(14)	2192.78(16)	8520.7(2)
<b>a (<math>\text{\AA}</math>)</b>	6.2422(2)	18.0541(18)	9.9751(2)	10.5213(4)	9.3102(5)	18.9491(3)
<b>b (<math>\text{\AA}</math>)</b>	22.8992(7)	13.4873(13)	12.6630(3)	12.7581(5)	15.1537(7)	41.3420(7)
<b>c (<math>\text{\AA}</math>)</b>	27.3841(8)	20.820(2)	14.8623(3)	16.4769(8)	16.4769(8)	13.8422(2)
<b><math>\alpha</math> (deg)</b>	90	90	93.610(1)	77.715(1)	105.875(2)	90
<b><math>\beta</math> (deg)</b>	94.7060(10)	97.380(3)	96.835(1)	74.447(1)	100.257(2)	128.2090(10)
<b><math>\gamma</math> (deg)</b>	90	90	98.716(1)	79.226(1)	91.511(2)	90
<b>Z</b>	4	4	2	2	2	4
<b><math>\rho</math> (calc. <math>\text{g cm}^{-3}</math>)</b>	1.217	1.263	1.2658	1.1084	1.227	1.192
<b><math>\mu</math> (<math>\text{mm}^{-1}</math>)</b>	0.078	3.271	0.636	0.272	0.606	0.399
<b>F(000)</b>	1522	1892	737.9	750.9	864.9	3268
<b>temp (K)</b>	180(2)	296(2)	296.15	296.15	180(2)	180(2)
<b>total no. reflex.</b>	71416	39876	54883	35450	43775	50375
<b>unique reflex.</b>	5642	8274	15270	7239	8341	9764
<b>Largest diff. peak and hole (<math>\text{e.\AA}^{-3}</math>)</b>	0.28/-0.21	2.74/-1.86	0.76/-0.28	0.32/-0.33	0.97/-0.93	0.33/-0.33
<b>Final R indices [<math>I &gt; 2\sigma(I)</math>]</b>	R1 = 0.0426	R1 = 0.0621,	R1 = 0.0375,	R1 = 0.0492,	R1 = 0.0536,	R1 = 0.0457
	wR2 = 0.1013	wR2 = 0.1816	wR2 = 0.0952	wR2 = 0.1321	wR2 = 0.1260	wR2 = 0.1374
<b>GOF</b>	1.017	1.134	1.016	1.059	1.073	1.122
<b>CCDC</b>	1452415	1019622	1019624	1452867	1452244	1018600

The  $\text{UO}_2[\text{L}^{\text{I}}]$  complex, which crystallizes in space group  $\text{P}2_1/\text{n}$ , is shown in **Figure 2.2**. Bond distances for the binding pocket can be found in **Table 2.2**. U-N distances are 2.560(7) and 2.546(8)  $\text{\AA}$ . U- $\text{O}_{\text{Ligand}}$  distances are 2.242(7) and 2.265(7). For the  $\text{UO}_2[\text{L}^{\text{I}}]$  complex, the distance from a mean plane ( $\text{L}_{\text{plane}}$ ), which is defined by atoms C22-C23-O1-O2, is 1.955  $\text{\AA}$ . Bond distances and angles for the binding pocket are found in **Table 2.2**. The  $\text{Cu}[\text{L}^{\text{I}}]$  complex is shown in **Figure 2.3**; Cu-N distances are found at 1.9304(16) and 1.9477(15)  $\text{\AA}$ . Cu-O ligand distances are found at 1.9091(12) and 1.8906(14)  $\text{\AA}$ . For the  $\text{Cu}^{2+}$  and  $\text{UO}_2^{2+}$  complexes the M-O and M-N bond distances agree with previously reported data.<sup>26,33</sup> For the  $\text{Cu}[\text{L}^{\text{I}}]$  complex, the

M-L<sub>plane</sub> distance is only 0.171 Å. As the XRD atomic coordinate data indicates, the Cu complex more closely resembles a planar system as compared to the uranyl complex.

**Table 2.2.** Selected bond distances (Å) and bond angles (deg) for [H<sub>2</sub>L<sup>I</sup>], UO<sub>2</sub>[L<sup>I</sup>](H<sub>2</sub>O), Cu[L<sup>I</sup>], VO[L<sup>I</sup>], Zn[L<sup>I</sup>](CH<sub>3</sub>OH), and Fe[L<sup>I</sup>]-O-Fe[L<sup>I</sup>]. Images show crystals from data collection.<sup>31</sup>



	[H <sub>2</sub> L <sup>I</sup> ]	Cu[L <sup>I</sup> ]	UO <sub>2</sub> [L <sup>I</sup> ]	VO[L <sup>I</sup> ]	Zn[L <sup>I</sup> ]	Fe[L <sup>I</sup> ]-O-Fe[L <sup>I</sup> ]
M-N1	--	1.92	2.54	2.05	2.07	2.11
M-N2	--	1.94	2.56	2.05	2.08	2.10
M-O1	--	1.92	2.27	1.93	1.95	1.92
M-O2	--	1.89	2.24	1.93	1.97	1.91
M-O3	---		2.45	1.59	2.11	1.76
O1-N1	2.59	2.79	2.73	2.74	2.85	2.76
N1-N2	2.70	2.58	2.71	2.59	2.65	2.62
N2-O2	2.61	2.81	2.75	2.75	2.85	2.77
O1-O2	3.41	2.66	4.42	2.65	2.89	2.80
O1-N2	3.64	3.85	4.43	3.76	3.99	3.87
O2-N1	4.23	3.81	4.40	3.83	3.92	3.85
O1-M1-N1	--	93.3	68.9	86.9	89.9	86.1
N1-M1-N2	--	83.8	64.1	78.3	79.5	76.8
N2-M1-O2	--	94.5	69.5	87.3	89.6	87.1
O2-M1-O1	--	88.7	157.5	86.9	94.9	93.9
M1-O3-M1	--	--	--	--	--	161.5
M1-Lplane*	--	0.178	1.96	0.983	0.837	0.583

L-plane defined by C4-C21-C22-C31

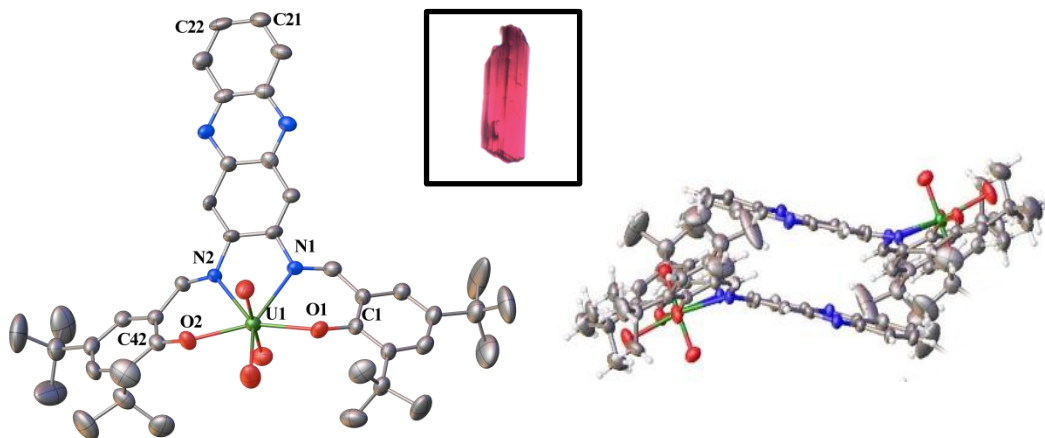


**Figure 2.2.** Projection of  $\text{UO}_2[\text{L}^1]$  complex. Hydrogen atoms have been omitted for clarity. Inset image obtained on a CRAIC 20/20 PV microspectrophotometer shows the crystal employed for X-ray data collection.<sup>30</sup>

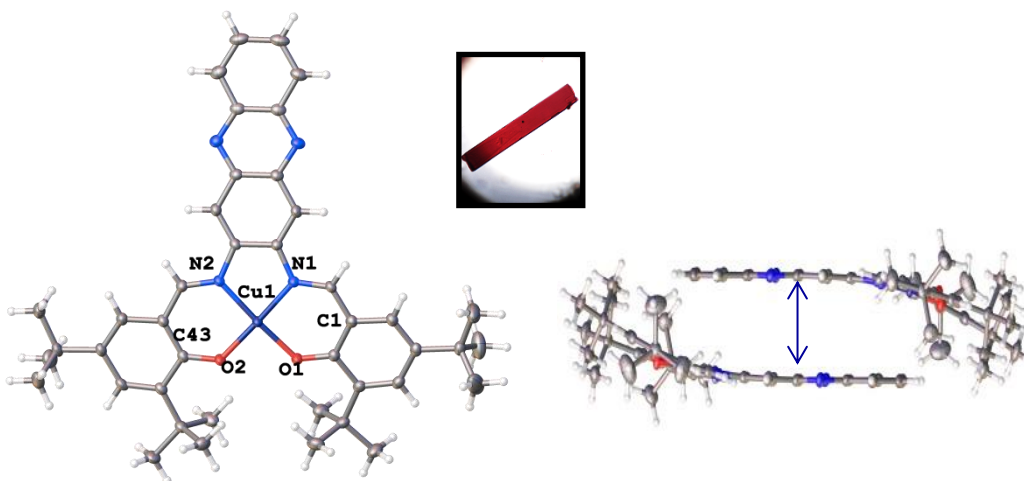


**Figure 2.3.** Projection of  $\text{Cu}[\text{L}^1]$  complex. Inset image obtained on the microspectrophotometer showing the crystal used for X-ray data collection.<sup>30</sup>

The smaller ionic radii of transition metals allows for improved planar pi orbital overlap as compared to the distortion of the conjugated system observed upon coordination of uranyl, resulting in a bathochromic shift of the charge transfer band in the uranyl complex. Complex  $\text{VO}[\text{L}^1]$ , shown in **Figure 2.4**, crystallizes in the triclinic space group  $\text{P}\bar{1}$ . This complex has a distorted square pyramidal geometry with the axial position being an oxo group on the vanadyl cation ( $\text{VO}^{2+}$ ). The geometry of the metal in the binding pocket is indicated by the bond angles

of O1-V-N1, N1-V-N2, N2-V-O2, O2-V-O1 of 86.94(8), 78.27(8), 87.31(8), and 86.90(7)° respectively, comparable to other vanadyl salen and salophen complexes (N1-V1-N2 77.3-78.7° and O1-V-N1, N2-V-O2, O2-V-O1 (86.3-88.8°).<sup>38-40</sup> The VO[L<sup>I</sup>] complex is skewed from square pyramidal geometry as compared to the Zn[L<sup>I</sup>](CH<sub>3</sub>OH) and Fe[L<sup>I</sup>]-O-Fe[L<sup>I</sup>] complexes, both of which are also square pyramidal geometries. The vanadium atom V-N1 and V-N2 bond distances are 2.050(2), 2.054(2) Å, respectively. These bond lengths are comparable to others in the literature (2.05-2.07 Å) for salen type complexes, but the lack of symmetry in the angles is unusual.<sup>38-40</sup> The twist in L<sup>I</sup> from the sterically hindered t-butyl groups causes a lack of symmetry in the binding pocket. The V-O1 and V-O2 bond distances of 1.929(2) and 1.930(2) Å respectively are comparable to literature (1.91-1.95 Å) which have greater variety than the vanadium nitrogen distances.<sup>38-40</sup>

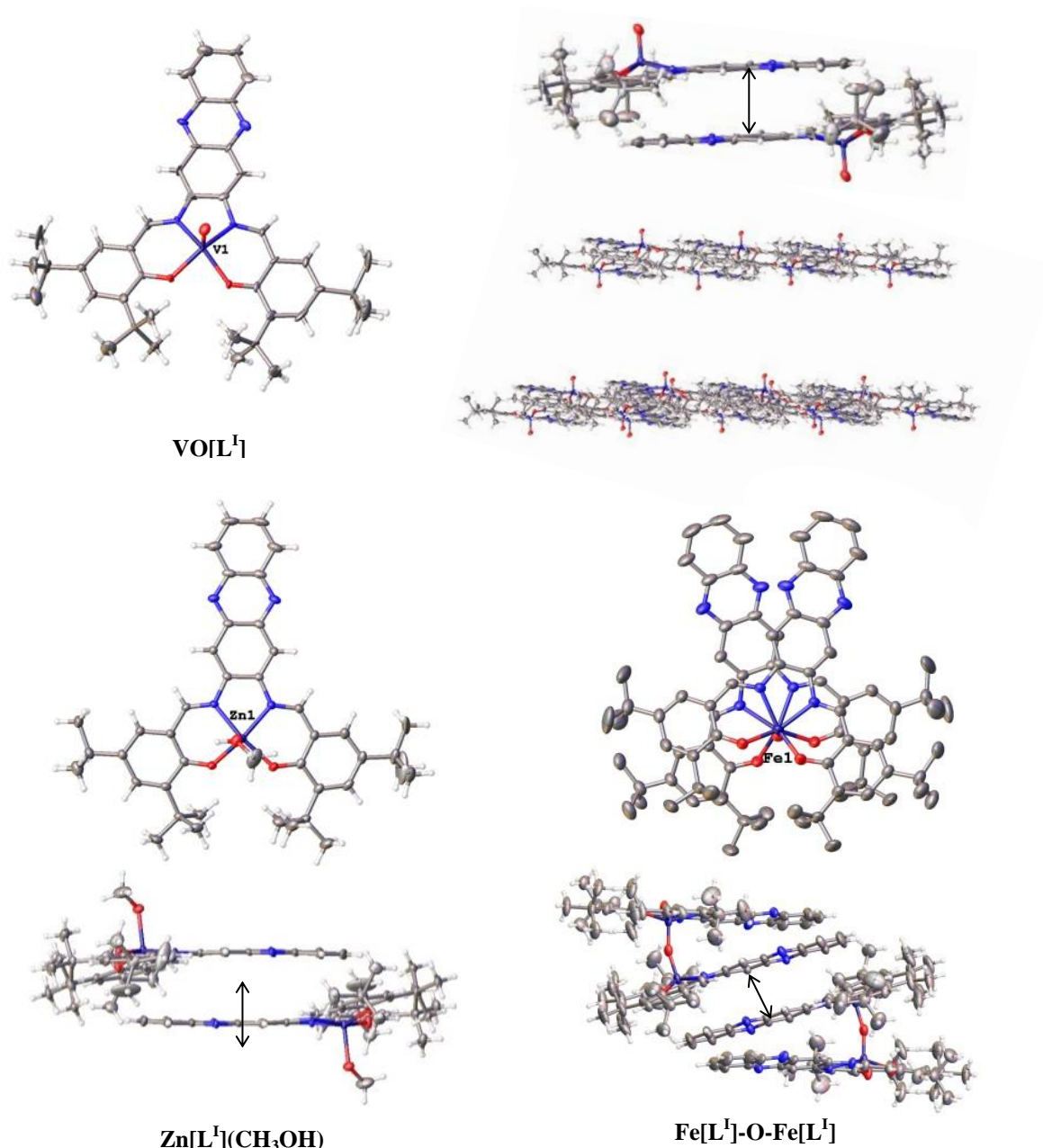


**Figure 2.4.** Projections of VO[L<sup>1</sup>], Zn[L<sup>1</sup>](CH<sub>3</sub>OH), and Fe[L<sup>1</sup>]-O-Fe[L<sup>1</sup>] complexes. Solid-state dimers and pseudo 2-D sheets are also shown. Transition metal shown in purple, carbon atoms shown in grey, nitrogen shown in blue, oxygen shown in red, hydrogen (when not omitted for clarity) are shown in white. All interstitial solvents were removed for clarity.<sup>31</sup>

This complex forms pseudo two-dimensional sheets involving a dimer held together by  $\pi$ - $\pi$  interactions in the solid state. These sheets are separated by 12.55 Å. The  $\pi$ - $\pi$  distance



between the P1-P2 rings on phenazine of the dimer is 3.36 Å. These electron rich systems prefer off-center parallel  $\pi$ - $\pi$  stacking. The M-P3 distance between the dimer phenazine rings is 3.235 Å, suggesting possible metal backbonding to the pi system of the ligand.

Complex  $\text{Zn}[\text{L}^{\text{I}}](\text{CH}_3\text{OH})$  crystallizes in the triclinic space group  $\text{P}\bar{1}$  and is shown in **Figure 2.4**. This complex has a square pyramidal geometry around the zinc atom with a coordinating neutral methanol molecule. This is observed by the close to  $90^\circ$  bond angles of the zinc to the O-N-N-O ligand donor atoms, O1-Zn-N1, N1-Zn-N2, N2-Zn-O2, O2-Zn-O1 are  $89.90(11)$ ,  $79.46(11)$ ,  $89.55(10)$ ,  $94.88(10)^\circ$  respectively. These bond angles are comparable to previously reported zinc structures with coordinating methanol or pyridine solvent ( $79.0$ - $95.5^\circ$ ).<sup>41-42</sup> The oxygen (O3) from the methanol is also approximately  $90^\circ$  from the equatorially bound ligand with O3-Zn-O1, O3-Zn-O2, O3-Zn-N1, O3-Zn-N2 angles of  $101.02(11)$ ,  $98.79(11)$ ,  $95.01(10)$  and  $105.18(11)^\circ$  respectively. This coordination solvent is quite labile, and the zinc metal quickly dissociates from the ligand under acidic conditions. The zinc atom binds less securely than the copper in the tetradentate binding pocket with Zn-N1, Zn-N2, Zn-O1, Zn-O2 bond distances of  $2.074(3)$ ,  $2.076(3)$ ,  $1.954(2)$ , and  $1.965(2)$  Å, respectively. These bond lengths are within  $\pm 0.03$  Å of the previously reported  $\text{Zn}(\text{salphenzine})(\text{DMSO})$  complex,<sup>33</sup> and within standard lengths of previously reported zinc salophen structures (Zn-O  $1.93$ - $1.97$  Å and Zn-N  $2.04$ - $2.09$  Å).<sup>41-43</sup>

Complex  $\text{Fe}[\text{L}^{\text{I}}]\text{-O-Fe}[\text{L}^{\text{I}}]$  crystallizes in the monoclinic space group  $\text{C}2/c$  and is shown in **Figure 2.4**. The iron(III) atom is in a square pyramidal geometry with the axial position being occupied by a bridging oxo group to a second, symmetry related, iron-ligand complex. This phenomenon is well documented in the literature, with 814 examples of mixed nitrogen and oxygen donor ligands with  $\mu$ -oxo geometries, and 28 examples of salen ligands with  $\mu$ -oxo

geometries reported in the Cambridge Crystallographic Data Center (CCDC).<sup>44</sup> The iron atom binds in the tetradentate binding pocket, but has the most distortion from square pyramidal as compared to the vanadyl and zinc structures with O1-Fe-N1, N1-Fe-N2, N2-Fe-O2, O2-Fe-O1 bond angles of 76.81(9), 87.14(10), 86.12(7), and 93.85(9)<sup>o</sup> respectively. These angles are comparable to other related examples in the literature (76.3-94.5<sup>o</sup>).<sup>45-46</sup> The Fe-N1, Fe-N2, Fe-O1, and Fe-O2 bond distances are also the longest of the transition metal structure in this M[L<sup>I</sup>] series with lengths of 2.1105(18), 2.100(3), 1.9216(17), and 1.906(2) Å, respectively. These distances are comparable to other Fe-salen dimers and elongated in comparison to some less sterically hindered complexes.<sup>45-47</sup> Of note is the lack of  $\pi$ -stacking in the dimer, and the Fe1-O3-Fe1 angle of 161.50(16)<sup>o</sup> which is comparable to other  $\mu$ -oxo species<sup>45-46</sup> but is well below the stereotypical limits observed of 175-180<sup>o</sup>.<sup>45-49</sup> This can be explained by steric hindrance of the substituted aldehyde moieties. The  $\pi$ - $\pi$  distance between the P1-P2 rings on the external dimer phenazine rings is 3.35 Å. The metal is 3.172 Å above the P3 ring.

Structurally, the uranyl metal complex UO<sub>2</sub>[L<sup>I</sup>] is most similar to the ligand geometry. The axial positions of the uranium coordination sphere are occupied by the two oxo “-yl” groups of the uranyl subunit. The uranium atom is bound further out in the pocket than the transition metals. These bond distances are consistently 0.5 Å longer than the transition metal analogues (**Table 2.2**). This puckering of the ligand causes a shift from a planar backbone and results in the uranium atom being 1.954(9) Å above the plane of the ligand as defined by C4-C21-C22-C31. This puckering, highlighted in **Figure 2.5**, is the explanation of the spectroscopic distinction between uranyl and the transition metal analogues.

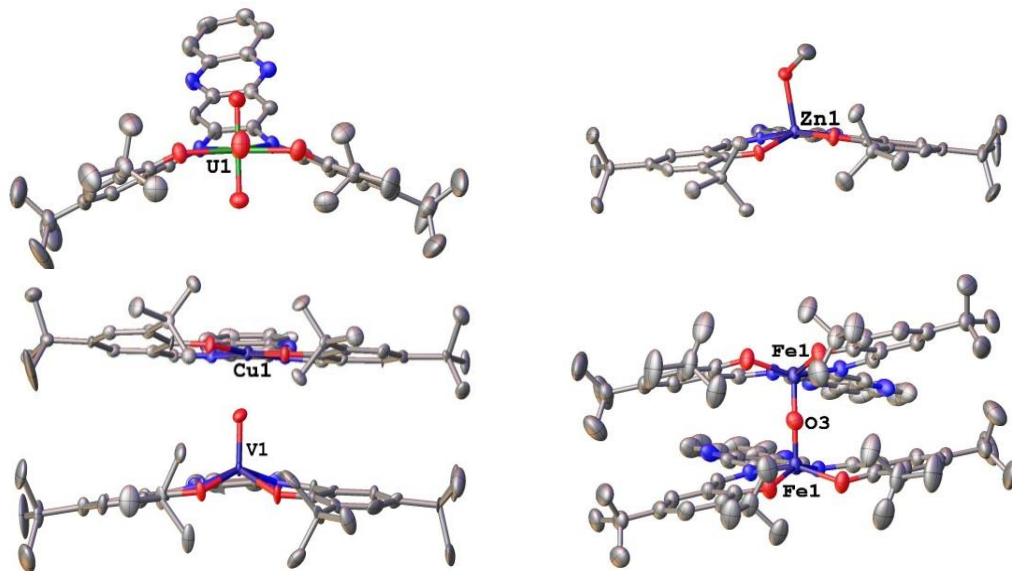


**Figure 2.5.** Projections of  $M[L^I]$  series highlighting the pucker of the tetradentate binding pocket. Carbon atoms shown in grey, nitrogen shown in blue, oxygen shown in red, transition metals shown in purple, uranium shown in green, and hydrogen omitted for clarity.<sup>31</sup>

The planarity of the ligand, regardless of the steric bulk in the 3-position of the aldehyde, observed in the transition metal complexes was surprising. The planarity of the transition metal structures can be observed most distinctly by the Cu- $L_{\text{plane}}$  distance of 0.178(3) Å. The VO[ $L^I$ ] structure is second only to the uranyl structure in distance from metal to ligand plane with V- $L_{\text{plane}}$  distance of 0.967(7) Å. The Zn- $L_{\text{plane}}$  distance of 0.837(2) Å above the ligand plane is accompanied by a twist in the O-N-N-O pocket, explaining the lability observed in this metal complex as compared to the other analogues. The iron atom is closer to the plane of the ligand, however, than Zn[ $L^I$ ](CH<sub>3</sub>OH) or VO[ $L^I$ ] structures, with a Fe- $L_{\text{plane}}$  distance of 0.583(2) Å. The iron atom is closer to the ligand plane than the other structures, while simultaneously having longer bond lengths suggesting that the *tert*-butyl groups in the 3 and 3' positions keep the pocket open wider than is strictly necessary for this metal centre.

## Spectroscopy

All UV measurements were done using a Cary 50 UV-Vis spectrometer and with pyridine as a solvent due to limitations of solubility. The  $\lambda_{\text{max}}$  values and molar absorptivities of the charge transfer bands for  $M[L^I]$  complexes are listed in **Table 2.3**. Ligand  $[H_2L^I]$  exhibits an absorption band at 420 nm. Upon 1:1 binding of  $UO_2^{2+}$  a 60 nm hypsochromic shift of the  $\pi$ - $\pi^*$  excitation to 369 nm is observed. A charge transfer band with a maximum absorbance at 470 nm ( $\epsilon = 1.95 \times 10^4 \text{ cm}^{-1} \text{ M}^{-1}$ ), a separation of 48 nm from the original ligand peak, and a shoulder at 520 nm are also observed in  $UO_2[L^I]$ . By comparison, the  $Cu[L^I]$  complex, exhibits a hypsochromic shift of the ligand peak of 24 nm and a charge transfer band at 521 nm ( $\epsilon = 1.95 \times 10^4 \text{ cm}^{-1} \text{ M}^{-1}$ ) with a shoulder at 455 nm, a peak separation of 98 nm between absorbance maxima.

**Table 2.3.** UV-Visible data for  $M[L^I]$  complexes and free base  $[H_2L^I]$ , 20  $\mu\text{M}$  in pyridine solution.<sup>31</sup>

$M$	$\lambda(\text{nm})$	$\epsilon(\times 10^4 \text{ cm}^{-1} \text{ M}^{-1})$
$[H_2L^I]$	420	1.80
$UO_2[L^I]$	369	2.64
	470	1.95
$Cu[L^I]$	394	1.62
	455	0.959
	521	1.95
$VO[L^I]$	375	1.59
	471	1.41
$Zn[L^I]$	387	1.79
	521	1.51
$Fe[L^I]-O-Fe[L^I]$	408	1.58
	511	0.926
$Co[L^I]$	338	1.88
	403	1.29
	509	1.35
$Ni[L^I]$	374	1.22
	408	1.08
	509	1.42

Compound [ $\text{H}_2\text{L}^{\text{I}}$ ] was complexed with other earth abundant transition metals  $\text{Cu}^{2+}$ ,  $\text{Zn}^{2+}$ ,  $\text{Fe}^{3+}$ ,  $\text{Co}^{2+}$ ,  $\text{Ni}^{2+}$ , and  $\text{VO}^{2+}$ . **Figure 2.6** combines the complexes and free-base, highlighting the differences between these compounds. The complex  $\text{Zn}[\text{L}^{\text{I}}]$  exhibits an absorbance feature at 520 nm ( $\epsilon = 1.51 \times 10^4 \text{ cm}^{-1} \text{ M}^{-1}$ ) with a hypsochromic shift of the ligand peak by 37 nm. The  $\text{Fe}[\text{L}^{\text{I}}]$ - $\text{O-Fe}[\text{L}^{\text{I}}]$  complex has a charge transfer band at 511 nm ( $9.26 \times 10^3 \text{ cm}^{-1} \text{ M}^{-1}$ ) after the templation condensation reaction, but shows no reaction when the  $\text{FeCl}_3$  free metal salt is introduced. The presence of a  $\text{Co}^{2+}$  ion ( $\text{Co}[\text{L}^{\text{I}}]$ ) induced a charge transfer band at 517 nm ( $\epsilon = 1.35 \times 10^4 \text{ cm}^{-1} \text{ M}^{-1}$ ), a peak separation of 93 nm, and a hypsochromic shift of the ligand peak by 12 nm. Introduction of the  $\text{Ni}^{2+}$  ion ( $\text{Ni}[\text{L}^{\text{I}}]$ ) induced a charge transfer band at 509 nm ( $\epsilon = 1.42 \times 10^4 \text{ cm}^{-1} \text{ M}^{-1}$ ), a peak separation of 85 nm, with a shoulder at 570 nm which was not present in any of the other complexes. A hypsochromic shift of 10 nm, along with an additional high energy peak was also observed. Complex  $\text{VO}[\text{L}^{\text{I}}]$ , which is the least likely contaminant in waste water samples, has a maximum at 471 nm ( $\epsilon = 1.47 \times 10^4 \text{ cm}^{-1} \text{ M}^{-1}$ ). The kinetics of binding of vanadyl was found to be much slower, over 24 hours, than the other transition metals. The  $\text{UO}_2[\text{L}^{\text{I}}]$  complex has greater than 30 nm of separation from all the transition metals, save  $\text{VO}[\text{L}^{\text{I}}]$ , and 50 nm separation between the ligand and complex absorbance. The difference in the common false positive copper and uranyl is 50 nm, and can easily be seen by the naked eye (**Figure 2.7**).

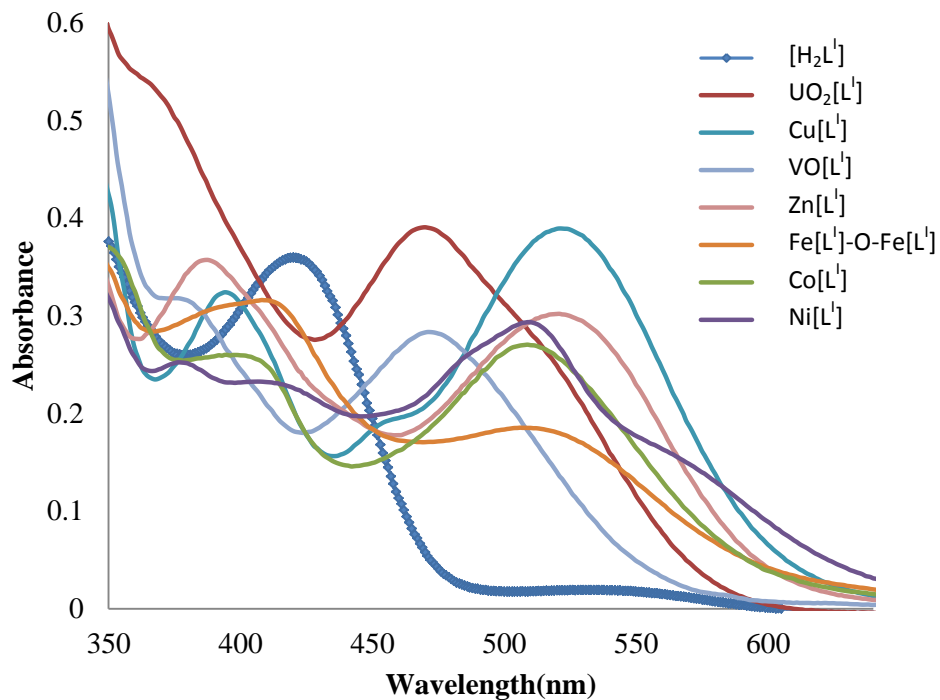


**Figure 2.6.** UV-Vis spectral changes of  $M[L^I]$  complexes at  $20 \mu\text{M}$  concentration in pyridine.<sup>31</sup>

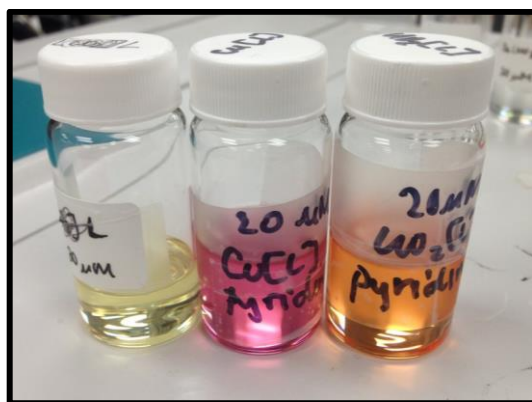


**Figure 2.7.** Vials with  $20 \mu\text{M}$  solutions of  $H_2L^I$ ,  $Cu[L^I]$  and  $UO_2[L^I]$  in pyridine.

The growth of these charge transfer peaks is visualized in the metal titration spectra. Each metal salt was added to  $20 \mu\text{M}$  solutions of the free base and are shown below in **Figures 2.8-2.13**. Of note are the extended mix times necessary for  $UO_2^{2+}$ . The rearrangement of the ligand

pocket to accommodate the larger atomic radius of uranium, coupled with the need for a fifth coordination site for a solvent molecule, requires extended periods of time.

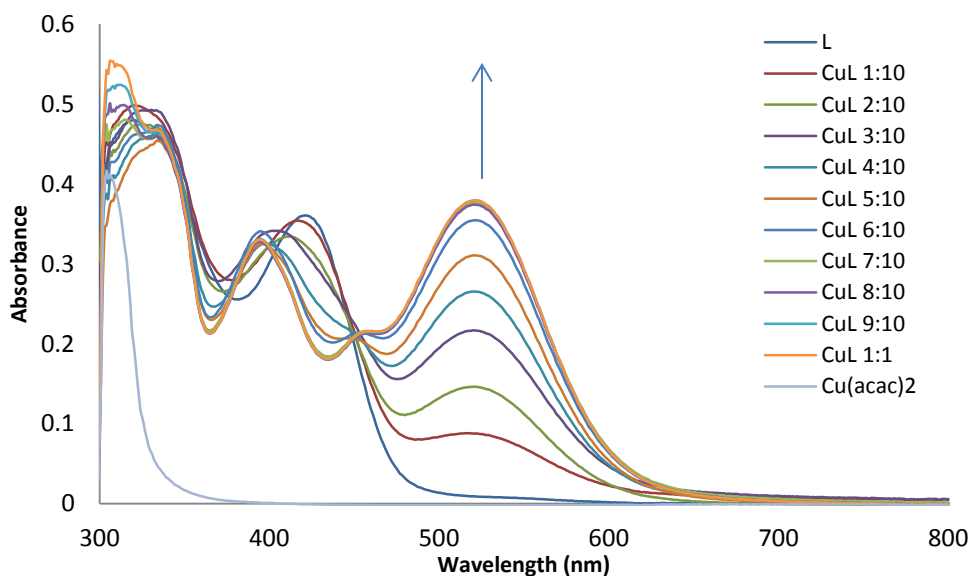


**Figure 2.8.**  $\text{Cu}(\text{acac})_2$  titration of the ligand in pyridine indicates a 1:1  $\text{Cu}^{2+}$  to  $\text{H}_2\text{L}^1$ .  $\text{H}_2\text{L}^1$  concentration was kept at  $20 \mu\text{M}$ . Spectra were obtained minutes after the solutions were made.<sup>30</sup>

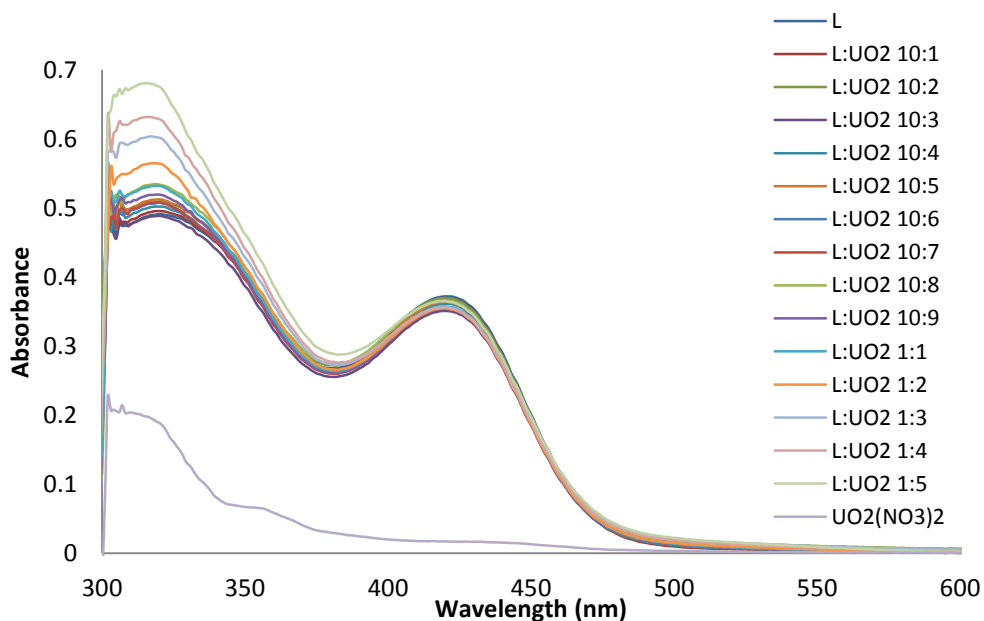


**Figure 2.9.**  $\text{UO}_2(\text{NO}_3)_2$  titration of the ligand in pyridine, indicating no binding.  $\text{H}_2\text{L}^1$  concentration was kept at  $20 \mu\text{M}$ . Spectra were obtained minutes after the solutions were made.<sup>30</sup>

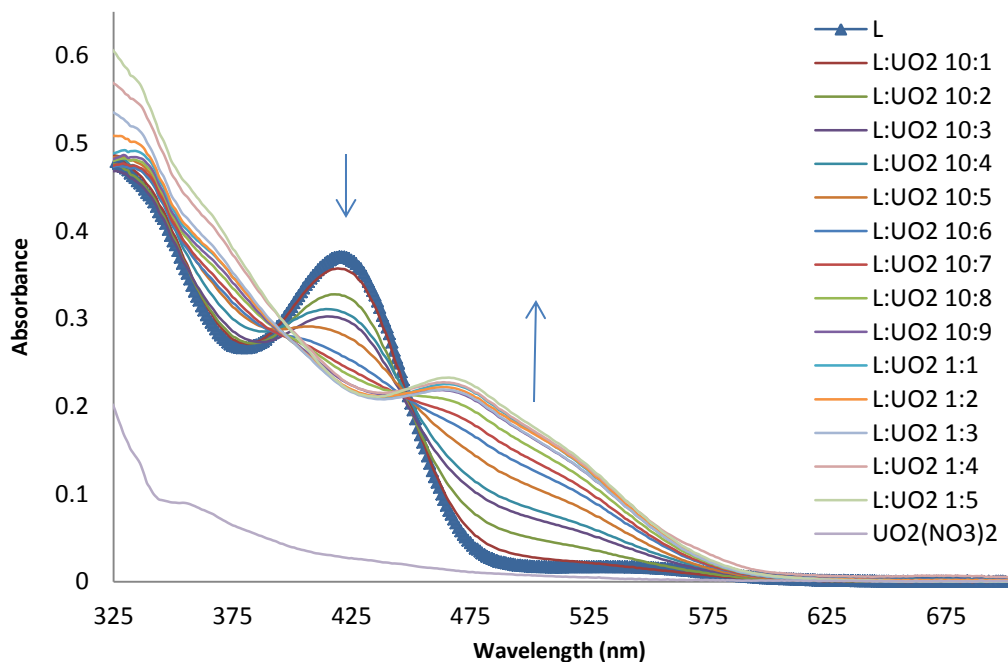


**Figure 2.10.**  $\text{UO}_2(\text{NO}_3)_2$  titration of the ligand in pyridine indicates a 1:1  $\text{UO}_2^{2+}$  to  $\text{H}_2\text{L}^1$  complex.  $\text{H}_2\text{L}^1$  concentration was kept at  $20 \mu\text{M}$ . Spectra were obtained after 3 days.<sup>30</sup>

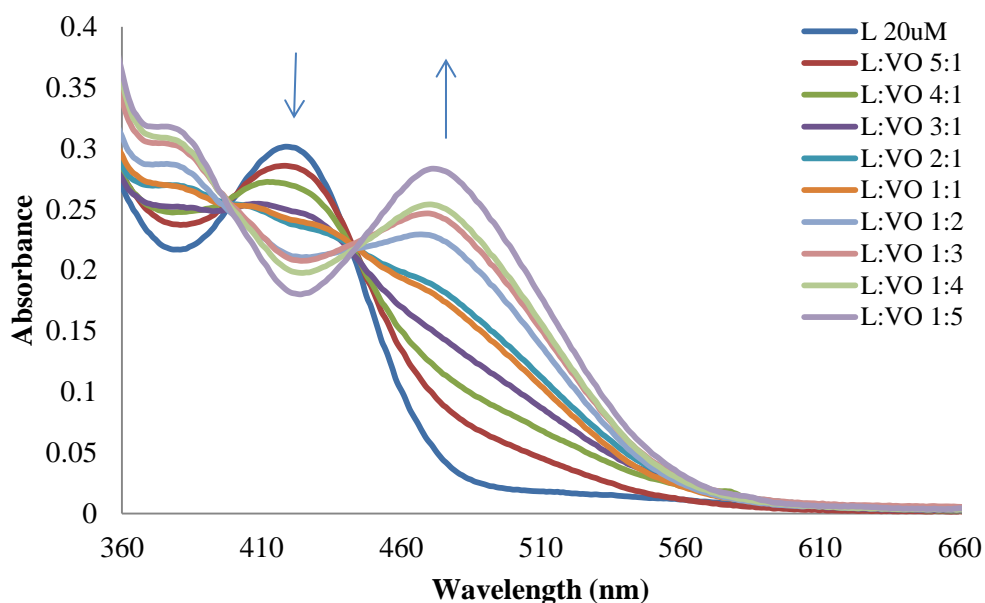


**Figure 2.11.** UV Vis spectrum of  $20 \mu\text{M}$  salphenazine [ $\text{H}_2\text{L}^1$ ] solution with varying  $\text{VO}(\text{acac})_2$  concentrations in pyridine after 72 hours stir time.<sup>31</sup>



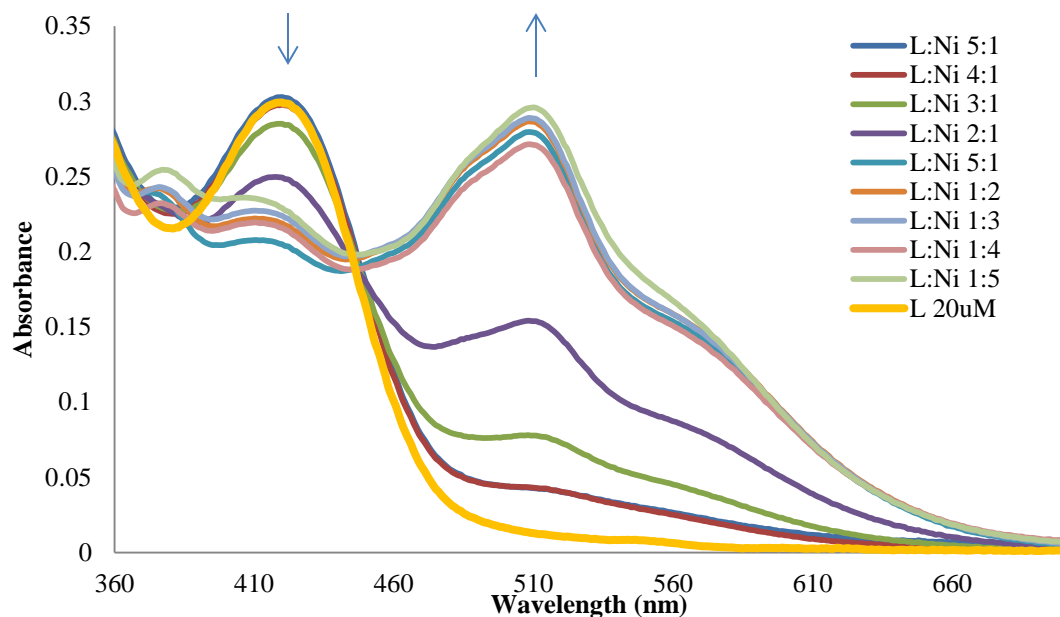


**Figure 2.12.** UV Vis spectrum of 20 μM salphenazine [H<sub>2</sub>L<sup>I</sup>] solution with varying Ni(acetate)<sub>2</sub> concentrations in pyridine after 15 minute stir time.<sup>31</sup>

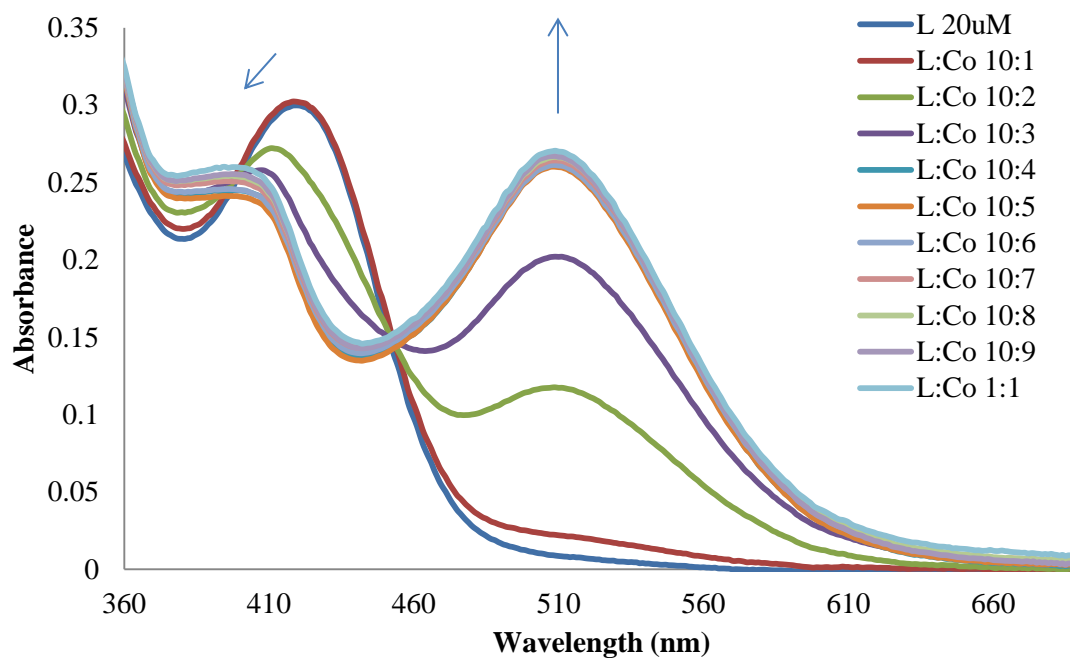
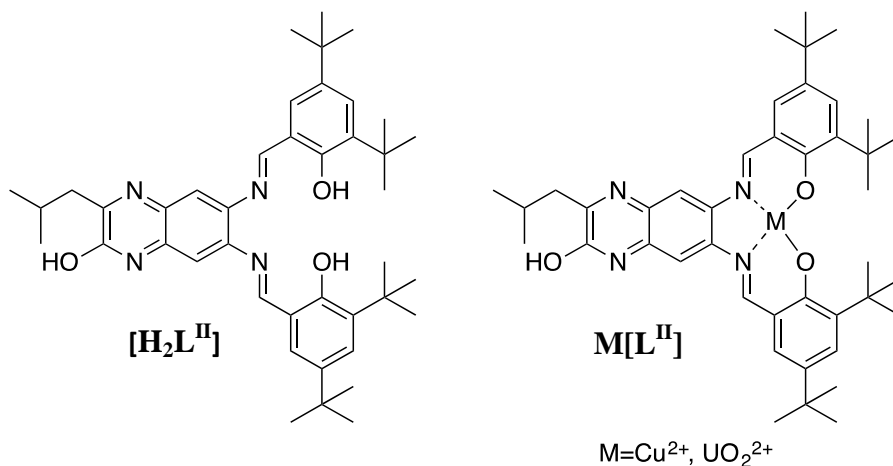


**Figure 2.13.** UV Vis spectrum of 20 μM salphenazine [H<sub>2</sub>L<sup>I</sup>] solution with varying Co(acetate)<sub>2</sub> concentrations in pyridine after 15 minute stir time.<sup>31</sup>

While extra time was necessary for the complexation of uranyl, in comparison to the other earth abundant first row transition metals, this chemistry represents a colorimetric chemosensor that can identify uranyl solutions over transition metal solutions. Further optimization of the binding geometry is necessary to create a rapid, on-site detection method.

## Electrochemistry

Cyclic voltammograms for the salphenazine compounds  $[\text{H}_2\text{L}^{\text{I}}]$ ,  $\text{UO}_2[\text{L}^{\text{I}}]$ , and  $\text{Cu}[\text{L}^{\text{I}}]$  are shown in **Figure 2.14**. The cyclic voltammograms of salqu compounds (**Scheme 2.2**)  $[\text{H}_2\text{L}^{\text{II}}]$ ,  $\text{UO}_2[\text{L}^{\text{II}}]$ , and  $\text{Cu}[\text{L}^{\text{II}}]$  are compared in **Figure 2.15**. The change in stability of ligand oxidation was also investigated. All compounds were studied at 1.0 mM concentration in a dichloromethane solution with 0.100 M of tetra-n-butylammonium perchlorate electrolyte. Experiments were run with a scan rate of 0.10-1.50  $\text{V s}^{-1}$  on a platinum working electrode vs. a  $\text{Ag}/\text{AgCl}$  reference electrode and a platinum wire counter electrode.



**Scheme 2.2.** Salqu  $[\text{H}_2\text{L}^{\text{II}}]$  and salqu complexes  $\text{M}[\text{L}^{\text{II}}]$ , synthesized according to literature procedure.<sup>31</sup>

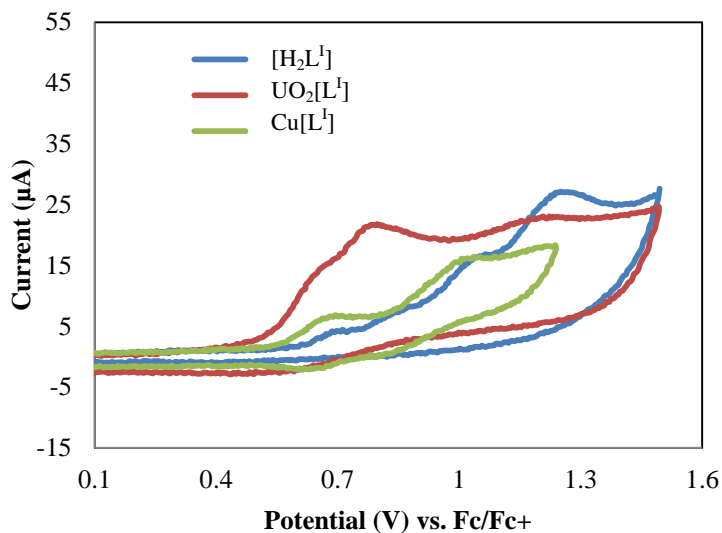


**Figure 2.14.** Cyclic voltammogram of  $[\text{H}_2\text{L}^{\text{I}}]$ ,  $\text{UO}_2[\text{L}^{\text{I}}]$ , and  $\text{Cu}[\text{L}^{\text{I}}]$ . Conditions: 0.5 mM ligand and complexes in dichloromethane, room temperature, tetra-n-butylammonium perchlorate (0.1 M) as electrolyte with a  $0.10 \text{ V s}^{-1}$  scan rate.<sup>31</sup>

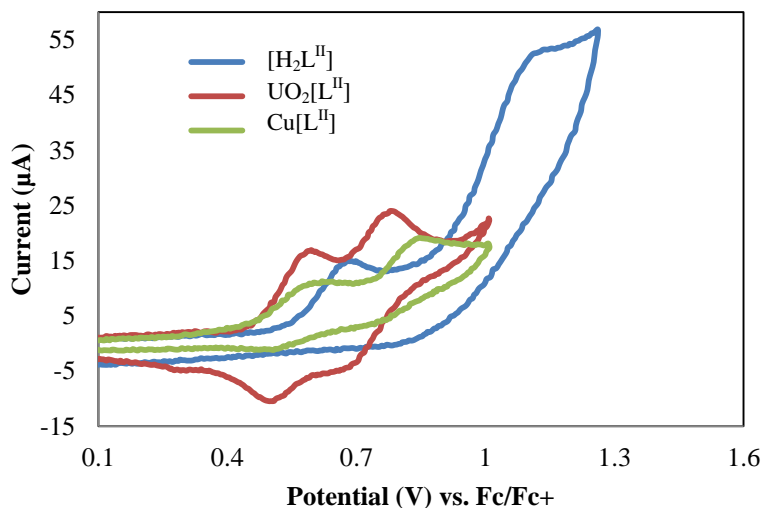


**Figure 2.15.** Cyclic voltammogram of  $[\text{H}_2\text{L}^{\text{II}}]$ ,  $\text{UO}_2[\text{L}^{\text{II}}]$ , and  $\text{Cu}[\text{L}^{\text{II}}]$ . Conditions: 1.0 mM ligand and complexes in dichloromethane, room temperature, tetra-n-butylammonium perchlorate (0.1 M) as electrolyte with a  $0.10 \text{ V s}^{-1}$  scan rate.<sup>31</sup>

The salphenazine  $[\text{L}^{\text{I}}]$  ligand shows four oxidation peaks, at  $E_p^{\text{ox,a}} = 0.72 \text{ V}$ ,  $E_p^{\text{ox,b}} = 0.89 \text{ V}$ ,  $E_p^{\text{ox,c}} = 1.07 \text{ V}$ , and  $E_p^{\text{ox,d}} = 1.27 \text{ V}$  as compared to the ferrocene ferrocenium redox couple as an internal standard, none of which are reversible. This result suggests  $[\text{H}_2\text{L}^{\text{I}}]$  can stabilize not

only the cationic radical on the phenol groups, but can further oxidize. Reduction peaks were not present in  $[\mathbf{H}_2\mathbf{L}^{\mathbf{I}}]$ . The same is not true for salqu  $[\mathbf{H}_2\mathbf{L}^{\mathbf{II}}]$ ; two oxidation peaks at  $E_p^{\text{ox,a}} = 0.68$  V and  $E_p^{\text{ox,b}} = 1.11$  V and two reduction peaks at  $E_p^{\text{red,a}} = -0.609$  V and  $E_p^{\text{red,b}} = -1.12$  V which are all not reversible are observed (shown in **Figure 2.20**). The two oxidation peaks are indicative of phenoxyl radicals formed from single electron oxidations.<sup>50-52</sup> The two reduction peaks are indicative of reduction of the imine nitrogen.<sup>50-52</sup>

One oxidation peak of  $[\mathbf{H}_2\mathbf{L}^{\mathbf{I}}]$  is not observed in the salphenazine complex  $\text{Cu}[\mathbf{L}^{\mathbf{I}}]$  which has oxidation peaks at  $E_p^{\text{ox,a}} = 0.63$  V,  $E_p^{\text{ox,b}} = 0.75$  V,  $E_p^{\text{ox,c}} = 1.16$  V. The three remaining oxidation peaks do not shift in oxidation potential from the ligand by more than  $E_p^{\text{ox}} = 0.050$  V suggesting minimal stabilization of the phenoxyl radicals formed upon oxidation by the copper ion.<sup>50</sup> Two of the oxidation peaks from  $[\mathbf{H}_2\mathbf{L}^{\mathbf{I}}]$  are absent from the complex  $\text{UO}_2[\mathbf{L}^{\mathbf{I}}]$  voltammogram. Two oxidation peaks at  $E_p^{\text{ox,a}} = 0.68$  V and  $E_p^{\text{ox,b}} = 0.98$  V remain and are now quasireversible, suggesting that the phenoxyl radicals are stabilized by the uranyl ion, with separation of the anodic of cathodic peaks of 60 and 100 mV respectively shown in **Figure 2.15**. A new reduction peak at  $E_p^{\text{red}} = -0.38$  V is observed in the complex  $\text{UO}_2[\mathbf{L}^{\mathbf{I}}]$  that is not present in the free base, suggesting that the uranyl ion stabilizes the  $\pi$ -system enough to reduce the imine nitrogen that could occur in the free base  $[\mathbf{H}_2\mathbf{L}^{\mathbf{I}}]$  (**Figures 2.16-2.17**).

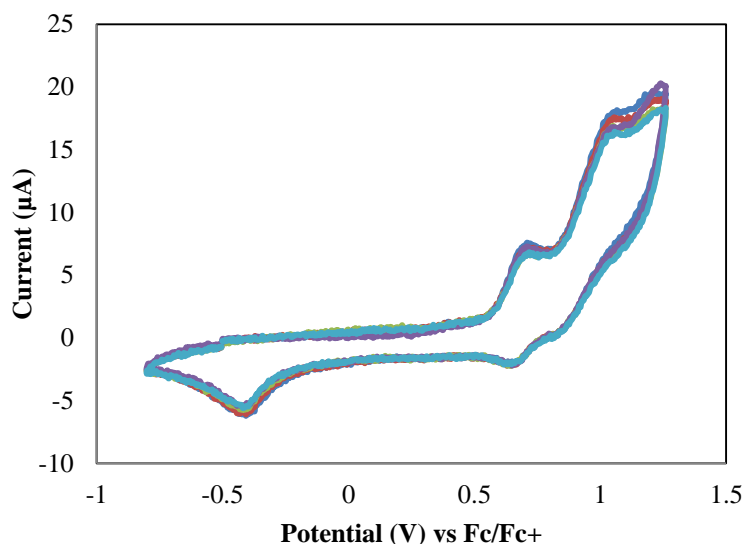


**Figure 2.16.** Cyclic voltammogram of  $\text{UO}_2[\text{L}^{\text{I}}]$  Conditions: 0.5 mM complex in dichloromethane, room temperature, tetra-n-butylammonium perchlorate (0.1 M) as electrolyte. Scan rate 0.100 V/s.<sup>31</sup>

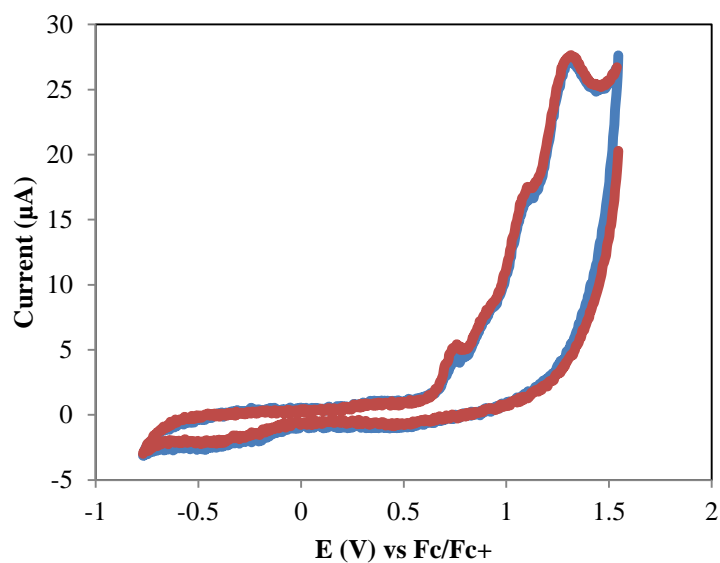


**Figure 2.17.** Cyclic voltammogram of Salphenazine  $[\text{H}_2\text{L}^{\text{I}}]$  Conditions: 0.5 mM ligand in dichloromethane, room temperature, tetra-n-butylammonium perchlorate (0.1 M) as electrolyte. Scan rate 0.100 V/s.<sup>31</sup>

The oxidation peaks in the salqu complexes  $\text{UO}_2[\text{L}^{\text{II}}]$  and  $\text{Cu}[\text{L}^{\text{II}}]$  become quasi-reversible suggesting that the phenoxyl radicals are stabilized by the metal ions.<sup>50</sup> Complex

$\text{Cu}[\text{L}^{\text{II}}]$  has two single electron oxidation peaks at  $E_p^{\text{ox,a}} = 0.56 \text{ V}$   $E_p^{\text{ox,b}} = 0.75 \text{ V}$  with anodic and cathodic peak potential separation values in the range of 50 – 70 mV (**Figure 2.18**). Complex  $\text{UO}_2[\text{L}^{\text{II}}]$  (**Figure 2.19**) has two single electron oxidation peaks at  $E_p^{\text{ox,a}} = 0.58 \text{ V}$ ,  $E_p^{\text{ox,b}} = 0.81 \text{ V}$  with anodic and cathodic peak potential separation values in the range of 20 – 50 mV that seem to be quasi-reversible at best. Both metal complexes show reversible ligand oxidation peaks at  $E_p^{\text{ox,a}}$  and  $E_p^{\text{ox,b}}$ , indicative of phenol type radical oxidation of the ligand.<sup>50</sup> The average shifts in the oxidation potential from the free base  $[\text{H}_2\text{L}^{\text{II}}]$  of  $E_p^{\text{ox}} = 0.12$  and  $E_p^{\text{ox}} = 0.032$  (**Figure 2.20**) observed in complexes  $\text{UO}_2[\text{L}^{\text{II}}]$  and  $\text{Cu}[\text{L}^{\text{II}}]$  suggest moderate stabilization of the phenoxyl radical. A third cathodic peak  $E_p^{\text{red,c}} = 0.31 \text{ V}$  present in complex  $\text{Cu}[\text{L}^{\text{II}}]$  which may be attributed to a Cu(III)-phenolate species that is present simultaneously with the Cu(II)-phenoxyl radical species.

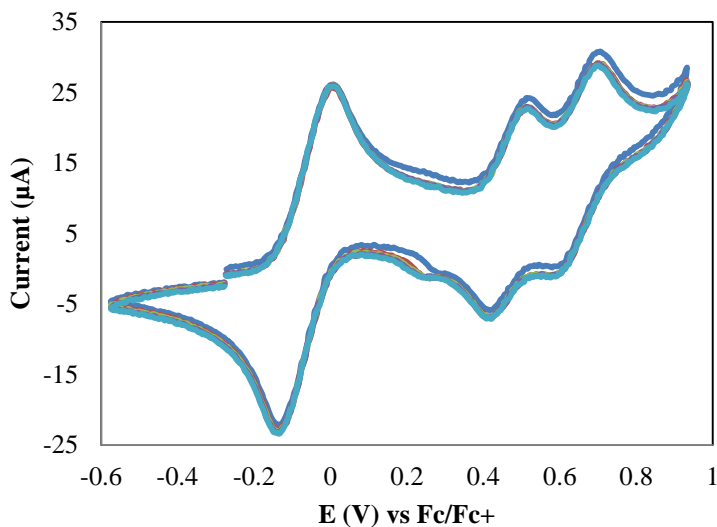


**Figure 2.18.** Cyclic voltammogram of  $\text{Cu}[\text{L}^{\text{II}}]$  Conditions: 1.0 mM ligand in dichloromethane, room temperature, tetra-n-butylammonium perchlorate (0.1 M) as electrolyte. Scan rate 0.100 V/s.<sup>31</sup>

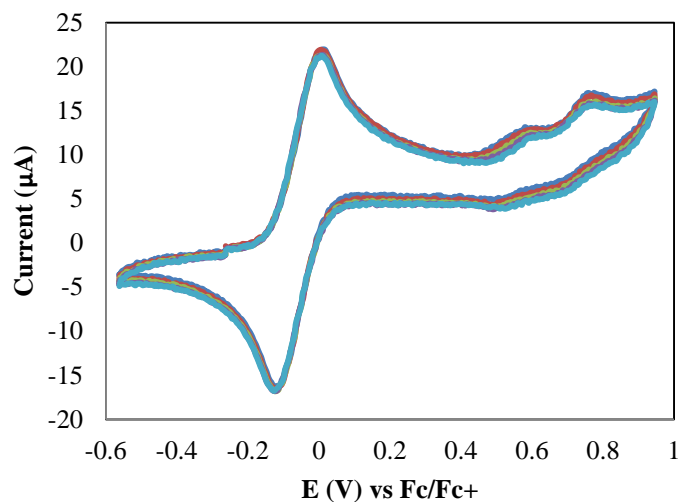


**Figure 2.19.** Cyclic Voltammogram of  $\text{UO}_2[\text{L}^{\text{II}}]$  Conditions: 1.0 mM ligand in dichloromethane, room temperature, tetra-*n*-butylammonium perchlorate (0.1 M) as electrolyte. Scan rate 0.100 V/s.<sup>31</sup>

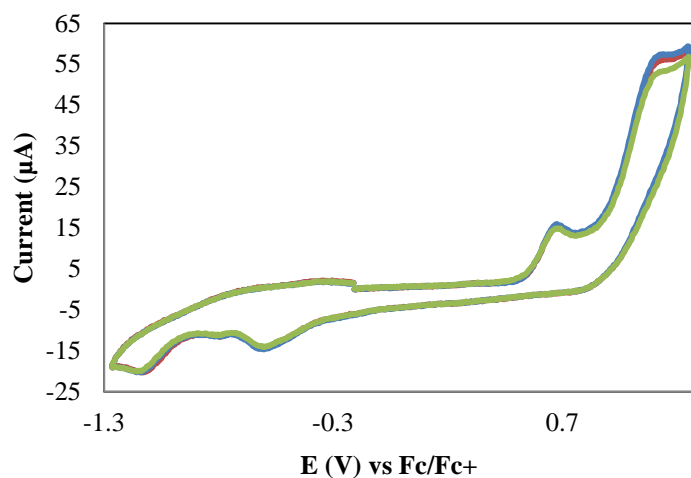


**Figure 2.20.** Cyclic Voltammogram of Salqu  $[\text{H}_2\text{L}^{\text{II}}]$  Conditions: 1.0 mM ligand in dichloromethane, room temperature, tetra-*n*-butylammonium perchlorate (0.1 M) as electrolyte. Scan rate 0.100 V/s.<sup>31</sup>

Complex  $\text{UO}_2[\text{L}^{\text{I}}]$  resulted in two reduction peaks, at  $E_p^{\text{red,a}} = -1.75$  V and  $E_p^{\text{red,b}} = -2.23$  V, both of which are visibly quasireversible in **Figure 2.21**. The  $\text{UO}_2[\text{L}^{\text{II}}]$  complex, has a reduction peak at  $E_p^{\text{red,a}} = -1.87$  V and  $E_p^{\text{red,b}} = -2.11$  V. The reduction of U(VI) to U(V) in

UO<sub>2</sub>[salophen] occurs at -1.67 V in pyridine and -1.55 in DMSO.<sup>51-52</sup> Complex UO<sub>2</sub>[L<sup>II</sup>] has an feature that is 0.20 V more negative than the reference UO<sub>2</sub>[salophen] for the U(VI)/U(V) redox couple, revealing a better stabilization of the uranyl complex in the salqu ligand, even without the presence of a coordinating solvent, than in previously reported salophen complexes.<sup>51-52</sup>

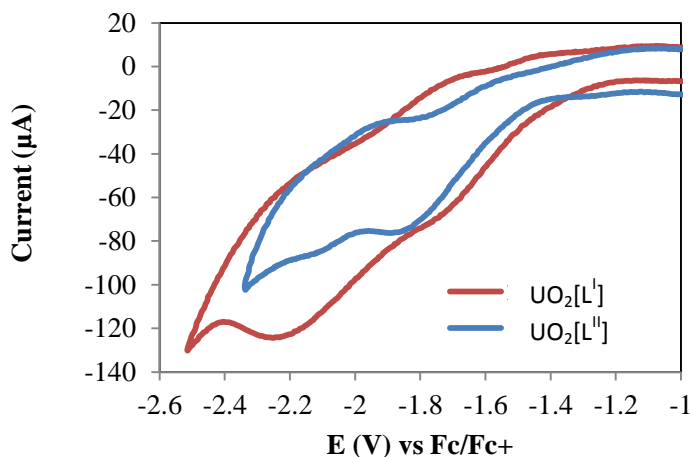


**Figure 2.21.** Cyclic Voltammogram of UO<sub>2</sub>[L<sup>I</sup>] and UO<sub>2</sub>[L<sup>II</sup>]. Conditions: 0.5 mM complex in dichloromethane, room temperature, tetra-n-butylammonium perchlorate (0.1 M) as electrolyte with the ferrocene redox couple as an internal standard.<sup>31</sup>

This stabilization is not as apparent in the UO<sub>2</sub>[L<sup>I</sup>] complex which had a feature that is 0.10 V to that of the reference UO<sub>2</sub>[salophen]. The second set of reduction peaks present in both UO<sub>2</sub>[L<sup>I</sup>] and UO<sub>2</sub>[L<sup>II</sup>] that was absent in UO<sub>2</sub>[salophen] may be due to not only a reduction of uranium to the pentavalent uranyl cation, but subsequent disproportionation to U(IV) and U(VI) or a rearrangement of the uranium geometry. If a coordinating solvent is removed from the coordination sphere, an additional oxidation peak may present itself.

### Microfluidic Detection

The electronic characterization shows that the aromatic M[L<sup>I</sup>] complexes have large molar extinction coefficients which allows these complexes to be measured at low



concentrations. Extending this fact and pairing with detection on a microspectrophotometer leads to the novel application of detection by spectral detection of metal-ligand complexes in mere picoliter volumes ( $4 \times 10^2$  pL) on a microfluidic chip (**Figure 2.22**).

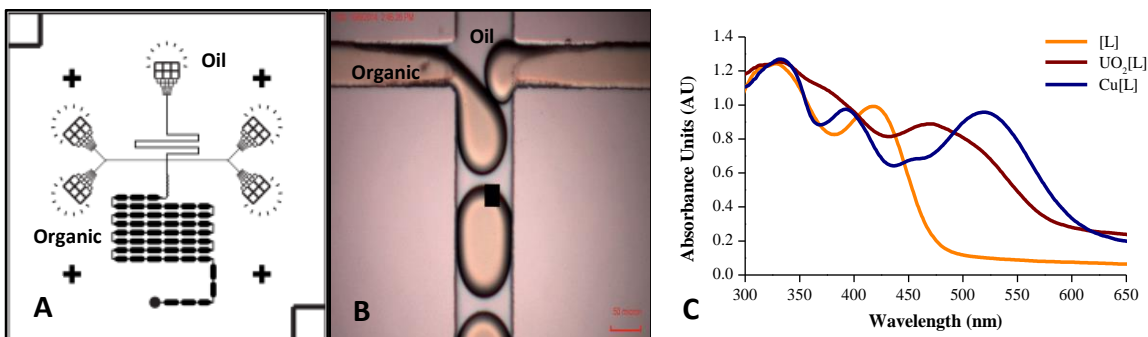


**Figure 2.22.** A. Droplet microchopper design. B. Oil and pyridine phases meet at a T-junction to form organic in oil droplets ( $\text{UO}_2(\text{NO}_3)_2$  and ligand). C. CRAIC spectra of complexes collected on chip with  $100 \mu\text{m}$  optical path length.<sup>30</sup>

Proof of concept for detection of these complexes within microfluidic droplets (pyridine droplets in perfluorocarbon oil) is shown in **Figure 2.22**. Spectra collected using the microdroplet system match well with spectra from macro-scale measurements (**Figure 2.23**). **Figure 22.24** shows an image from the microspectrophotometer showing the droplets and spectra obtained. Time consuming metal titrations can also be replicated in a fraction of the time with these methods. With a properly designed microfluidic device that includes exact mixing times, kinetics of metal binding could be determined.

Reducing sample volume by more than 6 orders of magnitude on this microchopper device<sup>34</sup> with concurrent spectroscopic detection (**Figure 2.22C**) could speed the ease of ligand screening within the field of environmental actinide sensing. By designing simple, easy-to-use devices, sample and waste volumes could be drastically reduced. The ability to reliably sense

actinide elements at a release event and quickly respond could play a large role in altering the current standards of immediate response in field detection procedures.

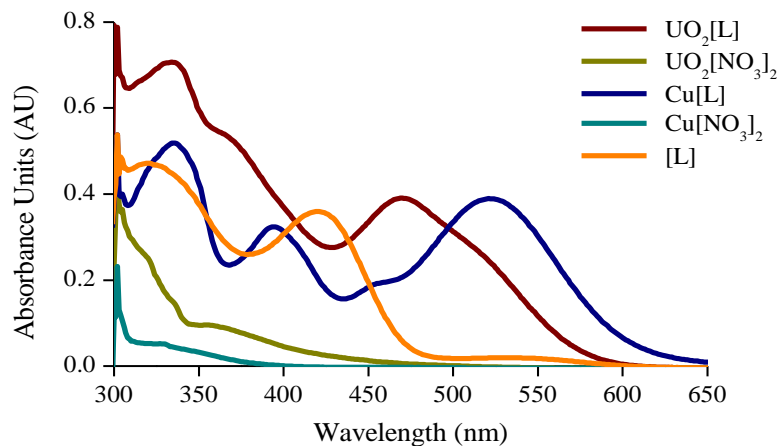


**Figure 2.23** UV-Vis spectrum of the metal starting materials  $[\text{Cu}(\text{NO}_3)_2]$ ,  $\text{UO}_2(\text{NO}_3)_2$ ,  $[\text{H}_2\text{L}^1]$ ,  $\text{Cu}[\text{L}^1]$ , and  $\text{UO}_2[\text{L}^1]$  complexes in pyridine at  $20 \mu\text{M}$ .<sup>30</sup>

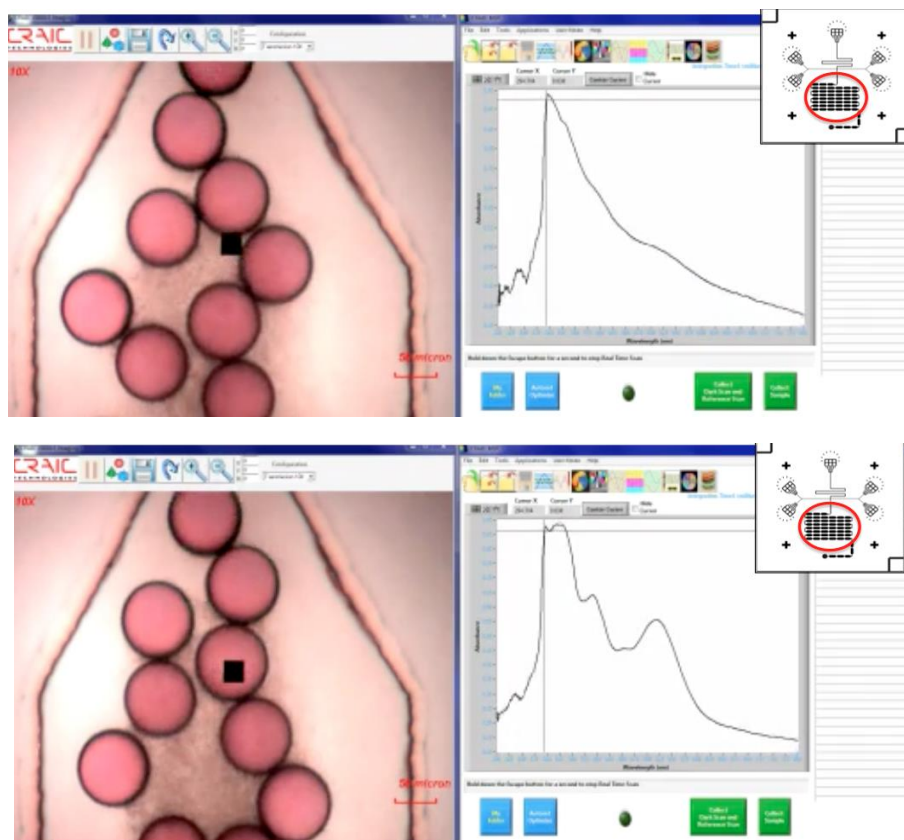


**Figure 2.24.** Images of the droplets corresponding real-time spectra showing the proof of concept that the spectra are maintained and only the droplets in the aperture are measured. Insets are the microchopper design with the position of the camera highlighted in red.

While current sensing methods for actinide elements have high selectivity and low limits of detection, they require large sample and reagent volumes and expensive instrumentation for assays that can take up to several days for the analysis to be completed.<sup>53</sup> By designing simple, easy-to-use devices, sample and waste volumes could be drastically reduced, opening up the potential for detection of the much more expensive and controlled neptunium or plutonium. This proof of concept requires less than 5 minutes to collect multiple spectra and determine sample composition in picoliter volumes if an adequate sensor were to be designed.

## Conclusions

The salphenazine ligand, with the O-N-N-O salen type bonding motif, has been synthesized and characterized in the presence of various first row transition metals and uranium in the most common oxidation state in aqueous solution ( $\text{UO}_2^{2+}$ ). Complexes have been characterized by x-ray crystallography and UV-visible spectroscopy, revealing the extended  $\pi$ -conjugation of these ligands results in differentiation of a uranyl signal as compared to these transition metal contaminants. The solid-state characterization of this series provides insight to the preferred coordination environment of uranyl in these conjugated systems. The  $\pi$ - $\pi$  stacking of all the observed systems is within the confines of typical graphene stacking distance of 3.21-3.50 Å. The metal centres often are within 3.0-3.2 Å above a conjugated ring, suggesting possible metal backbonding to the ring system. These insights can guide further design for ligands with extended conjugation to be used as on-site actinide chemosensors. The free bases, compounds  $[\text{H}_2\text{L}^{\text{I}}]$  and  $[\text{H}_2\text{L}^{\text{II}}]$ , along with the uranyl and copper complexes,  $\text{UO}_2[\text{L}^{\text{I}}]$ ,  $\text{Cu}[\text{L}^{\text{I}}]$ ,  $\text{UO}_2[\text{L}^{\text{II}}]$ , and  $\text{Cu}[\text{L}^{\text{II}}]$ , have been characterized by cyclic voltammetry. The extended  $\pi$ -conjugation that is deemed responsible for differentiation between metals in the spectroscopy

does not necessarily translate into a significant change in the U(V)/U(VI) redox couple, but may provide a secondary sensing method for chemosensors of this type.

## Materials and Methods

### Synthetic Details

*Caution! The uranium metal salts -  $UO_2(NO_3)_2 \cdot 6H_2O$  - used in this study contained depleted uranium, standard precautions for handling radioactive materials were followed.*

The reagents 1,5-difluoro-2,4-dinitrobenzene (97%, Matrix Scientific), leucine methyl ester hydrochloride (TCI), diisopropylethylamine (Aldrich), ammonium hydroxide (BDH), ammonium formate (97%, Aldrich), palladium 5% on carbon, dry, type 87L (Alpha Aesar), 3,5-di-tert-butylsalicylaldehyde (98%, TCI), 2,3-diaminophenazine (98%, Aldrich), copper (II) acetate hydrate (>98%, MC/B), copper(II) acetylacetonate (98% STREM), vanadium(IV) bis(acetylacetonato)oxide (98%, STREM), cobalt(II) acetate tetrahydrate (Mallinckrodt), nickel(II) acetate tetrahydrate (Aldrich), zinc acetate hydrate (Aldrich) and tetra-n-butylammonium perchlorate (Alfa Aesar, electrochemical grade) were used as received without further purification.  $UO_2(NO_3)_2 \cdot 6H_2O$  (98%, J. T. Baker) was recrystallized from an aqueous nitric acid solution, stored under hexanes and washed and dried before use. THF (BDH), chloroform (BDH), ethyl acetate (BDH), hexanes (BDH), acetone (BDH) and pyridine (anhydrous, Aldrich) were used as received with no further purification.

**Cu[L<sup>I</sup>]:** 50 ml of pyridine was placed in a round bottom flask charged with a stir bar and heated at 80 °C. A 0.2204 gram (0.9406 mmol) addition of 3,5-ditertbutyl salicylaldehyde was added to dissolve in the warmed solution. A 0.1253 gram (0.4787 mmol) addition of copper (II) acetylacetonate was dissolved in the warmed solution. In a separate beaker 0.0982 gram (0.4671

mmol) of 2,3-diaminophenazine was dissolved in about 25 ml of pyridine. The pyridine solution was added slowly with the aid of a syringe pump set to deliver 4 mL/hr. The reaction was allowed to proceed for 24 hours, and then the reaction mixture was allowed to come to room temperature and subsequently rotovapped to dryness. Column chromatography was performed with a mobile phase of 3:4 acetone to hexanes. This was set up in an attempt to isolate the red/maroon/violet spot seen on the TLC plate. Single crystals of X-ray diffraction quality were obtained after 2 days of slow evaporation. A THF solution containing ~50 mg was placed in several test tubes and then put in secondary containers for slow diffusion crystallization containing secondary solvents. Crystals were observed in the MeOH and EtOH slow evaporation chambers. CCDC: 1019624. HRMS (EI) m/z (M+H) calcd 703.3073, found 703.1739.

**UO<sub>2</sub>[L<sup>I</sup>]**: 50 ml of pyridine was placed in a round bottom flask charged with a stir bar and heated at 80 °C. A 0.2219 gram (0.9500 mmol) addition of 3,5-di-tert-butylsalicylaldehyde was added to dissolve in the warmed solution. A 0.2381 gram (0.4740 mmol) addition of UO<sub>2</sub>(NO<sub>3</sub>)<sub>2</sub>•6H<sub>2</sub>O was then added to the flask and allowed to dissolve in the warmed solution. Several increments totaling 0.0996 g (0.474 mmol) of 2,3 diaminophenazine was then added to the flask in equal increments over the course of 1 hour. The reaction was then allowed to heat for 24 hours. This mixture was purified by column chromatography using a 1:1 ratio of ethyl acetate to hexanes as the mobile phase. A THF solution containing ~50 mg was placed in several test tubes and then put in secondary containers for slow diffusion crystallization containing secondary solvents. Crystals were observed in the MeOH and EtOH slow evaporation chambers. CCDC: 1019622. HRMS (EI) m/z (M+H) calcd 911.4183 found 911.4117.

**[H<sub>2</sub>L<sup>I</sup>]:** UO<sub>2</sub>[L<sup>I</sup>] (100 mg) was dissolved in 20 mL of THF and added to 60 mL of chloroform. Nitric acid (80 mL, 1 M) was added to the red organic phase in a separatory funnel. The organic layer was washed a second time with deionized water (80 mL). The yellow organic layer was evaporated under reduced pressure and the ligand was separated from the monosubstituted side product via column chromatography (2:1 hexanes:ethyl acetate). Yield: 40%; orange crystals were grown from slow evaporation of the mobile phase. Products were confirmed via mass spec analysis HRMS (EI) m/z: (M+H) calcd 643.3934, found 643.3942. CCDC: 1452415.

**VO[L<sup>I</sup>]:** 2,3-diaminophenazine (231 mg, 1.10 mmol) was dissolved in 35 mL of pyridine and added slowly to a round bottom flask containing 3,5-ditertbutylsalicylaldehyde (507 mg, 2.17 mmol), vanadium(IV) bis(acetylacetonato)oxide (281 mg, 1.06 mmol), 20 mL of pyridine, and a stir bar. The reaction vessel was heated to 80 °C for 24 hours. The solvent was removed using a rotary evaporator, and the remaining solid dried in a vacuum oven at 60 °C overnight. This crude solid was purified using column chromatography (2:1 hexanes:ethyl acetate). Yield: 27.4 %; red crystals were grown from slow diffusion of methanol into a saturated solution in THF. CCDC: 1452867. HRMS (EI) m/z (M+H) calcd 708.3166, found 708.3269.

**Zn[L<sup>I</sup>]:** 2,3-diaminophenazine (197 mg, 0.940 mmol) was dissolved in 35 mL of pyridine and subsequently added slowly to a round bottom flask containing 3,5-ditertbutylsalicylaldehyde (505 mg, 2.18 mmol), zinc acetate dihydrate (237 mg, 1.04 mmol), 20 mL of pyridine, and a stir bar. The reaction vessel was heated to 80 °C for 24 hours. The solvent was removed using a rotary evaporator, and the remaining solid was dried in a vacuum oven at 60 °C overnight. This crude solid was purified using column chromatography (2:1 hexanes:ethyl acetate). Yield: 24.2 %; red crystals were grown from slow diffusion of methanol into a saturated

solution in THF. CCDC: 1452244. Metal complex formation was confirmed via UV spectroscopy,  $\lambda_{\text{max}} = 387 \text{ nm}$  ( $\epsilon = 1.79 \times 10^4 \text{ cm}^{-1} \text{ M}^{-1}$ ) and  $521 \text{ nm}$  ( $\epsilon = 1.51 \times 10^4 \text{ cm}^{-1} \text{ M}^{-1}$ ). IR spectroscopy, 3417.92(m), 2955.96(m), 1612.52(s), 1595.16(s), 1432.17(m), 1383.9(m), 1164.06(m), 1128.38(m), 1026.15(w), 983.71(w), 908.49(w), 870.88(w), 755.14(m), 677.99(w)  $\text{cm}^{-1}$ . HRMS (EI) m/z: (M+H) calcd 705.3069, found 643.3734. The HRMS matrix was found to be acidic and stripped the zinc out of the complex. The observed ion at 643.3734 m/z indicates the presence of the protonated free base.

**Fe[L<sup>I</sup>]-O-Fe[L<sup>I</sup>]:** 2,3-diaminophenazine (211 mg, 1.01 mmol) was dissolved in 35 mL of pyridine and subsequently added slowly to a round bottom flask containing 3,5-ditertbutylsalicylaldehyde (540. mg, 2.31 mmol), iron(III) trichloride hexahydrate (277 mg, 1.03 mmol), 20 mL of pyridine, and a stir bar. The reaction vessel was heated to 80 °C for 24 hours. The solvent was removed using a rotary evaporator. The remaining solid was dried in a vacuum at 60 °C oven overnight. The resulting crude solid was purified using column chromatography (4:3 hexanes:acetone). Yield: 21.2 %; red crystals were grown from slow evaporation of mobile phase. CCDC: 1018600. The dimer dissociates in acidic solution to  $[\text{FeL}^{\text{I}}]^+$ . HRMS (EI) m/z: ( $\text{M}^+$ ) calcd 696.3127, found 696.3117.

**Co[L<sup>I</sup>]:** 2,3-diaminophenazine (201 mg, 0.958 mmol) dissolved in 35 mL of pyridine was added slowly to a round bottom flask containing 3,5-ditertbutylsalicylaldehyde (541 mg, 2.31 mmol), cobalt(II) acetate hydrate (220. mg, 0.885 mmol), 20 mL of pyridine, and a stir bar. The reaction vessel was heated to 80 °C for 24 hours. The solvent was removed using a rotary evaporator, and the remaining solid was dried in a vacuum oven at 60 °C overnight. The resulting crude solid was purified using column chromatography (4:3 hexanes:acetone). Yield: 20.1 % HRMS (EI) m/z: (M+H) calcd 699.3109, found 699.3079.

**Ni[L<sup>I</sup>]:** 2,3-diaminophenazine (190. mg, 0.904 mmol) was dissolved in 35 mL of pyridine and added slowly to a round bottom flask containing 3,5-ditertbutylsalicylaldehyde (485 mg, 2.07 mmol), nickel(II) acetate hydrate (193 mg, 0.778 mmol), 20 mL of pyridine, and a stir bar. The reaction vessel was heated to 80 °C for 24 hours. The solvent was removed using a rotary evaporator, and the remaining solid was dried in a vacuum oven at 60 °C overnight. The crude solid was purified using column chromatography (2:1 hexanes:ethyl acetate). The mobile phase was evaporated under reduced pressure to yield a dark red solid. Yield: 36.9 %. HRMS (EI) m/z: (M+H) calcd 699.3209, found 699.3221.

Synthesis of 6,7-diamino-2-quinoxalinol and 3,5-ditertbutylsal-2-quinoxalinol (salqu) [H<sub>2</sub>L<sup>II</sup>], UO<sub>2</sub>[L<sup>II</sup>], and Cu[L<sup>II</sup>] were prepared using previously reported procedures.<sup>26, 54</sup> Purity was confirmed by HRMS and NMR spectroscopy.

### Crystallographic Details

Datasets were collected on a Bruker SMART APEX CCD X-ray diffractometer unit using Mo K $\alpha$  radiation, from crystals mounted in Paratone-N oil on glass fibers. SMART (v 5.624) was used for preliminary determination of cell constants and data collection control. [H<sub>2</sub>L<sup>I</sup>], Zn[L<sup>I</sup>] and Fe[L<sup>I</sup>]-O-Fe[L<sup>I</sup>] datasets were collected at 180 K, and UO<sub>2</sub>[L<sup>I</sup>], Cu[L<sup>I</sup>], and VO[L<sup>I</sup>] datasets were collected at 296 K. Determination of integrated intensities and global cell refinement were performed with the Bruker SAINT software package using a narrow-frame integration algorithm.<sup>55</sup> The program suite SHELXL (v 5.1) was used for space group determination, structure solution, and refinement. Refinement was performed against F<sup>2</sup> by weighted full-matrix least squares, and empirical absorption correction (SADABS) was applied.<sup>56</sup> The olex2.refinement package using Gauss-Newton minimization was used for further



refinement and to generate a solvent mask to account for the 3 methanol molecules in the unit cell of VO[L<sup>I</sup>] and for 2 interstitial THF molecules in the unit cell of Zn[L<sup>I</sup>].<sup>57</sup> Projections were generated using the Olex2.1-1 graphics program.<sup>57</sup> Complete lists of bond lengths, angles, refinement information, atomic coordinates, and hydrogen bonding are in Appendix I.

### **Spectroscopic Details**

UV-Vis experiments were performed on a Varian Cary 50 WinUV Spectrophotometer. Pyridine solutions for each titration were made individually and stirred for 5 minutes before data collection, unless otherwise noted. All solutions were 20  $\mu$ M in ligand.

### **Electrochemical Details**

Cyclic voltammetry experiments were performed using a Pine AFCBP1 bipotentiostat driven by a PC with the Aftermath software package. All experiments were completed with a Pt disk working electrode, a Pt wire counter electrode, and an Ag/AgCl reference electrode (BASi MF-2052). Solutions for cyclic voltammetry experiments were 1.0 mM in the salqu metal complex or ligand (M[L<sup>II</sup>] and [H<sub>2</sub>L<sup>II</sup>]), or 0.5 mM in the salphenazine metal complex or ligand (M[L<sup>I</sup>] and [H<sub>2</sub>L<sup>I</sup>]). All solutions were made in dichloromethane and contained 0.1 M tetra-n-butylammonium perchlorate (TBAP). Platinum electrodes were cleaned with piranha acid (H<sub>2</sub>SO<sub>4</sub>/H<sub>2</sub>O<sub>2</sub>), polished in between experiments, and all electrodes were stored according to factory suggestion. All experiments were performed at room temperature.

### **Microfluidic Device Fabrication**

Microdevices were fabricated using polydimethylsiloxane (PDMS) and soft lithography techniques.<sup>58-59</sup> The silicon wafer master design (**Figure 2.22**) was a previously established

droplet generating chip designed in house.<sup>58</sup> Wafers were pre-treated with 1 mL of chlorotrimethylsilane for 30 min. After mixing 10:1 base to curing agent of PDMS, the de-gassed mixture was cured on top of the wafer at 65°C overnight. Once cured, the PDMS was carefully peeled off the wafer and designated inlet/outlets were punched for sample and outlet wells. The PDMS along with a glass microscope slide was then washed with methanol, dried with a nitrogen air gun, and cleaned with scotch tape. Once cleaned, both the PDMS chip and the microscope slide were placed in an air plasma cleaner for 45 seconds (Harrick Plasma) and immediately placed on top of each other to bond together. 1.5cm OD Tygon tubing was inserted into the outlet well, and a blunt ended needle was inserted into the opposite end of the tubing. Aquapel (Pittsburgh Glass Works) was applied to each of the inlet channels of the chip and pulled through with a mild vacuum to surface treat the channels. Methanol was washed through as well to remove any excess Aquapel. Chips were then placed back into the 65 °C oven to dry for at least 4 hours. Solutions were flowed through the chips passively, via a handheld, 25 mL syringe connected to the needle in the tubing. Chips were taped to the imaging stage to hold them in place. Vacuum was applied to the chip on the stage and the droplets were imaged directly on the chip. In order to form oil in organic droplets, 1.8% w/w Krytox 157 FSL surfactant (Dupont) in HFE-7500 oil (3M) droplet carrier fluid was applied to the oil well.<sup>58</sup>

### **Microspectrophotometer Imaging**

UV–Visible data were acquired from microfluidic droplets and microwells using a CRAIC Technologies 20/20 PV microspectrophotometer. 400 picoliter droplets were generated on the microfluidic chip and the data were collected from 200 to 800 nm. Microwell data was also measured using the same parameters and fixed pathlength. The exposure time was auto-optimized by the CRAIC Minerva 8.7.3.12 software.

## References

1. Corner, A.; Venables, D.; Spence, A.; Poortinga, W.; Demski, C.; Pidgeon, N., Nuclear power, climate change and energy security: Exploring British public attitudes. *Energ. Policy* **2011**, *39* (9), 4823-4833.
2. Youinou, G. J., Powering sustainable low-carbon economies: Some facts and figures. *Renew. Sust. Energ. Rev.* **2016**, *53*, 1626-1633.
3. Visschers, V. H. M.; Siegrist, M., How a Nuclear Power Plant Accident Influences Acceptance of Nuclear Power: Results of a Longitudinal Study Before and After the Fukushima Disaster. *Risk Anal.* **2013**, *33* (2), 333-347.
4. Hess, G., Spotlight on Nuclear Power. *Chemical & Engineering News Archive* **2011**, *89* (29), 10.
5. Snow, M. S.; Snyder, D. C.; Clark, S. B.; Kelley, M.; Delmore, J. E., <sup>137</sup>Cs Activities and <sup>135</sup>Cs/<sup>137</sup>Cs Isotopic Ratios from Soils at Idaho National Laboratory: A Case Study for Contaminant Source Attribution in the Vicinity of Nuclear Facilities. *Environ. Sci. Technol.* **2015**, *49* (5), 2741-2748.
6. Whicker, F. W.; Schultz, V., *Radioecology: Nuclear Energy and the Environment*. CRC Press, Inc.: Boca Raton, Florida, 1982; Vol. 1.
7. Vega, F. A.; Covelo, E. F.; Andrade, M. L., Competitive sorption and desorption of heavy metals in mine soils: Influence of mine soil characteristics. *J. Colloid Interf. Sci.* **2005**, *298*, 582-592.
8. Hu, Z.; Gao, S., Upper crustal abundances of trace elements: A revision and update. *Chem. Geol.* **2008**, *253* (3-4), 205-221.

9. Sessler, J. L.; Melfi, P. J.; Seidel, D.; Gorden, A. E. V.; Ford, D. K.; Palmer, P. D.; Tait, C. D., Hexaphyrin(1.0.1.0.0.0). A new colorimetric actinide sensor. *Tetrahedron* **2004**, *60*, 11089-11097.
10. Gorden, A. E. V.; Xu, J.; Raymond, K. N.; Durbin, P., Rational Design of Sequestering Agents for Plutonium and Other Actinides. *Chem. Rev.* **2003**, *103*, 4207-4282.
11. Zaiter, A.; Amine, B.; Bouzidi, Y.; Belkhiri, L.; Boucekkine, A.; Ephritikhine, M., Selectivity of Azine Ligands Toward Lanthanide(III)/Actinide(III) Differentiation: A Relativistic DFT Based Rationalization. *Inorg. Chem.* **2014**, *53* (9), 4687-4697.
12. Gorden, A. E.; DeVore, M. A., II; Maynard, B. A., Coordination chemistry with f-element complexes for an improved understanding of factors that contribute to extraction selectivity. *Inorg. Chem.* **2013**, *52* (7), 3445-58.
13. Li, Y.; Lee, T.; Weerasiri, K.; Wang, T.; Buss, E. E.; McKee, M. L.; Gorden, A. E. V., 2-Quinoxalinol diamine Cu(II) complex: facilitating catalytic oxidation through dual mechanisms. *Dalton Trans.* **2014**, *43*, 13578-13583.
14. Weerasiri, K. C.; Gorden, A. E. V., Oxidation of Propargylic Alcohols with a 2-Quinoxalinol Salen Copper (II) Complex and tert-Butyl Hydroperoxide. *Eur. J. Org. Chem.* **2013**, 1546-1550.
15. Chen, T.; Cai, C., Selective Oxidation of benzyl alcohols to aldehydes with a salophen copper(II) complex and ter-butyl hydroperoxide at room temperature. *Synth. Commun.* **2015**, *45*, 1334-1341.
16. North, M.; Quek, S. C. Z.; Pridmore, N. E.; Whitwood, A. C.; Wu, X., Aluminum(salen) Complexes as Catalysts for the Kinetic Resolution of Terminal Epoxides via CO<sub>2</sub> Coupling. *ACS Catalysis* **2015**, *5* (6), 3398-3402.

17. Nishat, N.; Rasool, R.; Parveen, S.; Khan, S. A., New Antimicrobial Agents: The synthesis of schiff base polymers containing transition metals and their characterization and applications. *J. Appl. Polym. Sci.* **2011**, *122*, 2756-2764.
18. Murtinho, D.; da Rocha, Z. N.; Pires, A. S.; Jiménez, R. P.; Abrantes, A. M.; Laranjo, M.; Mamede, A. C.; Casalta-Lopes, J. E.; Botelho, M. F.; Pais, A. A. C. C.; Nunes, S. C. C.; Burrows, H. D.; Costa, T.; Silva Serra, M. E., Synthesis, characterization and assessment of the cytotoxic activity of Cu(II), Fe(III) and Mn(III) complexes of camphoric acid-derived salen ligands. *Appl. Organomet. Chem.* **2015**, *29* (7), 425-432.
19. Peng, Q.; Xie, M.; Huang, Y.; Lu, Z.; Cao, Y., Novel supramolecular polymers based on zinc-salen chromophores for efficient light-emitting diodes. *Macromol. Chem. Phys.* **2005**, *206*, 2373-2380.
20. Hwang, K. Y.; Lee, M. H.; Jang, H.; Sung, Y.; Lee, J. S.; Kim, S. H.; Do, Y., Aluminum-salen luminophores as new hole-blocking materials for phosphorescent OLEDs. *Dalton Trans.* **2008**, 1818-1820.
21. Ren, M.; Xu, Z.-L.; Bao, S.-S.; Wang, T.-T.; Zheng, Z.-H.; Ferreira, R. A. S.; Zheng, L.-M.; Carlos, L. D., Lanthanide salen-type complexes exhibiting single ion magnet and photoluminescent properties. *Dalton Trans.* **2016**, *45*, 2974-2982.
22. Zhou, D.; Sun, C.; Chen, C.; Cui, X.; Li, W., Research of a highly selective fluorescent chemosensor or aluminum(III) ions based on photoinduced electron transfer. *J. Mol. Struct.* **2015**, *1079*, 315-320.
23. Cheng, J.; Wei, K.; Ma, X.; Zhou, X.; Xiang, H., Synthesis and Photophysical Properties of Colorful Salen-Type Schiff Bases. *J. Phys. Chem. C* **2013**, *117*, 16552-16563.

24. Lin, H.-Y.; Chen, T.-Y.; Liu, C.-K.; Wu, A.-T., A fluorescent chemosensor based on naphthol for detection of  $Zn^{2+}$ . *Luminescence* **2016**, *31* (1), 236-240.
25. DeVore Li, M. A.; Kerns, S. A.; Gorden, A. E. V., Characterization of Quinoxolinol Salen Ligands as Selective Ligands for Chemosensors for Uranium. *Eur. J. Inorg. Chem.* **2015**, *2015* (34), 5708-5714.
26. Wu, X.; Bharara, M. S.; Bray, T. H.; Tate, B. K.; Gorden, A. E. V., Synthesis and characterization of 2-quinoxalinol Schiff-base metal complexes. *Inorg. Chim. Acta* **2009**, *362* (6), 1847-1854.
27. Bharara, M. S.; Heflin, K.; Tonks, S.; Strawbridge, K. L.; Gorden, A. E. V., Hydroxy- and alkoxy-bridged dinuclear uranyl-Schiff base complexes: hydrolysis, transamination and extraction studies. *Dalton Trans.* **2008**, *22*, 2966-73.
28. Cheng-Liang Xiao, C.-Z. W., Li-Yong Yuan, Bin Li, Hui He, Shuao Wang, Yu-Liang Zhao, Zhi-Fang Chai, Wei-Qun Shi, Excellent Selectivity for Actinides with a Tetradentate 2,9-Diamide-1,10 Phenanthroline Ligand in Highly Acidic Solution: A Hard-Soft Donor Combined Strategy. *Inorg. Chem.* **2014**, *53* (3), 1217-1720.
29. Mikhalyova, E. A.; Yakovenko, A. V.; Zeller, M.; Gavrilenko, K. S.; Lofland, S. E.; Addison, A. W.; Pavlishchuk, V. V., Structure, magnetic and luminescence properties of the lanthanide complexes  $Ln_2(\text{Salphen})_3 \cdot H_2O$  ( $Ln = Pr, Nd, Sm, Eu, Gd, Tb, Dy$ ;  $H_2\text{Salphen} = N,N'$ -bis(salicylidene)-1,2-phenylenediamine). *Inorg. Chim. Acta* **2014**, *414*, 97-104.
30. Maynard, B. A.; Brooks, J. C.; Hardy, E. E.; Easley, C. J.; Gorden, A. E. V., Synthesis, structural characterization, electronic spectroscopy, and microfluidic detection of  $Cu^{2+}$  and  $UO_2^{2+}$  [di-tert-butyl-salphenazine] complexes. *Dalton Trans.* **2015**, *44* (10), 4428-4430.

31. Hardy, E. E.; Eddy, M. A.; Maynard, B. A.; Gordon, A. E. V., Solid state  $\pi$ - $\pi$  stacking and higher order dimensional crystal packing, reactivity, and electrochemical behaviour of salphenazine actinide and transition metal complexes. *Dalton Trans.* **2016**, 45 (36), 14243-14251.
32. Bharara, M. S.; Tonks, S. A.; Gordon, A. E. V., Uranyl stabilized Schiff base complex. *Chem. Commun. (Camb.)* **2007**, (39), 4006-8.
33. Salassa, G.; Ryan, J. W.; Escudero-Adan, E. C.; Kleij, A. W., Spectroscopic properties of Zn(salphenazine) complexes and their application in small molecule organic solar cells. *Dalton Trans.* **2014**, 43 (1), 210-221.
34. Deal, K. S.; Easley, C. J., Self-Regulated, Droplet-Based Sample Chopper for Microfluidic Absorbance Detection. *Anal. Chem.* **2012**, (84), 1510.
35. Seemann, R.; Brinkmann, M.; Pfohl, T.; Herminghaus, S., Droplet based microfluidics. *Rep. Prog. Phys.* **2012**, 75 (1), 016601.
36. Teh, S.-Y.; Lin, R.; Hung, L.-H.; Lee, A. P., Droplet microfluidics. *Lab on a Chip* **2008**, 8 (2), 198-220.
37. Zhu, Y.; Fang, Q., Analytical detection techniques for droplet microfluidics—A review. *Anal. Chim. Acta* **2013**, 787, 24-35.
38. Zamian, J. R.; Dockal, E. R.; Castellano, G.; Oliva, G., Synthesis and Characterization of [N,N' - ethylenebis(3-ethoxysalicylideneaminato)] oxovanadium (IV). *Polyhedron* **1995**, 14, 2411.
39. WeberskiJr, M. P.; McLauchlan, C. C.; Hamaker, C. G., Synthesis and X-ray structural characterization of M(3,5-tbu<sub>2</sub>-salophen) (M= Cu, V=O). *Polyhedron* **2006**, 25, 119.

40. Zabierowski, P.; Szklarzewicz, J.; Grybos, R.; Modryl, B.; Nitek, N., Assemblies of salen-type oxidovanadium(IV) complexes: substituent effects and in vitro protein tyrosine phosphatase inhibition. *Dalton Trans.* **2014**, *43*, 17044.
41. Morris, G. A.; Zhou, H.; Stern, C. L.; Nguyen, S. T., A general high-yield route to bis(salicylaldimine) zinc(II) complexes: application to the synthesis of pyridine-modified salen-type zinc(II) complexes. *Inorg. Chem.* **2001**, *40*, 3222-3227.
42. Liuzzo, V.; Oberhauser, W.; Pucci, A., Synthesis of new red photoluminescent Zn(II)-salicylaldiminato complex. *Inorg. Chem. Commun.* **2010**, *13*, 686-688.
43. Germain, M. E.; Vargo, T. R.; Khalifah, P. G.; Knapp, M. J., Fluorescent Detection of Nitroaromatics and 2,3-dimethyl-2,3-dinitrobutane (DMNB) by a zinc complex: (salphen)Zn. *Inorg. Chem.* **2007**, *46*, 4422-4429.
44. Allen, F. H., The Cambridge Structural Database: a quarter of a million crystal structures and rising. *Acta Cryst.* **2002**, *B58*, 380-388.
45. Mayilmurugan, R.; Stoeckli-Evans, H.; Sleresh, E.; Palaniandavar, M., Chemoselective and biomimetic hydroxylation of hydrocarbons by non-heme  $\mu$ -oxo-bridged diiron(III) catalysts using *m*-CPBA as oxidant. *Dalton Trans.* **2009**, *26*, 5101.
46. Rusere, L. N.; Shalumova, T.; Tanski, J. M.; Tyler, L. A., Synthesis and crystal structures of Ni(II), Cu(II), and  $\mu$ -oxo-Fe(III) complexes of a salen type ligand: mononuclear versus multinuclear complex formation. *Polyhedron* **2009**, *28*, 3804.
47. Jana, S.; Chatterjee, S.; Chattopadhyay, S., Syntheses, characterization and X-ray crystal structures of hexa-coordinated monomeric and oxo-bridged dimeric Fe (II) compounds with salen type Schiff. *Polyhedron* **2012**, *48* (1), 189-198.



48. Veauthier, J. M.; Cho, W.-S.; Lynch, V. M.; Sessler, J. L., Calix[4]pyrrole Schiff base macrocycles. Novel binucleating ligands for u-oxo iron complexes. *Inorg. Chem.* **2004**, *43* (4), 1220-1228.
49. Whiteoak, C. J.; Rosales, R. T. M. d.; White, A. J. P.; Britovsek, G. J. P., Iron(II) complexes with tetradentate Bis(aminophenolate) ligands: synthesis and Characterization, Solution behavior, and Reactivity with O<sub>2</sub>. *Inorg. Chem.* **2010**, *49* (23), 11106-11117.
50. Asami, K.; Takashina, A.; Kobayashi, M.; Iwatsuki, S.; Yajima, T.; Kochem, A.; Gastel, M. V.; Tani, F.; Kohzuma, T.; Thomas, F.; Shimazaki, Y., Characterization of one-electron oxidized copper(II)-salophen-type complexes; effects of electronic and geometrical structures on reactivities. *Dalton Trans.* **2014**, *43*, 2283-2293.
51. Mizuoka, K.; Kim, S. Y.; Hasegawa, M.; Hoshi, T.; Uchiyama, G.; Ikeda, Y., Electrochemical and spectroelectrochemical studies on UO<sub>2</sub>(saloph)L (saloph = N, N'-disalicylidene-o-phenylenediaminate, L = Dimethylsulfoxide or N,N-Dimethylformamide). *Inorg. Chem.* **2003**, *42* (4), 1031.
52. Nocton, G.; Horeglad, P.; Vetere, V.; Pecaut, J.; Dubois, L.; Maldivi, P.; Edelstein, N.; Mazzanti, M., Synthesis, structure, and bonding of stable complexes of pentavalent uranyl. *J. Am. Chem. Soc.* **2010**, *132*, 495.
53. Lee, J. H.; Wang, Z.; Liu, J.; Lu, Y., Highly Sensitive and Selective Colorimetric Sensors for Uranyl (UO<sub>2</sub><sup>2+</sup>): Development and Comparison of Labeled and Label-Free DNzyme-Gold Nanoparticle Systems. *J. Am. Chem. Soc.* **2008**, *130* (43), 14217-14226.
54. Wu, X.; Gordon, A. E. V., An Efficient Method for Solution-Phase Parallel Synthesis of 2-Quinoxalinol Salen Schiff-Base Ligands. *J. Comb. Chem.* **2007**, *9*, 601.

55. Sheldrick, G. M., A Brief History of SHELX. *Acta Crystallogr., Sect. A: Found. Crystallogr.* **2008**, *A64*, 112.
56. Bruker AXS Inc.: Madison, Wisconsin, USA, 2001.
57. Dolomanov, O. V.; Bourhis, L. J.; Gildea, R. J.; Howard, J. A. K.; Puschmann, H., OLEX2: A complete structure solution, refinement and analysis program. *J. Appl. Cryst.* **2009**, *42*, 339-341.
58. Deal, K. S.; Easley, C. J., Self-Regulated, Droplet-Based Sample Chopper for Microfluidic Absorbance Detection. *Anal. Chem.* **2012**, *84* (3), 1510-1516.
59. Duffy, D. C.; McDonald, J. C.; Schueller, O. J. A.; Whitesides, G. M., Rapid Prototyping of Microfluidic Systems in Poly(dimethylsiloxane). *Anal. Chem.* **1998**, *70*, 4974-4984.

## **Chapter 3: An Unusual Example of Pyridine Donor Schiff Base Uranyl Complexes and Zinc Enhanced Ligand Emission**

Portions of this chapter are reproduced from Hardy, E. E.; Wyss, K. M.; Eddy, M. A.; Gordon, A. E. V., *Chem. Commun.* **2017**, 53, 5718-5720 with permission from the Royal Society of Chemistry.

### **Introduction**

Nuclear power is a major contributor and integral asset to carbon neutral energy production for ever-increasing energy demands.<sup>1</sup> Interest in fundamental actinide research has been on the rise to illuminate their fundamental chemistry and pave the way for enhanced nuclear fuel remediation techniques.<sup>2-5</sup> Recently, depleted uranium has been investigated for applications in catalysis to complete difficult chemical transformations.<sup>6-7</sup> Researchers have also sought to characterize the degree of actinide covalency both synthetically and computationally using ligands featuring nitrogen donors.<sup>8-9</sup> Examples of uranium coordination have included pyrrole nitrogen donors in the ligand environment, but only a handful have included the less strongly coordinating pyridine.<sup>10-11</sup> Sessler and co-workers have explored changes in ligand aromatic character when a pyridine moiety is bound to an actinide, further exploring uncommon coordination geometries.<sup>12</sup>

Previously, we have described highly conjugated, tetradentate, mixed nitrogen and oxygen donor systems designed as chemosensors in on-site detection for uranyl, the most environmentally available oxidation state of uranium in aqueous and acidic solutions.<sup>13-15</sup> Other nitrogen donor systems that have been explored also involve mixed oxygen and nitrogen coordination environments.<sup>16-19</sup> These systems often require multiple synthetic steps to prepare and are not always easily accessed or derivatized. The synthetic ease, in particular as compared to macrocyclic uranyl chelators, and the ability to change the electronic characteristics of the ligand environment easily made these Schiff base ligands an ideal scaffold for uranyl detection. The pentadentate coordination environment of a 2,6-bis[1-[(2-hydroxyphenyl)imino]ethyl]pyridine ( $[H_2L^{III}]$ ) ligand scaffold was designed to accommodate the larger atomic radius of uranium as the uranyl dioxo cation, while fully occupying its equatorial plane. Here, four new uranyl ( $UO_2^{2+}$ ) complexes utilizing this scaffold have been synthesized from successive condensation reactions and subsequent metal complexation.

Highly increased fluorescence was observed when  $[H_2L^{III}]$  was complexed with Zn(II). Zinc has been long known to be a biologically essential trace metal, which is imperative for development, immunity, and endocrine function.<sup>20-21</sup> Misregulation of zinc ions has been linked to various diseases, specifically Alzheimer's and other neurodegenerative diseases.<sup>22-23</sup> Designing molecules that selectively bind and sense zinc ions is therefore of great importance.<sup>24-25</sup> Recently, a common binding motif in many of these examples for biological imaging and ratiometric fluorescent sensing is the N-C-C-C-O binding pocket similar to that of a Salen ligand.<sup>26-30</sup> A few examples of pentadentate ligand systems with mixed oxo and aza donors have been reported for this purpose as well.<sup>31-32</sup> The characterization of solution phase

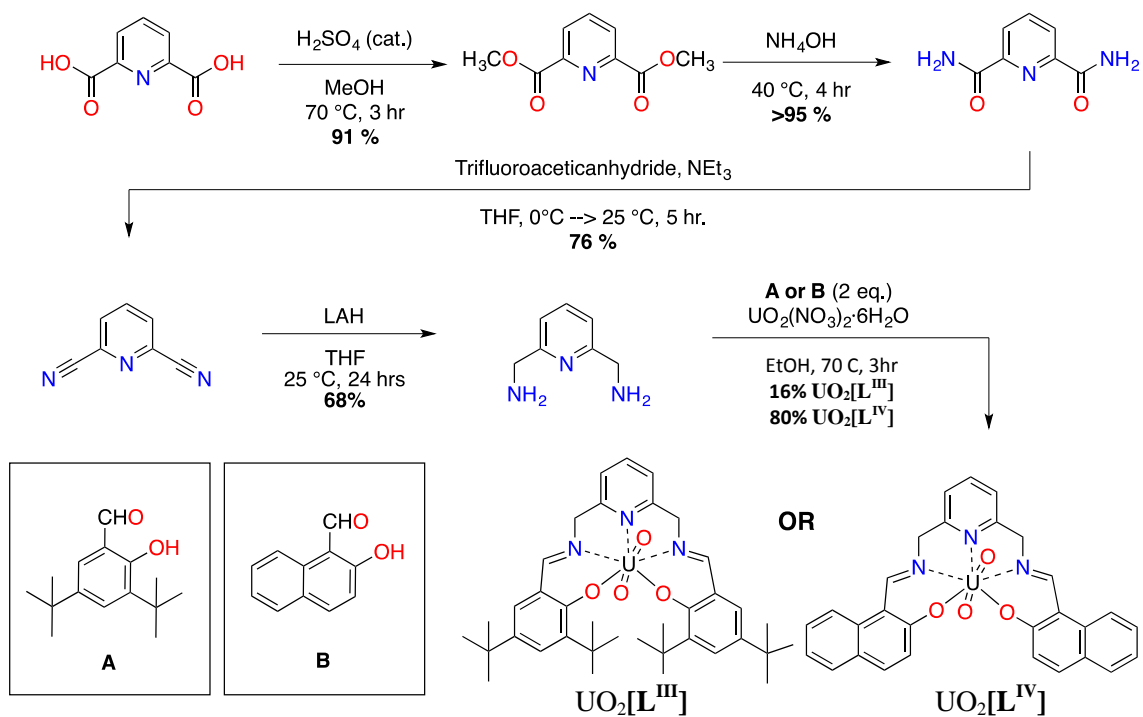
absorbance and increased emission of  $\text{Zn}[\text{L}^{\text{III}}]$ , in hopes of this system being of use for zinc sensing, is reported.

## Results and Discussion

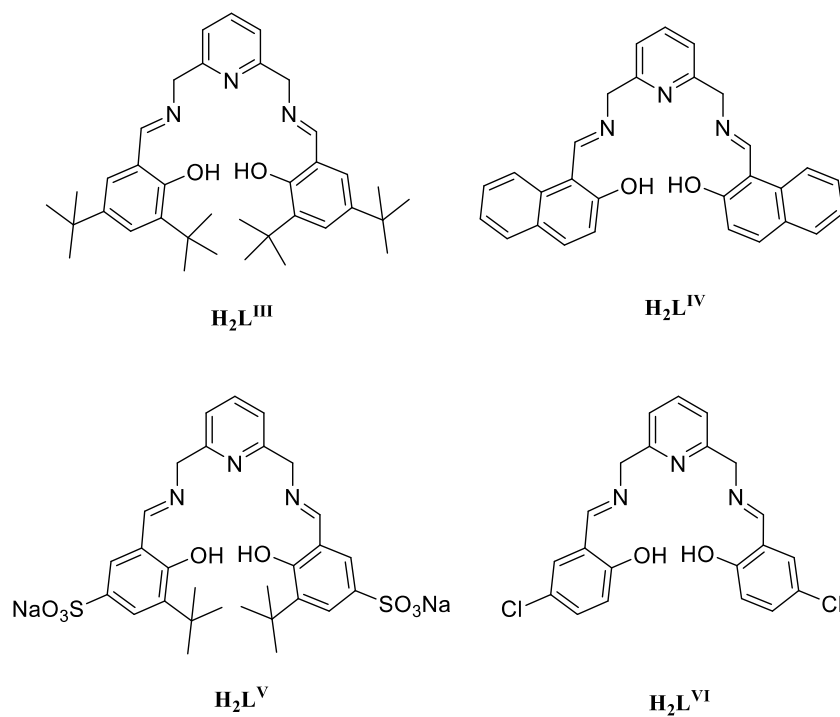
### Synthesis

The expansion and simultaneous change in  $\pi$ -overlap of the ligand in the tetradentate salen-type salqu and salphenazine ligands have been used to differentiate between actinide and transition metals of potential concern.<sup>13-15</sup> One limitation of the tetradentate binding geometry is the expansion of the binding pocket to accommodate the larger atomic radius of uranium often results in poor coordination kinetics and subsequently longer detection times. The dioxo cation uranyl has been shown to prefer a pentagonal bipyramidal binding geometry, explaining the presence of a coordinating solvent molecule in numerous reported solid-state structures. The observation of this preference led to the design of the expanded mixed oxygen and imine nitrogen coordination environment, coupled with a pyridine donor to occupy the fifth site.

As shown in **Scheme 3.1**, the 2,6-bis [1-[(2-hydroxy-3,5-ditert-butylphenyl)imino]ethyl]pyridine ( $[\text{H}_2\text{L}^{\text{III}}]$ ) and 2,6-bis[1-[(2-hydroxynaphthyl)imino]ethyl]pyridine ligands ( $[\text{H}_2\text{L}^{\text{IV}}]$ ) and the corresponding  $\text{UO}_2(\text{VI})$  complexes ( $\text{UO}_2[\text{L}^{\text{III}}]$ ,  $\text{UO}_2[\text{L}^{\text{IV}}]$ ) were designed and synthesized from a commercially available starting material, 2,6-pyridinedicarboxylic acid, to accommodate the larger atomic radius of uranium and fully occupy its equatorial plane.<sup>33</sup> Additionally 2,6-bis [1-[(2-hydroxy-3-tert-butyl-5-sulfophenyl)imino]ethyl]pyridine ( $[\text{H}_2\text{L}^{\text{V}}]$ ) and 2,6-bis [1-[(2-hydroxy-5-chlorophenyl)imino]ethyl]pyridine ( $[\text{H}_2\text{L}^{\text{VI}}]$ ) and uranyl complexes ( $\text{UO}_2[\text{L}^{\text{V}}]$  and  $\text{UO}_2[\text{L}^{\text{VI}}]$ ) were synthesized according to the same procedure (**Scheme 3.2**).



**Scheme 3.1.** Synthetic Scheme of  $\text{UO}_2\text{[L}^{\text{III}}\text{]}$  and  $\text{UO}_2\text{[L}^{\text{IV}}\text{]}$ <sup>33</sup>



**Scheme 3.2.** Representations of ligands  $[\text{H}_2\text{L}^{\text{III}}]$ ,  $[\text{H}_2\text{L}^{\text{IV}}]$ ,  $[\text{H}_2\text{L}^{\text{V}}]$ , and  $[\text{H}_2\text{L}^{\text{VI}}]$ .

## X-Ray Crystallography

The complex  $\text{UO}_2[\text{L}^{\text{III}}]$  (**Figure 3.1**) has U1-N1, U1-N2, U1-O1, and U1-O2 bond lengths of 2.532(2), 2.508(2), 2.2548(18), and 2.2604(18) respectively. These bond lengths are comparable ( $\pm 0.08$  Å) to previously synthesized tetradentate salen-type uranyl complexes.<sup>15, 34-35</sup> The U1-N3 bond length of 2.623(2) are comparable to other U-N bonds, and average of 2.59 Å from coordinating pyridine moieties in similar ligand environments.<sup>36-37</sup> The bond angles O1-U1-N1, N1-U1-N3, N3-U1-N2, N2-U1-O2, O2-U1-O1 of 69.54(7), 62.09(7), 61.81(7), 70.91(7), and 96.61(7) respectively describe a beautiful pentagonal bipyramidal coordination geometry around the uranium metal centre. The O3-U1-O4 angle of 175.83(9) is within previously reported ranges.<sup>10-12, 15, 34-38</sup> The crystallographic information for  $\text{UO}_2[\text{L}^{\text{III}}]$  and  $\text{UO}_2[\text{L}^{\text{IV}}]$  can be found in

### Table 3.1.

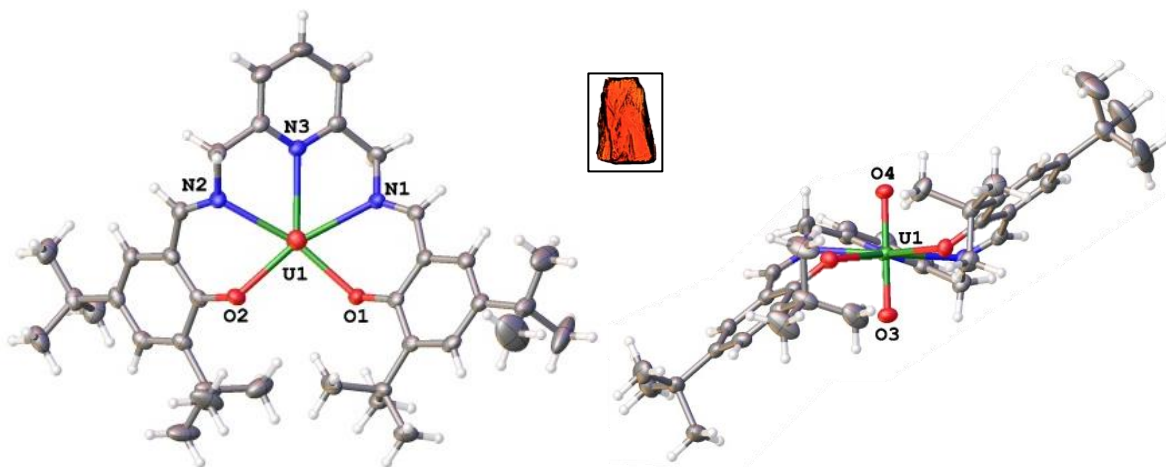


**Figure 3.1.** Projection of  $\text{UO}_2[\text{L}^{\text{III}}]$  is shown without the non-coordinating acetonitrile molecule. Hydrogen atoms are shown in white, nitrogen in blue, oxygen in red, and uranium in green. Inset image crystal dimensions: 0.2 x 0.09 x 0.03 mm.<sup>33</sup>

**Table 3.1.** Crystallographic data and details of data collection for  $\text{UO}_2[\text{L}^{\text{III}}]$  and  $\text{UO}_2[\text{L}^{\text{IV}}]$ .<sup>33</sup>

	$\text{UO}_2[\text{L}^{\text{III}}]\cdot\text{CH}_3\text{CN}$	$\text{UO}_2[\text{L}^{\text{IV}}]$
<b>Empirical formula</b>	$\text{C}_{40}\text{H}_{52}\text{N}_4\text{O}_4\text{U}$	$\text{C}_{29}\text{H}_{21}\text{N}_3\text{O}_4\text{U}$
<b>Formula weight (g/mol)</b>	890.88	713.54
<b>Crystal size/mm<sup>3</sup></b>	$0.06 \times 0.06 \times 0.02$	$0.12 \times 0.12 \times 0.04$
<b>Crystal system</b>	orthorhombic	monoclinic
<b>Space group</b>	Pccn	$\text{P}2_1/\text{c}$
<b>a/Å</b>	13.9974(3)	22.8062(10)
<b>b/Å</b>	23.5111(5)	7.2736(3)
<b>c/Å</b>	23.6244(5)	14.7805(6)
<b><math>\alpha/^\circ</math></b>	90	90
<b><math>\beta/^\circ</math></b>	90	97.3343(5)
<b><math>\gamma/^\circ</math></b>	90	90
<b>Volume/Å<sup>3</sup></b>	7774.7(3)	2431.78(18)
<b>Z</b>	8	4
<b><math>\rho_{\text{calc}}/\text{mg}/\text{mm}^3</math></b>	1.499	1.9488
<b><math>\text{m}/\text{mm}^{-1}</math></b>	4.217	6.72
<b>F(000)</b>	3496	1320.2
<b>Temperature/K</b>	180(2)	180.45
<b>Radiation</b>	MoK $\alpha$ ( $\lambda = 0.71073$ )	Mo K $\alpha$ ( $\lambda = 0.71073$ )
<b>Reflections collected</b>	93148	61345
<b>Independent reflections</b>	11887	8098
<b>Largest diff. peak/hole / e Å<sup>-3</sup></b>	1.37/-0.74	3.18/-5.58
<b>Final R indexes [<math>I \geq 2\sigma(I)</math>]</b>	$R_1 = 0.0305,$ $wR_2 = 0.0619$	$R_1 = 0.0359,$ $wR_2 = 0.0726$
<b>Goodness-of-fit on F<sup>2</sup></b>	1.01	1.084

The complex  $\text{UO}_2[\text{L}^{\text{IV}}]$  (Figure 3.2) has U1-N1, U1-N2, U1-O1, and U1-O2 bond lengths of 2.486(3), 2.525(3), 2.264(3), and 2.267(3) respectively. These bond lengths are comparable to previously synthesized tetradentate uranyl chemosensors and to  $\text{UO}_2[\text{L}^{\text{III}}]$ .<sup>15,34-35</sup> The U1-N3 bond length of 2.566(3) is slightly shortened from the t-butyl analogue,  $\text{UO}_2[\text{L}^{\text{III}}]$ , but only slightly shorter than the average U-N bond of 2.59 Å from other similar coordinating pyridine moieties in the literature.<sup>36-37</sup> The bond angles O1-U1-N1, N1-U1-N3, N3-U1-N2, N2-U1-O2, O2-U1-O1 of 69.83(10), 62.68(10), 62.99(9), 69.31(10), and 95.61(10) respectively describe a pentagonal bipyramidal coordination geometry around the uranium centre. The O3-



U1-O4 angle of 175.96(13) is also within previously reported ranges.<sup>10-12, 15, 34-37</sup> Dipicolinic acid (2,6-pyridinedicarboxylic acid) is a common coordination agent, and has been applied to the extraction of uranyl from acidic solutions.<sup>39</sup> The observed U-N<sub>py</sub> distance in UO<sub>2</sub>[L<sup>III</sup>] and UO<sub>2</sub>[L<sup>IV</sup>] is equivalent to, or shorter than, some examples of dipicolinic systems and their derivatives.<sup>10,38-39</sup>

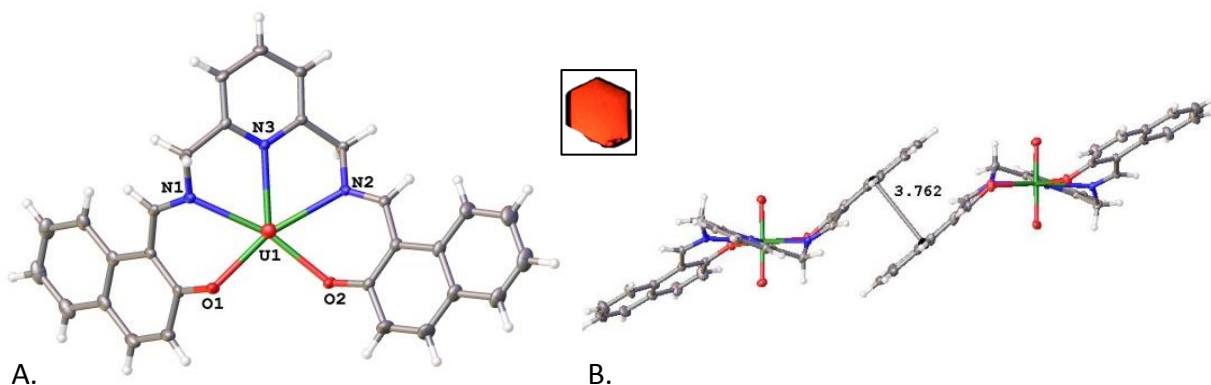


**Figure 3.2a.** Projection of UO<sub>2</sub>[L<sup>IV</sup>] is shown. Hydrogen atoms are shown in white, nitrogen in blue, oxygen in red, and uranium in green. Inset image is the crystal from the data collection. **Figure 3.2b.** Projections of UO<sub>2</sub>[L<sup>IV</sup>], highlighting pi-pi stacking in the solid-state. Inset crystal dimensions: 0.12 x 0.09 x 0.02 mm.<sup>33</sup>

The similarity of observed bond lengths and angles to tridentate and tetradentate systems discussed previously suggest that the preferred 5-coordinate binding in the equatorial plane is achieved without the necessity of significant ligand pocket expansion or solvent coordination. Thus, the improved coordination kinetics as compared to the ligand in Chapter 2, of a few seconds for UO<sub>2</sub>[L<sup>III</sup>], can be explained by this reduced need for ligand rearrangement. While UO<sub>2</sub>[L<sup>III</sup>] incorporated an interstitial acetonitrile solvent molecule, UO<sub>2</sub>[L<sup>IV</sup>] has  $\pi$ - $\pi$  stacking interactions that reduced the void volume and simultaneously the need for an interstitial solvent molecule. The parallel offset  $\pi$ - $\pi$  stacking interactions (3.76 Å) are highlighted in **Figure 3.2b** and are significantly longer than graphene (3.2-3.5 Å) and most examples of  $\pi$ - $\pi$  interactions.<sup>40-41</sup>

## Spectroscopy

Serial titrations of  $[\text{H}_2\text{L}^{\text{III}}]$  with the addition of  $\text{UO}_2^{2+}$  or other common transition metals in methanol and dichloromethane were completed for comparison. In the UV-visible spectra a shift of the maximum of the free base, 334 nm ( $\epsilon = 9,070 \text{ cm}^{-1} \text{ M}^{-1}$ ), to 356 nm ( $\epsilon = 7,005 \text{ cm}^{-1} \text{ M}^{-1}$ ) is observed upon the addition of  $\text{UO}_2$  as the nitrate salt in dichloromethane (**Figure 3.3**). This shift is accompanied by the growth of a charge transfer band at 419 nm ( $\epsilon = 3,454 \text{ cm}^{-1} \text{ M}^{-1}$ ) and a large shoulder centred at 512 nm ( $\epsilon = 1094 \text{ cm}^{-1} \text{ M}^{-1}$ ). These spectral changes are observed upon addition of 36 ppm of uranyl salt; modifying the ligand in future studies to include further conjugation would allow for a decrease in the limit of detection.

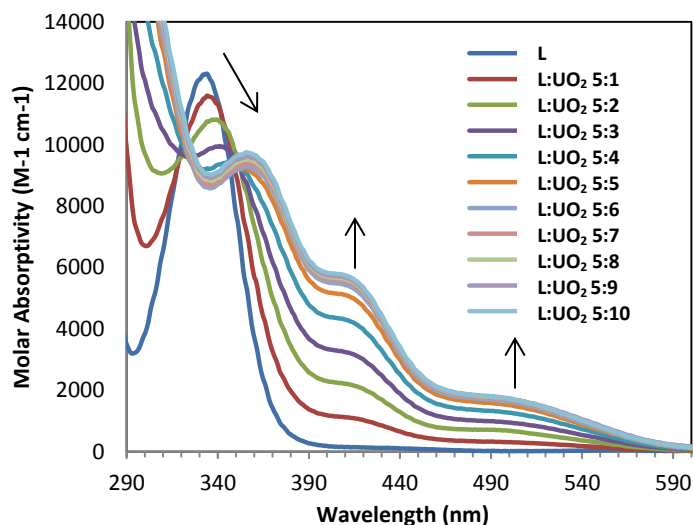


**Figure 3.3.** UV-Visible spectra of a serial titration of 0.123 mM  $[\text{H}_2\text{L}^{\text{III}}]$  in dichloromethane solution with an increasing ratios of  $\text{UO}_2(\text{NO}_3)_2$ , from 3:1 to 3:10  $\text{L}^{\text{III}}:\text{UO}_2$ .<sup>33</sup>

In an attempt to lower the limits of detection and characterize the potential effects of solvents, titrations in methanol (**Figure 3.4**) were also completed. Extinction coefficients were highest in non-coordinating solvents, but the metal salts are often not soluble in these solvents. Methanol was chosen to complete further metal titration experiments. Serial titrations of  $[\text{H}_2\text{L}^{\text{III}}]$

were completed by introducing a known amount of various metal salts ( $\text{UO}_2(\text{NO}_3)_2$ ,  $\text{Cu}(\text{C}_2\text{H}_3\text{O}_2)_2$ , etc...) to a solution of free base. Solutions consisted of 2 mL of 0.123 mM ligand, and approximately 30  $\mu\text{L}$  of 1.5 mM metal salt. The actual volumes and concentrations varied depending on stock solutions, but 1/5 equivalent of metal salt was added per addition. Serial titrations were completed in DCM, EtOH and MeOH. The solutions were shaken for 3 seconds and replaced in the spectrometer followed by collection of the absorbance spectrum or fluorescence spectrum. This was repeated until an excess of metal salt was present. The absorbance at 420 nm and 500 nm increased in intensity as the absorbance at 340 nm shifted to 350 nm and reduced in intensity, until a 1:1 ratio of metal to ligand was obtained.

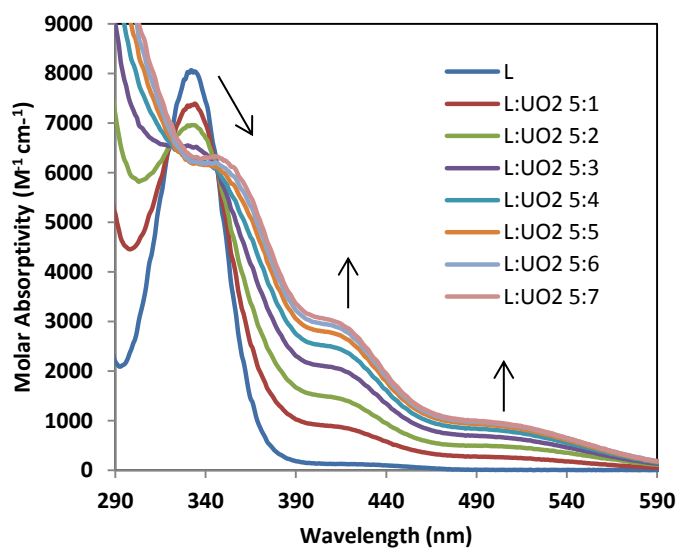


**Figure 3.4.** Absorbance spectrum of a serial titration completed via the general procedure of 0.123 mM  $\text{H}_2\text{L}^{\text{III}}$  in methanol solution with an increasing ratio of  $\text{UO}_2(\text{NO}_3)_2$ , from 5:1 to 5:7  $\text{L}^{\text{III}}:\text{UO}_2$ .<sup>33</sup>

Metal titration experiments from 0.2 equivalents of metal to 2 equivalents of common transition metal contaminants were completed using the same general procedure in methanol. The titration with copper(II) resulted in a decrease of the ligand peak at 384 nm and the growth

of a new charge transfer band at 399 nm ( $\epsilon = 5.77 \times 10^3 \text{ cm}^{-1} \text{ M}^{-1}$ ) growing charge transfer band at 600 ( $\epsilon = 3.47 \times 10^2 \text{ cm}^{-1} \text{ M}^{-1}$ ) nm (**Figure 3.5**). An isobestic point was observed at 360 nm. The addition of cobalt(II) resulted in the same decrease in ligand absorbance and an increase of absorbance at 415 nm ( $\epsilon = 5.11 \times 10^3 \text{ cm}^{-1} \text{ M}^{-1}$ ) (**Figure 3.6A**). The titrations of manganese(II), vanadyl(IV), and nickel(II) did not show significant changes in the absorbance spectra, suggesting that binding is not occurring strongly in methanol solution (**Figures 3.6B -3.6C**). Addition of zinc(II) resulted in reduction in the ligand peak and increase of a band at 386 nm ( $\epsilon = 7.21 \times 10^3 \text{ cm}^{-1} \text{ M}^{-1}$ ), and an isobestic point at 353 nm (**Figure 3.7**). The intensity of these absorbance features increased until a ratio of ligand to metal of 1:1.5 was reached, as shown in **Figure 3.8**.

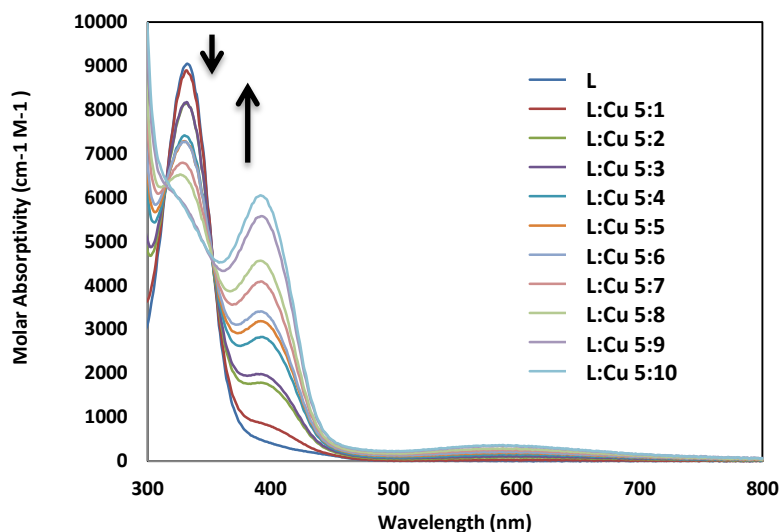


**Figure 3.5.** Absorbance spectrum of a serial titration completed via the general procedure of free base  $0.123 \text{ mM H}_2\text{L}^{\text{III}}$  in methanol solution with an increasing ratio of  $\text{Cu}(\text{C}_2\text{H}_3\text{O}_2)_2$ , from 5:1 to 5:10  $\text{L}^{\text{III}}:\text{Cu}$ .<sup>33</sup>

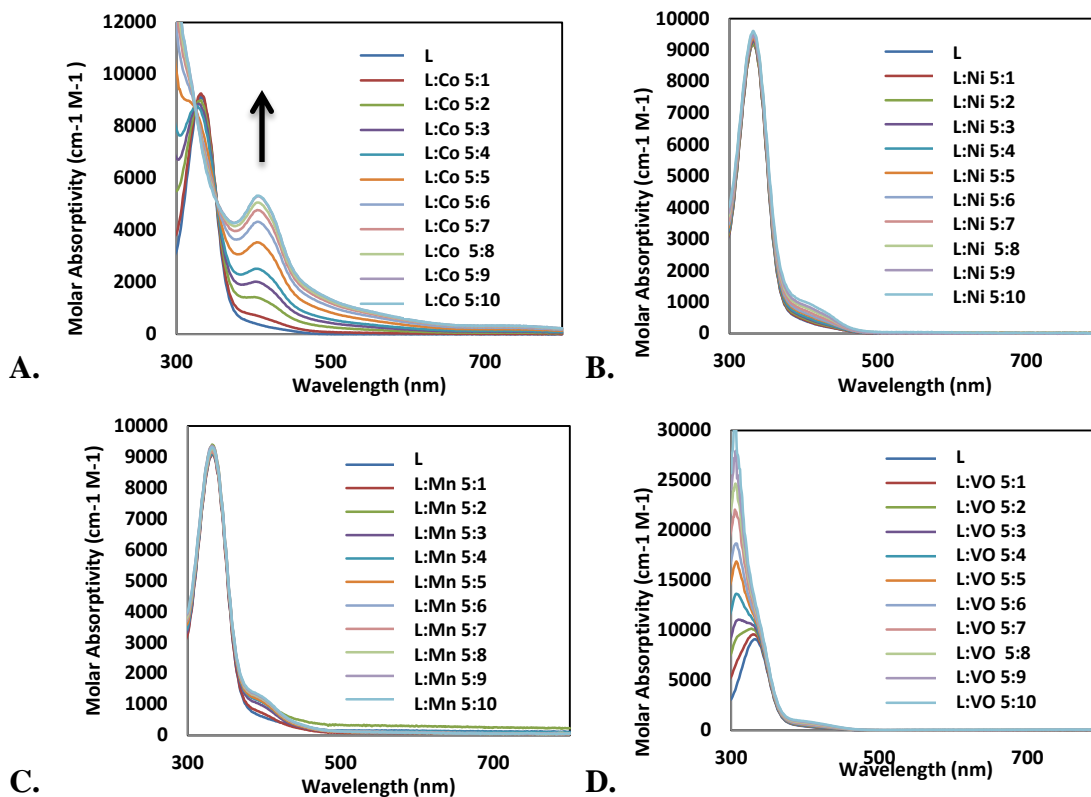


**Figure 3.6.** Absorbance spectrum of a serial titrations completed via the general procedure of free base  $0.123 \text{ mM H}_2\text{L}^{\text{III}}$  in methanol solution with an increasing ratio of  $\text{L}^{\text{III}}:\text{M}$  5:1 to 5:10, where M is equal to **A.**  $\text{Co}(\text{C}_2\text{H}_3\text{O}_2)_2$  **B.**  $\text{Ni}(\text{C}_2\text{H}_3\text{O}_2)_2$  **C.**  $\text{Mn}(\text{C}_2\text{H}_3\text{O}_2)_2$  **D.**  $\text{VO}(\text{acac})_2$ .

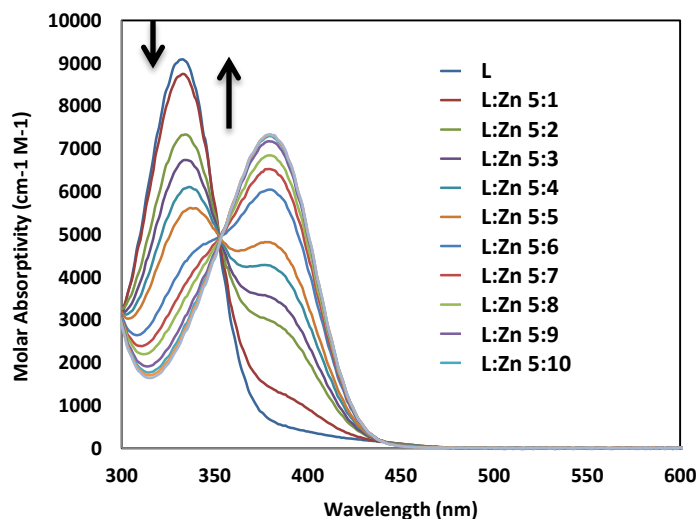


**Figure 3.7.** Absorbance spectrum of a serial titration completed via the general procedure of free base  $0.123 \text{ mM H}_2\text{L}^{\text{III}}$  in methanol solution with an increasing ratio of  $\text{Zn}(\text{C}_2\text{H}_3\text{O}_2)_2$ , from 5:1 to 5:10  $\text{L}^{\text{III}}:\text{Zn}$ .

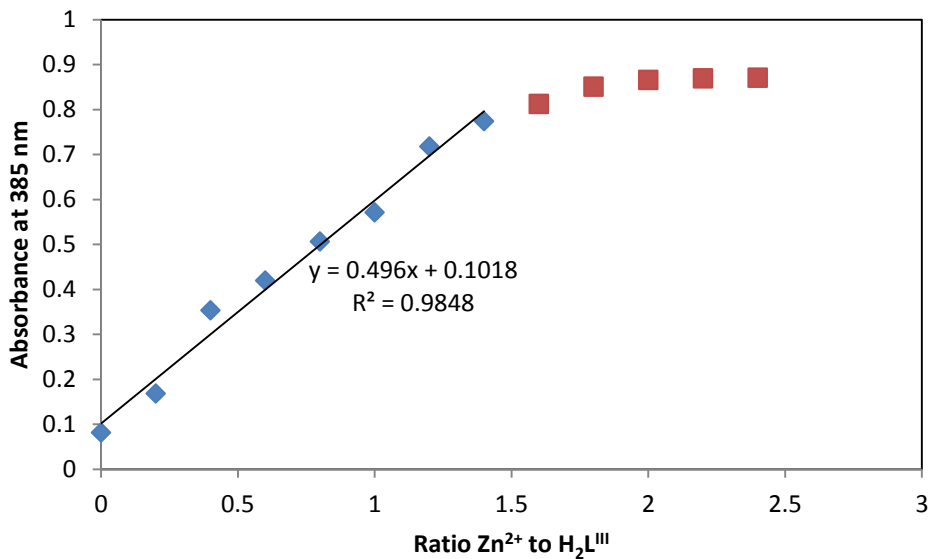


**Figure 3.8** Absorbance at 385 nm as a function of the ratio of Zn<sup>2+</sup> to 0.123 mM [H<sub>2</sub>L<sup>III</sup>].

Fluorescence measurements of the metal titration experiments above were completed using the same general procedure in methanol. The titration with uranyl(VI), copper(II), cobalt(II), and nickel(II) resulted in a quenching of emission resulting from excitation at 365 nm (**Figure 3.9**). Addition of zinc(II) and vanadyl(IV) resulted in an increase of emission (**Figure 3.10**). A summation of the solution fluorescence spectra of [H<sub>2</sub>L<sup>III</sup>] mixed with 1 equivalent of metal salt in methanol and images of the Zn[L<sup>III</sup>] emission is shown in **Figure 3.11**. The UO<sub>2</sub>, Cu, Co, Mn, and Ni metals ions all quenched the ligand fluorescence induced by 365 nm excitation, while Zn, and VO increased the fluorescence. Notably, Zn increased the fluorescence by a factor of 5.

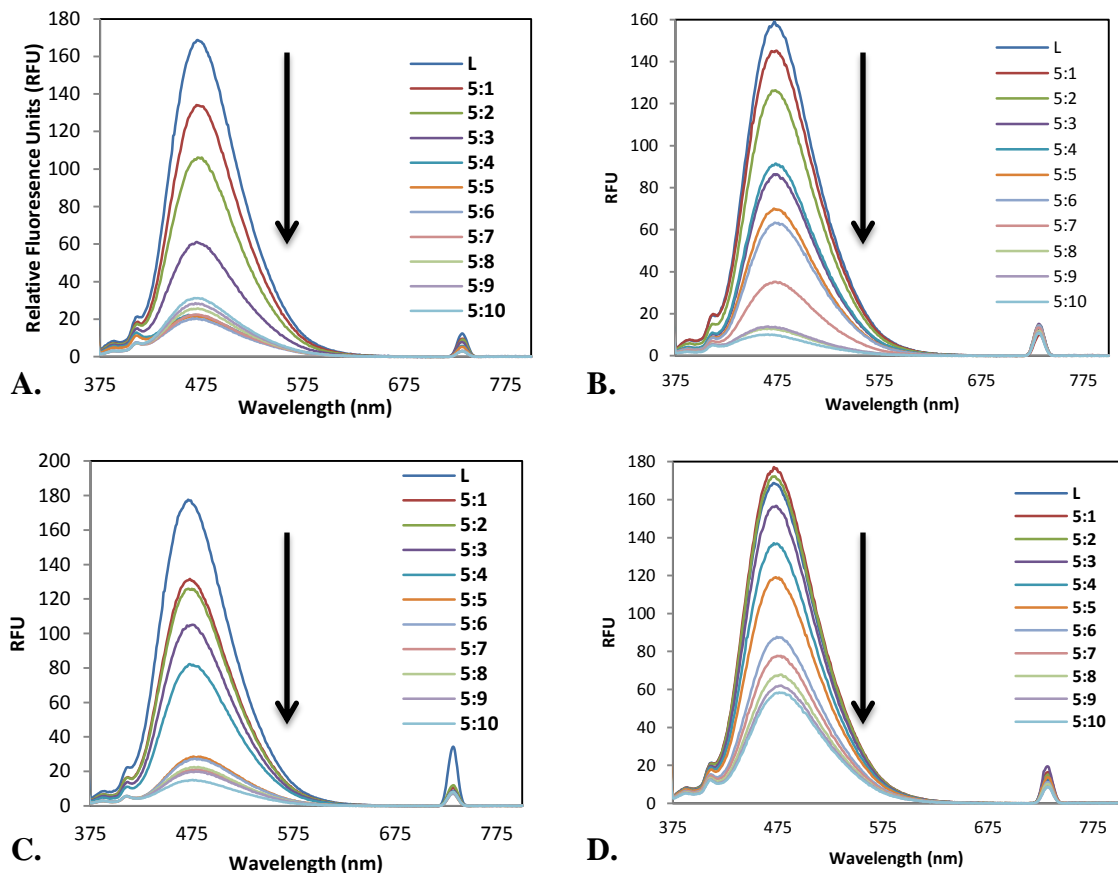


**Figure 3.9.** Emission spectrum of a serial titration completed via the general procedure of 0.123 mM  $H_2L^{III}$  in methanol solution with an increasing ratio of  $L^{III}$ :M from 5:1 to 5:10, where M is equal to **A.**  $UO_2$ , **B.** Cu, **C.** Co, **D.** Ni. Excited at 365 nm.

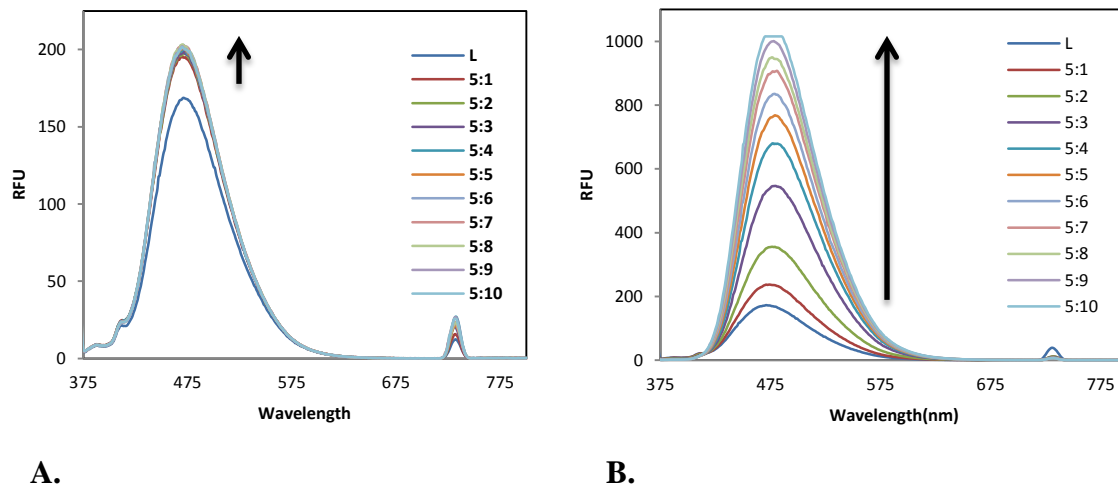


**Figure 3.10.** A. Emission spectrum of a serial titration completed via the general procedure of 0.123 mM  $H_2L^{III}$  in methanol solution with an increasing ratio of **A.**  $VO(acac)_2$  and **B.**  $Zn(C_2H_3O_2)_2$  from 5:1 to 5:10  $L^{III}$ :M. Excited at 365 nm.

After observing this increase in emission, the quantum yield of Zn[L<sup>III</sup>] was calculated using **Figure 3.12** and equation 1,

$$\Phi_X = \Phi_{ST} \left( \frac{\text{slope}_X}{\text{slope}_{ST}} \right) \left( \frac{\eta_X^2}{\eta_{ST}^2} \right) \quad (1)$$

Where the subscripts ST and X denote standard and unknown respectively,  $\Phi$  is the fluorescence quantum yield, Slope is the slope from the plot of fluorescence intensity vs absorbance, and  $\eta$  the refractive index of the solvent. In this case the solvent was constant, and  $\Phi_{ST}$  for anthracene was equal to 0.24 (24 %).<sup>42</sup> The quantum yield of Zn[L<sup>III</sup>] was calculated to be 0.016, or 1.6 %.

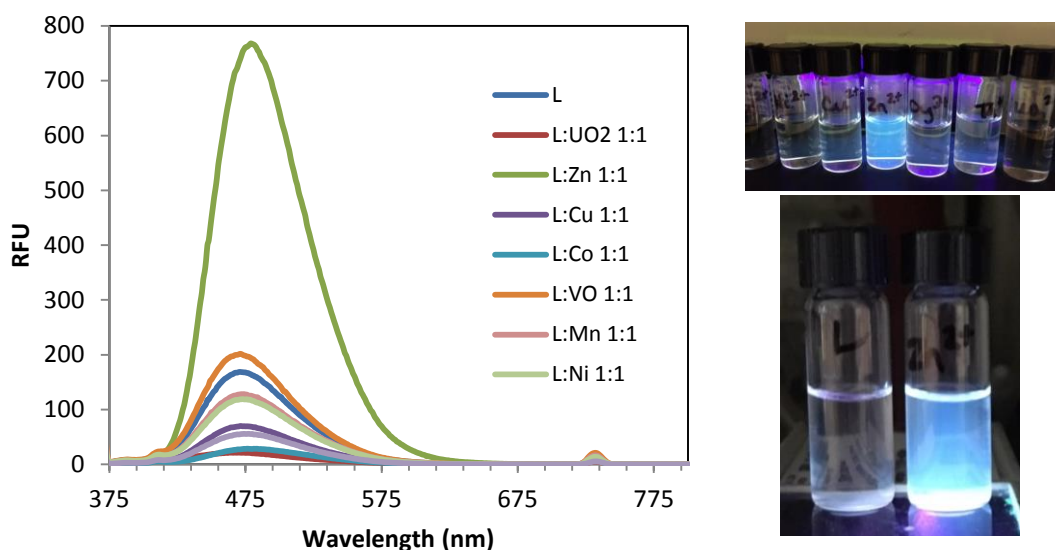


**Figure 3.11.** Solution fluorescence of a serial titration of 0.123 mM [H<sub>2</sub>L<sup>III</sup>] with indicated metal salts, shown is the 1:1 ratio in methanol solution at 365 nm excitation.<sup>33</sup>



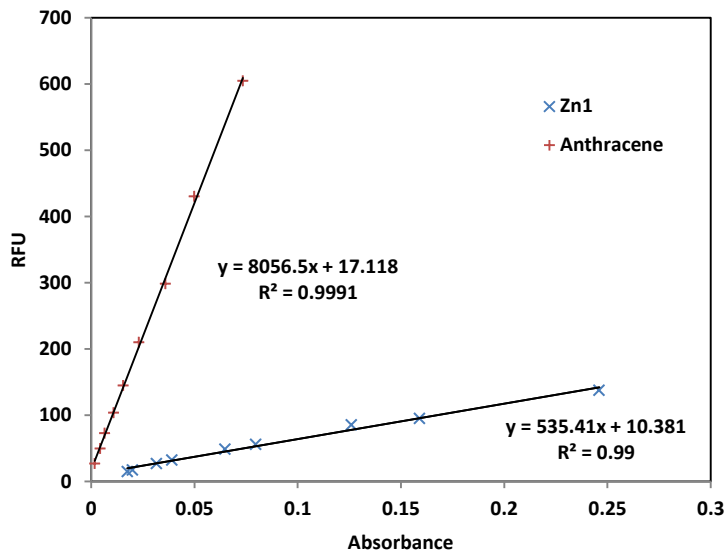


**Figure 3.12.** Zn[L<sup>III</sup>] fluorescence at 473 nm after excitation at 365 nm vs. absorbance value at 365 nm of 116, 87, 58, 43.5, 29.2, 21.8, 14.5, 10.9, 7.2, 5.5, 3.6, 2.7  $\mu$ M solutions in methanol and Anthracene fluorescence at 422 nm after excitation at 365 nm vs. absorbance value at 365 nm of 35.7, 23.8, 15.8, 10.6, 7.1, 4.7, 3.1, 2.0, 1.0  $\mu$ M solutions in methanol.<sup>33</sup>

Another representation of the Zn emission, in comparison to the other transition metals investigated, are shown in **Figure 3.13**. Adding two equivalents of the zinc metal maximized the emission intensity. An image suggesting a possible 1:1 zinc binding is shown in **Scheme 3.3**, but by comparing the molar ratio of free zinc metal added to free base the emission plateaus at 1.5 equivalents of metal. A possibility is that two ligands are binding three zinc ions, including acetate counter ions, creating supramolecular aggregates that emit more intensity than the 1:1 complex.

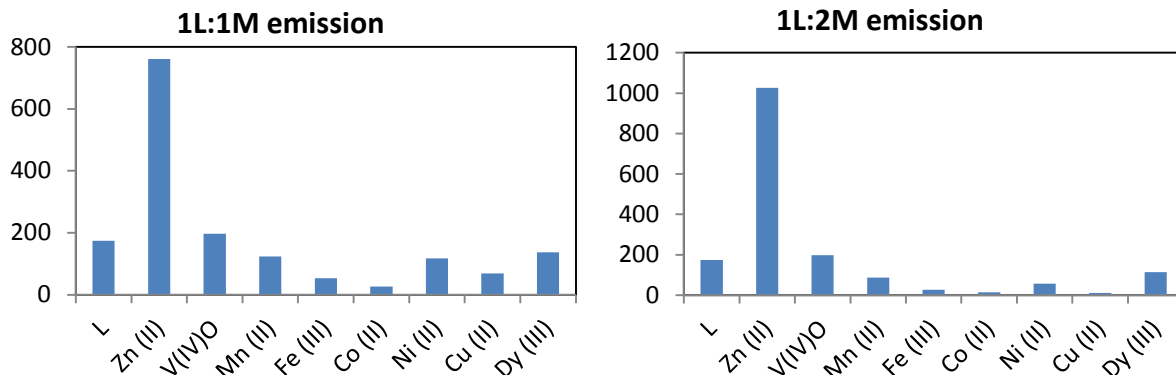
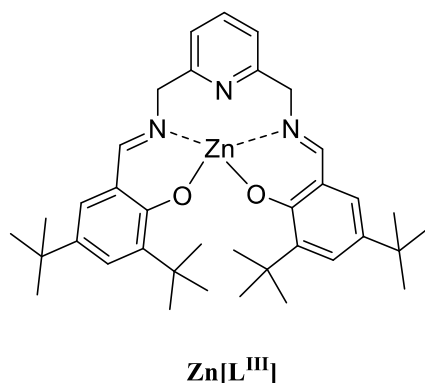


**Figure 3.13.** Zinc emission in comparison with the free base, 0.123 mM  $[\text{H}_2\text{L}^{\text{III}}]$ , and the indicated metal titrations.



**Scheme 3.3.** Potential zinc binding with  $[\text{H}_2\text{L}^{\text{III}}]$

Further studies on the selectivity of  $[\text{H}_2\text{L}^{\text{III}}]$  could ultimately lead to this ligand being tested in biological sensing of zinc ions. Additionally, the mercury and cadmium complexes of this system may be of interest. Both mercury and cadmium are common environmental contaminants that would be useful to identify through a fluorescence assay.

In an attempt to increase the extinction coefficient and reduce the limit of detection of the system, the naphthyl analogue ( $\text{UO}_2[\text{L}^{\text{IV}}]$ ) was synthesized. Absorbance is observed at 220 nm ( $\epsilon = 14,300 \text{ cm}^{-1} \text{ M}^{-1}$ ), at 322 nm ( $\epsilon = 4,021 \text{ cm}^{-1} \text{ M}^{-1}$ ), and at 366 nm ( $\epsilon = 2,710 \text{ cm}^{-1} \text{ M}^{-1}$ ), in the UV-visible spectrum of  $\text{UO}_2[\text{L}^{\text{IV}}]$  (**Figure 3.14**). While increasing the conjugation of organic molecules often increases their extinction coefficient, this was not observed with  $[\text{H}_2\text{L}^{\text{IV}}]$  due to

the  $sp^3$  hybridized carbon present in the backbone skeleton. The conjugation was locally increased, but the entire backbone was not conjugated, which resulted in no significant increase in absorbance.

The sulfonyl analogue ( $UO_2[L^V]$ ) was also synthesized. Such a ligand may provide a simple method for testing waste water streams. Attempts to make the free base  $[H_2L^V]$  were unsuccessful, probably due to the electron withdrawing and deactivating nature of the sulfonyl groups. When the metal is present to aid in coordination and organization, the reactions are more likely to go to completion. Crystallization of  $UO_2[L^V]$  was also attempted, but resulted in no crystals of quality for diffraction methods. The chloro- analogue  $UO_2[L^{VI}]$  was also synthesized and purified, but no increase in extinction coefficient was observed. While crystals of  $UO_2[L^{VI}]$  were grown several times, none were suitable for characterization by single crystal X-ray diffraction.

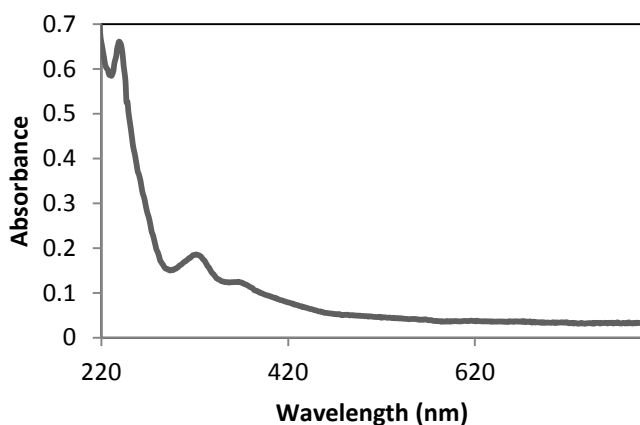


**Figure 3.14.** Absorbance spectrum of a 20  $\mu$ M solution of  $UO_2[L^{IV}]$  in DCM.

## Conclusions

In summary,  $UO_2[L^{III}]$  and  $UO_2[L^{IV}]$  complexes with uncommon pyridine coordination have been synthesized and characterized in solution and in the solid state. This pentadentate

binding ligand fully occupies the equatorial binding environment, removing the necessity of a coordinating solvent molecule or ligand rearrangement and allowing to quickly and selectively bind uranyl in a one-to-one fashion. The  $\text{UO}_2[\text{L}^{\text{V}}]$  and  $\text{UO}_2[\text{L}^{\text{VI}}]$  complexes were also synthesized, but their molar extinction coefficients were low. These complexes do have a distinct response for uranyl over common first-row transition metals in the UV, meaning synthetic addition of a chromophore may lead to this system being a useful, in-the-field sensor. The ligand  $[\text{H}_2\text{L}^{\text{III}}]$  showed a significant increase in fluorescence in the presence of zinc, inspiring interest in use as a zinc fluorescent sensor.<sup>25, 43</sup>

## Materials and Methods

### Experimental

*Caution! The  $\text{UO}_2(\text{NO}_3)_2 \cdot 6\text{H}_2\text{O}$  used in this study contained depleted uranium, standard precautions for handling radioactive materials or heavy metals were followed.*

All solvents not specifically mentioned were ACS grade from EMD and used as received with no further purification. Reagents methanol (HPLC grade, EMD), ethanol (200 proof, ACS grade, Pharmco-aaper), 2,6-pyridinedicarboxylic acid (99%, Acros), sulfuric acid (95-98%, Sigma Aldrich), sodium bicarbonate (EMD), sodium chloride (Macron), ammonium hydroxide (BDH), trifluoroacetic anhydride (>99%, Sigma Aldrich), palladium 5% on carbon, dry, type 87L (Alpha Aesar), Celite (Alpha Aesar), 3,5-di-tert-butylsalicylaldehyde (98%, TCI), 2-hydroxynaphthaldehyde (98%, Alpha Aesar), hydrochloric acid (ACS grade, Fischer Scientific), sodium hydroxide (ACS grade, EMD), copper(II) acetate hydrate (>98%, MC/B), zinc (II) acetate dihydrate (Sigma Aldrich), vanadium(IV) bis(acetylacetonato)oxide (98%, STREM),

cobalt(II) acetate tetrahydrate (Mallinckrodt), and nickel(II) acetate tetrahydrate (Sigma Aldrich) were used as received without further purification. Anhydrous dichloromethane (BDH) and tetrahydrofuran (Macron) were purchased, stored under argon, and dispensed from a solvent purification system. Triethylamine (99%, Alpha Aesar) was distilled and stored under argon until use.  $\text{UO}_2(\text{NO}_3)_2 \cdot 6\text{H}_2\text{O}$  (98%, J. T. Baker) was recrystallized from a nitric acid solution and stored under hexanes until use.

### **Dimethyl-2,6-pyridinedicarboxylate**

Methanol (320 mL) and 2,6-pyridinedicarboxylic acid (8.195 g, 49.03 mmol) were added to a round bottom flask, charged with a stir bar and gently warmed to 30 °C to aid in dissolution. Sulfuric acid (10 mL) was added slowly, followed by heating the flask to reflux for 4 hours. The reaction solution was quenched with  $\text{NaHCO}_3$  until a neutral pH was attained, followed by the extraction of the ester into dichloromethane (DCM). The ester was washed twice with brine solution and remaining solvent was removed under reduced pressure yielding a white powder (8.681 g, 44.48 mmol, 91 %).  $^1\text{H}$  NMR (400 MHz,  $\text{CDCl}_3$ )  $\delta$  4.37 (s, 6H), 8.041 (t, 1H,  $J = 7.8$  Hz), 8.332 (d, 2H,  $J = 7.6$  Hz); TOF MS (ESI)  $m/z$  ( $\text{M}^+ + 1$ ) Cald 196.0532, Found 196.0597.

### **2,6-pyridinedicarboxamide**

Ammonium hydroxide (50 mL) and dimethyl-2,6-pyridinedicarboxylate (3.053 g, 15.64 mmol) were added to a round bottom flask, charged with a stir bar and heated to 40 °C for 8 hours. Resulting white powder was filtered using cold deionized water. Product was dried at 60 °C overnight in a vacuum oven, yielding a matte white solid in quantitative yield (2.583g, 15.64 mmol).  $^1\text{H}$  NMR (400 MHz,  $\text{D}_6\text{-DMSO}$ )  $\delta$  7.717 (s, 2NH) 8.117-8.198 (m, 3H) 8.881 (s, 2NH); MS (ESI)  $m/z$  ( $\text{M}^+ + 1$ ) Cald 166.0538, Found 166.0642.

### **2,6-pyridinedicarbonitrile**

Dry THF (25 mL), 2,6-pyridinedicarboxamide (3.517 g, 21.29 mmol) and freshly distilled triethylamine (7 mL) were added to a round bottom flask, charged with a stir bar and cooled to 0 °C. Trifluoroacetic anhydride (8.75 mL) was added dropwise with stirring. Reaction vessel was stirred for 30 minutes in ice, and then allowed to warm to room temperature. Reaction was allowed to continue until judged complete, for 4 hours, and quenched with saturated sodium bicarbonate solution. Solution was filtered and washed with cold deionized water, yielding a shiny white solid (2.075 g, 16.08 mmol, 76 %). <sup>1</sup>H NMR (400 MHz, CDCl<sub>3</sub>) δ 7.924 (d, 2H, J = 8.0 Hz), 8.067 (t, 1H, J = 7.6 Hz); <sup>13</sup>C NMR (100 MHz, CDCl<sub>3</sub>) δ 115.41, 131.07, 135.40, 138.78; TOF MS (ESI) m/z (M<sup>+</sup> + 1) Cald 130.0327, Found 130.0420.

### **2,6-(dimethylamino)pyridine**

2,6-pyridinedicarbonitrile (0.989 g, 7.67 mmol) and dry tetrahydrofuran (100 mL) were added to a flame dried round bottom flask charged with a stir bar and allowed to dissolve. Lithium aluminum hydride (3.5 eq., 1.034 g, 27.2 mmol) was added to the reaction vessel slowly and allowed to stir at room temperature for 22 hours. The resulting solution was quenched slowly using cold isopropanol (60 mL), while stirring in an ice bath. The solution was stirred at room temperature for 2 additional hours and then filtered over Celite to remove excess aluminum salts, and solvent was removed from resulting filtrate under reduced pressure to yield a thick yellow oil (0.7239 g, 5.284 mmol, 69%). <sup>1</sup>H NMR (600 MHz, CDCl<sub>3</sub>) δ 1.676 (s, 4H), 3.967 (s, 4H), 7.145 (d, 2H, J = 7.8 Hz), 7.613 (t, 1H, J = 7.5Hz); <sup>13</sup>C NMR (151 MHz, CDCl<sub>3</sub>) δ 47.96, 119.48, 137.31, 161.56; TOF MS (ESI) m/z (M<sup>+</sup> + 1) Cald 138.0953, Found 138.0748.

### **2,6-bis[1-[(2-hydroxy-3,5-ditert-butylphenyl)imino]ethyl]pyridine ([H<sub>2</sub>L<sup>III</sup>])**

Ethanol (60 mL), 3,5-ditertbutylsalicylaldehyde (1.948 g, 8.325 mmol), 2,6-(dimethylamino)pyridine (0.5766 g, 4.209 mmol), trifluoroacetic acid (1 drop), and magnesium sulfate (1 g) were added to round bottom flask charged with a stir bar. The reaction vessel was heated to reflux for 18 hours until it was judged complete by TLC. Magnesium sulfate was removed via hot filtration, and the solvent was removed from the resulting filtrate under reduced pressure to yield a crude yellow oil. Crude product was purified with column chromatography with a gradient of 5% ethyl acetate in hexanes solution, followed by a 10% ethyl acetate in hexanes solution. The product was collected and concentrated under reduced pressure to yield a bright yellow solid (0.3404 g, 0.5982 mmol, 14.42%) <sup>1</sup>H NMR (400 MHz, CDCl<sub>3</sub>) δ 1.312 (s, 18H), 1.449 (s, 18H), 4.930 (s, 4H), 7.146 (s, 2H), 7.285 (d, 2H, *J* = 7.2 Hz), 7.408 (s, 2H), 7.686 (t, 1H, *J* = 7.5 Hz), 8.549 (s, 2H), 13.657 (s, 2OH); <sup>13</sup>C NMR (100 MHz, CDCl<sub>3</sub>) δ 29.604, 31.684, 34.314, 35.219, 65.204, 118.077, 120.587, 126.376, 127.413, 136.896, 137.850, 140.381, 158.164, 158.232, 168.179; TOF MS (ESI) *m/z* (*M*<sup>+</sup> + 1) *Calcd* 570.3981, *Found* 570.3319.

### **UO<sub>2</sub>[2,6-bis[1-[(2-hydroxy-3,5-ditert-butylphenyl)imino]ethyl]pyridine] (UO<sub>2</sub>[L<sup>III</sup>])**

Ethanol (50 mL) was added to 2,6-(dimethylamino)pyridine (0.3116 g, 2.258 mmol) in a round bottom flask charged with a stir bar, and stirred until dissolved with gentle warming. Magnesium sulfate and 3,5-ditert-butylsalicylaldehyde (1.949 g, 8.329 mmol) were added to the reaction vessel and heated to reflux for 18 hours. The resulting solution was filtered to remove the magnesium sulfate and transferred to a round bottom flask. Uranyl nitrate hexahydrate (1.082 g, 2.16 mmol) and trimethylamine (660 uL) were added to the reaction vessel and gently warmed to 40 °C for 3 hours, until the reaction was judged complete by TLC. The crude red solid, attained by removal of solvent through rotary evaporation, was purified using column

chromatography and DCM as eluent to produce a dark red solid (0.309g, 0.369 mmol, 16.3 %).  $^1\text{H}$  NMR (600 MHz,  $\text{CDCl}_3$ )  $\delta$  1.315 (s, 18H), 1.821 (s, 18H), 5.668 (s, 4H), 7.284 (s, 2H), 7.538 (d, 2H,  $J = 8.4$  Hz), 7.741 (s, 2H), 7.942 (t, 1H,  $J = 7.5$  Hz), 9.427 (s, 2H);  $^{13}\text{C}$  NMR (150 MHz,  $\text{CDCl}_3$ )  $\delta$  30.90, 31.74, 33.88, 35.93, 69.67, 120.19, 122.83, 127.87, 130.29, 139.29, 140.77, 160.96, 166.76, 169.75;  $^1\text{H}$  NMR (400 MHz,  $\text{CD}_3\text{CN}$ )  $\delta$  1.344 (s, 18H), 1.764 (s, 18H), 5.771 (s, 4H), 7.485 (d, 2H,  $J = 2.3$  Hz), 7.681 (d, 2H,  $J = 2.8$  Hz), 7.792 (s, 1H), 7.812 (s, 1H), 8.192 (t, 1H,  $J = 7.6$  Hz), 9.427 (s, 2H);  $^{13}\text{C}$  NMR (100 MHz,  $\text{CD}_3\text{CN}$ )  $\delta$  31.481, 32.211, 34.877, 36.969, 70.476, 122.188, 124.503, 129.769, 131.071, 140.353, 141.418, 124.564, 162.222, 167.512, 171.399; MS (ESI)  $m/z$  ( $M^+ + 1$ ) Calcd 838.4231, Found 838.4254. Single crystals of  $\text{UO}_2[\text{L}^{\text{III}}]$  were grown from slow evaporation of a concentrated solution of  $\text{UO}_2[\text{L}^{\text{III}}]$  in acetonitrile. CCDC: 1469301.

#### **$\text{UO}_2[2,6\text{-bis}[1\text{-}[(2\text{-hydroxy-naphthyl)imino]ethyl]pyridine]$ ( $\text{UO}_2[\text{L}^{\text{IV}}]$ )**

Ethanol (50 mL) was added to 2,6-(dimethylamino)pyridine (0.143 g, 1.04 mmol) in a round bottom flask charged with a stir bar, and stirred until dissolved with gentle warming. 2-hydroxynaphthaldehyde (0.385 g, 2.24 mmol) were added to the reaction vessel and heated to reflux for 9 hours. Uranyl nitrate hexahydrate (0.5126 g, 1.021 mmol) and trimethylamine (400  $\mu\text{L}$ ) were added to the reaction vessel and gently warmed to 40  $^\circ\text{C}$  for 12 hours, until the reaction was judged complete. The resulting solution was placed in ice to precipitate an orange solid was separated via vacuum filtration (0.5891 g, 0.826 mmol, 79.5 %).  $^1\text{H}$  NMR (400 MHz,  $d_6\text{-DMSO}$ )  $\delta$  6.154 (s, 4H), 7.305 (t, 2H,  $J = 7.3$  Hz), 7.424 (d, 2H,  $J = 9.0$  Hz), 7.585 (t, 2H,  $J = 7.6$  Hz), 7.893 (d, 2H,  $J = 8.0$  Hz), 7.990 (d, 2H,  $J = 7.8$  Hz), 8.213 (d, 2H,  $J = 9.0$  Hz), 8.353-8.382 (m, 3H), 10.581 (s, 2H);  $^{13}\text{C}$  NMR (150 MHz,  $d_6\text{-DMSO}$ )  $\delta$  69.074, 113.220, 121.487, 121.802, 123.255, 124.771, 127.753, 127.980, 129.102, 134.566, 136.351, 142.096, 161.565, 165.044,



170.347; TOF MS (ESI) m/z ( $M^+ + 1$ ) Cald 714.2040, Found 714.2008 . Single crystals of  $UO_2[L^{IV}]$  were grown from slow diffusion of hexanes into a concentrated solution of  $UO_2[L^{IV}]$  in DCM. CCDC: 1497023.

**$UO_2[2,6\text{-bis}[1\text{-}[(2\text{-hydroxy-3-tert-butyl-5-sulfo-phenyl)imino]ethyl]pyridine]$  ( $UO_2[L^V]$ )**

Methanol (120 mL) was added to 2,6-(dimethylamino)pyridine (0.3671 g, 2.679 mmol) in a round bottom flask charged with a stir bar. The reagent 5-sulfo-3-t-butylsalicylaldehyde (0.842 g, 3.00 mmol) was added to the reaction and stirred until dissolved with gentle warming. Uranyl acetate (0.5802 g, 1.495mmol) was then added to the reaction vessel which was heated to reflux for 18 hours. The resulting red solution was put in the freezer for three days. The yellow solid (residual starting material) was then filtered from the flask and the red solution was collected. The residual solvent was removed through rotary evaporation to produce a dark red solid.

**$UO_2[2,6\text{-bis}[1\text{-}[(2\text{-hydroxy-5-chlorophenyl)imino]ethyl]pyridine]$  ( $UO_2[L^{VI}]$ )**

Ethanol (80 mL) was added to 2,6-(dimethylamino)pyridine (0.4043 g, 2.951 mmol) in a round bottom flask charged with a stir bar, and stirred until dissolved with gentle warming. The reagent 5-chlorosalicylaldehyde (.4787 g, 3.057 mmol) were added to the reaction vessel and heated to reflux for 18 hours. Uranyl acetate hexahydrate (0.5788 g, 1.4917 mmol) was added to the reaction vessel and heated to reflux for 18 hours. The crude red solid, attained by filtration, was purified using column chromatography and 5% MeOH in DCM as the eluent to produce a red orange solid.

**NMR Spectroscopy:**  $^1H$  NMR spectra were recorded with a Bruker AC400 spectrometer at 400 or Bruker AC600 spectrometer at 600 MHz.  $^{13}C$  NMR spectra were recorded with a Bruker AC400 spectrometer at 100 or Bruker AC600 spectrometer 151 at MHz. NMR spectroscopic

data were collected using deuterated chloroform ( $\text{CDCl}_3$ ), deuterated dimethylsulfoxide ( $\text{D}_6$ -DMSO) or deuterated acetonitrile ( $\text{CD}_3\text{CN}$ ) and reported in parts per million relative to trimethylsilane (TMS,  $\delta$  0.00 ppm).

**X-ray Diffraction:** Suitable crystals were selected and mounted on a glass fiber using Paratone-n oil and data collection was completed on a 'Bruker APEX CCD' diffractometer. The crystal was kept at 180(2) K during unit cell and data collection. The structure was solved with the ShelXS structure solution program using Direct Methods<sup>44-45</sup> and refined with the ShelXL refinement package using Least Squares minimization<sup>44-45</sup>, or refined with the olex2.refine<sup>46</sup> refinement package using Gauss-Newton minimisation. Projections were created on Olex2 software.<sup>46</sup>

**Absorbance Spectroscopy:** All absorbance spectra were collected on a VARIAN Cary 50 WinUV Spectrometer with a xenon lamp with absorbance spectra from 200 nm to 900 nm with a 1 cm width quartz cuvette.

**Fluorescence Spectroscopy:** All fluorescence spectra were collected on a Shimadzu RF-5301 PC fluorospectrophotometer with a xenon lamp and a 1 cm width quartz cuvette with an excitation of 365 nm and an emission spectrum of 375–900 nm. Slit widths were set so that the maximum emission of the ligand could be maintained throughout the titration.

## References

1. Vasu, A.; Boswell, C., Carbon Pollution Emission Guidelines for Existing Stationary Sources: Electric Utility Generating Units. EPA, Ed. Federal Register: 2015; Vol. 80, pp 64661-65120.
2. Anderson, N. H.; Odoh, S. O.; Williams, U. J.; Lewis, A. J.; Wagner, G. L.; Lezama Pacheco, J.; Kozimor, S. A.; Gagliardi, L.; Schelter, E. J.; Bart, S. C., Investigation of the Electronic Ground States for a Reduced Pyridine(diimine) Uranium Series: Evidence for a Ligand Tetraanion Stabilized by a Uranium Dimer. *J. Am. Chem. Soc.* **2015**, *137* (14), 4690-4700.
3. Chatelain, L.; Scopelliti, R.; Mazzanti, M., Synthesis and Structure of Nitride-Bridged Uranium(III) Complexes. *J. Am. Chem. Soc.* **2016**, *138* (6), 1784-1787.
4. Bagus, P. S.; Nelin, C. J.; Hrovat, D. A.; Ilton, E. S., Covalent bonding in heavy metal oxides. *J. Chem. Phys.* **2017**, *146*, 134706.
5. Neidig, M. L.; Clark, D. L.; Martin, R. L., Covalency in f-element complexes. *Coord. Chem. Rev.* **2013**, *257* (2), 394-406.
6. Fox, A. R.; Bart, S. C.; Meyer, K.; Cummins, C. C., Towards uranium catalysts. *Nature* **2008**, *455* (7211), 341-349.
7. Halter, D. P.; Heinemann, F. W.; Bachmann, J.; Meyer, K., Uranium-mediated electrocatalytic dihydrogen production from water. *Nature* **2016**, *530* (7590), 317-321.
8. Arnold, P. L.; Farnaby, J. H.; White, R. C.; Kaltsoyannis, N.; Gardiner, M. G.; Love, J. B., Switchable [small pi]-coordination and C-H metallation in small-cavity macrocyclic uranium and thorium complexes. *Chem. Sci.* **2014**, *5* (2), 756-765.

9. Kaltsoyannis, N., Does covalency increase or decrease across the actinide series? Implications for minor actinide partitioning. *Inorg. Chem.* **2013**, *52* (7), 3407-13.
10. Copping, R.; Jeon, B.; Pemmaraju, C. D.; Wang, S.; Teat, S. J.; Janousch, M.; Tyliczszak, T.; Canning, A.; Grønbech-Jensen, N.; Prendergast, D.; Shuh, D. K., Toward Equatorial Planarity about Uranyl: Synthesis and Structure of Tridentate Nitrogen-Donor  $\{\text{UO}_2\}^{2+}$  Complexes. *Inorg. Chem.* **2014**, *53* (5), 2506-2515.
11. Kiernicki, J. J.; Cladis, D. P.; Fanwick, P. E.; Zeller, M.; Bart, S. C., Synthesis, Characterization, and Stoichiometric U–O Bond Scission in Uranyl Species Supported by Pyridine(diimine) Ligand Radicals. *J. Am. Chem. Soc.* **2015**, *137* (34), 11115-11125.
12. Ho, I. T.; Zhang, Z.; Ishida, M.; Lynch, V. M.; Cha, W.-Y.; Sung, Y. M.; Kim, D.; Sessler, J. L., A Hybrid Macrocyclic with a Pyridine Subunit Displays Aromatic Character upon Uranyl Cation Complexation. *J. Am. Chem. Soc.* **2014**, *136* (11), 4281-4286.
13. Bharara, M. S.; Heflin, K.; Tonks, S.; Strawbridge, K. L.; Gorden, A. E. V., Hydroxy- and alkoxy-bridged dinuclear uranyl-Schiff base complexes: hydrolysis, transamination and extraction studies. *Dalton Trans.* **2008**, *22*, 2966-73.
14. Maynard, B. A.; Brooks, J. C.; Hardy, E. E.; Easley, C. J.; Gorden, A. E. V., Synthesis, structural characterization, electronic spectroscopy, and microfluidic detection of  $\text{Cu}^{2+}$  and  $\text{UO}_2^{2+}$  [di-tert-butyl-salphenazine] complexes. *Dalton Trans.* **2015**, *44* (10), 4428-4430.
15. Hardy, E. E.; Eddy, M. A.; Maynard, B. A.; Gorden, A. E. V., Solid state  $\pi$ - $\pi$  stacking and higher order dimensional crystal packing, reactivity, and electrochemical behaviour of salphenazine actinide and transition metal complexes. *Dalton Trans.* **2016**, *45* (36), 14243-14251.

16. Bhatt, K. D.; Makwana, B. A.; Vyas, D. J.; Mishra, D. R.; Jain, V. K., Selective recognition by novel calix system: ICT based chemosensor for metal ions. *J. Lumin.* **2014**, *146*, 450-457.
17. Ho, I. T.; Sessler, J. L.; Gambhir, S. S.; Jokerst, J. V., Parts per billion detection of uranium with a porphyrinoid-containing nanoparticle and in vivo photoacoustic imaging. *Analyst* **2015**, *140* (11), 3731-3737.
18. Ansari, R.; Mosayebzadeh, Z., Construction of a new solid-state U(VI) ion-selective electrode based on polypyrrole conducting polymer. *J. Radioanal. Nucl. Chem.* **2013**, *299* (3), 1597-1605.
19. Gorden, A. E. V.; Xu, J.; Raymond, K. N.; Durbin, P., Rational Design of Sequestering Agents for Plutonium and Other Actinides. *Chem. Rev.* **2003**, *103*, 4207-4282.
20. Berg, J. M.; Shi, Y., The Galvanization of Biology: A Growing Appreciation for the Roles of Zinc. *Science* **1996**, *271* (5252), 1081-1085.
21. Frederickson, C. J.; Koh, J.-Y.; Bush, A. I., The neurobiology of zinc in health and disease. *Nature Rev. Neurosci.* **2005**, *6*, 449.
22. Bush, A.; Pettingell, W.; Multhaup, G.; d Paradis, M.; Vonsattel, J.; Gusella, J.; Beyreuther, K.; Masters, C.; Tanzi, R., Rapid induction of Alzheimer A beta amyloid formation by zinc. *Science* **1994**, *265* (5177), 1464-1467.
23. Noy, D.; Solomonov, I.; Sinkevich, O.; Arad, T.; Kjaer, K.; Sagi, I., Zinc-Amyloid  $\beta$  Interactions on a Millisecond Time-Scale Stabilize Non-fibrillar Alzheimer-Related Species. *J. Am. Chem. Soc.* **2008**, *130* (4), 1376-1383.
24. Chen, Y.; Bai, Y.; Han, Z.; He, W.; Guo, Z., Photoluminescence imaging of  $Zn^{2+}$  in living systems. *Chem. Soc. Rev.* **2015**, *44* (14), 4517-4546.

25. Aron, A. T.; Ramos-Torres, K. M.; Cotruvo, J. A.; Chang, C. J., Recognition- and Reactivity-Based Fluorescent Probes for Studying Transition Metal Signaling in Living Systems. *Acc. Chem. Res.* **2015**, *48* (8), 2434-2442.
26. Mandal, S.; Sikdar, Y.; Maiti, D. K.; Maiti, G. P.; Mandal, S. K.; Biswas, J. K.; Goswami, S., A new pyridoxal based fluorescence chemo-sensor for detection of Zn(II) and its application in bio imaging. *RSC Advances* **2015**, *5* (89), 72659-72669.
27. Maji, A.; Pal, S.; Lohar, S.; Mukhopadhyay, S. K.; Chattopadhyay, P., A new turn-on benzimidazole-based greenish-yellow fluorescent sensor for Zn<sup>2+</sup> ions at biological pH applicable in cell imaging. *New J. Chem.* **2017**, *41* (15), 7583-7590.
28. Formica, M.; Favi, G.; Fusi, V.; Giorgi, L.; Mantellini, F.; Micheloni, M., Synthesis and study of three hydroxypyrazole-based ligands: A ratiometric fluorescent sensor for Zn(II). *J. Lumin.* **2018**, *195*, 193-200.
29. Hosseini, M.; Ghafarloo, A.; Ganjali, M. R.; Faridbod, F.; Norouzi, P.; Niasari, M. S., A turn-on fluorescent sensor for Zn<sup>2+</sup> based on new Schiff's base derivative in aqueous media. *Sensors Actuators B: Chem.* **2014**, *198*, 411-415.
30. Dong, W.-K.; Akogun, S. F.; Zhang, Y.; Sun, Y.-X.; Dong, X.-Y., A reversible "turn-on" fluorescent sensor for selective detection of Zn<sup>2+</sup>. *Sensors Actuators B: Chem.* **2017**, *238*, 723.
31. Li, Q.-F.; Wang, J.-T.; Wu, S.; Ge, G.-W.; Huang, J.; Wang, Z.; Yang, P.; Lin, J., A water-soluble fluorescent chemosensor having a high affinity and sensitivity for Zn<sup>2+</sup> and its biological application. *Sensors Actuators B: Chem.* **2018**, *259*, 484-491.
32. Jung, J. M.; Lee, S. Y.; Nam, E.; Lim, M. H.; Kim, C., A highly selective turn-on chemosensor for Zn<sup>2+</sup> in aqueous media and living cells. *Sensors Actuators B: Chem.* **2017**, *244*, 1045-1053.

33. Hardy, E. E.; Wyss, K. M.; Eddy, M. A.; Gorden, A. E. V., An example of unusual pyridine donor Schiff base uranyl ( $\text{UO}_2^{2+}$ ) complexes. *Chem. Commun.* **2017**, 53 (42), 5718-5720.
34. Horeglad, P.; Nocton, G.; Filinchuk, Y.; Pecaut, J.; Mazzanti, M., Pentavalent uranyl stabilized by a dianionic bulky tetradentate ligand. *Chem. Commun.* **2009**, (14), 1843-1845.
35. Valkonen, A.; Lombardo, G. M.; Rissanen, K.; Punzo, F.; Cametti, M., X-Ray crystallographic and computational study on uranyl-salophen complexes bearing nitro groups. *Dalton Trans.* **2017**, 46 (16), 5240-5249.
36. Takao, K.; Tsushima, S.; Takao, S.; Scheinost, A. C.; Bernhard, G.; Ikeda, Y.; Hennig, C., X-ray Absorption Fine Structures of Uranyl(V) Complexes in a Nonaqueous Solution. *Inorg. Chem.* **2009**, 48 (20), 9602-9604.
37. Takao, K.; Kato, M.; Takao, S.; Nagasawa, A.; Bernhard, G.; Hennig, C.; Ikeda, Y., Molecular Structure and Electrochemical Behavior of Uranyl(VI) Complex with Pentadentate Schiff Base Ligand: Prevention of Uranyl(V) Cation–Cation Interaction by Fully Chelating Equatorial Coordination Sites. *Inorg. Chem.* **2010**, 49 (5), 2349-2359.
38. Lapka, J. L.; Paulenova, A.; Zakharov, L. N.; Alyapyshev, M. Y.; Babain, V. A., Coordination of uranium(VI) with N,N' -diethyl- N,N' -ditolyldipicolinamide. *IOP Conf. Series: Mat. Sci. Engin.* **2010**, 9 (1), 012029.
39. Gatto, C. C.; Lang, E. S.; Jagst, A.; Abram, U., Dioxouranium(VI) complexes with 2,6-acetylpyridinebenzoylhydrazones and -semicarbazones. *Inorg. Chim. Acta* **2004**, 357 (15), 4405-4412.

40. Paolucci, G.; Marangoni, G.; Bandoli, G.; Clemente, D. A., Reactivity of uranyl ion with quinquedentate chelating hydrazine derivatives. Part 2. 2,6-Diacetylpyridine bis(4-methoxybenzoylhydrazone). *J. Chem. Soc., Dalton Trans.* **1980**, (8), 1304-1311.
41. Martinez, C. R.; Iverson, B. L., Rethinking the term "pi-stacking". *Chem. Sci.* **2012**, 3 (7), 2191-2201.
42. Melhuish, W. H., Quantum Efficiencies of Fluorescence of Organic Substances: Effect of Solvent and Concentration of the Fluorescent Solute. *J. Phys.Chem.* **1961**, 65 (2), 229-235.
43. Carter, K. P.; Young, A. M.; Palmer, A. E., Fluorescent Sensors for Measuring Metal Ions in Living Systems. *Chem. Rev.* **2014**, 114 (8), 4564-4601.
44. Bruker, Bruker AXS Inc.: Madison, Wisconsin, USA, 2001.
45. Sheldrick, G. M., A Short History of SHELX. *Acta Crystallogr., Sect. A: Found. Crystallogr.* **2008**, A64, 112.
46. Dolomanov, O. V.; Bourhis, L. J.; Gildea, R. J.; Howard, J. A. K.; Puschmann, H., OLEX<sup>2</sup>: A complete structure solution, refinement and analysis program. *J. Appl. Cryst.* **2009**, 42, 339-341.



## **Chapter 4: Unusual Thorium Fluorescence and Tunable Ligand Emission of Naphthylsalophen Uranyl(VI), Thorium(IV), and Lanthanide(III) Sandwich Complexes**

Portions of this chapter are reproduced from Hardy, E. E.; Wyss, K. M.; Gorden, J. D.; Ariyaratna, I. R.; Miliordos, E.; Gorden, A. E. V., *Chem. Commun.*, **2017**, 53, 11984 and Hardy, E. E.; Wyss, K. M.; Keller, R. J.; Gorden, J. D.; Gorden, A. E. V., *Dalton Trans.*, **2018**, 47, 1337 with permission from the Royal Society of Chemistry.

### **Introduction**

Actinide and lanthanide compounds have been found to possess interesting near infrared fluorescence that have been explored for use in sensors and exploited in medicinal sensing technologies.<sup>1-2</sup> In particular, the distinctive properties of multi-nuclear lanthanide and actinide complexes are of interest for their use in biological imaging,<sup>3-4</sup> quantum computing,<sup>5-6</sup> single-molecule magnets (SMMs),<sup>7-10</sup> organic light emitting diodes (OLEDs),<sup>11-12</sup> and catalysis.<sup>13</sup> Additionally a variety of lanthanide molecular organic framework (Ln-MOF) and actinide molecular organic framework (An-MOF) structures have also been applied to separations or fluorescent sensors.<sup>14-18</sup>

Directed synthesis targeting multi-nuclear lanthanide and actinide species can be difficult, due to large coordination numbers, somewhat flexible coordination geometries, and high sensitivity to pH changes or counter anions.<sup>19-20</sup> As lanthanides have similar ionic radii and

are all typically found in the trivalent oxidation state, selective sensing or extraction of any given lanthanide is of great interest. As a host of applications have been found for the lanthanides, their purification is quite complex as they are often found together in natural ores as blends also often containing uranium and/or thorium, and hence, their separation has recently become a topic of intense study.<sup>21</sup> Lutetium, for example, has been studied for photodynamic breast cancer treatments and as a sensitizer for positron emission tomography (PET) scan detection.<sup>22-23</sup> While selective detection of many of the lanthanides have been investigated, discovery of new methodologies is still of great interest.<sup>24-25</sup>

Multidentate ligand systems coupled with highly absorbing organic ligands have been used to synthesize lanthanide and actinide complexes with intriguing fluorescence properties for use in some of the aforementioned applications.<sup>26-29</sup> Salen ligands have been employed as part of multidentate ligand systems and are attractive due to their relative ease of customization of the coordination environments.<sup>30-31</sup> There have been recent examples of double and triple decker sandwich complexes with salophen ligands and lanthanides, specifically Tb(III), Yb(III), and Dy(III).<sup>19, 32-36</sup> Concurrent to this work, triple-decker sandwich complexes with naphthylsalophen and lanthanides were reported by Sanudo and co-workers, but the focus of that paper was the magnetic properties of the complexes, not structural, and no systematic discussion of this coordination environment was presented.<sup>36</sup> There have also been examples of actinide salophen sandwich complexes that provide interesting electronic properties.<sup>37-40</sup>

Previously, we have introduced ligands with a salen core but featuring a further extended conjugated backbone incorporating phenazine or quinoxalinol moieties.<sup>41-45</sup> This addition of conjugation serves to enhance the change in  $\pi$ -overlap and increase visible absorption when bound to an actinide center. This also provides access to self-assembled multinuclear lanthanide

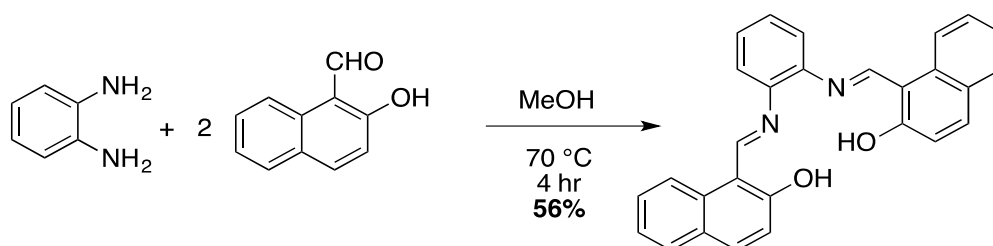
complexes. Here, we used extended conjugation on salophen ligands, in order to increase the electronic distinction between lanthanide and actinides and investigate the electronic properties of the resulting complexes. For that purpose, we have synthesized 1,1'-((1E,1'E)-(1,2-phenylenebis(azanylylidene))bis(methanylylidene))bis(naphthalen-2-ol) ( $[\text{H}_2\text{L}^{\text{VII}}]$ ), nicknamed naphthylsalophen. The ligand  $[\text{H}_2\text{L}^{\text{VII}}]$  was used to prepare lanthanide(III), cerium(IV), and thorium(IV) metal complexes. These were found to self-assemble as triple decker sandwich complexes of the type  $\text{Ln}_2[\text{L}^{\text{VII}}]_3$ , where  $\text{Ln} = \text{Pr(III)}, \text{Nd(III)}, \text{Sm(III)}, \text{Eu(III)}, \text{Gd(III)}, \text{Tb(III)}, \text{Dy(III)}, \text{Ho(III)}, \text{Er(III)}, \text{Yb(III)}, \text{or Lu(III)}$ ,<sup>46</sup> and double decker sandwiches of the type  $\text{M}[\text{L}^{\text{VII}}]_2$ , where  $\text{M} = \text{Ce(IV)} \text{ or } \text{Th(IV)}$ .<sup>47</sup>

Double decker sandwiches of the type  $\text{Th}[\text{L}^{\text{VII}}]_2$  resulted in the first fluorescent thorium compound reported to fluoresce in both the solid-state and solution. One fluorescent thorium solid-state compound and three examples of solution phase fluorescence have been described previously; however, many more examples of thorium quenching fluorescence exist.<sup>48-52</sup> Additionally, the triple-decker sandwich complexes of the type  $\text{Ln}_2[\text{L}^{\text{VII}}]_3$ , where  $\text{Ln} = \text{Pr(III)}, \text{Nd(III)}, \text{Sm(III)}, \text{Eu(III)}, \text{Gd(III)}, \text{Tb(III)}, \text{Dy(III)}, \text{Ho(III)}, \text{Er(III)}, \text{Yb(III)}, \text{or Lu(III)}$  were synthesized and structural characterization by single crystal X-ray diffraction is described for the complexes  $\text{Th}[\text{L}^{\text{VII}}]_2$ ,  $\text{Ce}[\text{L}^{\text{VII}}]_2$ ,  $\text{Nd}_2[\text{L}^{\text{VII}}]_3$ ,  $\text{Gd}_2[\text{L}^{\text{VII}}]_3$ ,  $\text{Tb}_2[\text{L}^{\text{VII}}]_3$ ,  $\text{Dy}_2[\text{L}^{\text{VII}}]_3$ ,  $\text{Ho}_2[\text{L}^{\text{VII}}]_3$ ,  $\text{Yb}_2[\text{L}^{\text{VII}}]_3$ , and  $\text{Lu}_2[\text{L}^{\text{VII}}]_3$ . The emission properties in both solution and solid-state are discussed, where tunable ligand emission in the solid state across the  $\text{Ln}_2[\text{L}^{\text{VII}}]_3$  series with a maximum at 556 nm for the  $\text{Sm}_2[\text{L}^{\text{VII}}]_3$  complex to 617 nm for  $\text{Er}_2[\text{L}^{\text{VII}}]_3$  was observed, as well as greatly increased ligand emission selectively for the complex  $\text{Lu}_2[\text{L}^{\text{VII}}]_3$ . The synthesis and interesting hydrogen bonding tetramer in the solid-state of a  $\text{UO}_2[\text{L}^{\text{VII}}]$  complex is also discussed.

## Results and Discussion

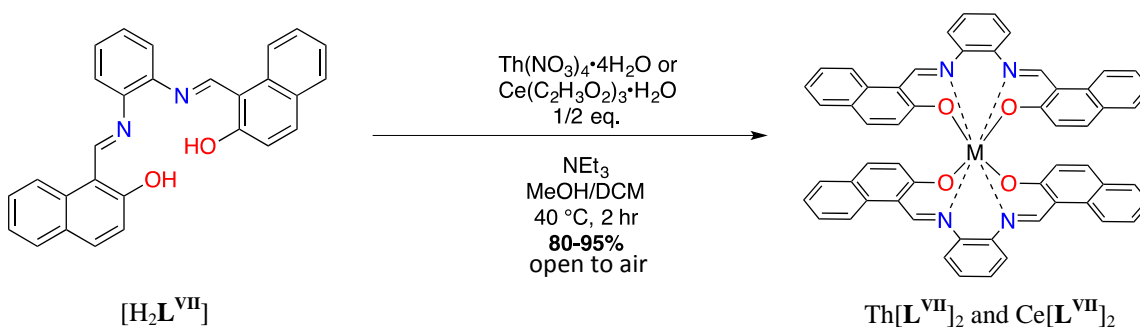
### Synthesis

The ligand [ $\text{H}_2\text{L}^{\text{VII}}$ ] was prepared reacting two equivalents of 2-hydroxynaphthaldehyde with 1,2-diaminobenzene in methanol. A precipitate formed after heating the solution to 70 °C for four hours and was isolated via vacuum filtration. The product was characterized and found to result in the desired ligand featuring a tetradentate binding pocket with two Schiff base imine donors and two phenol donors.



**Scheme 4.1.** Synthesis of  $\text{H}_2\text{L}^{\text{VII}}$ .

The synthesis of Ce(IV) and Th(IV) sandwich complexes with naphthylsalophen with this simple core but highly conjugated backbone is reported.  $\text{Ce}[\text{L}^{\text{VII}}]_2$ , and  $\text{Th}[\text{L}^{\text{VII}}]_2$  were synthesized through the addition of the metal salts to a warm methanol/dichloromethane solution of ligand and triethylamine (**Scheme 4.2**).



**Scheme 4.2.** Synthesis of  $\text{Th}[\text{L}^{\text{VII}}]_2$  and  $\text{Ce}[\text{L}^{\text{VII}}]_2$ .<sup>47</sup>

The  $\text{Ce}[\text{L}^{\text{VII}}]_2$  complex was initially synthesized from addition of 0.5 equivalents of Ce(III) acetate salt in warm methanol/dichloromethane with triethylamine as a base. Once coordinated, oxygen oxidizes the cerium ion to Ce(IV), which is subsequently stabilized by the naphthylsalophen ligands. The oxidation of Ce(III) to Ce(IV) was followed spectrophotometrically by adding 1 equivalent of Ce(III) acetate to a solution of free base in dimethylformamide under heating. The UV-visible spectra were recorded every two minutes for 36 minutes (**Figure 4.1**). A similar instance of stabilization of the Ce(IV) ion involved formation of a Ce(IV) sandwich complex in the presence of oxygen with good yields was reported by Schelter and co-workers.<sup>53</sup> The same  $\text{Ce}[\text{L}^{\text{VII}}]_2$  complex, as confirmed via a diamagnetic NMR spectrum, UV, and solid state elucidation can be synthesized using either Ce(III) salts or Ce(IV) salts in reactions with  $[\text{H}_2\text{L}^{\text{VII}}]$ . Further characterization of the stabilization of the Ce(III)/Ce(IV) redox couple by means of more detailed electrochemical analysis will be the subject of future work.

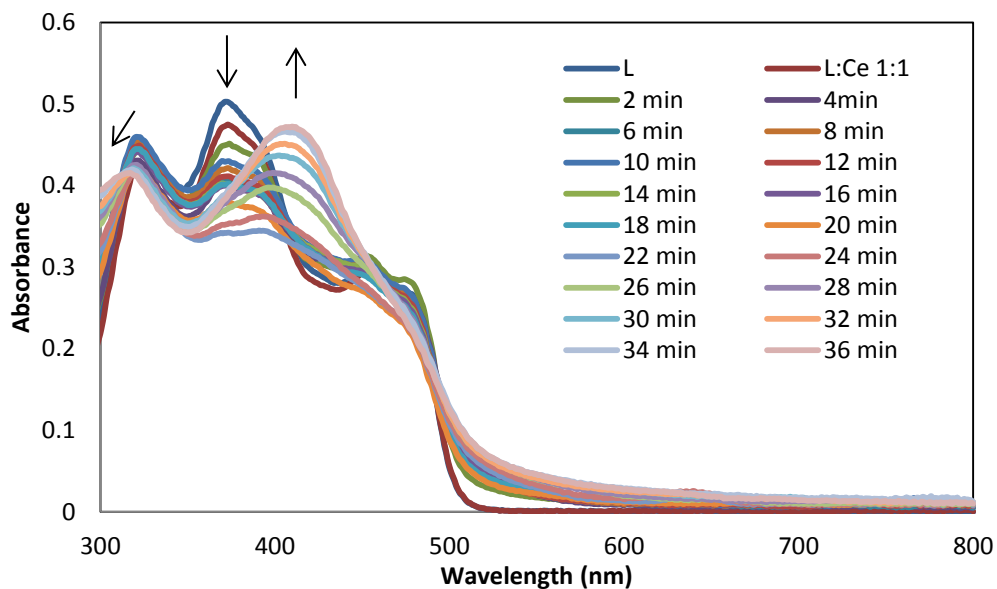
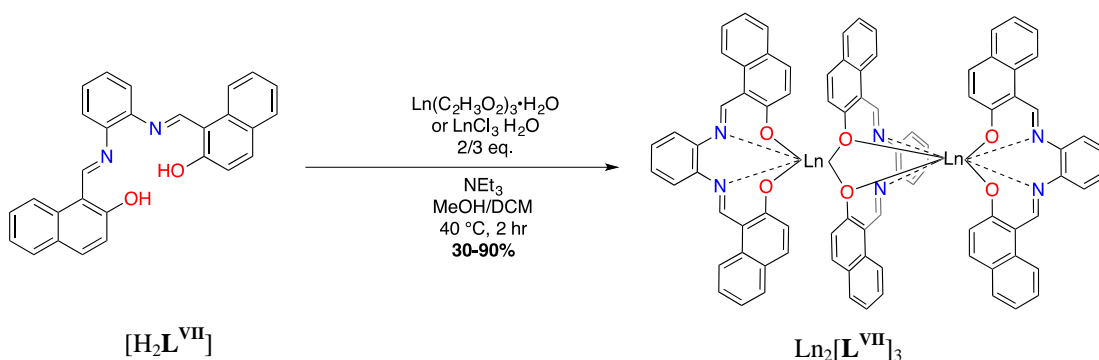
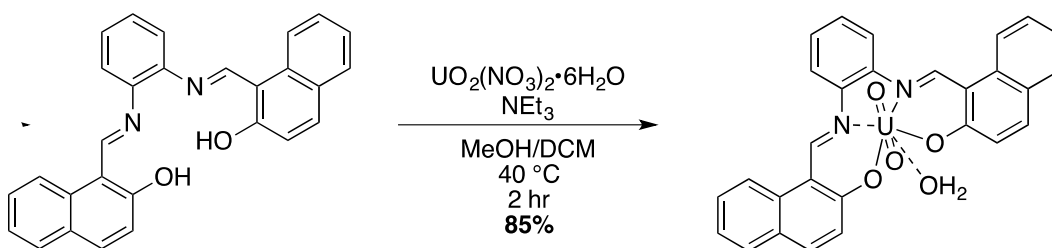


**Figure 4.1.** Solution phase absorbance of  $[\text{H}_2\text{L}^{\text{VII}}]$  ( $\lambda_{\text{max}}=324, 394, \text{ and } 446 \text{ nm}$ ) and spectrophotometric observation of the formation of  $\text{Ce}[\text{L}^{\text{VII}}]_2$  ( $\lambda_{\text{max}}=317, \text{ and } 417 \text{ nm}$ ).<sup>47</sup>

In addition, lanthanide salts (Pr(III), Nd(III), Sm(III), Eu(III), Gd(III), Tb(III), Dy(III), Ho(III), Er(III), Yb(III), or Lu(III)) were added to warm solutions of  $[H_2L^{VII}]$  in methanol (MeOH) and dichloromethane (DCM) mixture in the presence of triethylamine ( $NEt_3$ ) to afford  $Ln_2[L^{VII}]_3$  complexes (**Scheme 4.3**). Lastly, the synthesis of the  $UO_2[L^{VII}]$  complex was preformed by addition of recrystallized uranyl nitrate hexahydrate in methanol to a warm solution of  $[H_2L^{VII}]$  in DCM containing triethylamine (**Scheme 4.4**).



**Scheme 4.3.** Synthesis of  $Ln_2[L^{VII}]_3$  complexes, where Ln = Pr(III), Nd(III), Sm(III), Eu(III), Gd(III), Tb(III), Dy(III), Ho(III), Er(III), Yb(III), or Lu(III).<sup>46</sup>



**Scheme 4.4.** Synthesis of  $UO_2[L^{VII}]$  complex

## Crystallography

For each of the following compounds, crystals suitable for single crystal X-ray diffraction were selected and mounted on a glass fiber using Paratone-N oil and data set collection was

completed on a 'Bruker APEX CCD' diffractometer using Mo K $\alpha$  radiation. A full list of tables of bond lengths and angles for all compounds characterized by single crystal X-Ray diffraction can be found in Appendix I.

Crystals of [ $\text{H}_2\text{L}^{\text{VII}}$ ] suitable for X-Ray diffraction were grown from slow evaporation of a saturated 1:1 DCM and methanol solution. [ $\text{H}_2\text{L}^{\text{VII}}$ ] crystallized in the orthorhombic space group  $P2_12_12_1$  with an interstitial dichloromethane molecule in the asymmetric unit (**Figure 4.2**). The C-O1 bond length of 1.276(3) and C-O2 bond length of 1.338(3) show that the tautomerization of one phenol is the most stable form in the solid-state (**Scheme 4.5**). The longer C<sub>imine</sub>-N1 distance of 1.319(3) in comparison to C<sub>imine</sub>-N2 of 1.302(2) also confirms this assignment, although not as distinctly. This tautomerization has been observed and explained before for this system in solution using  $^1\text{H}$  NMR and IR, but this is the first crystal structure showing such phenomenon.<sup>54</sup> Crystallographic data for [ $\text{H}_2\text{L}^{\text{VII}}$ ],  $\text{Th}[\text{L}^{\text{VII}}]_2$ , and  $\text{Ce}[\text{L}^{\text{VII}}]_2$  are shown in **Table 4.1**.

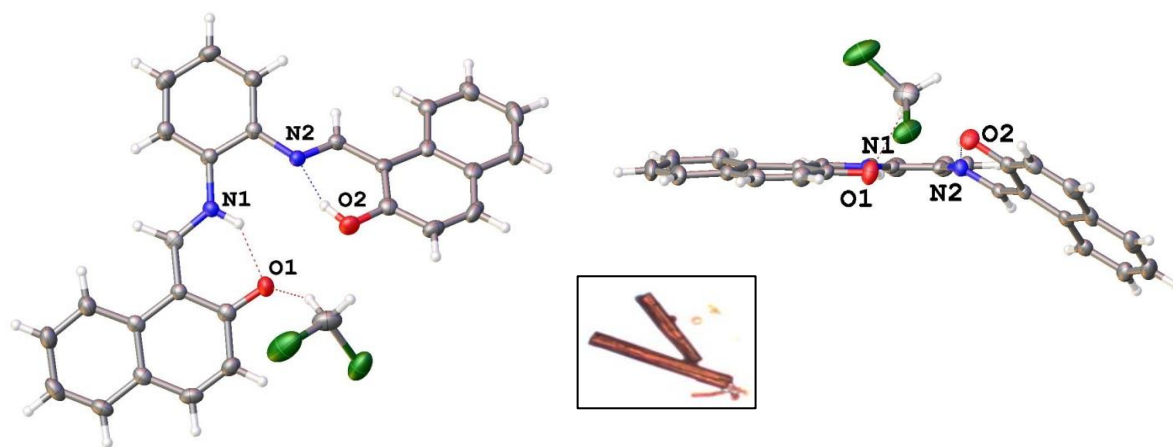
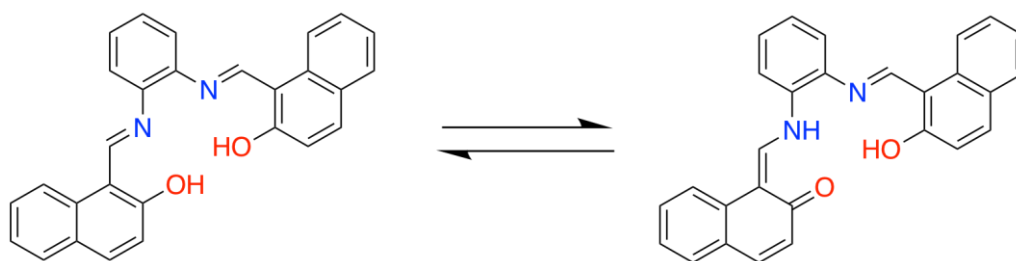


**Figure 4.2.** Projection of [ $\text{H}_2\text{L}^{\text{VII}}$ ] and interstitial DCM solvent molecule. Carbon atoms are shown in grey, nitrogen in blue, oxygen in red, and chlorine in green. Inset image of crystals.



**Scheme 4.5.** Tautomerization of  $[\text{H}_2\text{L}^{\text{VII}}]$  observed in the solid-state and solution  $^1\text{H}$  NMR.

**Table 4.1.** Crystallographic data and details of data collection of  $[\text{H}_2\text{L}^{\text{VII}}]$ ,  $\text{Th}[\text{L}^{\text{VII}}]_2$  and  $\text{Ce}[\text{L}^{\text{VII}}]_2$ .<sup>47</sup>

	$[\text{H}_2\text{L}^{\text{VII}}] \cdot \text{DCM}$	$\text{Th}[\text{L}^{\text{VII}}]_2 \cdot \frac{1}{2}\text{C}_7\text{H}_8$	$\text{Ce}[\text{L}^{\text{VII}}]_2 \cdot \text{H}_2\text{O} \cdot \frac{1}{2}\text{C}_6\text{H}_{14}$
<b>Empirical formula</b>	$\text{C}_{29}\text{H}_{22}\text{Cl}_2\text{N}_2\text{O}_2$	$\text{C}_{66.5}\text{H}_{47.5}\text{N}_4\text{O}_4\text{Th}$	$\text{C}_{59}\text{H}_{36}\text{CeN}_4\text{O}_5$
<b>Formula weight</b>	501.42	1198.68	1021.08
<b>Crystal size/mm<sup>3</sup></b>	$0.20 \times 0.04 \times 0.02$	$0.18 \times 0.12 \times 0.08$	$0.45 \times 0.15 \times 0.02$
<b>Crystal system</b>	orthorhombic	triclinic	monoclinic
<b>Space group</b>	$\text{P}2_12_12_1$	P-1	$\text{P}2_1/\text{n}$
<b>a/Å</b>	7.1378(10)	11.4987(3)	13.0103(8)
<b>b/Å</b>	16.682(2)	14.3613(4)	13.9521(8)
<b>c/Å</b>	20.056(3)	16.2765(5)	26.1970(15)
<b><math>\alpha/^\circ</math></b>	90	106.2205(11)	90
<b><math>\beta/^\circ</math></b>	90	90.8258(11)	99.6888(12)
<b><math>\gamma/^\circ</math></b>	90	94.1516(11)	90
<b>Volume/Å<sup>3</sup></b>	2388.1(6)	2572.39(13)	4687.5(5)
<b>Z</b>	4	2	4
<b><math>\rho_{\text{calc}}/\text{mg}/\text{mm}^3</math></b>	1.3945	1.5474	1.4468
<b><math>\text{m}/\text{mm}^{-1}</math></b>	0.303	2.955	1.028
<b>F(000)</b>	1041.6	1180.2	2064.4
<b>Temperature/K</b>	180.45	180.45	180.45
<b>Radiation</b>	Mo K $\alpha$	Mo K $\alpha$	Mo K $\alpha$
	( $\lambda = 0.71073$ )	( $\lambda = 0.71073$ )	( $\lambda = 0.71073$ )
<b>Reflections collected</b>	17603	53501	61172
<b>Independent reflections</b>	6177	8180	9966
<b>Goodness-of-fit on F<sup>2</sup></b>	1.036	1.06	1.068
<b>Final R indexes</b>	$R_1 = 0.0557,$	$R_1 = 0.0242,$	$R_1 = 0.0292,$
<b>[I] <math>\geq 2\sigma</math> (I)</b>	$wR_2 = 0.1176$	$wR_2 = 0.0489$	$wR_2 = 0.0699$
<b>Largest diff. peak/hole / e Å<sup>-3</sup></b>	0.64/-0.64	0.92/-0.91	0.78/-0.60

Crystals of  $\text{Th}[\text{L}^{\text{VII}}]_2$  suitable for X-ray diffraction were grown from slow diffusion of hexanes into a saturated toluene solution.  $\text{Th}[\text{L}^{\text{VII}}]_2$  crystallized in  $\text{P}\bar{1}$  with 1.5 toluene molecules per asymmetric unit, with one disordered toluene molecule lying on the mirror plane. The



resulting solid was characterized in the solid-state using single crystal diffraction and UV-Vis spectroscopy (**Figure 4.3**). The thorium atom has a distorted square antiprismatic coordination environment, with the coordinating oxygen and nitrogen on one ligand making up each square face of the coordination environment.  $\text{Th}[\text{L}^{\text{VII}}]_2$  has four Th-O bonds with lengths 2.254, 2.326, 2.282, and 2.289 Å. These Th-O bonds are 0.2 Å shorter than the average observed in similar thorium sandwich complexes, suggesting stronger interactions as compared to previously reported compounds.<sup>39,55-60</sup>

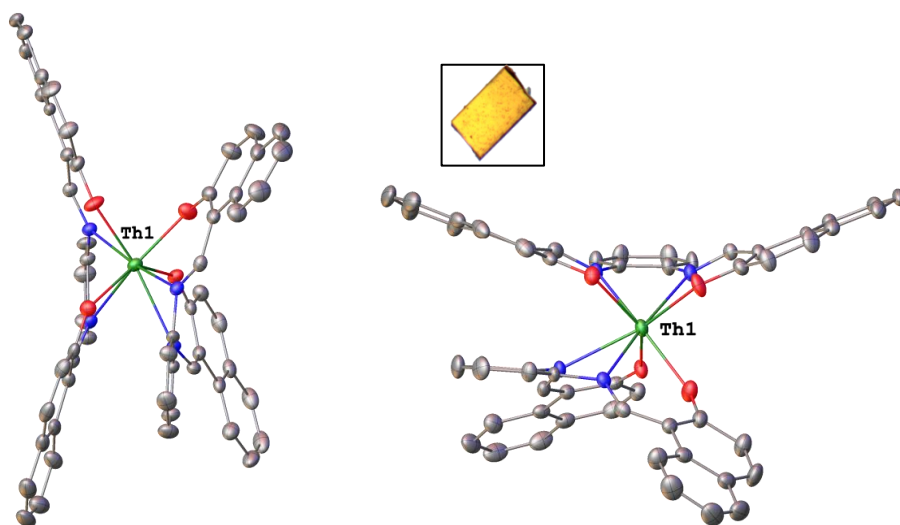


**Figure 4.3.** Projections of  $\text{Th}[\text{L}^{\text{VII}}]_2$  highlighting the 8-coordinate thorium(IV) metal center. Disordered interstitial toluene solvent molecule and hydrogen atoms have been removed for clarity. Carbon atoms are shown in grey, nitrogen in blue, oxygen in red, and thorium in green. Inset image of crystal of data collection.<sup>47</sup>

The shortened distances do not seem to be caused by  $\pi$ - $\pi$  overlap in the ligand systems, as there is distortion from planarity preventing  $\pi$ -stacking interactions. The average Th-N bond length of 2.63 Å ( $\pm 0.01$ ), is slightly longer (0.1 Å) than that in the reported porphyrin sandwich structure,<sup>14</sup> but comparable (within  $\pm 0.03$  Å) to many other 8 and 9 coordinate thorium sandwich complexes described previously.<sup>39,56-58</sup> The Th-N bond lengths are notably shorter (0.2 Å) than reported Th-N bond lengths in either tertiary amine containing ligands<sup>59</sup> or hydroxy

bridged species.<sup>60</sup> The coordination of the free base may be more properly explained as a negatively charged N donor and neutral carbonyl species, rather than a negatively charged phenol and neutral imine donor, to explain this uncommonly short Th-N bond lengths.

The  $\text{Ce}[\text{L}^{\text{VII}}]_2$  complex was found to be crystalline and ordered in  $\text{P2}_1/\text{n}$  space group, with one half of a disordered hexane molecule and one water molecule per asymmetric unit (**Figure 4.4**). The cerium(IV) atom also has a distorted square antiprismatic coordination environment. The average Ce-O bond length of 2.22 Å ( $\pm 0.02$ ) is within the standard deviation of the average Ce(IV)-O bond length in similar sandwich complexes reported in the literature.<sup>53, 61-62</sup> The  $\text{Ce}[\text{L}^{\text{VII}}]_2$  complex has Ce-N bond lengths of 2.571, 2.521, 2.580, and 2.519 Å. The Ce-O and Ce-N bond lengths in  $\text{Ce}[\text{L}^{\text{VII}}]_2$  are, on average, 0.2 Å shorter than reported Ce(III)-O and Ce(III)-N bond lengths, affirming the assignment as the tetrapositive  $\text{Ce}^{4+}$  ion.<sup>53, 61-63</sup>

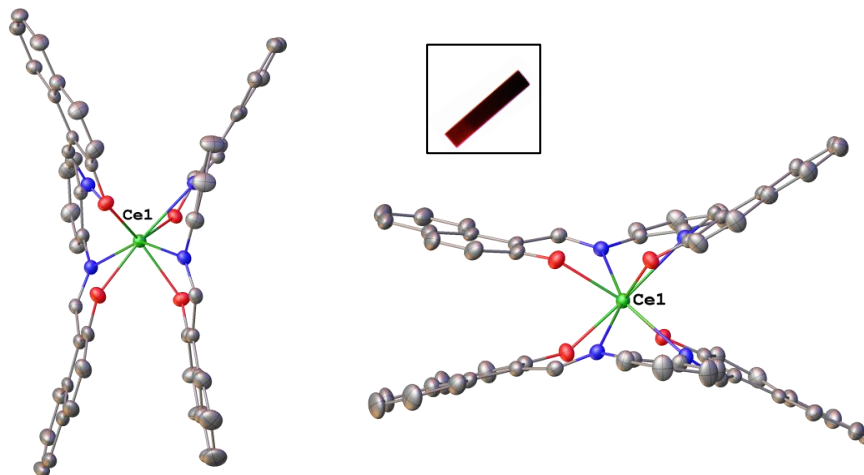


**Figure 4.4.** Projection of  $\text{Ce}[\text{L}^{\text{VII}}]_2$  highlighting the 8-coordinate cerium(IV) metal center. Disordered interstitial hexane and hydrogen atoms have been removed for clarity. Carbon atoms are shown in grey, nitrogen in blue, oxygen in red, and cerium in green.<sup>47</sup>

Nine of eleven of the  $\text{Ln}_2[\text{L}^{\text{VII}}]_3$  complexes, Nd(III), Eu(III), Gd(III), Tb(III), Dy(III), Ho(III), Er(III), Yb(III), and Lu(III), were crystallized from slow evaporation of saturated

methanol solutions. Crystallographic data for  $\text{Nd}_2[\text{L}^{\text{VII}}]_3$ ,  $\text{Gd}_2[\text{L}^{\text{VII}}]_3$ ,  $\text{Ho}_2[\text{L}^{\text{VII}}]_3$ , and  $\text{Yb}_2[\text{L}^{\text{VII}}]_3$  are reported in **Table 4.2**.

**Table 4.2.** Crystallographic data for  $\text{Nd}_2[\text{L}^{\text{VII}}]_3$ ,  $\text{Gd}_2[\text{L}^{\text{VII}}]_3$ ,  $\text{Ho}_2[\text{L}^{\text{VII}}]_3$ , and  $\text{Yb}_2[\text{L}^{\text{VII}}]_3$ .<sup>46</sup>

Identification code	$\text{Nd}_2[\text{L}^{\text{VII}}]_3 \cdot 2\text{MeOH}$	$\text{Gd}_2[\text{L}^{\text{VII}}]_3 \cdot 2\text{MeOH}$	$\text{Ho}_2[\text{L}^{\text{VII}}]_3 \cdot 3\text{MeOH}$	$\text{Yb}_2[\text{L}^{\text{VII}}]_3 \cdot \text{MeOH}$
<b>Emp. formula</b>	$\text{C}_{86}\text{H}_{62}\text{N}_6\text{O}_8\text{Nd}_2$	$\text{C}_{88}\text{H}_{66}\text{N}_6\text{O}_8\text{Gd}_2\text{Cl}_4$	$\text{C}_{87}\text{H}_{66}\text{N}_6\text{O}_9\text{Ho}_2$	$\text{C}_{86}\text{H}_{58}\text{N}_6\text{O}_7\text{Yb}_2$
<b>Formula weight</b>	1595.96	1791.85	1669.39	1791.38
<b>Crystal system</b>	monoclinic	triclinic	triclinic	monoclinic
<b>Space group</b>	$\text{P2}_1/\text{n}$	$\text{P}\bar{1}$	$\text{P}\bar{1}$	$\text{P2}_1/\text{c}$
<b>a/Å</b>	10.2700(4)	12.3985(2)	10.3525(1)	17.4061(8)
<b>b/Å</b>	42.4242 (19)	17.1412(3)	17.6031(2)	20.4222(10)
<b>c/Å</b>	17.3937(8)	17.7640(3)	18.9169(2)	20.6605(10)
<b><math>\alpha/^\circ</math></b>	90	87.7454(8)	82.6930(6)	90
<b><math>\beta/^\circ</math></b>	91.5379(11)	75.9048(7)	86.1741(6)	96.2697
<b><math>\gamma/^\circ</math></b>	90	85.8045(7)	82.4147(6)	90
<b>Volume/Å<sup>3</sup></b>	7575.6(6)	3650.92(11)	3385.05(6)	7300.3(6)
<b>Z</b>	4	2	2	4
<b><math>\rho_{\text{calc}}</math> (g cm<sup>-3</sup>)</b>	1.3992	1.6298	1.6377	1.6298
<b><math>\mu</math> (mm<sup>-1</sup>)</b>	1.415	2.013	2.39	2.756
<b>Temperature/K</b>	181.65	180.45	180.65	180.45
<b>Radiation (Å)</b>	0.71073	0.71073	0.71073	0.71073
<b>collected reflns</b>	66686	112543	127024	104807
<b>Indpdnt reflns</b>	10233	20486	20696	14938
<b>GoF (on F<sup>2</sup>)</b>	1.073	1.155	1.154	1.076
<b>R<sub>1</sub> [I=2<math>\sigma</math>(I)]</b>	0.0887	0.0362	0.0271	0.0576
<b>wR<sub>2</sub> [I=2<math>\sigma</math>(I)]</b>	0.2250	0.0841	0.0561	0.1027
<b>(<math>\Delta\rho</math>)<sub>max</sub>/<sub>min</sub> (e Å<sup>-3</sup>)</b>	2.05/-1.77	3.29/-2.30	3.23/-1.90	2.08/-1.79

While all the crystalline products were observed to form distinct 3L:2M complexes, four structures, one early, two middle, and one late lanthanide, will be discussed in detail here to highlight the key structural differences. These differences are likely due to the reduced ionic radii as caused by the lanthanide contraction (**Figure 4.5-4.8**).

The metal complex  $\text{Nd}_2[\text{L}^{\text{VII}}]_3$ , **Figure 4.5a-c**, crystallized in space group  $\text{P2}_1/\text{n}$  and contains two interstitial dichloromethane (DCM) molecules. The complex was found to have two neodymium atoms that are 8-coordinate, unlike all the other structures reported here and previously reported with this ligand framework.<sup>36,64</sup> **Figure 4.5a** clearly shows a hydrogen

bonding interaction with a length of 1.927 Å between a coordinating methanol (O7) on Nd2 and a phenol donor (O2) that is also bound to Nd1. This interaction is maintained throughout the lanthanide series structures. As pictured in **Figure 4.5b**, Nd1 exhibits a distorted square antiprismatic binding geometry, where all eight donor atoms come from two ligand moieties. The Nd-O bond lengths range from 2.302-2.622 Å, notably the phenolic donors (2.32 on average) are shorter than the bridging oxygen (2.50 on average) indicating a stronger interaction with the phenolic oxygen. The Nd-N bond lengths range from 2.590 to 2.651 Å. The internuclear distance between Nd1 and Nd2 is 4.017 Å (**Figure 4.5b**). These bond lengths are slightly longer, ~0.05 Å, than the average of previous examples of triple-decker Nd complexes with simple salen ligands,<sup>33,65-66</sup> but this difference may be due to the larger pi systems of the ligand rather than notable changes in the coordination environment. The second metal ion - Nd2 is 8-coordinate, but is likewise greatly distorted from the idealized square antiprismatic ligand environment. Four donor atoms are from one ligand, two oxygen donor atoms are from a second ligand, and two are occupied by coordinating methanol solvent molecules. The two phenol donors of the internal L are  $\mu$ -oxo groups. As shown in **Figure 4.5c**, the naphthyl rings are not observed to have any  $\pi$ -stacking interactions and are, in fact, greatly distorted from planarity. This is notably different from other salen Nd salen complexes found in the literature in which  $\pi$ - $\pi$  effects were significant reporting  $\pi$ - $\pi$  stacking distances at 3.929 and 3.836 Å.<sup>67</sup>

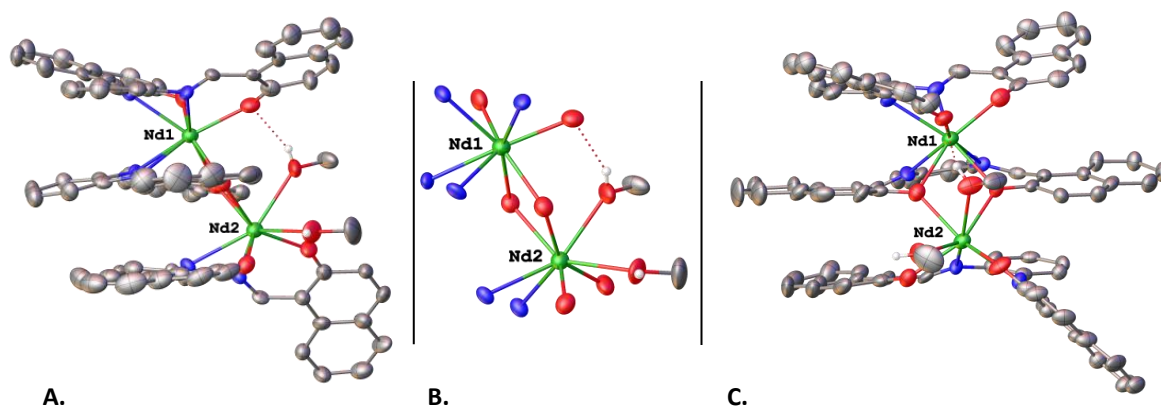


**Figure 4.5.** a. Projection of the side view of  $\text{Nd}_2[\text{L}^{\text{VII}}]_3$  b. Coordination spheres of Nd1 and Nd2 c. Projection of the front view of  $\text{Nd}_2[\text{L}^{\text{VII}}]_3$ . Interstitial solvent and hydrogen, except those involved in hydrogen bonding have been removed for clarity. Carbon atoms are shown in grey, nitrogen in blue, oxygen in red, and neodymium in green.<sup>46</sup>

The lanthanide example from the middle of the series,  $\text{Gd}_2[\text{L}^{\text{VII}}]_3$ , crystallized in  $\text{P}\bar{1}$  with two interstitial DCM molecules per asymmetric unit. This structure is shown in **Figure 4.6a-c**. While the  $\text{Nd}_2[\text{L}^{\text{VII}}]_3$  structure contains two coordinating methanol molecules, in  $\text{Gd}_2[\text{L}^{\text{VII}}]_3$  one methanol is coordinating to the metal center and the second methanol (O8) is hydrogen bonded to the coordinating methanol (O7) and the phenol oxygen (O2). The coordination sphere of Gd1, **Figure 4.6b**, is similar to that of Nd1, and is occupied by two tetradentate ligand equivalents. The second Gd atom, however, is seven coordinate and is observed to have a monocapped trigonal prismatic geometry. Four donor atoms are from one equivalent of ligand, two donors atoms are  $\mu$ -aryloxides from a second equivalent of ligand, and the final coordination site is occupied by a coordinating methanol. The Gd-O bond lengths range from 2.218-2.388 Å, with the bridged phenolic oxygen being presumably due to weaker interactions as judged by the longer lengths. The Gd-N bond lengths range from 2.487-2.562 Å. The Gd1-Gd2 distance of 3.915 Å and the Gd2-O7 distance of the coordinating methanol is 2.419 Å. While other examples of  $\text{Gd}_2[\text{L}^{\text{VII}}]_3$  salen type sandwich complexes have been prepared and characterized,<sup>33</sup> this is the first example of solid-state elucidation of this coordination environment for gadolinium. As

highlighted in **Figure 4.6a** and **Figure 4.6c**, the planarity of the naphthylsalophen ligand is better retained in the mid lanthanides. This planarity is greatly aided by the interaction with the additional hydrogen bonded methanol, as well as the smaller size of Gd in comparison to Nd. While the  $\pi$  systems of the second and third tier of the double sandwich are interacting and aligned well, the first tier ligand twists noticeably to the left as is highlighted in **Figure 4.6c**.

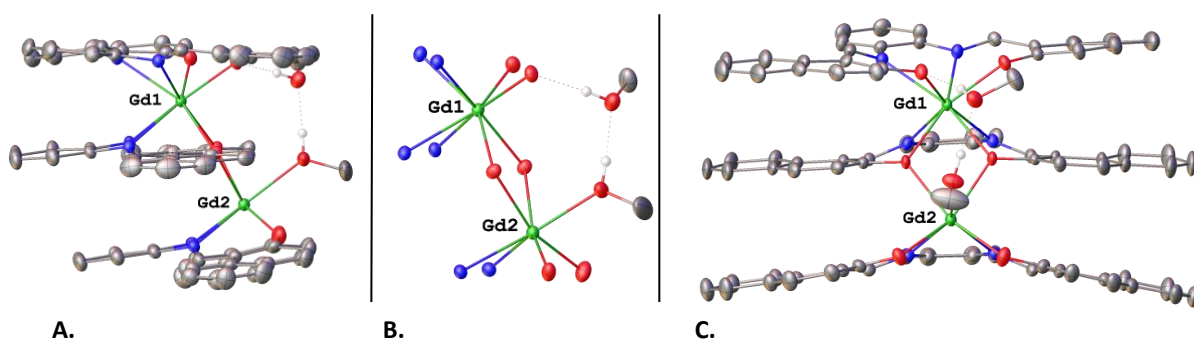


**Figure 4.6.** **a.** Projection of the side view of  $\text{Gd}_2[\text{L}^{\text{VII}}]_3$  **b.** Coordination spheres of Gd1 and Gd2 **c.** Projection of the front view of  $\text{Gd}_2[\text{L}^{\text{VII}}]_3$ . Interstitial solvent and hydrogen, except those involved in hydrogen bonding have been removed for clarity. Carbon atoms are shown in grey, nitrogen in blue, oxygen in red, and gadolinium in green.<sup>46</sup>

The complex of  $\text{Ho}_2[\text{L}^{\text{VII}}]_3$ , with Ho, a mid-to late lanthanide, has a similar geometry as  $\text{Gd}_2[\text{L}^{\text{VII}}]_3$ , crystallized in P1 without the interstitial DCM in all the other analogues reported, but incorporates an additional methanol into the hydrogen-bonding network (**Figure 4.7a-c**). The additional methanol allows for increased planarity in the triple-decker sandwich (**Figure 4.7a**). The coordination of Ho1 is again distorted square antiprismatic, as with Gd1. Ho2 is distorted monocapped trigonal prismatic, with a coordinating methanol, a coordinating L equivalent, and two bridging oxo groups (**Figure 4.7b**). The Ho-O bond lengths range from 2.187-2.351 Å, with the longer Ho-O lengths being the bridging phenols. The Ho-N bond lengths range from 2.444-2.538 Å and the Ho1-Ho2 are separated by 3.854 Å. These bond lengths are within 0.08 Å of previously reported Ho salen structures.<sup>67-68</sup> As with  $\text{Gd}_2[\text{L}^{\text{VII}}]_3$ , the two bottom tiers of the

sandwich generally maintain planarity and interact through  $\pi$ -stacking interaction and the top tier rotates to the left (**Figure 4.7c**).

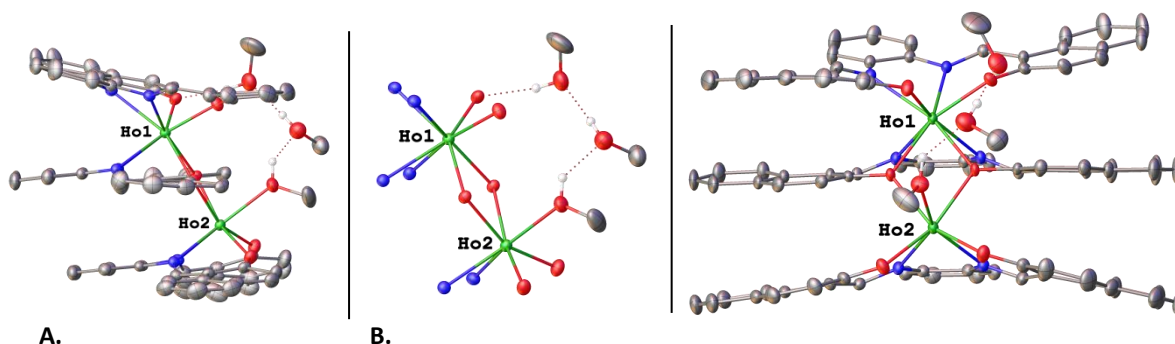


**Figure 4.7.** **a.** Projection of the side view of  $\text{Ho}_2[\text{L}^{\text{VII}}]_3$  **b.** Coordination environments of Ho1 and Ho2 **c.** Projection of the front view of  $\text{Ho}_2[\text{L}^{\text{VII}}]_3$ . Interstitial DCM and hydrogen atoms, except those involved in hydrogen bonding have been removed for clarity. Carbon atoms are shown in grey, nitrogen in blue, oxygen in red, and holmium in green.<sup>46</sup>

$\text{Yb}_2[\text{L}^{\text{VII}}]_3$ , the late lanthanide example, was found to crystallize in  $P2_1/c$  space group with two interstitial DCM molecules per asymmetric unit and is shown in **Figure 4.8a-c**. As highlighted in **Figure 4.8a**, the hydrogen bond between the coordinating methanol and phenol (2.159 Å) is elongated as compared to the  $\text{Nd}_2[\text{L}^{\text{VII}}]_3$ ,  $\text{Gd}_2[\text{L}^{\text{VII}}]_3$  and  $\text{Ho}_2[\text{L}^{\text{VII}}]_3$  cases, which coordinated an additional methanol. The coordination spheres of Yb1 and Yb2 are reminiscent of  $\text{Gd}_2[\text{L}^{\text{VII}}]_3$  and  $\text{Ho}_2[\text{L}^{\text{VII}}]_3$ . Yb1 has a distorted square antiprismatic coordination geometry, with all the donor atoms being from two equivalents of  $[\text{L}^{\text{VII}}]^{2-}$  (**Figure 4.8b**). Yb2 has a distorted monocapped trigonal prismatic geometry, with four donor atoms coming from one equivalent of  $[\text{L}^{\text{VII}}]^{2-}$ , two donor atoms are from a second equivalent of  $[\text{L}^{\text{VII}}]^{2-}$ , and the last donor atom is from a coordinating methanol. This is similar to that observed by Sanudo and co-workers, but a coordinating water molecule completed the coordination sphere for Yb2 rather than a methanol.<sup>36</sup> The Yb-O bond lengths range from 2.163-2.321 Å, which is within 0.01 Å of one previously reported Yb salen complex,<sup>36,69</sup> but is significantly shorter (~0.1 Å) than other

examples.<sup>19,70</sup> The Yb-N bond lengths range from 2.400-2.501 Å, and the Yb1-Yb2 distance is 3.778 Å, which are within previously reported ranges.<sup>19,36,70</sup> The planarity of  $[\mathbf{L}^{\text{VII}}]^{2-}$  is more distorted than the Gd and Ho structures, which had additional methanol incorporation, but is generally maintained (**Figure 4.8c**). The  $\pi$  systems in the second and third tiers stack well, while the first tier is rotated slightly to the right due to the hydrogen bonding interaction of the methanol.

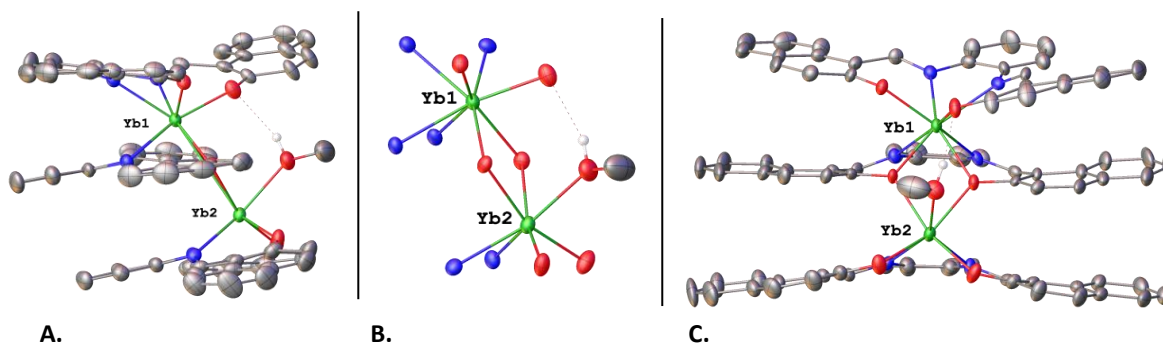


**Figure 4.8.** a. Projection of the side view of  $\text{Yb}_2[\mathbf{L}^{\text{VII}}]_3$  b. Coordination environments of Yb1 and Yb2 c. Projection of the front view of  $\text{Yb}_2[\mathbf{L}^{\text{VII}}]_3$ . Interstitial solvent and hydrogen, except those involved in hydrogen bonding have been removed for clarity. Carbon atoms are shown in grey, nitrogen in blue, oxygen in red, and ytterbium in green.<sup>46</sup>

The metal ion coordination in the  $\text{Eu}_2[\mathbf{L}^{\text{VII}}]_3$ ,  $\text{Tb}_2[\mathbf{L}^{\text{VII}}]_3$ ,  $\text{Dy}_2[\mathbf{L}^{\text{VII}}]_3$ , and  $\text{Lu}_2[\mathbf{L}^{\text{VII}}]_3$  complexes (**Figures 4.9-4.11 and 4.13**) are isostructural with  $\text{Yb}_2[\mathbf{L}^{\text{VII}}]_3$ , with small variations in the unit cell (crystallographic data displayed in **Table 4.3**).  $\text{Er}_2[\mathbf{L}^{\text{VII}}]_3$  is isostructural with  $\text{Gd}_2[\mathbf{L}^{\text{VII}}]_3$ , with small variations in the unit cell (**Figure 4.12**).



**Table 4.3.** Crystallographic Data for  $\text{Eu}_2[\text{L}^{\text{VII}}]_3$ ,  $\text{Tb}_2[\text{L}^{\text{VII}}]_3$ ,  $\text{Dy}_2[\text{L}^{\text{VII}}]_3$ ,  $\text{Er}_2[\text{L}^{\text{VII}}]_3$ , and  $\text{Lu}_2[\text{L}^{\text{VII}}]_3$ .<sup>46</sup>

Identification code	$\text{Eu}_2[\text{L}^{\text{VII}}]_3$ - MeOH-2DCM	$\text{Tb}_2[\text{L}^{\text{VII}}]_3$ - MeOH	$\text{Dy}_2[\text{L}^{\text{VII}}]_3$ - MeOH	$\text{Er}_2[\text{L}^{\text{VII}}]_3$ - 3MeOH	$\text{Lu}_2[\text{L}^{\text{VII}}]_3$ - MeOH
<b>Empirical formula</b>	$\text{C}_{87}\text{H}_{62}\text{Cl}_4\text{N}_6\text{O}_7\text{Eu}_2$	$\text{C}_{85}\text{H}_{58}\text{N}_6\text{O}_7\text{Tb}_2$	$\text{C}_{85}\text{H}_{58}\text{N}_6\text{O}_7\text{Dy}_2$	$\text{C}_{87}\text{H}_{66}\text{N}_6\text{O}_9\text{Er}_2$	$\text{C}_{85}\text{H}_{58}\text{N}_6\text{O}_7\text{Lu}_2$
<b>Formula weight</b>	1749.24	1593.29	1600.44	1674.04	1625.38
<b>Crystal system</b>	monoclinic	monoclinic	monoclinic	triclinic	monoclinic
<b>Space group</b>	$\text{P}2_1/\text{c}$	$\text{P}2_1/\text{c}$	$\text{P}2_1/\text{c}$	P-1	$\text{P}2_1/\text{c}$
<b>a/Å</b>	17.512(7)	17.4947(6)	17.4758(9)	10.309(2)	17.3981(17)
<b>b/Å</b>	20.500(8)	20.5096(7)	20.4943(11)	17.582(4)	20.4310(19)
<b>c/Å</b>	20.517(8)	20.6071(8)	20.6011(11)	18.939(4)	20.6803(19)
<b><math>\alpha/^\circ</math></b>	90	90	90	82.655(4)	90
<b><math>\beta/^\circ</math></b>	96.457(7)	96.4934(9)	96.445(1)	86.443(4)	96.1767(13)
<b><math>\gamma/^\circ</math></b>	90	90	90	82.386(4)	90
<b>Volume/Å<sup>3</sup></b>	7319(5)	7347.3(4)	7331.7(7)	3371.2(12)	7308.4(12)
<b>Z</b>	4	4	4	2	4
<b><math>\rho_{\text{calc}}</math> (g cm<sup>-3</sup>)</b>	1.5873	1.4404	1.4498	1.6490	1.4771
<b>m/mm-1</b>	1.907	1.969	2.082	2.542	2.745
<b>Temperature/K</b>	180.45	180.45	180.45	180.65	180.45
<b>Radiation</b>	0.71073	0.71073	0.71073	0.71073	0.71073
<b>collected reflns</b>	23881	107251	97079	26445	80420
<b>Independent reflns</b>	2833	16189	12348	8754	16055
<b>GoF (on F<sup>2</sup>)</b>	1.127	1.078	1.085	0.941	1.987
<b>R1 [I=2<math>\sigma</math>(I)]</b>	0.0682	0.0495	0.0622	0.0608	0.1491
<b>wR2 [I=2<math>\sigma</math>(I)]</b>	0.1750	0.0954	0.1037	0.1208	0.4186
<b>(<math>\Delta\rho</math>)max/(<math>\Delta\rho</math>)min (e Å<sup>-3</sup>)</b>	2.67/-0.79	3.04/-1.35	2.26/-3.45	2.74/-2.53	8.78/-2.86

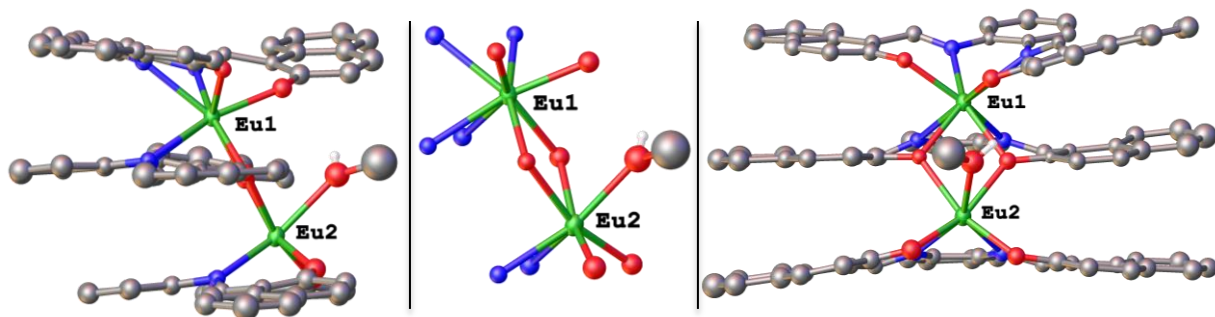


**Figure 4.9.** Projections of  $\text{Eu}_2[\text{L}^{\text{VII}}]_3$ . Carbon atoms shown in grey, hydrogen in white, oxygen in red, nitrogen in blue, and europium in green.<sup>46</sup>

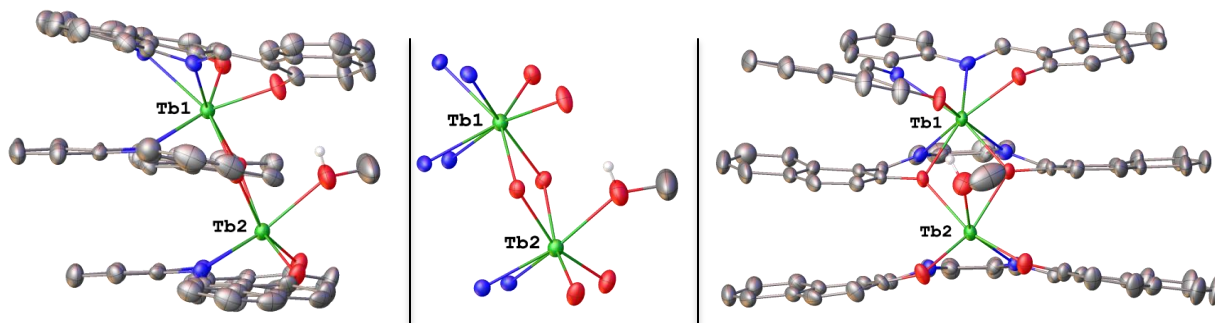


**Figure 4.10.** Projections of  $\text{Tb}_2[\text{L}^{\text{VII}}]_3$ . Carbon atoms shown in grey, hydrogen in white, oxygen in red, nitrogen in blue, and terbium in green.<sup>46</sup>

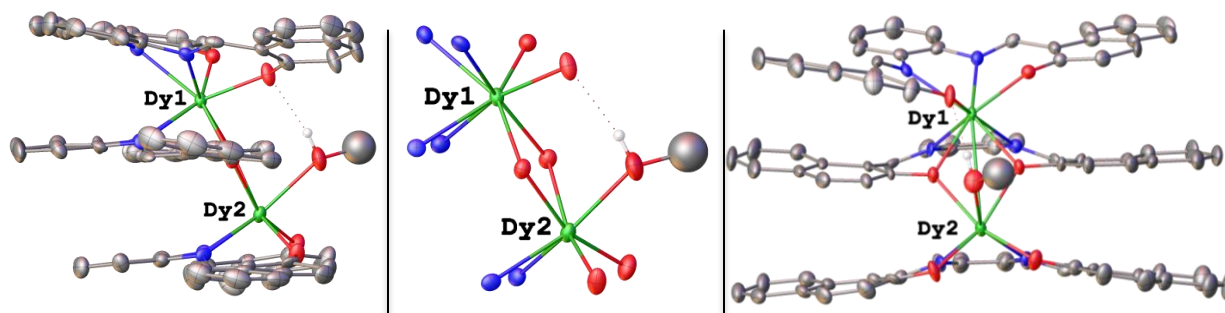


**Figure 4.11.** Projections of  $\text{Dy}_2[\text{L}^{\text{VII}}]_3$ . Carbon atoms shown in grey, hydrogen in white, oxygen in red, nitrogen in blue, and dysprosium in green.<sup>46</sup>

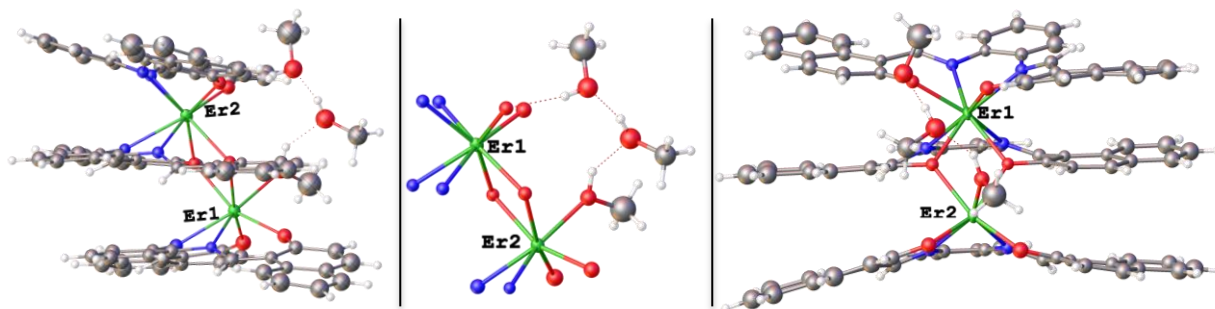


**Figure 4.12.** Projections of  $\text{Er}_2[\text{L}^{\text{VII}}]_3$ . Carbon atoms shown in grey, hydrogen in white, oxygen in red, nitrogen in blue, and erbium in green.<sup>46</sup>

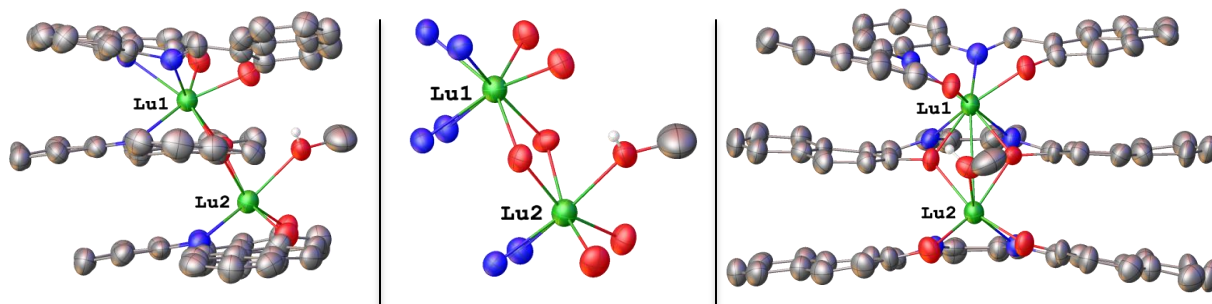


**Figure 4.13.** Projections of  $\text{Lu}_2[\text{L}^{\text{VII}}]_3$ . Carbon atoms shown in grey, hydrogen in white, oxygen in red, nitrogen in blue, and lutetium in green.<sup>46</sup>

As is highlighted in **Figures 4.5-4.13**, the lanthanide contraction is evident in the coordination environments of  $\text{Nd}_2[\text{L}^{\text{VII}}]_3$ ,  $\text{Gd}_2[\text{L}^{\text{VII}}]_3$ , and  $\text{Yb}_2[\text{L}^{\text{VII}}]_3$ . The contraction is obvious when looking at the bond angles and lengths, which can be found in **Table 4.4** and **Table 4.5**, respectively. The bond lengths and angles of  $\text{Eu}_2[\text{L}^{\text{VII}}]_3$  and  $\text{Dy}_2[\text{L}^{\text{VII}}]_3$  are comparable to previously reported salen sandwich complexes.<sup>34, 71-73</sup> Bond angles generally widen and bond lengths shorten from early (Nd) to late (Yb) lanthanides, which is consistent with the lanthanide contraction and smaller size of the late lanthanides. In particular, these changes are most evident in the O-M-O angles, which span from  $111.0^\circ$  in  $\text{Nd}_2[\text{L}^{\text{VII}}]_3$  to  $90.25^\circ$  in  $\text{Yb}_2[\text{L}^{\text{VII}}]_3$ . The M1-M2 distances consistently decrease from  $4.017 \text{ \AA}$  to  $3.778 \text{ \AA}$ , highlighting the contraction. In fact, the contraction is evident in all the bond lengths (**Table 4.5**).

**Table 4.4.** Selected bond angles (deg) of Ln<sub>2</sub>[L<sup>VII</sup>]<sub>3</sub> complexes<sup>46</sup>

	Nd <sub>2</sub> [L <sup>VII</sup> ] <sub>3</sub>	Gd <sub>2</sub> [L <sup>VII</sup> ] <sub>3</sub>	Tb <sub>2</sub> [L <sup>VII</sup> ] <sub>3</sub>	Dy <sub>2</sub> [L <sup>VII</sup> ] <sub>3</sub>	Ho <sub>2</sub> [L <sup>VII</sup> ] <sub>3</sub>	Yb <sub>2</sub> [L <sup>VII</sup> ] <sub>3</sub>	Lu <sub>2</sub> [L <sup>VII</sup> ] <sub>3</sub>
<b>O1-M1-N1</b>	69.1	71.44	71.52	72.08	71.70	74.86	74.6
<b>N1-M1-N2</b>	64.0	64.54	65.19	65.37	66.00	66.04	65.3
<b>N2-M1-O2</b>	69.1	70.24	73.54	74.02	72.65	72.47	75.3
<b>O2-M1-O1</b>	89.2	80.89	84.48	83.72	81.74	81.90	81.4
<b>O3-M1-N3</b>	68.2	68.71	68.79	69.07	69.95	69.23	70.7
<b>N3-M1-N4</b>	61.3	63.02	63.14	63.23	63.32	64.55	63.5
<b>N4-M1-O4</b>	68.4	69.20	68.81	68.78	68.89	69.89	69.3
<b>O4-M1-O3</b>	71.3	69.21	69.84	69.57	68.85	68.84	69.1
<b>O3-M2-O4</b>	70.1	68.77	70.34	70.28	69.20	69.83	70.0
<b>O5-M2-N5</b>	67.6	72.81	73.49	73.97	73.77	74.64	75.5
<b>N5-M2-N6</b>	62.0	65.51	66.02	66.26	66.30	66.93	66.3
<b>N6-M2-O6</b>	68.0	72.75	73.47	73.61	73.03	75.38	75.0
<b>O6-M2-O5</b>	111.0	93.85	93.90	92.20	93.00	90.25	88.4

**Table 4.5.** Selected bond lengths (Å) of Ln<sub>2</sub>[L<sup>VII</sup>]<sub>3</sub> complexes<sup>46</sup>

	Nd <sub>2</sub> [L <sup>VII</sup> ] <sub>3</sub>	Gd <sub>2</sub> [L <sup>VII</sup> ] <sub>3</sub>	Tb <sub>2</sub> [L <sup>VII</sup> ] <sub>3</sub>	Dy <sub>2</sub> [L <sup>VII</sup> ] <sub>3</sub>	Ho <sub>2</sub> [L <sup>VII</sup> ] <sub>3</sub>	Yb <sub>2</sub> [L <sup>VII</sup> ] <sub>3</sub>	Lu <sub>2</sub> [L <sup>VII</sup> ] <sub>3</sub>
<b>M1-N1</b>	2.590	2.500	2.489	2.466	2.477	2.419	2.37
<b>M1-N2</b>	2.600	2.530	2.472	2.463	2.445	2.445	2.37
<b>M1-O1</b>	2.302	2.275	2.271	2.255	2.241	2.234	2.22
<b>M1-O2</b>	2.373	2.318	2.281	2.267	2.232	2.210	2.22
<b>M1-N3</b>	2.609	2.562	2.559	2.553	2.538	2.483	2.48
<b>M1-N4</b>	2.651	2.549	2.537	2.524	2.533	2.501	2.46
<b>M1-O3</b>	2.458	2.379	2.350	2.345	2.351	2.321	2.31
<b>M1-O4</b>	2.440	2.368	2.379	2.362	2.338	2.301	2.32
<b>M2-O3</b>	2.514	2.386	2.357	2.339	2.330	2.275	2.28
<b>M2-O4</b>	2.455	2.388	2.343	2.327	2.339	2.295	2.30
<b>M2-N5</b>	2.637	2.487	2.461	2.447	2.448	2.400	2.39
<b>M2-N6</b>	2.631	2.493	2.463	2.445	2.444	2.410	2.37
<b>M2-O5</b>	2.280	2.237	2.211	2.119	2.187	2.163	2.20
<b>M2-O6</b>	2.331	2.218	2.218	2.203	1.196	2.167	2.18
<b>M2-O7</b>	2.594	2.419	2.467	2.443	2.383	2.392	2.37
<b>M1-M2</b>	4.017	3.915	3.858	3.838	3.854	3.778	3.77

Crystals of UO<sub>2</sub>[L<sup>VII</sup>] were grown from slow diffusion of hexanes into a saturated solution of UO<sub>2</sub>[L<sup>VII</sup>] in toluene. The compound UO<sub>2</sub>[L<sup>VII</sup>] was observed to crystallize in the P2<sub>1</sub>/n space group with four interstitial dichloromethane molecules. Two distinct UO<sub>2</sub>[L<sup>VII</sup>] units are found in the asymmetric unit and are shown in **Figure 4.14**. These two units are symmetrically related to two other complexes, resulting in a tetrad of UO<sub>2</sub>[L<sup>VII</sup>] complexes held

together through hydrogen bonding interactions with a H---O distance of 1.923 and 2.032 Å (Figure 4.15). The average U-O<sub>yl</sub> bond length is 1.777 Å, which is easily within the normal range for the -yl oxo groups bound to a uranium hexavalent ion. The hydrogen bonding interactions to these -yl oxygen are reminiscent of Lewis acid interactions of -yl oxygen in compounds made by Arnold and Bart that proved to easily reduce uranyl(VI) to uranyl(V).<sup>74-76</sup> These compounds always showed a lengthening of the U-O<sub>yl</sub> bond, which unfortunately was not observed in UO<sub>2</sub>[L<sup>VII</sup>]. The average U-N<sub>imine</sub> bond lengths of 2.515 Å, U-O<sub>H<sub>2</sub>O</sub> bond lengths of 2.450 Å, and the U-O<sub>phenol</sub> bond lengths of 2.286 Å are within normal ranges. Of note is the U-O<sub>phenol</sub> distance of 2.311(3) Å, which is slightly lengthened and is participating in hydrogen bonding with the coordinating water molecule of the next complex.

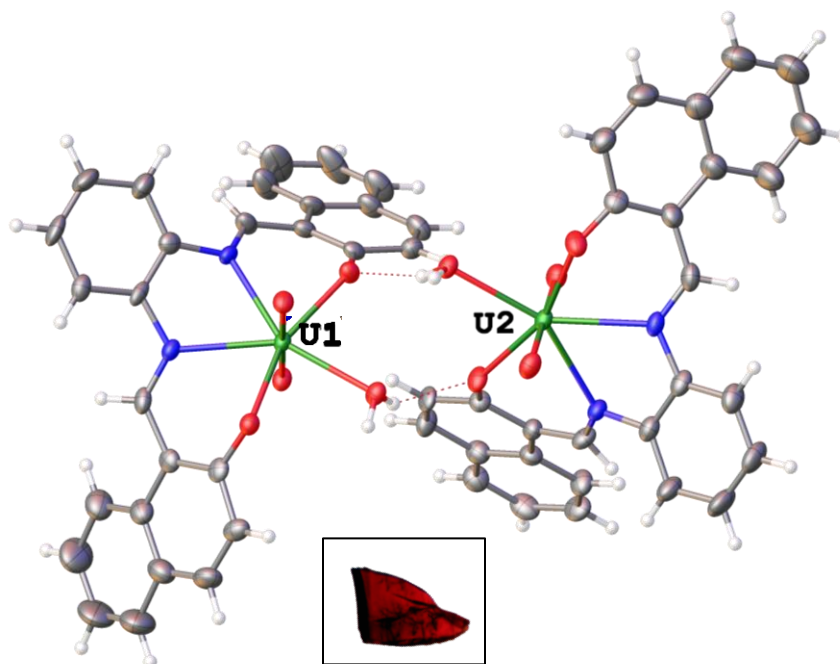


**Figure 4.14.** Projection of the asymmetric unit of UO<sub>2</sub>[L<sup>VII</sup>]. Carbon atoms are shown in grey, oxygen in red, nitrogen in blue, hydrogen in white, and uranium in green.

These hydrogen bonding interactions observed in the complex UO<sub>2</sub>[L<sup>VII</sup>], paired with pi stacking of the naphthalene rings of 4.304 Å, affords an interesting supramolecular stacking

structure with void channels that are filled with interstitial DCM in the solid-state structure (**Figure 4.15**). These channels have been observed in metal organic frameworks (MOFs) and were of interest for applications in that area.<sup>77-78</sup> These stacking interactions are off-set, which is common in structures such as these, but is an artifact of the packing rather than an interaction that would allow this structure to maintain these tetramers in solution and therefore limits their application.

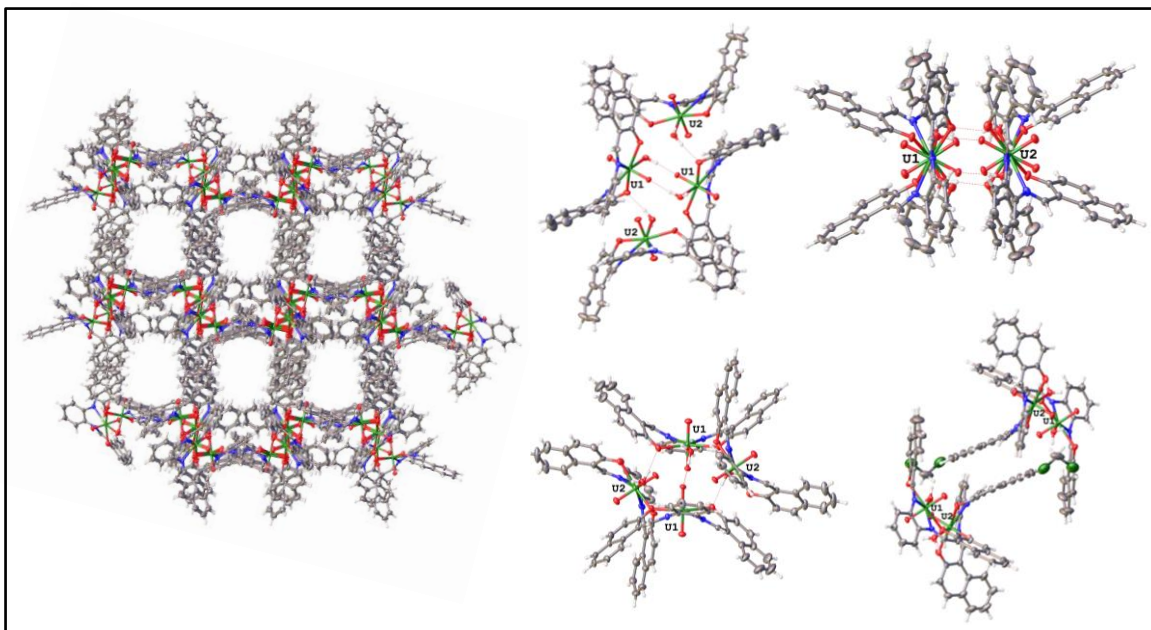


**Figure 4.15.** Projections of the  $\text{UO}_2[\text{L}^{\text{VII}}]$  complex highlighting the hydrogen bonded tetramers and pi-pi stacking interactions resulting in an interesting supramolecular structure. Interstitial dichloromethane molecules have been removed for clarity.

### Uncharacteristic Thorium(IV) Emission

Absorbance and fluorescence spectra for  $\text{Th}[\text{L}^{\text{VII}}]_2$ , and  $\text{Ce}[\text{L}^{\text{VII}}]_2$  were collected both from the solutions and in the solid-state, resulting in unexpected emissive properties of the  $\text{Th}[\text{L}^{\text{VII}}]_2$  complex. Thus far,  $\text{Th}[\text{L}^{\text{VII}}]_2$  is the first example of a fluorescent thorium compound in both solution and solid-state. Images of  $\text{Th}[\text{L}^{\text{VII}}]_2$  fluorescence under ambient light and with 365 nm excitation are shown in **Figure 4.16**. All fluorescence is quenched in solution and solid state

for  $\text{Ce}[\text{L}^{\text{VII}}]_2$  with 365 nm excitation. In solution, two absorbance peaks at 335 nm and 387 nm, with a shoulder centered on 440 nm are observed in the UV-visible spectrum (**Figure 4.17**). In dichloromethane solution the absorbance of the complex  $\text{Th}[\text{L}^{\text{VII}}]_2$  features two absorbance peaks at 333 nm and 391 nm, with a shoulder centered on 440 nm, and an emission peak at 473 nm. In the solid-state, an absorbance peak centered at 488 nm, and an emission peak at 537 nm are observed. A broad emission feature is observed in solution and solid-state  $\text{Th}[\text{L}^{\text{VII}}]_2$  at the same excitation wavelength. This is highly unusual for a Th(IV) complex (**Figure 4.18**).

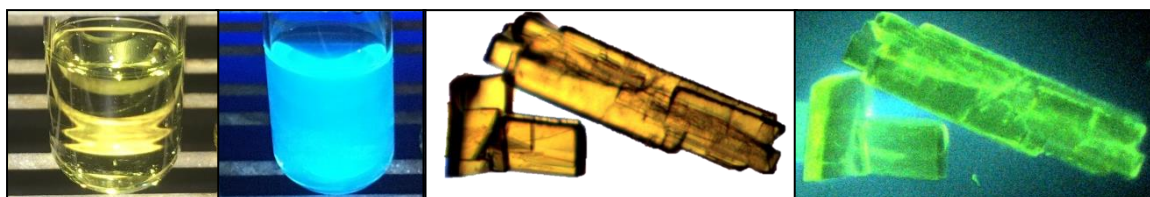
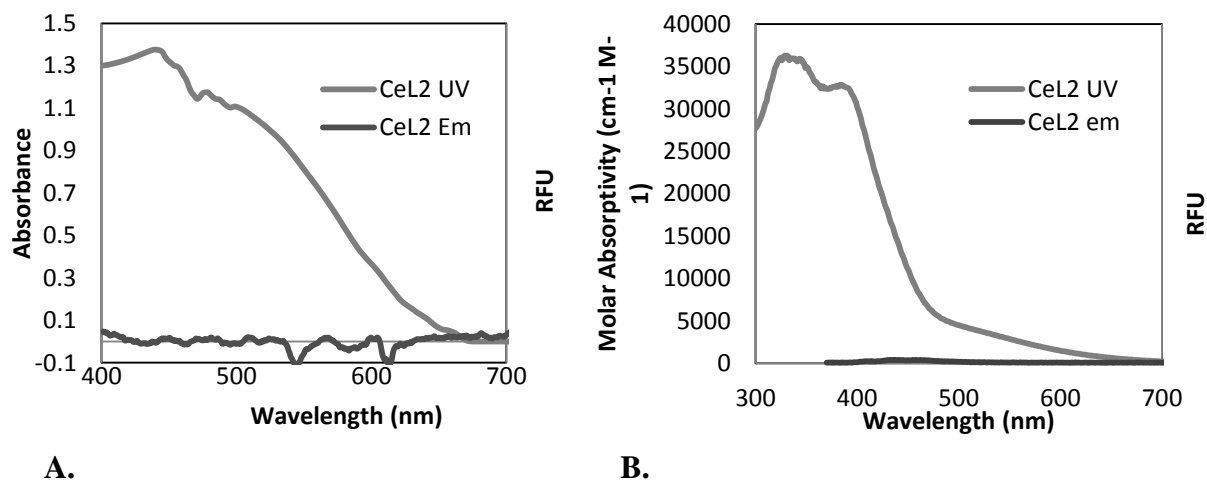


**Figure 4.16.** Absorption and emission of a 40  $\mu\text{M}$   $\text{CHCl}_3$  solution of  $\text{Th}[\text{L}^{\text{VII}}]_2$  and in single crystals under white light and under 365 nm excitation.<sup>47</sup>



**A.**

**B.**

**Figure 4.17.** **A.** Solid-state absorbance and emission spectra with excitation at 365 nm of  $\text{Ce}[\text{L}^{\text{VII}}]_2$ . **B.** Solution phase absorbance and emission spectra of  $\text{Ce}[\text{L}^{\text{VII}}]_2$  in dichloromethane with excitation at 365 nm.<sup>47</sup>

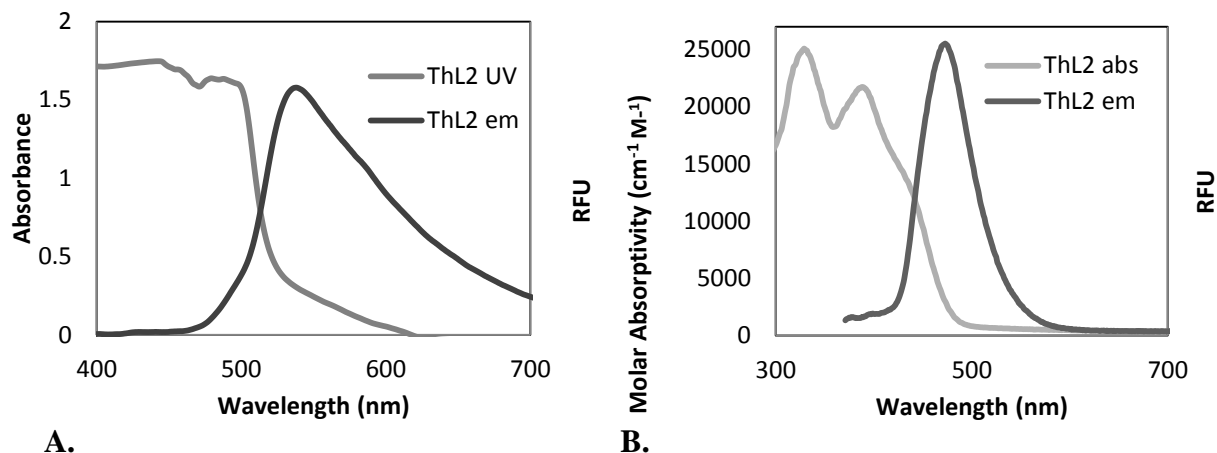
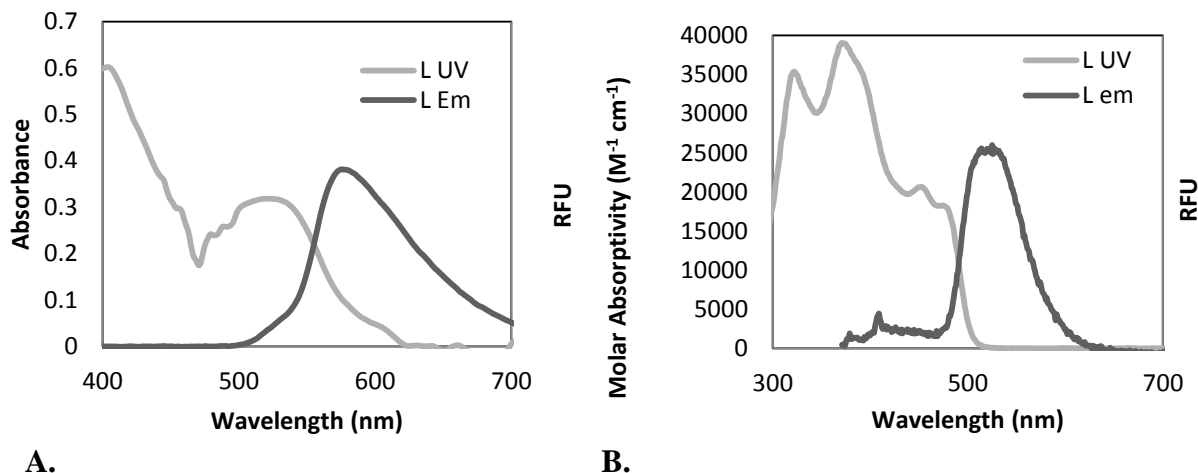


**Figure 4.18.** **A.** Solid-state absorbance emission spectra with excitation at 365 nm of  $\text{Th}[\text{L}^{\text{VII}}]_2$ . **B.** Solution phase absorbance and emission spectra of  $\text{Th}[\text{L}^{\text{VII}}]_2$  in acetonitrile with excitation at 365 nm.<sup>47</sup>

To compare the observed emission and quenching of the  $\text{Ce}[\text{L}^{\text{VII}}]_2$  and  $\text{Th}[\text{L}^{\text{VII}}]_2$  complexes, the UV-visible spectrum and emission spectrum of the ligand were measured. In dichloromethane solutions of the free base, four absorbance peaks at 326 nm, 375 nm, 456, and 476 nm are observed, with an emission peak at 517 nm. In the solid-state an absorbance peak at 520 nm and an emission peak at 575 nm are observed (**Figure 4.19**). As the Th(IV) ion is non-emissive, the emission can be assigned to a charge transfer state within the ligand framework in agreement with our theoretical calculations described below and comparison to ligand emission in solution and solid-state. Most examples characterized as fluorescent sensors for thorium are “turn-off” chemosensors, due to  $f^0$  ground state of Th(IV).<sup>79-80</sup> One fluorescent thorium solid-state compound and three examples of solution phase fluorescence have been described previously, while many more examples of thorium quenching fluorescence exist.<sup>49-52, 80</sup>





**A.** **Figure 4.19.** A. Solid-state absorbance emission spectra with excitation at 365 nm of  $[\text{H}_2\text{L}^{\text{VII}}]$ . B. Solution phase absorbance and emission spectra of  $\text{H}_2[\text{L}^{\text{VII}}]_2$  in acetonitrile with excitation at 365 nm.<sup>47</sup>

The emission from  $\text{Th}[\text{L}^{\text{VII}}]_2$  was characterized in a variety of solvents in solution phase, as well as two distinct solid-state crystal systems (**Figure 4.20**). The emission of  $\text{Th}[\text{L}^{\text{VII}}]_2$  was found to be highly solvent dependent, and is summarized in **Table 4.6**. While solvent dependent fluorescence is not uncommon,<sup>81-82</sup> the change in emission of  $\text{Th}[\text{L}^{\text{VII}}]_2$  extends from 461 nm to 502 nm in solution, to as high as 537 nm observed in the solid-state.  $\text{Th}[\text{L}^{\text{VII}}]_2$  in chloroform and toluene, the non-coordinating solvents, were found to have emission bands near 460 nm, while in the coordinating solvents emission closer to 500 nm was observed. The quantum yield of  $\text{Th}[\text{L}^{\text{VII}}]_2$  in chloroform is 2.5%, and the coordinating solvents are non-fluorescent by comparison.

We hypothesize that the distortion caused by coordinating solvents in solution causes these changes in emission to longer wavelength, and reduces the quantum yield. This claim is substantiated by the more bulky coordinating solvents causes the emission to shift the most, especially methanol which is capable of hydrogen bonding. Further, the solid-state emissions from crystals that are formally distorted by the packing structure are both at longer wavelength.

Another possibility is the equilibrium between an 8 and 9 coordinate thorium metal center occurs in solution. Crystals in coordinating solvents, acetonitrile and DMSO, were grown and collected. All species were 8 coordinate in the solid-state, but loss of symmetry in the NMR does suggest an equilibrium between the 8 and 9 coordinate species.

**Table 4.6.** Emission wavelengths and quantum yields of 45 ( $\pm 0.5$ )  $\mu\text{M}$  solutions of  $\text{Th}[\text{L}^{\text{VII}}]_2$  in indicated solvents and solid-state crystals.<sup>47</sup>

	$\lambda_{\text{em}}$	$\phi_f$
<b><math>\text{CHCl}_3</math></b>	461	2.50 %
<b>Tol</b>	464	0.50 %
<b>ACN</b>	473	0.70 %
<b>DMF</b>	487	0 %
<b>DMSO</b>	487	0 %
<b>MeOH</b>	502	0 %
<b>Tol-xtal</b>	523	--
<b>DCM-xtal</b>	537	--

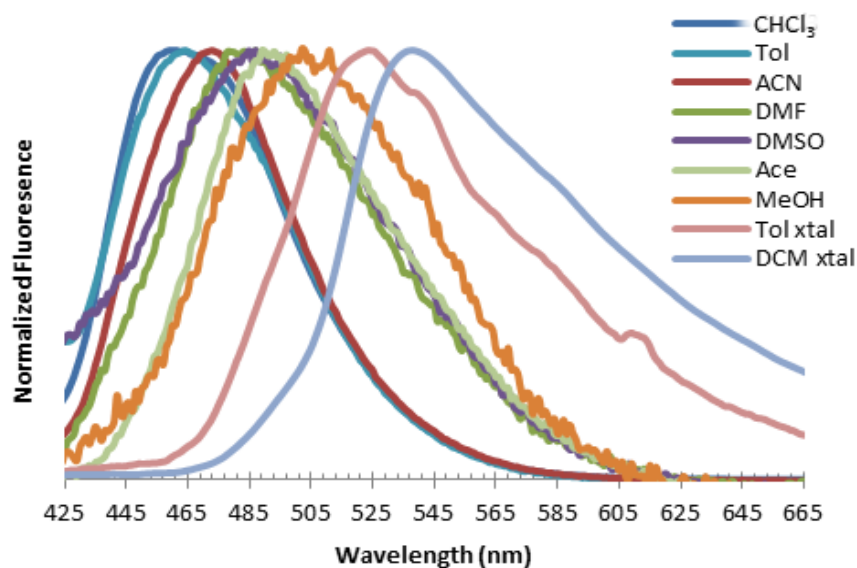


**Figure 4.20.** Normalized solution and solid-state emission of  $\text{Th}[\text{L}^{\text{VII}}]_2$  with 365 nm excitation in indicated solvent.<sup>47</sup>

In an attempt to explain our observations, a collaborator performed density functional theory (DFT) and time-dependent DFT (TD-DFT) calculations. The Th-O, Th-N, Ce-O, and Ce-

N bond lengths in the optimized structure range within 2.295-2.317, 2.648-2.691, 2.241-2.255, and 2.606-2.651 Å, respectively. The agreement (within  $\pm 0.05$  Å) with the experimental values validates the employed methodology. The ground state of both  $\text{Ce}[\text{L}^{\text{VII}}]_2$  and  $\text{Th}[\text{L}^{\text{VII}}]_2$  complexes were found to be closed-shell singlets with substantial Ce(IV) and Th(IV) character.

**Figure 4.21** shows the highest occupied molecular orbital (HOMO) and lowest unoccupied molecular orbital (LUMO) for both complexes. Note the HOMO and LUMO for  $\text{Th}[\text{L}^{\text{VII}}]_2$  are localized on the ligands. On the other hand, the HOMO of  $\text{Ce}[\text{L}^{\text{VII}}]_2$  is on the ligand but the LUMO is purely on cerium. The orbital resembling the LUMO of  $\text{Th}[\text{L}^{\text{VII}}]_2$  is the eighth unoccupied orbital of  $\text{Ce}[\text{L}^{\text{VII}}]_2$ .

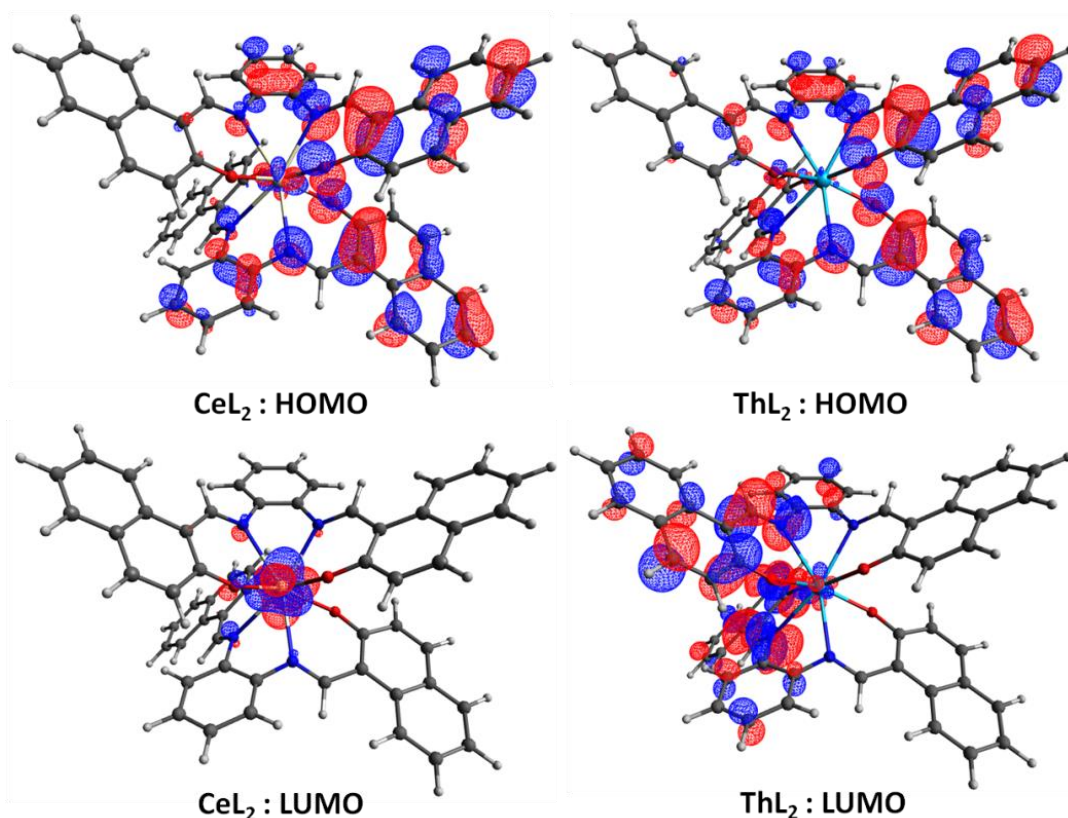


**Figure 4.21.** Ground state HOMO and LUMO of  $\text{Ce}[\text{L}^{\text{VII}}]_2$  and  $\text{Th}[\text{L}^{\text{VII}}]_2$ .<sup>47</sup>

The vertical excitation energies of all electronic states of singlet spin multiplicity up to 3.5 eV are calculated at the TD-DFT level. The energy levels for the  $\text{Ce}[\text{L}^{\text{VII}}]_2$  and  $\text{Th}[\text{L}^{\text{VII}}]_2$  complexes are compared in **Figure 4.22**. Within the present energy range all excitations of the  $\text{Th}[\text{L}^{\text{VII}}]_2$  complex pertain mostly to "local" excitations within the ligands (blue lines). The electronic state with the largest transition probability is shown with a green wider line at 3.43 eV or 361 nm, which matches favorably with the experimental wavelength of 365 nm.

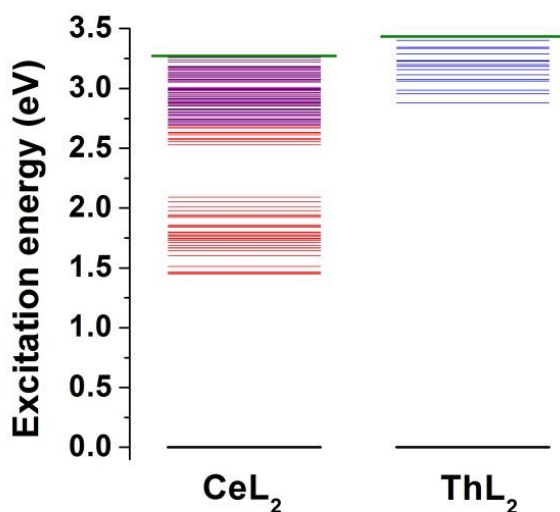


**Figure 4.22.** Vertically excited electronic levels of  $\text{Ce}[\text{L}^{\text{VII}}]_2$  and  $\text{Th}[\text{L}^{\text{VII}}]_2$ .<sup>47</sup>

The  $\text{Ce}[\text{L}^{\text{VII}}]_2$  complex also has energy levels with a similar energy separation from the ground state (purple lines of **Figure 4.22**) that are not highly localized; the involved orbitals also have some cerium contribution. Most importantly,  $\text{Ce}[\text{L}^{\text{VII}}]_2$  possesses several other electronic excitations corresponding to pure intra-molecular electron transfer from the ligands to the metal (red lines of **Figure 4.22**). Access to these additional electronic states allow the slow relaxation to the lower states,<sup>83</sup> usually resulting from conical intersections or inter-system crossings which finally leads to fluorescence quenching.

## Tunable Ligand Emission of $\text{Ln}_2[\text{L}^{\text{VII}}]_3$

The solution phase absorbance spectra of  $\text{Pr}_2[\text{L}^{\text{VII}}]_3$ ,  $\text{Nd}_2[\text{L}^{\text{VII}}]_3$ ,  $\text{Sm}_2[\text{L}^{\text{VII}}]_3$ ,  $\text{Eu}_2[\text{L}^{\text{VII}}]_3$ ,  $\text{Gd}_2[\text{L}^{\text{VII}}]_3$ ,  $\text{Tb}_2[\text{L}^{\text{VII}}]_3$ ,  $\text{Dy}_2[\text{L}^{\text{VII}}]_3$ ,  $\text{Ho}_2[\text{L}^{\text{VII}}]_3$ ,  $\text{Er}_2[\text{L}^{\text{VII}}]_3$ ,  $\text{Yb}_2[\text{L}^{\text{VII}}]_3$ , and  $\text{Lu}_2[\text{L}^{\text{VII}}]_3$  were measured in solution phase in chloroform ( $\text{CHCl}_3$ ) and in the solid state as crystalline solids using a microspectrophotometer. The  $\text{Ln}_2[\text{L}^{\text{VII}}]_3$  complexes have very similar electronic absorption spectra in solution with absorbance bands at 335 and 395 nm, and a shoulder at 440 nm. The absorption spectra of  $\text{Nd}_2[\text{L}^{\text{VII}}]_3$ ,  $\text{Gd}_2[\text{L}^{\text{VII}}]_3$ ,  $\text{Ho}_2[\text{L}^{\text{VII}}]_3$  and  $\text{Yb}_2[\text{L}^{\text{VII}}]_3$  are highlighted in **Figure 4.23**.  $\text{Gd}_2[\text{L}^{\text{VII}}]_3$  has a distinct third absorption feature centered at 450 nm, rather than a shoulder that is observed for the other three examples.

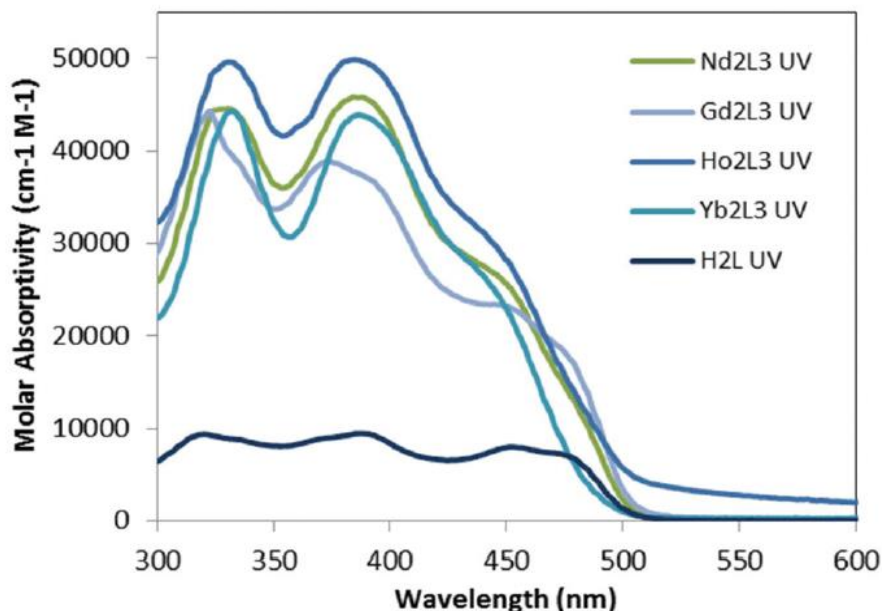


**Figure 4.23.** Absorption spectra of 15  $\mu\text{M}$  solutions of  $\text{Nd}_2[\text{L}^{\text{VII}}]_3$ ,  $\text{Gd}_2[\text{L}^{\text{VII}}]_3$ ,  $\text{Ho}_2[\text{L}^{\text{VII}}]_3$ ,  $\text{Yb}_2[\text{L}^{\text{VII}}]_3$  and  $[\text{H}_2\text{L}^{\text{VII}}]$  in  $\text{CHCl}_3$ .<sup>46</sup>

The molar absorptivities of these  $\text{Ln}_2[\text{L}^{\text{VII}}]_3$  complexes are significant and on the order of  $10^4$ , which is in agreement with similar structures previously reported.<sup>36, 64</sup> The extinction

coefficients for the described series range from  $1.5 \times 10^4 \text{ cm}^{-1} \text{ M}^{-1}$  for  $\text{Lu}_2[\text{L}^{\text{VII}}]_3$  to  $5.4 \times 10^4 \text{ cm}^{-1} \text{ M}^{-1}$  for  $\text{Sm}_2[\text{L}^{\text{VII}}]_3$ , which is consistently larger than the previously reported  $[\text{1M:1L}]^+$  example.<sup>64</sup> The solution phase emission spectra of  $\text{Nd}_2[\text{L}^{\text{VII}}]_3$ ,  $\text{Gd}_2[\text{L}^{\text{VII}}]_3$ ,  $\text{Ho}_2[\text{L}^{\text{VII}}]_3$  and  $\text{Yb}_2[\text{L}^{\text{VII}}]_3$  are highlighted in **Figure 4.24**, with the strongest emission at 406 nm, 434 nm, 406 nm, and 460 nm respectively, attributed to a  $\pi$  to  $\pi^*$  excitation. The emissions at 434 nm and 460 nm are present in all four complexes, with varying intensities, suggesting similar emission transitions. The solution phase fluorescence is dominated by ligand-to-ligand excitation and emission, which explains these similarities in the emission spectra of various lanthanides as well as the broad signal.

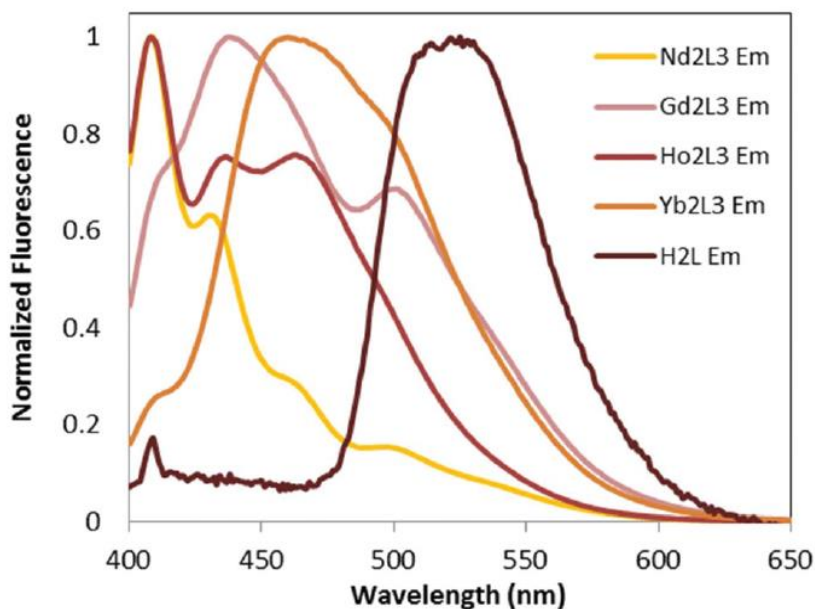


**Figure 4.24.** Normalized emission spectra of 15  $\mu\text{M}$  solutions of  $\text{Nd}_2[\text{L}^{\text{VII}}]_3$ ,  $\text{Gd}_2[\text{L}^{\text{VII}}]_3$ ,  $\text{Ho}_2[\text{L}^{\text{VII}}]_3$ ,  $\text{Yb}_2[\text{L}^{\text{VII}}]_3$  and  $[\text{H}_2\text{L}^{\text{VII}}]$  in  $\text{CHCl}_3$  with excitation at 365 nm.<sup>46</sup>

The emission spectra of the  $\text{Ln}_2[\text{L}^{\text{VII}}]_3$  complexes were sensitive to concentration, suggesting the formation of aggregates in solution. As the concentration increased, the emission was found to decrease, possibly due to self-quenching between different units in the aggregate.

Solutions with concentrations lower than 15  $\mu\text{M}$  were linear with respect to concentration vs. intensity, and thus, used to calculate the quantum yields of the  $\text{Ln}_2[\text{L}^{\text{VII}}]_3$  complexes. Experiments on solution phase fluorescence for the remaining seven complexes were conducted (Figures 4.25-4.27), and were dominated by ligand based emissions.

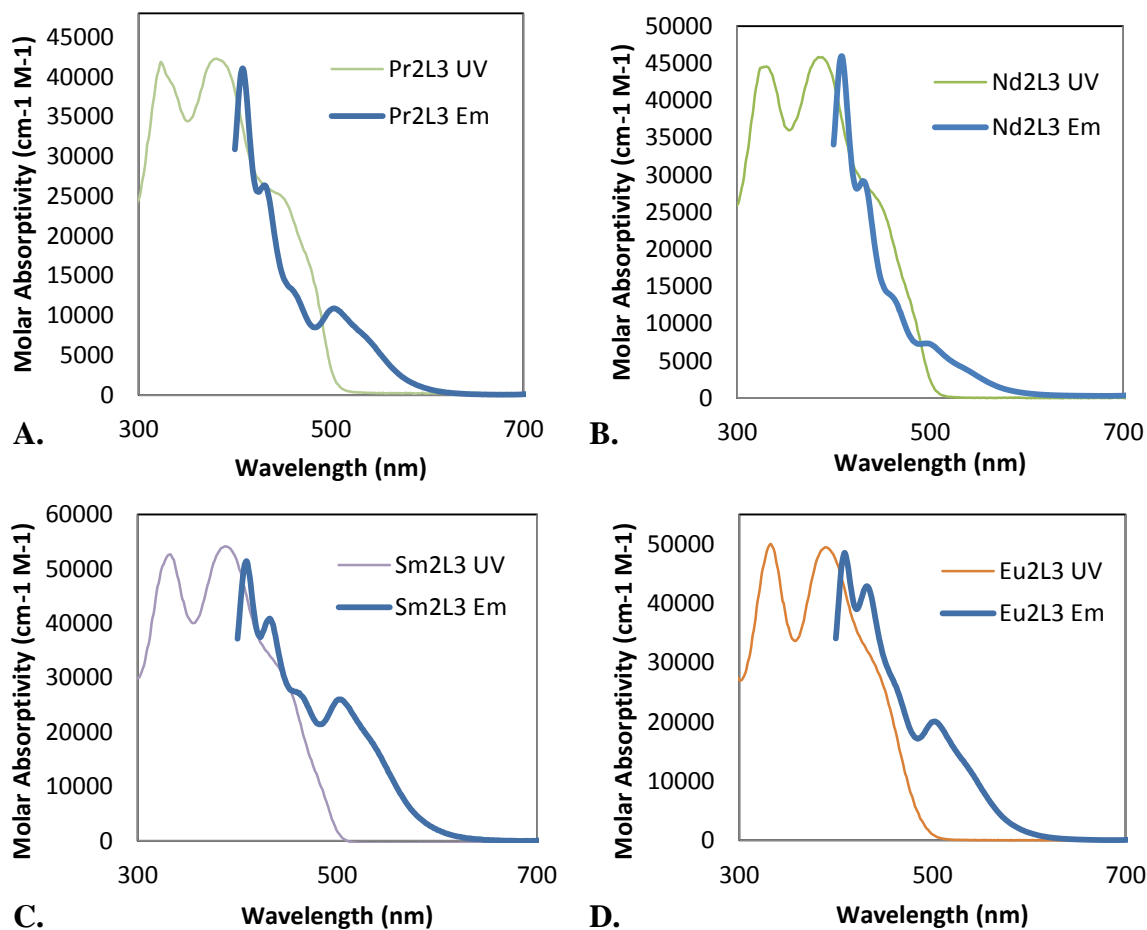


**Figure 4.25.** Solution phase absorbance and emission after 365 nm excitation of 15  $\mu\text{M}$   $\text{CHCl}_3$  solutions of **A.**  $\text{Pr}_2[\text{L}^{\text{VII}}]_3$  **B.**  $\text{Nd}_2[\text{L}^{\text{VII}}]_3$  **C.**  $\text{Sm}_2[\text{L}^{\text{VII}}]_3$  **D.**  $\text{Eu}_2[\text{L}^{\text{VII}}]_3$

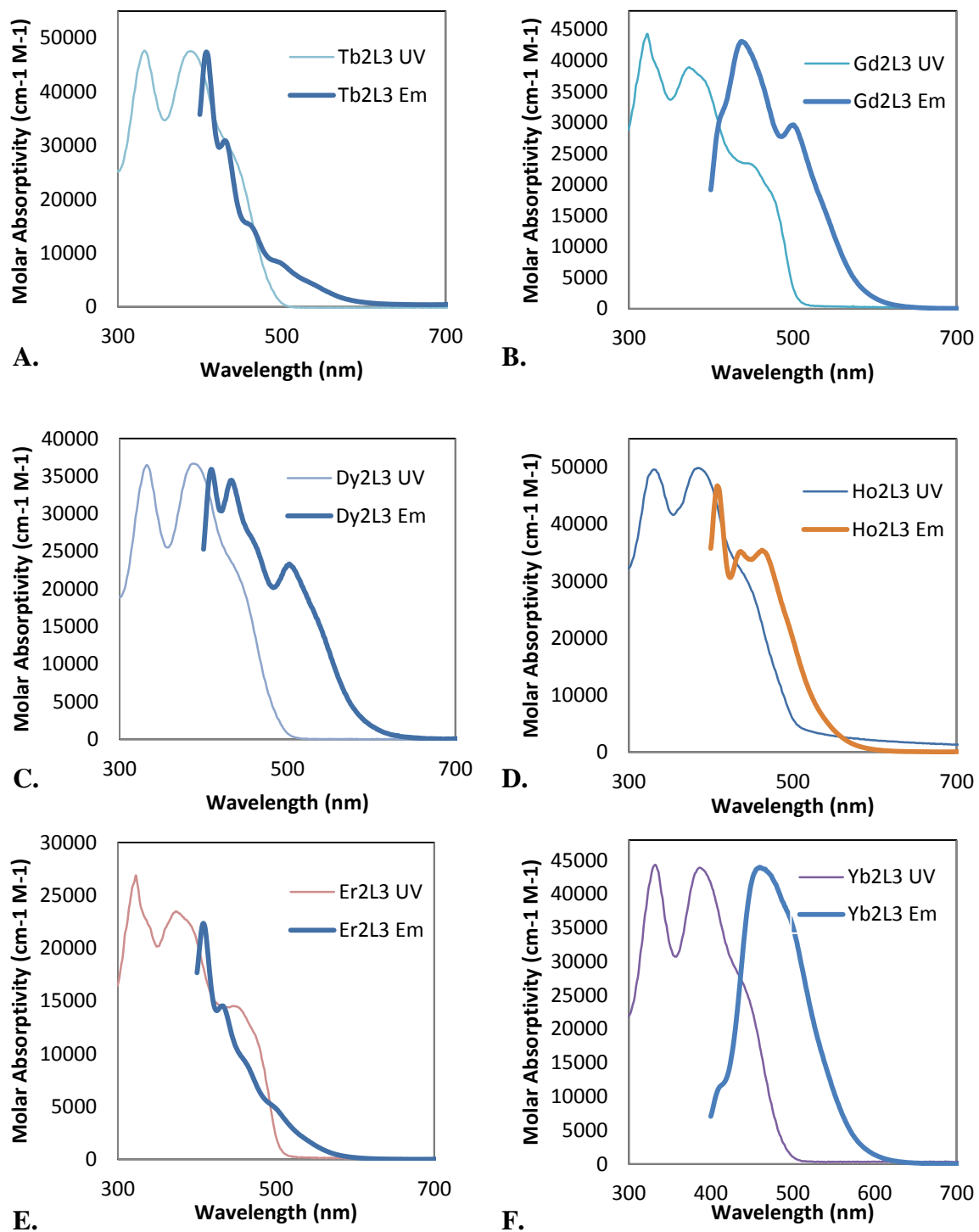


**Figure 4.26.** Solution phase absorbance and emission after 365 nm excitation of 15  $\mu\text{M}$   $\text{CHCl}_3$  solutions of **A.**  $\text{Gd}_2[\text{L}^{\text{VII}}]_3$  **B.**  $\text{Tb}_2[\text{L}^{\text{VII}}]_3$  **C.**  $\text{Dy}_2[\text{L}^{\text{VII}}]_3$  **D.**  $\text{Ho}_2[\text{L}^{\text{VII}}]_3$  **E.**  $\text{Er}_2[\text{L}^{\text{VII}}]_3$  **F.**  $\text{Yb}_2[\text{L}^{\text{VII}}]_3$ <sup>46</sup>



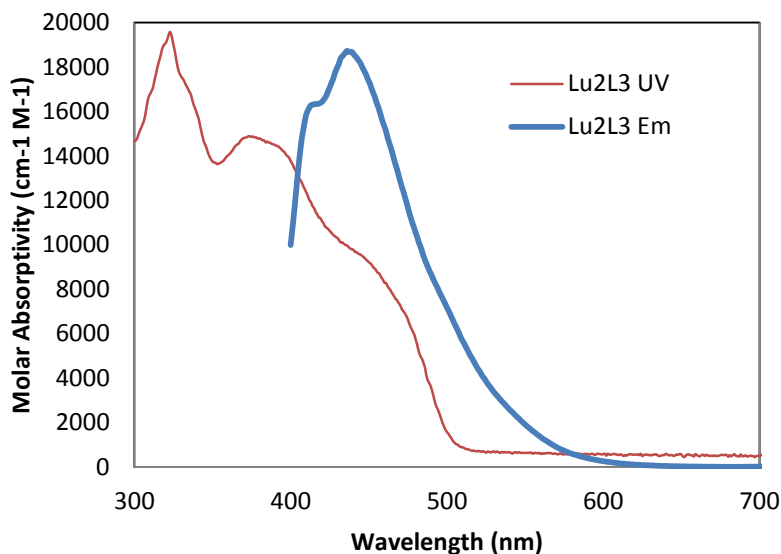


**Figure 4.27.** Solution phase absorbance and emission after 365 nm excitation of  $\text{Lu}_2[\text{L}^{\text{VII}}]_3$  (15  $\mu\text{M}$  in  $\text{CHCl}_3$ ).<sup>46</sup>

The emission quantum yields in  $\text{CHCl}_3$  solutions were obtained (**Table 4.6**) using **Equation 4.1**. Notably, the quantum yields for  $\text{Er}_2[\text{L}^{\text{VII}}]_3$  and  $\text{Lu}_2[\text{L}^{\text{VII}}]_3$  are 3.4% and 2.7 %, respectively.

$$\Phi_X = \Phi_{ST} \left( \frac{\text{slope}_X}{\text{slope}_{ST}} \right) \left( \frac{\eta_X^2}{\eta_{ST}^2} \right) \quad \text{(Equation 4.1)}$$

The subscripts ST and X denote standard and unknown respectively,  $\Phi$  is the fluorescence quantum yield. Slope is the slope from the plot of fluorescence intensity vs absorbance, and  $\eta$  the refractive index of the solvent. In this case the solvent was held constant, and  $\Phi_{ST}$  was equal to 24 %.<sup>84</sup> The calculated quantum yields are tabulated in **Table 4.7**. The plot used to calculate quantum yield is shown in **Figure 4.28**. The intercepts of the lines of best fit are not zero, indicating there may be self-quenching or solvent effects occurring in this system.

**Table 4.7.** Quantum yields of  $\text{Ln}_2[\text{L}^{\text{VII}}]_3$  complexes in  $\text{CHCl}_3$  solution.<sup>46</sup>

Metal Ion	$\Phi$
Dy	0.20%
Eu	0.25%
Gd	0.36%
Ho	1.00%
Lu	2.17%
Er	3.40%
Pr	0.33%
Tb	0.22%
Yb	0.38%

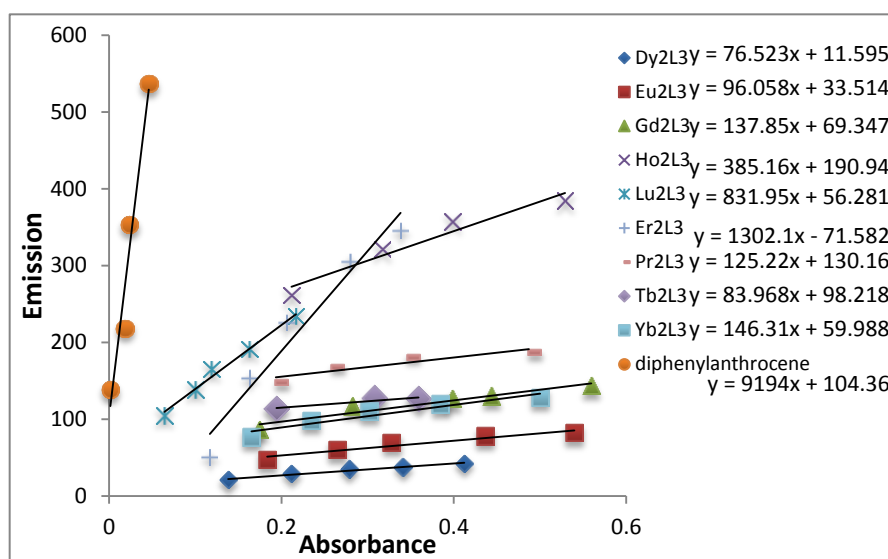


**Figure 4.28.** Quantum Yield Plot of  $\text{Ln}_2[\text{L}^{\text{VII}}]_3$  complexes<sup>46</sup>

Solid-state absorbance and emission of all eleven complexes were conducted (**Figures 4.29-4.31**). The observed emission, which lacks the stereotypical sharp fluorescence of the lanthanides, is broad and can be attributed to ligand-based excitation. The small changes in coordination environment, which cause no distinct changes in absorption properties, provide tunable emission in the solid-state. The absorbance and emission of  $\text{Lu}_2[\text{L}^{\text{VII}}]_3$  in the solid-state, as well as an inset image of  $\text{Lu}_2\text{L}_3$  under ambient light and 365 nm excitation, shown in **Figure**

**4.29.** The solid-state absorbance and emission of each  $\text{Ln}_2[\text{L}^{\text{VII}}]_3$  complex, as well as images of the crystals under ambient and 365 nm light were observed.

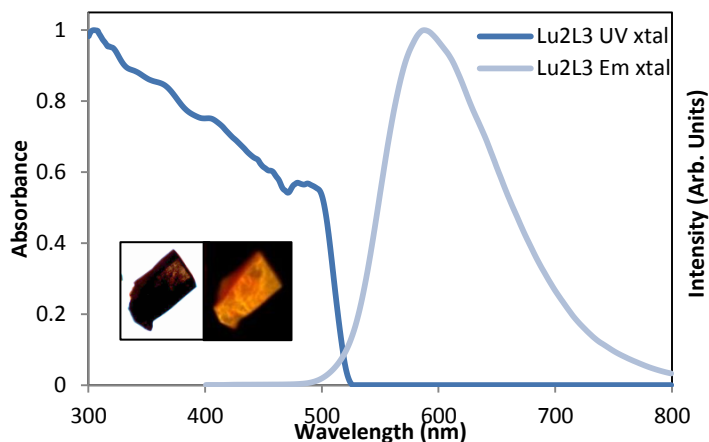


**Figure 4.29.** Solid-state absorbance and emission of a single crystal of  $\text{Lu}_2[\text{L}^{\text{VII}}]_3$ . Inset image of  $\text{Lu}_2[\text{L}^{\text{VII}}]_3$  single crystal under ambient light and with 365 nm excitation.<sup>46</sup>

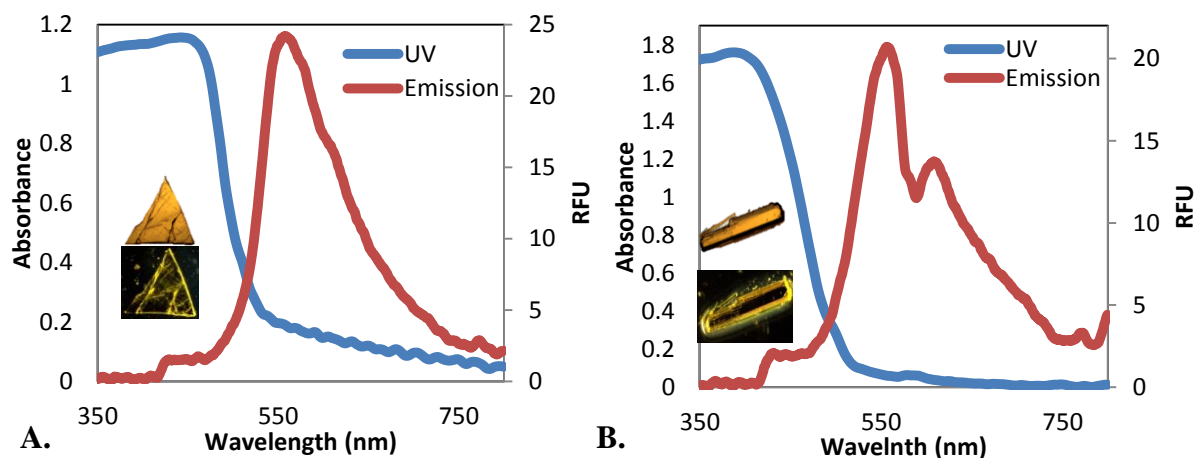


**Figure 4.30.** Solid-state absorbance and emission after 365 nm excitation of **A.**  $\text{Pr}_2[\text{L}^{\text{VII}}]_3$ . And **B.**  $\text{Nd}_2[\text{L}^{\text{VII}}]_3$  Images of single crystals taken on a CRAIC Microspectrophotometer under ambient light and 365 nm light.<sup>46</sup>

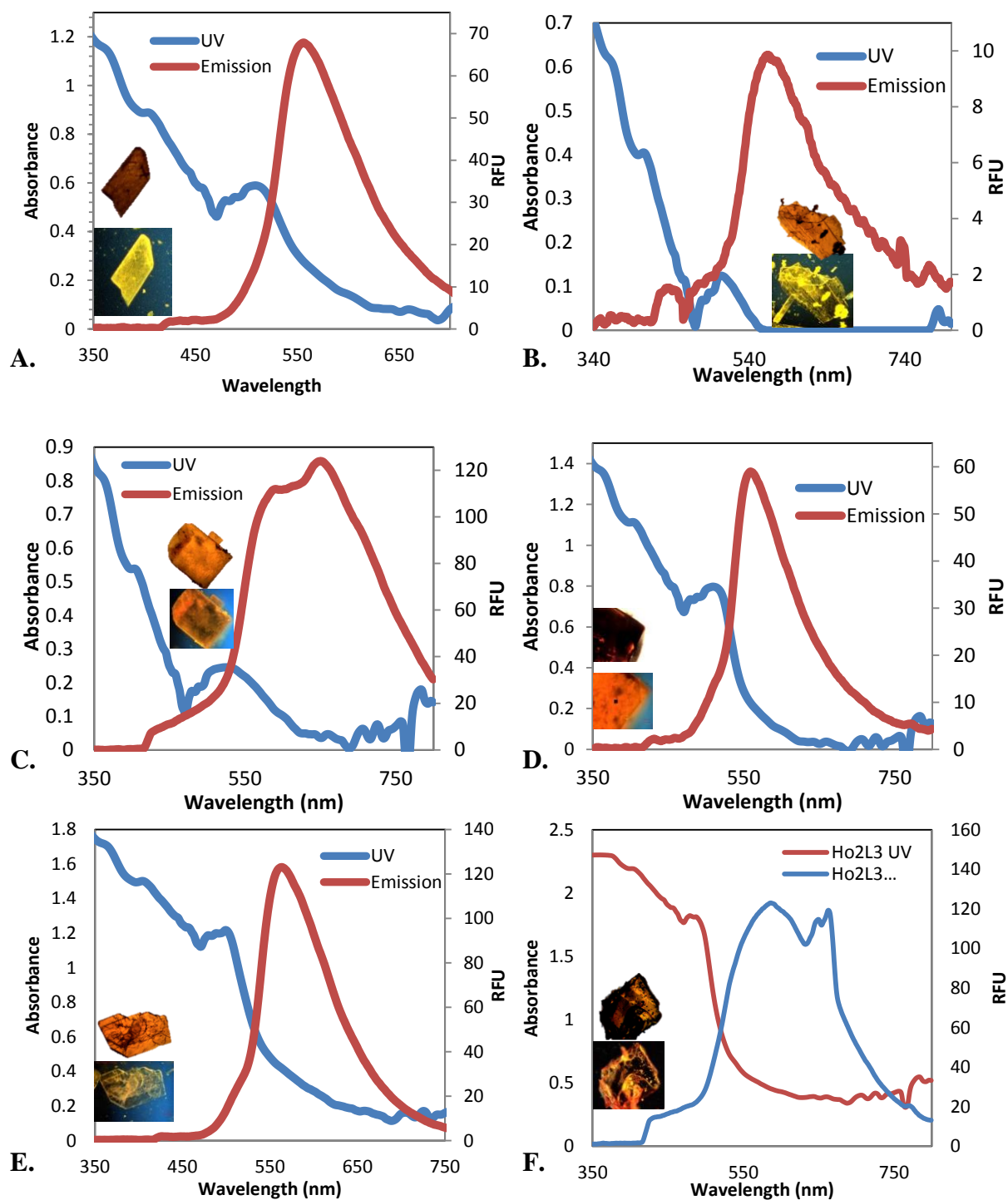


**Figure 4.31.** Solid-state absorbance and emission after 365 nm excitation of **A.**  $\text{Sm}_2[\text{L}^{\text{VII}}]_3$  **B.**  $\text{Eu}_2[\text{L}^{\text{VII}}]_3$  **C.**  $\text{Gd}_2[\text{L}^{\text{VII}}]_3$  **D.**  $\text{Tb}_2[\text{L}^{\text{VII}}]_3$  **E.**  $\text{Dy}_2[\text{L}^{\text{VII}}]_3$  **F.**  $\text{Ho}_2[\text{L}^{\text{VII}}]_3$ . Images of single crystals of taken on a CRAIC Microspectrophotometer under ambient light and 365 nm light.<sup>46</sup>

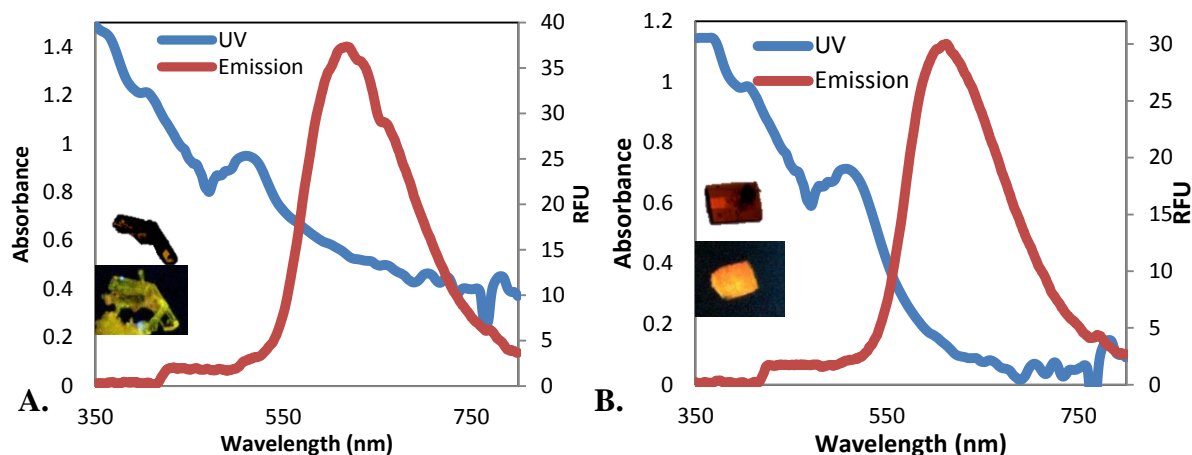


**Figure 4.32.** Solid state absorbance and emission after 365 nm excitation of **A.**  $\text{Er}_2[\text{L}^{\text{VII}}]_3$  **B.**  $\text{Yb}_2[\text{L}^{\text{VII}}]_3$ . Images of single crystals taken on a CRAIC Microspectrophotometer under ambient light and 365 nm light.<sup>46</sup>

As highlighted in **Figure 4.33**, while all the lanthanide analogues fluoresce in the solid-state, the  $\text{Lu}_2[\text{L}^{\text{VII}}]_3$  complex emits 1000 times more strongly than any other of the eleven  $\text{Ln}_2[\text{L}^{\text{VII}}]_3$  complexes observed. This significant increase in fluorescence is surprising, as the changes in bond lengths from Lu to Yb, the next closest in size, are within an average of 0.02 Å. The lanthanide contraction is again evident in the change in emission, as it goes from emission at 556 nm to 617 nm from early to late lanthanides (**Table 4.8**). As the lanthanide ions get smaller, the ligands in the triple-decker sandwich are pulled closer together from early to late lanthanides, reducing the energy from the ground and excited states, until the optimum distance is achieved on reaching lutetium.

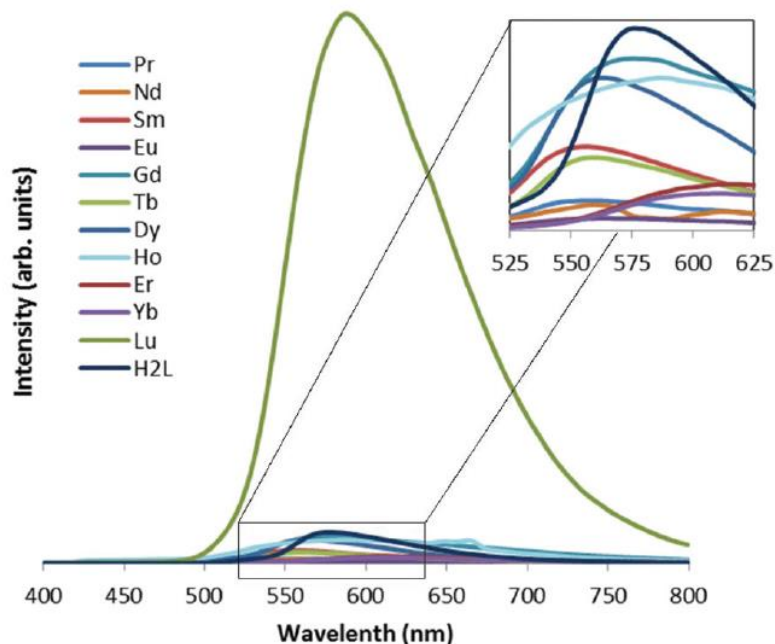


**Figure 4.33.** Solid-state emission spectra of the  $\text{Ln}_2[\text{L}^{\text{VII}}]_3$  complexes with excitation at 365 nm.<sup>46</sup>

**Table 4.8.** Emission wavelengths of  $\text{Ln}_2[\text{L}^{\text{VII}}]_3$  species in solid-state.<sup>46</sup>

Metal	Max Wavelength (nm)
Sm	556
Pr	558
Nd	559
Tb	559
Eu	563
Dy	564
Gd	575
Ho	587
Lu	588
Yb	611
Er	617

## Conclusions

In summary, three new mononuclear complexes  $\text{UO}_2[\text{L}^{\text{VII}}]$ ,  $\text{Ce}[\text{L}^{\text{VII}}]_2$ , and  $\text{Th}[\text{L}^{\text{VII}}]_2$  and eleven lanthanide double decker sandwich complexes ( $\text{Ln}_2[\text{L}^{\text{VII}}]_3$ ), where Ln = Pr(III), Nd(III),

Sm(III), Eu(III), Gd(III), Tb(III), Dy(III), Ho(III), Er(III), Yb(III), or Lu(III), were synthesized and characterized in the solid-state and in solution.

$\text{Th}[\text{L}^{\text{VII}}]_2$  was observed to fluoresce in both solid-state and solution phase, but  $\text{Ce}[\text{L}^{\text{VII}}]_2$  was not. DFT calculations indicated that this is due to fluorescence quenching in the case of cerium. Unlike  $\text{Th}[\text{L}^{\text{VII}}]_2$ ,  $\text{Ce}[\text{L}^{\text{VII}}]_2$  was found to possess appropriate electronic states, which can facilitate a non-radiative decay from the involved excited to the lower electronic states. Solvent dependence of emission was observed and may be due to solvent coordination in the 8- and 9-coordinate equilibrium of  $\text{Th}[\text{L}^{\text{VII}}]_2$  in solution. The uncommonly short M-N<sub>imine</sub> bond lengths may be due to a stronger imine donor than typically is observed in salen-like compounds.

The structural differences in the  $\text{Nd}_2[\text{L}^{\text{VII}}]_3$ ,  $\text{Gd}_2[\text{L}^{\text{VII}}]_3$ ,  $\text{Tb}_2[\text{L}^{\text{VII}}]_3$ ,  $\text{Dy}_2[\text{L}^{\text{VII}}]_3$ ,  $\text{Ho}_2[\text{L}^{\text{VII}}]_3$ ,  $\text{Yb}_2[\text{L}^{\text{VII}}]_3$ , and  $\text{Lu}_2[\text{L}^{\text{VII}}]_3$  analogues are minimal and can be attributed to the decreasing size of the lanthanide series. The small differences in structure afforded similar absorbance spectra, but differences in the emission properties were observed in solution. These differences were more apparent in the solid-state luminescence with  $\text{Sm}_2[\text{L}^{\text{VII}}]_3$  emission at 556 nm to  $\text{Er}_2[\text{L}^{\text{VII}}]_3$  emission at 617 nm. Lutetium exhibited a significant increase in fluorescent signal as compared to the other  $\text{Ln}_2[\text{L}^{\text{VII}}]_3$  complexes in the solid state, suggesting that the late lanthanides provide a scaffold to closely hold the naphthylsalophen ligands in a rigid structure to maximize ligand to ligand excitation and emission.

The complex  $\text{UO}_2[\text{L}^{\text{VII}}]$  was synthesized and characterized in the solid-state and may show promise as a colorimetric chemosensor similar to those species discussed in Chapters 2 and 3 in the future. Interesting hydrogen bonded tetramers of the complex  $(\text{UO}_2[\text{L}^{\text{VII}}])_4$  were observed, but seem to be a solid-state phenomenon.

## Experimental Details

### General considerations

*Caution! Standard precautions for handling radioactive materials or heavy metals, such as  $\text{Th}(\text{NO}_3)_4 \cdot 6\text{H}_2\text{O}$  as used in this study, were followed.*

Any solvents not specifically identified were ACS grade, purchased from EMD, and used as received without further purification. The reagents toluene (HPLC grade, BDH), dimethylsulfoxide (99%, Macron), dimethylformamide (99.9%, EMD), acetonitrile (99.5%, BDH), chloroform (99.8%, BDH), methanol (HPLC grade, EMD), 1,2-diaminobenzene (99.5%, Aldrich), 2-hydroxynaphthaldehyde (98%, Alpha Aesar), cerium(III) acetate (99.9%, STREM), samarium(III) chloride hydrate (99.9%, STREM), lutetium(III) chloride (99.9%, STREM), praseodymium(III) chloride (99.9%, STREM), terbium(III) chloride hexahydrate (99.9%, STREM), ytterbium(III) acetate hydrate (99.9%, STREM), holmium(III) chloride hydrate (99.9%, STREM) europium(III) acetate hydrate (99.9%, STREM), erbium(III) chloride hydrate (99.9%, STREM), neodymium(III) chloride hexahydrate (99.9%, STREM), dysprosium(III) acetate hydrate (99.9%, STREM), and  $\text{Th}(\text{NO}_3)_4 \cdot 6\text{H}_2\text{O}$  (99%, Fluka) were used as received without further purification. Anhydrous dichloromethane (BDH) was purchased, stored under argon, and dispensed from a solvent purification system. Triethylamine (99%, Alpha Aesar) was distilled and stored under argon until use. Deuterated dimethylsulfoxide (DMSO) and chloroform were purchased from Cambridge Isotope and stored in a desiccator when not in use.

### Synthetic Details

**Naphthylsalophen** [ $\text{H}_2\text{L}^{\text{VII}}$ ]: 1,2-diaminobenzene (0.433 g, 7.23 mmol) and 2-hydroxynaphthaldehyde (1.32 g, 15.0 mmol) were added to 150 mL of MeOH, heated to reflux



temperature, and stirred for 6 hours. The solution was observed to change from yellow to dark orange and a precipitate formed. The solution was allowed to cool to room temperature. The resulting solid was filtered and washed with hexanes to yield a bright orange powder (2.54 g, 84%).  $^1\text{H}$  NMR (600 MHz,  $\text{CDCl}_3$ )  $\delta$  7.18 (d, 2H,  $J = 9.2$  Hz), 7.34 (t, 2H,  $J = 7.4$  Hz), 7.44-7.39 (m, 4H), 7.51 (t, 2H,  $J = 8.2$  Hz), 7.73 (d, 2H,  $J = 7.9$  Hz), 7.82 (d, 2H,  $J = 9.2$  Hz), 8.14 (d, 2H,  $J = 8.5$  Hz), 9.46 (d, 2H,  $J = 3.6$  Hz), 15.08 (s, 2OH);  $^{13}\text{C}$  NMR (151 MHz,  $\text{CDCl}_3$ )  $\delta$  109.40, 119.03, 119.15, 122.09, 123.63, 127.42, 127.51, 128.08, 129.41, 133.21, 136.67, 139.73, 156.17, 169.08; TOF MS (ESI)  $m/z$  ( $\text{M}^+ + 1$ ) Calcd 417.1525, Found 417.1550. CCDC: 1523762.

**Ce[L<sup>VII</sup>]<sub>2</sub>**: The naphthylsalophen ligand [ $\text{H}_2\text{L}^{\text{VII}}$ ] (867 mg, 2.08 mmol) and  $\text{NEt}_3$  (1.0 mL) were added to minimal amount of DCM (120 mL) and allowed to dissolve in a 250 mL round bottom flask.  $\text{Ce}(\text{OAc})_3 \cdot \text{H}_2\text{O}$  (342 mg, 1.08 mmol) was then added to the flask with minimal amount (80 mL) of MeOH to dissolve the salt after some stirring. The reaction was heated to 40 °C and stirred for 6 hours. The solution volume was reduced by half by rotary evaporation, and the precipitate, a reddish brown solid, was filtered off and collected. Crystals suitable for x-ray diffraction were grown in five days from layering a saturated toluene solution of  $\text{Ce}[\text{L}^{\text{VII}}]_2$  with hexanes. (976 mg, 94%).  $^1\text{H}$  NMR (600 MHz,  $\text{CDCl}_3$ )  $\delta$  6.33 (d, 4H,  $J = 9.0$  Hz), 7.25-7.27 (m, 4H), 7.30-7.35 (m, 8H), 7.53 (s, 4H), 7.55 (s, 4H), 7.73 (d, 4H,  $J = 7.7$  Hz), 7.97 (d, 4H,  $J = 8.4$  Hz), 9.63 (s, 4H) ppm;  $^{13}\text{C}$  NMR (151 MHz,  $\text{CDCl}_3$ )  $\delta$  114.27, 118.80, 120.09, 122.55, 122.94, 127.15, 127.20, 127.83, 128.88, 133.81, 134.77, 146.74, 156.11, 168.82 ppm; TOF MS (ESI)  $m/z$  ( $\text{M}^+ + 1$ ) Calcd 969.1791, Found 969.1705. CCDC 1523760.

**Pr<sub>2</sub>[L<sup>VII</sup>]<sub>3</sub>**: The naphthylsalophen ligand [ $\text{H}_2\text{L}^{\text{VII}}$ ] (209 mg, 0.503 mmol) and  $\text{NEt}_3$  (600  $\mu\text{L}$ ) were added to 40 mL of DCM and 40 mL of MeOH in a 100 mL round bottom flask and allowed to stir until dissolved.  $\text{PrCl}_3 \cdot 7\text{H}_2\text{O}$  (141 mg, 0.378 mmol) was then added to the flask. The reaction

was heated to 40 °C, and allowed to stir for 4 hours. The solution volume was reduced by half through the use of a rotary evaporator, and the subsequent solution was allowed to evaporate slowly. Orange needles were filtered after 18 hours (230 mg, 88%). TOF MS (ESI)  $m/z$  ( $M^+ + 1$ ) Calcd 1621.7329, Found 1621.7505 ; Elem. Anal. For  $C_{87}H_{68}N_6Pr_2O_{10}$  Calcd (Found): C, 63.74 (63.61); H, 4.18 (3.83); N, 5.13 (5.18).

**Nd<sub>2</sub>[L<sup>VII</sup>]<sub>3</sub>**: The naphthylsalophen ligand [ $H_2L^{VII}$ ] (204 mg, 0.490 mmol) and  $NEt_3$  (600  $\mu$ L) were added to 40 mL of DCM and 40 mL of MeOH in a 100 mL round bottom flask and allowed to stir until dissolved.  $NdCl_3 \cdot 6H_2O$  (181 mg, 0.505 mmol) was then added to the flask. The reaction was heated to 40 °C, and allowed to stir for 4 hours. The solution volume was reduced by half through the use of a rotary evaporator, and the subsequent solution was allowed to evaporate slowly. Orange needle crystals suitable for x-ray diffraction were filtered after 18 hours (235 mg, 92%). TOF MS (ESI)  $m/z$  ( $M^+ + 1$ ) Calcd 1531.2408, Found 1531.2390; Elem. Anal. for  $C_{87}H_{64}Cl_2N_6Nd_2O_8$  Calcd % (Found %): C, 62.17 (62.02); H, 3.84 (3.88); N, 5.00 (5.11). CCDC: 1555710.

**Sm<sub>2</sub>[L<sup>VII</sup>]<sub>3</sub>**: The naphthylsalophen ligand [ $H_2L^{VII}$ ] (202 mg, 0.486 mmol) and  $NEt_3$  (600  $\mu$ L) were added to 40 mL of DCM and 40 mL of MeOH in a 100 mL round bottom flask and allowed to stir until dissolved.  $Sm(OAc)_3 \cdot H_2O$  (166 mg, 0.505 mmol) was then added to the flask. The reaction was heated to 40 °C, and allowed to stir for 4 hours. The solution volume was reduced by half through the use of a rotary evaporator, and the subsequent solution was allowed to evaporate slowly. Orange solid was filtered after 18 hours (74 mg, 29%). TOF MS (ESI)  $m/z$  ( $M^+ + 1$ ) Calcd, 1545.2579 Found 1545.2465; Elem. Anal. for  $C_{88}H_{68}Cl_2N_6O_9Sm_2$  Calcd % (Found %): C, 61.27 (61.11); H, 3.97 (3.80); N, 4.87 (4.88).

**Eu<sub>2</sub>[L<sup>VII</sup>]<sub>3</sub>**: The naphthylsalophen ligand [H<sub>2</sub>L<sup>VII</sup>] (208 mg, 0.500 mmol) and NEt<sub>3</sub> (600 μL) were added to 40 mL of DCM and 40 mL of MeOH in a 100 mL round bottom flask and allowed to stir until dissolved. Eu(OAc)<sub>3</sub>•H<sub>2</sub>O (165 mg, 0.501 mmol) was then added to the flask. The reaction was heated to 40 °C, and allowed to stir for 4 hours. The solution volume was reduced by half through the use of a rotary evaporator, and the subsequent solution was allowed to evaporate slowly. Solid orange block crystals suitable for x-ray diffraction were filtered after 36 hours (121 mg, 46%). TOF MS (ESI) m/z (M<sup>+</sup> + 1) Calcd 1547.2581, Found 1547.2603. Elem. Anal. for C<sub>87</sub>H<sub>62</sub>Cl<sub>4</sub>Eu<sub>2</sub>N<sub>6</sub>O<sub>7</sub> Calcd % (Found %): C, 59.74 (59.51); H, 3.57 (3.62); N, 4.80 (4.75).

**Gd<sub>2</sub>[L<sup>VII</sup>]<sub>3</sub>**: The naphthylsalophen ligand [H<sub>2</sub>L<sup>VII</sup>] (201 mg, 0.483 mmol) and NEt<sub>3</sub> (600 μL) were added to 40 mL of DCM and 40 mL of MeOH in a 100 mL round bottom flask and allowed to stir until dissolved. Gd(OAc)<sub>3</sub>•H<sub>2</sub>O (196 mg, 0.744 mmol) was then added to the flask. The reaction was heated to 40 °C, and allowed to stir for 4 hours. The solution volume was reduced by half through the use of a rotary evaporator, and the subsequent solution was allowed to evaporate slowly. Solid orange block crystals suitable for x-ray diffraction were filtered after 18 hours (150. mg, 59%). TOF MS (ESI) m/z (M<sup>+</sup> + 1) Calcd 1559.2695, Found 1559.2788. Elem. Anal. for C<sub>86</sub>H<sub>68</sub>Gd<sub>2</sub>N<sub>6</sub>O<sub>11</sub> Calcd % (Found %): C, 61.63 (61.49); H, 4.09 (4.11); N, 5.01 (5.20). CCDC: 1523761.

**Tb<sub>2</sub>[L<sup>VII</sup>]<sub>3</sub>**: The naphthylsalophen ligand [H<sub>2</sub>L<sup>VII</sup>] (202 mg, 0.486 mmol) and NEt<sub>3</sub> (600 μL) were added to 40 mL of DCM and 40 mL of MeOH in a 100 mL round bottom flask and allowed to stir until dissolved. TbCl<sub>3</sub>•6H<sub>2</sub>O (188 mg, 0.504 mmol) was then added to the flask. The reaction was heated to 40 °C, and allowed to stir for 4 hours. The solution volume was reduced by half through the use of a rotary evaporator, and the subsequent solution was allowed to evaporate

slowly. Solid orange block crystals suitable for x-ray diffraction were filtered after 18 hours (224 mg, 85%). TOF MS (ESI)  $m/z$  ( $M^+ + 1$ ) Calcd 1562.2690, Found 1562.2859. Elem. Anal. for  $C_{85}H_{58}N_6O_7Tb_2$  Calcd % (Found %): C, 64.08 (63.85); H, 3.67 (3.56); N, 5.27 (5.25). CCDC: 1555317.

**Dy<sub>2</sub>[L<sup>VII</sup>]<sub>3</sub>**: The naphthylsalophen ligand [ $H_2L^{VII}$ ] (207 mg, 0.498 mmol) and  $NEt_3$  (600  $\mu$ L) were added to 40 mL of DCM and 40 mL of MeOH in a 100 mL round bottom flask and allowed to stir until dissolved.  $Dy(OAc)_3 \cdot 6H_2O$  (171 mg, 0.504 mmol) was then added to the flask. The reaction was heated to 40 °C, and allowed to stir for 4 hours. The solution volume was reduced by half through the use of a rotary evaporator, and the subsequent solution was allowed to evaporate slowly. Solid orange block crystals suitable for x-ray diffraction were filtered after 18 hours (260 mg, 98%). TOF MS (ESI)  $m/z$  ( $M^+ + 1$ ) Calcd 1569.2799, Found 1569.2994; Elem. Anal. for  $C_{85}H_{58}Dy_2N_6O_7$  Calcd % (Found %): C, 63.79 (63.32); H, 3.65 (3.72); N, 5.25 (5.30). CCDC: 1555316.

**Ho<sub>2</sub>[L<sup>VII</sup>]<sub>3</sub>**: The naphthylsalophen ligand [ $H_2L^{VII}$ ] (205 mg, 0.494 mmol) and  $NEt_3$  (600  $\mu$ L) were added to 40 mL of DCM and 40 mL of MeOH in a 100 mL round bottom flask and allowed to stir until dissolved.  $HoCl_3 \cdot 6H_2O$  (189 mg, 0.4979 mmol) was then added to the flask. The reaction was heated to 40 °C, and allowed to stir for 4 hours. The solution volume was reduced by half through the use of a rotary evaporator, and the subsequent solution was allowed to evaporate slowly. A brown colored solid was filtered after 18 hours (220 mg, 83%). Dark brown crystals suitable for x-ray diffraction grew from slow evaporation of methanol. TOF MS (ESI)  $m/z$  ( $M^+ + 1$ ) Calcd. 1572.2711, Found 1561.3846. Elem. Anal. for  $C_{90}H_{76}Cl_{10}N_6O_7Ho_2$  Calcd % (Found %): C, 51.43 (51.06); H, 3.64 (3.69); N, 4.00 (4.01). CCDC:1555027.

**Er<sub>2</sub>[L<sup>VII</sup>]<sub>3</sub>**: The naphthylsalophen ligand [H<sub>2</sub>L<sup>VII</sup>] (208 mg, 0.499 mmol) and NEt<sub>3</sub> (600 μL) were added to 40 mL of DCM and 40 mL of MeOH in a 100 mL round bottom flask and allowed to stir until dissolved. ErCl<sub>3</sub>•H<sub>2</sub>O (171 mg, 0.6264 mmol) was then added to the flask. The reaction was heated to 40 °C, and allowed to stir for 4 hours. The solution volume was reduced by half by rotary evaporation and was allowed to evaporate slowly. The resulting yellow solid was filtered (248 mg, 96%). TOF MS (ESI) m/z (M<sup>+</sup> + 1) Calcd 1577.2827, Found 1577.2870. Elem. Anal. for C<sub>109</sub>H<sub>125</sub>Cl<sub>6</sub>N<sub>9</sub>O<sub>15</sub>Er<sub>2</sub> Calcd % (Found %): C, 55.06 (54.81); H, 5.45 (5.25); N, 5.45 (5.84).

**Yb<sub>2</sub>[L<sup>VII</sup>]<sub>3</sub>**: The naphthylsalophen ligand [H<sub>2</sub>L<sup>VII</sup>] (208 mg, 0.500 mmol) and NEt<sub>3</sub> (600 uL) were added to 40 mL of DCM and 40 mL of MeOH in a 100 mL round bottom flask and allowed to stir until dissolved. Yb(OAc)<sub>3</sub>•H<sub>2</sub>O (175 mg, 0. mmol) was then added to the flask. The reaction was heated to 40 °C, and allowed to stir for 4 hours. The solution volume was reduced by half through the use of a rotary evaporator, and the subsequent solution was allowed to evaporate slowly. The reaction was heated to 40 °C, and allowed to stir for 4 hours. The solution volume was reduced by half by rotary evaporation and was allowed to evaporate slowly. Solid orange block crystals suitable for x-ray diffraction were filtered after 18 hours (141 mg, 52 %). CCDC:1555028. TOF MS (ESI) m/z (M<sup>+</sup> + 1) Calcd 1590.2974, Found 1590.2826; Elem. Anal. for C<sub>85</sub>H<sub>58</sub>N<sub>6</sub>O<sub>7</sub>Yb<sub>2</sub> Calcd % (Found %): C, 62.96 (62.14); H, 3.61 (3.65); N, 5.18 (5.25).

**Lu<sub>2</sub>[L<sup>VII</sup>]<sub>3</sub>**: The naphthylsalophen ligand [H<sub>2</sub>L<sup>VII</sup>] (210 mg, 0.506 mmol) and NEt<sub>3</sub> (600 uL) were added to 40 mL of DCM and 40 mL of MeOH in a 100 mL round bottom flask and allowed to stir until dissolved. Lu(OAc)<sub>3</sub>•H<sub>2</sub>O (173 mg, 0.490 mmol) was then added to the flask. The reaction was heated to 40 °C, and allowed to stir for 4 hours. The solution volume was reduced by half through the use of a rotary evaporator, and the subsequent solution was allowed to evaporate slowly. Solid orange block crystals suitable for x-ray diffraction were filtered after 18

hours (279 mg, quantitative yield). TOF MS (ESI)  $m/z$  ( $M^+ + 1$ ) Calcd 1594.3031, Found 1594.3022; Elem. Anal. for  $C_{85}H_{60}Lu_2N_6O_8$  Calcd % (Found %): C, 62.12 (61.69); H, 3.68 (3.64); N, 5.11 (5.18). CCDC: 1555720.

**Th[L<sup>VII</sup>]<sub>2</sub>**: The naphthylsalophen ligand [ $H_2L^{VII}$ ] (414 mg, 0.995 mmol) and  $NEt_3$  (1.0 mL) were added to 100 mL of DCM and 50 mL of MeOH in a 250 mL round bottom flask. The mixture was stirred until all the solids were dissolved. Thorium nitrate (214 mg, 0.415 mmol) was then added to the flask. The reaction was heated to 40 °C and heated with stirring for 5.5 hours. The solution volume was reduced by half by rotary evaporation, and subsequently put in ice for 30 minutes. A yellow solid precipitated. This was filtered off and rinsed with hexanes (333 mg, 76 %). Crystals suitable for x-ray diffraction were grown in 3 days from layering a saturated toluene solution of  $Th[L^{VII}]_2$  with hexanes. <sup>1</sup>H NMR (600 MHz,  $CDCl_3$ )  $\delta$  6.53 (d, 4H,  $J = 9.0$  Hz), 7.15 (s, 4H), 7.27 (t, 4H,  $J = 7.2$  Hz), 7.46 (t, 4H,  $J = 7.2$  Hz), 7.56 (d, 4H,  $J = 9.0$  Hz), 7.67 (d, 4H,  $J = 7.8$  Hz), 7.94 (d, 4H,  $J = 8.4$  Hz), 9.30 (s, 4H) ppm; <sup>13</sup>C NMR (151 MHz,  $CDCl_3$ )  $\delta$  113.73, 119.62, 119.67, 122.78, 124.44, 127.43, 127.47, 127.53, 129.27, 134.54, 136.00, 145.93, 158.68, 167.15 ppm; TOF MS (ESI)  $m/z$  ( $M^+ + 1$ ) Calcd 1061.3117, Found 1061.3773. CCDC: 1548265.

**UO<sub>2</sub>[L<sup>VII</sup>]**: The naphthylsalophen ligand [ $H_2L^{VII}$ ] (970. mg, 2.33 mmol) and  $NEt_3$  (1 mL) were added to 40 mL of DCM and 20 mL of MeOH in a 100 mL round bottom flask. The mixture was stirred until all the solids were dissolved. Uranyl nitrate hexahydrate (963 mg, 2.27 mmol) was then added to the flask. The reaction was heated to 40 °C and heated with stirring for 2 hours. The solution volume was reduced by half by rotary evaporation, and subsequently put in ice for 30 minutes. A yellow solid precipitated. This was filtered off and rinsed with hexanes (132 mg, 83%). Crystals suitable for x-ray diffraction were grown in 3 days from layering a saturated toluene solution of  $UO_2[L^{VII}]$  with hexanes. The <sup>1</sup>H NMR (600 MHz,  $d_6$ -DMSO)  $\delta$  7.31 (t, 2H,  $J$

= 7.4 Hz), 7.38 (d, 2H,  $J = 9.1$  Hz), 7.53-7.55 (m, 4H), 7.85-7.88 (m, 4H), 8.20 (d, 2H,  $J = 8.1$  Hz), 8.36 (d, 2H,  $J = 8.5$  Hz), 10.20 (s, 2H) ppm;  $^{13}\text{C}$  NMR (151 MHz,  $d_6$ -DMSO)  $\delta$  114.72, 120.33, 121.36, 122.92, 124.20, 127.03, 127.91, 128.49, 128.75, 134.49, 137.12, 147.38, 160.09, 171.33 ppm; TOF MS (ESI)  $m/z$  ( $M^+ + 1$ ) Cald 685.1774, Found 685.1777, ( $M(\text{H}_2\text{O})^+ + 1$ ) Cald 703.1880, Found 703.1902. **Crystal Data** for  $\text{UO}_2[\text{L}^{\text{VII}}]$ :  $\text{C}_{60}\text{H}_{48}\text{Cl}_8\text{N}_4\text{O}_{10}\text{U}_2$  ( $M = 1744.75$ ): monoclinic, space group  $\text{P}2_1/\text{n}$  (no. 14),  $a = 15.4659(12)$  Å,  $b = 19.3294(14)$  Å,  $c = 22.2346(16)$  Å,  $\beta = 106.655(1)^\circ$ ,  $V = 6368.1(8)$  Å<sup>3</sup>,  $Z = 4$ ,  $T = 180.0$  K,  $\mu(\text{Mo K}\alpha) = 5.476$  mm<sup>-1</sup>,  $D_{\text{calc}} = 1.8197$  g/mm<sup>3</sup>, 74217 reflections measured ( $2.84 \leq 2\Theta \leq 51.52$ ), 12168 unique ( $R_{\text{int}} = 0.0706$ ,  $R_{\text{sigma}} = 0.0463$ ) which were used in all calculations. The final  $R_1$  was 0.0440 ( $I \geq 2\sigma(I)$ ) and  $wR_2$  was 0.1031 (all data). CCDC: 1827293.

### Single Crystal X-ray Diffraction

Crystals suitable for single crystal X-ray diffraction were selected and mounted on a glass fiber using Paratone-N oil and data set collection was completed on a 'Bruker APEX CCD' diffractometer using Mo K $\alpha$  radiation. The crystal was kept at 180 K during unit cell and data collection. SMART (v. 5.624) was used for preliminary determination of cell constants and data collection control. Determination of integrated intensities and global cell refinement were performed with the Bruker SAINT software package, and empirical absorption correction (SADABS) was applied. The structures were solved with the ShelXS structure solution program using Direct Methods<sup>85-86</sup> and refined with the olex2.refine refinement package using Gauss-Newton minimisation.<sup>87-88</sup> Carbon atoms in coordinating methanol molecules in  $\text{Dy}_2[\text{L}^{\text{VII}}]_3$ ,  $\text{Tb}_2[\text{L}^{\text{VII}}]_3$ ,  $\text{Lu}_2[\text{L}^{\text{VII}}]_3$  were refined isotropically, as attempts to model disorder resulted in non-convergence. A disordered interstitial toluene on an inversion center was modeled for  $\text{Th}[\text{L}^{\text{VII}}]_2$ . A half of a highly disordered interstitial hexane was modeled over two positions for  $\text{Ce}[\text{L}^{\text{VII}}]_2$ .

Solvent masks for poorly resolved and highly disordered interstitial DCM and water molecules were generated for  $\text{Yb}_2[\text{L}^{\text{VII}}]_3$ ,  $\text{Ho}_2[\text{L}^{\text{VII}}]_3$ ,  $\text{Dy}_2[\text{L}^{\text{VII}}]_3$ ,  $\text{Tb}_2[\text{L}^{\text{VII}}]_3$ ,  $\text{Lu}_2[\text{L}^{\text{VII}}]_3$  using Olex<sup>2</sup>.<sup>88</sup> Attempts to converge the  $\text{Eu}_2[\text{L}^{\text{VII}}]_3$  and  $\text{Er}_2[\text{L}^{\text{VII}}]_3$  solutions with the rigor to publish in the Cambridge Crystallographic Data Center were unsuccessful, even by allowing coordinating solvent to be isotropically refined. Projections were created on Olex2.1.<sup>87</sup>

### **NMR Spectroscopy**

<sup>1</sup>H NMR spectra were recorded with a Bruker spectrometer at 600 MHz. <sup>13</sup>C NMR spectra were recorded with a Bruker spectrometer at 151 MHz. NMR spectroscopic data were collected using deuterated chloroform ( $\text{CDCl}_3$ ) or deuterated DMSO ( $D_6$ -DMSO).

### **Absorbance Spectroscopy**

All solution phase absorbance spectra were collected on a VARIAN Cary 50 WinUV Spectrometer with a xenon lamp with absorbance spectra from 200 nm to 900 nm with a 1 cm width quartz cuvette. Solid-state absorbance spectra were collected on a 20/20 PV CRAIC microspectrophotometer with a xenon lamp for transmission/absorbance measurements, with optimized exposure times from single crystals of each respective complex.

### **Fluorescence Spectroscopy**

All solution phase fluorescence spectra were collected on a Shimadzu RF-5301 PC fluorospectrophotometer with a xenon lamp and a 1 cm width quartz cuvette with an excitation of 365 nm and an emission spectrum of 400–900 nm. Slit widths were set so that the maximum emission of the ligand could be seen, and held constant throughout. Solid-state fluorescence spectra were collected on a 20/20 PV CRAIC microspectrophotometer with a mercury lamp for



fluorescence measurements. Samples were excited with 365 nm light with optimized exposure times from single crystals of each respective complex.

### **Computational Details**

The B3LYP functional was chosen combined with the correlation consistent cc-pVDZ basis set for C, N, H, and O atoms. For Ce and Th, the Stuttgart relativistic small-core effective core potentials (RSC-ECP) and their companion basis sets were used. The inner 27 and 80 electrons are represented by the RSC-ECP for Ce and Th, respectively. A set of 5s5p4d3f/Ce and 8s7p6d4f/Th Gaussian basis functions were employed for the rest of the electrons.

The experimental geometries were used as initial structures to optimize the geometry at the B3LYP level. The Gaussian16 package was invoked for this reason.<sup>89</sup> No other low-lying structures (isomers) were located. The TD-DFT calculations for the excited states were done with NWChem.<sup>90</sup> The vertical excitation energies and transition dipole moments were obtained with TD-DFT.

## References

1. Comby, S.; Surender, E. M.; Kotova, O.; Truman, L. K.; Molloy, J. K.; Gunnlaugsson, T., Lanthanide-Functionalized Nanoparticles as MRI and Luminescent Probes for Sensing and/or Imaging Applications. *Inorg. Chem.* **2014**, *53* (4), 1867-1879.
2. Martinić, I.; Eliseeva, S. V.; Petoud, S., Near-infrared Emitting Probes for Biological Omaging: Organic Fluorophores, Quantum Dots, Fluorescent Proteins, Lanthanide(III) Complexes and Nanomaterials. *J. Lumin.* **2017**, *189*, 19-43.
3. Zhang, L.; Tan, C.; Wang, Q.; Zhang, C. C., Anion/Cation Induced Optical Switches Based on Luminescent Lanthanide ( $Tb^{3+}$  and  $Eu^{3+}$ ) Hydrogels. *Photochem. Photobiol.* **2011**, *87* (5), 1036-1041.
4. Werts, M. H. V., Woudenberg, Richard H., Emmerink, Peter G., van Gassel, Rob, Hofstraat, Johannes W., Verhoeven, Jan W., A Near-Infrared Luminescent Label Based on YbIII Ions and Its Application in a Fluoroimmunoassay. *Angew. Chem. Int. Ed.* **2000**, *39* (24), 1521-3773.
5. McAdams, S. G.; Ariciu, A.-M.; Kostopoulos, A. K.; Walsh, J. P. S.; Tuna, F., Molecular single-ion magnets based on lanthanides and actinides: Design considerations and new advances in the context of quantum technologies. *Coord. Chem. Rev.* **2017**, *346*, 216-239.
6. Vincent, R.; Klyatskaya, S.; Ruben, M.; Wernsdorfer, W.; Balestro, F., Electronic read-out of a single nuclear spin using a molecular spin transistor. *Nature* **2012**, *488* (7411), 357-360.
7. Ishikawa, N.; Sugita, M.; Ishikawa, T.; Koshihara, S.-y.; Kaizu, Y., Lanthanide Double-Decker Complexes Functioning as Magnets at the Single-Molecular Level. *J. Am. Chem. Soc.* **2003**, *125* (29), 8694-8695.

8. Rinehart, J. D.; Long, J. R., Slow Magnetic Relaxation in a Trigonal Prismatic Uranium(III) Complex. *J. Am. Chem. Soc.* **2009**, *131* (35), 12558-12559.
9. Sorace, L.; Benelli, C.; Gatteschi, D., Lanthanides in molecular magnetism: old tools in a new field. *Chem. Soc. Rev.* **2011**, *40* (6), 3092-3104.
10. Woodruff, D. N.; Winpenny, R. E. P.; Layfield, R. A., Lanthanide Single-Molecule Magnets. *Chem. Rev.* **2013**, *113* (7), 5110-5148.
11. Lima, P. P.; Paz, F. A. A.; Brites, C. D. S.; Quirino, W. G.; Legnani, C.; Costa e Silva, M.; Ferreira, R. A. S.; Júnior, S. A.; Malta, O. L.; Cremona, M.; Carlos, L. D., White OLED based on a temperature sensitive  $\text{Eu}^{3+}/\text{Tb}^{3+}$   $\beta$ -diketonate complex. *Org. Electron.* **2014**, *15* (3), 798-808.
12. Yao, L.; Zhang, S.; Wang, R.; Li, W.; Shen, F.; Yang, B.; Ma, Y., Highly Efficient Near-Infrared Organic Light-Emitting Diode Based on a Butterfly-Shaped Donor–Acceptor Chromophore with Strong Solid-State Fluorescence and a Large Proportion of Radiative Excitons. *Angew. Chem. Int. Ed.* **2014**, *53* (8), 2119-2123.
13. Maynard, B. A.; Tutson, C. D.; Lynn, K. S.; Pugh, C. W.; Gorden, A. E. V., Actinide ( $\text{Th}^{4+}$  and  $\text{UO}_2^{2+}$ ) assisted oxidative coupling of ortho-phenylenediamine in the presence of oxygen. *Tetrahedron Lett.* **2016**, *57* (4), 472-475.
14. Cui, Y.; Chen, B.; Qian, G., Lanthanide metal-organic frameworks for luminescent sensing and light-emitting applications. *Coord. Chem. Rev.* **2014**, *273*, 76-86.
15. Liu, X.; Lin, H.; Xiao, Z.; Fan, W.; Huang, A.; Wang, R.; Zhang, L.; Sun, D., Multifunctional lanthanide-organic frameworks for fluorescent sensing, gas separation and catalysis. *Dalton Trans.* **2016**, *45* (9), 3743-3749.

16. Muller, J. M.; Galley, S. S.; Albrecht-Schmitt, T. E.; Nash, K. L., Characterization of Lanthanide Complexes with Bis-1,2,3-triazole-bipyridine Ligands Involved in Actinide/Lanthanide Separation. *Inorg. Chem.* **2016**, *55* (21), 11454-11461.
17. Li, P.; Vermeulen, N. A.; Gong, X.; Malliakas, C. D.; Stoddart, J. F.; Hupp, J. T.; Farha, O. K., Design and Synthesis of a Water-Stable Anionic Uranium-Based Metal–Organic Framework (MOF) with Ultra Large Pores. *Angew. Chem.* **2016**, *128* (35), 10514-10518.
18. Li, Y.-J.; Wang, Y.-L.; Liu, Q.-Y., The Highly Connected MOFs Constructed from Nonanuclear and Trinuclear Lanthanide-Carboxylate Clusters: Selective Gas Adsorption and Luminescent pH Sensing. *Inorg. Chem.* **2017**, *56* (4), 2159-2164.
19. Yan, P.-F.; Chen, S.; Chen, P.; Zhang, J.-W.; Li, G.-M., Novel quadridentate salen type triple-decker sandwich ytterbium complexes with near infrared luminescence. *CrystEngComm* **2011**, *13* (1), 36-39.
20. Yang, X.; Jones, R. A.; Wong, W.-K., Anion dependant self-assembly and the first X-ray structure of a neutral homoleptic lanthanide salen complex  $Tb_4(\text{salen})_6$ . *Chem. Commun.* **2008**, (28), 3266-3268.
21. Zhao, X.; Wong, M.; Mao, C.; Trieu, T. X.; Zhang, J.; Feng, P.; Bu, X., Size-Selective Crystallization of Homochiral Camphorate Metal–Organic Frameworks for Lanthanide Separation. *J. Am. Chem. Soc.* **2014**, *136* (36), 12572-12575.
22. Chatziioannou, A. F.; Cherry, S. R.; Shao, Y.; Silverman, R. W.; Meadors, K.; Farquhar, T. H.; Pedarsani, M.; Phelps, M. E., Performance Evaluation of microPET: A High-Resolution Lutetium Oxyorthosilicate PET Scanner for Animal Imaging. *J. Nucl. Med.* **1999**, *40* (7), 1164-1175.

23. Blumenkranz, M. S.; Woodburn, K. W.; Qing, F.; Verdooner, S.; Kessel, D.; Miller, R., Lutetium texaphyrin (Lu-Tex): a potential new agent for ocular fundus angiography and photodynamic therapy. *Am. J. Ophthalmol.* **2000**, *129* (3), 353-362.
24. Hosseini, M.; Ganjali, M. R.; Aboufazeli, F.; Faridbod, F.; Goldooz, H.; Badiei, A.; Norouzi, P., A selective fluorescent bulk sensor for lutetium based on hexagonal mesoporous structures. *Sensors Actuators B: Chem.* **2013**, *184*, 93-99.
25. Zamani, H. A.; Rohani, M.; Zangeneh-Asadabadi, A.; Saleh Zabihi, M.; Ganjali, M. R.; Salavati-Niasari, M., A novel lutetium(III) PVC membrane sensor based on a new symmetric S–N Schiff's base for Lu(III) analysis in real sample. *Mat. Sci. Engin. C* **2010**, *30* (6), 917-920.
26. Bunzli, J.-C. G.; Piguet, C., Taking advantage of luminescent lanthanide ions. *Chem. Soc. Rev.* **2005**, *34* (12), 1048-1077.
27. Cable, M. L.; Kirby, J. P.; Levine, D. J.; Manary, M. J.; Gray, H. B.; Ponce, A., Detection of Bacterial Spores with Lanthanide–Macrocyclic Binary Complexes. *J. Am. Chem. Soc.* **2009**, *131* (27), 9562-9570.
28. Utochnikova, V. V.; Kalyakina, A. S.; Bushmarinov, I. S.; Vashchenko, A. A.; Marciniak, L.; Kaczmarek, A. M.; Van Deun, R.; Brase, S.; Kuzmina, N. P., Lanthanide 9-anthracenate: solution processable emitters for efficient purely NIR emitting host-free OLEDs. *J. Mat. Chem. C* **2016**, *4* (41), 9848-9855.
29. Sun, L.-N.; Yu, J.-B.; Zheng, G.-L.; Zhang, H.-J.; Meng, Q.-G.; Peng, C.-Y.; Fu, L.-S.; Liu, F.-Y.; Yu, Y.-N., Syntheses, Structures and Near-IR Luminescent Studies on Ternary Lanthanide (Er(III), Ho(III), Yb(III), Nd(III)) Complexes Containing 4,4,5,5,6,6,6-Heptafluoro-1-(2-thienyl)hexane-1,3-dionate. *Eur. J. Inorg. Chem.* **2006**, *2006* (19), 3962-3973.

30. Vigato, P. A.; Tamburini, S., The challenge of cyclic and acyclic schiff bases and related derivatives. *Coord. Chem. Rev.* **2004**, *248* (17–20), 1717-2128.
31. Feng, W.; Zhang, Y.; Zhang, Z.; Lü, X.; Liu, H.; Shi, G.; Zou, D.; Song, J.; Fan, D.; Wong, W.-K.; Jones, R. A., Anion-Induced Self-Assembly of Luminescent and Magnetic Homoleptic Cyclic Tetranuclear  $\text{Ln}_4(\text{Salen})_4$  and  $\text{Ln}_4(\text{Salen})_2$  Complexes ( $\text{Ln} = \text{Nd}, \text{Yb}, \text{Er}, \text{or Gd}$ ). *Inorg. Chem.* **2012**, *51* (21), 11377-11386.
32. Yang; Jones, R. A., Anion Dependent Self-Assembly of “Tetra-Decker” and “Triple-Decker” Luminescent Tb(III) Salen Complexes. *J. Am. Chem. Soc.* **2005**, *127* (21), 7686-7687.
33. Mikhalyova, E. A.; Yakovenko, A. V.; Zeller, M.; Gavrilenko, K. S.; Lofland, S. E.; Addison, A. W.; Pavlishchuk, V. V., Structure, magnetic and luminescence properties of the lanthanide complexes  $\text{Ln}_2(\text{Salphen})_3 \cdot \text{H}_2\text{O}$  ( $\text{Ln} = \text{Pr}, \text{Nd}, \text{Sm}, \text{Eu}, \text{Gd}, \text{Tb}, \text{Dy}$ ;  $\text{H}_2\text{Salphen} = \text{N}, \text{N}'$ -bis(salicylidene)-1,2-phenylenediamine). *Inorg. Chim. Acta* **2014**, *414*, 97-104.
34. Chien, Y.-L.; Chang, M.-W.; Tsai, Y.-C.; Lee, G.-H.; Sheu, W.-S.; Yang, E.-C., New salen-type dysprosium(III) double-decker and triple-decker complexes. *Polyhedron* **2015**, *102*, 8-15.
35. Canaj, A. B.; Siczek, M.; Otreba, M.; Lis, T.; Lorusso, G.; Evangelisti, M.; Milios, C. J., Building 1D lanthanide chains and non-symmetrical  $[\text{Ln}_2]$  "triple-decker" clusters using salen-type ligands: magnetic cooling and relaxation phenomena. *Dalton Trans.* **2016**, *45* (46), 18591-18602.
36. Dogaheh, S. G.; Khanmohammadi, H.; Sanudo, E. C., Double-decker luminescent ytterbium and erbium SMMs with symmetric and asymmetric Schiff base ligands. *New J. Chem.* **2017**, *41* (18), 10101-10111.

37. Mougel, V.; Pecaut, J.; Mazzanti, M., New polynuclear U(IV)-U(V) complexes from U(IV) mediated uranyl(V) disproportionation. *Chem. Commun.* **2012**, 48 (6), 868-870.
38. Wu, X.; Bharara, M. S.; Bray, T. H.; Tate, B. K.; Gorden, A. E. V., Synthesis and characterization of 2-quinoxalinol Schiff-base metal complexes. *Inorg. Chim. Acta* **2009**, 362 (6), 1847-1854.
39. Stobbe, B. C.; Powell, D. R.; Thomson, R. K., Schiff base thorium(IV) and uranium(IV) chloro complexes: synthesis, substitution and oxidation chemistry. *Dalton Trans.* **2017**, 46 (15), 4888-4892.
40. Meihaus, K. R.; Long, J. R., Actinide-based single-molecule magnets. *Dalton Trans.* **2015**, 44 (6), 2517-2528.
41. Wu, X.; Bharara, M. S.; Bray, T. H.; Tate, B. K.; Gorden, A. E. V., Synthesis and characterization of 2-quinoxalinol Schiff-base metal complexes. *Inorg. Chim. Acta* **2009**, 362 (6), 1847-1854.
42. Maynard, B. A.; Brooks, J. C.; Hardy, E. E.; Easley, C. J.; Gorden, A. E. V., Synthesis, structural characterization, electronic spectroscopy, and microfluidic detection of Cu<sup>2+</sup> and UO<sub>2</sub><sup>2+</sup> [di-tert-butyl-salphenazine] complexes. *Dalton Trans.* **2015**, 44 (10), 4428-4430.
43. DeVore II, M. A.; Kerns, S. A.; Gorden, A. E. V., Characterization of Quinoxalinol Salen Ligands as Selective Ligands for Chemosensors for Uranium. *Eur. J. Inorg. Chem.* **2015**, 2015 (34), 5708-5714.
44. Hardy, E. E.; Eddy, M. A.; Maynard, B. A.; Gorden, A. E. V., Solid state [small pi]-[small pi] stacking and higher order dimensional crystal packing, reactivity, and electrochemical behaviour of salphenazine actinide and transition metal complexes. *Dalton Trans.* **2016**, 45 (36), 14243-14251.

45. Hardy, E. E.; Wyss, K. M.; Eddy, M. A.; Gorden, A. E. V., An example of unusual pyridine donor Schiff base uranyl ( $\text{UO}_2^{2+}$ ) complexes. *Chem. Commun.* **2017**, 53(42), 5718-5720.
46. Hardy, E. E.; Wyss, K. M.; Keller, R. J.; Gorden, J. D.; Gorden, A. E. V., Tunable ligand emission of naphthylsalophen triple-decker dinuclear lanthanide(III) sandwich complexes. *Dalton Trans.* **2018**, 47 (4), 1337-1346.
47. Hardy, E. E.; Wyss, K. M.; Gorden, J. D.; Ariyaratna, I. R.; Miliordos, E.; Gorden, A. E. V., Th(IV) and Ce(IV) naphthylsalophen sandwich complexes: characterization of unusual thorium fluorescence in solution and solid-state. *Chem. Commun.* **2017**, 53 (88), 11984-11987.
48. Maynard, B. A.; Sykora, R. E.; Mague, J. T.; Gorden, A. E., Actinide tetracyanoplatinates: synthesis and structural characterization with uncharacteristic Th-NC coordination and thorium fluorescence. *Chem Commun (Camb)* **2010**, 46 (27), 4944-6.
49. Kunkely, H.; Vogler, A., Photoluminescence of thorium(IV) 2-methyl-8-quinolinolate. *Chem. Phys. Lett.* **1999**, 304 (3-4), 187-190.
50. Knör, G.; Strasser, A., Coexisting intraligand fluorescence and phosphorescence of hafnium(IV) and thorium(IV) porphyrin complexes in solution. *Inorg. Chem. Commun.* **2002**, 5 (11), 993-995.
51. Adelani, P. O.; Albrecht-Schmitt, T. E., Comparison of Thorium(IV) and Uranium(VI) Carboxyphosphonates. *Inorg. Chem.* **2010**, 49 (12), 5701-5705.
52. Wen, J.; Dong, L.; Hu, S.; Li, W.; Li, S.; Wang, X., Fluorogenic Thorium Sensors Based on 2,6-Pyridinedicarboxylic Acid-Substituted Tetraphenylethenes with Aggregation-Induced Emission Characteristics. *Chemistry – An Asian Journal* **2016**, 11 (1), 49-53.



53. Williams, U. J.; Mahoney, B. D.; Lewis, A. J.; DeGregorio, P. T.; Carroll, P. J.; Schelter, E. J., Single Crystal to Single Crystal Transformation and Hydrogen-Atom Transfer upon Oxidation of a Cerium Coordination Compound. *Inorg. Chem.* **2013**, *52* (8), 4142-4144.
54. Popović, Z.; Roje, V.; Pavlović, G.; Matković-Čalogović, D.; Giester, G., The first example of coexistence of the ketoamino–enolimino forms of diamine Schiff base naphthaldimine parts: the crystal and molecular structure of N,N'-bis(1-naphthaldimine)-o-phenylenediamine chloroform (1/1) solvate at 200 K. *J. Mol. Struct.* **2001**, *597* (1), 39-47.
55. Tutson, C. D.; Gorden, A. E. V., Thorium coordination: A comprehensive review based on coordination number. *Coord. Chem. Rev.* **2017**, *333*, 27-43.
56. Dormond, A.; Belkalem, B.; Charpin, P.; Lance, M.; Vigner, D.; Folcher, G.; Guillard, R., Thorium and uranium porphyrins. Synthesis and crystal structure of bis(acetylacetonato)(2,3,7,8,12,13,17,18-octaethylporphyrinato)thorium(IV). *Inorg. Chem.* **1986**, *25* (26), 4785-4790.
57. Abram, U.; Gatto, C. C.; Bonfada, E.; Schulz Lang, E., Bis{diacetylpyridinebis(benzoylhydrazonato)}thorium(IV) – a novel thorium chelate with coordination number 10. *Inorg. Chem. Commun.* **2002**, *5* (7), 461-463.
58. Hill, R. J.; Rickard, C. E. F., The crystal structure of bis[N,N'-o-phenylenebis(salicylaldiminato)] thorium(IV). *J. Inorg. Nucl. Chem.* **1978**, *40* (12), 2029-2032.
59. Mora, E.; Maria, L.; Biswas, B.; Camp, C.; Santos, I. C.; Pécaut, J.; Cruz, A.; Carretas, J. M.; Marçalo, J.; Mazzanti, M., Diamine Bis(phenolate) as Supporting Ligands in Organoactinide(IV) Chemistry. Synthesis, Structural Characterization, and Reactivity of Stable Dialkyl Derivatives. *Organometallics* **2013**, *32* (5), 1409-1422.

60. Aghabozorg, H.; Palenik, R. C.; Palenik, G. J., A ten-coordinate oxo-bridged thorium complex with an unusual coordination polyhedron. *Inorg. Chim. Acta* **1983**, *76*, L259-L260.
61. Szłyk, E.; Wojtczak, A.; Dobrzańska, L.; Barwiołek, M., X-ray crystal structure and nuclear Overhauser effect studies of cerium(IV) complexes with Schiff bases obtained from N,N'-(1R,2R)(-)-1,2-cyclohexanediamine and benzaldehyde derivatives. *Polyhedron* **2008**, *27* (2), 765-776.
62. Gottfriedsen, J.; Spoida, M.; Blaurock, S., Synthesis and Structure of the Cerium Schiff-Base Complexes [Ce(Salen')<sub>2</sub>] and [(THF)<sub>2</sub>KCe(Salen')<sub>2</sub>]. *Z. Anorg. Allg. Chem.* **2008**, *634* (3), 514-518.
63. Terzis, A.; Mentzafos, D.; Tajmir-Riahi, H. A., Eight-coordination. Synthesis and structure of the schiff-base chelate bis(N,N'-disalicylidene-1,2-phenylenediamino)cerium(IV). *Inorg. Chim. Acta* **1984**, *84* (2), 187-193.
64. Taha, Z. A.; Ajlouni, A. M.; Al Momani, W.; Al-Ghzawi, A. A., Syntheses, characterization, biological activities and photophysical properties of lanthanides complexes with a tetradentate Schiff base ligand. *Spectrochimica Acta Part A: Molecular and Biomolecular Spectroscopy* **2011**, *81* (1), 570-577.
65. Uh, H.; Badger, P. D.; Geib, S. J.; Petoud, S., Synthesis and Solid-State, Solution, and Luminescence Properties of Near-Infrared-Emitting Neodymium(3+) Complexes Formed with Ligands Derived from Salophen. *Helv. Chim. Acta* **2009**, *92* (11), 2313-2329.
66. Panayiotidou, L.; Drouza, C.; Arabatzis, N.; Lianos, P.; Stathatos, E.; Viskadourakis, Z.; Giapintzakis, J.; Keramidas, A. D., Structure, reactivity, luminescence and magnetism of dinuclear Ln<sup>3+</sup> complexes produced by the Ln<sup>3+</sup>-assisted hydrolysis of 3,6-bis(2-pyridyl)tetrazine. *Polyhedron* **2013**, *64*, 308-320.

67. Li, Q.; Yan, P.; Chen, P.; Hou, G.; Li, G., Salen Type Sandwich Triple-Decker Tri- and Di-nuclear Lanthanide Complexes. *Journal of Inorganic and Organometallic Polymers and Materials* **2012**, *22* (5), 1174-1181.
68. Koo, B. H.; Lim, K. S.; Ryu, D. W.; Lee, W. R.; Koh, E. K.; Hong, C. S., Synthesis, structures and magnetic characterizations of isostructural tetranuclear Ln<sub>4</sub> clusters (Ln = Dy, Ho, and Eu). *Dalton Trans.* **2013**, *42* (19), 7204-7209.
69. Liu, T.-Q.; Yan, P.-F.; Luan, F.; Li, Y.-X.; Sun, J.-W.; Chen, C.; Yang, F.; Chen, H.; Zou, X.-Y.; Li, G.-M., Near-IR Luminescence and Field-Induced Single Molecule Magnet of Four Salen-type Ytterbium Complexes. *Inorg. Chem.* **2015**, *54* (1), 221-228.
70. Yang, X.-P.; Jones, R. A.; Oye, M. M.; Holmes, A. L.; Wong, W.-K., Near Infrared Luminescence and Supramolecular Structure of a Helical Triple-Decker Yb(III) Schiff Base Cluster. *Crystal Growth & Design* **2006**, *6* (9), 2122-2125.
71. Koo, B. H.; Lim, K. S.; Ryu, D. W.; Lee, W. R.; Koh, E. K.; Hong, C. S., A unique tetranuclear Er(III)<sub>4</sub> cluster exhibiting field-induced single-molecule magnetism. *Chem. Commun.* **2012**, *48* (19), 2519-2521.
72. Yang, F.; Yan, P.; Li, Q.; Chen, P.; Li, G., Salen-Type Triple-Decker Trinuclear Dy<sub>3</sub> Complexes Showing Slow Magnetic Relaxation Behavior. *Eur. J. Inorg. Chem.* **2012**, *2012* (27), 4287-4293.
73. Zhu, J.; Song, H.-F.; Yan, P.-F.; Hou, G.-F.; Li, G.-M., Slow relaxation processes of salen type Dy<sub>2</sub> complex and 1D ionic spiral Dy<sub>n</sub> coordination polymer. *CrystEngComm* **2013**, *15* (9), 1747-1752.
74. Arnold, P. L.; Hollis, E.; Nichol, G. S.; Love, J. B.; Griveau, J.-C.; Caciuffo, R.; Magnani, N.; Maron, L.; Castro, L.; Yahia, A.; Odoh, S. O.; Schreckenbach, G., Oxo-

Functionalization and Reduction of the Uranyl Ion through Lanthanide-Element Bond Homolysis: Synthetic, Structural, and Bonding Analysis of a Series of Singly Reduced Uranyl–Rare Earth  $5f_1$ – $4f_n$  Complexes. *J. Am. Chem. Soc.* **2013**, *135* (10), 3841-3854.

75. Kiernicki, J. J.; Cladis, D. P.; Fanwick, P. E.; Zeller, M.; Bart, S. C., Synthesis, Characterization, and Stoichiometric U–O Bond Scission in Uranyl Species Supported by Pyridine(diimine) Ligand Radicals. *J. Am. Chem. Soc.* **2015**, *137* (34), 11115-11125.

76. Arnold, P. L.; Pécharman, A.-F.; Lord, R. M.; Jones, G. M.; Hollis, E.; Nichol, G. S.; Maron, L.; Fang, J.; Davin, T.; Love, J. B., Control of Oxo-Group Functionalization and Reduction of the Uranyl Ion. *Inorg. Chem.* **2015**, *54* (7), 3702-3710.

77. Hao, Z.; Song, X.; Zhu, M.; Meng, X.; Zhao, S.; Su, S.; Yang, W.; Song, S.; Zhang, H., One-dimensional channel-structured Eu-MOF for sensing small organic molecules and  $\text{Cu}^{2+}$  ion. *J. Mat. Chem. A* **2013**, *1* (36), 11043-11050.

78. Wang, L. L.; Luo, F.; Dang, L. L.; Li, J. Q.; Wu, X. L.; Liu, S. J.; Luo, M. B., Ultrafast high-performance extraction of uranium from seawater without pretreatment using an acylamide- and carboxyl-functionalized metal-organic framework. *Journal of Materials Chemistry A* **2015**, *3* (26), 13724-13730.

79. Singh, H.; Sindhu, J.; Khurana, J. M., Synthesis of novel fluorescence xanthene–aminoquinoline conjugates, determination of dipole moment and selective fluorescence chemosensor for  $\text{Th}^{4+}$  ions. *Opt. Mater.* **2015**, *42*, 449-457.

80. Maynard, B. A.; Sykora, R. E.; Mague, J. T.; Gordon, A. E. V., Actinide tetracyanoplatinates: synthesis and structural characterization with uncharacteristic Th-NC coordination and thorium fluorescence. *Chem. Commun.* **2010**, *46* (27), 4944-4946.

81. Yu, C.; Wu, Q.; Wang, J.; Wei, Y.; Hao, E.; Jiao, L., Red to Near-Infrared Isoindole BODIPY Fluorophores: Synthesis, Crystal Structures, and Spectroscopic and Electrochemical Properties. *J. Org. Chem.* **2016**, *81* (9), 3761-3770.
82. Sathyaraj, G.; Nair, B. U., Unusual solvent dependent emission property of two new ruthenium(II) complexes. *Inorg. Chim. Acta* **2013**, *402*, 75-82.
83. Kowalczyk, T.; Lin, Z.; Voorhis, T. V., Fluorescence Quenching by Photoinduced Electron Transfer in the Zn<sup>2+</sup> Sensor Zinpyr-1: A Computational Investigation. *J. Phys. Chem. A* **2010**, *114* (38), 10427-10434.
84. Heinrich, G.; Schoof, S.; Gusten, H., 9,10-diphenylanthracene as a fluorescence quantum yield standard. *J. Photochem.* **1974**, *3* (2), 315-320.
85. Bruker Bruker AXS Inc.: Madison, Wisconsin, USA, 2001.
86. Sheldrick, G. M., *Acta Crystallogr., Sect. A: Found. Crystallogr.* **2008**, *A64*, 112.
87. Dolomanov, O. V.; Bourhis, L. J.; Gildea, R. J.; Howard, J. A. K.; Puschmann, H., OLEX2: A complete structure solution, refinement and analysis program. *J. Appl. Cryst.* **2009**, *42*, 339-341.
88. Bourhis, L. J.; Dolomanov, O. V.; Gildea, R. J.; Howard, J. A. K.; Puschmann, H., The anatomy of a comprehensive constrained, restrained refinement program for the modern computing environment - Olex2 dissected. *Acta Crystallogr.* **2015**, *A71* (1), 59-75.
89. Frisch, M. J.; Trucks, G. W.; Schlegel, H. B.; Scuseria, G. E.; Robb, M. A.; Cheeseman, J. R.; Scalmani, G.; Barone, V.; Petersson, G. A.; Nakatsuji, H.; Li, X.; Caricato, M.; Marenich, A. V.; Bloino, J.; Janesko, B. G.; Gomperts, R.; Mennucci, B.; Hratchian, H. P.; Ortiz, J. V.; Izmaylov, A. F.; Sonnenberg, J. L.; Williams; Ding, F.; Lipparini, F.; Egidi, F.; Goings, J.; Peng, B.; Petrone, A.; Henderson, T.; Ranasinghe, D.; Zakrzewski, V. G.; Gao, J.; Rega, N.; Zheng, G.;

Liang, W.; Hada, M.; Ehara, M.; Toyota, K.; Fukuda, R.; Hasegawa, J.; Ishida, M.; Nakajima, T.; Honda, Y.; Kitao, O.; Nakai, H.; Vreven, T.; Throssell, K.; Montgomery Jr., J. A.; Peralta, J. E.; Ogliaro, F.; Bearpark, M. J.; Heyd, J. J.; Brothers, E. N.; Kudin, K. N.; Staroverov, V. N.; Keith, T. A.; Kobayashi, R.; Normand, J.; Raghavachari, K.; Rendell, A. P.; Burant, J. C.; Iyengar, S. S.; Tomasi, J.; Cossi, M.; Millam, J. M.; Klene, M.; Adamo, C.; Cammi, R.; Ochterski, J. W.; Martin, R. L.; Morokuma, K.; Farkas, O.; Foresman, J. B.; Fox, D. J. *Gaussian 16*, Wallingford, CT, 2016.

90. Valiev, M.; Bylaska, E. J.; Govind, N.; Kowalski, K.; Straatsma, T. P.; Van Dam, H. J. J.; Wang, D.; Nieplocha, J.; Apra, E.; Windus, T. L.; de Jong, W. A., NWChem: A comprehensive and scalable open-source solution for large scale molecular simulations. *Comput. Phys. Commun.* **2010**, *181* (9), 1477-1489.

## Chapter 5: Conclusions and Future Work

### Conclusions

The systematic characterization by X-ray crystallography and UV-visible spectroscopy salphenazine ligand ( $H_2L^I$ , shown in **Figure 5.1**), containing the O-N-N-O salen type bonding motif and corresponding metal complexes was achieved. These complexes revealed the extended  $\pi$ -conjugation of these ligands results in differentiation of a uranyl ( $UO_2^{2+}$ ) signal as compared to other +2 metal ions or transition metals. The solid-state characterization of this series provides insight to the preferred coordination environment of the uranyl ion in these conjugated systems. These insights can guide further design improvements in the development of ligands with extended conjugation to be used as on-site actinide chemosensors.

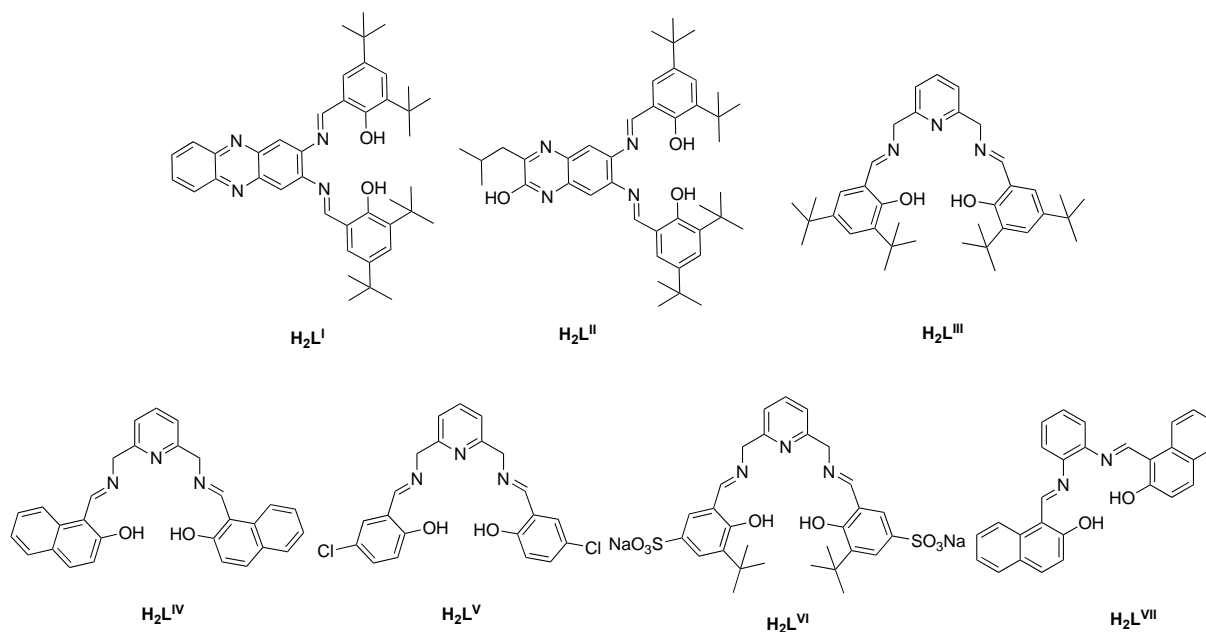


**Figure 5.1.** Projection of ligands discussed in this work

The pentadentate binding of the new ligands  $\text{H}_2\text{L}^{\text{III}}\text{-H}_2\text{L}^{\text{VI}}$ , which fully occupy the uranyl equatorial plane, removed the necessity of a coordinating solvent molecule or ligand rearrangement allowing to quickly and selectively bind uranyl in a one-to-one fashion. The  $\text{UO}_2[\text{L}^{\text{III}}]$  and  $\text{UO}_2[\text{L}^{\text{IV}}]$  complexes with uncommon pyridine coordination were synthesized and characterized in solution and in the solid state and found to have short U- $\text{N}_{\text{py}}$  distances as compared to the literature. These complexes have a distinct response for uranyl over common first-row transition metals in the UV and provide an example of uncommon binding for uranyl. The pyridine moiety and pentadentate coordination environment were shown to increase binding kinetics and affinity for uranyl of this system.

Eleven lanthanide double decker sandwich complexes ( $\text{Ln}_2[\text{L}^{\text{VII}}]_3$ ) were synthesized and characterized in the solid-state and in solution. The minimal structural differences in the  $\text{Nd}_2[\text{L}^{\text{VII}}]_3$ ,  $\text{Eu}_2[\text{L}^{\text{VII}}]_3$ ,  $\text{Gd}_2[\text{L}^{\text{VII}}]_3$ ,  $\text{Tb}_2[\text{L}^{\text{VII}}]_3$ ,  $\text{Dy}_2[\text{L}^{\text{VII}}]_3$ ,  $\text{Ho}_2[\text{L}^{\text{VII}}]_3$ ,  $\text{Er}_2[\text{L}^{\text{VII}}]_3$ ,  $\text{Yb}_2[\text{L}^{\text{VII}}]_3$ , and  $\text{Lu}_2[\text{L}^{\text{VII}}]_3$  analogues resulted in tunable solution emission properties, but it is more apparent in the solid-state luminescence with  $\text{Sm}_2[\text{L}^{\text{VII}}]_3$  emission at 556 nm to  $\text{Er}_2[\text{L}^{\text{VII}}]_3$  emission at 617 nm. Lutetium exhibited a large increase in fluorescence as compared to the other  $\text{Ln}_2[\text{L}^{\text{VII}}]_3$  complexes in the solid state, providing a rare opportunity to differentiate one of the 14 lanthanides. The completeness of this solid-state series is quite uncommon in the literature, and allows for a rare example of explaining differing properties through small changes in the coordination environment.

The complex  $\text{Th}[\text{L}^{\text{VII}}]_2$  was observed to fluoresce in both solid-state and solution phase, which at this point is unprecedented in the literature. This is the first reported example of a compound containing thorium that exhibits emission in the solid-state and solution. The quenching of the isoelectronic  $\text{Ce}[\text{L}^{\text{VII}}]_2$  complex was explained by the possible quenching

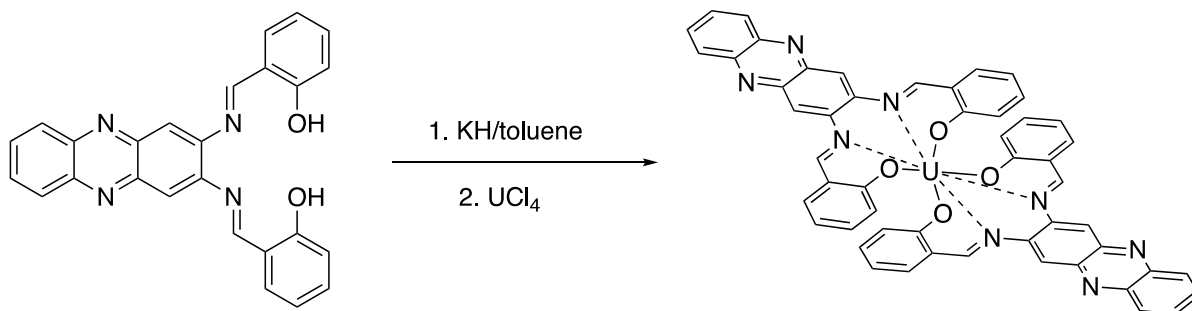


pathway involving the Ce(III)/(IV) redox couple, which is inaccessible in the thorium analogue. Solvent dependence of emission was observed and may be due to solvent coordination in the 8 and 9-coordinate equilibrium of  $\text{Th}[\text{L}^{\text{VII}}]_2$  in solution, and adds to the knowledge about the coordination chemistry of thorium. The  $\text{UO}_2 [\text{L}^{\text{VII}}]$  complex was found to crystallize in a hydrogen bonded tetramer, with coordinated water molecules hydrogen bonding to the  $-\text{yl}$  oxygen of the symmetrically inequivalent U atom. This finding was intriguing and suggests further study of  $-\text{yl}$  activation with naphthylsalophen derivatives may be of interest.

## Future Work

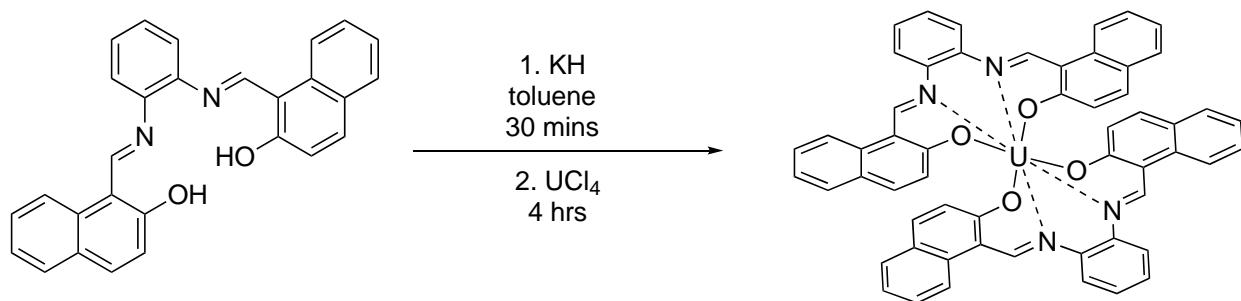
### U(IV) Complexes with Redox Active Ligands

The use of redox active ligands to stabilize low valent uranium has been of interest as the basis for new catalysts in recent years.<sup>1-4</sup> Such redox-active ligands would allow for electrons to be stored not only in the metal center, but also in the ligand framework for possible future use in multielectron catalysis.<sup>5</sup> The ligands described in Chapter 2 and Chapter 4 are prime candidates for this type of chemistry and could be explored for these purposes. A proposed synthesis for a U(IV) compound using  $\text{H}_2\text{L}^{\text{I}}$  is shown below in **Scheme 5.1**.



**Scheme 5.1.** General synthetic scheme for U(IV) salphenazine complex,  $\text{U}[\text{L}^{\text{I}}]_2$ .

Through deprotonation of the free base ( $\text{H}_2\text{L}^{\text{I}}$ ) using the strong base potassium hydride, products with the more difficult to complex  $\text{UCl}_4$  can be obtained. Precautions to rigorously exclude water and air from the reaction flask must be taken. Another proposed synthesis, incorporating  $\text{H}_2\text{L}^{\text{VII}}$ , is shown in **Scheme 5.2**. Single crystals of these should be obtained for detailed characterization as a solid. Single crystals suitable for X-ray diffraction of the earlier structures were obtained through slow diffusion of hexanes into toluene for similar systems, and should be one combination attempted. Crystals of analogous systems were also grown from slow diffusion of hexanes into DCM and ether into acetonitrile.

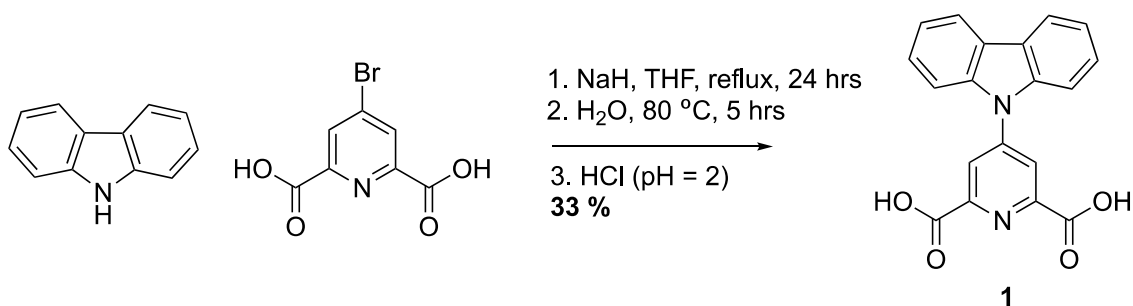


**Scheme 5.2.** General synthetic scheme for naphthylsalophen U(IV) complex,  $\text{U}[\text{L}^{\text{VII}}]_2$ .

Once these compounds and the derivatives thereof are synthesized and characterized, the electrochemical analysis of these species would also be of great interest. As mentioned in Chapter 2, the extended conjugation of the pi-system can provide stabilization of the U(V)/U(VI) redox couple. Investigation the U(III)/(IV) couple may be useful as many proposed uranium catalysts use the III/IV couple in their proposed mechanisms. Stabilization of any of these reduction potentials would be of intense interest and are similar to examples in the literature from actinide coordination chemistry research groups such as those of Polly Arnold, Marienella Mazzanti, and Suzanne Bart.<sup>2, 4, 6</sup> Understanding uranium chemistry at these oxidation states can also be used as model for plutonium and neptunium chemistry, which are more often found in their low valent states.<sup>7-8</sup>

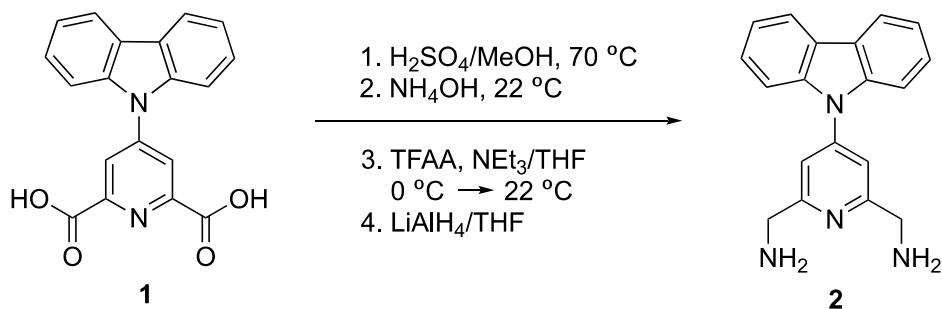
### Increasing the Extinction Coefficient of $[H_2L^{III}]$

As was discussed in Chapter 3, the pentadentate binding environment of  $H_2L^{III}$  increases the binding kinetics, but there is a significant loss in extinction coefficient and consequently, signal to noise. One avenue to remedy this issue would be to add a fluorophore, or a more highly absorbing tag, into the synthetic pathway. Ana DeBettencourt-Dias and coworkers recently published a synthesis to form compound **1**, shown below as an antenna to bind lanthanide ions and absorb light in the visible spectrum.<sup>9</sup> The amine in **Scheme 5.3** is readily available and the brominated dipicolinic acid derivative is commercially available. This could be reacted with an acidic work-up to achieve the synthesis of **1**.



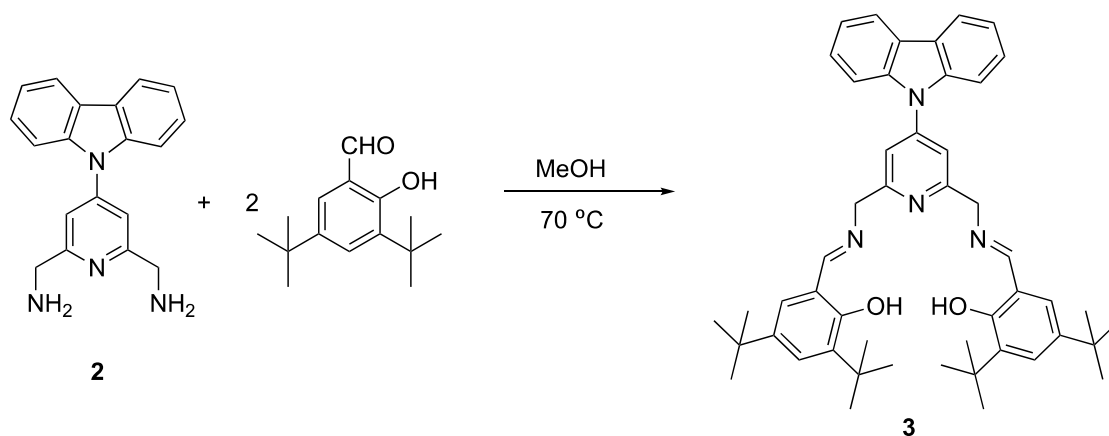
**Scheme 5.3.** Synthetic scheme for form compound **1**.<sup>9</sup>

Using compound **1** as a starting material in the synthetic pathway for ligands like those from Chapter 3 could yield a new ligand system with an increased extinction coefficient, without altering the binding pocket that previously resulted in such fast binding kinetics. The addition of the tertiary amine should be tolerant to the conditions listed in **Scheme 5.4** and should result in the formation of compound **2**, a diamine; however, optimization of the conditions may not be straightforward.



**Scheme 5.4.** Proposed synthetic scheme to form compound **2**

After formation of **2**, synthesizing **3** (**Scheme 5.5**) or derivatives thereof would allow ligands like those described in Chapter 3 to absorb more light, and the limit of detection for uranyl should be decreased. Compound **3** contains  $\text{sp}^3$  hybridized carbon atoms that are easily oxidized and this could complicate the synthetic pathway. Due to this complexity, synthesis of compound **3** may require additional optimization, especially during purification. The salicylaldehyde shown below in **Scheme 5.5** is 3,5-ditert-butylsalicylaldehyde, but other salicylaldehyde starting materials may be chosen to change the electronic character of the ligand. These compounds would also be more soluble than the salphenazine derivatives described in Chapter 2. This could eliminate the use of pyridine as a solvent while still providing a stronger absorption on complexation. If compound **3** has a high molar extinction coefficient and can be synthesized in a reasonable yield, and also quickly bind uranyl, then it could be useful in possible applications such as color changing paints, incorporation onto solid-state supports, and in-the-field detection of uranyl.



**Scheme 5.5.** Synthesis for formation of **3**, a derivative of  $[\text{H}_2\text{L}^{\text{III}}]$ .

### Naphthylsalophen Derivatives

One new direction for research would be the preparation and characterization of the naphthylsalophen analogues  $[\text{H}_2\text{L}^{\text{VIII}}]$  to  $[\text{H}_2\text{L}^{\text{XII}}]$ , featuring examples of strongly and mildly electron donating or withdrawing groups, and the corresponding metal complexes. These derivatives would be of interest in probing the electronic effects of systematic modification to the ligand, and could be easily synthesized and utilized to investigate the electronic properties of thorium emission, cerium oxidation state stabilization, and lanthanide antenna effect. An example of proposed naphthylsalophen derivatives can be found in **Figure 5.2**. The necessary diamines for the synthesis of  $[\text{H}_2\text{L}^{\text{VIII}}]$ ,  $[\text{H}_2\text{L}^{\text{X}}]$ , and  $[\text{H}_2\text{L}^{\text{XI}}]$  are commercially available. The diamine necessary for  $[\text{H}_2\text{L}^{\text{IX}}]$ , 1,2-diamino-4-methoxybenzene, can be synthesized by the reduction of the inexpensive and commercially available 1,2-dinitro-4-methoxybenzene via **Scheme 5.7**.

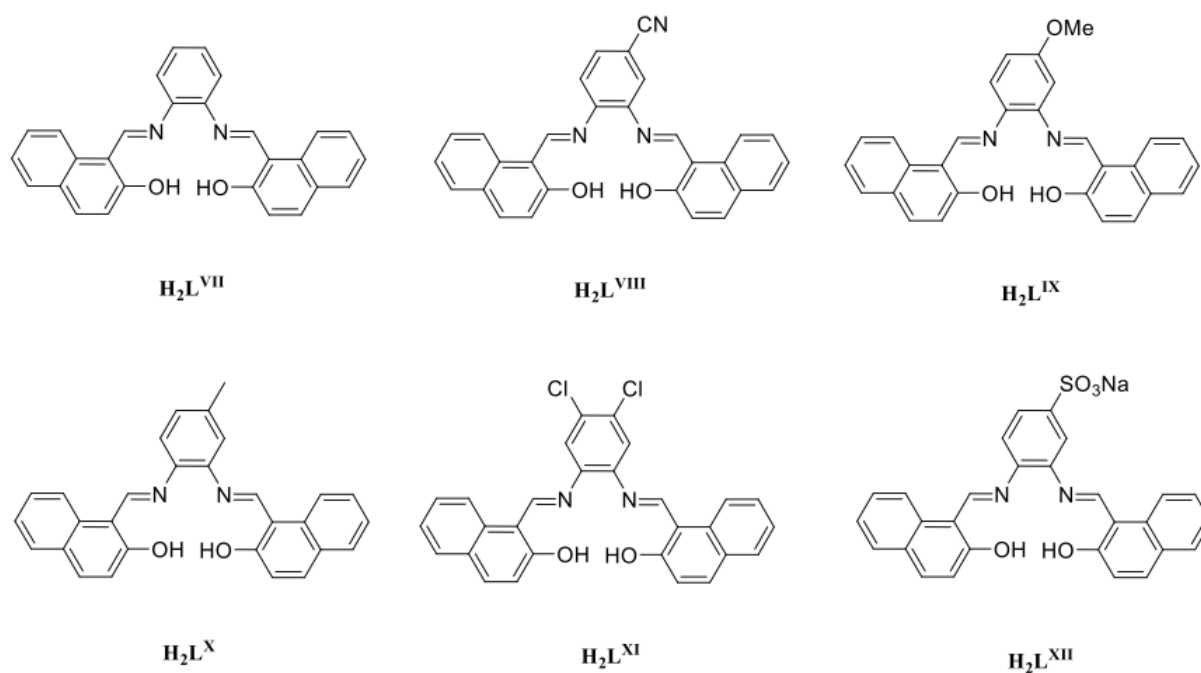
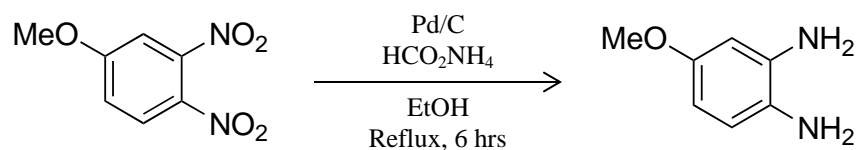
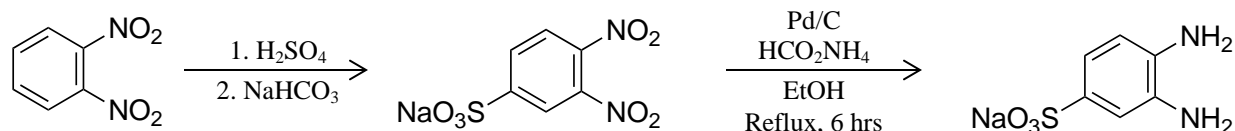


**Figure 5.2.** Proposed naphthylsalophen derivatives



**Scheme 5.7.** Synthetic scheme for the formation of 1,2-diamino-4-methoxybenzene.

A water-soluble analogue would be especially useful in this library of naphthylsalophen ligands. The diamine necessary for  $[\text{H}_2\text{L}^{\text{XII}}]$ , 1,2-diamino-4-sulfobenzene, can be synthesized through the sulfonation and reduction of 1,2-dinitrobenzene, shown in **Scheme 5.8**. If formation of this ligand could be achieved, sensing of uranyl in contaminated ground water could be investigated.



**Scheme 5.8.** Proposed synthetic scheme for the formation of 1,2-diamino-4-sulfobenzene.

Differences in the steric hindrance of groups may also be of interest, as the multi-decker sandwiches complexes may be disrupted and could lead to interesting electronics and packing effects. The derivatives suggested in **Figure 5.2** minimize the steric influence of the additional groups, but *t*-butyl or isopropyl analogues may elucidate the steric factor with these systems. Once a library of naphthylsalophen derivatives is synthesized and characterized, attempts to coordinate these ligands to uranyl, thorium, cerium, and lanthanides should be attempted.

The differences and ability to tune unusual emission from a thorium complex with these compounds would be of interest. The cerium(IV) analogues of these compounds would also be of interest to see if the same stabilization of the Ce(III)/Ce(IV) redox couple is observed (further explained below). If the lanthanide derivatives of these ligands were to be synthesized, particular care and urgency should be applied to the ytterbium, erbium, and neodymium complexes. These could be investigated for their possible use as near infrared (NIR) emitters and may have potential biological imaging applications. The gadolinium complexes may also be of interest, if the magnetic properties of these compounds were to be characterized using a variable temperature magnetometer. Multimetallc lanthanide compounds that self-assemble in a predictable fashion are uncommon and this system could be a good model to further explore f-block coordination chemistry. Compounds of this type have been used in medicinal applications as well as for molecular machines and single molecule magnets,<sup>10-11</sup> and would have interesting applications in addition to their interesting fundamental chemistry.

## Ceric(IV) Ammonium Nitrate (CAN) Oxidations and Ce[L<sup>VII</sup>]<sub>2</sub> Derivatives

Tangential to this, a completely new direction to be explored would be to characterize the coordination chemistry and unusual oxidation state stabilization of Ce[L<sup>VII</sup>]<sub>2</sub> introduced in Chapter 4. Electrochemical analysis of Ce[L<sup>VII</sup>]<sub>2</sub>, as well as the cerium complexes with naphthylsalophen derivatives mentioned earlier in this chapter (**Figure 5.1**), would be an interesting endeavor. Cerium is most commonly found as the Ce(III) salt and, in fact, ceric ammonium nitrate (CAN) oxidations using Ce(IV) as a single electron oxidant are prevalent in organic chemistry.<sup>12-13</sup> These oxidations often take place in mixed solvent systems and require stoichiometric amounts of cerium.<sup>13</sup> The cerium-containing compound is a single-electron oxidant, reducing the cerium metal from Ce(IV) to Ce(III) and must often be added in excess to do common oxidation transformations.<sup>12</sup> There are examples of catalytic CAN oxidations, but they require a co-oxidant to regenerate the reactive Ce(IV) species. The ability to use an organic scaffold that would be able to use molecular oxygen to regenerate the active cerium species would reduce the overall amounts of cerium salts required, as well as the need for mixed organic and aqueous reaction mixtures. Both of these would, in turn, reduce the overall amounts of waste generated.

Understanding the coordination chemistry of cerium compounds and producing a compound that can shift the redox potentials of this useful metal would be of great interest towards this end. Using an organic compound to stabilize the Ce(IV) oxidation state has been witnessed and explained by Eric Shelter and coworkers,<sup>14-15</sup> but further investigation into the compound presented here (Ce[L<sup>VII</sup>]) may lead to another example of shifting the Ce(III)/Ce(IV) redox potential.<sup>14</sup> The stabilization that Shelter and coworkers found amounted to be 1.2 V; this



large stabilization is likely occurring in the Ce[L<sup>VII</sup>] system as well, and would be of great interest as the focus of future study. If the Ce[L<sup>VII</sup>] ligand system could be properly tuned, it could be used as a catalyst to oxidize organic materials and then be regenerated in-situ using molecular oxygen as the oxidant rather than as a sacrificial oxidant. This is a potentially greener way to carry out oxidations and as this ligand is very soluble in organic solvents, would eliminate the need for mixed solvent systems that are often necessary for CAN oxidations. This Ce(III)/Ce(IV) redox chemistry is also of great interest as a model for Pu(III)/Pu(IV) oxidation chemistry.<sup>7</sup>

### Macrocyclic Chemosensors

Another way to overcome binding kinetics and overcome the need for the fifth coordinating solvent in the uranyl binding sphere would be to make a macrocycle that will eliminate the need for coordinating solvent. Many research groups have employed this strategy but key examples are from the Sessler group.<sup>16-17</sup> The binding pocket of **4** has the same number of atoms that are present in the recently published macrocycle (**5**) which enabled the a parts per billion sensor of uranyl.<sup>17</sup> These compounds require many synthetic steps and are not trivial to isolate.<sup>17</sup> The size of the coordination pocket is highlighted below in **Figure 5.2**. Synthesis of this compound **4** with the inclusion of the highly fluorescent quinoxalinol backbone would be of interest spectroscopically and has a reasonable chance to bind uranyl quickly and efficiently.

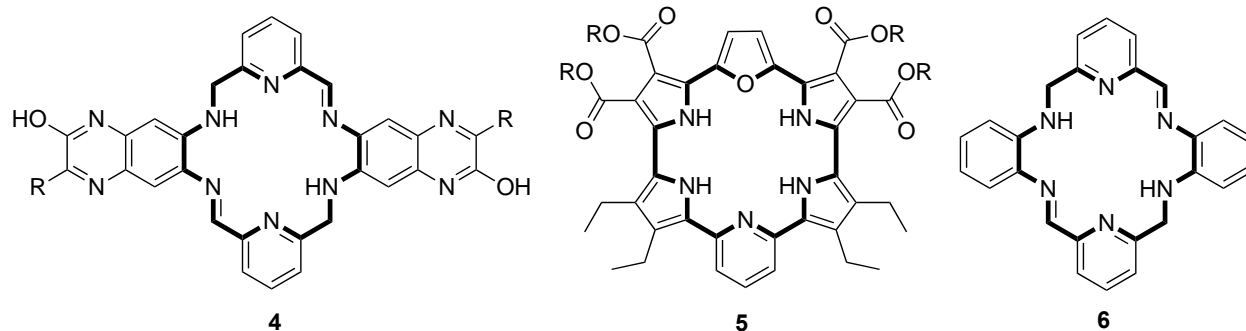
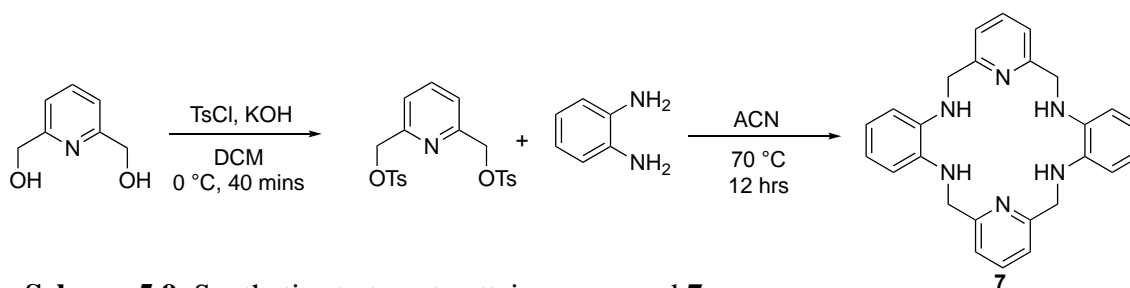


**Figure 5.3.** Proposed salqu derivatized macrocyle (compound **4**), parts per billion sensor for uranyl (compound **5**) reported by Sessler and Jokerst, and proposed benzene derivatized macrocycle (compound **6**).<sup>17</sup>

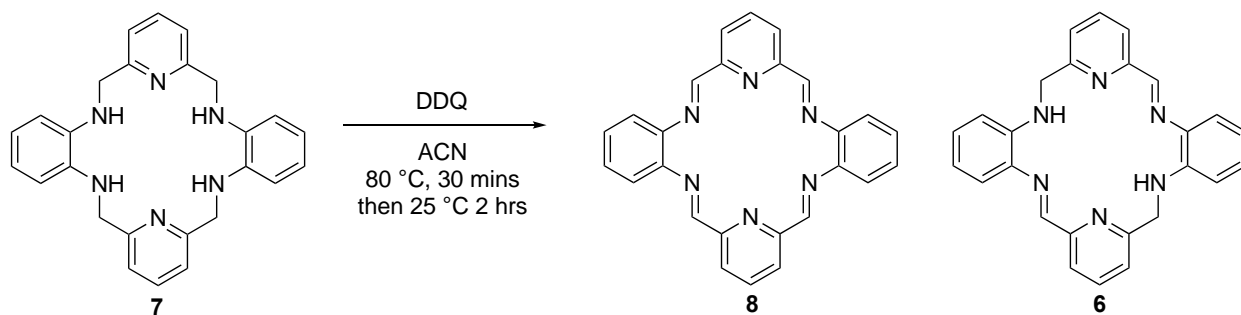
In order to attain **4** the model **6** would be useful to synthesize first, as the reagents necessary are commercially available and plentiful. Two possible synthetic routes will be described here. The synthesis of tetraamine **7** can be achieved through the synthetic pathway described in **Scheme 5.9**. First, tosyl chloride could be added to 2,6-pyridinedimethanol under basic conditions to result in a tosylated pyridine starting material. A simple S<sub>N</sub>2 type reaction with a desired diamine (1,2-diaminobenzene) could then be conducted to yield **7**. These compounds will require synthetic optimization and will form many polymeric byproducts.



**Scheme 5.9.** Synthetic strategy to attain compound **7**

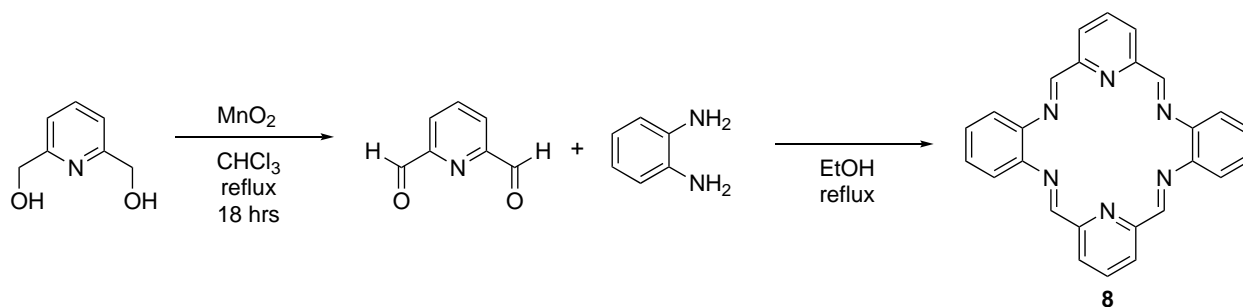
This compound may prove difficult to isolate as amines can be difficult to separate with column chromatography, but recrystallization could be attempted. These syntheses are not trivial and often require multiple columns and complexation with a metal center may aid in separation. Previous examples of metal templation with these “aza-crown” type compounds have been

achieved using strontium triflate, and may be useful here.<sup>18-19</sup> Further oxidation with 2,3-dichloro-5,6-dicyano-1,4-benzoquinone (DDQ) of the amines may also result in a product that is more amiable to column chromatography and is shown in **Scheme 5.10**. It is likely that a mixture of products **6** and **8** will be formed and need to be isolated. These compounds will be extremely polar contain free amines, which are notoriously difficult to separate by column chromatography. The optimization for compound **6** with the commercially available starting materials listed in **Scheme 5.9** will be useful before attempts to make the quinoxalinol derivative (compound **4**) are made.



**Scheme 5.10.** Synthetic strategy to synthesize compounds **8** and **6**.

Another, more direct route to form **8** may be achieved through oxidation of the 2,6-pyridinedimethanol starting material using a soft oxidant  $\text{MnO}_2$  in chloroform (**Scheme 5.11**). The resulting 2,6-pyridinedicarboxaldehyde could then be added to 1,2-diaminobenzene and after four successive condensation reactions formation of **8** could be achieved. As with any macrocycle synthesis, polymerization rather than cyclization may occur and high dilution could be used to limit the possible polymerization or side products. Regardless, the conditions for the cyclization will need to be optimized.



**Scheme 5.11.** Proposed alternate synthetic strategy to form compound **8**.

Any of the macrocyclic compounds (**6**, **7**, or **8**) would be of interest if bound to uranyl and the best synthetic route to form these compounds could then be applied using quinoxalino diamine derivatives to yield macrocycle **4**. Similar compounds have also been used with f-block elements in recent years and have been extremely successful sequestration agents with photoacoustic medical applications.<sup>17,20</sup> Few crystal structures exist of these particular compounds and solid-state characterization of these compounds would be of interest in their own right, as well as the potential use in detection of actinides.

The proposed projects described here are potential avenues to learn about the fundamental coordination chemistry of actinides. The insights from the research described and proposed in this work may lead to a better understanding of environmental incorporation, selective detection, or selective extraction of these metal ions. This knowledge could potentially be applied as new waste remediation technologies or in new applications such as single molecule magnets or catalysis. New actinide properties and unexpected results are often achieved, as was reported in this work, due to the comparatively small amount of fundamental research and flexibility in both oxidation state and coordination environment of the actinides.

## References

1. Anderson, N. H.; Odoh, S. O.; Yao, Y.; Williams, U. J.; Schaefer, B. A.; Kiernicki, J. J.; Lewis, A. J.; Goshert, M. D.; Fanwick, P. E.; Schelter, E. J.; Walensky, J. R.; Gagliardi, L.; Bart, S. C., Harnessing redox activity for the formation of uranium tris(imido) compounds. *Nat. Chem.* **2014**, *6* (10), 919-926.
2. Kiernicki, J. J.; Cladis, D. P.; Fanwick, P. E.; Zeller, M.; Bart, S. C., Synthesis, Characterization, and Stoichiometric U–O Bond Scission in Uranyl Species Supported by Pyridine(diimine) Ligand Radicals. *J. Am. Chem. Soc.* **2015**, *137* (34), 11115-11125.
3. Anderson, N. H.; Odoh, S. O.; Williams, U. J.; Lewis, A. J.; Wagner, G. L.; Lezama Pacheco, J.; Kozimor, S. A.; Gagliardi, L.; Schelter, E. J.; Bart, S. C., Investigation of the Electronic Ground States for a Reduced Pyridine(diimine) Uranium Series: Evidence for a Ligand Tetraanion Stabilized by a Uranium Dimer. *J. Am. Chem. Soc.* **2015**, *137* (14), 4690-4700.
4. Bell, N. L.; Shaw, B.; Arnold, P. L.; Love, J. B., Uranyl to Uranium(IV) Conversion through Manipulation of Axial and Equatorial Ligands. *J. Am. Chem. Soc.* **2018**, *140* (9), 3378-3384.
5. Fox, A. R.; Bart, S. C.; Meyer, K.; Cummins, C. C., Towards uranium catalysts. *Nature* **2008**, *455* (7211), 341-349.
6. Camp, C.; Toniolo, D.; Andrez, J.; Pecaut, J.; Mazzanti, M., A versatile route to homo- and hetero-bimetallic 5f-5f and 3d-5f complexes supported by a redox active ligand framework. *Dalton Trans.* **2017**, *46* (34), 11145-11148.
7. Gorden, A. E. V.; Xu, J.; Raymond, K. N.; Durbin, P., Rational Design of Sequestering Agents for Plutonium and Other Actinides. *Chem. Rev.* **2003**, *103*, 4207-4282.

8. Panak, P. J.; Geist, A., Complexation and Extraction of Trivalent Actinides and Lanthanides by Triazinylpyridine N-Donor Ligands. *Chem. Rev.* **2013**, *113* (2), 1199-1236.
9. Monteiro, J. H. S. K.; de Bettencourt-Dias, A.; Sigoli, F. A., Estimating the Donor–Acceptor Distance To Tune the Emission Efficiency of Luminescent Lanthanide Compounds. *Inorg. Chem.* **2017**, *56* (2), 709-712.
10. Werts, M. H. V.; Woudenberg, R. H.; Emmerink, P. G.; van Gassel, R.; Hofstraat, J. W.; Verhoeven, J. W., A Near-Infrared Luminescent Label Based on Yb(III) Ions and Its Application in a Fluoroimmunoassay. *Angew. Chem. Int. Ed.* **2000**, *39* (24), 1521-3773.
11. Ishikawa, N.; Sugita, M.; Ishikawa, T.; Koshihara, S.-y.; Kaizu, Y., Lanthanide Double-Decker Complexes Functioning as Magnets at the Single-Molecular Level. *J. Am. Chem. Soc.* **2003**, *125* (29), 8694-8695.
12. Nair, V.; Deepthi, A., Cerium(IV) Ammonium Nitrate: A Versatile Single-Electron Oxidant. *Chem. Rev.* **2007**, *107* (5), 1862-1891.
13. Sridharan, V.; Menéndez, J. C., Cerium(IV) Ammonium Nitrate as a Catalyst in Organic Synthesis. *Chem. Rev.* **2010**, *110* (6), 3805-3849.
14. Williams, U. J.; Mahoney, B. D.; Lewis, A. J.; DeGregorio, P. T.; Carroll, P. J.; Schelter, E. J., Single Crystal to Single Crystal Transformation and Hydrogen-Atom Transfer upon Oxidation of a Cerium Coordination Compound. *Inorg. Chem.* **2013**, *52* (8), 4142-4144.
15. Piro, N. A.; Robinson, J. R.; Walsh, P. J.; Schelter, E. J., The electrochemical behavior of cerium(III/IV) complexes: Thermodynamics, kinetics and applications in synthesis. *Coord. Chem. Rev.* **2014**, *260*, 21-36.

16. Ho, I. T.; Zhang, Z.; Ishida, M.; Lynch, V. M.; Cha, W.-Y.; Sung, Y. M.; Kim, D.; Sessler, J. L., A Hybrid Macrocyclic with a Pyridine Subunit Displays Aromatic Character upon Uranyl Cation Complexation. *J. Am. Chem. Soc.* **2014**, *136* (11), 4281-4286.
17. Ho, I. T.; Sessler, J. L.; Gambhir, S. S.; Jokerst, J. V., Parts per billion detection of uranium with a porphyrinoid-containing nanoparticle and in vivo photoacoustic imaging. *Analyst* **2015**, *140* (11), 3731-3737.
18. Bell, T. W.; Guzzo, F., Isolation and conformation of a fully unsaturated nitrogen analogue of 18-crown-6. *J. Chem. Soc., Chem. Commun.* **1986**, (10), 769-771.
19. Bell, T. W.; Guzzo, F.; Drew, M. G. B., Molecular architecture. 1. Sodium, potassium, and strontium complexes of a hexaazamacrocyclic; an 18-crown-6/torand analog. *J. Am. Chem. Soc.* **1991**, *113* (8), 3115-3122.
20. Benetollo, F.; Bombieri, G.; Fonda, K. K.; Polo, A.; Quagliano, J. R.; Vallarino, L. M., Complexes of the lanthanide(III) ions with an aromatic six-nitrogen-donor macrocyclic ligand. *Inorg. Chem.* **1991**, *30* (6), 1345-1353.

## Appendix 1: Crystallographic Tables

### Data Collection: single crystal X-ray diffraction

The X-ray diffraction datasets were collected at 180K, on a Bruker SMART APEX CCD X-ray diffractometer unit using Mo K $\alpha$  radiation, from crystals mounted in Paratone-N oil on glass fibers, with the exception of VO[L<sup>I</sup>], which was mounted in epoxy on a glass fiber and collected at 273 K. SMART (v 5.624) was used for preliminary determination of cell constants and data collection control. Determination of integrated intensities and global cell refinement were performed with the Bruker SAINT software package using a narrow-frame integration algorithm for all data sets. Refinement was performed against  $F^2$  by weighted full-matrix least squares, and empirical absorption correction (SADABS) was applied.<sup>1</sup> The program suite ShelXTL (v 5.1) was used for space group determination, and structure solution and refinement for H<sub>2</sub>[L<sup>I</sup>], UO<sub>2</sub>[L<sup>I</sup>], Cu[L<sup>I</sup>], VO[L<sup>I</sup>], Zn[L<sup>I</sup>], Fe[L<sup>I</sup>]-O-Fe[L<sup>I</sup>].<sup>2</sup> For data sets UO<sub>2</sub>[L<sup>III</sup>], UO<sub>2</sub>[L<sup>IV</sup>], H<sub>2</sub>[L<sup>VII</sup>], Th[L<sup>VII</sup>]<sub>2</sub>, Ce[L<sup>VII</sup>]<sub>2</sub>, Nd<sub>2</sub>[L<sup>VII</sup>]<sub>3</sub>, Gd<sub>2</sub>[L<sup>VII</sup>]<sub>3</sub>, Ho<sub>2</sub>[L<sup>VII</sup>]<sub>3</sub>, Yb<sub>2</sub>[L<sup>VII</sup>]<sub>3</sub>, Eu<sub>2</sub>[L<sup>VII</sup>]<sub>3</sub>, Tb<sub>2</sub>[L<sup>VII</sup>]<sub>3</sub>, Dy<sub>2</sub>[L<sup>VII</sup>]<sub>3</sub>, Er<sub>2</sub>[L<sup>VII</sup>]<sub>3</sub>, Lu<sub>2</sub>[L<sup>VII</sup>]<sub>3</sub>, UO<sub>2</sub>[L<sup>VII</sup>] the program suite ShelXTL (v 5.1) was used for space group determination, and structure solution<sup>2</sup> and were refined with Olex2.refine package using Gauss-Newton minimization.<sup>3</sup>

An interstitial ethyl acetate molecule on an inversion center and a disordered t-butyl group were modeled for the H<sub>2</sub>[L<sup>I</sup>] data set. Two interstitial THF molecules were removed using SQUEEZE for the data set Fe[L<sup>I</sup>]-O-Fe[L<sup>I</sup>]. Solvent masks for interstitial



methanol and DCM for the data sets VO[L<sup>I</sup>], Yb<sub>2</sub>[L<sup>VII</sup>]<sub>3</sub>, Tb<sub>2</sub>[L<sup>VII</sup>]<sub>3</sub>, Dy<sub>2</sub>[L<sup>VII</sup>]<sub>3</sub> and Lu<sub>2</sub>[L<sup>VII</sup>]<sub>3</sub> were generated by Olex2.1.<sup>3-4</sup> A disordered toluene molecule on a mirror plane was modeled for the Th[L<sup>VII</sup>]<sub>2</sub> data set. One half an equivalent of a disordered interstitial hexanes molecule was modeled for the Ce[L<sup>VII</sup>]<sub>2</sub> data set. Disordered DCM molecule was modeled over two positions for the Gd<sub>2</sub>[L<sup>VII</sup>]<sub>3</sub> dataset. Only the metal atoms were refined anisotropically for the Er<sub>2</sub>[L<sup>VII</sup>]<sub>3</sub> and Eu<sub>2</sub>[L<sup>VII</sup>]<sub>3</sub> datasets due to low resolution, and resulted in the structures being useful for discussion but unpublishable. The carbon atoms on the coordinating methanol molecules on the Yb<sub>2</sub>[L<sup>VII</sup>]<sub>3</sub>, Tb<sub>2</sub>[L<sup>VII</sup>]<sub>3</sub>, Dy<sub>2</sub>[L<sup>VII</sup>]<sub>3</sub>, and Lu<sub>2</sub>[L<sup>VII</sup>]<sub>3</sub> datasets was set as an idealized methyl group and refined isotropically to allow for data convergence. All projections were generated in the Olex2.1-1 graphics program.<sup>4</sup>

## H<sub>2</sub>[L<sup>I</sup>]

**Crystallographic Table 1** Fractional Atomic Coordinates ( $\times 10^4$ ) and Equivalent Isotropic Displacement Parameters ( $\text{\AA}^2 \times 10^3$ ) for H<sub>2</sub>[L<sup>I</sup>]. U<sub>eq</sub> is defined as 1/3 of the trace of the orthogonalised U<sub>ij</sub> tensor.

Atom	x	y	z	U(eq)
C1	6188(3)	6822.0(8)	1866.4(7)	23.1(4)
N1	2784(2)	6263.1(7)	2334.9(6)	25.3(4)
O1	5574(2)	7089.4(6)	2272.1(5)	33.1(4)
C2	7814(3)	7079.0(8)	1609.3(7)	21.9(4)
N2	2317(2)	6652.3(7)	3252.1(6)	27.2(4)
O2	3940(2)	7705.4(6)	3283.5(5)	35.8(4)
C3	8827(3)	7669.2(8)	1772.6(7)	25.6(5)
N3	-3479(2)	5020.1(7)	2404.7(6)	27.5(4)
C4	7084(3)	8145.7(9)	1766.6(8)	36.4(5)
N4	-3907(2)	5432.9(7)	3376.4(6)	29.6(4)
C5	9969(3)	7613.8(9)	2288.8(7)	32.2(5)
C6	10500(4)	7869.7(9)	1431.3(8)	42.0(6)
C7	8441(3)	6774.7(8)	1206.0(7)	24.1(4)
C8	7558(3)	6239.3(8)	1035.4(7)	25.3(4)
C13	5951(3)	6007.6(8)	1295.0(7)	25.5(5)
C14	5231(3)	6289.2(8)	1705.5(7)	22.9(4)
C15	3537(3)	6022.5(8)	1959.5(7)	25.0(5)
C16	1055(3)	6021.2(8)	2568.9(7)	23.1(4)
C17	-403(3)	5631.7(8)	2359.5(7)	25.0(5)
C18	-2102(3)	5412.5(8)	2623.6(7)	23.3(4)
C19	-5060(3)	4830.7(8)	2673.2(7)	27.0(5)
C20	-6584(3)	4417.6(9)	2463.2(8)	33.3(5)
C21	-8210(3)	4227.4(9)	2724.7(8)	37.6(6)
C22	-8423(3)	4432.7(9)	3204.4(9)	38.5(6)
C23	-7009(3)	4827.0(9)	3417.7(8)	35.4(5)
C24	-5280(3)	5037.5(8)	3158.3(8)	28.0(5)
C25	-2323(3)	5619.4(8)	3110.0(7)	25.4(5)
C26	-810(3)	6035.1(8)	3316.8(7)	27.9(5)
C27	831(3)	6226.7(8)	3060.3(7)	24.7(4)
C28	3351(3)	6562.8(9)	3669.6(7)	27.7(5)
C29	4845(3)	6985.9(8)	3902.0(7)	26.5(5)
C30	6045(3)	6825.1(9)	4336.5(7)	30.2(5)
C31	7510(3)	7200.5(9)	4574.0(7)	29.4(5)

C32	8876(3)	7043.9(10)	5046.6(7)	36.4(5)
C33	8122(4)	6479.4(11)	5272.2(8)	51.0(7)
C34	8729(4)	7532.8(11)	5427.5(8)	46.9(6)
C35	11229(4)	6975.6(13)	4929.5(9)	56.7(7)
C36	7747(3)	7749.8(9)	4355.2(7)	30.3(5)
C37	6604(3)	7940.9(9)	3929.8(7)	27.5(5)
C38	6956(3)	8546.0(9)	3708.8(7)	31.1(5)
C39	4847(3)	8899.1(10)	3678.8(9)	42.6(6)
C40	8668(4)	8899.3(10)	4015.9(8)	43.7(6)
C41	7750(4)	8477.9(10)	3197.9(8)	40.0(6)
C42	5107(3)	7541.4(9)	3699.2(7)	26.3(5)
C43S	7042(8)	4618(2)	4496.1(15)	118.9(15)
C44S	8738(14)	4920(3)	4454(2)	84(2)
C45S	8267(13)	4726(3)	5012(3)	74.4(18)
O46S	7458(8)	4552.6(19)	5368.2(17)	90.6(14)
O3S	10000	5000	5000	85.3(10)
C9	8373(3)	5926.9(9)	590.5(7)	30.4(5)
C1A	9667(12)	5354(3)	796(2)	50(2)
C1b	10628(9)	5739(3)	705.6(19)	55(2)
C2A	9950(16)	6267(3)	326(3)	67(3)
C2b	8347(11)	6381(2)	145.3(16)	45.4(17)
C3A	6512(16)	5700(5)	263(4)	62(3)
C3b	6953(15)	5432(4)	400(4)	63(3)

**Crystallographic Table 2** Anisotropic Displacement Parameters ( $\text{\AA}^2 \times 10^3$ ) for  $\text{H}_2[\text{L}^1]$ .

The Anisotropic displacement factor exponent takes the form:

$$-2\pi^2 [h^2 a^{*2} U_{11} + 2hka^* b^* U_{12} + \dots]$$

Atom	$U_{11}$	$U_{22}$	$U_{33}$	$U_{12}$	$U_{13}$	$U_{23}$
C1	22.6(10)	25.4(11)	21.2(10)	4.3(8)	0.8(8)	-4.6(8)
N1	20.8(8)	29.1(9)	26.0(9)	-1.5(7)	1.9(7)	1.2(7)
O1	31.5(8)	35.5(8)	33.9(8)	-6.6(6)	12.7(6)	-10.6(7)
C2	21.8(10)	21.4(10)	22.4(11)	0.4(8)	1.0(8)	-0.2(8)
N2	25.6(9)	30.3(9)	25.5(9)	-5.4(7)	1.6(8)	-3.6(7)
O2	41.5(9)	35.4(8)	28.1(8)	-10.0(7)	-11.1(7)	1.6(7)
C3	28.3(11)	22(1)	26.8(11)	-2.0(8)	4.6(9)	-4.1(8)
N3	23.3(9)	24.0(9)	34.9(10)	-0.8(7)	0.8(8)	-2.6(7)
C4	41.4(13)	24.1(11)	42.4(13)	3.9(9)	-5.1(11)	-3.9(10)
N4	27.4(9)	29.0(9)	33.1(10)	-4.5(7)	6.2(8)	-1.4(8)
C5	30.8(11)	28.4(12)	36.7(12)	1.5(9)	-2.6(10)	-7.2(9)
C6	50.8(14)	32.0(13)	45.0(14)	-16.5(11)	15.1(12)	-10.1(10)

C7	25.4(10)	26.2(11)	20.9(10)	-1.4(8)	3.6(8)	1.0(9)
C8	26.9(10)	24.9(11)	23.7(11)	-0.4(9)	0.5(9)	-1.4(9)
C13	27.4(10)	23.1(11)	25.8(11)	-3.7(8)	0.9(9)	-3.0(9)
C14	21.9(10)	24.7(11)	22.1(11)	0.5(8)	1.2(8)	1.2(8)
C15	23.5(10)	24.7(11)	26.2(11)	-1.3(8)	-2.0(9)	-0.0(9)
C16	19.3(10)	23.6(10)	26.4(11)	0.1(8)	1.4(8)	1.2(9)
C17	23.7(10)	28.9(11)	22.3(11)	1.1(9)	1.8(9)	-2.1(8)
C18	21(1)	21.3(10)	27.1(11)	2.2(8)	-1.1(9)	-0.4(8)
C19	22.7(10)	21.8(10)	36.2(12)	2.7(8)	1.1(9)	2.5(9)
C20	27.8(11)	26.7(11)	44.7(14)	-2.8(9)	-1.2(10)	-5.3(10)
C21	28.4(11)	27.3(12)	56.3(16)	-5.7(9)	-1.0(11)	0.4(11)
C22	30.6(12)	32.7(12)	52.9(15)	-6(1)	8.2(11)	6.9(11)
C23	33.3(12)	34.4(12)	39.4(13)	-4.8(10)	8.9(10)	2.3(10)
C24	25.0(11)	22.6(11)	36.6(12)	-1.0(9)	2.6(9)	2.8(9)
C25	23.2(10)	25.2(11)	27.9(11)	1.5(8)	2.7(9)	1.2(9)
C26	28.8(11)	30.7(11)	24.4(11)	-4.0(9)	3.4(9)	-3.7(9)
C27	23.3(10)	22.6(10)	27.6(11)	-2.0(8)	-1.1(9)	-0.1(8)
C28	28.3(11)	27.9(11)	27.6(12)	-3.1(9)	7.1(9)	0.1(9)
C29	25.1(10)	30.2(11)	24.2(11)	-3.0(9)	2.0(9)	-3.2(9)
C30	30.5(11)	33.5(12)	26.6(11)	0.3(9)	2.8(9)	0.9(9)
C31	26.4(11)	37.0(12)	24.9(11)	2.1(9)	2.2(9)	-2.8(9)
C32	32.9(12)	47.4(14)	27.9(12)	4.9(10)	-3.3(10)	-0.1(10)
C33	58.5(16)	52.4(15)	39.5(14)	6.0(13)	-11.1(12)	9.2(12)
C34	53.1(15)	58.6(16)	27.7(13)	-2.0(12)	-4.6(11)	1.3(11)
C35	37.2(13)	82(2)	49.2(16)	14.6(13)	-5.6(12)	2.0(14)
C36	26.5(11)	38.7(13)	25.4(11)	-4.0(9)	0.3(9)	-8.1(9)
C37	26.6(10)	33.3(12)	22.8(11)	-1.8(9)	3.3(9)	-5.5(9)
C38	35.5(12)	30.0(11)	27.8(12)	-4.7(9)	1.8(9)	-3.3(9)
C39	44.8(13)	35.9(13)	46.6(15)	0.9(11)	0.5(11)	-2.6(11)
C40	48.0(14)	36.9(13)	45.2(14)	-12.8(11)	-2.4(11)	-6.4(11)
C41	46.4(14)	39.0(13)	35.4(13)	-9.9(11)	7.3(11)	0.3(10)
C42	25.3(10)	34.0(12)	19.5(11)	-1.9(9)	0.2(9)	-1.8(9)
C43S	129(4)	134(4)	89(3)	33(3)	-15(3)	26(3)
C44S	125(6)	79(5)	46(4)	-8(4)	-10(4)	14(3)
C45S	97(5)	53(4)	76(5)	25(4)	23(5)	11(4)
O46S	125(4)	78(3)	72(3)	7(3)	30(3)	11(2)
O3S	113(3)	65(2)	82(2)	13(2)	31(2)	12.5(17)
C9	33.7(11)	31.2(12)	27.2(12)	-4.1(9)	7.4(9)	-9.0(9)
C1A	61(4)	46(4)	44(3)	24(4)	12(3)	-6(3)
C1b	55(3)	68(5)	42(3)	26(3)	4(3)	-13(3)
C2A	109(8)	49(4)	51(5)	-18(4)	48(5)	-21(3)
C2b	60(4)	52(3)	24(3)	4(3)	6(2)	-7(2)
C3A	54(4)	90(8)	39(5)	19(5)	-9(3)	-42(5)
C3b	64(5)	60(5)	68(6)	-22(4)	31(4)	-41(4)

**Crystallographic Table 3** Bond Lengths for  $\text{H}_2[\text{L}^1]$ .

Atom	Atom	Length/Å	Atom	Atom	Length/Å
C1	O1	1.351(2)	C23	C24	1.424(3)
C1	C2	1.410(3)	C25	C26	1.425(3)
C1	C14	1.413(3)	C26	C27	1.361(3)
N1	C15	1.289(2)	C28	C29	1.454(3)
N1	C16	1.413(2)	C29	C30	1.402(3)
C2	C3	1.543(3)	C29	C42	1.403(3)
C2	C7	1.389(3)	C30	C31	1.378(3)
N2	C27	1.417(2)	C31	C32	1.533(3)
N2	C28	1.282(2)	C31	C36	1.406(3)
O2	C42	1.353(2)	C32	C33	1.524(3)
C3	C4	1.540(3)	C32	C34	1.538(3)
C3	C5	1.535(3)	C32	C35	1.537(3)
C3	C6	1.528(3)	C36	C37	1.386(3)
N3	C18	1.349(2)	C37	C38	1.535(3)
N3	C19	1.350(2)	C37	C42	1.419(3)
N4	C24	1.352(2)	C38	C39	1.541(3)
N4	C25	1.346(2)	C38	C40	1.535(3)
C7	C8	1.408(3)	C38	C41	1.530(3)
C8	C13	1.382(3)	C43S	C44S	1.277(8)
C8	C9	1.535(3)	C43S	C45S	1.570(8)
C13	C14	1.402(3)	C44S	C45S	1.641(10)
C14	C15	1.448(3)	C44S	O3S1	1.642(6)
C16	C17	1.367(3)	C45S	O46S	1.202(7)
C16	C27	1.443(3)	C45S	O3S1	1.253(9)
C17	C18	1.423(3)	C9	C1A	1.617(6)
C18	C25	1.431(3)	C9	C1b	1.481(5)
C19	C20	1.428(3)	C9	C2A	1.489(6)
C19	C24	1.428(3)	C9	C2b	1.601(5)
C20	C21	1.361(3)	C9	C3A	1.501(10)
C21	C22	1.412(3)	C9	C3b	1.505(8)
C22	C23	1.360(3)			

 $^1/2$ -X,1-Y,1-Z**Crystallographic Table 4** Bond Angles for  $\text{H}_2[\text{L}^1]$ .

Atom	Atom	Atom	Angle/°	Atom	Atom	Atom	Angle/°
C2	C1	O1	119.05(16)	C29	C28	N2	122.78(18)
C14	C1	O1	120.42(17)	C30	C29	C28	118.37(18)
C14	C1	C2	120.53(17)	C42	C29	C28	121.47(17)
C16	N1	C15	122.43(16)	C42	C29	C30	120.16(17)
C3	C2	C1	121.04(16)	C31	C30	C29	121.60(19)
C7	C2	C1	116.66(16)	C32	C31	C30	123.63(19)

C7	C2	C3	122.31(16)	C36	C31	C30	116.47(18)
C28	N2	C27	119.16(16)	C36	C31	C32	119.88(17)
C4	C3	C2	110.19(15)	C33	C32	C31	111.82(17)
C5	C3	C2	110.05(15)	C34	C32	C31	110.01(17)
C5	C3	C4	110.04(16)	C34	C32	C33	107.76(18)
C6	C3	C2	111.74(16)	C35	C32	C31	108.84(17)
C6	C3	C4	107.37(16)	C35	C32	C33	109.3(2)
C6	C3	C5	107.38(16)	C35	C32	C34	109.08(19)
C19	N3	C18	116.06(16)	C37	C36	C31	125.15(18)
C25	N4	C24	116.14(17)	C38	C37	C36	122.42(17)
C8	C7	C2	124.93(18)	C42	C37	C36	116.44(18)
C13	C8	C7	116.39(17)	C42	C37	C38	121.12(17)
C9	C8	C7	121.53(17)	C39	C38	C37	110.22(16)
C9	C8	C13	122.07(17)	C40	C38	C37	112.04(16)
C14	C13	C8	122.00(17)	C40	C38	C39	107.82(17)
C13	C14	C1	119.47(17)	C41	C38	C37	109.63(16)
C15	C14	C1	121.42(17)	C41	C38	C39	110.13(17)
C15	C14	C13	119.10(17)	C41	C38	C40	106.93(17)
C14	C15	N1	122.11(17)	C29	C42	O2	120.83(16)
C17	C16	N1	124.98(17)	C37	C42	O2	119.01(17)
C27	C16	N1	115.55(16)	C37	C42	C29	120.16(17)
C27	C16	C17	119.44(17)	C45S	C43S	C44S	69.5(5)
C18	C17	C16	121.04(18)	C45S	C44S	C43S	63.7(5)
C17	C18	N3	118.88(17)	O3S1	C44S	C43S	108.5(5)
C25	C18	N3	121.84(17)	O3S1	C44S	C45S	44.9(3)
C25	C18	C17	119.27(17)	C44S	C45S	C43S	46.8(3)
C20	C19	N3	119.08(18)	O46S	C45S	C43S	118.2(7)
C24	C19	N3	122.05(17)	O46S	C45S	C44S	164.6(8)
C24	C19	C20	118.87(18)	O3S1	C45S	C43S	114.4(6)
C21	C20	C19	120.1(2)	O3S1	C45S	C44S	67.6(5)
C22	C21	C20	120.94(19)	O3S1	C45S	O46S	127.5(7)
C23	C22	C21	120.9(2)	C44S	O3S	C44S1	180
C24	C23	C22	120.1(2)	C45S	O3S	C44S	67.5(4)
C19	C24	N4	121.85(17)	C45S	O3S	C44S1	112.5(4)
C23	C24	N4	119.04(19)	C45S1	O3S	C44S	112.5(4)
C23	C24	C19	119.11(18)	C45S1	O3S	C44S1	67.5(4)
C18	C25	N4	122.05(17)	C45S1	O3S	C45S	180
C26	C25	N4	119.28(17)	C2A	C9	C1A	105.2(4)
C26	C25	C18	118.66(17)	C2b	C9	C1b	107.5(3)
C27	C26	C25	120.82(18)	C3A	C9	C1A	105.5(4)
C16	C27	N2	117.33(16)	C3A	C9	C2A	113.6(5)
C26	C27	N2	121.87(17)	C3b	C9	C1b	112.1(4)
C26	C27	C16	120.73(17)	C3b	C9	C2b	104.8(4)

<sup>1</sup>2-X,1-Y,1-Z

**Crystallographic Table 5** Hydrogen Atom Coordinates ( $\text{\AA}^2 \times 10^4$ ) and Isotropic Displacement Parameters ( $\text{\AA}^2 \times 10^3$ ) for  $\text{H}_2[\text{L}^1]$ .

Atom	x	y	z	U(eq)
H1	4640(30)	6885(5)	2397(5)	49.7(5)
H2	3190(30)	7423(3)	3173(5)	53.6(6)
H4a	6413(14)	8192(4)	1432.5(12)	54.7(8)
H4b	5989(11)	8032(3)	1985(4)	54.7(8)
H4c	7739(5)	8516.3(15)	1878(4)	54.7(8)
H5a	8936(5)	7486(5)	2517.6(11)	48.4(8)
H5b	11131(13)	7327(4)	2284.7(12)	48.4(8)
H5c	10568(17)	7993.5(15)	2394(2)	48.4(8)
H6a	11658(12)	7580(3)	1434(4)	63.0(9)
H6b	9821(6)	7911(6)	1097.6(13)	63.0(9)
H6c	11096(17)	8247(3)	1544(3)	63.0(9)
H7	9548(3)	6940.4(8)	1032.1(7)	28.9(5)
H13	5315(3)	5646.6(8)	1192.0(7)	30.6(6)
H15	2962(3)	5658.4(8)	1845.8(7)	30.0(5)
H17	-281(3)	5505.4(8)	2032.5(7)	30.0(5)
H20	-6461(3)	4275.6(9)	2140.8(8)	40.0(6)
H21	-9216(3)	3952.5(9)	2582.3(8)	45.1(7)
H22	-9569(3)	4293.6(9)	3380.7(9)	46.2(7)
H23	-7176(3)	4962.3(9)	3740.3(8)	42.4(6)
H26	-948(3)	6180.3(8)	3637.7(7)	33.5(6)
H28	3133(3)	6205.1(9)	3834.0(7)	33.2(6)
H30	5844(3)	6448.3(9)	4470.5(7)	36.2(6)
H33a	6600(8)	6514(3)	5331(5)	76.5(10)
H33b	8310(20)	6154.0(15)	5047(3)	76.5(10)
H33c	8971(17)	6407(4)	5583(3)	76.5(10)
H34a	9280(20)	7897.6(18)	5298(2)	70.4(9)
H34b	7227(5)	7586(4)	5497(4)	70.4(9)
H34c	9589(19)	7427(3)	5730(2)	70.4(9)
H35a	11349(6)	6647(5)	4704(5)	85.0(11)
H35b	11707(9)	7335(3)	4777(6)	85.0(11)
H35c	12132(5)	6901(7)	5233.1(12)	85.0(11)
H36	8771(3)	8010.3(9)	4511.2(7)	36.4(6)
H39a	3723(7)	8682(3)	3485(4)	63.9(9)
H39b	4406(12)	8963(5)	4009.8(9)	63.9(9)
H39c	5073(7)	9277(3)	3522(5)	63.9(9)
H40a	8193(11)	8965(6)	4343.8(19)	65.6(9)
H40b	10026(7)	8682(3)	4043(5)	65.6(9)
H40c	8878(17)	9276(3)	3857(3)	65.6(9)
H41a	9148(11)	8281(5)	3224.1(9)	60.1(8)
H41b	6714(11)	8245(5)	2991.9(17)	60.1(8)
H41c	7900(20)	8864.3(10)	3050(2)	60.1(8)
H1Aa	10910(40)	5474(3)	1015(10)	75(3)
H1Ab	8710(20)	5109(8)	977(11)	75(3)

H1Ac	10160(50)	5132(9)	521(2)	75(3)
H1ba	11517(13)	6079(4)	802(12)	83(3)
H1bb	10696(12)	5456(12)	975(8)	83(3)
H1bc	11160(20)	5556(14)	416(4)	83(3)
H2Aa	9320(30)	6643(8)	222(14)	101(5)
H2Ab	11250(30)	6335(16)	544(6)	101(5)
H2Ac	10320(60)	6047(9)	37(9)	101(5)
H2ba	6865(12)	6505(10)	54(7)	68(3)
H2bb	9220(40)	6722(6)	246(4)	68(3)
H2bc	8940(40)	6194(4)	-136(4)	68(3)
H3Aa	5670(40)	5430(14)	448(5)	93(5)
H3Ab	5600(40)	6027(5)	144(13)	93(5)
H3Ac	7051(16)	5495(16)	-16(8)	93(5)
H3ba	7060(50)	5109(7)	635(7)	94(4)
H3bb	5460(17)	5567(5)	355(13)	94(4)
H3bc	7410(40)	5298(11)	85(8)	94(4)

**Crystallographic Table 6** Atomic Occupancy for  $\text{H}_2[\text{L}^1]$

Atom	Occupancy	Atom	Occupancy	Atom	Occupancy
C44S	0.5	C45S	0.5	O46S	0.5
C1A	0.463(9)	H1Aa	0.463(9)	H1Ab	0.463(9)
H1Ac	0.463(9)	C1b	0.537(9)	H1ba	0.537(9)
H1bb	0.537(9)	H1bc	0.537(9)	C2A	0.463(9)
H2Aa	0.463(9)	H2Ab	0.463(9)	H2Ac	0.463(9)
C2b	0.537(9)	H2ba	0.537(9)	H2bb	0.537(9)
H2bc	0.537(9)	C3A	0.463(9)	H3Aa	0.463(9)
H3Ab	0.463(9)	H3Ac	0.463(9)	C3b	0.537(9)
H3ba	0.537(9)	H3bb	0.537(9)	H3bc	0.537(9)



**UO<sub>2</sub>[L<sup>I</sup>]**

**Crystallographic Table 7** Crystal data and structure refinement for **UO<sub>2</sub>[L<sup>I</sup>]**

Empirical formula	C <sub>42</sub> H <sub>45</sub> N <sub>4</sub> O <sub>7</sub> U
Formula weight	955.85
Temperature/K	296(2)
Crystal system	monoclinic
Space group	P2 <sub>1</sub> /n
a/Å	18.0541(18)
b/Å	13.4873(13)
c/Å	20.820(2)
α/°	90.00
β/°	97.380(3)
γ/°	90.00
Volume/Å <sup>3</sup>	5027.6(9)
Z	4
ρ <sub>calc</sub> /mg/mm <sup>3</sup>	1.263
m/mm <sup>-1</sup>	3.271
F(000)	1892.0
Crystal size/mm <sup>3</sup>	? × ? × ?
Radiation	MoKα (λ = 0.71073)
2θ range for data collection	2.82 to 49.1°
Index ranges	-20 ≤ h ≤ 19, -15 ≤ k ≤ 15, -24 ≤ l ≤ 24
Reflections collected	39876
Independent reflections	8274 [R <sub>int</sub> = 0.0770, R <sub>sigma</sub> = 0.0612]
Data/restraints/parameters	8274/0/499
Goodness-of-fit on F <sup>2</sup>	1.134
Final R indexes [I ≥ 2σ (I)]	R <sub>1</sub> = 0.0610, wR <sub>2</sub> = 0.1816
Final R indexes [all data]	R <sub>1</sub> = 0.0809, wR <sub>2</sub> = 0.1931
Largest diff. peak/hole / e Å <sup>-3</sup>	2.74/-1.86

**Crystallographic Table 8** Fractional Atomic Coordinates (×10<sup>4</sup>) and Equivalent Isotropic Displacement Parameters (Å<sup>2</sup>×10<sup>3</sup>) for **UO<sub>2</sub>[L<sup>I</sup>]**. U<sub>eq</sub> is defined as 1/3 of the trace of the orthogonalised U<sub>ij</sub> tensor.

Atom	x	y	z	U(eq)
U1	1462.3(2)	1585.6(3)	1714.81(19)	31.01(16)
O1S	2118(7)	8436(8)	2287(9)	121(6)
N1	352(4)	2570(6)	1150(4)	28.6(18)
O2S	2773(13)	6646(17)	1255(11)	213(12)

N4	1786(5)	3053(6)	1035(4)	32.4(19)
O3	2713(4)	1702(5)	1702(4)	42.9(19)
O4	1509(4)	2443(6)	2379(4)	46.0(19)
O5	1414(5)	780(6)	1044(4)	44.9(19)
C100	-637(6)	1324(7)	1170(5)	33(2)
N2	-397(5)	5993(6)	716(4)	36(2)
N3	1134(5)	6502(6)	767(4)	37(2)
O11	1925(5)	366(7)	2543(4)	62(3)
O10	385(4)	955(5)	1960(3)	39.1(18)
C2	-301(6)	763(7)	1695(5)	33(2)
C3	-310(5)	2230(7)	967(5)	31(2)
C4	492(6)	3579(7)	992(5)	33(2)
C5	-47(5)	4295(7)	912(5)	34(2)
C6	153(5)	5303(7)	802(5)	31(2)
C7	-184(6)	6928(8)	652(5)	35(2)
C8	-730(7)	7689(9)	547(6)	48(3)
C9	-512(8)	8643(8)	498(6)	49(3)
C10	245(7)	8907(8)	560(6)	44(3)
C11	774(7)	8216(8)	670(6)	44(3)
C12	585(6)	7197(7)	702(5)	34(2)
C13	914(6)	5551(7)	803(5)	31(2)
C14	1447(6)	4784(7)	876(5)	33(2)
C15	1260(6)	3831(7)	952(5)	32(2)
C16	2361(6)	3154(8)	743(6)	38(3)
C17	3042(6)	2598(8)	819(5)	35(2)
C18	3203(6)	1893(8)	1301(5)	33(2)
C19	3922(6)	1412(8)	1378(5)	36(2)
C20	4398(6)	1676(8)	949(6)	43(3)
C21	4257(6)	2389(9)	455(6)	43(3)
C22	3572(6)	2841(8)	405(6)	42(3)
C23	4838(7)	2612(10)	-1(7)	58(3)
C24	5002(11)	1665(14)	-345(10)	105(7)
C25	5578(9)	2930(17)	408(9)	102(6)
C26	4590(12)	3392(19)	-469(12)	169(15)
C27	4114(6)	587(9)	1879(6)	44(3)
C28	3595(9)	-315(9)	1705(7)	67(4)
C29	4919(8)	218(12)	1898(8)	78(5)
C30	4021(8)	924(11)	2566(6)	64(4)

C31	-1371(6)	1141(8)	884(5)	36(2)
C32	-1785(6)	383(8)	1102(6)	41(3)
C33	-1443(6)	-160(8)	1637(6)	42(3)
C34	-725(6)	-20(8)	1938(5)	36(2)
C35	-400(7)	-663(9)	2515(6)	53(3)
C36	-183(10)	5(13)	3106(7)	86(5)
C37	-971(10)	-1431(12)	2685(8)	87(5)
C38	304(8)	-1195(11)	2355(7)	71(4)
C39	-2578(7)	142(10)	788(7)	56(3)
C40	-2798(9)	716(17)	171(9)	113(7)
C41	-3127(8)	419(18)	1247(10)	112(7)
C42	-2643(10)	-953(13)	633(13)	142(10)

**Crystallographic Table 9** Anisotropic Displacement Parameters ( $\text{\AA}^2 \times 10^3$ ) for  $\text{UO}_2[\text{L}]$ .

The Anisotropic displacement factor exponent takes the form: -

$$2\pi^2[h^2a^2U_{11}+2hka*b*U_{12}+\dots]$$

Atom	$U_{11}$	$U_{22}$	$U_{33}$	$U_{23}$	$U_{13}$	$U_{12}$
U1	28.9(2)	28.1(2)	35.1(3)	3.44(17)	0.21(16)	0.47(17)
O1S	62(7)	82(9)	216(17)	55(9)	13(9)	17(6)
N1	25(4)	23(4)	38(5)	6(4)	4(4)	1(3)
O2S	180(20)	260(30)	180(20)	-111(18)	-56(16)	13(16)
N4	28(5)	25(4)	44(5)	5(4)	3(4)	2(4)
O3	37(4)	39(4)	54(5)	16(4)	10(4)	14(3)
O4	41(4)	43(5)	53(5)	-11(4)	5(4)	-2(4)
O5	57(5)	42(5)	36(4)	-1(3)	4(4)	3(4)
C100	31(6)	29(5)	39(6)	1(4)	5(5)	2(4)
N2	26(4)	28(5)	52(6)	1(4)	-3(4)	3(4)
N3	45(5)	27(5)	39(5)	4(4)	7(4)	0(4)
O11	48(5)	69(6)	67(6)	37(5)	2(4)	9(4)
O10	33(4)	42(4)	41(4)	16(3)	-1(3)	-4(3)
C2	36(6)	32(6)	32(6)	-2(4)	4(5)	-5(5)
C3	30(6)	29(5)	32(6)	2(4)	1(4)	-3(4)
C4	32(6)	20(5)	47(7)	6(4)	3(5)	5(4)
C5	16(5)	31(6)	54(7)	4(5)	1(4)	3(4)
C6	30(5)	32(5)	31(6)	5(4)	0(4)	2(4)
C7	43(6)	28(5)	33(6)	-4(4)	-1(5)	9(5)
C8	38(6)	44(7)	60(8)	2(6)	-3(6)	8(5)
C9	66(9)	25(6)	57(8)	-2(5)	11(6)	19(5)
C10	54(8)	26(6)	53(7)	0(5)	11(6)	3(5)

C11	60(8)	27(6)	44(7)	2(5)	8(6)	-2(5)
C12	44(6)	28(6)	30(6)	1(4)	0(5)	4(5)
C13	34(6)	33(6)	25(5)	7(4)	0(4)	-1(4)
C14	35(6)	26(5)	38(6)	-4(5)	4(5)	2(4)
C15	29(5)	24(5)	43(6)	1(4)	-3(5)	7(4)
C16	42(6)	29(6)	42(6)	1(5)	8(5)	3(5)
C17	32(6)	33(6)	42(6)	6(5)	11(5)	2(5)
C18	34(6)	35(6)	34(6)	1(5)	11(5)	2(4)
C19	29(5)	37(6)	43(6)	0(5)	5(5)	0(4)
C20	36(6)	46(7)	47(7)	1(5)	7(5)	11(5)
C21	37(6)	48(7)	46(7)	2(5)	13(5)	5(5)
C22	40(6)	38(6)	48(7)	7(5)	11(5)	3(5)
C23	51(8)	66(9)	59(8)	7(7)	20(6)	4(7)
C24	96(14)	138(18)	95(14)	-34(12)	59(12)	-14(12)
C25	75(11)	152(17)	87(13)	-12(12)	42(10)	-47(12)
C26	118(17)	220(30)	190(20)	160(20)	117(18)	95(18)
C27	35(6)	48(7)	49(7)	10(6)	8(5)	10(5)
C28	94(11)	43(8)	64(9)	10(7)	10(8)	8(7)
C29	55(9)	90(11)	91(11)	38(9)	18(8)	39(8)
C30	79(10)	75(10)	34(7)	9(7)	-1(6)	20(8)
C31	35(6)	33(6)	38(6)	-5(5)	2(5)	-1(5)
C32	29(6)	43(6)	51(7)	-14(5)	3(5)	-4(5)
C33	36(6)	41(6)	51(7)	1(5)	12(5)	-14(5)
C34	40(6)	36(6)	34(6)	2(5)	6(5)	0(5)
C35	64(8)	49(7)	44(7)	13(6)	2(6)	-13(6)
C36	109(14)	99(13)	46(9)	6(8)	-5(8)	-11(10)
C37	91(12)	93(12)	76(11)	34(9)	5(9)	-35(10)
C38	76(10)	65(9)	70(10)	31(8)	6(8)	18(8)
C39	35(7)	62(8)	71(9)	-2(7)	2(6)	-5(6)
C40	57(10)	170(20)	99(14)	29(14)	-25(10)	-24(12)
C41	40(9)	180(20)	118(16)	-3(15)	18(9)	-7(11)
C42	59(11)	74(13)	270(30)	-53(16)	-44(14)	-18(9)

**Crystallographic Table 10 Bond Lengths for UO<sub>2</sub>[L<sup>I</sup>].**

Atom	Atom	Length/Å	Atom	Atom	Length/Å
U1	N1	2.561(8)	C11	C12	1.419(14)
U1	N4	2.546(8)	C13	C14	1.407(14)
U1	O3	2.268(7)	C14	C15	1.345(14)

U1	O4	1.796(8)	C16	C17	1.431(14)
U1	O5	1.763(7)	C17	C18	1.385(14)
U1	O11	2.451(8)	C17	C22	1.407(14)
U1	O10	2.241(7)	C18	C19	1.442(15)
N1	C3	1.291(12)	C19	C20	1.364(15)
N1	C4	1.430(12)	C19	C27	1.533(15)
N4	C15	1.410(13)	C20	C21	1.407(16)
N4	C16	1.276(13)	C21	C22	1.370(15)
O3	C18	1.317(12)	C21	C23	1.534(16)
C100	C2	1.402(14)	C23	C24	1.51(2)
C100	C3	1.444(14)	C23	C25	1.55(2)
C100	C31	1.404(14)	C23	C26	1.46(2)
N2	C6	1.356(13)	C27	C28	1.550(18)
N2	C7	1.330(14)	C27	C29	1.532(16)
N3	C12	1.358(13)	C27	C30	1.530(17)
N3	C13	1.347(13)	C31	C32	1.377(15)
O10	C2	1.316(12)	C32	C33	1.409(16)
C2	C34	1.434(14)	C32	C39	1.529(15)
C4	C5	1.365(13)	C33	C34	1.378(15)
C4	C15	1.440(14)	C34	C35	1.535(15)
C5	C6	1.433(14)	C35	C36	1.534(19)
C6	C13	1.415(14)	C35	C37	1.535(18)
C7	C8	1.421(15)	C35	C38	1.533(19)
C7	C12	1.426(15)	C39	C40	1.51(2)
C8	C9	1.353(16)	C39	C41	1.51(2)
C9	C10	1.403(17)	C39	C42	1.51(2)
C10	C11	1.333(16)			

**Crystallographic Table 11** Bond Angles for  $\text{UO}_2[\text{L}^1]$ .

Atom	Atom	Atom	Angle/°	Atom	Atom	Atom	Angle/°
N4	U1	N1	64.1(3)	N3	C13	C6	121.2(9)
O3	U1	N1	132.9(2)	N3	C13	C14	120.2(9)
O3	U1	N4	68.8(3)	C14	C13	C6	118.5(9)
O3	U1	O11	78.8(3)	C15	C14	C13	122.5(10)
O4	U1	N1	88.6(3)	N4	C15	C4	117.2(9)
O4	U1	N4	86.3(3)	C14	C15	N4	123.4(9)
O4	U1	O3	90.9(3)	C14	C15	C4	119.4(9)

O4	U1	O11	85.0(4)	N4	C16	C17	129.1(10)
O4	U1	O10	91.4(3)	C18	C17	C16	122.6(9)
O5	U1	N1	89.9(3)	C18	C17	C22	120.5(10)
O5	U1	N4	91.7(3)	C22	C17	C16	116.9(10)
O5	U1	O3	88.9(3)	O3	C18	C17	119.8(9)
O5	U1	O4	177.9(4)	O3	C18	C19	120.6(9)
O5	U1	O11	97.0(3)	C17	C18	C19	119.5(9)
O5	U1	O10	89.5(3)	C18	C19	C27	121.6(9)
O11	U1	N1	147.9(3)	C20	C19	C18	116.3(10)
O11	U1	N4	146.3(3)	C20	C19	C27	121.9(10)
O10	U1	N1	69.5(2)	C19	C20	C21	126.0(10)
O10	U1	N4	133.6(3)	C20	C21	C23	120.9(10)
O10	U1	O3	157.5(2)	C22	C21	C20	115.9(10)
O10	U1	O11	79.2(3)	C22	C21	C23	123.2(11)
C3	N1	U1	126.2(6)	C21	C22	C17	121.8(10)
C3	N1	C4	117.0(8)	C21	C23	C24	108.6(12)
C4	N1	U1	116.6(6)	C21	C23	C25	108.9(11)
C15	N4	U1	116.5(6)	C24	C23	C25	106.7(14)
C16	N4	U1	127.4(7)	C26	C23	C21	112.2(11)
C16	N4	C15	116.1(9)	C26	C23	C24	110.7(17)
C18	O3	U1	140.5(7)	C26	C23	C25	109.6(17)
C2	C100	C3	122.2(9)	C19	C27	C28	109.4(10)
C31	C100	C2	121.7(10)	C29	C27	C19	112.6(10)
C31	C100	C3	115.1(9)	C29	C27	C28	107.1(11)
C7	N2	C6	116.6(9)	C29	C27	C30	106.9(11)
C13	N3	C12	116.5(9)	C30	C27	C19	112.2(10)
C2	O10	U1	141.0(6)	C30	C27	C28	108.5(11)
C100	C2	C34	118.4(9)	C32	C31	C100	120.9(10)
O10	C2	C100	120.6(9)	C31	C32	C33	116.4(10)
O10	C2	C34	120.9(9)	C31	C32	C39	122.3(11)
N1	C3	C100	127.8(9)	C33	C32	C39	121.2(10)
N1	C4	C15	115.9(8)	C34	C33	C32	125.4(10)
C5	C4	N1	123.8(9)	C2	C34	C35	121.6(10)
C5	C4	C15	120.3(9)	C33	C34	C2	117.0(10)
C4	C5	C6	120.0(9)	C33	C34	C35	121.4(10)
N2	C6	C5	118.5(9)	C34	C35	C36	109.2(11)
N2	C6	C13	122.2(9)	C34	C35	C38	109.8(10)
C13	C6	C5	119.3(9)	C36	C35	C38	108.4(12)

N2	C7	C8	119.7(10)	C37	C35	C34	111.2(11)
N2	C7	C12	121.8(9)	C37	C35	C36	108.7(12)
C12	C7	C8	118.5(10)	C37	C35	C38	109.5(12)
C9	C8	C7	119.7(11)	C40	C39	C32	112.6(11)
C8	C9	C10	121.6(11)	C41	C39	C32	109.4(12)
C11	C10	C9	120.4(11)	C41	C39	C40	106.8(14)
C10	C11	C12	120.9(12)	C42	C39	C32	109.9(11)
N3	C12	C7	121.5(9)	C42	C39	C40	108.3(16)
N3	C12	C11	119.7(10)	C42	C39	C41	109.8(15)
C11	C12	C7	118.8(10)				

**Crystallographic Table 12** Torsion Angles for  $\text{UO}_2[\text{L}^1]$ .

A	B	C	D	Angle/°	A	B	C	D	Angle/°
U1	N1	C3	C100	17.0(15)	C3	C100	C31	C32	-170.6(10)
U1	N1	C4	C5	-155.6(9)	C4	N1	C3	C100	-166.7(10)
U1	N1	C4	C15	21.1(12)	C4	C5	C6	N2	179.1(10)
U1	N4	C15	C4	-26.8(12)	C4	C5	C6	C13	-2.4(16)
U1	N4	C15	C14	149.4(9)	C5	C4	C15	N4	-179.5(10)
U1	N4	C16	C17	-14.4(17)	C5	C4	C15	C14	4.1(17)
U1	O3	C18	C17	36.3(16)	C5	C6	C13	N3	-173.3(10)
U1	O3	C18	C19	-146.9(8)	C5	C6	C13	C14	3.5(15)
U1	O10	C2	C100	-27.9(16)	C6	N2	C7	C8	178.8(10)
U1	O10	C2	C34	152.4(8)	C6	N2	C7	C12	-2.8(15)
N1	U1	N4	C15	26.3(7)	C6	C13	C14	C15	-0.8(15)
N1	U1	N4	C16	-151.4(10)	C7	N2	C6	C5	176.4(10)
N1	U1	O3	C18	-37.8(12)	C7	N2	C6	C13	-2.2(15)
N1	U1	O10	C2	39.1(10)	C7	C8	C9	C10	-1.2(19)
N1	C4	C5	C6	175.2(10)	C8	C7	C12	N3	-176.4(10)
N1	C4	C15	N4	3.6(14)	C8	C7	C12	C11	2.3(15)
N1	C4	C15	C14	-172.8(10)	C8	C9	C10	C11	0.0(19)
N4	U1	N1	C3	151.9(9)	C9	C10	C11	C12	2.4(18)
N4	U1	N1	C4	-24.4(7)	C10	C11	C12	N3	175.2(11)
N4	U1	O3	C18	-41.0(10)	C10	C11	C12	C7	-3.6(17)
N4	U1	O10	C2	40.7(12)	C12	N3	C13	C6	-2.8(14)
N4	C16	C17	C18	-7.1(19)	C12	N3	C13	C14	-179.5(9)
N4	C16	C17	C22	176.8(11)	C12	C7	C8	C9	0.0(17)
O3	U1	N1	C3	148.5(8)	C13	N3	C12	C7	-2.1(15)
O3	U1	N1	C4	-27.8(8)	C13	N3	C12	C11	179.2(10)

O3	U1	N4	C15	-156.4(8)	C13	C14	C15	N4	-179.1(10)
O3	U1	N4	C16	25.9(9)	C13	C14	C15	C4	-3.0(16)
O3	U1	O10	C2	-137.0(10)	C15	N4	C16	C17	167.8(11)
O3	C18	C19	C20	-178.4(10)	C15	C4	C5	C6	-1.4(17)
O3	C18	C19	C27	6.5(16)	C16	N4	C15	C4	151.2(10)
O4	U1	N1	C3	-121.5(8)	C16	N4	C15	C14	-32.6(15)
O4	U1	N1	C4	62.2(7)	C16	C17	C18	O3	1.2(17)
O4	U1	N4	C15	-63.9(7)	C16	C17	C18	C19	-175.6(10)
O4	U1	N4	C16	118.3(9)	C16	C17	C22	C21	177.0(11)
O4	U1	O3	C18	-126.7(10)	C17	C18	C19	C20	-1.6(16)
O4	U1	O10	C2	127.0(11)	C17	C18	C19	C27	-176.7(10)
O5	U1	N1	C3	60.0(9)	C18	C17	C22	C21	0.7(18)
O5	U1	N1	C4	-116.3(7)	C18	C19	C20	C21	1.8(18)
O5	U1	N4	C15	115.4(7)	C18	C19	C27	C28	63.7(14)
O5	U1	N4	C16	-62.3(9)	C18	C19	C27	C29	-177.4(12)
O5	U1	O3	C18	51.2(10)	C18	C19	C27	C30	-56.7(14)
O5	U1	O10	C2	-51.1(11)	C19	C20	C21	C22	-0.7(18)
C100	C2	C34	C33	-0.6(15)	C19	C20	C21	C23	-179.4(12)
C100	C2	C34	C35	-179.5(10)	C20	C19	C27	C28	-111.1(12)
C100	C31	C32	C33	2.6(16)	C20	C19	C27	C29	7.8(17)
C100	C31	C32	C39	-178.0(10)	C20	C19	C27	C30	128.4(12)
N2	C6	C13	N3	5.2(15)	C20	C21	C22	C17	-0.6(17)
N2	C6	C13	C14	-178.0(9)	C20	C21	C23	C24	58.7(17)
N2	C7	C8	C9	178.4(11)	C20	C21	C23	C25	-57.0(17)
N2	C7	C12	N3	5.2(16)	C20	C21	C23	C26	-178.6(17)
N2	C7	C12	C11	-176.1(10)	C22	C17	C18	O3	177.2(10)
N3	C13	C14	C15	176.0(10)	C22	C17	C18	C19	0.4(16)
O11	U1	N1	C3	-43.1(11)	C22	C21	C23	C24	-119.9(15)
O11	U1	N1	C4	140.5(7)	C22	C21	C23	C25	124.4(15)
O11	U1	N4	C15	-139.3(7)	C22	C21	C23	C26	3(2)
O11	U1	N4	C16	43.0(12)	C23	C21	C22	C17	178.0(11)
O11	U1	O3	C18	148.5(11)	C27	C19	C20	C21	176.9(11)
O11	U1	O10	C2	-148.3(11)	C31	C100	C2	O10	-179.2(10)
O10	U1	N1	C3	-29.4(8)	C31	C100	C2	C34	0.5(15)
O10	U1	N1	C4	154.2(8)	C31	C100	C3	N1	-179.7(10)
O10	U1	N4	C15	24.5(9)	C31	C32	C33	C34	-2.9(17)
O10	U1	N4	C16	-153.2(8)	C31	C32	C39	C40	8.4(19)
O10	U1	O3	C18	137.2(10)	C31	C32	C39	C41	-110.2(15)



O10	C2	C34	C33	179.0(10)	C31	C32	C39	C42	129.2(16)
O10	C2	C34	C35	0.2(16)	C32	C33	C34	C2	1.9(17)
C2	C100	C3	N1	11.4(17)	C32	C33	C34	C35	-179.2(11)
C2	C100	C31	C32	-1.6(16)	C33	C32	C39	C40	-172.3(14)
C2	C34	C35	C36	59.0(15)	C33	C32	C39	C41	69.1(16)
C2	C34	C35	C37	178.9(12)	C33	C32	C39	C42	-51.5(19)
C2	C34	C35	C38	-59.7(15)	C33	C34	C35	C36	-119.9(13)
C3	N1	C4	C5	27.7(15)	C33	C34	C35	C37	0.1(17)
C3	N1	C4	C15	-155.6(10)	C33	C34	C35	C38	121.4(13)
C3	C100	C2	O10	-11.0(16)	C39	C32	C33	C34	177.7(11)
C3	C100	C2	C34	168.7(9)					

**Crystallographic Table 13** Hydrogen Atom Coordinates ( $\text{\AA}\times 10^4$ ) and Isotropic Displacement Parameters ( $\text{\AA}^2\times 10^3$ ) for  $\text{UO}_2[\text{L}^1]$ .

Atom	x	y	z	U(eq)
H25	-612	2614	668	37
H24	-544	4127	929	41
H23	-1236	7532	512	58
H1	-873	9135	421	58
H22	379	9569	524	53
H2	1274	8404	726	53
H21	1948	4943	871	40
H3	2334	3660	437	45
H14	4858	1357	987	51
H4	3455	3322	88	50
H5	4598	1525	-680	158
H6	5055	1128	-40	158
H7	5457	1741	-534	158
H8	5956	3024	128	153
H10	5735	2424	720	153
H9	5502	3540	628	153
H12	4951	3472	-766	253
H13	4539	4004	-244	253
H11	4117	3211	-705	253
H16	3697	-592	1300	100
H15	3083	-104	1667	100
H17	3684	-807	2039	100
H19	5258	755	2015	117

H20	4993	-29	1478	117
H18	5009	-305	2211	117
H30A	4164	396	2865	95
H30B	3508	1096	2585	95
H30C	4331	1492	2678	95
H45	-1581	1538	543	43
H35	-1726	-653	1802	50
H26	-614	368	3200	129
H28	197	462	3014	129
H27	2	-396	3472	129
H29	-749	-1837	3037	130
H30	-1123	-1840	2314	130
H31	-1399	-1096	2811	130
H33	170	-1662	2012	106
H34	534	-1539	2733	106
H32	647	-718	2222	106
H36	-2429	618	-116	169
H37	-2830	1408	270	169
H38	-3274	486	-32	169
H41	-3609	149	1092	168
H40	-3161	1128	1272	168
H39	-2959	157	1669	168
H43	-3066	-1064	312	212
H44	-2705	-1316	1019	212
H42	-2197	-1173	469	212

#### Refinement model description

Number of restraints - 0, number of constraints - unknown.

Details:

##### 1. Others

Fixed Uiso: H25(0.037) H24(0.041) H23(0.058) H1(0.058) H22(0.053) H2(0.053)  
H21(0.04) H3(0.045) H14(0.051) H4(0.05) H5(0.158) H6(0.158) H7(0.158)  
H8(0.153) H10(0.153) H9(0.153) H12(0.253) H13(0.253) H11(0.253) H16(0.1)  
H15(0.1) H17(0.1) H19(0.117) H20(0.117) H18(0.117) H30A(0.095) H30B(0.095)  
H30C(0.095) H45(0.043) H35(0.05) H26(0.129) H28(0.129) H27(0.129) H29(0.13)  
H30(0.13) H31(0.13) H33(0.106) H34(0.106) H32(0.106) H36(0.169) H37(0.169)  
H38(0.169) H41(0.168) H40(0.168) H39(0.168) H43(0.212) H44(0.212) H42(0.212)

Fixed X: H25(-0.0612) H24(-0.0544) H23(-0.1236) H1(-0.0873) H22(0.0379)  
H2(0.1274) H21(0.1948) H3(0.2334) H14(0.4858) H4(0.3455) H5(0.4598) H6(0.5055)  
H7(0.5457) H8(0.5956) H10(0.5735) H9(0.5502) H12(0.4951) H13(0.4539)  
H11(0.4117) H16(0.3697) H15(0.3083) H17(0.3684) H19(0.5258) H20(0.4993)  
H18(0.5009) H30A(0.4164) H30B(0.3508) H30C(0.4331) H45(-0.1581) H35(-0.1726)  
H26(-0.0614) H28(0.0197) H27(0.0002) H29(-0.0749) H30(-0.1123) H31(-0.1399)  
H33(0.017) H34(0.0534) H32(0.0647) H36(-0.2429) H37(-0.283) H38(-0.3274) H41(-  
0.3609) H40(-0.3161) H39(-0.2959) H43(-0.3066) H44(-0.2705) H42(-0.2197)  
Fixed Y: H25(0.2614) H24(0.4127) H23(0.7532) H1(0.9135) H22(0.9569)  
H2(0.8404) H21(0.4943) H3(0.366) H14(0.1357) H4(0.3322) H5(0.1525) H6(0.1128)  
H7(0.1741) H8(0.3024) H10(0.2424) H9(0.354) H12(0.3472) H13(0.4004)  
H11(0.3211) H16(-0.0592) H15(-0.0104) H17(-0.0807) H19(0.0755) H20(-0.0029)  
H18(-0.0305) H30A(0.0396) H30B(0.1096) H30C(0.1492) H45(0.1538) H35(-0.0653)  
H26(0.0368) H28(0.0462) H27(-0.0396) H29(-0.1837) H30(-0.184) H31(-0.1096)  
H33(-0.1662) H34(-0.1539) H32(-0.0718) H36(0.0618) H37(0.1408) H38(0.0486)  
H41(0.0149) H40(0.1128) H39(0.0157) H43(-0.1064) H44(-0.1316) H42(-0.1173)  
Fixed Z: H25(0.0668) H24(0.0929) H23(0.0512) H1(0.0421) H22(0.0524)  
H2(0.0726) H21(0.0871) H3(0.0437) H14(0.0987) H4(0.0088) H5(-0.068) H6(-0.004)  
H7(-0.0534) H8(0.0128) H10(0.072) H9(0.0628) H12(-0.0766) H13(-0.0244) H11(-  
0.0705) H16(0.13) H15(0.1667) H17(0.2039) H19(0.2015) H20(0.1478) H18(0.2211)  
H30A(0.2865) H30B(0.2585) H30C(0.2678) H45(0.0543) H35(0.1802) H26(0.32)  
H28(0.3014) H27(0.3472) H29(0.3037) H30(0.2314) H31(0.2811) H33(0.2012)  
H34(0.2733) H32(0.2222) H36(-0.0116) H37(0.027) H38(-0.0032) H41(0.1092)  
H40(0.1272) H39(0.1669) H43(0.0312) H44(0.1019) H42(0.0469)

## Cu[L<sup>I</sup>]

**Crystallographic Table 14** Crystal data and structure refinement for Cu[L<sup>I</sup>]

Formula	C <sub>42</sub> H <sub>48</sub> CuN <sub>4</sub> O <sub>2</sub>
D <sub>calc</sub> /g cm <sup>-3</sup>	1.274
μ/mm <sup>-1</sup>	0.636
Formula Weight	704.39
Colour	Red
Shape	Prism
Size/mm <sup>3</sup>	0.48 × 0.11 × 0.05
T/K	180(2)
Crystal System	Triclinic
Space Group	<i>P</i> <sup>-1</sup>
<i>a</i> /°Å	9.9751(2)
<i>b</i> /°	12.6630(3)
<i>c</i> /°	14.8623(3)
<i>α</i> /°	93.6100(10)
<i>β</i> /°	96.8350(10)
<i>γ</i> /°	98.7160(10)
<i>V</i> /° <sup>3</sup>	1836.17(7)
<i>Z</i>	2
Θ <sub>min</sub> /°	1.38
Θ <sub>max</sub> /°	26.77
Measured Refl.	60413
Independent Refl.	7756
Reflections Used	6595
<i>R</i> <sub>int</sub>	0.0333
Parameters	454
Restraints	0
Largest Peak	0.925
Deepest Hole	-0.422
GooF	1.062
<i>wR</i> 2(all data)	0.0966
<i>wR</i> 2	0.0924
<i>R</i> 1(all data)	0.0465
<i>R</i> 1	0.0365

**Crystallographic Table 15** Fractional Atomic Coordinates (×10<sup>4</sup>) and Equivalent Isotropic Displacement Parameters (°Å<sup>2</sup> × 10<sup>3</sup>) for Cu[L<sup>I</sup>]. *U*<sub>eq</sub> is defined as 1/3 of the trace of the orthogonalised *U*<sub>ij</sub> tensor.

Atom	X	Y	Z	U(eq)
Cu1	-34.8(2)	9894.14(17)	3409.36(14)	7.76(8)

O2	-646.1(13)	10812.6(10)	2549.2(9)	22.9(3)
O1	-1372.4(13)	8750.6(10)	2809.7(9)	24.1(3)
N1	588.6(15)	9024.8(12)	4345(1)	18.0(3)
C3	-3235.1(19)	7306.3(16)	1497.6(13)	24.2(4)
N4	5471.4(16)	11198.0(13)	6253.3(11)	23.1(3)
N3	4452.3(16)	9069.5(13)	6656.1(11)	23.7(3)
N2	1449.6(15)	10983.9(12)	4003.7(10)	17.7(3)
C16	1790.7(18)	9523.4(14)	4912.7(12)	17.7(4)
C27	2288.2(18)	10608.6(14)	4713.9(12)	17.5(4)
C28	1706.0(19)	11965.6(14)	3766.8(12)	19.8(4)
C29	998.2(19)	12396.8(14)	3027.6(12)	20.1(4)
C43	-122.2(18)	11788.1(14)	2426.6(12)	19.0(4)
C37	-663.1(19)	12281.2(15)	1643.1(12)	20.1(4)
C36	-99.0(19)	13318.1(15)	1536.1(13)	22.1(4)
C31	988.2(19)	13946.8(15)	2130.2(13)	21.9(4)
C30	1511.9(19)	13475.5(15)	2864.0(13)	22.4(4)
C32	1516(2)	15084.3(15)	1897.2(14)	25.9(4)
C35	352(2)	15754.7(17)	1855.0(18)	38.1(5)
C34	2026(2)	15012.7(19)	961.7(16)	39.2(5)
C33	2697(2)	15652.5(17)	2588.3(17)	37.7(5)
C38	-1808(2)	11645.7(15)	945.4(13)	22.9(4)
C41	-1302(2)	10660.0(18)	533.4(14)	34.4(5)
C40	-3098(2)	11297.0(18)	1389.9(15)	32.8(5)
C39	-2209(2)	12309.9(18)	157.7(15)	34.5(5)
C26	3487.7(19)	11152.2(15)	5171.1(12)	20.9(4)
C25	4265.3(19)	10661.9(15)	5844.6(12)	19.9(4)
C18	3756.9(19)	9592.4(15)	6046.1(12)	20.2(4)
C19	5648.7(19)	9611.1(16)	7076.5(12)	22.7(4)
C20	6433(2)	9106.4(18)	7742.6(13)	28.6(4)
C21	7645(2)	9636.1(19)	8175.4(14)	31.3(5)
C22	8161(2)	10687.6(19)	7974.3(14)	31.2(5)
C23	7451(2)	11198.4(17)	7336.8(14)	28.4(4)
C24	6165.1(19)	10677.2(16)	6873.5(12)	22.3(4)
C17	2502.2(19)	9047.7(15)	5569.3(13)	21.8(4)
C14	-1085.7(19)	7423.9(15)	3867.0(13)	20.7(4)
C1	-1681.0(18)	7780.3(14)	3036.6(13)	19.8(4)
C2	-2645.7(18)	7006.0(15)	2436.5(13)	21.0(4)
C4	-4160(2)	6347.5(18)	939.3(15)	35.6(5)
C6	-2070(2)	7673.1(18)	939.1(14)	30.9(5)
C5	-4094(2)	8202.1(19)	1618.6(16)	35.2(5)
C7	-3006.8(19)	5999.8(15)	2728.0(13)	22.8(4)
C8	-2483.1(19)	5651.4(15)	3570.4(13)	21.5(4)
C13	-1523.9(19)	6368.2(15)	4111.4(13)	22.3(4)

C9	-2928(2)	4494.5(15)	3793.5(14)	25.1(4)
C10	-4474(3)	4182(2)	3670(3)	66.5(9)
C15	13.9(18)	8047.6(14)	4448.7(12)	19.2(4)
C11	-2341(4)	3735(2)	3154(2)	60.1(8)
C12	-2397(3)	4299(2)	4772.4(19)	55.0(7)

**Crystallographic Table 16** Anisotropic Displacement Parameters ( $\times 10^4$ ) **Cu[L<sup>I</sup>]**. The Anisotropic displacement factor exponent takes the form:  $-2\pi^2[h2a * 2 U11 + \dots + 2hka \times b \times U12]$

Atom	U11	U22	U33	U23	U13	U12
Cu1	22.10(13)	15.05(12)	14.70(12)	3.27(8)	-2.47(8)	1.40(8)
O2	27.3(7)	18.9(7)	19.8(7)	6.2(5)	-5.0(5)	0.0(5)
O1	28.0(7)	18.4(7)	22.3(7)	4.3(5)	-7.0(6)	-0.8(5)
N1	20.5(8)	17.6(7)	15.0(7)	1.5(6)	-0.5(6)	2.4(6)
C3	23(1)	24.7(10)	22.5(10)	1.0(8)	-2.8(8)	0.7(8)
N4	23.7(8)	23.6(8)	20.7(8)	-1.1(6)	-0.1(6)	2.7(7)
N3	23.9(8)	28.2(9)	18.6(8)	5.8(7)	-1.1(6)	4.7(7)
N2	21.3(8)	16.8(7)	14.7(7)	2.6(6)	-0.2(6)	3.5(6)
C16	19.2(9)	18.1(9)	15.2(9)	0.6(7)	0.8(7)	2.6(7)
C27	22.0(9)	17.5(9)	13.4(8)	1.8(7)	1.6(7)	5.1(7)
C28	23.5(9)	17.3(9)	17.5(9)	0.9(7)	0.2(7)	1.9(7)
C29	24.1(9)	18.5(9)	18.1(9)	3.8(7)	2.1(7)	4.8(7)
C43	22.5(9)	17.9(9)	17.6(9)	3.2(7)	3.6(7)	5.2(7)
C37	22.7(9)	21.7(9)	17.5(9)	4.1(7)	3.2(7)	6.7(7)
C36	24.3(10)	23.6(10)	20.8(10)	9.0(8)	2.6(7)	8.7(8)
C31	24(1)	17.9(9)	25.3(10)	6.4(7)	4.1(8)	4.9(7)
C30	23.6(10)	18.1(9)	24.8(10)	3.3(7)	0.0(8)	2.8(7)
C32	27.4(10)	19.8(9)	31.4(11)	11.0(8)	2.3(8)	4.2(8)
C35	35.7(12)	24.2(11)	56.3(15)	12.1(10)	4.7(11)	8.6(9)
C34	43.2(13)	36.3(13)	38.7(13)	14.5(10)	11.2(10)	-0.5(10)
C33	40.2(13)	23.6(11)	45.7(14)	12.5(10)	-5.3(10)	-2.3(9)
C38	27.2(10)	23.4(10)	17.7(9)	5.1(7)	-1.3(8)	5.0(8)
C41	46.1(13)	33.7(12)	21.9(11)	-3.2(9)	-5.9(9)	12(1)
C40	24.9(10)	39.2(12)	31.8(12)	6.1(9)	-1.2(9)	-0.5(9)
C39	38.6(12)	35.1(12)	27.1(11)	10.6(9)	-9.1(9)	4(1)
C26	25.8(10)	16.5(9)	19.8(9)	2.9(7)	0.6(7)	2.6(7)
C25	21.3(9)	21.7(9)	16.0(9)	-1.7(7)	0.0(7)	4.4(7)
C18	21.6(9)	23.5(9)	15.5(9)	2.5(7)	1.2(7)	4.4(7)
C19	22.1(9)	31.4(11)	15.5(9)	0.7(8)	2.3(7)	7.2(8)
C20	28.3(11)	38.6(12)	20(1)	4.6(8)	0.3(8)	10.7(9)
C21	26.9(11)	48.9(13)	19.4(10)	-0.2(9)	-2.1(8)	15.9(10)
C22	22.1(10)	47.1(13)	22.5(10)	-8.6(9)	-3.1(8)	8.7(9)

C23	25.3(10)	32.6(11)	25.4(11)	-7.1(8)	1.1(8)	4.0(8)
C24	22.4(9)	28.3(10)	16.4(9)	-3.1(8)	1.0(7)	7.8(8)
C17	25.3(10)	19.1(9)	20.4(10)	6.2(7)	0.4(8)	1.6(7)
C14	22.2(9)	18.2(9)	21.6(10)	1.0(7)	2.0(7)	4.4(7)
C1	19.7(9)	18.5(9)	21.3(9)	1.4(7)	2.1(7)	3.6(7)
C2	18.2(9)	21.7(9)	22.3(10)	0.2(7)	0.9(7)	3.3(7)
C4	36.5(12)	36.2(12)	26.8(11)	1.0(9)	-7.1(9)	-7.4(10)
C6	30.4(11)	37.1(12)	23.8(11)	6.3(9)	0.0(8)	1.9(9)
C5	30.6(11)	39.4(13)	34.6(12)	1.3(10)	-7.0(9)	11.9(10)
C7	19.6(9)	21.2(9)	26.2(10)	-2.1(8)	1.9(8)	0.9(7)
C8	21.7(9)	18.0(9)	25.8(10)	1.5(7)	6.1(8)	4.2(7)
C13	24.5(10)	19.4(9)	23.5(10)	4.0(7)	2.1(8)	4.9(7)
C9	25.7(10)	19.4(9)	29.5(11)	4.1(8)	4.6(8)	0.2(8)
C10	39.1(15)	55.3(18)	107(3)	42.3(18)	8.4(16)	-1.2(13)
C15	23.1(9)	17.4(9)	17.7(9)	4.1(7)	0.5(7)	5.8(7)
C11	96(2)	27.6(13)	61.9(19)	6.5(12)	30.6(17)	10.3(14)
C12	78(2)	32.1(13)	47.3(16)	14.1(11)	-10.7(4)	-5.3(13)

**Crystallographic Table 17** Bond Lengths in Å for **Cu[L<sup>I</sup>]**

Atom	Atom	Å	Atom	Atom	Å
Cu1	O2	1.8909(12)	C31	C30	1.364(3)
Cu1	O1	1.9079(13)	C31	C32	1.532(3)
Cu1	N1	1.9305(15)	C32	C33	1.524(3)
Cu1	N2	1.9475(15)	C32	C35	1.536(3)
O2	C43	1.299(2)	C32	C34	1.539(3)
O1	C1	1.296(2)	C38	C39	1.534(3)
N1	C15	1.309(2)	C38	C40	1.535(3)
N1	C16	1.418(2)	C38	C41	1.535(3)
C3	C5	1.536(3)	C26	C25	1.424(3)
C3	C4	1.538(3)	C25	C18	1.435(3)
C3	C6	1.539(3)	C18	C17	1.418(3)
C3	C2	1.542(3)	C19	C20	1.431(3)
N4	C25	1.343(2)	C19	C24	1.434(3)
N4	C24	1.352(2)	C20	C21	1.356(3)
N3	C19	1.344(2)	C21	C22	1.416(3)
N3	C18	1.344(2)	C22	C23	1.368(3)
N2	C28	1.310(2)	C23	C24	1.425(3)
N2	C27	1.419(2)	C14	C15	1.414(3)
C16	C17	1.363(3)	C14	C13	1.425(3)
C16	C27	1.450(2)	C14	C1	1.434(3)
C27	C26	1.366(3)	C1	C2	1.443(3)
C28	C29	1.418(3)	C2	C7	1.381(3)

C29	C30	1.431(3)	C7	C8	1.421(3)
C29	C43	1.434(3)	C8	C13	1.359(3)
C43	C37	1.443(2)	C8	C9	1.534(3)
C37	C36	1.375(3)	C9	C10	1.519(3)
C37	C38	1.537(3)	C9	C11	1.536(3)
C36	C31	1.418(3)	C9	C12	1.536(3)

**Crystallographic Table 18** Bond Angles in ° for Cu[L<sup>1</sup>]

Atom	Atom	Atom	Angle/°	Atom	Atom	Atom	Angle/°
O2	Cu1	O1	89.19(5)	C31	C32	C34	108.48(17)
O2	Cu1	N1	176.50(6)	C35	C32	C34	109.18(18)
O1	Cu1	N1	93.26(6)	C39	C38	C40	107.49(17)
O2	Cu1	N2	93.50(6)	C39	C38	C41	107.14(17)
O1	Cu1	N2	175.04(6)	C40	C38	C41	110.14(17)
N1	Cu1	N2	84.24(6)	C39	C38	C37	111.88(16)
C43	O2	Cu1	129.18(12)	C40	C38	C37	110.92(16)
C1	O1	Cu1	128.99(12)	C41	C38	C37	109.19(16)
C15	N1	C16	121.28(15)	C27	C26	C25	120.61(17)
C15	N1	Cu1	124.84(12)	N4	C25	C26	119.25(17)
C16	N1	Cu1	113.84(11)	N4	C25	C18	121.80(17)
C5	C3	C4	107.91(17)	C26	C25	C18	118.92(16)
C5	C3	C6	110.12(17)	N3	C18	C17	118.30(17)
C4	C3	C6	106.81(17)	N3	C18	C25	122.19(17)
C5	C3	C2	109.76(16)	C17	C18	C25	119.47(16)
C4	C3	C2	111.93(16)	N3	C19	C20	119.00(18)
C6	C3	C2	110.26(15)	N3	C19	C24	121.92(17)
C25	N4	C24	116.07(16)	C20	C19	C24	119.08(18)
C19	N3	C18	116.09(17)	C21	C20	C19	120.1(2)
C28	N2	C27	121.75(16)	C20	C21	C22	120.96(19)
C28	N2	Cu1	124.57(12)	C23	C22	C21	120.98(19)
C27	N2	Cu1	113.63(11)	C22	C23	C24	120.0(2)
C17	C16	N1	125.35(17)	N4	C24	C23	119.18(18)
C17	C16	C27	120.23(17)	N4	C24	C19	121.92(17)
N1	C16	C27	114.35(15)	C23	C24	C19	118.91(17)
C26	C27	N2	126.27(16)	C16	C17	C18	120.60(17)
C26	C27	C16	120.14(16)	C15	C14	C13	116.33(16)
N2	C27	C16	113.53(15)	C15	C14	C1	123.08(17)
N2	C28	C29	126.28(17)	C13	C14	C1	120.43(17)
C28	C29	C30	116.47(17)	O1	C1	C14	122.68(17)
C28	C29	C43	123.27(17)	O1	C1	C2	119.92(16)
C30	C29	C43	120.15(16)	C14	C1	C2	117.39(16)
O2	C43	C29	122.89(16)	C7	C2	C1	118.03(17)



O2	C43	C37	119.10(16)	C7	C2	C3	121.79(17)
C29	C43	C37	117.99(16)	C1	C2	C3	120.18(16)
C36	C37	C43	117.83(17)	C2	C7	C8	125.23(18)
C36	C37	C38	121.80(16)	C13	C8	C7	116.32(17)
C43	C37	C38	120.36(16)	C13	C8	C9	123.62(17)
C37	C36	C31	125.35(17)	C7	C8	C9	119.89(17)
C30	C31	C36	116.81(17)	C8	C13	C14	122.40(17)
C30	C31	C32	124.63(18)	C10	C9	C8	112.12(18)
C36	C31	C32	118.54(16)	C10	C9	C11	108.3(2)
C31	C30	C29	121.82(18)	C8	C9	C11	108.79(17)
C33	C32	C31	112.48(16)	C10	C9	C12	107.4(2)
C33	C32	C35	108.61(18)	C8	C9	C12	112.64(17)
C31	C32	C35	109.85(16)	C11	C9	C12	107.3(2)
C33	C3	C3	108.18(18)	N1	C15	C1	126.45(17)

## VO[L<sup>I</sup>]

**Crystallographic Table 19** Crystal data and structure refinement for VO[L<sup>I</sup>]

Empirical formula	C <sub>42</sub> H <sub>48</sub> N <sub>4</sub> O <sub>3</sub> V
Formula weight	707.82
Temperature/K	296.15
Crystal system	triclinic
Space group	P-1
a/Å	10.5213(4)
b/Å	12.7581(5)
c/Å	16.9448(6)
α/°	77.715(1)
β/°	74.447(1)
γ/°	79.226(1)
Volume/Å <sup>3</sup>	2120.59(14)
Z	2
ρ <sub>calc</sub> /mg/mm <sup>3</sup>	1.1084
m/mm <sup>-1</sup>	0.272
F(000)	750.9
Crystal size/mm <sup>3</sup>	0.6 × 0.08 × 0.08
Radiation	Mo Kα (λ = 0.71073)
2θ range for data collection	3.3 to 49.42°
Index ranges	-12 ≤ h ≤ 12, -15 ≤ k ≤ 15, -19 ≤ l ≤ 19
Reflections collected	35450
Independent reflections	7239 [R <sub>int</sub> = 0.0414, R <sub>sigma</sub> = 0.0397]
Data/restraints/parameters	7239/0/462
Goodness-of-fit on F <sup>2</sup>	2.571
Final R indexes [I ≥ 2σ (I)]	R <sub>1</sub> = 0.1090, wR <sub>2</sub> = 0.3205
Final R indexes [all data]	R <sub>1</sub> = 0.1280, wR <sub>2</sub> = 0.3266
Largest diff. peak/hole / e Å <sup>-3</sup>	3.47/-0.47

**Crystallographic Table 20** Fractional Atomic Coordinates (×10<sup>4</sup>) and Equivalent Isotropic Displacement Parameters (Å<sup>2</sup>×10<sup>3</sup>) for VO[L<sup>I</sup>]. U<sub>eq</sub> is defined as 1/3 of the trace of the orthogonalised U<sub>ij</sub> tensor.

Atom	x	y	z	U(eq)
V1	4939.4(11)	5939.1(9)	1615.2(6)	21.8(4)
O2	4715(4)	6483(4)	2631(3)	26.8(10)
O1	4101(4)	4726(4)	2300(3)	28.2(11)
N2	6752(5)	6499(4)	1213(3)	21.8(12)

N1	6004(5)	4884(4)	832(3)	22.4(12)
N3	9706(5)	4813(5)	-1606(3)	28.7(13)
N4	10561(5)	6552(5)	-1166(3)	28.6(13)
C1	5224(6)	7265(5)	2787(4)	22.1(14)
C14	6401(6)	7638(5)	2265(4)	25.1(14)
C2	4613(7)	7718(5)	3520(4)	26.2(15)
C13	6948(7)	8442(5)	2470(4)	28.9(15)
C8	6385(7)	8885(6)	3162(4)	31.4(16)
C7	5208(7)	8505(5)	3678(4)	30.4(16)
C16	7592(6)	6126(5)	494(4)	21.3(13)
C27	7169(6)	5253(5)	261(4)	21.5(14)
C26	7857(6)	4839(5)	-437(4)	25.2(14)
C17	8729(6)	6538(5)	16(4)	24.6(14)
C25	9023(6)	5251(5)	-929(4)	24.1(14)
C18	9463(6)	6115(5)	-703(4)	24.2(14)
C24	10807(6)	5234(6)	-2057(4)	28.2(15)
C23	11591(7)	4785(6)	-2760(4)	36.8(18)
C20	12403(7)	6530(7)	-2353(5)	42.8(19)
C19	11228(6)	6117(6)	-1840(4)	29.1(16)
C22	12712(7)	5215(7)	-3223(4)	40.7(19)
C21	13108(8)	6072(7)	-3028(5)	45(2)
C29	4539(6)	3494(5)	1347(4)	25.7(15)
C30	4241(7)	2562(5)	1139(4)	30.1(16)
C28	5618(6)	3987(5)	786(4)	25.5(15)
C31	3293(7)	1980(5)	1660(4)	29.3(15)
O3	3974(5)	6712(4)	1082(3)	32.1(11)
C15	7121(6)	7208(5)	1541(4)	24.5(14)
C3	3322(7)	7345(6)	4106(4)	36.0(18)
C9	6927(8)	9780(6)	3410(5)	41.3(19)
C5	3612(8)	6122(6)	4466(4)	42.3(19)
C4	2210(8)	7549(7)	3646(5)	45(2)
C6	2840(10)	7958(8)	4850(5)	59(3)
C11	5894(10)	10793(6)	3434(6)	58(3)
C10	8216(10)	10074(9)	2789(7)	80(4)
C12	7238(12)	9385(8)	4266(6)	71(3)
C32	3006(7)	920(6)	1478(5)	35.3(17)
C34	1527(9)	845(8)	1732(7)	65(3)
C33	3476(11)	858(8)	564(6)	68(3)

C37	2866(7)	3236(6)	2669(4)	30.9(16)
C36	2643(7)	2336(6)	2416(4)	32.7(16)
C38	2154(7)	3527(6)	3523(4)	36.0(17)
C41	3188(8)	3365(7)	4052(4)	42.1(19)
C40	1494(8)	4717(7)	3451(5)	45(2)
C39	1067(10)	2817(8)	3982(5)	64(3)
C35	3727(13)	-31(7)	1957(8)	88(4)
C42	3841(6)	3866(5)	2103(4)	26.1(15)

**Crystallographic Table 21** Anisotropic Displacement Parameters ( $\text{\AA}^2 \times 10^3$ ) for VO[L<sup>I</sup>].  
The Anisotropic displacement factor exponent takes the form: -  
 $2\pi^2[h^2a^{*2}U_{11}+2hka^*b^*U_{12}+\dots]$

Atom	U <sub>11</sub>	U <sub>22</sub>	U <sub>33</sub>	U <sub>12</sub>	U <sub>13</sub>	U <sub>23</sub>
V1	23.3(6)	24.1(6)	19.8(6)	-8.2(4)	-3.0(4)	-6.2(4)
O2	30(2)	31(3)	22(2)	-13(2)	0.4(19)	-10.3(19)
O1	32(3)	31(3)	23(2)	-16(2)	1(2)	-8(2)
N2	25(3)	21(3)	18(3)	-3(2)	-3(2)	-5(2)
N1	24(3)	26(3)	18(3)	-10(2)	-3(2)	-3(2)
N3	30(3)	34(3)	20(3)	-3(3)	-4(2)	-5(2)
N4	23(3)	34(3)	25(3)	-8(2)	-2(2)	1(2)
C1	23(3)	22(3)	22(3)	-6(3)	-5(3)	-4(3)
C14	29(4)	23(3)	25(3)	-6(3)	-5(3)	-6(3)
C2	34(4)	25(4)	20(3)	-6(3)	-6(3)	-5(3)
C13	30(4)	29(4)	29(4)	-11(3)	-2(3)	-8(3)
C8	36(4)	28(4)	33(4)	-10(3)	-5(3)	-10(3)
C7	40(4)	27(4)	25(4)	-9(3)	-3(3)	-9(3)
C16	23(3)	23(3)	19(3)	-5(3)	-4(3)	-4(3)
C27	21(3)	22(3)	19(3)	-6(3)	-3(3)	0(3)
C26	29(4)	25(4)	22(3)	-5(3)	-5(3)	-5(3)
C17	24(3)	25(4)	24(3)	-8(3)	-3(3)	-4(3)
C25	24(3)	25(4)	21(3)	-1(3)	-3(3)	-3(3)
C18	23(3)	25(4)	22(3)	-5(3)	-5(3)	2(3)
C24	24(4)	37(4)	18(3)	-1(3)	-4(3)	3(3)
C23	32(4)	47(5)	24(4)	7(3)	-4(3)	-4(3)
C20	32(4)	54(5)	35(4)	-13(4)	1(3)	4(4)
C19	22(3)	39(4)	20(3)	-2(3)	-3(3)	4(3)
C22	27(4)	59(5)	24(4)	5(4)	1(3)	2(4)
C21	26(4)	66(6)	30(4)	-3(4)	3(3)	3(4)
C29	27(4)	26(4)	25(3)	-10(3)	-4(3)	-2(3)

C30	32(4)	28(4)	31(4)	-9(3)	-6(3)	-7(3)
C28	28(4)	29(4)	21(3)	-9(3)	-3(3)	-7(3)
C31	29(4)	25(4)	35(4)	-10(3)	-9(3)	-1(3)
O3	32(3)	34(3)	31(3)	-4(2)	-8(2)	-5(2)
C15	25(3)	20(3)	29(4)	-8(3)	-2(3)	-6(3)
C3	40(4)	40(4)	27(4)	-17(3)	7(3)	-14(3)
C9	45(5)	44(5)	40(4)	-24(4)	4(4)	-21(4)
C5	56(5)	42(5)	29(4)	-21(4)	0(4)	-5(3)
C4	34(4)	45(5)	53(5)	-10(4)	3(4)	-15(4)
C6	68(6)	68(6)	40(5)	-32(5)	21(4)	-31(4)
C11	81(7)	31(5)	66(6)	-20(4)	-4(5)	-22(4)
C10	70(7)	87(8)	97(8)	-56(6)	21(6)	-58(7)
C12	102(8)	66(7)	69(6)	-31(6)	-38(6)	-24(5)
C32	37(4)	25(4)	46(4)	-11(3)	-14(3)	1(3)
C34	57(6)	62(6)	89(7)	-32(5)	-13(5)	-29(5)
C33	79(7)	52(6)	85(7)	-32(5)	1(6)	-40(5)
C37	29(4)	36(4)	28(4)	-13(3)	-5(3)	1(3)
C36	33(4)	32(4)	35(4)	-19(3)	-7(3)	3(3)
C38	35(4)	45(5)	27(4)	-20(3)	2(3)	-3(3)
C41	52(5)	44(5)	26(4)	-8(4)	-6(4)	-2(3)
C40	31(4)	65(6)	38(4)	-4(4)	-4(3)	-17(4)
C39	65(6)	83(7)	44(5)	-51(6)	20(5)	-18(5)
C35	121(10)	26(5)	146(11)	-16(5)	-92(9)	3(6)
C42	27(4)	27(4)	28(4)	-12(3)	-7(3)	-3(3)

**Crystallographic Table 22 Bond Lengths for VO[L<sup>I</sup>].**

Atom	Atom	Length/Å	Atom	Atom	Length/Å
V1	O2	1.931(4)	C25	C18	1.429(9)
V1	O1	1.928(4)	C24	C23	1.420(9)
V1	N2	2.054(5)	C24	C19	1.432(10)
V1	N1	2.056(5)	C23	C22	1.367(10)
V1	O3	1.600(5)	C20	C19	1.426(10)
O2	C1	1.319(7)	C20	C21	1.366(11)
O1	C42	1.307(7)	C22	C21	1.372(12)
N2	C16	1.415(8)	C29	C30	1.418(9)
N2	C15	1.319(8)	C29	C28	1.422(9)
N1	C27	1.430(8)	C29	C42	1.424(9)
N1	C28	1.308(8)	C30	C31	1.362(9)

N3	C25	1.352(8)	C31	C32	1.548(9)
N3	C24	1.341(8)	C31	C36	1.405(10)
N4	C18	1.353(8)	C3	C5	1.555(11)
N4	C19	1.341(9)	C3	C4	1.527(11)
C1	C14	1.413(9)	C3	C6	1.545(10)
C1	C2	1.424(9)	C9	C11	1.525(12)
C14	C13	1.408(9)	C9	C10	1.532(11)
C14	C15	1.418(9)	C9	C12	1.531(12)
C2	C7	1.382(9)	C32	C34	1.515(11)
C2	C3	1.541(9)	C32	C33	1.509(12)
C13	C8	1.353(9)	C32	C35	1.508(11)
C8	C7	1.413(10)	C37	C36	1.386(10)
C8	C9	1.544(9)	C37	C38	1.529(10)
C16	C27	1.435(8)	C37	C42	1.439(9)
C16	C17	1.378(9)	C38	C41	1.545(10)
C27	C26	1.366(9)	C38	C40	1.541(11)
C26	C25	1.408(9)	C38	C39	1.531(10)
C17	C18	1.410(9)			

**Crystallographic Table 23** Bond Angles for VO[L<sup>1</sup>].

Atom	Atom	Atom	Angle/°	Atom	Atom	Atom	Angle/°
O1	V1	O2	86.81(18)	C19	C24	N3	121.7(6)
N2	V1	O2	87.49(19)	C19	C24	C23	118.9(6)
N2	V1	O1	141.4(2)	C22	C23	C24	119.6(8)
N1	V1	O2	147.9(2)	C21	C20	C19	119.9(8)
N1	V1	O1	86.81(19)	C24	C19	N4	121.9(6)
N1	V1	N2	78.2(2)	C20	C19	N4	119.5(7)
O3	V1	O2	108.7(2)	C20	C19	C24	118.6(6)
O3	V1	O1	111.0(2)	C21	C22	C23	121.8(7)
O3	V1	N2	107.0(2)	C22	C21	C20	121.2(7)
O3	V1	N1	102.9(2)	C28	C29	C30	116.3(6)
C1	O2	V1	131.3(4)	C42	C29	C30	121.2(6)
C42	O1	V1	130.8(4)	C42	C29	C28	122.4(6)
C16	N2	V1	114.9(4)	C31	C30	C29	121.3(6)
C15	N2	V1	124.9(4)	C29	C28	N1	126.2(6)
C15	N2	C16	120.1(5)	C32	C31	C30	122.5(6)
C27	N1	V1	114.8(4)	C36	C31	C30	116.8(6)
C28	N1	V1	124.4(4)	C36	C31	C32	120.4(6)

C28	N1	C27	120.6(5)	C14	C15	N2	126.4(6)
C24	N3	C25	116.7(6)	C5	C3	C2	108.8(6)
C19	N4	C18	116.4(6)	C4	C3	C2	110.9(6)
C14	C1	O2	121.8(5)	C4	C3	C5	110.8(6)
C2	C1	O2	119.6(5)	C6	C3	C2	111.1(6)
C2	C1	C14	118.5(5)	C6	C3	C5	107.1(6)
C13	C14	C1	120.3(6)	C6	C3	C4	108.0(7)
C15	C14	C1	123.1(6)	C11	C9	C8	109.5(6)
C15	C14	C13	116.6(6)	C10	C9	C8	111.3(6)
C7	C2	C1	117.8(6)	C10	C9	C11	108.6(7)
C3	C2	C1	120.5(5)	C12	C9	C8	109.9(6)
C3	C2	C7	121.7(6)	C12	C9	C11	109.8(7)
C8	C13	C14	122.3(6)	C12	C9	C10	107.7(8)
C7	C8	C13	116.9(6)	C34	C32	C31	111.0(6)
C9	C8	C13	124.5(6)	C33	C32	C31	111.4(6)
C9	C8	C7	118.6(6)	C33	C32	C34	107.5(7)
C8	C7	C2	124.2(6)	C35	C32	C31	108.9(6)
C27	C16	N2	114.9(5)	C35	C32	C34	109.3(8)
C17	C16	N2	125.7(5)	C35	C32	C33	108.8(8)
C17	C16	C27	119.4(5)	C38	C37	C36	121.9(6)
C16	C27	N1	113.1(5)	C42	C37	C36	116.9(6)
C26	C27	N1	125.7(6)	C42	C37	C38	121.1(6)
C26	C27	C16	121.2(6)	C37	C36	C31	125.8(6)
C25	C26	C27	119.8(6)	C41	C38	C37	108.8(6)
C18	C17	C16	120.3(6)	C40	C38	C37	111.4(6)
C26	C25	N3	118.8(6)	C40	C38	C41	108.4(6)
C18	C25	N3	121.5(6)	C39	C38	C37	111.9(6)
C18	C25	C26	119.7(6)	C39	C38	C41	108.7(6)
C17	C18	N4	118.7(6)	C39	C38	C40	107.6(7)
C25	C18	N4	121.7(6)	C29	C42	O1	121.8(6)
C25	C18	C17	119.5(6)	C37	C42	O1	120.3(6)
C23	C24	N3	119.4(6)	C37	C42	C29	117.8(6)

**Crystallographic Table 24** Hydrogen Atom Coordinates ( $\text{\AA}\times 10^4$ ) and Isotropic Displacement Parameters ( $\text{\AA}^2\times 10^3$ ) for **VO[L<sup>I</sup>]**.

Atom	<i>x</i>	<i>y</i>	<i>z</i>	<i>U</i> (eq)
H13	7723(7)	8676(5)	2118(4)	34.6(18)
H7	4807(7)	8805(5)	4155(4)	36.4(19)

H26	7555(6)	4287(5)	-588(4)	30.2(17)
H17	9014(6)	7097(5)	167(4)	29.5(17)
H23	11344(7)	4202(6)	-2905(4)	44(2)
H20	12689(7)	7109(7)	-2228(5)	51(2)
H22	13219(7)	4917(7)	-3684(4)	49(2)
H21	13872(8)	6347(7)	-3360(5)	54(2)
H30	4703(7)	2345(5)	637(4)	36.1(19)
H28	6095(6)	3638(5)	345(4)	30.6(17)
H15	7934(6)	7450(5)	1271(4)	29.4(17)
H5a	3940(50)	5717(8)	4019(5)	63(3)
H5b	4270(40)	6019(8)	4780(30)	63(3)
H5c	2806(14)	5876(12)	4820(30)	63(3)
H4a	2040(40)	8309(9)	3440(30)	67(3)
H4b	2480(20)	7150(30)	3190(20)	67(3)
H4c	1416(17)	7310(40)	4022(10)	67(3)
H6a	3540(20)	7860(40)	5140(20)	89(4)
H6b	2610(60)	8715(11)	4652(6)	89(4)
H6c	2070(40)	7680(40)	5220(20)	89(4)
H11a	5710(50)	11040(30)	2894(12)	87(4)
H11b	5090(20)	10626(14)	3830(30)	87(4)
H11c	6230(30)	11350(18)	3590(40)	87(4)
H10a	8880(30)	9450(20)	2770(40)	120(6)
H10b	8050(20)	10330(60)	2246(13)	120(6)
H10c	8530(50)	10630(50)	2960(30)	120(6)
H12a	6430(15)	9260(60)	4677(9)	106(5)
H12b	7850(60)	8730(30)	4256(14)	106(5)
H12c	7630(70)	9930(30)	4400(20)	106(5)
H34a	1192(16)	900(60)	2308(12)	97(4)
H34b	1073(12)	1420(30)	1400(30)	97(4)
H34c	1379(11)	160(20)	1650(40)	97(4)
H33a	3130(60)	1520(20)	246(7)	102(4)
H33b	4431(10)	770(60)	407(11)	102(4)
H33c	3160(60)	260(40)	456(10)	102(4)
H36	2008(7)	1931(6)	2779(4)	39(2)
H41a	3640(40)	2636(14)	4080(30)	63(3)
H41b	3820(30)	3860(30)	3800(18)	63(3)
H41c	2743(10)	3500(40)	4602(11)	63(3)
H40a	2171(8)	5185(7)	3270(30)	67(3)



H40b	950(40)	4859(13)	3060(30)	67(3)
H40c	950(40)	4847(13)	3984(9)	67(3)
H39a	370(30)	2970(40)	3690(20)	96(4)
H39b	1441(17)	2067(8)	4010(40)	96(4)
H39c	710(50)	2970(40)	4535(15)	96(4)
H35a	4670(13)	-20(40)	1770(40)	131(6)
H35b	3450(60)	10(40)	2539(10)	131(6)
H35c	3520(70)	-693(7)	1870(40)	131(6)

**Crystallographic Table 25** Solvent masks information for VO[L<sup>1</sup>].

**Number X Y Z Volume Electron count**

1	0.000	0.500	0.500	341.2	59.5
2	0.000	0.500	0.000	82.4	0.2

Refinement model description

Number of restraints - 0, number of constraints - 72.

Details:

1. Fixed Uiso

At 1.2 times of:

All C(H) groups

At 1.5 times of:

All C(H,H,H) groups

2.a Aromatic/amide H refined with riding coordinates:

C13(H13), C7(H7), C26(H26), C17(H17), C23(H23), C20(H20), C22(H22), C21(H21), C30(H30), C28(H28), C15(H15), C36(H36)

2.b Idealised Me refined as rotating group:

C5(H5a,H5b,H5c), C4(H4a,H4b,H4c), C6(H6a,H6b,H6c), C11(H11a,H11b,H11c), C10(H10a,H10b,H10c), C12(H12a,H12b,H12c), C34(H34a,H34b,H34c), C33(H33a,H33b, H33c), C41(H41a,H41b,H41c), C40(H40a,H40b,H40c), C39(H39a,H39b,H39c), C35(H35a, H35b,H35c)

## Zn[L<sup>I</sup>]

**Crystallographic Table 26** Crystal data and structure refinement for Zn[L<sup>I</sup>]

Empirical formula	C <sub>43</sub> H <sub>52</sub> N <sub>4</sub> O <sub>3</sub> Zn
Formula weight	738.31
Temperature/K	180.45
Crystal system	triclinic
Space group	P-1
a/Å	9.3102(5)
b/Å	15.1537(7)
c/Å	16.4769(8)
α/°	105.875(2)
β/°	100.257(2)
γ/°	91.511(2)
Volume/Å <sup>3</sup>	2193.30(19)
Z	2
ρ <sub>calc</sub> /mg/mm <sup>3</sup>	1.1179
m/mm <sup>-1</sup>	0.599
F(000)	784.9
Crystal size/mm <sup>3</sup>	0.2 × 0.1 × 0.1
Radiation	Mo Kα (λ = 0.71073)
2θ range for data collection	3.26 to 51.44°
Index ranges	-11 ≤ h ≤ 11, -18 ≤ k ≤ 18, -20 ≤ l ≤ 20
Reflections collected	43775
Independent reflections	8341 [R <sub>int</sub> = 0.0552, R <sub>sigma</sub> = 0.0462]
Data/restraints/parameters	8341/1/476
Goodness-of-fit on F <sup>2</sup>	1.064
Final R indexes [I >= 2σ (I)]	R <sub>1</sub> = 0.0467, wR <sub>2</sub> = 0.1086
Final R indexes [all data]	R <sub>1</sub> = 0.0614, wR <sub>2</sub> = 0.1186
Largest diff. peak/hole / e Å <sup>-3</sup>	0.59/-0.61

**Crystallographic Table 27** Fractional Atomic Coordinates (×10<sup>4</sup>) and Equivalent Isotropic Displacement Parameters (Å<sup>2</sup>×10<sup>3</sup>) for Zn[L<sup>I</sup>]. U<sub>eq</sub> is defined as 1/3 of the trace of the orthogonalised U<sub>ij</sub> tensor.

Atom	x	y	z	U(eq)
Zn1	3184.2(3)	3244.4(2)	2731.92(18)	22.58(10)
O1	3995(2)	2082.2(12)	2815.9(11)	25.9(4)
O2	2306(2)	2779.8(13)	1514.3(11)	29.2(4)
O3	5039(2)	3993.9(14)	2623.7(12)	32.1(5)

N1	3529(2)	3706.8(13)	4061.3(12)	18.5(4)
N2	1606(2)	4185.7(13)	2895.9(12)	19.7(4)
N4	146(2)	6635.7(14)	5118.6(14)	26.5(5)
N3	2384(2)	6225.3(14)	6345.9(13)	23.5(5)
C15	4360(3)	3320.0(16)	4568.9(15)	20.2(5)
C6	5055(3)	2488.3(17)	4322.0(15)	20.9(5)
C1	4801(3)	1887.8(17)	3457.0(16)	20.5(5)
C2	5469(3)	1018.5(17)	3319.2(16)	22.7(5)
C3	6379(3)	854.5(17)	4006.9(17)	24.6(6)
C4	6674(3)	1443.6(17)	4860.3(16)	23.9(6)
C5	5986(3)	2242.6(18)	4997.0(16)	25.1(6)
C11	7718(3)	1162.3(19)	5564.2(18)	30.4(6)
C13	9277(3)	1179(2)	5377(2)	40.8(8)
C12	7727(4)	1811(2)	6458.7(18)	45.0(8)
C14	7258(3)	179(2)	5568(2)	41.2(8)
C7	5118(3)	301.0(17)	2426.8(16)	25.0(6)
C8	5627(3)	676(2)	1734.5(18)	33.7(7)
C9	3467(3)	27.1(19)	2164.3(18)	31.3(6)
C10	5881(4)	-581.9(19)	2436.2(19)	38.0(7)
C16	2798(3)	4494.4(16)	4390.4(15)	18.8(5)
C27	1696(3)	4734.9(16)	3751.0(15)	18.0(5)
C28	579(3)	4272.9(17)	2277.1(16)	22.6(5)
C29	332(3)	3750.0(17)	1394.1(15)	22.3(5)
C30	-860(3)	3990.3(19)	846.1(17)	28.3(6)
C31	-1264(3)	3521(2)	-9.3(17)	29.6(6)
C35	-2543(3)	3754(2)	-619.9(19)	41.6(8)
C37	-2050(4)	3876(2)	-1419.0(19)	46.4(8)
C38	-3746(4)	2973(4)	-885(4)	112(2)
C36	-3140(5)	4654(4)	-195(2)	103(2)
C32	-465(3)	2759.9(19)	-319.0(16)	28.6(6)
C33	705(3)	2480.5(18)	165.6(16)	24.8(6)
C39	1514(3)	1638(2)	-211.6(17)	31.1(6)
C42	786(4)	1120(2)	-1141.2(19)	44.4(8)
C41	1521(4)	953(2)	330(2)	48.0(9)
C40	3095(3)	1946(2)	-212.3(19)	40.9(8)
C34	1171(3)	3007.1(18)	1054.1(16)	22.8(6)
C26	858(3)	5450.8(17)	4011.1(16)	23.8(6)
C25	1033(3)	5962.8(16)	4888.3(16)	21.3(5)

C24	353(3)	7097.5(17)	5961.2(18)	26.7(6)
C19	1484(3)	6897.7(17)	6583.0(17)	26.3(6)
C18	2160(3)	5752.7(16)	5509.2(16)	20.2(5)
C17	3035(3)	5016.1(16)	5229.3(15)	19.9(5)
C20	1630(3)	7396.0(19)	7462.8(18)	33.8(7)
C21	701(3)	8056(2)	7705(2)	40.9(8)
C22	-396(3)	8266(2)	7096(2)	42.0(8)
C23	-579(3)	7805.4(19)	6244(2)	36.6(7)
C43	5261(4)	4059(3)	1810(2)	62.5(11)

**Crystallographic Table 28** Anisotropic Displacement Parameters ( $\text{\AA}^2 \times 10^3$ ) for **Zn[L<sup>1</sup>]**.

The Anisotropic displacement factor exponent takes the form: -

$$2\pi^2[h^2a^2U_{11}+2hka*b*U_{12}+...]$$

Atom	U <sub>11</sub>	U <sub>22</sub>	U <sub>33</sub>	U <sub>12</sub>	U <sub>13</sub>	U <sub>23</sub>
Zn1	26.03(18)	22.46(17)	17.66(16)	6.54(12)	3.51(12)	3.04(12)
O1	36.7(11)	21.2(9)	17.7(9)	10.2(8)	3.2(8)	2.7(7)
O2	32.0(11)	32.8(11)	17.7(9)	10.5(8)	1.2(8)	0.4(8)
O3	30.8(11)	40.0(12)	26.1(10)	-1.9(9)	3.1(9)	12.5(9)
N1	21.8(11)	15.6(10)	17.1(10)	4.2(8)	4.2(8)	2.3(8)
N2	23.0(11)	18.0(11)	18.3(10)	4.3(8)	4.2(9)	4.6(8)
N4	25.9(12)	17.7(11)	34.2(13)	4.7(9)	9.8(10)	1.9(10)
N3	26.3(12)	20.3(11)	21.4(11)	-0.6(9)	8.7(9)	-0.5(9)
C15	24.9(13)	18.8(13)	14.8(12)	1.7(10)	4(1)	1.4(10)
C6	24.1(13)	19.2(13)	21.1(13)	4.2(10)	6.4(10)	6.8(10)
C1	21.0(13)	20.4(13)	22.5(13)	2.5(10)	9.3(10)	6.8(10)
C2	25.0(14)	21.0(13)	23.8(13)	3.5(11)	10.0(11)	5.8(11)
C3	25.1(14)	19.5(13)	32.0(14)	9.2(11)	10.3(11)	8.0(11)
C4	23.5(14)	23.5(14)	26.0(14)	5.0(11)	4.9(11)	8.7(11)
C5	28.8(14)	26.0(14)	19.1(13)	5.7(11)	3.2(11)	4.6(11)
C11	29.7(15)	29.6(15)	33.1(15)	10.7(12)	2.9(12)	12.2(12)
C13	29.0(16)	44.4(19)	52(2)	8.5(14)	3.6(14)	21.2(16)
C12	52(2)	50(2)	29.0(16)	23.8(16)	-3.5(14)	9.3(14)
C14	43.3(19)	44.6(19)	40.8(18)	4.3(15)	1.4(14)	24.8(15)
C7	30.7(15)	19.9(13)	24.8(13)	6.7(11)	10.0(11)	3.7(11)
C8	42.1(17)	32.6(16)	27.8(15)	3.5(13)	17.1(13)	4.3(12)
C9	36.5(16)	26.1(15)	28.1(15)	1.0(12)	10.4(12)	0.1(12)
C10	50.6(19)	25.2(15)	35.5(16)	12.8(14)	12.0(14)	0.9(13)
C16	20.0(13)	15.0(12)	21.2(12)	0.9(10)	5.5(10)	4(1)

C27	18.8(12)	14.8(12)	20.1(12)	0.4(10)	5.6(10)	3.7(10)
C28	24.7(14)	21.3(13)	23.7(13)	6.4(11)	6.3(11)	7.9(11)
C29	23.0(13)	25.7(14)	19.1(12)	0.2(11)	2.8(10)	8.6(11)
C30	26.8(14)	35.0(16)	26.3(14)	8.4(12)	7.7(11)	11.6(12)
C31	19.4(14)	47.2(18)	25.0(14)	0.9(12)	2.9(11)	15.8(13)
C35	27.1(16)	73(2)	29.7(16)	8.5(15)	2.8(13)	24.2(16)
C37	47(2)	66(2)	28.7(16)	12.3(17)	1.0(14)	22.6(16)
C38	30(2)	179(5)	145(5)	-37(3)	-38(3)	114(4)
C36	105(4)	181(5)	36(2)	111(4)	13(2)	41(3)
C32	24.8(14)	40.0(16)	17.6(13)	-5.8(12)	3.5(11)	3.9(12)
C33	21.7(13)	32.4(15)	19.2(13)	-4.1(11)	4.2(10)	6.1(11)
C39	30.5(15)	35.7(16)	20.3(13)	1.1(12)	3.6(11)	-2.1(12)
C42	41.0(18)	50(2)	29.7(16)	3.7(15)	3.4(14)	-7.3(14)
C41	71(2)	26.8(16)	43.0(19)	6.4(16)	13.6(17)	1.7(14)
C40	31.1(16)	53(2)	30.6(16)	4.9(14)	7.3(13)	-2.1(14)
C34	20.8(13)	26.8(14)	21.4(13)	-3.4(11)	4.3(10)	8.1(11)
C26	24.1(14)	22.3(13)	22.0(13)	5.5(11)	0.7(10)	3.6(11)
C25	20.9(13)	13.9(12)	28.4(14)	-0.2(10)	7.2(11)	3.4(10)
C24	26.4(14)	17.7(13)	34.4(15)	-1.0(11)	13.9(12)	-0.1(11)
C19	26.5(14)	18.5(13)	32.8(15)	-3.7(11)	16.1(12)	-0.8(11)
C18	21.8(13)	15.1(12)	22.1(13)	-1.3(10)	7.5(10)	0.5(10)
C17	19.7(13)	20.2(13)	18.8(12)	2.7(10)	3(1)	4.2(10)
C20	38.0(17)	30.2(15)	29.2(15)	-1.3(13)	14.4(13)	-2.9(12)
C21	44.1(19)	32.9(17)	40.0(18)	-4.9(14)	26.4(15)	-9.8(14)
C22	35.1(17)	29.3(16)	57(2)	2.3(13)	28.0(16)	-7.7(15)
C23	30.5(16)	24.6(15)	52.6(19)	5.3(12)	18.2(14)	0.4(13)
C43	61(2)	91(3)	43(2)	-19(2)	7.3(18)	35(2)

**Crystallographic Table 29** Bond Lengths for **Zn[L<sup>1</sup>]**.

Atom	Atom	Length/Å	Atom	Atom	Length/Å
Zn1	O1	1.9637(17)	C7	C9	1.534(4)
Zn1	O2	1.9499(17)	C7	C10	1.534(4)
Zn1	O3	2.1024(19)	C16	C27	1.463(3)
Zn1	N1	2.0713(19)	C16	C17	1.367(3)
Zn1	N2	2.075(2)	C27	C26	1.371(3)
O1	C1	1.291(3)	C28	C29	1.428(3)
O2	C34	1.299(3)	C29	C30	1.423(4)

O3	C43	1.421(4)	C29	C34	1.431(4)
N1	C15	1.305(3)	C30	C31	1.372(4)
N1	C16	1.415(3)	C31	C35	1.532(4)
N2	C27	1.413(3)	C31	C32	1.415(4)
N2	C28	1.306(3)	C35	C37	1.524(4)
N4	C25	1.345(3)	C35	C38	1.523(5)
N4	C24	1.349(3)	C35	C36	1.521(5)
N3	C19	1.355(3)	C32	C33	1.379(4)
N3	C18	1.344(3)	C33	C39	1.538(4)
C15	C6	1.424(3)	C33	C34	1.444(3)
C6	C1	1.440(3)	C39	C42	1.538(4)
C6	C5	1.424(3)	C39	C41	1.543(4)
C1	C2	1.450(3)	C39	C40	1.532(4)
C2	C3	1.374(4)	C26	C25	1.419(3)
C2	C7	1.545(3)	C25	C18	1.436(3)
C3	C4	1.419(4)	C24	C19	1.432(4)
C4	C5	1.367(4)	C24	C23	1.429(4)
C4	C11	1.537(4)	C19	C20	1.420(4)
C11	C13	1.538(4)	C18	C17	1.422(3)
C11	C12	1.530(4)	C20	C21	1.364(4)
C11	C14	1.542(4)	C21	C22	1.406(5)
C7	C8	1.544(4)	C22	C23	1.364(4)

**Crystallographic Table 30 Bond Angles for Zn[L<sup>I</sup>].**

Atom	Atom	Atom	Angle/°	Atom	Atom	Atom	Angle/°
O2	Zn1	O1	94.93(7)	C17	C16	C27	119.7(2)
O3	Zn1	O1	101.34(8)	C16	C27	N2	115.0(2)
O3	Zn1	O2	98.66(8)	C26	C27	N2	125.7(2)
N1	Zn1	O1	89.46(7)	C26	C27	C16	119.4(2)
N1	Zn1	O2	164.37(8)	C29	C28	N2	127.0(2)
N1	Zn1	O3	95.17(8)	C30	C29	C28	115.8(2)
N2	Zn1	O1	152.16(8)	C34	C29	C28	124.2(2)
N2	Zn1	O2	89.89(8)	C34	C29	C30	120.0(2)
N2	Zn1	O3	105.01(8)	C31	C30	C29	122.2(3)
N2	Zn1	N1	79.46(8)	C35	C31	C30	123.8(3)
C1	O1	Zn1	130.08(16)	C32	C31	C30	116.6(2)
C34	O2	Zn1	131.72(16)	C32	C31	C35	119.5(2)
C43	O3	Zn1	120.97(19)	C37	C35	C31	110.7(2)

C15	N1	Zn1	123.74(16)	C38	C35	C31	108.8(3)
C16	N1	Zn1	114.68(15)	C38	C35	C37	109.3(3)
C16	N1	C15	121.6(2)	C36	C35	C31	111.2(3)
C27	N2	Zn1	114.74(15)	C36	C35	C37	106.8(3)
C28	N2	Zn1	124.29(17)	C36	C35	C38	109.9(4)
C28	N2	C27	121.0(2)	C33	C32	C31	125.0(2)
C24	N4	C25	116.9(2)	C39	C33	C32	122.2(2)
C18	N3	C19	117.2(2)	C34	C33	C32	118.0(2)
C6	C15	N1	127.0(2)	C34	C33	C39	119.8(2)
C1	C6	C15	123.6(2)	C42	C39	C33	112.3(2)
C5	C6	C15	116.0(2)	C41	C39	C33	110.0(2)
C5	C6	C1	120.3(2)	C41	C39	C42	107.3(2)
C6	C1	O1	123.1(2)	C40	C39	C33	109.8(2)
C2	C1	O1	119.5(2)	C40	C39	C42	108.0(2)
C2	C1	C6	117.4(2)	C40	C39	C41	109.3(3)
C3	C2	C1	117.9(2)	C29	C34	O2	122.8(2)
C7	C2	C1	120.0(2)	C33	C34	O2	119.1(2)
C7	C2	C3	122.0(2)	C33	C34	C29	118.0(2)
C4	C3	C2	125.7(2)	C25	C26	C27	121.4(2)
C5	C4	C3	116.2(2)	C26	C25	N4	119.3(2)
C11	C4	C3	119.6(2)	C18	C25	N4	121.6(2)
C11	C4	C5	124.2(2)	C18	C25	C26	119.1(2)
C4	C5	C6	122.4(2)	C19	C24	N4	121.8(2)
C13	C11	C4	108.9(2)	C23	C24	N4	119.2(3)
C12	C11	C4	111.9(2)	C23	C24	C19	118.9(2)
C12	C11	C13	108.9(2)	C24	C19	N3	121.0(2)
C14	C11	C4	110.3(2)	C20	C19	N3	119.8(3)
C14	C11	C13	108.5(2)	C20	C19	C24	119.2(2)
C14	C11	C12	108.2(2)	C25	C18	N3	121.5(2)
C8	C7	C2	111.4(2)	C17	C18	N3	119.7(2)
C9	C7	C2	110.2(2)	C17	C18	C25	118.9(2)
C9	C7	C8	109.3(2)	C18	C17	C16	121.3(2)
C10	C7	C2	111.3(2)	C21	C20	C19	119.9(3)
C10	C7	C8	107.5(2)	C22	C21	C20	121.2(3)
C10	C7	C9	107.0(2)	C23	C22	C21	121.0(3)
C27	C16	N1	114.6(2)	C22	C23	C24	119.8(3)
C17	C16	N1	125.7(2)				

**Crystallographic Table 31** Hydrogen Atom Coordinates ( $\text{\AA}\times 10^4$ ) and Isotropic Displacement Parameters ( $\text{\AA}^2\times 10^3$ ) for **Zn[L<sup>1</sup>]**.

Atom	x	y	z	U(eq)
H15	4519(3)	3626.1(16)	5167.0(15)	24.2(6)
H3a	6853(3)	298.1(17)	3901.7(17)	29.5(7)
H5	6135(3)	2648.6(18)	5562.8(16)	30.1(7)
H13a	9613(9)	1810(3)	5416(13)	61.2(11)
H13b	9937(5)	956(14)	5798(8)	61.2(11)
H13c	9275(5)	780(11)	4797(5)	61.2(11)
H12a	8375(19)	1597(9)	6891(2)	67.5(13)
H12b	8080(20)	2434(4)	6481(5)	67.5(13)
H12c	6732(6)	1819(12)	6577(6)	67.5(13)
H14a	7916(14)	14(6)	6029(9)	61.8(11)
H14b	6251(9)	152(4)	5665(13)	61.8(11)
H14c	7310(20)	-255(3)	5013(5)	61.8(11)
H8a	6695(4)	797(12)	1872(7)	50.5(10)
H8b	5338(18)	221(6)	1171(3)	50.5(10)
H8c	5172(16)	1249(7)	1721(8)	50.5(10)
H9a	3265(4)	-455(9)	1615(6)	46.9(10)
H9b	3138(5)	-204(12)	2606(6)	46.9(10)
H9c	2944(3)	565(4)	2104(12)	46.9(10)
H10a	5586(17)	-835(8)	2874(9)	57.0(11)
H10b	5600(18)	-1034(5)	1871(4)	57.0(11)
H10c	6945(4)	-441(3)	2569(13)	57.0(11)
H28	-75(3)	4733.6(17)	2430.9(16)	27.1(7)
H30	-1394(3)	4492.1(19)	1080.3(17)	34.0(7)
H37a	-1242(16)	4358(11)	-1248(2)	69.6(13)
H37b	-1720(20)	3296(5)	-1735(8)	69.6(13)
H37c	-2870(7)	4053(15)	-1788(7)	69.6(13)
H38a	-3355(13)	2396(7)	-1160(20)	168(3)
H38b	-4100(30)	2914(19)	-376(5)	168(3)
H38c	-4560(20)	3106(15)	-1290(20)	168(3)
H36a	-3420(40)	4617(11)	343(13)	155(3)
H36b	-2386(16)	5161(5)	-70(20)	155(3)
H36c	-4000(30)	4762(15)	-582(11)	155(3)
H32	-756(3)	2415.1(19)	-905.2(16)	34.3(7)
H42a	790(20)	1531(5)	-1508(3)	66.6(12)
H42b	1328(14)	585(9)	-1351(5)	66.6(12)



H42c	-227(8)	913(13)	-1157(3)	66.6(12)
H41a	1970(20)	397(7)	59(8)	72.1(13)
H41b	2090(20)	1237(6)	910(5)	72.1(13)
H41c	513(4)	787(12)	363(12)	72.1(13)
H40a	3618(7)	1405(2)	-431(13)	61.4(12)
H40b	3094(3)	2354(12)	-582(11)	61.4(12)
H40c	3585(8)	2274(13)	375(3)	61.4(12)
H26	145(3)	5607.7(17)	3595.2(16)	28.5(7)
H17	3800(3)	4884.1(16)	5633.6(15)	23.8(6)
H20	2374(3)	7269.6(19)	7881.9(18)	40.6(8)
H21	796(3)	8381(2)	8296(2)	49.0(9)
H22	-1020(3)	8735(2)	7282(2)	50.4(10)
H23	-1324(3)	7954.9(19)	5839(2)	44.0(9)
H43a	5490(30)	3459(6)	1470(7)	93.8(17)
H43b	4370(11)	4246(18)	1507(7)	93.8(17)
H43c	6077(19)	4517(14)	1893(2)	93.8(17)
H3	5880(30)	3910(20)	2960(20)	65(12)

**Crystallographic Table 32** Solvent masks information for **Zn[L<sup>1</sup>]**.

Number	X	Y	Z	Volume	Electron count	Content
1	-0.267	-0.290	0.291	177.6	35.4	2 MeOH
2	0.267	0.290	0.709	177.6	35.6	2 MeOH
3	0.309	0.856	0.975	35.5	0.0	?
4	0.691	0.144	0.025	35.5	0.0	?

Refinement model description

Number of restraints - 1, number of constraints - 76.

Details:

N/A

**Fe[L<sup>I</sup>]-O-Fe[L<sup>I</sup>]**

**Crystallographic Table 33** Crystal data and structure refinement for **Fe[L<sup>I</sup>]-O-Fe[L<sup>I</sup>]**

Empirical formula	C <sub>92</sub> H <sub>112</sub> Fe <sub>2</sub> N <sub>8</sub> O <sub>7</sub>
Formula weight	1553.60
Temperature/K	180(2)
Crystal system	monoclinic
Space group	C2/c
a/Å	18.9491(3)
b/Å	41.3420(7)
c/Å	13.8422(2)
α/°	90.00
β/°	128.2090(10)
γ/°	90.00
Volume/Å <sup>3</sup>	8520.7(2)
Z	4
ρ <sub>calc</sub> /mg/mm <sup>3</sup>	1.136
m/mm <sup>-1</sup>	0.399
F(000)	3088.0
Crystal size/mm <sup>3</sup>	0.1 × 0.1 × 0.08
Radiation	MoKα (λ = 0.71073)
2θ range for data collection	1.98 to 55.48°
Index ranges	-24 ≤ h ≤ 24, -52 ≤ k ≤ 53, -16 ≤ l ≤ 17
Reflections collected	50375
Independent reflections	9764 [R <sub>int</sub> = 0.0359, R <sub>sigma</sub> = 0.0360]
Data/restraints/parameters	9764/0/505
Goodness-of-fit on F <sup>2</sup>	1.033
Final R indexes [I >= 2σ (I)]	R <sub>1</sub> = 0.0557, wR <sub>2</sub> = 0.1510
Final R indexes [all data]	R <sub>1</sub> = 0.0845, wR <sub>2</sub> = 0.1739
Largest diff. peak/hole / e Å <sup>-3</sup>	0.74/-0.55

**Crystallographic Table 34** Fractional Atomic Coordinates (×10<sup>4</sup>) and Equivalent Isotropic Displacement Parameters (Å<sup>2</sup>×10<sup>3</sup>) for **Fe[L<sup>I</sup>]-O-Fe[L<sup>I</sup>]**. U<sub>eq</sub> is defined as 1/3 of the trace of the orthogonalised U<sub>ij</sub> tensor.

Atom	x	y	z	U(eq)
Fe1	9557.1(2)	1191.68(7)	5962.5(3)	34.58(13)
C1	9638.9(14)	464.1(5)	5967(2)	32.5(5)
C2	9476.0(15)	141.5(6)	5953(2)	36.5(5)
C6	11214(3)	-1164.5(7)	7212(3)	72.3(11)

C11	11186.8(16)	351.9(6)	6804(2)	38.2(5)
C12	10504.5(15)	568.9(5)	6345(2)	33.3(5)
C3	10166.2(16)	-91.1(5)	6375(2)	36.5(5)
C4	10663(2)	-613.2(6)	6786(2)	48.4(7)
C10	11038.2(16)	17.7(6)	6833(2)	37.7(5)
C9	11533.2(19)	-505.1(6)	7230(3)	47.3(6)
C5	10517(2)	-950.1(7)	6802(3)	66.0(9)
C8	12220(2)	-737.1(7)	7634(3)	61.9(8)
C7	12058(3)	-1057.0(8)	7629(3)	73.8(10)
N1	9029.3(12)	719.6(4)	5635.5(18)	33.1(4)
N2	10558.7(13)	903.1(4)	6179.8(19)	35.1(4)
C13	11204.7(16)	1012.4(6)	6182(2)	39.8(6)
C14	11320.4(16)	1338.5(6)	5965(2)	40.1(6)
C15	12086.6(16)	1401.6(6)	6035(3)	43.7(6)
C19	10685.2(16)	1587.6(6)	5615(2)	40.2(6)
C16	12249.7(16)	1701.9(6)	5799(3)	44.8(6)
C18	10864.8(17)	1906.2(6)	5409(3)	46.3(6)
C17	11630.4(17)	1948.1(6)	5508(3)	48.4(7)
C20	8269.4(15)	665.1(6)	5426(2)	35.8(5)
C22	7674.6(15)	1231.4(6)	4920(3)	41.7(6)
C26	6863.1(16)	786.6(6)	5043(2)	42.6(6)
C21	7605.6(15)	898.8(6)	5125(2)	38.5(5)
C23	6998.9(16)	1449.3(6)	4692(3)	50.7(7)
C25	6203.1(16)	993.0(7)	4788(3)	46.5(6)
C24	6304.8(17)	1322.5(7)	4636(3)	52.3(7)
C27	13058.0(18)	1781.5(7)	5843(3)	51.1(7)
C28	13619(2)	1480.2(8)	6082(4)	66.0(9)
C29	13650(2)	2029.3(9)	6865(3)	72.1(10)
C30	12726(2)	1927.0(8)	4605(3)	66.0(9)
C31	10215.8(19)	2184.9(6)	5091(3)	58.9(8)
C32	10141(3)	2230.6(8)	6121(4)	76.5(11)
C33	10546(2)	2506.3(7)	4944(4)	82.5(13)
C34	9290(2)	2115.2(8)	3864(4)	73.7(11)
C35	7071.8(19)	1812.6(7)	4540(4)	74.9(12)
C36	7949(2)	1942.7(8)	5733(5)	94.7(15)
C37	7050(2)	1872.7(9)	3435(4)	94.6(15)
C38	6292(3)	2004.3(8)	4339(6)	112.1(19)
C39	5384.9(19)	885.4(8)	4689(3)	59.0(8)

C42	5295(3)	521(1)	4637(6)	107.3(18)
C40	5468(3)	1018.5(12)	5772(5)	96.4(14)
C41	4528(2)	1022.0(15)	3509(5)	116.9(19)
N4	11721.5(15)	-190.2(5)	7261(2)	47.1(5)
N3	9979.5(15)	-405.8(5)	6350(2)	45.0(5)
O2	9946.1(11)	1530.8(4)	5457.6(19)	46.4(5)
O1	8330.4(11)	1336.0(4)	4939.3(18)	46.7(5)
O3	10000	1260.2(6)	7500	43.5(6)
O6	2875(3)	458.4(15)	6590(5)	179(2)
C53	2753(5)	489.7(15)	5544(7)	136(2)
C55	3313(7)	247(3)	5530(7)	254(6)
C57	3331(5)	108(3)	6972(11)	226(6)
C56	3731(12)	71(4)	6606(14)	335(10)

**Crystallographic Table 35** Anisotropic Displacement Parameters ( $\text{\AA}^2 \times 10^3$ ) for **Fe[L<sup>I</sup>]-O-Fe[L<sup>I</sup>]**. The Anisotropic displacement factor exponent takes the form: -  
 $2\pi^2[h^2a^2U_{11}+2hka*b*U_{12}+\dots]$

Atom	U <sub>11</sub>	U <sub>22</sub>	U <sub>33</sub>	U <sub>23</sub>	U <sub>13</sub>	U <sub>12</sub>
Fe1	33.81(19)	21.82(19)	53.3(3)	7.26(14)	29.53(18)	4.60(12)
C1	38.5(11)	24.9(11)	33.3(12)	5.1(9)	21.8(10)	6.1(8)
C2	39.0(12)	27.4(12)	38.1(13)	2.6(10)	21.3(11)	1.6(9)
C6	95(3)	27.5(14)	62(2)	11.1(13)	32.0(19)	21.2(15)
C11	43.3(12)	34.4(13)	45.3(14)	9.9(11)	31.6(11)	10.1(10)
C12	43.1(12)	25.7(11)	39.5(13)	5.4(9)	29.8(11)	5.7(9)
C3	49.0(13)	24.2(11)	31.4(12)	4.7(9)	22.4(11)	7.8(9)
C4	65.3(17)	28.0(13)	35.3(14)	4.8(10)	22.7(13)	13.0(11)
C10	48.4(13)	32.1(12)	36.6(13)	9.2(10)	28.3(11)	12.2(10)
C9	61.9(16)	33.2(13)	48.0(16)	11.6(12)	34.6(14)	17.8(12)
C5	77(2)	29.5(14)	56.7(19)	6.0(13)	24.1(16)	9.1(13)
C8	75(2)	43.0(16)	71(2)	20.4(15)	46.9(18)	28.4(15)
C7	85(2)	48.3(19)	79(2)	19.0(17)	46(2)	35.4(18)
N1	32.8(9)	24.1(9)	41.8(11)	4.1(8)	22.7(9)	3.7(7)
N2	38.4(10)	25.7(10)	48.2(12)	8.5(8)	30.3(9)	6.5(7)
C13	39.1(12)	32.2(12)	55.0(16)	9.1(11)	32.7(12)	8.2(9)
C14	37.6(12)	33.7(13)	50.8(15)	9.1(11)	28.2(11)	2.9(9)
C15	37.8(12)	39.3(14)	55.4(16)	6.6(12)	29.4(12)	1.4(10)
C19	39.2(12)	32.1(12)	52.4(15)	10.9(11)	29.9(12)	3.9(9)
C16	38.0(12)	43.2(14)	51.3(16)	4.9(12)	26.7(12)	-6.4(10)
C18	41.7(13)	32.7(13)	58.8(17)	11.9(12)	28.2(12)	0.9(10)

C17	43.8(13)	36.4(14)	58.3(17)	10.0(12)	28.3(13)	-4.9(11)
C20	40.7(12)	24.9(11)	43.6(14)	0.5(10)	27.0(11)	-0.8(9)
C22	30.7(11)	32.7(13)	51.5(16)	0.5(11)	20.4(11)	1.8(9)
C26	39.2(12)	36.7(13)	53.3(16)	-6.7(11)	29.3(12)	-6.8(10)
C21	34.8(11)	31.0(12)	48.2(15)	-1(1)	25.0(11)	-1.2(9)
C23	33.8(12)	33.6(13)	70.4(19)	-2.8(13)	25.1(13)	2(1)
C25	34.5(12)	50.4(16)	54.2(16)	-11.3(13)	27.3(12)	-5.9(11)
C24	34.5(12)	42.8(15)	73(2)	-9.4(14)	29.6(13)	1.9(10)
C27	42.4(13)	51.8(16)	60.5(18)	0.9(14)	32.5(13)	-11.7(12)
C28	55.5(17)	68(2)	95(3)	10.6(18)	57.2(18)	0.0(15)
C29	51.7(17)	84(3)	80(2)	-19.6(19)	40.3(17)	-27.0(16)
C30	66.3(19)	62(2)	78(2)	4.6(17)	48.7(18)	-17.0(15)
C31	48.4(15)	30.1(14)	90(2)	20.0(14)	38.9(16)	5.7(11)
C32	81(2)	38.1(17)	124(3)	9.1(19)	71(2)	16.1(15)
C33	66(2)	33.4(16)	136(4)	26.8(19)	57(2)	4.0(14)
C34	47.9(16)	49.5(18)	97(3)	33.8(18)	31.9(17)	9.6(13)
C35	42.1(15)	32.4(15)	133(3)	2.3(18)	45.7(19)	6.6(11)
C36	57.7(19)	39.6(18)	157(4)	-27(2)	52(2)	-9.0(14)
C37	63(2)	53(2)	139(4)	42(2)	48(2)	15.8(16)
C38	65(2)	39.8(18)	217(6)	-2(2)	80(3)	12.6(15)
C39	47.2(15)	67(2)	77(2)	-11.6(16)	45.1(16)	-9.0(13)
C42	108(3)	75(3)	206(5)	-42(3)	131(4)	-38(2)
C40	116(3)	99(3)	129(4)	-23(3)	103(3)	-16(3)
C41	38.8(18)	173(5)	120(4)	26(3)	40(2)	-13(2)
N4	57.7(13)	37.8(12)	55.4(14)	16.4(10)	39.8(12)	19.6(10)
N3	53.0(12)	26.3(10)	40.0(12)	3.0(9)	20.8(10)	4.9(9)
O2	45.4(9)	29.2(9)	74.6(13)	19.3(8)	42(1)	10.0(7)
O1	34.5(8)	29.2(9)	72.8(13)	11.0(8)	31.3(9)	5.9(7)
O3	49.8(14)	27.9(12)	60.7(17)	0	38.1(13)	0
O6	161(4)	246(6)	170(4)	71(4)	123(4)	91(4)
C53	205(7)	100(4)	152(6)	14(4)	136(6)	18(4)
C55	299(12)	347(14)	104(5)	83(7)	119(7)	211(11)
C57	117(5)	264(11)	317(14)	204(11)	144(7)	86(6)
C56	410(20)	349(19)	274(15)	78(13)	229(17)	256(18)

**Crystallographic Table 36 Bond Lengths for Fe[L<sup>I</sup>]-O-Fe[L<sup>I</sup>].**

Atom	Atom	Length/Å	Atom	Atom	Length/Å
Fe1	N1	2.1105(19)	C16	C27	1.530(3)

Fe1	N2	2.1000(18)	C18	C17	1.381(4)
Fe1	O2	1.9064(17)	C18	C31	1.537(4)
Fe1	O1	1.9216(16)	C20	C21	1.429(3)
Fe1	O3	1.7619(5)	C22	C21	1.427(3)
C1	C2	1.367(3)	C22	C23	1.432(3)
C1	C12	1.446(3)	C22	O1	1.301(3)
C1	N1	1.416(3)	C26	C21	1.417(3)
C2	C3	1.425(3)	C26	C25	1.368(4)
C6	C5	1.388(5)	C23	C24	1.373(4)
C6	C7	1.395(5)	C23	C35	1.535(4)
C11	C12	1.365(3)	C25	C24	1.409(4)
C11	C10	1.416(3)	C25	C39	1.536(4)
C12	N2	1.415(3)	C27	C28	1.535(4)
C3	C10	1.428(4)	C27	C29	1.531(4)
C3	N3	1.343(3)	C27	C30	1.537(4)
C4	C9	1.429(4)	C31	C32	1.529(5)
C4	C5	1.423(4)	C31	C33	1.535(4)
C4	N3	1.346(3)	C31	C34	1.536(5)
C10	N4	1.348(3)	C35	C36	1.544(5)
C9	C8	1.424(4)	C35	C37	1.524(6)
C9	N4	1.343(3)	C35	C38	1.543(4)
C8	C7	1.357(5)	C39	C42	1.513(5)
N1	C20	1.301(3)	C39	C40	1.512(5)
N2	C13	1.303(3)	C39	C41	1.531(5)
C13	C14	1.428(3)	O3	Fe1 <sup>1</sup>	1.7619(5)
C14	C15	1.418(3)	O6	C53	1.324(7)
C14	C19	1.422(3)	O6	C57	1.601(10)
C15	C16	1.367(4)	C53	C55	1.471(9)
C19	C18	1.433(3)	C55	C56	1.384(13)
C19	O2	1.299(3)	C57	C56	1.153(12)
C16	C17	1.411(4)			

<sup>1</sup>2-X,+Y,3/2-Z

**Crystallographic Table 37** Bond Angles for Fe[L<sup>1</sup>]-O-Fe[L<sup>1</sup>].

Atom	Atom	Atom	Angle/°	Atom	Atom	Atom	Angle/°
N2	Fe1	N1	76.81(7)	C17	C18	C19	117.4(2)
O2	Fe1	N1	147.22(9)	C17	C18	C31	122.7(2)
O2	Fe1	N2	87.14(7)	C18	C17	C16	125.1(2)

O2	Fe1	O1	93.86(7)	N1	C20	C21	127.0(2)
O1	Fe1	N1	86.12(7)	C21	C22	C23	118.1(2)
O1	Fe1	N2	148.88(9)	O1	C22	C21	121.4(2)
O3	Fe1	N1	102.48(9)	O1	C22	C23	120.6(2)
O3	Fe1	N2	101.84(7)	C25	C26	C21	121.4(2)
O3	Fe1	O2	108.74(9)	C22	C21	C20	122.5(2)
O3	Fe1	O1	107.20(7)	C26	C21	C20	117.0(2)
C2	C1	C12	119.6(2)	C26	C21	C22	120.5(2)
C2	C1	N1	126.3(2)	C22	C23	C35	120.1(2)
N1	C1	C12	114.17(19)	C24	C23	C22	117.8(2)
C1	C2	C3	120.7(2)	C24	C23	C35	122.0(2)
C5	C6	C7	121.6(3)	C26	C25	C24	117.0(2)
C12	C11	C10	120.5(2)	C26	C25	C39	123.6(3)
C11	C12	C1	120.5(2)	C24	C25	C39	119.3(2)
C11	C12	N2	125.1(2)	C23	C24	C25	125.1(2)
N2	C12	C1	114.44(18)	C16	C27	C28	112.2(2)
C2	C3	C10	119.1(2)	C16	C27	C29	108.9(3)
N3	C3	C2	118.9(2)	C16	C27	C30	109.3(2)
N3	C3	C10	122.1(2)	C28	C27	C30	108.0(3)
C5	C4	C9	118.9(3)	C29	C27	C28	109.3(3)
N3	C4	C9	121.9(2)	C29	C27	C30	109.2(3)
N3	C4	C5	119.2(3)	C32	C31	C18	110.2(3)
C11	C10	C3	119.4(2)	C32	C31	C33	107.3(3)
N4	C10	C11	118.8(2)	C32	C31	C34	110.7(3)
N4	C10	C3	121.8(2)	C33	C31	C18	111.6(2)
C8	C9	C4	119.3(3)	C33	C31	C34	107.2(3)
N4	C9	C4	122.0(2)	C34	C31	C18	109.9(3)
N4	C9	C8	118.7(3)	C23	C35	C36	108.8(3)
C6	C5	C4	119.1(3)	C23	C35	C38	111.7(3)
C7	C8	C9	120.4(3)	C37	C35	C23	110.4(3)
C8	C7	C6	120.7(3)	C37	C35	C36	111.0(3)
C1	N1	Fe1	115.90(14)	C37	C35	C38	107.9(3)
C20	N1	Fe1	121.36(15)	C38	C35	C36	106.9(3)
C20	N1	C1	120.8(2)	C42	C39	C25	111.8(2)
C12	N2	Fe1	115.37(14)	C42	C39	C41	107.6(4)
C13	N2	Fe1	124.60(16)	C40	C39	C25	109.1(3)
C13	N2	C12	120.03(19)	C40	C39	C42	110.4(4)
N2	C13	C14	126.4(2)	C40	C39	C41	108.3(4)

C15	C14	C13	116.3(2)	C41	C39	C25	109.5(3)
C15	C14	C19	120.3(2)	C9	N4	C10	116.1(2)
C19	C14	C13	123.2(2)	C3	N3	C4	116.1(2)
C16	C15	C14	121.6(2)	C19	O2	Fe1	133.86(15)
C14	C19	C18	118.6(2)	C22	O1	Fe1	128.09(16)
O2	C19	C14	121.6(2)	Fe1 <sup>1</sup>	O3	Fe1	161.51(15)
O2	C19	C18	119.8(2)	C53	O6	C57	98.2(6)
C15	C16	C17	116.9(2)	O6	C53	C55	107.9(6)
C15	C16	C27	123.7(2)	C56	C55	C53	106.4(7)
C17	C16	C27	119.4(2)	C56	C57	O6	110.0(10)
C19	C18	C31	120.0(2)	C57	C56	C55	108.0(11)

<sup>1</sup>2-X,+Y,3/2-Z

**Crystallographic Table 38** Hydrogen Atom Coordinates ( $\text{\AA}\times 10^4$ ) and Isotropic Displacement Parameters ( $\text{\AA}^2\times 10^3$ ) for  $\text{Fe}[\text{L}^1]\text{-O-Fe}[\text{L}^1]$ .

Atom	<i>x</i>	<i>y</i>	<i>z</i>	U(eq)
H2	8897	72	5660	44
H6	11115	-1390	7210	87
H11	11765	426	7107	46
H5	9949	-1027	6535	79
H8	12795	-667	7909	74
H7	12524	-1209	7911	89
H13	11642	860	6345	48
H15	12497	1231	6252	52
H17	11749	2159	5368	58
H20	8142	446	5478	43
H26	6823	563	5167	51
H24	5858	1468	4484	63
H28A	13847	1385	6875	99
H28B	14126	1542	6098	99
H28C	13244	1322	5427	99
H29A	13298	2224	6703	108
H29B	14163	2085	6889	108
H29C	13867	1937	7658	108
H30A	12296	1779	3938	99
H30B	13238	1960	4603	99
H30C	12433	2135	4482	99
H32A	9920	2030	6230	115



H32B	9722	2407	5906	115
H32C	10733	2283	6888	115
H33A	10111	2677	4722	124
H33B	10608	2485	4295	124
H33C	11129	2562	5720	124
H34A	9040	1918	3941	111
H34B	9352	2085	3217	111
H34C	8887	2298	3651	111
H36A	8464	1830	5884	142
H36B	7940	1906	6425	142
H36C	8000	2175	5647	142
H37A	7547	1756	3547	142
H37B	7112	2105	3362	142
H37C	6478	1796	2687	142
H38A	6357	2234	4237	168
H38B	6305	1976	5053	168
H38C	5719	1924	3600	168
H42A	5274	437	3958	161
H42B	4741	462	4507	161
H42C	5811	428	5413	161
H40A	6003	928	6536	145
H40B	4933	960	5694	145
H40C	5521	1255	5790	145
H41A	4588	1257	3484	175
H41B	4014	974	3493	175
H41C	4433	922	2794	175
H53A	2927	710	5481	163
H53B	2112	456	4838	163
H55A	2938	103	4806	304
H55B	3766	353	5497	304
H57A	3738	87	7878	272
H57B	2860	-61	6628	272
H56A	3743	-162	6444	402
H56B	4357	146	7222	402

## Refinement model description

Number of restraints - 0, number of constraints - unknown.

Details:

### 1. Others

Fixed U12: O3(0)

Fixed U23: O3(0)

Fixed Uiso: H2(0.044) H6(0.087) H11(0.046) H5(0.079) H8(0.074) H7(0.089)  
H13(0.048) H15(0.052) H17(0.058) H20(0.043) H26(0.051) H24(0.063) H28A(0.099)  
H28B(0.099) H28C(0.099) H29A(0.108) H29B(0.108) H29C(0.108) H30A(0.099)  
H30B(0.099) H30C(0.099) H32A(0.115) H32B(0.115) H32C(0.115) H33A(0.124)  
H33B(0.124) H33C(0.124) H34A(0.111) H34B(0.111) H34C(0.111) H36A(0.142)  
H36B(0.142) H36C(0.142) H37A(0.142) H37B(0.142) H37C(0.142) H38A(0.168)  
H38B(0.168) H38C(0.168) H42A(0.161) H42B(0.161) H42C(0.161) H40A(0.145)  
H40B(0.145) H40C(0.145) H41A(0.175) H41B(0.175) H41C(0.175) H53A(0.163)  
H53B(0.163) H55A(0.304) H55B(0.304) H57A(0.272) H57B(0.272) H56A(0.402)  
H56B(0.402)

Fixed X: H2(0.8897) H6(1.1115) H11(1.1765) H5(0.9949) H8(1.2795) H7(1.2524)  
H13(1.1642) H15(1.2497) H17(1.1749) H20(0.8142) H26(0.6823) H24(0.5858)  
H28A(1.3847) H28B(1.4126) H28C(1.3244) H29A(1.3298) H29B(1.4163)  
H29C(1.3867)

H30A(1.2296) H30B(1.3238) H30C(1.2433) H32A(0.992) H32B(0.9722) H32C(1.0733)  
H33A(1.0111) H33B(1.0608) H33C(1.1129) H34A(0.904) H34B(0.9352) H34C(0.8887)  
H36A(0.8464) H36B(0.794) H36C(0.8) H37A(0.7547) H37B(0.7112) H37C(0.6478)  
H38A(0.6357) H38B(0.6305) H38C(0.5719) H42A(0.5274) H42B(0.4741)  
H42C(0.5811)

H40A(0.6003) H40B(0.4933) H40C(0.5521) H41A(0.4588) H41B(0.4014)  
H41C(0.4433)

O3(1) H53A(0.2927) H53B(0.2112) H55A(0.2938) H55B(0.3766) H57A(0.3738)  
H57B(0.286) H56A(0.3743) H56B(0.4357)

Fixed Y: H2(0.0072) H6(-0.139) H11(0.0426) H5(-0.1027) H8(-0.0667) H7(-  
0.1209) H13(0.086) H15(0.1231) H17(0.2159) H20(0.0446) H26(0.0563) H24(0.1468)  
H28A(0.1385) H28B(0.1542) H28C(0.1322) H29A(0.2224) H29B(0.2085)  
H29C(0.1937)

H30A(0.1779) H30B(0.196) H30C(0.2135) H32A(0.203) H32B(0.2407) H32C(0.2283)  
H33A(0.2677) H33B(0.2485) H33C(0.2562) H34A(0.1918) H34B(0.2085)  
H34C(0.2298)

H36A(0.183) H36B(0.1906) H36C(0.2175) H37A(0.1756) H37B(0.2105) H37C(0.1796)  
H38A(0.2234) H38B(0.1976) H38C(0.1924) H42A(0.0437) H42B(0.0462)  
H42C(0.0428)

H40A(0.0928) H40B(0.096) H40C(0.1255) H41A(0.1257) H41B(0.0974) H41C(0.0922)  
H53A(0.071) H53B(0.0456) H55A(0.0103) H55B(0.0353) H57A(0.0087) H57B(-  
0.0061)

H56A(-0.0162) H56B(0.0146)

Fixed Z: H2(0.566) H6(0.721) H11(0.7107) H5(0.6535) H8(0.7909) H7(0.7911)  
H13(0.6345) H15(0.6252) H17(0.5368) H20(0.5478) H26(0.5167) H24(0.4484)  
H28A(0.6875) H28B(0.6098) H28C(0.5427) H29A(0.6703) H29B(0.6889)  
H29C(0.7658)  
H30A(0.3938) H30B(0.4603) H30C(0.4482) H32A(0.623) H32B(0.5906) H32C(0.6888)  
H33A(0.4722) H33B(0.4295) H33C(0.572) H34A(0.3941) H34B(0.3217) H34C(0.3651)  
H36A(0.5884) H36B(0.6425) H36C(0.5647) H37A(0.3547) H37B(0.3362)  
H37C(0.2687)  
H38A(0.4237) H38B(0.5053) H38C(0.36) H42A(0.3958) H42B(0.4507) H42C(0.5413)  
H40A(0.6536) H40B(0.5694) H40C(0.579) H41A(0.3484) H41B(0.3493) H41C(0.2794)  
O3(0.75) H53A(0.5481) H53B(0.4838) H55A(0.4806) H55B(0.5497) H57A(0.7878)  
H57B(0.6628) H56A(0.6444) H56B(0.7222)

**UO<sub>2</sub>[L<sup>III</sup>]**

**Crystallographic Table 39** Crystal data and structure refinement for **UO<sub>2</sub>[L<sup>III</sup>]**

Empirical formula	C <sub>40</sub> H <sub>52</sub> N <sub>3</sub> O <sub>4</sub> U
Formula weight	876.87
Temperature/K	180(2)
Crystal system	orthorhombic
Space group	Pccn
a/Å	13.9974(3)
b/Å	23.5111(5)
c/Å	23.6244(5)
α/°	90
β/°	90
γ/°	90
Volume/Å <sup>3</sup>	7774.7(3)
Z	8
ρ <sub>calc</sub> /mg/mm <sup>3</sup>	1.498
m/mm <sup>-1</sup>	4.217
F(000)	3496.0
Crystal size/mm <sup>3</sup>	0.06 × 0.06 × 0.02
Radiation	MoKα (λ = 0.71073)
2θ range for data collection	3.386 to 61.054°
Index ranges	-19 ≤ h ≤ 19, -23 ≤ k ≤ 33, -32 ≤ l ≤ 33
Reflections collected	93148
Independent reflections	11882 [R <sub>int</sub> = 0.0538, R <sub>sigma</sub> = 0.0376]
Data/restraints/parameters	11882/0/446
Goodness-of-fit on F <sup>2</sup>	1.010
Final R indexes [I ≥ 2σ (I)]	R <sub>1</sub> = 0.0305, wR <sub>2</sub> = 0.0619
Final R indexes [all data]	R <sub>1</sub> = 0.0569, wR <sub>2</sub> = 0.0699
Largest diff. peak/hole / e Å <sup>-3</sup>	1.37/-0.74

**Crystallographic Table 40** Fractional Atomic Coordinates (×10<sup>4</sup>) and Equivalent Isotropic Displacement Parameters (Å<sup>2</sup>×10<sup>3</sup>) for **UO<sub>2</sub>[L<sup>III</sup>]**. U<sub>eq</sub> is defined as 1/3 of the trace of the orthogonalised U<sub>ij</sub> tensor.

Atom	x	y	z	U(eq)
U1	6576.3(2)	3772.4(2)	2540.7(2)	20.73(3)
O1	5726.4(13)	3283.4(8)	3189.2(7)	25.9(4)
O2	5323.3(13)	4029.0(8)	1993.8(7)	27.0(4)
O3	6737.5(13)	3175.0(8)	2089.2(8)	29.4(4)
O4	6506.5(13)	4379.8(8)	2995.7(8)	27.6(4)
N1	7681.9(15)	3246.6(10)	3208.1(9)	25.0(5)
N2	7136.6(16)	4464.9(9)	1804.3(9)	25.5(5)
N4	6545(3)	5110(2)	5271.0(18)	97.0(15)
N3	8415.1(15)	3971.3(11)	2461.0(8)	23.9(4)
C17	9050(2)	3616.3(12)	2710.9(11)	26.8(6)

C16	8620.7(19)	3097.4(13)	2975.2(12)	30.0(6)
C15	7535(2)	3152.6(12)	3734.6(11)	26.7(6)
C14	6639.3(19)	3223.7(12)	4035.3(11)	25.5(6)
C13	6676(2)	3201.3(12)	4635.3(11)	29.4(6)
C8	5863(2)	3225.5(12)	4959.0(11)	29.0(6)
C7	4995(2)	3246.4(12)	4666.7(12)	29.4(6)
C2	4901.5(19)	3260.7(11)	4080.5(11)	24.8(5)
C1	5749.7(19)	3263.8(11)	3751.0(11)	24.2(6)
C3	3917(2)	3276.1(13)	3797.5(12)	30.3(6)
C4	3808(2)	3843.7(14)	3471.6(15)	42.1(8)
C6	3104(2)	3249.5(16)	4232.8(14)	41.7(8)
C5	3802(2)	2771.4(13)	3393.1(12)	33.1(7)
C12	5871(2)	3199.1(15)	5611.7(12)	39.9(8)
C10	5233(4)	3671(2)	5849.8(17)	97.4(19)
C9	5508(4)	2625(2)	5801.8(15)	93.2(19)
C11	6854(3)	3303(2)	5847.8(15)	77.1(15)
C18	10034(2)	3734.4(14)	2711.6(14)	38.3(8)
C19	10329(2)	4239.4(17)	2470.1(12)	43.1(8)
C20	9688(2)	4599.4(14)	2222.1(12)	36.3(7)
C21	8732(2)	4448.1(12)	2215.3(11)	27.4(6)
C22	7983(2)	4806.9(13)	1932.6(12)	31.5(6)
C23	6818(2)	4486.4(12)	1296.1(11)	27.9(6)
C24	5961(2)	4216.6(12)	1082.3(11)	26.6(6)
C37	5223(2)	4017.3(12)	1435.2(10)	25.0(5)
C32	4361(2)	3830.4(12)	1170.9(11)	28.6(6)
C31	4324(2)	3823.5(12)	582.1(11)	30.3(6)
C26	5074(2)	4000.5(12)	227.4(11)	28.7(6)
C27	4970(2)	3960.5(13)	-418.3(12)	33.8(7)
C29	4041(3)	4250.5(16)	-608.0(14)	50.4(9)
C28	5809(3)	4240.4(16)	-725.3(12)	46.9(9)
C30	4921(3)	3325.3(14)	-577.9(12)	43.3(8)
C25	5875(2)	4205.8(12)	489.0(11)	28.6(6)
C33	3499(2)	3641.5(17)	1524.6(13)	41.3(8)
C36	3754(3)	3123.8(18)	1879.7(14)	53.9(10)
C34	2630(2)	3482(2)	1155.3(15)	66.7(13)
C35	3182(2)	4136(2)	1907.1(16)	61.5(12)
C38	6078(4)	4773(2)	4275.1(17)	77.8(14)
C39	6357(3)	4965.9(18)	4832.1(18)	57.7(10)

**Crystallographic Table 41** Anisotropic Displacement Parameters ( $\text{\AA}^2 \times 10^3$ ) for  $\text{UO}_2[\text{L}^{\text{III}}]$ . The Anisotropic displacement factor exponent takes the form: -  $2\pi^2[h^2a^2U_{11}+2hka*b*U_{12}+\dots]$

Atom	$U_{11}$	$U_{22}$	$U_{33}$	$U_{23}$	$U_{13}$	$U_{12}$
U1	20.01(5)	17.24(5)	24.94(5)	-0.96(4)	-0.56(3)	-1.05(4)
O1	23.1(10)	25.3(11)	29.3(9)	4.0(8)	0.9(7)	-1.8(8)
O2	23.1(10)	29.9(11)	27.9(9)	-2.4(8)	-3.9(7)	-0.6(9)

O3	31.1(11)	24.5(11)	32.5(10)	-6.4(8)	3.1(8)	-2.0(9)
O4	31.7(11)	22.3(10)	28.8(9)	-5.0(8)	-2.7(8)	2.5(9)
N1	21.9(12)	19.6(12)	33.7(11)	4.3(9)	1.6(9)	0.1(9)
N2	28.4(12)	17.6(12)	30.4(11)	1.1(9)	-4.7(9)	-5(1)
N4	120(4)	96(4)	75(3)	-20(3)	-34(3)	14(3)
N3	24.4(11)	21.8(11)	25.5(10)	-3.0(8)	0.0(9)	-4.9(9)
C17	26.0(14)	28.2(16)	26.2(12)	-2.9(11)	3.1(10)	0.1(12)
C16	23.6(15)	26.9(16)	39.5(15)	2.2(12)	3.4(11)	5.3(12)
C15	23.7(14)	20.7(15)	35.7(14)	3.1(11)	-1.9(11)	-1.7(11)
C14	25.6(14)	19.4(14)	31.5(13)	4.2(11)	1.2(11)	-2.5(12)
C13	27.6(15)	26.9(16)	33.7(13)	3.7(12)	-3.0(11)	-4.1(12)
C8	31.5(15)	24.6(15)	31.0(13)	2.8(12)	2.5(11)	-6.8(13)
C7	30.1(16)	20.4(15)	37.7(14)	1.9(12)	7.7(11)	-4.3(12)
C2	24.7(14)	13.8(13)	35.8(13)	1.6(11)	2.5(11)	-0.3(11)
C1	25.7(14)	15.3(13)	31.5(13)	2.5(11)	0.9(10)	-2.3(11)
C3	21.9(14)	25.7(16)	43.1(15)	5.8(13)	0.7(12)	-0.4(12)
C4	32.4(17)	31.4(19)	62(2)	9.8(16)	-8.8(15)	2.9(14)
C6	24.7(16)	47(2)	53.1(19)	-2.4(16)	3.7(14)	-0.8(15)
C5	25.7(15)	31.9(17)	41.8(15)	3.2(13)	-2.7(12)	-7.8(13)
C12	39.8(18)	50(2)	30.2(14)	0.3(14)	2.4(13)	-12.6(16)
C10	106(4)	142(5)	44(2)	-29(3)	5(2)	30(4)
C9	145(5)	93(4)	42(2)	27(2)	-17(2)	-73(4)
C11	69(3)	127(4)	35.4(18)	4(2)	-9.8(18)	-45(3)
C18	28.6(16)	47(2)	39.5(15)	2.7(14)	-5.8(12)	2.7(16)
C19	21.8(15)	62(2)	45.7(17)	5.8(17)	-0.3(13)	-11.8(15)
C20	33.9(17)	37.3(19)	37.8(15)	2.1(13)	0.4(13)	-13.2(14)
C21	31.9(15)	23.5(15)	26.6(12)	-3.8(11)	-0.8(11)	-8.1(12)
C22	36.5(17)	22.5(16)	35.6(14)	2.5(12)	-6.3(12)	-10.9(13)
C23	32.6(15)	21.8(15)	29.2(13)	2.1(11)	-1.3(11)	-1.4(12)
C24	26.2(14)	21.3(15)	32.2(13)	0.1(11)	-6.5(11)	0.4(12)
C37	26.1(14)	20.6(14)	28.3(12)	-3.8(11)	-3.9(11)	4.8(12)
C32	25.0(14)	27.4(16)	33.4(13)	-6.0(12)	-3.8(10)	3.6(12)
C31	28.2(15)	27.7(16)	35.0(14)	-8.4(12)	-7.2(11)	2.5(12)
C26	36.6(16)	20.3(14)	29.2(13)	-1.4(11)	-7.8(11)	3.8(12)
C27	46.5(19)	26.4(16)	28.7(13)	-2.7(12)	-9.2(12)	-3.4(14)
C29	58(2)	47(2)	46.9(18)	3.2(17)	-23.4(17)	4.9(19)
C28	63(2)	49(2)	28.8(14)	0.8(15)	-5.9(15)	-13.5(19)
C30	62(2)	34.3(19)	33.8(15)	-7.5(14)	-1.0(15)	-5.6(17)
C25	33.0(16)	24.2(16)	28.6(13)	2.1(11)	-3.5(11)	-0.9(12)
C33	23.7(15)	63(2)	37.3(15)	-15.5(15)	0.9(12)	-4.0(16)
C36	48(2)	71(3)	43.0(18)	-4.5(18)	9.6(16)	-26(2)
C34	31.3(19)	117(4)	52(2)	-21(2)	-1.1(16)	-24(2)
C35	30.4(19)	95(4)	59(2)	-31(2)	3.2(16)	17(2)
C38	119(4)	57(3)	57(2)	-17(2)	-9(3)	6(3)
C39	67(3)	48(2)	59(2)	-8(2)	-7(2)	6(2)

**Crystallographic Table 42 Bond Lengths for UO<sub>2</sub>[L<sup>III</sup>].**

Atom	Atom	Length/Å	Atom	Atom	Length/Å
U1	O1	2.2548(18)	C3	C4	1.548(4)
U1	O2	2.2603(18)	C3	C6	1.535(4)
U1	O3	1.7780(19)	C3	C5	1.532(4)
U1	O4	1.7901(18)	C12	C10	1.531(6)
U1	N1	2.532(2)	C12	C9	1.511(5)
U1	N2	2.508(2)	C12	C11	1.505(5)
U1	N3	2.623(2)	C18	C19	1.381(5)
O1	C1	1.328(3)	C19	C20	1.366(5)
O2	C37	1.327(3)	C20	C21	1.385(4)
N1	C16	1.467(3)	C21	C22	1.502(4)
N1	C15	1.280(3)	C23	C24	1.447(4)
N2	C22	1.464(3)	C24	C37	1.409(4)
N2	C23	1.282(3)	C24	C25	1.407(4)
N4	C39	1.122(5)	C37	C32	1.427(4)
N3	C17	1.355(4)	C32	C31	1.392(4)
N3	C21	1.338(4)	C32	C33	1.534(4)
C17	C16	1.497(4)	C31	C26	1.407(4)
C17	C18	1.404(4)	C26	C27	1.535(4)
C15	C14	1.451(4)	C26	C25	1.368(4)
C14	C13	1.419(4)	C27	C29	1.536(4)
C14	C1	1.418(4)	C27	C28	1.529(4)
C13	C8	1.372(4)	C27	C30	1.542(4)
C8	C7	1.398(4)	C33	C36	1.521(5)
C8	C12	1.543(4)	C33	C34	1.543(4)
C7	C2	1.391(4)	C33	C35	1.538(5)
C2	C1	1.420(4)	C38	C39	1.445(5)
C2	C3	1.532(4)			

**Crystallographic Table 43 Bond Angles for UO<sub>2</sub>[L<sup>III</sup>].**

Atom	Atom	Atom	Angle/°	Atom	Atom	Atom	Angle/°
O1	U1	O2	96.61(6)	O1	C1	C2	121.8(2)
O1	U1	N1	69.53(7)	C14	C1	C2	118.3(2)
O1	U1	N2	165.27(7)	C2	C3	C4	109.0(2)
O1	U1	N3	131.10(7)	C2	C3	C6	111.9(2)
O2	U1	N1	163.87(7)	C6	C3	C4	107.2(3)
O2	U1	N2	70.91(7)	C5	C3	C2	110.4(2)
O2	U1	N3	132.29(7)	C5	C3	C4	110.3(3)
O3	U1	O1	94.12(8)	C5	C3	C6	108.0(2)
O3	U1	O2	88.07(8)	C10	C12	C8	109.5(3)
O3	U1	O4	175.83(9)	C9	C12	C8	109.3(3)
O3	U1	N1	84.86(8)	C9	C12	C10	110.1(4)
O3	U1	N2	93.27(8)	C11	C12	C8	111.7(3)
O3	U1	N3	88.47(8)	C11	C12	C10	106.2(4)
O4	U1	O1	88.28(8)	C11	C12	C9	110.0(3)

O4	U1	O2	95.05(8)	C19	C18	C17	117.6(3)
O4	U1	N1	92.80(8)	C20	C19	C18	120.9(3)
O4	U1	N2	85.16(8)	C19	C20	C21	118.7(3)
O4	U1	N3	87.38(8)	N3	C21	C20	122.0(3)
N1	U1	N3	62.09(7)	N3	C21	C22	115.6(2)
N2	U1	N1	123.90(7)	C20	C21	C22	122.3(3)
N2	U1	N3	61.81(7)	N2	C22	C21	110.4(2)
C1	O1	U1	133.14(17)	N2	C23	C24	126.7(3)
C37	O2	U1	130.17(16)	C37	C24	C23	123.2(2)
C16	N1	U1	115.51(16)	C25	C24	C23	115.3(3)
C15	N1	U1	126.26(19)	C25	C24	C37	121.4(2)
C15	N1	C16	117.8(2)	O2	C37	C24	120.2(2)
C22	N2	U1	117.78(16)	O2	C37	C32	122.1(2)
C23	N2	U1	124.48(19)	C24	C37	C32	117.6(2)
C23	N2	C22	117.0(2)	C37	C32	C33	121.0(2)
C17	N3	U1	120.18(18)	C31	C32	C37	118.2(3)
C21	N3	U1	120.37(18)	C31	C32	C33	120.8(3)
C21	N3	C17	119.2(2)	C32	C31	C26	124.3(3)
N3	C17	C16	114.9(2)	C31	C26	C27	120.2(3)
N3	C17	C18	121.5(3)	C25	C26	C31	116.5(2)
C18	C17	C16	123.7(3)	C25	C26	C27	123.3(3)
N1	C16	C17	108.7(2)	C26	C27	C29	110.1(3)
N1	C15	C14	126.5(3)	C26	C27	C30	107.9(2)
C13	C14	C15	117.0(2)	C29	C27	C30	108.7(3)
C1	C14	C15	122.3(2)	C28	C27	C26	111.8(2)
C1	C14	C13	120.5(2)	C28	C27	C29	108.7(3)
C8	C13	C14	121.7(3)	C28	C27	C30	109.6(3)
C13	C8	C7	116.5(2)	C26	C25	C24	121.8(3)
C13	C8	C12	123.3(3)	C32	C33	C34	112.5(3)
C7	C8	C12	120.1(3)	C32	C33	C35	109.1(3)
C2	C7	C8	125.0(3)	C36	C33	C32	110.3(3)
C7	C2	C1	117.8(2)	C36	C33	C34	107.6(3)
C7	C2	C3	121.3(2)	C36	C33	C35	110.4(3)
C1	C2	C3	120.8(2)	C35	C33	C34	106.8(3)
O1	C1	C14	119.8(2)	N4	C39	C38	177.7(5)

**Crystallographic Table 44** Hydrogen Bonds for  $\text{UO}_2[\text{L}^{\text{III}}]$ .

D	H	A	d(D-H)/Å	d(H-A)/Å	d(D-A)/Å	D-H-A/°
C23	H23	N4 <sup>1</sup>	0.95	2.71	3.642(5)	167.5
C38	H38B	O4	0.98	2.61	3.217(4)	120.4
C38	H38B	O4	0.98	2.61	3.217(4)	120.4
C38	H38B	O4	0.98	2.61	3.217(4)	120.4
C38	H38B	O4	0.98	2.61	3.217(4)	120.4

<sup>1</sup> $3/2-X,+Y,-1/2+Z$



**Crystallographic Table 45** Torsion Angles for **UO<sub>2</sub>[L<sup>III</sup>]**.

<b>A</b>	<b>B</b>	<b>C</b>	<b>D</b>	<b>Angle/°</b>	<b>A</b>	<b>B</b>	<b>C</b>	<b>D</b>	<b>Angle/°</b>
U1	O1	C1	C14	-45.0(4)	C7	C2	C3	C4	116.1(3)
U1	O1	C1	C2	137.3(2)	C7	C2	C3	C6	-2.3(4)
U1	O2	C37	C24	-44.9(4)	C7	C2	C3	C5	-122.5(3)
U1	O2	C37	C32	138.0(2)	C1	C14	C13	C8	-0.9(4)
U1	N1	C16	C17	49.9(3)	C1	C2	C3	C4	-63.5(3)
U1	N1	C15	C14	13.1(4)	C1	C2	C3	C6	178.1(3)
U1	N2	C22	C21	41.9(3)	C1	C2	C3	C5	57.8(3)
U1	N2	C23	C24	14.3(4)	C3	C2	C1	O1	0.4(4)
U1	N3	C17	C16	5.3(3)	C3	C2	C1	C14	-177.3(2)
U1	N3	C17	C18	-175.2(2)	C12	C8	C7	C2	-178.8(3)
U1	N3	C21	C20	172.5(2)	C18	C17	C16	N1	145.8(3)
U1	N3	C21	C22	-7.5(3)	C18	C19	C20	C21	-0.2(5)
O2	C37	C32	C31	-179.0(3)	C19	C20	C21	N3	2.4(4)
O2	C37	C32	C33	1.0(4)	C19	C20	C21	C22	-177.6(3)
N1	C15	C14	C13	-168.2(3)	C20	C21	C22	N2	159.0(3)
N1	C15	C14	C1	17.2(5)	C21	N3	C17	C16	179.7(2)
N2	C23	C24	C37	17.7(5)	C21	N3	C17	C18	-0.8(4)
N2	C23	C24	C25	-167.3(3)	C22	N2	C23	C24	-175.7(3)
N3	C17	C16	N1	-34.7(3)	C23	N2	C22	C21	-128.8(3)
N3	C17	C18	C19	2.8(4)	C23	C24	C37	O2	-5.6(4)
N3	C21	C22	N2	-21.0(3)	C23	C24	C37	C32	171.6(3)
C17	N3	C21	C20	-1.9(4)	C23	C24	C25	C26	-175.4(3)
C17	N3	C21	C22	178.1(2)	C24	C37	C32	C31	3.8(4)
C17	C18	C19	C20	-2.3(5)	C24	C37	C32	C33	-176.2(3)
C16	N1	C15	C14	-174.4(3)	C37	C24	C25	C26	-0.2(4)
C16	C17	C18	C19	-177.7(3)	C37	C32	C31	C26	-1.4(4)
C15	N1	C16	C17	-123.4(3)	C37	C32	C33	C36	-62.4(4)
C15	C14	C13	C8	-175.6(3)	C37	C32	C33	C34	177.5(3)
C15	C14	C1	O1	-5.5(4)	C37	C32	C33	C35	59.1(4)
C15	C14	C1	C2	172.2(3)	C32	C31	C26	C27	178.3(3)
C14	C13	C8	C7	2.9(4)	C32	C31	C26	C25	-1.9(4)
C14	C13	C8	C12	179.6(3)	C31	C32	C33	C36	117.6(3)
C13	C14	C1	O1	-179.9(2)	C31	C32	C33	C34	-2.6(5)
C13	C14	C1	C2	-2.2(4)	C31	C32	C33	C35	-120.9(3)
C13	C8	C7	C2	-1.9(4)	C31	C26	C27	C29	52.0(4)
C13	C8	C12	C10	132.7(4)	C31	C26	C27	C28	173.0(3)
C13	C8	C12	C9	-106.6(4)	C31	C26	C27	C30	-66.5(4)
C13	C8	C12	C11	15.4(5)	C31	C26	C25	C24	2.7(4)
C8	C7	C2	C1	-1.1(4)	C27	C26	C25	C24	-177.5(3)
C8	C7	C2	C3	179.3(3)	C25	C24	C37	O2	179.6(3)
C7	C8	C12	C10	-50.7(4)	C25	C24	C37	C32	-3.1(4)
C7	C8	C12	C9	70.0(4)	C25	C26	C27	C29	-127.8(3)
C7	C8	C12	C11	-168.0(3)	C25	C26	C27	C28	-6.8(4)

C7	C2	C1	O1	-179.3(2)	C25	C26	C27	C30	113.7(3)
C7	C2	C1	C14	3.1(4)	C33	C32	C31	C26	178.6(3)

**Crystallographic Table 46** Hydrogen Atom Coordinates ( $\text{\AA}\times 10^4$ ) and Isotropic Displacement Parameters ( $\text{\AA}^2\times 10^3$ ) for  $\text{UO}_2[\text{L}^{\text{III}}]$ .

Atom	x	y	z	U(eq)
H16A	8551	2794	2688	36
H16B	9042	2955	3281	36
H15	8066	3023	3950	32
H13	7279	3169	4817	35
H7	4425	3251	4885	35
H4A	3874	4163	3736	63
H4B	3177	3858	3292	63
H4C	4304	3870	3180	63
H6A	3151	2895	4449	63
H6B	2488	3263	4036	63
H6C	3153	3574	4491	63
H5A	4336	2766	3125	50
H5B	3200	2809	3185	50
H5C	3796	2416	3611	50
H10A	5254	3662	6264	146
H10B	4575	3613	5722	146
H10C	5463	4041	5715	146
H9A	5910	2325	5639	140
H9B	4847	2574	5674	140
H9C	5533	2602	6216	140
H11A	6825	3305	6262	116
H11B	7091	3672	5714	116
H11C	7286	3001	5721	116
H18	10479	3476	2872	46
H19	10987	4338	2476	52
H20	9894	4947	2057	44
H22A	7804	5126	2185	38
H22B	8244	4969	1578	38
H23	7181	4702	1033	33
H31	3754	3690	408	36
H29A	3496	4072	-417	76
H29B	3968	4210	-1019	76
H29C	4064	4655	-509	76
H28A	5831	4646	-629	70
H28B	5726	4197	-1135	70
H28C	6406	4058	-608	70
H30A	5496	3132	-441	65
H30B	4881	3288	-990	65
H30C	4355	3153	-404	65
H25	6387	4345	264	34

H36A	3980	2818	1632	81
H36B	3188	2995	2087	81
H36C	4259	3225	2149	81
H34A	2792	3153	918	100
H34B	2459	3805	914	100
H34C	2088	3385	1400	100
H35A	2640	4015	2140	92
H35B	2991	4460	1672	92
H35C	3714	4249	2153	92
H38A	5820	4386	4301	117
H38B	6637	4774	4025	117
H38C	5589	5028	4122	117

**UO<sub>2</sub>[L<sup>IV</sup>]**

**Crystallographic Table 47** Crystal data and structure refinement for UO<sub>2</sub>[L<sup>IV</sup>].

Empirical formula	C <sub>29</sub> H <sub>21</sub> N <sub>3</sub> O <sub>4</sub> U
Formula weight	713.54
Temperature/K	180.45
Crystal system	monoclinic
Space group	P2 <sub>1</sub> /c
a/Å	22.8062(10)
b/Å	7.2736(3)
c/Å	14.7805(6)
α/°	90
β/°	97.3343(5)
γ/°	90
Volume/Å <sup>3</sup>	2431.78(18)
Z	4
ρ <sub>calc</sub> /mg/mm <sup>3</sup>	1.9488
m/mm <sup>-1</sup>	6.720
F(000)	1320.2
Crystal size/mm <sup>3</sup>	0.12 × 0.12 × 0.04
Radiation	Mo Kα (λ = 0.71073)
2θ range for data collection	3.6 to 63.04°
Index ranges	-33 ≤ h ≤ 33, -10 ≤ k ≤ 10, -21 ≤ l ≤ 21
Reflections collected	61345
Independent reflections	8098 [R <sub>int</sub> = 0.0473, R <sub>sigma</sub> = 0.0295]
Data/restraints/parameters	8098/0/333
Goodness-of-fit on F <sup>2</sup>	1.084
Final R indexes [I ≥ 2σ (I)]	R <sub>1</sub> = 0.0359, wR <sub>2</sub> = 0.0726
Final R indexes [all data]	R <sub>1</sub> = 0.0427, wR <sub>2</sub> = 0.0755
Largest diff. peak/hole / e Å <sup>-3</sup>	3.18/-5.58

**Crystallographic Table 48** Fractional Atomic Coordinates (×10<sup>4</sup>) and Equivalent Isotropic Displacement Parameters (Å<sup>2</sup>×10<sup>3</sup>) for UO<sub>2</sub>[L<sup>IV</sup>]. U<sub>eq</sub> is defined as 1/3 of the trace of the orthogonalised U<sub>ij</sub> tensor.

Atom	x	y	z	U(eq)
U1	2665.70(6)	6702.81(17)	3444.78(8)	11.33(4)
O2	2136.0(12)	7009(4)	2047.1(18)	17.0(5)
N1	3348.1(15)	7175(4)	4877(2)	15.4(6)
N2	1903.7(14)	4179(4)	3165(2)	13.1(5)

N3	2567.2(14)	4501(4)	4773(2)	12.7(5)
C16	2222.4(16)	1657(5)	5326(2)	15.1(6)
C12	3100.6(18)	6796(5)	5724(2)	17.6(7)
C10	4217.0(17)	8071(5)	4181(3)	15.8(7)
C13	2784.3(16)	4964(5)	5633(2)	13.6(6)
C17	2290.3(16)	2866(5)	4620(2)	12.5(6)
C15	2440.4(18)	2166(6)	6211(3)	18.4(7)
C14	2723.0(18)	3845(5)	6371(2)	16.9(7)
C9	4855.3(18)	8040(5)	4312(3)	18.6(7)
C6	6105(2)	8122(6)	4530(4)	31.4(10)
C2	4239(2)	9706(6)	2745(3)	24.1(8)
C11	3904.7(18)	7518(5)	4933(3)	16.3(7)
C1	3909.9(18)	8868(5)	3394(3)	17.9(7)
C4	5168.0(19)	8844(6)	3631(3)	21.7(8)
C3	4840(2)	9677(6)	2857(3)	25.2(9)
C7	5804(2)	7308(6)	5196(4)	29.6(10)
C8	5193.4(19)	7258(6)	5080(3)	22.8(8)
C5	5795(2)	8846(6)	3757(3)	28.1(9)
C20	1173.9(17)	5694(5)	2060(3)	16.3(7)
C18	2084.2(18)	2459(5)	3636(3)	15.9(7)
C19	1398.8(16)	4216(5)	2666(2)	15.3(7)
C21	556.4(17)	5688(6)	1688(3)	20.0(7)
C28	1348(2)	8183(7)	1038(3)	30.9(10)
C29	1566.0(17)	6964(5)	1745(3)	16.2(7)
C27	775(2)	8159(6)	656(3)	30.4(10)
C25	-238(2)	6881(7)	564(3)	30.1(10)
C26	358.6(19)	6932(6)	967(3)	23.6(8)
C24	-629(2)	5666(8)	862(4)	34.7(11)
O4	3167.7(12)	5102(4)	3040.0(18)	17.9(5)
O3	2151.1(13)	8170(4)	3898(2)	19.6(5)
C22	131.8(19)	4501(7)	1993(3)	29.2(10)
C23	-446(2)	4490(8)	1590(4)	34.6(11)
O1	3322.6(13)	8957(4)	3251(2)	20.7(6)

**Crystallographic Table 49** Anisotropic Displacement Parameters ( $\text{\AA}^2 \times 10^3$ ) for  $\text{UO}_2[\text{L}^{\text{IV}}]$ . The Anisotropic displacement factor exponent takes the form: -  $2\pi^2[h^2a^2U_{11}+2hka*b*U_{12}+...$

Atom	$U_{11}$	$U_{22}$	$U_{33}$	$U_{12}$	$U_{13}$	$U_{23}$
U1	13.96(6)	9.98(6)	9.63(6)	-0.66(5)	-0.14(4)	1.18(5)
O2	14.8(12)	21.6(14)	13.9(12)	-1.3(10)	-0.8(9)	5.2(10)

N1	21.7(16)	12.1(13)	12.3(13)	-3.5(11)	1.0(12)	-0.6(10)
N2	18.3(15)	11.1(13)	9.9(13)	-1.6(11)	2.0(11)	-0.4(10)
N3	14.6(14)	12.0(13)	11.2(13)	0.2(11)	0.4(10)	-0.4(10)
C16	16.2(16)	12.8(15)	15.9(15)	-1.1(13)	0.1(12)	3.0(13)
C12	24.8(18)	17.6(16)	10.2(15)	-2.5(15)	0.9(13)	-1.6(13)
C10	20.0(17)	12.3(16)	14.8(15)	-4.3(13)	1.5(13)	-0.2(12)
C13	14.5(15)	14.8(15)	11.4(14)	2.0(13)	1.2(12)	-0.5(12)
C17	14.0(15)	10.6(14)	12.8(15)	0.8(11)	1.4(12)	1.2(11)
C15	21.1(18)	20.8(17)	14.0(16)	-0.9(14)	4.7(14)	5.2(13)
C14	20.3(18)	20.6(17)	10.0(15)	0.9(14)	2.4(13)	1.0(13)
C9	21.8(18)	12.7(16)	21.2(18)	-2.0(13)	1.6(14)	-5.0(13)
C6	17.2(19)	27(2)	50(3)	2.3(16)	4.9(19)	-14(2)
C2	33(2)	22.2(19)	17.2(17)	-9.2(17)	1.9(16)	2.9(15)
C11	22.4(18)	11.0(15)	14.4(16)	-1.8(13)	-2.2(13)	1.1(12)
C1	19.7(18)	15.4(16)	17.8(17)	-6.5(14)	-1.1(14)	1.0(13)
C4	23(2)	16.7(17)	26(2)	-4.9(15)	5.9(16)	-7.5(15)
C3	31(2)	26(2)	20.7(19)	-10.6(17)	8.7(16)	-2.2(16)
C7	22(2)	22(2)	43(3)	5.5(16)	-4.1(19)	-6.3(19)
C8	22.8(19)	14.8(17)	30(2)	-1.8(14)	-1.9(16)	-1.5(15)
C5	25(2)	24(2)	38(2)	-5.0(17)	11.7(19)	-10.5(18)
C20	14.9(16)	18.1(16)	15.5(16)	1.0(13)	0.1(13)	0.3(13)
C18	24.2(19)	8.5(15)	14.2(16)	0.3(13)	-0.8(13)	1.6(12)
C19	14.1(16)	18.1(16)	13.3(15)	-1.5(13)	0.5(12)	2.0(13)
C21	14.8(17)	25.1(19)	19.3(18)	4.4(15)	-1.1(14)	-1.6(15)
C28	31(2)	32(2)	28(2)	-1.6(19)	-5.0(18)	14.4(19)
C29	16.6(17)	17.5(17)	13.5(15)	1.6(13)	-2.1(12)	0.3(13)
C27	29(2)	25(2)	34(2)	3.9(18)	-8.6(18)	11.2(18)
C25	22(2)	36(3)	30(2)	10.3(18)	-6.7(17)	-1.4(19)
C26	18.0(18)	26(2)	25(2)	6.4(15)	-4.0(15)	0.6(16)
C24	15(2)	49(3)	38(3)	7.3(19)	-3.6(18)	-8(2)
O4	15.0(12)	22.4(13)	15.6(12)	1.8(11)	-0.5(9)	-0.8(11)
O3	22.9(14)	15.6(12)	20.6(13)	3.0(11)	3.7(11)	-1.1(11)
C22	17.3(19)	41(3)	29(2)	-3.1(18)	1.1(16)	5.6(19)
C23	17(2)	47(3)	39(3)	-2.1(19)	3.0(18)	1(2)
O1	21.6(14)	20.1(13)	19.1(13)	-6.1(11)	-3.2(11)	7.6(11)

**Crystallographic Table 50 Bond Lengths for UO<sub>2</sub>[L<sup>IV</sup>].**

Atom	Atom	Length/Å	Atom	Atom	Length/Å
U1	O2	2.267(3)	C9	C4	1.430(6)
U1	N1	2.486(3)	C9	C8	1.409(6)
U1	N2	2.525(3)	C6	C7	1.401(7)
U1	N3	2.565(3)	C6	C5	1.369(8)
U1	O4	1.789(3)	C2	C1	1.428(5)
U1	O3	1.780(3)	C2	C3	1.360(6)
U1	O1	2.264(3)	C1	O1	1.331(5)
O2	C29	1.320(5)	C4	C3	1.421(6)
N1	C12	1.464(5)	C4	C5	1.419(6)
N1	C11	1.286(5)	C7	C8	1.382(6)
N2	C18	1.465(5)	C20	C19	1.450(5)
N2	C19	1.286(5)	C20	C21	1.445(5)
N3	C13	1.348(4)	C20	C29	1.406(5)
N3	C17	1.352(4)	C21	C26	1.426(6)
C16	C17	1.388(5)	C21	C22	1.414(6)
C16	C15	1.389(5)	C28	C29	1.412(6)
C12	C13	1.513(5)	C28	C27	1.356(7)
C10	C9	1.444(6)	C27	C26	1.421(7)
C10	C11	1.451(5)	C25	C26	1.415(6)
C10	C1	1.404(5)	C25	C24	1.367(8)
C13	C14	1.382(5)	C24	C23	1.396(8)
C17	C18	1.501(5)	C22	C23	1.375(6)
C15	C14	1.387(6)			

**Crystallographic Table 51 Bond Angles for UO<sub>2</sub>[L<sup>IV</sup>].**

Atom	Atom	Atom	Angle/°	Atom	Atom	Atom	Angle/°
N1	U1	O2	164.84(10)	C18	C17	C16	123.5(3)
N2	U1	O2	69.31(10)	C14	C15	C16	119.9(3)
N2	U1	N1	125.66(10)	C15	C14	C13	118.4(3)
N3	U1	O2	132.07(10)	C4	C9	C10	119.0(4)
N3	U1	N1	62.70(10)	C8	C9	C10	123.6(4)
N3	U1	N2	62.99(9)	C8	C9	C4	117.5(4)
O4	U1	O2	92.78(11)	C5	C6	C7	120.2(4)
O4	U1	N1	90.97(11)	C3	C2	C1	121.3(4)
O4	U1	N2	85.90(11)	C10	C11	N1	125.5(3)
O4	U1	N3	88.38(11)	C2	C1	C10	118.9(4)

O3	U1	O2	89.08(12)	O1	C1	C10	122.5(3)
O3	U1	N1	88.15(12)	O1	C1	C2	118.5(4)
O3	U1	N2	91.39(12)	C3	C4	C9	118.8(4)
O3	U1	N3	87.69(11)	C5	C4	C9	119.5(4)
O3	U1	O4	175.94(13)	C5	C4	C3	121.6(4)
O1	U1	O2	95.60(10)	C4	C3	C2	121.6(4)
O1	U1	N1	69.84(10)	C8	C7	C6	120.0(5)
O1	U1	N2	163.42(10)	C7	C8	C9	121.9(4)
O1	U1	N3	132.31(10)	C4	C5	C6	120.9(4)
O1	U1	O4	88.10(12)	C21	C20	C19	118.9(3)
O1	U1	O3	95.31(12)	C29	C20	C19	120.1(3)
C29	O2	U1	133.9(2)	C29	C20	C21	120.4(4)
C12	N1	U1	115.8(2)	C17	C18	N2	109.0(3)
C11	N1	U1	126.0(3)	C20	C19	N2	126.1(3)
C11	N1	C12	117.8(3)	C26	C21	C20	118.9(4)
C18	N2	U1	113.4(2)	C22	C21	C20	123.6(4)
C19	N2	U1	128.8(3)	C22	C21	C26	117.5(4)
C19	N2	C18	117.8(3)	C27	C28	C29	122.0(4)
C13	N3	U1	120.6(2)	C20	C29	O2	123.0(3)
C17	N3	U1	120.4(2)	C28	C29	O2	118.2(4)
C17	N3	C13	119.0(3)	C28	C29	C20	118.6(4)
C15	C16	C17	118.5(3)	C26	C27	C28	121.5(4)
C13	C12	N1	108.7(3)	C24	C25	C26	120.9(4)
C11	C10	C9	118.6(3)	C27	C26	C21	118.6(4)
C1	C10	C9	120.3(3)	C25	C26	C21	119.6(4)
C1	C10	C11	120.5(4)	C25	C26	C27	121.8(4)
C12	C13	N3	114.7(3)	C23	C24	C25	120.0(4)
C14	C13	N3	122.4(3)	C23	C22	C21	121.6(5)
C14	C13	C12	122.9(3)	C22	C23	C24	120.4(5)
C16	C17	N3	121.8(3)	C1	O1	U1	127.9(2)
C18	C17	N3	114.6(3)				

**Crystallographic Table 52** Hydrogen Atom Coordinates ( $\text{\AA}\times 10^4$ ) and Isotropic Displacement Parameters ( $\text{\AA}^2\times 10^3$ ) for  $\text{UO}_2[\text{L}^{\text{IV}}]$ .

Atom	x	y	z	U(eq)
H16	2031.1(16)	506(5)	5206(2)	18.2(7)
H12a	3420.9(18)	6759(5)	6243(2)	21.2(8)
H12b	2819.9(18)	7781(5)	5840(2)	21.2(8)
H15	2396.0(18)	1366(6)	6705(3)	22.1(9)



H14	2870.9(18)	4217(5)	6973(2)	20.3(8)
H6	6525(2)	8172(6)	4615(4)	37.6(12)
H2	4034(2)	10295(6)	2224(3)	28.9(10)
H11	4130.7(18)	7398(5)	5516(3)	19.6(8)
H3	5045(2)	10227(6)	2407(3)	30.2(10)
H7	6020(2)	6790(6)	5727(4)	35.5(12)
H8	4995.8(19)	6680(6)	5532(3)	27.4(10)
H5	6003(2)	9356(6)	3299(3)	33.7(11)
H18a	1746.6(18)	1594(5)	3587(3)	19.1(8)
H18b	2407.7(18)	1880(5)	3350(3)	19.1(8)
H19	1149.7(16)	3177(5)	2697(2)	18.3(8)
H28	1611(2)	9045(7)	822(3)	37.1(12)
H27	649(2)	8980(6)	170(3)	36.5(12)
H25	-369(2)	7702(7)	81(3)	36.1(12)
H24	-1026(2)	5622(8)	573(4)	41.7(13)
H22	248.4(19)	3692(7)	2488(3)	35.1(12)
H23	-722(2)	3678(8)	1809(4)	41.6(13)

$\text{H}_2[\text{L}^{\text{VII}}]$ **Crystallographic Table 53** Crystal data and structure refinement for  $\text{H}_2[\text{L}^{\text{VII}}]$ 

Empirical formula	$\text{C}_{29}\text{H}_{22}\text{N}_2\text{O}_2\text{Cl}_2$
Formula weight	501.42
Temperature/K	180.45
Crystal system	orthorhombic
Space group	$P2_12_12_1$
$a/\text{\AA}$	7.1378(10)
$b/\text{\AA}$	16.682(2)
$c/\text{\AA}$	20.056(3)
$\alpha/^\circ$	90
$\beta/^\circ$	90
$\gamma/^\circ$	90
Volume/ $\text{\AA}^3$	2388.1(6)
Z	4
$\rho_{\text{calc}}/\text{mg}/\text{mm}^3$	1.3945
$m/\text{mm}^{-1}$	0.303
F(000)	1041.6
Crystal size/ $\text{mm}^3$	$0.4 \times 0.3 \times 0.06$
Radiation	Mo $K\alpha$ ( $\lambda = 0.71073$ )
$2\Theta$ range for data collection	4.06 to $57.4^\circ$
Index ranges	$-9 \leq h \leq 9, -22 \leq k \leq 22, -27 \leq l \leq 22$
Reflections collected	17603
Independent reflections	6177 [ $R_{\text{int}} = 0.0539, R_{\text{sigma}} = 0.0733$ ]
Data/restraints/parameters	6177/0/318
Goodness-of-fit on $F^2$	1.036
Final R indexes [ $I \geq 2\sigma(I)$ ]	$R_1 = 0.0556, wR_2 = 0.1167$
Final R indexes [all data]	$R_1 = 0.0869, wR_2 = 0.1284$
Largest diff. peak/hole / $e \text{\AA}^{-3}$	0.65/-0.64
Flack parameter	-0.10(7)

**Crystallographic Table 54** Fractional Atomic Coordinates ( $\times 10^4$ ) and Equivalent Isotropic Displacement Parameters ( $\text{\AA}^2 \times 10^3$ ) for  $\text{H}_2[\text{L}^{\text{VII}}]$ .  $U_{\text{eq}}$  is defined as 1/3 of the trace of the orthogonalised  $U_{\text{H}}$  tensor.

Atom	$x$	$y$	$z$	$U(\text{eq})$
Cl1	2694.3(12)	711.1(5)	7279.7(4)	54.7(2)
Cl2	-91.0(15)	-266.7(6)	6613.8(5)	76.7(3)
O1	3838(3)	758.8(10)	5454.9(9)	33.6(4)

O2	1504(3)	2189.6(10)	5876(1)	32.6(4)
N1	3053(3)	998.7(10)	4218.4(10)	21.9(4)
N2	2093(3)	2498.5(10)	4636.3(10)	23.0(4)
C6	5919(4)	-2672.6(15)	4246.2(15)	39.4(7)
C5	6087(4)	-2349.1(14)	4870.4(15)	33.2(6)
C4	5436(3)	-1559.6(13)	5008.4(13)	26.1(5)
C9	4655(3)	-1092.2(13)	4496.0(12)	22.9(5)
C10	4117(3)	-267.4(13)	4633.9(12)	21.3(5)
C11	3519(3)	241.4(13)	4125.5(12)	22.0(5)
C12	2486(3)	1554.4(13)	3731.9(11)	21.1(5)
C17	1991(3)	2330.3(13)	3943.7(12)	21.0(5)
C18	2578(3)	3218.5(12)	4818.0(12)	22.2(5)
C19	2632(3)	3464.1(13)	5505.2(11)	21.5(5)
C20	3239(3)	4264.4(14)	5691.5(12)	25.0(5)
C25	3177(3)	4491.4(14)	6371.5(13)	29.2(6)
C24	3724(4)	5278.1(17)	6556.7(15)	39.2(7)
C23	4318(4)	5817.7(16)	6089.2(17)	42.1(7)
C3	5601(4)	-1234.0(15)	5666.9(14)	31.3(6)
C2	5040(4)	-485.3(15)	5807.1(14)	31.0(6)
C1	4296(3)	43.1(13)	5300.7(13)	25.8(5)
C8	4444(4)	-1455.5(14)	3863.3(14)	31.2(6)
C7	5067(4)	-2223.7(15)	3746.3(15)	37.3(6)
C13	2429(4)	1369.6(14)	3054.7(12)	27.3(5)
C14	1881(4)	1939.5(15)	2595.4(13)	31.5(6)
C15	1343(4)	2700.5(15)	2804.2(13)	32.6(6)
C16	1387(4)	2888.8(14)	3474.6(13)	28.5(6)
C26	2578(4)	3930.1(16)	6853.7(14)	35.3(6)
C27	2049(3)	3175.4(15)	6680.7(13)	31.6(6)
C28	2069(3)	2938.2(14)	6007.5(13)	26.7(5)
C22	4395(4)	5593.0(15)	5419.0(14)	32.8(6)
C21	3879(3)	4843.3(14)	5222.4(14)	27.2(5)
C29	966(4)	681(2)	6663.7(16)	50.0(8)

**Crystallographic Table 55** Anisotropic Displacement Parameters ( $\text{\AA}^2 \times 10^3$ ) for  $\text{H}_2[\text{L}^{\text{VII}}]$ .

The Anisotropic displacement factor exponent takes the form: -

$$2\pi^2[h^2a^2U_{11}+2hka*b*U_{12}+...]$$

Atom	$U_{11}$	$U_{22}$	$U_{33}$	$U_{12}$	$U_{13}$	$U_{23}$
Cl1	65.3(5)	63.6(5)	35.2(4)	-23.4(4)	0.2(4)	-0.8(4)
Cl2	85.4(7)	89.7(7)	55.0(6)	-48.7(6)	-16.8(5)	20.5(5)

O1	51.3(11)	23.7(8)	25.8(10)	0.6(8)	-0.2(8)	-2.6(7)
O2	40.7(10)	31.1(9)	25.8(11)	-3.0(8)	4.3(9)	5.7(8)
N1	24.1(9)	20.4(9)	21.2(11)	-1.9(7)	0.6(8)	-0.1(8)
N2	26.1(10)	21.2(9)	21.6(11)	1.9(8)	0.2(8)	1.2(8)
C6	45.0(16)	20.5(12)	53(2)	4.5(11)	11.6(14)	-2.7(12)
C5	35.6(14)	22.2(12)	41.8(18)	3.1(10)	2.2(12)	8.0(11)
C4	22.6(11)	21.5(11)	34.2(16)	0.4(9)	2.6(10)	2.1(10)
C9	20.0(11)	19.5(10)	29.2(15)	-1.6(8)	3.5(10)	4.1(10)
C10	18.9(10)	20.4(10)	24.7(14)	-2.0(8)	0.4(9)	0.1(9)
C11	21.2(10)	19.6(10)	25.2(14)	-3.7(8)	1.1(10)	0.6(10)
C12	18.6(10)	22.2(10)	22.4(13)	-3.3(9)	-0.1(10)	4.0(9)
C17	20.8(11)	22.9(11)	19.2(13)	-4.9(9)	1.7(9)	0.4(9)
C18	20(1)	22.6(11)	23.8(13)	2.8(9)	4(1)	4.2(9)
C19	17.7(10)	23.3(10)	23.6(13)	5.1(9)	-0.8(9)	1.4(9)
C20	18.3(10)	28.3(12)	28.4(14)	6.9(9)	-3.5(9)	-3(1)
C25	26.3(12)	32.6(13)	28.6(15)	11.2(10)	-5.5(10)	-4.4(11)
C24	37.6(14)	43.5(16)	36.6(17)	9.2(12)	-8.7(13)	-16.0(14)
C23	36.4(14)	30.1(14)	60(2)	2.7(11)	-10.3(14)	-15.2(14)
C3	30.2(13)	30.7(12)	33.1(17)	-0.5(10)	-1.0(11)	12.6(11)
C2	34.7(13)	34.6(13)	23.8(14)	-1.5(11)	0.1(11)	1.7(11)
C1	24.9(11)	23.4(11)	29.3(15)	-3.4(9)	3.4(10)	2.2(10)
C8	37.3(14)	26.1(12)	30.2(15)	1.0(11)	0.3(11)	-2.0(11)
C7	47.8(16)	27.5(13)	36.5(17)	3.2(12)	6.2(13)	-6.4(12)
C13	29.9(12)	24.7(11)	27.4(14)	-1.2(10)	2.5(11)	-0.3(10)
C14	35.5(13)	38.4(13)	20.8(15)	-2.4(11)	2.2(11)	1.9(11)
C15	39.7(14)	32.4(13)	25.8(15)	-1.5(11)	-3.4(12)	9.0(11)
C16	35.5(13)	21.5(11)	28.6(15)	0.3(10)	-2.5(11)	2.8(10)
C26	33.1(13)	49.2(16)	23.5(15)	10.7(12)	-2.9(12)	-7.3(12)
C27	30.9(13)	42.1(14)	21.9(14)	8.1(11)	4.2(11)	4.5(11)
C28	21.9(11)	28.4(12)	29.6(15)	4.4(9)	-1.9(10)	1.9(10)
C22	32.1(13)	25.1(12)	41.1(17)	3.3(10)	-4.3(12)	0.5(11)
C21	22.7(11)	26.5(11)	32.2(15)	3.4(9)	-3.7(10)	1.0(11)
C29	52.2(17)	52.3(18)	45.6(19)	-2.4(15)	-0.7(15)	22.2(15)

**Crystallographic Table 56** Bond Lengths for  $\text{H}_2[\text{L}^{\text{VII}}]$ .

Atom	Atom	Length/Å	Atom	Atom	Length/Å
C11	C29	1.747(3)	C17	C16	1.392(3)
C12	C29	1.755(3)	C18	C19	1.438(3)

O1	C1	1.276(3)	C19	C20	1.453(3)
O2	C28	1.338(3)	C19	C28	1.395(3)
N1	C11	1.319(3)	C20	C25	1.416(3)
N1	C12	1.405(3)	C20	C21	1.423(3)
N2	C17	1.419(3)	C25	C24	1.419(4)
N2	C18	1.302(3)	C25	C26	1.412(4)
C6	C5	1.369(4)	C24	C23	1.367(4)
C6	C7	1.392(4)	C23	C22	1.396(4)
C5	C4	1.424(3)	C3	C2	1.341(4)
C4	C9	1.405(3)	C2	C1	1.446(4)
C4	C3	1.433(4)	C8	C7	1.376(3)
C9	C10	1.455(3)	C13	C14	1.380(3)
C9	C8	1.414(4)	C14	C15	1.391(4)
C10	C11	1.394(3)	C15	C16	1.381(4)
C10	C1	1.440(4)	C26	C27	1.359(4)
C12	C17	1.407(3)	C27	C28	1.407(4)
C12	C13	1.393(3)	C22	C21	1.362(3)

**Crystallographic Table 57** Bond Angles for  $\text{H}_2[\text{L}^{\text{VII}}]$ .

Atom	Atom	Atom	Angle/°	Atom	Atom	Atom	Angle/°
C12	N1	C11	127.3(2)	C21	C20	C25	117.7(2)
C18	N2	C17	118.05(19)	C24	C25	C20	119.4(2)
C7	C6	C5	119.0(2)	C26	C25	C20	119.4(2)
C4	C5	C6	120.9(2)	C26	C25	C24	121.2(2)
C9	C4	C5	120.0(2)	C23	C24	C25	121.0(3)
C3	C4	C5	120.2(2)	C22	C23	C24	119.7(3)
C3	C4	C9	119.8(2)	C2	C3	C4	121.4(2)
C10	C9	C4	119.4(2)	C1	C2	C3	122.0(3)
C8	C9	C4	117.4(2)	C10	C1	O1	122.6(2)
C8	C9	C10	123.2(2)	C2	C1	O1	119.6(2)
C11	C10	C9	121.2(2)	C2	C1	C10	117.7(2)
C1	C10	C9	119.6(2)	C7	C8	C9	121.2(2)
C1	C10	C11	119.2(2)	C8	C7	C6	121.3(3)
C10	C11	N1	123.9(2)	C14	C13	C12	120.4(2)
C17	C12	N1	118.0(2)	C15	C14	C13	120.4(2)
C13	C12	N1	122.6(2)	C16	C15	C14	119.6(2)
C13	C12	C17	119.4(2)	C15	C16	C17	120.8(2)
C12	C17	N2	117.7(2)	C27	C26	C25	121.6(2)

C16	C17	N2	123.0(2)	C28	C27	C26	120.2(2)
C16	C17	C12	119.3(2)	C19	C28	O2	122.1(2)
C19	C18	N2	122.5(2)	C27	C28	O2	116.7(2)
C20	C19	C18	121.1(2)	C27	C28	C19	121.3(2)
C28	C19	C18	120.3(2)	C21	C22	C23	121.0(3)
C28	C19	C20	118.6(2)	C22	C21	C20	121.2(3)
C25	C20	C19	119.0(2)	C12	C29	Cl1	111.72(16)
C21	C20	C19	123.3(2)				

**Crystallographic Table 58** Hydrogen Bonds for  $\text{H}_2[\text{L}^{\text{VII}}]$ .

D	H	A	d(D-H)/Å	d(H-A)/Å	d(D-A)/Å	D-H-A/°
O2	H2	N2	0.80(3)	1.82(3)	2.574(3)	156(3)

**Crystallographic Table 59** Hydrogen Atom Coordinates ( $\text{Å} \times 10^4$ ) and Isotropic Displacement Parameters ( $\text{Å}^2 \times 10^3$ ) for  $\text{H}_2[\text{L}^{\text{VII}}]$ .

Atom	x	y	z	U(eq)
H2	1570(50)	2158(18)	5480(17)	48.8(7)
H6	6378(4)	-3195.9(15)	4155.5(15)	47.3(8)
H5	6646(4)	-2655.6(14)	5216.5(15)	39.9(7)
H11	3441(3)	30.7(13)	3686.3(12)	26.4(6)
H18	2909(3)	3596.3(12)	4483.7(12)	26.6(6)
H24	3676(4)	5432.4(17)	7012.4(15)	47.1(8)
H23	4678(4)	6343.0(16)	6219.7(17)	50.5(9)
H3	6118(4)	-1555.5(15)	6011.8(14)	37.6(7)
H2a	5136(4)	-296.4(15)	6252.6(14)	37.2(7)
H8	3863(4)	-1164.2(14)	3512.8(14)	37.4(7)
H7	4911(4)	-2451.9(15)	3315.8(15)	44.8(8)
H13	2769(4)	848.0(14)	2908.2(12)	32.8(6)
H14	1872(4)	1811.2(15)	2133.9(13)	37.9(7)
H15	947(4)	3088.6(15)	2487.4(13)	39.2(7)
H16	1000(4)	3405.9(14)	3617.5(13)	34.2(7)
H26	2544(4)	4083.6(16)	7309.7(14)	42.3(7)
H27	1665(3)	2807.2(15)	7015.3(13)	38.0(7)
H22	4813(4)	5968.5(15)	5095.5(14)	39.3(7)
H21	3947(3)	4704.1(14)	4763.7(14)	32.6(6)
H29a	-2(4)	1089(2)	6763.5(16)	60.0(9)
H29b	1533(4)	816(2)	6227.3(16)	60.0(9)
H1	3103(3)	1175.6(10)	4631.3(10)	26.3(5)

## Refinement model description

Number of restraints - 0, number of constraints - 42.

### Details:

#### 1. Fixed Uiso

At 1.2 times of:

All C(H) groups, All C(H,H) groups, All N(H) groups

At 1.5 times of:

All O(H) groups

#### 2.a Secondary CH2 refined with riding coordinates:

C29(H29a,H29b)

#### 2.b Aromatic/amide H refined with riding coordinates:

N1(H1), C6(H6), C5(H5), C11(H11), C18(H18), C24(H24), C23(H23), C3(H3),  
C2(H2a), C8(H8), C7(H7), C13(H13), C14(H14), C15(H15), C16(H16), C26(H26),  
C27(H27), C22(H22), C21(H21)

## Th[L<sup>VII</sup>]<sub>2</sub>

**Crystallographic Table 60** Crystal data and structure refinement for Th[L<sup>VII</sup>]<sub>2</sub>

Empirical formula	C <sub>66.5</sub> H <sub>47.5</sub> N <sub>4</sub> O <sub>4</sub> Th
Formula weight	1198.68
Temperature/K	180.45
Crystal system	triclinic
Space group	P-1
a/Å	11.4987(3)
b/Å	14.3613(4)
c/Å	16.2765(5)
α/°	106.2205(11)
β/°	90.8258(11)
γ/°	94.1516(11)
Volume/Å <sup>3</sup>	2572.39(13)
Z	2
ρ <sub>calc</sub> /mg/mm <sup>3</sup>	1.5474
m/mm <sup>-1</sup>	2.955
F(000)	1180.2
Crystal size/mm <sup>3</sup>	0.18 × 0.12 × 0.08
Radiation	Mo Kα (λ = 0.71073)
2θ range for data collection	2.6 to 48.22°
Index ranges	-13 ≤ h ≤ 13, -16 ≤ k ≤ 16, -18 ≤ l ≤ 18
Reflections collected	53501
Independent reflections	8180 [R <sub>int</sub> = 0.0498, R <sub>sigma</sub> = 0.0396]
Data/restraints/parameters	8180/3/686
Goodness-of-fit on F <sup>2</sup>	1.060
Final R indexes [I ≥ 2σ (I)]	R <sub>1</sub> = 0.0242, wR <sub>2</sub> = 0.0489
Final R indexes [all data]	R <sub>1</sub> = 0.0330, wR <sub>2</sub> = 0.0516
Largest diff. peak/hole / e Å <sup>-3</sup>	0.92/-0.91

**Crystallographic Table 61** Fractional Atomic Coordinates (×10<sup>4</sup>) and Equivalent Isotropic Displacement Parameters (Å<sup>2</sup>×10<sup>3</sup>) for Th[L<sup>VII</sup>]<sub>2</sub>. U<sub>eq</sub> is defined as 1/3 of the trace of the orthogonalised U<sub>ij</sub> tensor.

Atom	x	y	z	U(eq)
Th1	105.71(10)	5047.97(10)	2558.78(8)	18.78(5)
O1	-621.3(17)	5380.9(16)	1388.0(13)	21.4(5)
O3	207.8(18)	5808.6(16)	3993.1(13)	22.8(5)
O4	1803.9(18)	4430.9(17)	2831.8(14)	28.0(6)



N3	399(2)	6951(2)	2905.6(16)	18.6(6)
N4	1928(2)	5814(2)	1950.7(16)	18.8(6)
N2	-1484(2)	4086(2)	3193.3(16)	18.5(6)
N1	-1985(2)	5709.5(19)	2808.4(16)	17.9(6)
O2	-246.0(19)	3440.0(18)	1737.1(14)	28.9(6)
C40	890(3)	7271(2)	2228(2)	19.2(8)
C19	-1227(3)	2380(2)	2444(2)	22.0(8)
C10	-2247(3)	6345(2)	1563(2)	19.7(8)
C45	1692(3)	6681(2)	1726(2)	20.6(8)
C48	4540(3)	4377(2)	1675.8(19)	18.2(8)
C12	-2506(3)	5541(2)	3549.0(19)	17.4(8)
C11	-2588(3)	6117(2)	2344(2)	19.9(8)
C2	-1056(3)	6097(2)	302(2)	24.7(8)
C9	-3009(3)	6884(2)	1186(2)	20.8(8)
C16	-2592(3)	4539(3)	4525(2)	24.5(8)
C4	-2758(3)	7004(2)	368(2)	24.8(8)
C20	-1533(3)	1392(2)	2472(2)	24.2(8)
C27	-348(3)	1748(3)	1072(2)	34.8(10)
C29	-178(3)	6562(3)	4549(2)	22.2(8)
C17	-2208(3)	4717(2)	3771(2)	19.0(8)
C56	2837(3)	4204(3)	2534(2)	24.0(8)
C13	-3240(3)	6165(3)	4075(2)	26.8(9)
C31	-806(3)	7235(3)	5994(2)	31.7(10)
C1	-1287(3)	5941(2)	1111(2)	18.7(8)
C53	5055(3)	3642(3)	1945(2)	24.3(8)
C41	600(3)	8106(3)	2019(2)	26.2(9)
C47	3411(3)	4683(2)	2000(2)	19.7(8)
C3	-1760(3)	6609(2)	-48(2)	28.0(9)
C39	97(3)	7608(3)	3584(2)	22.5(8)
C50	6196(3)	4433(2)	773(2)	25.7(9)
C8	-4024(3)	7291(2)	1572(2)	29.3(9)
C49	5137(3)	4750(2)	1062(2)	23.6(8)
C54	4446(3)	3211(3)	2516(2)	31.0(9)
C51	6724(3)	3733(3)	1068(2)	29.4(9)
C28	-587(3)	2559(3)	1769(2)	25.4(9)
C44	2168(3)	6944(3)	1042(2)	26.3(9)
C18	-1714(3)	3159(3)	3054(2)	20.5(8)
C38	-335(3)	7442(2)	4361(2)	20.2(8)

C37	-811(3)	8231(3)	4995(2)	25.3(9)
C46	2965(3)	5519(2)	1817.4(19)	19.1(8)
C15	-3328(3)	5161(3)	5029(2)	33.9(10)
C32	-1016(3)	8128(3)	5827(2)	27.4(9)
C52	6149(3)	3336(3)	1632(2)	29.0(9)
C55	3384(3)	3468(3)	2796(2)	28.0(9)
C25	-1285(3)	609(3)	1763(2)	30.7(9)
C35	-1566(3)	9826(3)	5458(3)	41(1)
C21	-2047(3)	1164(3)	3174(2)	34.7(10)
C30	-424(3)	6480(3)	5384(2)	27.2(9)
C43	1899(3)	7787(3)	855(2)	32.5(9)
C24	-1626(3)	-351(3)	1772(3)	40.9(11)
C36	-1124(3)	9090(3)	4833(2)	33.6(9)
C5	-3507(3)	7510(3)	-21(2)	33.8(10)
C42	1106(3)	8369(3)	1343(2)	30.5(9)
C14	-3659(3)	5958(3)	4801(2)	33.7(9)
C22	-2345(3)	217(3)	3162(3)	43.7(11)
C33	-1448(3)	8894(3)	6459(2)	40.3(11)
C26	-700(3)	826(3)	1072(2)	39.8(10)
C7	-4732(3)	7771(3)	1169(3)	35.5(10)
C34	-1714(3)	9725(3)	6279(3)	45.4(12)
C6	-4473(3)	7868(3)	364(3)	37.5(10)
C23	-2153(3)	-542(3)	2459(3)	44.6(11)
C58S	4787(4)	8330(3)	5026(3)	50.8(12)
C59S	3832(4)	7670(3)	4740(3)	65.3(14)
C63S	5255(4)	8778(4)	4452(3)	64.5(14)
C62S	4763(5)	8614(4)	3643(3)	73.7(16)
C57S	5301(5)	8528(4)	5915(3)	81.7(17)
C60S	3348(4)	7486(4)	3946(4)	83.7(18)
C61S	3809(5)	7978(4)	3390(3)	77.3(16)
C66S	-6167(6)	9853(5)	-21(7)	105(3)
C64S	-6210(14)	10433(9)	1544(8)	136(6)
C67S	-5552(9)	9616(5)	-796(6)	111(3)
C65S	-5610(8)	10226(5)	764(6)	104(2)

**Crystallographic Table 62** Anisotropic Displacement Parameters ( $\text{\AA}^2 \times 10^3$ ) for  $\text{Th}[\text{L}^{\text{VII}}]_2$ . The Anisotropic displacement factor exponent takes the form: -  $2\pi^2[h^2a^2U_{11}+2hka*b*U_{12}+\dots]$

Atom	$U_{11}$	$U_{22}$	$U_{33}$	$U_{12}$	$U_{13}$	$U_{23}$
------	----------	----------	----------	----------	----------	----------

Th1	17.92(8)	22.71(8)	19.14(8)	5.72(5)	5.11(5)	10.30(6)
O1	19.7(12)	29.6(15)	18.0(12)	8.4(11)	4(1)	10.2(11)
O3	26.7(13)	26.3(15)	18.6(12)	5.3(11)	3.4(10)	10.4(11)
O4	21.2(13)	38.8(16)	34.3(14)	14.7(12)	9.4(11)	23.6(13)
N3	15.6(14)	23.7(18)	18.2(15)	3.8(13)	5.2(12)	7.9(14)
N4	18.7(15)	21.5(17)	18.6(15)	5.8(13)	3.3(12)	8.2(13)
N2	17.9(15)	20.4(18)	19.7(15)	3.7(13)	1.4(12)	9.4(13)
N1	16.7(14)	19.3(16)	19.0(15)	3.6(12)	6.2(12)	6.9(13)
O2	35.3(14)	26.2(16)	26.7(14)	3.7(12)	11.7(11)	9.1(12)
C40	19.2(18)	16(2)	21.5(19)	0.3(15)	1.6(15)	4.8(16)
C19	21.5(19)	21(2)	23(2)	4.3(16)	-3.0(16)	5.8(17)
C10	19.6(18)	19(2)	20.8(19)	1.8(15)	-1.4(15)	6.1(16)
C45	18.8(18)	23(2)	22.6(19)	6.4(16)	5.1(15)	9.6(17)
C48	15.1(17)	19(2)	18.1(18)	2.0(15)	0.3(15)	1.5(16)
C12	13.8(17)	20(2)	19.1(18)	1.9(15)	2.3(14)	5.5(16)
C11	19.5(18)	16(2)	23.3(19)	2.9(15)	3.2(16)	3.9(16)
C2	28(2)	26(2)	20.3(19)	2.5(17)	4.1(16)	6.0(17)
C9	22.7(19)	15(2)	25(2)	-1.0(15)	-5.6(16)	6.6(16)
C16	29(2)	24(2)	23.7(19)	3.4(17)	9.2(16)	11.4(17)
C4	31(2)	18(2)	25(2)	-2.2(17)	-6.2(17)	7.1(17)
C20	20.5(19)	22(2)	30(2)	2.0(16)	-5.4(16)	8.2(18)
C27	43(2)	28(2)	33(2)	6.6(19)	10.4(19)	6.2(19)
C29	14.7(18)	34(2)	16.9(19)	-0.1(16)	-0.4(15)	5.1(17)
C17	15.4(17)	20(2)	19.3(18)	1.8(15)	4.9(15)	2.2(16)
C56	18.4(19)	31(2)	24(2)	4.8(16)	-0.5(16)	8.4(17)
C13	26(2)	30(2)	27(2)	11.5(17)	8.1(17)	10.2(18)
C31	19.4(19)	58(3)	17(2)	1.6(19)	2.5(16)	10(2)
C1	22.3(19)	16.3(19)	16.6(18)	-1.2(15)	-3.6(15)	4.1(15)
C53	22.3(19)	30(2)	19.5(19)	5.3(17)	-2.4(16)	4.4(17)
C41	28(2)	26(2)	27(2)	8.9(17)	10.1(17)	9.0(17)
C47	18.2(18)	24(2)	17.7(18)	5.2(15)	0.1(15)	5.6(16)
C3	40(2)	26(2)	21(2)	-2.5(18)	-4.5(18)	11.0(17)
C39	19.4(18)	20(2)	29(2)	2.3(16)	0.0(16)	8.0(18)
C50	20.8(19)	28(2)	23(2)	-1.7(17)	5.3(16)	0.0(17)
C8	30(2)	25(2)	37(2)	4.7(17)	-1.7(18)	13.7(18)
C49	21.8(19)	23(2)	24.9(19)	3.7(16)	2.2(16)	3.7(16)
C54	30(2)	37(2)	33(2)	17.6(18)	0.0(18)	18.8(19)
C51	17.5(19)	39(2)	25(2)	8.3(18)	1.7(16)	-2.3(19)

C28	25(2)	27(2)	23(2)	7.1(17)	-0.3(17)	4.2(18)
C44	27(2)	32(2)	24(2)	13.6(17)	13.4(16)	11.5(18)
C18	19.1(18)	26(2)	18.7(19)	0.3(16)	1.3(15)	10.9(17)
C38	17.9(18)	25(2)	16.8(18)	0.3(16)	3.1(15)	5.2(16)
C37	17.1(18)	27(2)	27(2)	-4.3(16)	2.8(16)	1.1(18)
C46	20.0(19)	22(2)	17.5(18)	2.7(16)	4.0(15)	9.0(16)
C15	37(2)	44(3)	22(2)	3(2)	14.1(18)	10.9(19)
C32	18.9(19)	38(2)	21(2)	-2.5(17)	3.7(16)	2.3(18)
C52	24(2)	34(2)	28(2)	11.6(17)	-3.3(17)	4.3(18)
C55	27(2)	35(2)	31(2)	10.3(18)	6.2(17)	21.0(18)
C25	24(2)	24(2)	41(2)	2.6(17)	-4.7(18)	5.5(19)
C35	38(2)	30(3)	51(3)	2.0(19)	15(2)	4(2)
C21	39(2)	26(2)	42(2)	3.0(18)	5.4(19)	13(2)
C30	21.6(19)	44(3)	21(2)	2.6(18)	0.1(16)	16.5(19)
C43	38(2)	36(2)	32(2)	10.2(19)	15.0(18)	20.9(19)
C24	40(2)	21(2)	56(3)	5.3(19)	-4(2)	1(2)
C36	36(2)	30(2)	31(2)	-1.5(19)	13.4(18)	2.5(19)
C5	49(3)	24(2)	30(2)	2(2)	-13(2)	12.2(18)
C42	42(2)	21(2)	35(2)	11.3(18)	11.9(19)	15.1(18)
C14	34(2)	34(3)	33(2)	10.4(19)	16.4(18)	5.9(19)
C22	45(3)	33(3)	59(3)	1(2)	11(2)	23(2)
C33	34(2)	49(3)	29(2)	-3(2)	9.9(19)	-3(2)
C26	48(2)	28(3)	37(2)	8(2)	11(2)	-4(2)
C7	27(2)	26(2)	54(3)	8.6(18)	-7(2)	11(2)
C34	39(2)	42(3)	40(3)	0(2)	18(2)	-13(2)
C6	47(3)	25(2)	43(3)	5(2)	-21(2)	14(2)
C23	42(2)	22(2)	72(3)	0(2)	3(2)	16(2)
C58S	51(3)	47(3)	55(3)	3(2)	4(2)	16(2)
C59S	55(3)	59(3)	77(4)	-14(3)	14(3)	16(3)
C63S	58(3)	56(3)	70(4)	-13(3)	2(3)	7(3)
C62S	98(4)	60(4)	59(4)	-10(3)	12(3)	13(3)
C57S	90(4)	75(4)	81(4)	6(3)	-18(3)	25(3)
C60S	48(3)	103(5)	74(4)	-18(3)	-1(3)	-10(4)
C61S	81(4)	83(4)	55(3)	4(3)	-8(3)	-1(3)
C66S	70(4)	55(4)	207(8)	-11(4)	-54(6)	73(5)
C64S	260(20)	60(9)	90(10)	36(11)	67(12)	22(8)
C67S	134(8)	52(4)	157(8)	-3(5)	-68(6)	51(5)
C65S	96(6)	54(4)	175(8)	5(4)	-33(6)	57(5)

**Crystallographic Table 63** Bond Lengths for **Th[L<sup>VII</sup>]<sub>2</sub>**.

Atom	Atom	Length/Å	Atom	Atom	Length/Å
Th1	O1	2.254(2)	C29	C38	1.403(5)
Th1	O3	2.282(2)	C29	C30	1.427(4)
Th1	O4	2.289(2)	C56	C47	1.395(4)
Th1	N3	2.627(3)	C56	C55	1.427(5)
Th1	N4	2.630(3)	C13	C14	1.382(5)
Th1	N2	2.608(3)	C31	C32	1.419(5)
Th1	N1	2.644(2)	C31	C30	1.354(5)
Th1	O2	2.326(2)	C53	C54	1.420(5)
O1	C1	1.311(4)	C53	C52	1.417(4)
O3	C29	1.312(4)	C41	C42	1.382(4)
O4	C56	1.318(4)	C47	C46	1.442(4)
N3	C40	1.417(4)	C39	C38	1.440(4)
N3	C39	1.307(4)	C50	C49	1.374(4)
N4	C45	1.434(4)	C50	C51	1.400(5)
N4	C46	1.295(4)	C8	C7	1.374(5)
N2	C17	1.433(4)	C54	C55	1.349(4)
N2	C18	1.293(4)	C51	C52	1.363(5)
N1	C12	1.426(4)	C44	C43	1.382(5)
N1	C11	1.297(4)	C38	C37	1.449(5)
O2	C28	1.313(4)	C37	C32	1.424(5)
C40	C45	1.408(4)	C37	C36	1.401(5)
C40	C41	1.395(4)	C15	C14	1.374(5)
C19	C20	1.451(5)	C32	C33	1.407(5)
C19	C28	1.403(5)	C25	C24	1.410(5)
C19	C18	1.427(5)	C25	C26	1.415(5)
C10	C11	1.451(4)	C35	C36	1.380(5)
C10	C9	1.447(4)	C35	C34	1.396(5)
C10	C1	1.405(4)	C21	C22	1.372(5)
C45	C44	1.381(4)	C43	C42	1.386(5)
C48	C53	1.414(4)	C24	C23	1.364(5)
C48	C47	1.459(4)	C5	C6	1.347(5)
C48	C49	1.421(4)	C22	C23	1.375(5)
C12	C17	1.394(4)	C33	C34	1.359(6)
C12	C13	1.396(4)	C7	C6	1.389(5)
C2	C1	1.422(4)	C58S	C59S	1.382(6)

C2	C3	1.351(5)	C58S	C63S	1.370(6)
C9	C4	1.421(4)	C58S	C57S	1.498(6)
C9	C8	1.418(5)	C59S	C60S	1.347(7)
C16	C17	1.393(4)	C63S	C62S	1.376(6)
C16	C15	1.381(5)	C62S	C61S	1.356(7)
C4	C3	1.414(5)	C60S	C61S	1.385(7)
C4	C5	1.416(5)	C66S	C67S	1.425(8)
C20	C25	1.416(5)	C66S	C65S	1.369(8)
C20	C21	1.401(5)	C64S	C65S	1.422(10)
C27	C28	1.427(5)	C67S	C65S <sup>1</sup>	1.336(9)
C27	C26	1.356(5)			

<sup>1</sup>-1-X,2-Y,-Z

**Crystallographic Table 64** Bond Angles for Th[L<sup>VII</sup>]<sub>2</sub>.

Atom	Atom	Atom	Angle/°	Atom	Atom	Atom	Angle/°
O3	Th1	O1	135.40(8)	C30	C29	C38	119.2(3)
O4	Th1	O1	132.65(8)	C12	C17	N2	116.6(3)
O4	Th1	O3	84.21(8)	C16	C17	N2	122.7(3)
N3	Th1	O1	75.34(8)	C16	C17	C12	120.7(3)
N3	Th1	O3	67.17(8)	C47	C56	O4	121.9(3)
N3	Th1	O4	110.38(8)	C55	C56	O4	117.9(3)
N4	Th1	O1	76.15(7)	C55	C56	C47	120.1(3)
N4	Th1	O3	104.69(8)	C14	C13	C12	119.9(3)
N4	Th1	O4	67.66(8)	C30	C31	C32	121.9(3)
N4	Th1	N3	61.61(8)	C10	C1	O1	122.3(3)
N2	Th1	O1	110.22(7)	C2	C1	O1	118.1(3)
N2	Th1	O3	75.51(8)	C2	C1	C10	119.5(3)
N2	Th1	O4	103.54(8)	C54	C53	C48	118.7(3)
N2	Th1	N3	125.47(8)	C52	C53	C48	120.0(3)
N2	Th1	N4	170.99(8)	C52	C53	C54	121.3(3)
N1	Th1	O1	68.12(8)	C42	C41	C40	121.1(3)
N1	Th1	O3	78.30(8)	C56	C47	C48	119.0(3)
N1	Th1	O4	159.18(8)	C46	C47	C48	119.1(3)
N1	Th1	N3	73.06(8)	C46	C47	C56	121.7(3)
N1	Th1	N4	127.74(8)	C4	C3	C2	121.7(3)
N1	Th1	N2	61.26(8)	C38	C39	N3	126.8(3)
O2	Th1	O1	83.66(8)	C51	C50	C49	121.5(3)

O2	Th1	O3	134.37(8)	C7	C8	C9	121.4(3)
O2	Th1	O4	79.63(8)	C50	C49	C48	120.9(3)
O2	Th1	N3	158.17(8)	C55	C54	C53	122.2(3)
O2	Th1	N4	107.86(8)	C52	C51	C50	118.8(3)
O2	Th1	N2	67.47(8)	C19	C28	O2	122.7(3)
O2	Th1	N1	104.75(8)	C27	C28	O2	119.0(3)
C1	O1	Th1	145.0(2)	C27	C28	C19	118.2(3)
C29	O3	Th1	140.23(19)	C43	C44	C45	121.3(3)
C56	O4	Th1	144.0(2)	C19	C18	N2	128.7(3)
C40	N3	Th1	113.26(19)	C39	C38	C29	120.4(3)
C39	N3	Th1	128.5(2)	C37	C38	C29	119.9(3)
C39	N3	C40	118.1(3)	C37	C38	C39	119.3(3)
C45	N4	Th1	112.75(19)	C32	C37	C38	119.0(3)
C46	N4	Th1	130.0(2)	C36	C37	C38	123.9(3)
C46	N4	C45	117.2(3)	C36	C37	C32	117.1(3)
C17	N2	Th1	112.25(19)	C47	C46	N4	127.4(3)
C18	N2	Th1	130.3(2)	C14	C15	C16	120.6(3)
C18	N2	C17	117.4(3)	C37	C32	C31	118.8(3)
C12	N1	Th1	112.66(18)	C33	C32	C31	121.2(3)
C11	N1	Th1	129.4(2)	C33	C32	C37	120.0(4)
C11	N1	C12	117.9(3)	C51	C52	C53	121.3(3)
C28	O2	Th1	143.8(2)	C54	C55	C56	120.5(3)
C45	C40	N3	116.8(3)	C24	C25	C20	119.1(4)
C41	C40	N3	124.2(3)	C26	C25	C20	118.3(3)
C41	C40	C45	119.0(3)	C26	C25	C24	122.5(4)
C28	C19	C20	120.6(3)	C34	C35	C36	119.9(4)
C18	C19	C20	118.5(3)	C22	C21	C20	121.2(4)
C18	C19	C28	120.4(3)	C31	C30	C29	121.1(4)
C9	C10	C11	118.7(3)	C42	C43	C44	119.9(3)
C1	C10	C11	121.2(3)	C23	C24	C25	121.4(4)
C1	C10	C9	119.5(3)	C35	C36	C37	121.9(4)
C40	C45	N4	116.7(3)	C6	C5	C4	121.1(4)
C44	C45	N4	124.1(3)	C43	C42	C41	119.6(3)
C44	C45	C40	119.1(3)	C15	C14	C13	120.6(3)
C47	C48	C53	119.4(3)	C23	C22	C21	121.2(4)
C49	C48	C53	117.3(3)	C34	C33	C32	120.9(4)
C49	C48	C47	123.2(3)	C25	C26	C27	122.5(4)
C17	C12	N1	116.6(3)	C6	C7	C8	120.6(4)

C13	C12	N1	124.4(3)	C33	C34	C35	120.2(4)
C13	C12	C17	118.9(3)	C7	C6	C5	120.2(3)
C10	C11	N1	127.6(3)	C22	C23	C24	119.3(4)
C3	C2	C1	121.0(3)	C63S	C58S	C59S	116.7(4)
C4	C9	C10	118.9(3)	C57S	C58S	C59S	121.5(5)
C8	C9	C10	124.2(3)	C57S	C58S	C63S	121.8(4)
C8	C9	C4	116.8(3)	C60S	C59S	C58S	122.7(5)
C15	C16	C17	119.2(3)	C62S	C63S	C58S	121.6(4)
C3	C4	C9	119.2(3)	C61S	C62S	C63S	120.1(5)
C5	C4	C9	119.9(3)	C61S	C60S	C59S	119.4(5)
C5	C4	C3	120.9(3)	C60S	C61S	C62S	119.4(5)
C25	C20	C19	118.9(3)	C65S	C66S	C67S	122.3(7)
C21	C20	C19	123.4(3)	C65S <sup>1</sup>	C67S	C66S	119.3(7)
C21	C20	C25	117.7(3)	C64S	C65S	C66S	122.9(11)
C26	C27	C28	121.1(4)	C67S <sup>1</sup>	C65S	C66S	118.4(8)
C38	C29	O3	122.9(3)	C67S <sup>1</sup>	C65S	C64S	118.7(12)
C30	C29	O3	117.9(3)				

<sup>1</sup>-1-X,2-Y,-Z

**Crystallographic Table 65** Hydrogen Atom Coordinates ( $\text{\AA}\times 10^4$ ) and Isotropic Displacement Parameters ( $\text{\AA}^2\times 10^3$ ) for **Th[L<sup>VII</sup>]<sub>2</sub>**.

Atom	x	y	z	U(eq)
H11	-3340(3)	6285(2)	2538(2)	23.9(10)
H2	-396(3)	5838(2)	2(2)	29.6(10)
H16	-2350(3)	3997(3)	4690(2)	29.4(10)
H27	64(3)	1855(3)	601(2)	41.8(12)
H13	-3450(3)	6730(3)	3934(2)	32.2(10)
H31	-936(3)	7166(3)	6550(2)	38.1(12)
H41	47(3)	8500(3)	2347(2)	31.4(10)
H3	-1580(3)	6706(2)	-587(2)	33.6(11)
H39	171(3)	8264(3)	3563(2)	26.9(10)
H50	6578(3)	4695(2)	364(2)	30.8(10)
H8	-4218(3)	7231(2)	2121(2)	35.2(11)
H49	4799(3)	5224(2)	848(2)	28.3(10)
H54	4796(3)	2727(3)	2707(2)	37.2(11)
H51	7470(3)	3538(3)	879(2)	35.2(11)
H44	2692(3)	6537(3)	692(2)	31.5(10)
H18	-2285(3)	2971(3)	3406(2)	24.5(10)



H46	3491(3)	5897(2)	1570.9(19)	23.0(9)
H15	-3607(3)	5036(3)	5537(2)	40.7(11)
H52	6489(3)	2843(3)	1819(2)	34.8(11)
H55	2998(3)	3156(3)	3172(2)	33.6(11)
H35	-1770(3)	10401(3)	5330(3)	49.2(13)
H21	-2193(3)	1674(3)	3668(2)	41.7(12)
H30	-319(3)	5886(3)	5514(2)	32.7(11)
H43	2256(3)	7966(3)	393(2)	39.0(11)
H24	-1484(3)	-876(3)	1289(3)	49.1(13)
H36	-1029(3)	9167(3)	4276(2)	40.4(11)
H5	-3326(3)	7600(3)	-563(2)	40.6(12)
H42	911(3)	8945(3)	1214(2)	36.7(11)
H14	-4181(3)	6371(3)	5147(2)	40.5(11)
H22	-2690(3)	84(3)	3648(3)	52.5(13)
H33	-1556(3)	8830(3)	7019(2)	48.3(13)
H26	-549(3)	305(3)	588(2)	47.8(12)
H7	-5405(3)	8039(3)	1442(3)	42.7(12)
H34	-2001(3)	10238(3)	6714(3)	54.5(14)
H6	-4979(3)	8187(3)	85(3)	45.0(12)
H23	-2386(3)	-1192(3)	2452(3)	53.5(13)
H59S	3503(4)	7333(3)	5118(3)	78.3(17)
H63S	5935(4)	9212(4)	4615(3)	77.4(17)
H62S	5091(5)	8947(4)	3262(3)	88.4(19)
H57a	4760(14)	8250(20)	6261(7)	122(3)
H57b	6044(16)	8230(20)	5892(4)	122(3)
H57c	5430(30)	9232(4)	6172(9)	122(3)
H60S	2695(4)	7023(4)	3770(4)	100(2)
H61S	3460(5)	7870(4)	2835(3)	92.7(19)
H66S	-6994(6)	9749(5)	-50(7)	126(3)
H64a	-6840(60)	10850(70)	1510(30)	204(10)
H64b	-6540(80)	9823(10)	1640(40)	204(10)
H64c	-5660(20)	10770(70)	2019(11)	204(10)
H67S	-5963(9)	9348(5)	-1331(6)	133(3)

**Crystallographic Table 66** Atomic Occupancy for  $\text{Th}[\text{L}^{\text{VII}}]_2$ .

<i>Atom</i>	<i>Occupancy</i>	<i>Atom</i>	<i>Occupancy</i>	<i>Atom</i>	<i>Occupancy</i>
C64S	0.500000	H64a	0.500000	H64b	0.500000
H64c	0.500000				

## Refinement model description

Number of restraints - 3, number of constraints - 94.

Details:

### 1. Others

Fixed Sof: C64S(0.5) H64a(0.5) H64b(0.5) H64c(0.5)

**Ce[L<sup>VII</sup>]<sub>2</sub>**

**Crystallographic Table 67** Crystal data and structure refinement for **Ce[L<sup>VII</sup>]<sub>2</sub>**

Empirical formula	C <sub>59</sub> H <sub>36</sub> CeN <sub>4</sub> O <sub>5</sub>
Formula weight	1021.08
Temperature/K	180.45
Crystal system	monoclinic
Space group	P2 <sub>1</sub> /n
a/Å	13.0103(8)
b/Å	13.9521(8)
c/Å	26.1970(15)
α/°	90
β/°	99.6888(12)
γ/°	90
Volume/Å <sup>3</sup>	4687.5(5)
Z	4
ρ <sub>calc</sub> /mg/mm <sup>3</sup>	1.4468
m/mm <sup>-1</sup>	1.028
F(000)	2064.4
Crystal size/mm <sup>3</sup>	0.45 × 0.15 × 0.02
Radiation	Mo Kα (λ = 0.71073)
2θ range for data collection	3.16 to 53.46°
Index ranges	-16 ≤ h ≤ 15, -17 ≤ k ≤ 17, -33 ≤ l ≤ 32
Reflections collected	61172
Independent reflections	9966 [R <sub>int</sub> = 0.0428, R <sub>sigma</sub> = 0.0340]
Data/restraints/parameters	9966/0/621
Goodness-of-fit on F <sup>2</sup>	1.068
Final R indexes [I >= 2σ (I)]	R <sub>1</sub> = 0.0292, wR <sub>2</sub> = 0.0699
Final R indexes [all data]	R <sub>1</sub> = 0.0442, wR <sub>2</sub> = 0.0769
Largest diff. peak/hole / e Å <sup>-3</sup>	0.78/-0.60

**Crystallographic Table 68** Fractional Atomic Coordinates (×10<sup>4</sup>) and Equivalent Isotropic Displacement Parameters (Å<sup>2</sup>×10<sup>3</sup>) for **Ce[L<sup>VII</sup>]<sub>2</sub>**. U<sub>eq</sub> is defined as 1/3 of the trace of the orthogonalised U<sub>ij</sub> tensor.

Atom	x	y	z	U(eq)
Ce1	1318.5(1)	924.77(10)	1757.27(5)	16.96(5)
O1	2153.0(13)	1636.4(12)	2452.6(6)	20.5(4)
O2	218.8(13)	2157.9(13)	1776.9(7)	22.6(4)
N4	472.8(16)	112.9(14)	2439.2(8)	19.3(4)

C39	2988.5(19)	-1063.5(17)	2130.4(10)	19.4(5)
O4	-210.9(14)	285.7(13)	1391.0(7)	25.3(4)
N1	2969.9(16)	1761.5(15)	1562.4(8)	19.7(5)
N2	1130.1(16)	1872.6(15)	927.5(8)	19.3(4)
O3	1949.3(14)	-80.5(12)	1234.8(7)	22.9(4)
N3	2356.2(16)	-437.6(15)	2274.5(8)	18.7(4)
C46	-520.0(19)	3.7(18)	2434.2(10)	21.0(5)
C9	4885(2)	2432.3(17)	2724.8(10)	21.6(5)
C11	3738.4(19)	2143.0(18)	1878.7(10)	21.4(5)
C19	-626(2)	2491.1(18)	912.6(10)	21.4(5)
C53	-3244(2)	260.7(19)	1688.0(12)	29.4(6)
C29	2767(2)	-616.6(18)	1203.3(10)	20.6(5)
C8	5785(2)	2590.0(18)	2500.9(11)	26.0(6)
C20	-1563(2)	2823.2(19)	578.0(11)	25.6(6)
C37	4149.1(19)	-1752.9(17)	1555.7(10)	20.0(5)
C12	2995(2)	1815.7(19)	1021.7(10)	22.2(6)
C40	2174(2)	-483.5(18)	2794.6(10)	20.3(5)
C10	3890.0(19)	2133.1(17)	2432.7(9)	19.0(5)
C45	1183.8(19)	-187.4(18)	2881.2(10)	20.6(5)
C56	-1155(2)	301.1(18)	1506.0(11)	24.7(6)
C47	-1348.4(19)	231.7(18)	2015.1(10)	21.7(5)
C17	2031(2)	1838.1(18)	685.4(10)	21.8(6)
C35	5527(2)	-2890(2)	1874.3(11)	27.7(6)
C42	2694(2)	-761(2)	3709.7(11)	30.6(7)
C18	300.1(19)	2305.4(18)	696.2(10)	21.7(5)
C38	3300.9(19)	-1118.8(17)	1628.3(10)	18.7(5)
C16	1999(2)	1792(2)	151.9(10)	28.5(6)
C32	4439(2)	-1827.3(19)	1058.2(10)	25.4(6)
C52	-4287(2)	219(2)	1780.9(14)	36.5(7)
C43	1721(2)	-462(2)	3797.7(11)	31.4(7)
C34	5788(2)	-2974(2)	1379.2(11)	29.3(6)
C4	4988(2)	2541.8(19)	3272.3(11)	24.6(6)
C1	3072.5(19)	1889.4(17)	2700(1)	19.3(5)
C31	3890(2)	-1274(2)	646.2(11)	32.8(7)
C44	976(2)	-169.2(19)	3387.6(10)	26.5(6)
C36	4729(2)	-2299.6(19)	1959.7(11)	24.4(6)
C48	-2409(2)	231.1(18)	2112.9(11)	25.0(6)
C21	-1670(2)	2843(2)	33.5(11)	34.2(7)

C25	-2421(2)	3140(2)	806.4(12)	32.1(7)
C6	6792(2)	3009(2)	3329.1(12)	32.7(7)
C5	5945(2)	2847(2)	3559.7(11)	31.1(6)
C30	3090(2)	-690(2)	712.2(11)	30.3(7)
C28	-597(2)	2460.2(18)	1452(1)	21.9(6)
C33	5257(2)	-2450(2)	984.5(12)	31.2(7)
C14	3874(2)	1757(2)	282.8(12)	39.6(8)
C27	-1472(2)	2805(2)	1661.4(11)	32.1(7)
C41	2920(2)	-764.7(19)	3211.9(11)	26.4(6)
C54	-3012(2)	320(2)	1178.8(12)	35.0(7)
C3	4123(2)	2301(2)	3516.9(11)	28.8(6)
C51	-4502(2)	171(2)	2272.5(14)	39.6(8)
C15	2917(2)	1754(2)	-46.9(11)	36.6(7)
C7	6715(2)	2858(2)	2797.4(12)	30.1(6)
C50	-3690(2)	174(2)	2691.6(13)	35.6(7)
C23	-3382(3)	3541(3)	-40.3(14)	48.5(9)
C26	-2341(2)	3119(2)	1349.2(12)	37.1(7)
C55	-2020(2)	344(2)	1086.9(12)	32.4(7)
C13	3911(2)	1774(2)	814.6(11)	30.9(7)
C49	-2668(2)	203(2)	2615.4(12)	30.0(6)
C22	-2555(3)	3205(3)	-264.5(13)	45.6(8)
C24	-3325(2)	3495(2)	483.3(14)	42.5(8)
C2	3217(2)	1968.1(19)	3246.4(10)	24.6(6)
O5s	-207(2)	742(2)	-412.4(11)	76.0(9)
C59s	5082(7)	60(5)	4725(3)	164(6)
C58s	6109(7)	503(6)	4711(4)	164(4)
C57s	6480(10)	598(6)	4228(3)	209(6)

**Crystallographic Table 69** Anisotropic Displacement Parameters ( $\text{\AA}^2 \times 10^3$ ) for  $\text{Ce}[\text{L}^{\text{VII}}]_2$ . The Anisotropic displacement factor exponent takes the form: -  $2\pi^2[h^2a^*{}^2U_{11}+2hka^*b^*U_{12}+\dots]$

Atom	$U_{11}$	$U_{22}$	$U_{33}$	$U_{12}$	$U_{13}$	$U_{23}$
Ce1	17.85(8)	19.76(8)	13.02(8)	-0.55(6)	1.86(5)	1.49(6)
O1	19.6(9)	24.5(9)	17.9(9)	-3.0(7)	4.6(7)	-1.2(7)
O2	23.4(9)	27.8(9)	15.6(9)	4.6(8)	0.9(7)	-0.2(8)
N4	21.8(11)	20.3(11)	15.3(11)	-0.6(9)	1.9(9)	2.0(9)
C39	19.0(12)	20.3(13)	18.1(13)	-1.4(10)	1.2(10)	3.4(10)
O4	24.6(10)	30.5(10)	19.8(10)	-5.6(8)	1.0(8)	1.3(8)
N1	20.0(11)	25.3(11)	13.8(11)	1.8(9)	3.1(9)	2.1(9)

N2	20.6(11)	22.5(11)	14.7(11)	-2.4(9)	3.0(9)	1.5(9)
O3	26.0(9)	25.3(9)	17.0(9)	4.6(8)	2.2(8)	0.1(8)
N3	20.1(10)	22.8(11)	13.3(11)	-1.1(9)	2.6(9)	1.0(9)
C46	23.8(13)	20.5(13)	19.3(14)	-1.9(10)	5.9(11)	0.1(10)
C9	22.1(13)	16.9(12)	24.5(14)	2.8(10)	0.1(11)	-0.7(10)
C11	20.6(13)	22.6(13)	21.4(14)	0.6(11)	5.1(11)	2.7(11)
C19	22.1(13)	20.7(13)	20.0(14)	-0.1(10)	-0.4(11)	1.7(10)
C53	23.7(14)	20.2(13)	41.8(18)	-2.1(11)	-2.0(13)	0.1(12)
C29	22.5(13)	20.1(12)	19.3(14)	-3.2(10)	3.9(11)	-0.4(10)
C8	25.6(14)	24.3(14)	27.8(16)	-2.3(11)	3.7(12)	-2.0(12)
C20	23.7(13)	24.0(13)	26.7(15)	-4.7(11)	-2.7(11)	3.0(12)
C37	19.2(12)	20.4(12)	20.6(14)	-4.8(10)	3.5(11)	1.7(11)
C12	24.0(13)	28.3(14)	15.0(13)	-2.0(11)	5.3(11)	3.9(11)
C40	23.7(13)	20.9(13)	15.7(13)	-0.7(10)	2.1(11)	1.4(10)
C10	20.7(12)	19.2(12)	16.4(13)	1.7(10)	1.2(10)	-1.6(10)
C45	22.5(13)	20.3(12)	18.6(14)	-1.2(10)	2.1(11)	2.7(10)
C56	22.4(13)	21.5(13)	28.2(15)	-5.5(11)	-1.2(11)	1.3(11)
C47	20.9(13)	18.1(12)	24.9(15)	-4.1(10)	0.3(11)	-0.2(11)
C17	26.2(14)	23.6(13)	16.5(13)	-1.3(11)	6.0(11)	3.8(11)
C35	22.2(13)	28.7(14)	31.4(16)	1.3(11)	2.4(12)	4.9(12)
C42	37.6(16)	35.7(16)	15.5(14)	6.4(13)	-4.3(12)	1.6(12)
C18	25.7(13)	22.9(13)	15.6(13)	-3.1(11)	1.4(11)	3.4(11)
C38	19.6(12)	17.6(12)	19.0(13)	-2.9(10)	3.6(10)	0.2(10)
C16	30.1(15)	37.6(16)	17.1(14)	-0.5(12)	2.2(12)	3.0(12)
C32	26.5(14)	28.3(14)	23.0(15)	-0.5(11)	8.9(12)	2.0(12)
C52	22.4(14)	24.4(14)	59(2)	-2.3(12)	-2.2(14)	-1.0(14)
C43	42.1(17)	37.2(16)	15.5(14)	5.4(14)	6.4(13)	3.2(12)
C34	23.1(14)	30.3(15)	36.5(17)	4.1(12)	11.3(13)	1.7(13)
C4	24.0(13)	24.7(14)	22.9(15)	3.5(11)	-2.1(11)	-1.5(11)
C1	21.0(13)	17.3(12)	18.6(13)	2.2(10)	0.4(10)	-0.6(10)
C31	38.7(17)	41.9(16)	20.4(15)	6.8(14)	13.1(13)	4.6(13)
C44	29.5(15)	31.3(15)	19.9(14)	3.3(12)	7.7(12)	1.7(12)
C36	22.1(13)	28.6(14)	23.1(15)	0.1(11)	5.5(11)	1.3(12)
C48	20.9(13)	17.3(12)	35.7(16)	-4.7(10)	1.5(12)	0.4(11)
C21	32.5(16)	39.5(17)	28.1(16)	-3.8(13)	-2.2(13)	4.9(14)
C25	27.1(15)	32.1(15)	35.2(18)	2.8(12)	-0.4(13)	3.1(13)
C6	23.9(14)	27.2(15)	41.6(19)	-0.7(12)	-10.3(13)	-2.9(13)
C5	30.0(15)	32.4(15)	26.6(16)	0.4(12)	-7.2(12)	-3.0(13)

C30	39.3(17)	33.9(15)	18.5(15)	6.5(13)	7.0(13)	7.5(12)
C28	23.5(13)	20.7(13)	20.8(14)	1(1)	1.6(11)	1.0(11)
C33	29.8(15)	38.1(16)	29.2(16)	2.5(13)	15.0(13)	1.0(13)
C14	31.2(16)	65(2)	25.7(16)	4.6(15)	14.2(13)	11.5(15)
C27	31.9(15)	39.7(16)	25.5(16)	8.9(13)	6.9(13)	0.4(13)
C41	26.6(14)	30.1(15)	21.2(15)	4.7(11)	0.9(12)	1.2(11)
C54	26.0(15)	32.6(16)	40.7(19)	-4.9(12)	-11.4(13)	3.5(14)
C3	32.8(15)	36.7(16)	15.9(14)	4.1(13)	1.3(12)	-0.0(12)
C51	22.6(15)	29.0(16)	69(2)	-3.8(12)	12.5(16)	-6.5(16)
C15	39.1(17)	58(2)	15.1(15)	3.0(15)	10.2(13)	4.8(14)
C7	22.2(14)	27.8(14)	39.5(18)	-1.2(12)	3.3(13)	-1.9(13)
C50	30.0(16)	28.8(15)	51(2)	-1.9(13)	16.0(15)	-3.3(14)
C23	33.6(18)	58(2)	46(2)	7.3(16)	-16.1(16)	11.5(18)
C26	28.0(15)	43.4(18)	40.6(19)	12.2(13)	8.4(14)	-0.1(15)
C55	33.2(16)	34.5(16)	26.3(16)	-7.5(13)	-4.4(13)	4.7(13)
C13	26.0(15)	45.2(17)	21.9(15)	1.2(13)	4.8(12)	5.1(13)
C49	25.1(14)	27.4(15)	37.5(18)	-3.3(12)	5.2(13)	-2.3(13)
C22	40.5(19)	60(2)	31.2(19)	0.7(16)	-10.1(15)	10.3(16)
C24	26.4(16)	48(2)	50(2)	9.8(14)	-2.4(15)	5.6(17)
C2	24.3(13)	30.9(15)	18.8(14)	1.8(12)	4.4(11)	1.1(11)
O5s	51.6(16)	114(3)	55.2(18)	-22.1(16)	-12.2(14)	2.7(17)
C59s	118(5)	76(4)	260(13)	55(4)	-82(8)	-97(8)
C58s	134(6)	108(6)	225(10)	50(5)	-43(7)	-74(7)
C57s	421(18)	101(5)	94(5)	148(8)	8(8)	9(4)

**Crystallographic Table 70** Bond Lengths for Ce[L<sup>VII</sup>]<sub>2</sub>.

Atom	Atom	Length/Å	Atom	Atom	Length/Å
Ce1	O1	2.1948(17)	C12	C13	1.391(4)
Ce1	O2	2.2437(17)	C40	C45	1.407(3)
Ce1	N4	2.519(2)	C40	C41	1.391(4)
Ce1	O4	2.2433(17)	C10	C1	1.410(3)
Ce1	N1	2.571(2)	C45	C44	1.398(4)
Ce1	N2	2.521(2)	C56	C47	1.402(4)
Ce1	O3	2.2117(17)	C56	C55	1.435(4)
Ce1	N3	2.580(2)	C47	C48	1.446(3)
Ce1	C56	3.291(3)	C17	C16	1.393(4)
Ce1	C28	3.281(3)	C35	C34	1.400(4)
O1	C1	1.309(3)	C35	C36	1.374(4)

O2	C28	1.313(3)	C42	C43	1.388(4)
N4	C46	1.299(3)	C42	C41	1.384(4)
N4	C45	1.418(3)	C16	C15	1.381(4)
C39	N3	1.299(3)	C32	C31	1.418(4)
C39	C38	1.443(3)	C32	C33	1.413(4)
O4	C56	1.313(3)	C52	C51	1.365(5)
N1	C11	1.300(3)	C43	C44	1.383(4)
N1	C12	1.424(3)	C34	C33	1.356(4)
N2	C17	1.424(3)	C4	C5	1.408(4)
N2	C18	1.295(3)	C4	C3	1.426(4)
O3	C29	1.315(3)	C1	C2	1.416(4)
N3	C40	1.423(3)	C31	C30	1.355(4)
C46	C47	1.439(4)	C48	C49	1.413(4)
C9	C8	1.413(4)	C21	C22	1.374(4)
C9	C10	1.450(3)	C25	C26	1.409(4)
C9	C4	1.426(4)	C25	C24	1.418(4)
C11	C10	1.431(3)	C6	C5	1.362(4)
C19	C20	1.452(4)	C6	C7	1.396(4)
C19	C18	1.439(4)	C28	C27	1.428(4)
C19	C28	1.408(4)	C14	C15	1.391(4)
C53	C52	1.418(4)	C14	C13	1.386(4)
C53	C48	1.419(4)	C27	C26	1.352(4)
C53	C54	1.419(4)	C54	C55	1.353(4)
C29	C38	1.397(4)	C3	C2	1.351(4)
C29	C30	1.423(4)	C51	C50	1.390(4)
C8	C7	1.374(4)	C50	C49	1.378(4)
C20	C21	1.410(4)	C23	C22	1.391(5)
C20	C25	1.423(4)	C23	C24	1.363(5)
C37	C38	1.452(3)	C59s	C59s <sup>1</sup>	1.503(19)
C37	C32	1.420(4)	C59s	C58s	1.479(14)
C37	C36	1.415(4)	C58s	C57s	1.435(13)
C12	C17	1.407(4)			

<sup>1</sup>1-X,-Y,1-Z

**Crystallographic Table 71 Bond Angles for Ce[L<sup>VII</sup>]<sub>2</sub>.**

Atom	Atom	Atom	Angle/°	Atom	Atom	Atom	Angle/°
O2	Ce1	O1	82.09(6)	C36	C37	C32	117.2(2)



N4	Ce1	O1	80.15(6)	C17	C12	N1	117.2(2)
N4	Ce1	O2	88.41(6)	C13	C12	N1	123.4(2)
O4	Ce1	O1	144.50(6)	C13	C12	C17	119.3(2)
O4	Ce1	O2	77.96(7)	C45	C40	N3	116.5(2)
O4	Ce1	N4	70.29(6)	C41	C40	N3	123.9(2)
N1	Ce1	O1	69.28(6)	C41	C40	C45	119.5(2)
N1	Ce1	O2	102.34(6)	C11	C10	C9	119.4(2)
N1	Ce1	N4	145.52(7)	C1	C10	C9	119.2(2)
N1	Ce1	O4	143.74(6)	C1	C10	C11	121.3(2)
N2	Ce1	O1	116.18(6)	C40	C45	N4	116.3(2)
N2	Ce1	O2	69.37(6)	C44	C45	N4	124.4(2)
N2	Ce1	N4	148.94(7)	C44	C45	C40	119.2(2)
N2	Ce1	O4	83.64(6)	O4	C56	Ce1	29.48(11)
N2	Ce1	N1	63.50(6)	C47	C56	Ce1	98.86(16)
O3	Ce1	O1	128.11(6)	C47	C56	O4	122.8(2)
O3	Ce1	O2	143.59(6)	C55	C56	Ce1	139.15(19)
O3	Ce1	N4	113.92(7)	C55	C56	O4	117.9(2)
O3	Ce1	O4	83.00(7)	C55	C56	C47	119.2(2)
O3	Ce1	N1	75.85(7)	C56	C47	C46	120.7(2)
O3	Ce1	N2	77.96(7)	C48	C47	C46	118.7(2)
N3	Ce1	O1	75.83(6)	C48	C47	C56	119.9(2)
N3	Ce1	O2	146.33(6)	C12	C17	N2	115.8(2)
N3	Ce1	N4	63.17(6)	C16	C17	N2	124.2(2)
N3	Ce1	O4	106.25(6)	C16	C17	C12	120.0(2)
N3	Ce1	N1	93.32(6)	C36	C35	C34	120.6(3)
N3	Ce1	N2	143.68(6)	C41	C42	C43	120.1(3)
N3	Ce1	O3	69.02(6)	C19	C18	N2	125.9(2)
C56	Ce1	O1	128.03(6)	C29	C38	C39	121.4(2)
C56	Ce1	O2	66.52(6)	C37	C38	C39	119.3(2)
C56	Ce1	N4	59.60(7)	C37	C38	C29	119.2(2)
C56	Ce1	O4	16.74(7)	C15	C16	C17	119.9(3)
C56	Ce1	N1	154.42(7)	C31	C32	C37	118.8(2)
C56	Ce1	N2	90.93(7)	C33	C32	C37	119.5(2)
C56	Ce1	O3	99.25(7)	C33	C32	C31	121.7(2)
C56	Ce1	N3	108.54(6)	C51	C52	C53	121.2(3)
C28	Ce1	O1	98.99(6)	C44	C43	C42	120.0(3)
C28	Ce1	O2	17.06(6)	C33	C34	C35	119.3(3)
C28	Ce1	N4	93.55(6)	C5	C4	C9	119.7(2)

C28	Ce1	O4	64.70(6)	C3	C4	C9	118.6(2)
C28	Ce1	N1	106.32(6)	C3	C4	C5	121.7(3)
C28	Ce1	N2	59.18(6)	C10	C1	O1	121.5(2)
C28	Ce1	O3	127.50(6)	C2	C1	O1	118.4(2)
C28	Ce1	N3	156.60(6)	C2	C1	C10	120.0(2)
C28	Ce1	C56	56.43(6)	C30	C31	C32	121.9(3)
C1	O1	Ce1	144.66(16)	C43	C44	C45	120.6(2)
C28	O2	Ce1	132.87(15)	C35	C36	C37	121.6(3)
C46	N4	Ce1	126.73(17)	C47	C48	C53	119.3(3)
C45	N4	Ce1	114.15(15)	C49	C48	C53	117.4(2)
C45	N4	C46	119.0(2)	C49	C48	C47	123.3(2)
C38	C39	N3	126.2(2)	C22	C21	C20	120.9(3)
C56	O4	Ce1	133.78(17)	C26	C25	C20	119.2(3)
C11	N1	Ce1	129.64(16)	C24	C25	C20	119.2(3)
C12	N1	Ce1	112.42(15)	C24	C25	C26	121.5(3)
C12	N1	C11	117.9(2)	C7	C6	C5	119.3(3)
C17	N2	Ce1	113.49(15)	C6	C5	C4	121.5(3)
C18	N2	Ce1	126.90(16)	C31	C30	C29	120.6(3)
C18	N2	C17	119.4(2)	O2	C28	Ce1	30.07(11)
C29	O3	Ce1	142.02(16)	C19	C28	Ce1	98.96(16)
C39	N3	Ce1	130.07(17)	C19	C28	O2	122.9(2)
C40	N3	Ce1	112.28(15)	C27	C28	Ce1	138.44(18)
C40	N3	C39	117.6(2)	C27	C28	O2	118.0(2)
C47	C46	N4	126.7(2)	C27	C28	C19	119.1(2)
C10	C9	C8	123.7(2)	C34	C33	C32	121.8(3)
C4	C9	C8	117.2(2)	C13	C14	C15	120.0(3)
C4	C9	C10	119.1(2)	C26	C27	C28	121.1(3)
C10	C11	N1	127.0(2)	C42	C41	C40	120.5(3)
C18	C19	C20	119.5(2)	C55	C54	C53	122.0(3)
C28	C19	C20	119.6(2)	C2	C3	C4	122.0(2)
C28	C19	C18	120.5(2)	C50	C51	C52	119.7(3)
C48	C53	C52	119.5(3)	C14	C15	C16	120.4(3)
C54	C53	C52	121.7(3)	C6	C7	C8	120.9(3)
C54	C53	C48	118.9(3)	C49	C50	C51	120.6(3)
C38	C29	O3	122.3(2)	C24	C23	C22	119.6(3)
C30	C29	O3	117.6(2)	C27	C26	C25	122.0(3)
C30	C29	C38	120.1(2)	C54	C55	C56	120.8(3)
C7	C8	C9	121.3(3)	C14	C13	C12	120.4(3)

C21	C20	C19	123.2(3)	C50	C49	C48	121.5(3)
C25	C20	C19	118.9(2)	C23	C22	C21	121.2(3)
C25	C20	C21	117.9(3)	C23	C24	C25	121.1(3)
C32	C37	C38	119.3(2)	C3	C2	C1	120.8(2)
C36	C37	C38	123.5(2)	C57s	C58s	C59s	120.0(9)

**Crystallographic Table 72** Hydrogen Atom Coordinates ( $\text{\AA}\times 10^4$ ) and Isotropic Displacement Parameters ( $\text{\AA}^2\times 10^3$ ) for  $\text{Ce}[\text{L}^{\text{VII}}]_2$ .

Atom	x	y	z	U(eq)
H39	3272.5(19)	-1529.1(17)	2379.3(10)	23.2(6)
H46	-720.0(19)	-253.2(18)	2738.7(10)	25.2(6)
H11	4255.1(19)	2462.9(18)	1725.6(10)	25.6(7)
H8	5748(2)	2509.1(18)	2138.2(11)	31.2(7)
H35	5906(2)	-3245(2)	2153.8(11)	33.2(7)
H42	3205(2)	-964(2)	3991.6(11)	36.7(8)
H18	303.0(19)	2519.8(18)	352.3(10)	26.0(7)
H16	1348(2)	1787(2)	-75.1(10)	34.2(7)
H52	-4845(2)	225(2)	1495.9(14)	43.8(9)
H43	1568(2)	-459(2)	4139.7(11)	37.7(8)
H34	6331(2)	-3393(2)	1320.2(11)	35.1(8)
H31	4089(2)	-1314(2)	314.1(11)	39.3(8)
H44	316(2)	46.6(19)	3450.5(10)	31.8(7)
H36	4561(2)	-2257.2(19)	2298.2(11)	29.3(7)
H21	-1123(2)	2604(2)	-129.4(11)	41.1(8)
H6	7429(2)	3222(2)	3528.3(12)	39.2(8)
H5	6001(2)	2942(2)	3922.4(11)	37.3(8)
H30	2742(2)	-328(2)	428.1(11)	36.4(8)
H33	5441(2)	-2504(2)	649.7(12)	37.4(8)
H14	4502(2)	1746(2)	143.5(12)	47.5(9)
H27	-1443(2)	2814(2)	2026.2(11)	38.6(8)
H41	3591(2)	-960.8(19)	3154.9(11)	31.6(7)
H54	-3570(2)	344(2)	894.0(12)	42.1(8)
H3	4185(2)	2378(2)	3881.2(11)	34.5(7)
H51	-5204(2)	135(2)	2327.9(14)	47.5(9)
H15	2894(2)	1726(2)	-411.0(11)	43.9(9)
H7	7313(2)	2942(2)	2638.1(12)	36.1(8)
H50	-3841(2)	155(2)	3033.9(13)	42.8(9)
H23	-3983(3)	3800(3)	-251.0(14)	58.2(11)

H26	-2914(2)	3333(2)	1500.6(12)	44.5(9)
H55	-1894(2)	390(2)	740.9(12)	38.9(8)
H13	4565(2)	1758(2)	1038.9(11)	37.1(8)
H49	-2125(2)	204(2)	2907.4(12)	36.0(8)
H22	-2603(3)	3226(3)	-630.3(13)	54.8(10)
H24	-3901(2)	3705(2)	634.3(14)	51(1)
H2	2670(2)	1784.3(19)	3425(1)	29.5(7)

### Refinement model description

Number of restraints - 0, number of constraints - 72.

#### Details:

##### 1. Fixed Uiso

At 1.2 times of:

All C(H) groups

##### 2.a Aromatic/amide H refined with riding coordinates:

C39(H39), C46(H46), C11(H11), C8(H8), C35(H35), C42(H42), C18(H18), C16(H16), C52(H52), C43(H43), C34(H34), C31(H31), C44(H44), C36(H36), C21(H21), C6(H6), C5(H5), C30(H30), C33(H33), C14(H14), C27(H27), C41(H41), C54(H54), C3(H3), C51(H51), C15(H15), C7(H7), C50(H50), C23(H23), C26(H26), C55(H55), C13(H13), C49(H49), C22(H22), C24(H24), C2(H2)

**Nd<sub>2</sub>[L<sup>VII</sup>]<sub>3</sub>**

**Crystallographic Table 73** Crystal data and structure refinement for **Nd<sub>2</sub>[L<sup>VII</sup>]<sub>3</sub>**

Empirical formula	C <sub>88</sub> H <sub>66</sub> Cl <sub>4</sub> N <sub>6</sub> Nd <sub>2</sub> O <sub>8</sub>
Formula weight	1765.82
Temperature/K	181.65
Crystal system	monoclinic
Space group	P2 <sub>1</sub> /n
a/Å	10.2688(4)
b/Å	42.4193(19)
c/Å	17.3908(8)
α/°	90
β/°	91.5390(11)
γ/°	90
Volume/Å <sup>3</sup>	7572.6(6)
Z	4
ρ <sub>calc</sub> /mg/mm <sup>3</sup>	1.5487
m/mm <sup>-1</sup>	1.560
F(000)	3555.3
Crystal size/mm <sup>3</sup>	0.2 × 0.1 × 0.02
Radiation	Mo Kα (λ = 0.71073)
2θ range for data collection	1.92 to 42.08°
Index ranges	-10 ≤ h ≤ 10, -42 ≤ k ≤ 42, -17 ≤ l ≤ 17
Reflections collected	56265
Independent reflections	8193 [R <sub>int</sub> = 0.0678, R <sub>sigma</sub> = 0.0459]
Data/restraints/parameters	8193/6/981
Goodness-of-fit on F <sup>2</sup>	1.079
Final R indexes [I ≥ 2σ (I)]	R <sub>1</sub> = 0.0758, wR <sub>2</sub> = 0.1625
Final R indexes [all data]	R <sub>1</sub> = 0.0852, wR <sub>2</sub> = 0.1704
Largest diff. peak/hole / e Å <sup>-3</sup>	1.53/-1.37

**Crystallographic Table 74** Fractional Atomic Coordinates (×10<sup>4</sup>) and Equivalent Isotropic Displacement Parameters (Å<sup>2</sup>×10<sup>3</sup>) for **Nd<sub>2</sub>[L<sup>VII</sup>]<sub>3</sub>**. U<sub>eq</sub> is defined as 1/3 of the trace of the orthogonalised U<sub>ij</sub> tensor.

Atom	x	y	z	U(eq)
Nd1	1397.9(6)	1180.33(16)	3016.0(4)	37.3(2)
Nd2	4770.0(6)	1299.12(15)	1934.3(4)	35.0(2)
O3	2761(7)	984.1(18)	1936(4)	35.1(19)

O8	5712(8)	902.7(18)	1236(5)	42(2)
N9	6396(8)	1528(2)	968(5)	32(2)
O10	3328(7)	1516.2(19)	2893(4)	40(2)
C11	30(10)	1346(3)	1236(6)	29(3)
O12	594(8)	1659(2)	3457(5)	43(2)
N14	-461(9)	929(2)	2138(5)	33(2)
C16	2545(10)	758(3)	1431(7)	32(3)
N18	6597(8)	1658(2)	2514(5)	32(2)
N19	3811(9)	1853(2)	1500(6)	34(2)
O20	5687(7)	1075.4(19)	3076(5)	43(2)
O21	400(8)	767(2)	3596(5)	49(2)
C22	3683(10)	1787(3)	3213(7)	34(3)
C23	5931(10)	864(3)	504(8)	38(3)
C24	6368(12)	1145(3)	3703(7)	41(3)
C25	7244(11)	1655(3)	3162(7)	35(3)
C26	6883(10)	1903(3)	2002(7)	34(3)
N27	395(8)	1525(2)	1890(5)	29(2)
C28	-399(10)	1036(3)	1358(7)	33(3)
N29	3482(8)	1337(2)	624(5)	30(2)
C30	7066(10)	1429(3)	3776(6)	32(3)
C31	2892(10)	1105(3)	295(6)	29(3)
C32	-1372(10)	731(3)	2290(6)	31(3)
C33	7190(11)	2213(3)	2219(8)	44(3)
C34	6353(10)	1110(3)	16(7)	34(3)
C37	-573(12)	568(3)	3592(7)	43(3)
C38	3611(10)	2077(3)	1968(7)	38(3)
C39	3839(11)	2064(3)	2795(7)	36(3)
C40	3465(10)	1637(3)	229(7)	36(3)
C41	3588(10)	1904(3)	699(7)	35(3)
C42	-3628(11)	307(3)	2481(7)	37(3)
C43	7754(12)	1275(3)	5106(8)	48(3)
C44	6799(10)	1841(3)	1197(7)	34(3)
C45	-517(10)	945(3)	0(6)	33(3)
C46	-689(12)	358(3)	4244(7)	45(3)
C47	7133(13)	981(3)	4967(7)	50(4)
C48	8357(13)	1334(4)	5835(8)	56(4)
C49	6593(11)	1044(3)	-779(6)	37(3)
C50	1596(12)	10(3)	-134(8)	48(3)

C51	2601(12)	564(3)	-692(7)	43(3)
C52	7707(11)	1505(3)	4518(6)	36(3)
C53	-671(10)	839(3)	736(6)	30(3)
C54	-1507(11)	551(3)	2992(7)	36(3)
C55	7262(12)	2386(3)	917(8)	47(3)
C56	3359(11)	1668(3)	-560(7)	37(3)
C58	2686(10)	795(3)	633(7)	33(3)
C59	6039(12)	488(3)	-562(8)	43(3)
C60	6490(12)	917(3)	4301(7)	50(4)
C61	6991(11)	2083(3)	664(7)	43(3)
C62	3493(12)	2199(3)	345(7)	42(3)
C63	8911(13)	1848(3)	5416(7)	54(4)
C64	258(10)	1823(3)	1869(7)	37(3)
C65	-98(10)	1252(3)	-119(7)	35(3)
C66	1922(11)	253(3)	396(7)	40(3)
C67	192(11)	1450(3)	493(7)	39(3)
C68	2276(12)	323(3)	-1184(7)	41(3)
C69	7377(13)	2449(3)	1701(8)	53(4)
C70	6448(12)	728(3)	-1049(7)	43(3)
C71	853(13)	2608(3)	2861(9)	57(4)
C72	654(11)	1955(3)	3242(8)	43(3)
C73	4159(11)	2352(3)	3196(7)	42(3)
C74	-4595(12)	90(3)	2550(8)	46(3)
C75	4318(12)	2354(3)	3997(8)	50(4)
C76	3318(13)	2229(3)	-433(8)	52(4)
C77	4354(12)	2642(3)	2803(8)	49(4)
C78	-2658(12)	119(3)	3684(8)	49(4)
C80	1775(11)	220(3)	1200(7)	38(3)
C81	-2589(11)	327(3)	3031(7)	40(3)
C82	6771(13)	656(3)	-1814(7)	49(3)
C83	797(11)	2494(3)	1515(9)	49(4)
C84	4146(12)	2065(4)	4399(8)	62(4)
C86	-4614(13)	-122(3)	3158(9)	55(4)
C87	-1674(12)	151(3)	4279(7)	48(3)
C88	5788(12)	552(3)	194(7)	44(3)
C89	-3664(12)	-107(3)	3723(9)	53(4)
C90	8324(12)	1797(3)	4693(8)	48(3)
C92	7314(13)	1191(3)	-2056(7)	53(4)

C93	2395(10)	540(3)	106(7)	33(3)
C95	1773(12)	42(3)	-912(7)	41(3)
C96	2062(11)	460(3)	1695(7)	35(3)
C97	807(12)	2198(4)	3823(8)	59(4)
C99	983(14)	2806(3)	1330(10)	68(4)
C101	574(11)	2049(3)	2460(8)	41(3)
C103	4608(15)	2916(4)	3204(10)	73(5)
C104	8943(14)	1615(4)	5977(8)	62(4)
C108	706(11)	2379(3)	2276(8)	47(4)
C109	7192(15)	885(3)	-2312(8)	62(4)
C111	7025(13)	1277(3)	-1304(7)	50(4)
C113	3845(11)	1785(3)	4031(7)	45(3)
C120	1029(14)	3023(4)	1928(12)	72(5)
C122	4605(15)	2643(4)	4386(9)	70(5)
C132	983(15)	2936(4)	2671(12)	76(5)
Cl4	-1658(4)	172.7(11)	-3334(3)	89.3(14)
Cl6	488(5)	610.1(13)	-3346(4)	123(2)
Cl13	9567(7)	3928(2)	1334(4)	164(3)
Cl35	7682(11)	3689(3)	2441(5)	226(5)
O1	3316(8)	861(2)	3626(5)	53(2)
O2	1481(9)	1283(2)	4504(4)	56(3)
C3	6729(11)	1413(3)	313(7)	43(3)
C4	3252(13)	1961(3)	-887(8)	52(4)
C5	3355(13)	557(3)	3953(9)	61(4)
C6	896(13)	2508(4)	3643(10)	61(4)
C7	-189(14)	291(4)	-2892(8)	65(4)
C8	1365(18)	1076(4)	5146(8)	88(6)
C10	8840(20)	3950(8)	2390(20)	232(19)
C1	4731(18)	2917(4)	4006(10)	83(5)

**Crystallographic Table 75** Anisotropic Displacement Parameters ( $\text{\AA}^2 \times 10^3$ ) for  $\text{Nd}_2[\text{L}^{\text{VII}}]_3$ . The Anisotropic displacement factor exponent takes the form: -  $2\pi^2[h^2a^2U_{11}+2hka*b*U_{12}+\dots]$

Atom	$U_{11}$	$U_{22}$	$U_{33}$	$U_{12}$	$U_{13}$	$U_{23}$
Nd1	31.5(4)	46.1(5)	34.3(4)	-3.1(3)	-0.6(3)	-0.2(3)
Nd2	28.7(4)	40.9(4)	35.2(4)	-0.3(3)	-0.4(3)	-0.1(3)
O3	36(5)	35(5)	34(5)	-7(4)	-3(4)	-3(4)
O8	45(5)	41(5)	39(6)	-2(4)	-4(4)	17(4)
N9	27(5)	35(6)	34(6)	-3(4)	-5(4)	10(5)



O10	40(5)	42(5)	39(5)	-5(4)	-4(4)	1(4)
C11	34(7)	28(7)	25(7)	4(5)	0(5)	-3(6)
O12	43(5)	49(6)	38(5)	-11(4)	4(4)	-3(4)
N14	33(6)	28(5)	37(6)	-5(5)	-9(4)	4(5)
C16	20(6)	23(7)	52(9)	0(5)	-3(5)	1(6)
N18	25(5)	35(6)	35(6)	-7(4)	3(5)	7(5)
N19	30(6)	27(6)	45(7)	10(4)	-10(5)	0(5)
O20	29(5)	50(5)	51(6)	-5(4)	0(4)	-3(4)
O21	33(5)	74(6)	38(5)	-12(5)	-11(4)	11(5)
C22	19(6)	51(9)	34(8)	3(6)	3(5)	-8(7)
C23	18(6)	40(8)	56(9)	2(5)	-16(6)	9(7)
C24	42(8)	34(8)	47(8)	7(6)	2(7)	-10(6)
C25	22(6)	48(8)	35(7)	6(5)	-2(6)	9(6)
C26	26(6)	39(8)	37(8)	1(5)	3(5)	0(6)
N27	30(5)	21(6)	36(6)	0(4)	-9(4)	3(4)
C28	27(6)	33(7)	38(8)	4(5)	5(5)	6(6)
N29	28(5)	44(6)	17(5)	-2(5)	-3(4)	-1(5)
C30	23(6)	50(8)	23(7)	13(6)	1(5)	-1(6)
C31	22(6)	48(8)	17(6)	8(6)	-1(5)	-1(6)
C32	25(6)	35(7)	32(7)	-4(6)	-11(5)	-6(6)
C33	30(7)	55(9)	48(8)	-5(6)	-6(6)	6(7)
C34	24(6)	41(8)	37(8)	12(5)	-8(5)	-7(6)
C37	38(8)	57(9)	34(8)	8(7)	3(6)	9(7)
C38	24(7)	36(8)	54(9)	-13(6)	3(6)	7(7)
C39	33(7)	35(8)	39(8)	4(6)	2(6)	-12(6)
C40	26(7)	36(8)	44(8)	1(5)	-1(5)	5(6)
C41	22(6)	36(8)	46(8)	-5(5)	-7(5)	-5(6)
C42	38(7)	41(8)	33(7)	-3(6)	1(6)	5(6)
C43	40(8)	48(9)	55(9)	1(7)	-5(7)	-1(7)
C44	19(6)	44(8)	38(8)	11(5)	-5(5)	-8(6)
C45	35(7)	36(8)	29(7)	2(6)	-5(5)	-8(6)
C46	31(7)	64(9)	39(8)	3(7)	-1(6)	19(7)
C47	57(9)	62(10)	32(8)	15(7)	3(7)	19(7)
C48	60(9)	73(11)	35(8)	-3(8)	-9(7)	3(7)
C49	29(7)	54(9)	27(7)	11(6)	-9(5)	3(6)
C50	45(8)	33(8)	66(10)	-11(6)	3(7)	1(7)
C51	53(8)	34(8)	42(8)	-8(6)	-7(6)	-6(6)
C52	36(7)	46(8)	28(7)	15(6)	9(5)	9(6)

C53	31(7)	33(7)	27(7)	-3(5)	0(5)	4(6)
C54	32(7)	39(7)	37(7)	0(6)	-2(6)	5(6)
C55	43(8)	32(8)	67(10)	-7(6)	-5(7)	12(7)
C56	44(8)	32(7)	35(8)	-2(6)	-6(6)	-4(6)
C58	24(6)	37(8)	38(8)	1(5)	1(5)	-7(6)
C59	48(8)	24(7)	57(9)	-1(6)	-2(7)	-7(6)
C60	51(8)	56(9)	44(9)	-8(7)	-6(7)	20(7)
C61	40(7)	55(9)	33(7)	0(6)	0(6)	21(7)
C62	49(8)	27(7)	49(9)	1(6)	5(6)	0(6)
C63	61(9)	67(10)	34(8)	-4(7)	-3(7)	-9(7)
C64	18(6)	53(9)	41(8)	-14(6)	0(5)	-5(7)
C65	21(6)	52(8)	31(7)	7(6)	1(5)	7(6)
C66	27(7)	34(8)	57(9)	-2(6)	-12(6)	5(7)
C67	28(7)	36(7)	54(9)	-5(5)	-3(6)	-1(7)
C68	51(8)	38(8)	33(7)	-6(6)	-2(6)	-4(6)
C69	57(9)	51(9)	51(9)	-13(7)	-3(7)	-3(8)
C70	41(8)	51(9)	37(8)	12(6)	-4(6)	-6(7)
C71	47(9)	42(9)	83(12)	-14(7)	9(8)	-17(8)
C72	22(7)	53(9)	54(9)	2(6)	0(6)	-9(7)
C73	28(7)	50(9)	47(9)	-2(6)	-3(6)	-14(7)
C74	34(8)	51(8)	52(9)	-5(7)	-9(6)	13(7)
C75	34(8)	65(10)	51(9)	-16(7)	1(6)	-7(8)
C76	59(9)	49(9)	46(9)	-8(7)	-5(7)	12(7)
C77	53(8)	42(8)	52(9)	-9(7)	2(7)	-21(7)
C78	37(8)	50(8)	60(9)	9(7)	3(7)	16(7)
C80	38(7)	38(8)	39(8)	-6(6)	8(6)	0(6)
C81	27(7)	43(8)	50(8)	6(6)	4(6)	5(6)
C82	57(9)	39(8)	49(9)	6(6)	-4(7)	-11(7)
C83	32(7)	42(9)	74(11)	-3(6)	-1(7)	-3(7)
C84	37(8)	103(13)	45(9)	1(8)	7(7)	-10(9)
C86	39(8)	51(9)	76(10)	-6(7)	5(8)	1(8)
C87	40(8)	64(9)	41(8)	3(7)	12(6)	20(7)
C88	42(8)	50(9)	40(8)	9(6)	-5(6)	16(7)
C89	36(8)	38(8)	86(11)	-10(6)	9(8)	20(7)
C90	40(8)	50(9)	54(9)	-2(6)	-2(7)	-3(7)
C92	63(9)	63(10)	34(8)	3(7)	9(7)	15(7)
C93	28(7)	35(7)	37(8)	2(5)	-1(5)	-10(6)
C95	49(8)	34(8)	40(8)	-9(6)	-3(6)	-18(6)

C96	34(7)	33(7)	37(7)	4(6)	1(5)	-4(6)
C97	37(8)	86(12)	55(9)	-15(8)	11(7)	-34(9)
C99	67(10)	45(10)	91(13)	-8(8)	-19(9)	10(9)
C101	24(7)	28(7)	70(10)	-3(5)	-2(6)	-7(7)
C103	81(11)	51(10)	87(13)	-19(8)	11(9)	-23(9)
C104	66(10)	76(11)	43(9)	-3(9)	-5(7)	-2(8)
C108	22(7)	51(9)	68(10)	-8(6)	3(6)	-20(8)
C109	88(11)	53(10)	44(9)	-3(8)	5(8)	3(8)
C111	66(9)	52(9)	32(8)	8(7)	0(7)	-1(7)
C113	33(7)	50(9)	50(9)	-19(6)	-5(6)	-2(7)
C120	50(10)	45(10)	122(16)	-8(7)	0(10)	-1(11)
C122	80(11)	70(12)	61(11)	-15(9)	5(9)	-37(10)
C132	63(11)	46(11)	120(16)	-16(8)	13(10)	-42(10)
Cl4	70(3)	93(3)	106(4)	4(2)	4(2)	-32(3)
Cl6	99(4)	90(4)	183(6)	-6(3)	34(4)	52(4)
Cl13	113(5)	237(9)	141(6)	15(5)	-6(4)	-17(6)
Cl35	230(10)	281(12)	165(8)	-46(9)	-47(7)	108(8)
O1	43(5)	69(6)	46(5)	-1(5)	-2(4)	33(5)
O2	71(6)	76(7)	21(5)	0(5)	4(4)	-15(5)
C3	31(7)	63(9)	35(8)	8(6)	5(6)	4(7)
C4	66(10)	47(9)	41(8)	-8(7)	-2(7)	15(7)
C5	41(8)	42(8)	99(12)	6(6)	1(8)	30(8)
C6	47(9)	53(10)	82(13)	-15(7)	20(8)	-31(9)
C7	68(10)	71(11)	57(10)	-2(8)	18(8)	15(8)
C8	114(15)	120(15)	29(9)	22(12)	4(9)	16(9)
C10	59(14)	230(30)	410(50)	-64(18)	50(20)	-180(30)
C1	113(15)	66(12)	69(12)	-19(10)	-4(10)	-46(10)

**Crystallographic Table 76 Bond Lengths for Nd<sub>2</sub>[L<sup>VII</sup>]<sub>3</sub>.**

Atom	Atom	Length/Å	Atom	Atom	Length/Å
Nd1	O3	2.514(8)	C43	C52	1.414(17)
Nd1	O10	2.455(8)	C44	C61	1.400(16)
Nd1	O12	2.331(9)	C45	C53	1.369(15)
Nd1	N14	2.637(9)	C45	C65	1.390(16)
Nd1	O21	2.280(9)	C46	C87	1.342(17)
Nd1	N27	2.631(9)	C47	C60	1.347(18)
Nd1	O1	2.594(8)	C48	C104	1.353(19)
Nd1	O2	2.622(8)	C49	C70	1.428(17)

Nd2	O3	2.458(7)	C49	C111	1.425(17)
Nd2	O8	2.302(9)	C50	C66	1.417(17)
Nd2	N9	2.590(9)	C50	C95	1.378(17)
Nd2	O10	2.440(8)	C51	C68	1.370(16)
Nd2	N18	2.600(9)	C51	C93	1.413(16)
Nd2	N19	2.651(9)	C52	C90	1.419(17)
Nd2	O20	2.373(8)	C54	C81	1.465(16)
Nd2	C22	3.258(11)	C55	C61	1.383(17)
Nd2	N29	2.609(8)	C55	C69	1.390(18)
O3	C16	1.315(13)	C56	C4	1.369(17)
O8	C23	1.310(15)	C58	C93	1.442(15)
N9	C44	1.446(14)	C59	C70	1.396(17)
N9	C3	1.292(15)	C59	C88	1.373(17)
O10	C22	1.325(14)	C62	C76	1.365(17)
C11	N27	1.409(14)	C63	C90	1.396(17)
C11	C28	1.405(15)	C63	C104	1.389(19)
C11	C67	1.380(16)	C64	C101	1.436(17)
O12	C72	1.311(15)	C65	C67	1.384(16)
N14	C28	1.433(14)	C66	C80	1.418(17)
N14	C32	1.291(14)	C66	C93	1.412(16)
C16	C58	1.407(16)	C68	C95	1.386(16)
C16	C96	1.437(16)	C70	C82	1.414(17)
N18	C25	1.292(14)	C71	C108	1.413(18)
N18	C26	1.403(14)	C71	C132	1.43(2)
N19	C38	1.269(15)	C71	C6	1.42(2)
N19	C41	1.422(15)	C72	C97	1.447(18)
O20	C24	1.312(14)	C72	C101	1.418(18)
O21	C37	1.308(15)	C73	C75	1.399(18)
C22	C39	1.392(17)	C73	C77	1.421(18)
C22	C113	1.428(17)	C74	C86	1.389(18)
C23	C34	1.419(17)	C75	C84	1.42(2)
C23	C88	1.435(17)	C75	C122	1.427(19)
C24	C30	1.406(17)	C76	C4	1.386(18)
C24	C60	1.424(17)	C77	C103	1.378(18)
C25	C30	1.449(16)	C78	C81	1.441(17)
C26	C33	1.400(17)	C78	C87	1.433(18)
C26	C44	1.426(16)	C78	C89	1.412(17)
N27	C64	1.271(14)	C80	C96	1.360(16)

C28	C53	1.390(15)	C82	C109	1.379(18)
N29	C31	1.285(14)	C83	C99	1.374(19)
N29	C40	1.446(14)	C83	C108	1.418(19)
C30	C52	1.468(16)	C84	C113	1.381(19)
C31	C58	1.458(16)	C86	C89	1.368(19)
C32	C54	1.450(16)	C92	C109	1.375(19)
C33	C69	1.364(18)	C92	C111	1.398(18)
C34	C49	1.437(16)	C97	C6	1.36(2)
C34	C3	1.435(17)	C99	C120	1.39(2)
C37	C46	1.450(17)	C101	C108	1.443(18)
C37	C54	1.400(16)	C103	C1	1.40(2)
C38	C39	1.452(17)	C120	C132	1.35(2)
C39	C73	1.441(16)	C122	C1	1.35(2)
C40	C41	1.400(16)	Cl4	C7	1.748(15)
C40	C56	1.379(16)	Cl6	C7	1.724(14)
C41	C62	1.398(16)	Cl13	C10	2.00(3)
C42	C74	1.361(16)	Cl35	C10	1.63(2)
C42	C81	1.416(16)	O1	C5	1.407(14)
C43	C47	1.415(18)	O2	C8	1.429(16)
C43	C48	1.418(18)			

**Crystallographic Table 77 Bond Angles for Nd<sub>2</sub>[L<sup>VII</sup>]<sub>3</sub>.**

Atom	Atom	Atom	Angle/°	Atom	Atom	Atom	Angle/°
O10	Nd1	O3	70.1(2)	C69	C33	C26	123.0(13)
O12	Nd1	O3	138.0(3)	C49	C34	C23	119.7(11)
O12	Nd1	O10	79.4(3)	C3	C34	C23	121.8(11)
N14	Nd1	O3	80.9(3)	C3	C34	C49	117.9(11)
N14	Nd1	O10	139.2(3)	C46	C37	O21	118.1(11)
N14	Nd1	O12	106.6(3)	C54	C37	O21	123.0(11)
O21	Nd1	O3	110.0(3)	C54	C37	C46	118.8(12)
O21	Nd1	O10	149.1(3)	C39	C38	N19	125.7(11)
O21	Nd1	O12	111.0(3)	C38	C39	C22	122.1(10)
O21	Nd1	N14	67.6(3)	C73	C39	C22	119.4(11)
N27	Nd1	O3	80.9(3)	C73	C39	C38	118.4(11)
N27	Nd1	O10	85.0(3)	C41	C40	N29	115.8(10)
N27	Nd1	O12	68.0(3)	C56	C40	N29	123.8(10)
N27	Nd1	N14	62.0(3)	C56	C40	C41	120.4(11)
N27	Nd1	O21	125.8(3)	C40	C41	N19	117.3(10)

O1	Nd1	O3	72.6(3)	C62	C41	N19	125.1(10)
O1	Nd1	O10	74.5(3)	C62	C41	C40	117.6(11)
O1	Nd1	O12	126.4(3)	C81	C42	C74	121.3(11)
O1	Nd1	N14	123.8(3)	C48	C43	C47	119.5(12)
O1	Nd1	O21	76.3(3)	C52	C43	C47	118.6(12)
O1	Nd1	N27	150.7(3)	C52	C43	C48	121.8(12)
O2	Nd1	O3	142.0(3)	C26	C44	N9	116.7(10)
O2	Nd1	O10	89.1(3)	C61	C44	N9	122.4(10)
O2	Nd1	O12	62.2(3)	C61	C44	C26	120.7(11)
O2	Nd1	N14	130.0(3)	C65	C45	C53	119.4(10)
O2	Nd1	O21	72.2(3)	C87	C46	C37	121.0(12)
O2	Nd1	N27	130.1(3)	C60	C47	C43	122.2(12)
O2	Nd1	O1	71.3(3)	C104	C48	C43	120.1(13)
O8	Nd2	O3	88.2(3)	C70	C49	C34	118.6(11)
N9	Nd2	O3	139.5(3)	C111	C49	C34	123.2(11)
N9	Nd2	O8	69.1(3)	C111	C49	C70	118.1(11)
O10	Nd2	O3	71.3(2)	C95	C50	C66	122.1(12)
O10	Nd2	O8	155.1(3)	C93	C51	C68	121.3(12)
O10	Nd2	N9	135.7(3)	C43	C52	C30	119.3(11)
N18	Nd2	O3	156.3(3)	C90	C52	C30	124.5(11)
N18	Nd2	O8	108.9(3)	C90	C52	C43	116.2(11)
N18	Nd2	N9	64.0(3)	C45	C53	C28	120.3(10)
N18	Nd2	O10	87.6(3)	C37	C54	C32	121.4(10)
N19	Nd2	O3	100.2(3)	C81	C54	C32	118.0(10)
N19	Nd2	O8	131.0(3)	C81	C54	C37	120.3(11)
N19	Nd2	N9	74.0(3)	C69	C55	C61	120.0(12)
N19	Nd2	O10	68.4(3)	C4	C56	C40	120.2(11)
N19	Nd2	N18	81.3(3)	C31	C58	C16	121.1(10)
O20	Nd2	O3	95.5(3)	C93	C58	C16	121.3(11)
O20	Nd2	O8	89.2(3)	C93	C58	C31	116.6(10)
O20	Nd2	N9	116.4(3)	C88	C59	C70	120.4(11)
O20	Nd2	O10	79.3(3)	C47	C60	C24	121.5(13)
O20	Nd2	N18	69.1(3)	C55	C61	C44	120.1(12)
O20	Nd2	N19	136.8(3)	C76	C62	C41	121.6(12)
C22	Nd2	O3	92.4(3)	C104	C63	C90	121.5(14)
C22	Nd2	O8	168.8(3)	C101	C64	N27	128.3(12)
C22	Nd2	N9	116.3(3)	C67	C65	C45	121.1(11)
C22	Nd2	O10	21.3(3)	C80	C66	C50	122.8(11)

C22	Nd2	N18	67.6(3)	C93	C66	C50	118.3(12)
C22	Nd2	N19	60.0(3)	C93	C66	C80	118.8(11)
C22	Nd2	O20	79.5(3)	C65	C67	C11	119.8(11)
N29	Nd2	O3	68.2(3)	C95	C68	C51	121.1(12)
N29	Nd2	O8	78.2(3)	C55	C69	C33	119.9(13)
N29	Nd2	N9	74.3(3)	C59	C70	C49	121.0(11)
N29	Nd2	O10	105.7(3)	C82	C70	C49	119.3(12)
N29	Nd2	N18	130.2(3)	C82	C70	C59	119.7(12)
N29	Nd2	N19	61.3(3)	C132	C71	C108	120.7(15)
N29	Nd2	O20	159.5(3)	C6	C71	C108	118.8(13)
N29	Nd2	C22	112.4(3)	C6	C71	C132	120.5(14)
Nd2	O3	Nd1	107.7(3)	C97	C72	O12	119.1(13)
C16	O3	Nd1	130.8(6)	C101	C72	O12	122.6(11)
C16	O3	Nd2	121.4(6)	C101	C72	C97	118.3(13)
C23	O8	Nd2	133.6(7)	C75	C73	C39	120.3(12)
C44	N9	Nd2	110.5(7)	C77	C73	C39	122.3(12)
C3	N9	Nd2	128.4(8)	C77	C73	C75	117.4(11)
C3	N9	C44	120.6(10)	C86	C74	C42	122.0(12)
Nd2	O10	Nd1	110.3(3)	C84	C75	C73	118.2(12)
C22	O10	Nd1	132.9(7)	C122	C75	C73	119.5(14)
C22	O10	Nd2	116.7(6)	C122	C75	C84	122.3(14)
C28	C11	N27	117.4(10)	C4	C76	C62	119.5(12)
C67	C11	N27	123.2(10)	C103	C77	C73	120.9(14)
C67	C11	C28	119.1(10)	C87	C78	C81	117.6(11)
C72	O12	Nd1	136.1(7)	C89	C78	C81	120.4(12)
C28	N14	Nd1	111.8(6)	C89	C78	C87	122.1(12)
C32	N14	Nd1	131.4(7)	C96	C80	C66	121.7(11)
C32	N14	C28	116.8(9)	C54	C81	C42	124.5(11)
C58	C16	O3	123.9(10)	C78	C81	C42	116.3(11)
C96	C16	O3	118.7(10)	C78	C81	C54	119.1(11)
C96	C16	C58	117.2(10)	C109	C82	C70	121.5(12)
C25	N18	Nd2	132.8(8)	C108	C83	C99	124.3(14)
C26	N18	Nd2	110.4(7)	C113	C84	C75	122.9(13)
C26	N18	C25	116.8(9)	C89	C86	C74	119.6(12)
C38	N19	Nd2	123.0(8)	C78	C87	C46	123.1(12)
C41	N19	Nd2	117.5(7)	C59	C88	C23	121.4(12)
C41	N19	C38	119.4(10)	C86	C89	C78	120.3(13)
C24	O20	Nd2	142.6(8)	C63	C90	C52	120.5(13)

C37	O21	Nd1	147.8(7)	C111	C92	C109	122.0(13)
O10	C22	Nd2	42.0(5)	C58	C93	C51	122.5(11)
C39	C22	Nd2	97.6(7)	C66	C93	C51	118.3(10)
C39	C22	O10	123.1(10)	C66	C93	C58	119.2(11)
C113	C22	Nd2	130.0(8)	C68	C95	C50	118.8(11)
C113	C22	O10	115.8(11)	C80	C96	C16	121.7(11)
C113	C22	C39	121.0(11)	C6	C97	C72	122.4(15)
C34	C23	O8	123.5(11)	C120	C99	C83	117.7(16)
C88	C23	O8	117.5(11)	C72	C101	C64	120.4(11)
C88	C23	C34	118.9(12)	C108	C101	C64	120.7(12)
C30	C24	O20	121.9(11)	C108	C101	C72	118.7(12)
C60	C24	O20	119.2(11)	C1	C103	C77	121.3(16)
C60	C24	C30	118.7(11)	C63	C104	C48	119.7(13)
C30	C25	N18	125.4(11)	C83	C108	C71	115.2(13)
C33	C26	N18	124.9(11)	C101	C108	C71	121.2(13)
C44	C26	N18	118.6(10)	C101	C108	C83	123.4(12)
C44	C26	C33	116.4(11)	C92	C109	C82	119.4(13)
C11	N27	Nd1	113.1(6)	C92	C111	C49	119.7(13)
C64	N27	Nd1	127.9(8)	C84	C113	C22	118.3(13)
C64	N27	C11	118.9(9)	C132	C120	C99	122.2(15)
N14	C28	C11	117.4(10)	C1	C122	C75	122.1(15)
C53	C28	C11	120.3(10)	C120	C132	C71	119.6(15)
C53	C28	N14	122.2(10)	C5	O1	Nd1	131.0(7)
C31	N29	Nd2	124.3(7)	C8	O2	Nd1	132.0(9)
C40	N29	Nd2	118.0(7)	C34	C3	N9	125.5(12)
C40	N29	C31	117.7(9)	C76	C4	C56	120.3(12)
C25	C30	C24	124.9(11)	C97	C6	C71	120.6(13)
C52	C30	C24	118.9(11)	C16	C7	C14	112.2(9)
C52	C30	C25	116.2(11)	C135	C10	C113	108.2(15)
C58	C31	N29	125.8(10)	C122	C1	C103	118.6(14)
C54	C32	N14	127.0(10)				

**Crystallographic Table 78** Hydrogen Atom Coordinates ( $\text{\AA}\times 10^4$ ) and Isotropic Displacement Parameters ( $\text{\AA}^2\times 10^3$ ) for  $\text{Nd}_2[\text{L}^{\text{VII}}]_3$ .

Atom	x	y	z	U(eq)
H25	7889(11)	1812(3)	3241(7)	42(3)
H31	2560(10)	1137(3)	-214(6)	35(3)
H32	-2023(10)	699(3)	1900(6)	37(3)



H33	7271(11)	2261(3)	2752(8)	53(4)
H38	3284(10)	2269(3)	1759(7)	46(4)
H42	-3650(11)	448(3)	2055(7)	45(4)
H45	-694(10)	809(3)	-425(6)	40(3)
H46	-58(12)	367(3)	4653(7)	54(4)
H47	7172(13)	825(3)	5358(7)	61(4)
H48	8348(13)	1177(4)	6224(8)	68(5)
H50	1244(12)	-182(3)	54(8)	58(4)
H51	2972(12)	751(3)	-892(7)	52(4)
H53	-965(10)	630(3)	821(6)	36(3)
H55	7370(12)	2551(3)	555(8)	57(4)
H56	3361(11)	1486(3)	-877(7)	44(4)
H59	5933(12)	280(3)	-754(8)	51(4)
H60	6109(12)	715(3)	4228(7)	61(4)
H61	6935(11)	2039(3)	129(7)	52(4)
H62	3552(12)	2384(3)	653(7)	50(4)
H63	9296(13)	2047(3)	5527(7)	65(4)
H64	-98(10)	1906(3)	1402(7)	45(4)
H65	-9(10)	1327(3)	-630(7)	42(4)
H67	502(11)	1658(3)	403(7)	47(4)
H68	2399(12)	348(3)	-1720(7)	49(4)
H69	7585(13)	2655(3)	1875(8)	64(4)
H74	-5277(12)	84(3)	2170(8)	55(4)
H76	3241(13)	2432(3)	-661(8)	62(4)
H77	4309(12)	2646(3)	2257(8)	59(4)
H80	1467(11)	26(3)	1399(7)	45(4)
H82	6696(13)	444(3)	-1990(7)	58(4)
H83	725(11)	2346(3)	1105(9)	59(4)
H84	4242(12)	2065(4)	4944(8)	74(5)
H86	-5283(13)	-276(3)	3181(9)	66(4)
H87	-1721(12)	19(3)	4719(7)	58(4)
H88	5514(12)	386(3)	519(7)	53(4)
H89	-3682(12)	-249(3)	4145(9)	64(5)
H90	8338(12)	1958(3)	4315(8)	58(4)
H92	7604(13)	1348(3)	-2401(7)	64(4)
H95	1553(12)	-125(3)	-1256(7)	49(4)
H96	1940(11)	430(3)	2230(7)	42(3)
H97	848(12)	2137(4)	4349(8)	71(5)

H99	1076(14)	2870(3)	811(10)	82(5)
H103	4700(15)	3108(4)	2930(10)	87(6)
H104	9376(14)	1652(4)	6458(8)	74(5)
H109	7396(15)	832(3)	-2825(8)	74(5)
H111	7117(13)	1490(3)	-1144(7)	60(4)
H113	3748(11)	1595(3)	4315(7)	53(4)
H120	1095(14)	3241(4)	1809(12)	87(6)
H122	4709(15)	2642(4)	4930(9)	84(6)
H132	1038(15)	3090(4)	3068(12)	91(6)
H1	4108(13)	913(15)	3500(50)	79(4)
H2	1280(110)	1472(6)	4659(12)	84(4)
H3	7268(11)	1540(3)	3(7)	52(4)
H4	3133(13)	1980(3)	-1429(8)	62(4)
H5a	3790(80)	412(5)	3600(20)	91(6)
H5b	3840(80)	565(5)	4450(30)	91(6)
H5c	2465(13)	484(10)	4030(50)	91(6)
H6	987(13)	2660(4)	4042(10)	73(5)
H7a	-344(14)	346(4)	-2349(8)	78(5)
H7b	434(14)	113(4)	-2895(8)	78(5)
H8a	520(50)	970(20)	5120(40)	131(9)
H8b	2060(70)	917(18)	5140(40)	131(9)
H8c	1440(120)	1197(6)	5624(8)	131(9)
H10a	9540(20)	3904(8)	2780(20)	280(20)
H10b	8500(20)	4163(8)	2480(20)	280(20)
H1a	4901(18)	3108(4)	4277(10)	99(6)

#### Refinement model description

Number of restraints - 6, number of constraints - 124.

Details:

##### 1. Fixed Uiso

At 1.2 times of:

All C(H) groups, All C(H,H) groups

At 1.5 times of:

All C(H,H,H) groups, All O(H) groups

##### 2. Restrained distances

O1-H1

0.87 with sigma of 0.01

O2-H2

0.87 with sigma of 0.01

C5-H1

1.885032 with sigma of 0.02

Nd1-H1

3.118054 with sigma of 0.02

C8-H2

1.895625 with sigma of 0.02

Nd1-H2

3.131953 with sigma of 0.02

3.a Secondary CH2 refined with riding coordinates:

C7(H7a,H7b), C10(H10a,H10b)

3.b Aromatic/amide H refined with riding coordinates:

C25(H25), C31(H31), C32(H32), C33(H33), C38(H38), C42(H42), C45(H45),  
C46(H46), C47(H47), C48(H48), C50(H50), C51(H51), C53(H53), C55(H55),  
C56(H56),

C59(H59), C60(H60), C61(H61), C62(H62), C63(H63), C64(H64), C65(H65),  
C67(H67), C68(H68), C69(H69), C74(H74), C76(H76), C77(H77), C80(H80),  
C82(H82),

C83(H83), C84(H84), C86(H86), C87(H87), C88(H88), C89(H89), C90(H90),  
C92(H92), C95(H95), C96(H96), C97(H97), C99(H99), C103(H103), C104(H104),  
C109(H109), C111(H111), C113(H113), C120(H120), C122(H122), C132(H132),  
C3(H3),

C4(H4), C6(H6), C1(H1a)

3.c Idealised Me refined as rotating group:

C5(H5a,H5b,H5c), C8(H8a,H8b,H8c)

## Gd<sub>2</sub>[L<sup>VII</sup>]<sub>3</sub>

### Crystallographic Table 79 Crystal data and structure refinement for Gd<sub>2</sub>[L<sup>VII</sup>]<sub>3</sub>

Empirical formula	C <sub>88</sub> H <sub>66</sub> Cl <sub>4</sub> Gd <sub>2</sub> N <sub>6</sub> O <sub>8</sub>
Formula weight	1791.85
Temperature/K	180.45
Crystal system	triclinic
Space group	P-1
a/Å	12.3985(2)
b/Å	17.1412(3)
c/Å	17.7640(3)
α/°	87.7454(8)
β/°	75.9048(7)
γ/°	85.8045(7)
Volume/Å <sup>3</sup>	3650.92(11)
Z	2
ρ <sub>calc</sub> /mg/mm <sup>3</sup>	1.6298
m/mm <sup>-1</sup>	2.013
F(000)	1794.2
Crystal size/mm <sup>3</sup>	0.28 × 0.21 × 0.1
Radiation	Mo Kα (λ = 0.71073)
2θ range for data collection	2.38 to 59.14°
Index ranges	-17 ≤ h ≤ 17, -23 ≤ k ≤ 23, -24 ≤ l ≤ 24
Reflections collected	112543
Independent reflections	20486 [R <sub>int</sub> = 0.0390, R <sub>sigma</sub> = 0.0280]
Data/restraints/parameters	20486/3/1003
Goodness-of-fit on F <sup>2</sup>	1.155
Final R indexes [I >= 2σ (I)]	R <sub>1</sub> = 0.0362, wR <sub>2</sub> = 0.0841
Final R indexes [all data]	R <sub>1</sub> = 0.0509, wR <sub>2</sub> = 0.1042
Largest diff. peak/hole / e Å <sup>-3</sup>	3.29/-2.30

### Crystallographic Table 80 Fractional Atomic Coordinates (×10<sup>4</sup>) and Equivalent Isotropic Displacement Parameters (Å<sup>2</sup>×10<sup>3</sup>) for Gd<sub>2</sub>[L<sup>VII</sup>]<sub>3</sub>. U<sub>eq</sub> is defined as 1/3 of of the trace of the orthogonalised U<sub>ij</sub> tensor.

Atom	x	y	z	U(eq)
Gd1	13714.93(13)	13048.58(9)	-2942.27(9)	14.34(4)
Gd2	12554.98(14)	10973.24(10)	-2841.57(9)	16.15(4)
O3	13469(2)	11845.5(14)	-2226.1(14)	17.5(5)

O4	13004(2)	12125.7(14)	-3621.9(14)	17.8(5)
N3	12203(2)	13212.1(17)	-1677.5(17)	16.8(5)
N5	11084(3)	11177.8(18)	-1621.6(17)	18.8(6)
N4	11758(2)	13498.8(17)	-3063.3(16)	16.3(5)
N6	10692(2)	11445.9(18)	-3039.1(17)	17.9(6)
C29	13560(3)	11748(2)	-1492.0(19)	16.3(6)
N2	13930(3)	14060.8(18)	-4035.4(17)	18.3(6)
C68	10233(3)	11761(2)	-1683(2)	19.1(7)
O1	15008(2)	13147.4(15)	-2241.6(15)	20.4(5)
O2	15312(2)	12727.8(15)	-3895.5(14)	20.2(5)
N1	13651(3)	14437.2(18)	-2543.4(17)	18.3(6)
C48	11654(3)	13128(2)	-5072(2)	21.9(7)
C71	8610(3)	12912(3)	-1894(3)	28.9(8)
C73	10024(3)	11901(2)	-2425(2)	18.1(6)
C38	12965(3)	12230(2)	-891.4(19)	17.3(6)
C47	11950(3)	12956(2)	-4340.3(19)	17.0(6)
C56	12720(3)	12328(2)	-4284.9(19)	16.9(6)
C46	11368(3)	13392(2)	-3660(2)	18.2(6)
C39	12160(3)	12846(2)	-1023(2)	19.1(7)
C17	13355(3)	14792(2)	-3802(2)	18.7(7)
C66	11758(3)	10217(2)	-757(2)	21.8(7)
C67	10998(3)	10816(2)	-955(2)	21.6(7)
O6	12243(2)	10281.5(16)	-3787.8(16)	24.5(6)
C40	11352(3)	13810(2)	-1714(2)	19.0(7)
O5	12679(3)	9924.6(17)	-2069.2(16)	28.4(6)
C4	14521(3)	13950(2)	-8(2)	24.3(8)
C58	13171(4)	9129(2)	-1080(2)	29.1(9)
C45	11101(3)	13949(2)	-2438(2)	18.8(7)
C37	13076(3)	12076(2)	-106(2)	21.3(7)
C28	15483(3)	12697(2)	-4655(2)	18.6(7)
C12	13220(3)	14996(2)	-3022(2)	19.3(7)
C72	9218(3)	12485(2)	-2519(2)	23.2(7)
C75	10866(3)	10956(2)	-4344(2)	20.1(7)
C82	11765(4)	10057(3)	-5674(2)	30.9(9)
C30	14265(3)	11106(2)	-1317(2)	22.3(7)
C53	12132(3)	12654(2)	-5716(2)	25.3(8)
O7	14481(2)	10551.4(17)	-3394.9(19)	30.5(6)
C77	9626(3)	11701(3)	-5100(2)	26.0(8)

C74	10321(3)	11365(2)	-3655(2)	19.7(7)
C44	10297(3)	14540(2)	-2513(2)	26.8(8)
C19	15005(3)	13258(2)	-5101(2)	19.2(7)
C54	12914(4)	12024(3)	-5636(2)	26.5(8)
C57	12531(3)	9777(2)	-1327(2)	23.2(7)
C32	13775(4)	11425(2)	48(2)	25.0(8)
C20	15153(3)	13142(2)	-5924(2)	22.9(7)
C55	13199(3)	11866(2)	-4949(2)	21.9(7)
C1	14876(3)	13451(2)	-1564(2)	19.7(7)
C84	11773(3)	10400(2)	-4363(2)	21.1(7)
C41	10825(4)	14281(3)	-1090(2)	28.4(8)
C70	8814(4)	12780(3)	-1168(2)	30.1(9)
C76	10441(3)	11100(2)	-5033(2)	20.5(7)
C65	11682(3)	10040(2)	59(2)	23.9(7)
C78	9263(4)	11826(3)	-5768(3)	32.0(9)
C31	14363(4)	10956(2)	-576(2)	27.2(8)
C11	13785(3)	14639(2)	-1875(2)	20.0(7)
C18	14404(3)	13957(2)	-4763(2)	19.9(7)
C13	12597(4)	15689(2)	-2750(2)	25.7(8)
C49	10903(4)	13771(3)	-5171(3)	32.1(9)
C81	10901(4)	10645(2)	-5700(2)	27.5(8)
C79	9700(5)	11361(3)	-6413(3)	41.0(11)
C69	9625(3)	12212(2)	-1062(2)	25.5(8)
C83	12180(4)	9939(2)	-5037(2)	26.5(8)
C26	16363(4)	11974(3)	-5823(2)	27.6(8)
C51	11088(5)	13415(3)	-6505(3)	44.7(13)
C59	13070(4)	8946(2)	-319(3)	31.6(9)
C10	14191(3)	14135(2)	-1326(2)	18.9(7)
C80	10509(5)	10785(3)	-6377(3)	39.0(11)
C60	12334(4)	9394(2)	277(2)	27.6(8)
C25	15808(3)	12481(2)	-6279(2)	24.9(8)
C16	12845(3)	15285(2)	-4285(2)	25.1(8)
C5	14283(4)	14161(3)	779(2)	33.1(9)
C21	14594(4)	13627(3)	-6396(2)	31.1(9)
C61	12262(4)	9218(3)	1071(3)	35.4(10)
C15	12251(4)	15972(2)	-4010(3)	30.4(9)
C2	15477(3)	13076(2)	-1035(2)	24.8(8)
C9	13957(3)	14364(2)	-522(2)	21.7(7)

C27	16215(3)	12081(2)	-5049(2)	25.3(8)
C43	9754(4)	14989(3)	-1883(3)	35.1(10)
C64	11012(4)	10498(3)	664(2)	33.4(9)
C3	15314(4)	13323(2)	-295(2)	28.0(8)
C24	15887(4)	12327(3)	-7067(2)	34.7(10)
C36	12561(4)	12569(3)	520(2)	33.5(9)
C50	10629(5)	13899(3)	-5880(3)	41.6(12)
C8	13141(4)	14956(3)	-209(2)	27.8(8)
C6	13495(4)	14747(3)	1064(2)	35.5(10)
C42	10022(4)	14862(3)	-1177(3)	36.1(10)
C22	14697(5)	13469(3)	-7162(3)	40.9(11)
C14	12128(4)	16172(2)	-3244(3)	29.9(9)
C62	11570(5)	9653(3)	1641(3)	40.0(11)
C63	10950(5)	10305(3)	1432(3)	41.8(12)
C52	11827(4)	12815(3)	-6431(2)	37.3(11)
C33	13883(4)	11272(3)	820(3)	37.8(11)
C35	12691(5)	12406(3)	1257(3)	43.1(12)
C7	12918(4)	15147(3)	564(3)	35.1(10)
Cl4	17991.9(17)	13322.4(13)	-4091.0(9)	78.8(6)
Cl3	17384(2)	14758.5(11)	-3270.3(14)	85.1(6)
C87	16923(5)	13891(3)	-3525(3)	46.6(13)
Cl2	17764(2)	13102.0(16)	-9103.0(12)	96.1(7)
Cl1	19776(2)	12537.6(18)	-8622(2)	114.7(9)
O8	16154(3)	11403.4(17)	-3347.1(18)	28.5(6)
C23	15335(5)	12814(3)	-7502(3)	42.7(12)
C34	13342(5)	11743(3)	1409(3)	45.3(13)
C85	14893(6)	9804(4)	-3681(6)	77(3)
C88A	19015(12)	13414(6)	-9252(6)	55(3)
C86	16731(5)	11473(3)	-2763(3)	40.6(11)
C88B	18398(7)	12422(6)	-8566(6)	36(2)

**Crystallographic Table 81** Anisotropic Displacement Parameters ( $\text{\AA}^2 \times 10^3$ ) for  $\text{Gd}_2[\text{L}^{\text{VI}}]_3$ . The Anisotropic displacement factor exponent takes the form: -  
 $2\pi^2[h^2a^{*2}U_{11}+2hka^*b^*U_{12}+\dots]$

Atom	$U_{11}$	$U_{22}$	$U_{33}$	$U_{12}$	$U_{13}$	$U_{23}$
Gd1	16.29(8)	15.25(8)	11.39(7)	0.34(6)	-3.48(6)	-0.91(5)
Gd2	17.06(8)	16.72(8)	15.22(8)	0.13(6)	-5.30(6)	-0.57(6)
O3	24.6(13)	17.3(12)	11.6(10)	-1.0(9)	-6.7(9)	-0.1(9)

O4	24.9(13)	18.4(12)	12.4(11)	-2.1(10)	-8.8(9)	0.9(9)
N3	16.5(13)	18.4(14)	14.9(13)	1.9(11)	-3.4(11)	-1.9(11)
N5	17.8(14)	20.6(15)	18.7(14)	-1.3(11)	-5.8(11)	0.3(11)
N4	18.3(14)	16.6(13)	13.1(12)	0.5(11)	-2.8(11)	1.1(10)
N6	15.4(13)	19.7(14)	18.1(14)	0.1(11)	-3.6(11)	-0.8(11)
C29	17.6(15)	19.1(16)	13.8(14)	-3.9(12)	-6.3(12)	1.2(12)
N2	20.0(14)	18.1(14)	17.0(13)	0.3(11)	-5.3(11)	-0.1(11)
C68	17.1(16)	22.2(17)	17.4(16)	-0.5(13)	-3.4(13)	1.3(13)
O1	22.1(13)	23.2(13)	17.5(12)	1.3(10)	-8(1)	-5.2(10)
O2	19.6(12)	23.7(13)	15.7(11)	3.9(10)	-2.5(9)	-3.2(10)
N1	22.4(15)	17.0(14)	15.7(13)	1.5(11)	-5.5(11)	-0.6(11)
C48	24.3(18)	26.0(18)	18.2(16)	-10.1(14)	-9.2(14)	5.5(14)
C71	22.9(19)	30(2)	32(2)	6.5(16)	-5.6(16)	-2.0(17)
C73	16.8(16)	20.7(17)	16.4(15)	-0.3(13)	-3.5(12)	-0.2(13)
C38	20.7(16)	19.3(16)	12.8(14)	-3.6(13)	-5.8(12)	4.0(12)
C47	17.4(16)	20.6(16)	14.5(15)	-4.8(13)	-6.5(12)	2.2(12)
C56	18.8(16)	18.7(16)	14.8(15)	-3.9(13)	-6.4(12)	1.6(12)
C46	17.7(16)	18.4(16)	18.8(16)	-0.4(12)	-5.5(13)	2.5(13)
C39	19.7(16)	23.7(17)	13.5(15)	-1.0(13)	-3.1(12)	-2.3(13)
C17	21.4(17)	15.8(16)	18.1(16)	-1.9(13)	-3.2(13)	1.5(12)
C66	22.5(17)	25.5(18)	18.2(16)	-4.7(14)	-6.7(14)	5.9(14)
C67	21.8(17)	26.6(19)	16.7(16)	-4.4(14)	-4.7(13)	2.5(14)
O6	27.2(14)	22.7(13)	26.9(14)	4.8(11)	-14.2(11)	-5.7(11)
C40	18.2(16)	21.2(17)	16.3(15)	1.9(13)	-2.2(13)	-2.3(13)
O5	38.3(16)	24.4(14)	20.7(13)	5.9(12)	-6.4(12)	2.4(11)
C4	30(2)	27.3(19)	17.8(17)	-6.0(15)	-8.2(15)	-2.6(14)
C58	43(2)	18.3(18)	27(2)	2.3(16)	-11.9(18)	0.6(15)
C45	16.2(16)	21.1(17)	17.2(15)	1.1(13)	-1.0(12)	0.2(13)
C37	28.0(19)	25.6(18)	12.0(15)	-6.5(15)	-7.2(13)	3.1(13)
C28	18.1(16)	21.9(17)	15.2(15)	-1.8(13)	-2.1(12)	-3.0(13)
C12	23.7(17)	15.7(16)	18.9(16)	-1.5(13)	-6.1(13)	1.2(13)
C72	21.3(17)	25.7(19)	21.9(17)	1.7(14)	-5.3(14)	-0.1(14)
C75	18.6(16)	21.2(17)	21.5(17)	-2.3(13)	-6.7(13)	-0.7(13)
C82	41(2)	28(2)	25.2(19)	5.0(17)	-10.6(17)	-10.4(16)
C30	27.9(19)	20.3(17)	20.6(17)	1.6(14)	-10.5(15)	1.2(13)
C53	31(2)	34(2)	13.6(16)	-12.0(16)	-8.1(14)	4.6(14)
O7	19.9(13)	23.4(14)	46.7(18)	1.2(11)	-4.8(13)	-10.0(13)
C77	25.0(19)	32(2)	22.9(18)	0.6(15)	-9.8(15)	-2.0(15)



C74	16.2(16)	21.8(17)	21.2(16)	-0.0(13)	-5.1(13)	1.0(13)
C44	24.5(19)	28(2)	27.1(19)	6.6(15)	-6.7(15)	2.0(15)
C19	19.5(16)	23.4(17)	12.5(14)	-4.4(13)	1.3(12)	-0.3(13)
C54	31(2)	33(2)	15.6(16)	-7.3(16)	-4.4(15)	-3.2(15)
C57	28.5(19)	19.8(17)	22.8(18)	-3.9(14)	-9.5(15)	4.9(14)
C32	36(2)	24.9(19)	18.1(17)	-6.6(16)	-13.7(15)	6.8(14)
C20	25.3(18)	28.9(19)	14.4(15)	-8.1(15)	-2.9(13)	-1.0(14)
C55	23.6(18)	23.9(18)	18.4(16)	-4.0(14)	-4.2(14)	-2.9(14)
C1	20.2(17)	22.3(17)	18.3(16)	-4.2(13)	-7.2(13)	-0.2(13)
C84	23.0(18)	20.0(17)	22.8(17)	-4.5(14)	-8.9(14)	-2.9(13)
C41	32(2)	31(2)	18.8(17)	8.1(17)	-1.0(15)	-6.3(15)
C70	26(2)	33(2)	26(2)	5.9(16)	1.5(16)	-6.1(16)
C76	20.6(17)	21.6(17)	20.6(17)	-5.6(13)	-6.1(14)	-0.9(13)
C65	25.5(19)	26.8(19)	21.5(17)	-7.1(15)	-8.8(15)	4.3(14)
C78	33(2)	37(2)	28(2)	-0.3(18)	-14.4(18)	3.4(17)
C31	35(2)	23.5(19)	27.7(19)	1.5(16)	-17.8(17)	4.3(15)
C11	20.7(17)	19.9(17)	19.0(16)	1.2(13)	-4.0(13)	-5.4(13)
C18	20.5(17)	22.3(17)	16.9(15)	-3.8(13)	-4.4(13)	2.5(13)
C13	36(2)	18.8(17)	22.9(18)	2.9(15)	-9.0(16)	-3.2(14)
C49	38(2)	33(2)	28(2)	-2.3(18)	-15.2(18)	8.9(17)
C81	35(2)	25.7(19)	24.6(19)	-0.9(16)	-11.9(16)	-3.8(15)
C79	52(3)	47(3)	30(2)	4(2)	-23(2)	-3(2)
C69	26.0(19)	32(2)	16.8(16)	2.4(16)	-2.4(14)	-3.2(15)
C83	30(2)	21.2(18)	29(2)	4.2(15)	-10.7(16)	-7.2(15)
C26	28(2)	32(2)	20.8(18)	-0.4(16)	-0.8(15)	-11.7(15)
C51	58(3)	61(3)	22(2)	-15(3)	-23(2)	14(2)
C59	48(3)	20.0(19)	31(2)	2.0(17)	-19.0(19)	2.6(16)
C10	20.2(16)	21.2(17)	16.1(15)	-0.7(13)	-5.2(13)	-3.8(13)
C80	58(3)	39(3)	24(2)	4(2)	-18(2)	-9.2(18)
C60	36(2)	27(2)	23.7(18)	-8.1(17)	-14.8(17)	5.3(15)
C25	23.6(18)	34(2)	15.7(16)	-6.8(15)	0.9(14)	-6.8(14)
C16	28.8(19)	26.9(19)	19.5(17)	1.2(15)	-7.1(15)	4.5(14)
C5	41(2)	42(2)	18.3(18)	-6(2)	-9.2(17)	-1.8(17)
C21	34(2)	41(2)	18.3(18)	-1.7(18)	-5.5(16)	-1.1(16)
C61	55(3)	29(2)	28(2)	-4(2)	-21(2)	7.9(17)
C15	35(2)	22.6(19)	34(2)	4.2(16)	-12.2(18)	6.9(16)
C2	26.7(19)	27.6(19)	23.0(18)	2.3(15)	-12.5(15)	-2.2(15)
C9	23.9(18)	24.8(18)	17.8(16)	-3.1(14)	-6.8(14)	-1.7(14)

C27	24.5(19)	29(2)	21.2(18)	4.7(15)	-3.2(15)	-8.6(15)
C43	31(2)	32(2)	38(2)	13.1(18)	-3.9(18)	-2.1(18)
C64	38(2)	41(2)	21.2(19)	2.7(19)	-9.4(17)	4.9(17)
C3	33(2)	30(2)	25.1(19)	0.1(16)	-15.2(17)	-1.5(16)
C24	40(2)	46(3)	16.7(18)	-7(2)	-0.4(17)	-10.1(17)
C36	42(3)	40(2)	17.8(18)	0(2)	-7.9(17)	0.1(17)
C50	50(3)	44(3)	38(3)	-4(2)	-26(2)	18(2)
C8	28(2)	30(2)	25.8(19)	-2.0(16)	-4.7(16)	-7.0(16)
C6	43(3)	44(3)	17.8(18)	-8(2)	-0.7(17)	-10.6(17)
C42	37(2)	33(2)	31(2)	13.0(19)	2.5(18)	-9.3(18)
C22	51(3)	55(3)	18.2(19)	-3(2)	-11.2(19)	1.8(19)
C14	36(2)	17.7(18)	35(2)	4.5(16)	-7.7(18)	-0.5(16)
C62	54(3)	47(3)	23(2)	-7(2)	-17(2)	7.4(19)
C63	48(3)	56(3)	20(2)	3(2)	-7.2(19)	1(2)
C52	48(3)	50(3)	18.2(18)	-12(2)	-14.9(19)	3.7(18)
C33	52(3)	42(3)	23(2)	2(2)	-19(2)	8.3(18)
C35	55(3)	55(3)	18(2)	2(2)	-9(2)	-5(2)
C7	36(2)	41(3)	26(2)	-1.9(19)	-1.3(18)	-11.9(18)
Cl4	88.3(13)	101.4(14)	40.6(8)	56.2(11)	-20.1(8)	-12.9(8)
Cl3	104.8(16)	55.1(10)	107.8(16)	-7.4(10)	-45.6(13)	-20.2(10)
C87	40(3)	48(3)	47(3)	-10(2)	3(2)	-6(2)
Cl2	120.6(19)	106.6(17)	57.1(11)	12.3(15)	-17.5(12)	-16.4(11)
Cl1	65.2(13)	115(2)	161(3)	-5.2(13)	-17.9(15)	-28.6(19)
O8	31.2(15)	23.4(14)	34.1(15)	1.3(12)	-15.1(13)	-0.7(12)
C23	52(3)	60(3)	16.8(19)	-6(2)	-8.3(19)	-6(2)
C34	63(3)	61(3)	15.8(19)	0(3)	-19(2)	5(2)
C85	32(3)	50(4)	142(9)	9(3)	-3(4)	-48(5)
C88A	101(10)	28(5)	26(5)	-16(5)	8(5)	-7(4)
C86	40(3)	46(3)	41(3)	9(2)	-24(2)	-12(2)
C88B	19(4)	44(5)	43(5)	-14(4)	2(3)	-2(4)

**Crystallographic Table 82 Bond Lengths for Gd<sub>2</sub>[L<sup>VII</sup>]<sub>3</sub>.**

Atom	Atom	Length/Å	Atom	Atom	Length/Å
Gd1	O3	2.379(2)	C75	C74	1.430(5)
Gd1	O4	2.368(2)	C75	C84	1.414(5)
Gd1	N3	2.562(3)	C75	C76	1.452(5)
Gd1	N4	2.549(3)	C82	C81	1.423(6)
Gd1	N2	2.530(3)	C82	C83	1.355(6)

Gd1	O1	2.275(2)	C30	C31	1.364(5)
Gd1	O2	2.318(2)	C53	C54	1.425(6)
Gd1	N1	2.500(3)	C53	C52	1.422(5)
Gd2	O3	2.386(2)	O7	C85	1.411(7)
Gd2	O4	2.388(2)	C77	C76	1.411(5)
Gd2	N5	2.487(3)	C77	C78	1.373(5)
Gd2	N6	2.493(3)	C44	C43	1.388(6)
Gd2	O6	2.218(3)	C19	C20	1.449(5)
Gd2	O5	2.237(3)	C19	C18	1.436(5)
Gd2	O7	2.419(3)	C54	C55	1.363(5)
O3	C29	1.339(4)	C32	C31	1.413(6)
O4	C56	1.336(4)	C32	C33	1.422(5)
N3	C39	1.290(4)	C20	C25	1.418(6)
N3	C40	1.427(4)	C20	C21	1.421(6)
N5	C68	1.421(5)	C1	C10	1.411(5)
N5	C67	1.299(5)	C1	C2	1.440(5)
N4	C46	1.292(4)	C84	C83	1.426(5)
N4	C45	1.424(4)	C41	C42	1.387(6)
N6	C73	1.420(4)	C70	C69	1.388(6)
N6	C74	1.301(4)	C76	C81	1.420(5)
C29	C38	1.401(5)	C65	C60	1.421(6)
C29	C30	1.426(5)	C65	C64	1.413(6)
N2	C17	1.421(5)	C78	C79	1.396(7)
N2	C18	1.296(5)	C11	C10	1.437(5)
C68	C73	1.413(5)	C13	C14	1.384(6)
C68	C69	1.400(5)	C49	C50	1.387(6)
O1	C1	1.299(4)	C81	C80	1.410(6)
O2	C28	1.317(4)	C79	C80	1.365(7)
N1	C12	1.418(4)	C26	C25	1.419(6)
N1	C11	1.301(4)	C26	C27	1.361(5)
C48	C47	1.448(5)	C51	C50	1.392(8)
C48	C53	1.411(6)	C51	C52	1.352(8)
C48	C49	1.424(6)	C59	C60	1.427(6)
C71	C72	1.383(6)	C10	C9	1.450(5)
C71	C70	1.381(6)	C60	C61	1.413(6)
C73	C72	1.396(5)	C25	C24	1.413(5)
C38	C39	1.452(5)	C16	C15	1.382(6)
C38	C37	1.448(4)	C5	C6	1.369(7)

C47	C56	1.403(5)	C21	C22	1.372(6)
C47	C46	1.451(5)	C61	C62	1.364(7)
C56	C55	1.427(5)	C15	C14	1.386(6)
C17	C12	1.410(5)	C2	C3	1.361(5)
C17	C16	1.406(5)	C9	C8	1.409(6)
C66	C67	1.434(5)	C43	C42	1.380(7)
C66	C57	1.411(6)	C64	C63	1.377(6)
C66	C65	1.451(5)	C24	C23	1.373(7)
O6	C84	1.298(4)	C36	C35	1.374(6)
C40	C45	1.404(5)	C8	C7	1.380(6)
C40	C41	1.396(5)	C6	C7	1.401(7)
O5	C57	1.303(4)	C22	C23	1.393(8)
C4	C5	1.412(5)	C62	C63	1.399(7)
C4	C9	1.418(5)	C33	C34	1.357(7)
C4	C3	1.424(6)	C35	C34	1.402(8)
C58	C57	1.436(5)	C14	C87	1.720(6)
C58	C59	1.353(6)	C13	C87	1.745(6)
C45	C44	1.395(5)	C12	C88A	1.634(14)
C37	C32	1.422(5)	C12	C88B	1.740(11)
C37	C36	1.415(6)	C11	C88A	2.139(13)
C28	C19	1.410(5)	C11	C88B	1.713(9)
C28	C27	1.427(5)	O8	C86	1.410(5)
C12	C13	1.402(5)			

**Crystallographic Table 83 Bond Angles for Gd<sub>2</sub>[L<sup>VII</sup>]<sub>3</sub>.**

Atom	Atom	Atom	Angle/°	Atom	Atom	Atom	Angle/°
O4	Gd1	O3	69.21(8)	C3	C4	C9	119.2(3)
N3	Gd1	O3	68.71(9)	C59	C58	C57	121.6(4)
N3	Gd1	O4	103.24(9)	C40	C45	N4	116.1(3)
N4	Gd1	O3	103.88(9)	C44	C45	N4	124.5(3)
N4	Gd1	O4	69.20(9)	C44	C45	C40	119.2(3)
N4	Gd1	N3	63.01(9)	C32	C37	C38	119.3(3)
N2	Gd1	O3	162.36(9)	C36	C37	C38	123.0(4)
N2	Gd1	O4	93.84(9)	C36	C37	C32	117.6(3)
N2	Gd1	N3	122.10(9)	C19	C28	O2	123.1(3)
N2	Gd1	N4	73.08(9)	C27	C28	O2	118.4(3)
O1	Gd1	O3	81.39(9)	C27	C28	C19	118.4(3)
O1	Gd1	O4	141.27(9)	C17	C12	N1	116.3(3)

O1	Gd1	N3	88.17(9)	C13	C12	N1	124.1(3)
O1	Gd1	N4	144.99(9)	C13	C12	C17	119.4(3)
O1	Gd1	N2	111.34(10)	C73	C72	C71	120.8(4)
O2	Gd1	O3	101.11(9)	C84	C75	C74	122.0(3)
O2	Gd1	O4	80.69(9)	C76	C75	C74	118.4(3)
O2	Gd1	N3	166.19(9)	C76	C75	C84	119.6(3)
O2	Gd1	N4	130.11(9)	C83	C82	C81	121.5(4)
O2	Gd1	N2	70.24(9)	C31	C30	C29	121.0(4)
O2	Gd1	O1	80.89(9)	C54	C53	C48	119.2(3)
N1	Gd1	O3	132.77(9)	C52	C53	C48	119.6(4)
N1	Gd1	O4	147.27(9)	C52	C53	C54	121.3(4)
N1	Gd1	N3	72.46(10)	C85	O7	Gd2	126.7(4)
N1	Gd1	N4	80.65(10)	C78	C77	C76	121.8(4)
N1	Gd1	N2	64.54(10)	C75	C74	N6	127.7(3)
N1	Gd1	O1	71.44(9)	C43	C44	C45	120.6(4)
N1	Gd1	O2	111.42(10)	C20	C19	C28	119.5(3)
O4	Gd2	O3	68.77(8)	C18	C19	C28	121.5(3)
N5	Gd2	O3	81.16(9)	C18	C19	C20	119.0(3)
N5	Gd2	O4	115.08(9)	C55	C54	C53	121.2(4)
N6	Gd2	O3	116.69(9)	O5	C57	C66	123.1(3)
N6	Gd2	O4	78.77(9)	C58	C57	C66	118.6(3)
N6	Gd2	N5	65.51(10)	C58	C57	O5	118.3(4)
O6	Gd2	O3	157.93(10)	C31	C32	C37	118.8(3)
O6	Gd2	O4	95.37(9)	C33	C32	C37	119.4(4)
O6	Gd2	N5	120.34(10)	C33	C32	C31	121.7(4)
O6	Gd2	N6	72.75(10)	C25	C20	C19	119.8(4)
O5	Gd2	O3	97.79(10)	C21	C20	C19	123.0(4)
O5	Gd2	O4	161.92(10)	C21	C20	C25	117.0(3)
O5	Gd2	N5	72.81(10)	C54	C55	C56	120.9(4)
O5	Gd2	N6	118.90(11)	C10	C1	O1	123.5(3)
O5	Gd2	O6	93.85(10)	C2	C1	O1	118.1(3)
O7	Gd2	O3	79.76(9)	C2	C1	C10	118.5(3)
O7	Gd2	O4	84.00(10)	C75	C84	O6	122.8(3)
O7	Gd2	N5	145.51(10)	C83	C84	O6	118.3(3)
O7	Gd2	N6	148.95(11)	C83	C84	C75	118.9(3)
O7	Gd2	O6	83.48(10)	C42	C41	C40	120.1(4)
O7	Gd2	O5	81.64(11)	C69	C70	C71	120.0(4)
Gd2	O3	Gd1	110.49(9)	C77	C76	C75	123.8(3)

C29	O3	Gd1	123.9(2)	C81	C76	C75	119.1(3)
C29	O3	Gd2	123.5(2)	C81	C76	C77	117.0(3)
Gd2	O4	Gd1	110.80(9)	C60	C65	C66	119.7(4)
C56	O4	Gd1	120.7(2)	C64	C65	C66	123.3(4)
C56	O4	Gd2	127.3(2)	C64	C65	C60	117.0(4)
C39	N3	Gd1	127.7(2)	C79	C78	C77	120.6(4)
C40	N3	Gd1	114.2(2)	C32	C31	C30	121.7(4)
C40	N3	C39	118.0(3)	C10	C11	N1	126.2(3)
C68	N5	Gd2	114.3(2)	C19	C18	N2	126.6(3)
C67	N5	Gd2	128.3(3)	C14	C13	C12	120.4(4)
C67	N5	C68	117.4(3)	C50	C49	C48	119.8(4)
C46	N4	Gd1	124.9(2)	C76	C81	C82	119.1(4)
C45	N4	Gd1	115.5(2)	C80	C81	C82	121.0(4)
C45	N4	C46	119.4(3)	C80	C81	C76	119.9(4)
C73	N6	Gd2	114.4(2)	C80	C79	C78	119.3(4)
C74	N6	Gd2	127.0(2)	C70	C69	C68	120.7(4)
C74	N6	C73	118.4(3)	C84	C83	C82	121.5(4)
C38	C29	O3	122.8(3)	C27	C26	C25	121.2(4)
C30	C29	O3	118.0(3)	C52	C51	C50	120.0(4)
C30	C29	C38	119.2(3)	C60	C59	C58	121.7(4)
C17	N2	Gd1	113.1(2)	C11	C10	C1	121.2(3)
C18	N2	Gd1	127.4(2)	C9	C10	C1	119.6(3)
C18	N2	C17	119.1(3)	C9	C10	C11	119.1(3)
C73	C68	N5	117.0(3)	C79	C80	C81	121.4(4)
C69	C68	N5	123.9(3)	C59	C60	C65	118.6(4)
C69	C68	C73	119.0(3)	C61	C60	C65	119.9(4)
C1	O1	Gd1	128.4(2)	C61	C60	C59	121.5(4)
C28	O2	Gd1	131.2(2)	C26	C25	C20	118.7(3)
C12	N1	Gd1	114.9(2)	C24	C25	C20	120.3(4)
C11	N1	Gd1	123.7(2)	C24	C25	C26	121.0(4)
C11	N1	C12	120.1(3)	C15	C16	C17	120.8(4)
C53	C48	C47	119.6(4)	C6	C5	C4	121.4(4)
C49	C48	C47	122.2(4)	C22	C21	C20	121.4(4)
C49	C48	C53	118.3(3)	C62	C61	C60	121.5(4)
C70	C71	C72	120.2(4)	C14	C15	C16	120.1(4)
C68	C73	N6	116.6(3)	C3	C2	C1	121.4(4)
C72	C73	N6	124.2(3)	C10	C9	C4	119.4(3)
C72	C73	C68	119.1(3)	C8	C9	C4	117.6(3)

C39	C38	C29	121.5(3)	C8	C9	C10	122.9(3)
C37	C38	C29	119.9(3)	C26	C27	C28	121.8(4)
C37	C38	C39	118.4(3)	C42	C43	C44	120.0(4)
C56	C47	C48	119.5(3)	C63	C64	C65	121.6(4)
C46	C47	C48	119.2(3)	C2	C3	C4	121.1(4)
C46	C47	C56	121.1(3)	C23	C24	C25	120.7(4)
C47	C56	O4	122.4(3)	C35	C36	C37	121.4(4)
C55	C56	O4	118.0(3)	C51	C50	C49	121.2(5)
C55	C56	C47	119.6(3)	C7	C8	C9	121.5(4)
C47	C46	N4	125.2(3)	C7	C6	C5	119.2(4)
C38	C39	N3	124.6(3)	C43	C42	C41	120.4(4)
C12	C17	N2	117.1(3)	C23	C22	C21	121.1(5)
C16	C17	N2	123.7(3)	C15	C14	C13	120.4(4)
C16	C17	C12	118.9(3)	C63	C62	C61	119.0(4)
C57	C66	C67	122.2(3)	C62	C63	C64	120.9(5)
C65	C66	C67	118.1(4)	C51	C52	C53	121.1(5)
C65	C66	C57	119.7(3)	C34	C33	C32	121.0(4)
C66	C67	N5	127.1(4)	C34	C35	C36	120.4(5)
C84	O6	Gd2	137.3(2)	C6	C7	C8	120.6(4)
C45	C40	N3	116.6(3)	C13	C87	C14	111.8(3)
C41	C40	N3	123.6(3)	C22	C23	C24	119.5(4)
C41	C40	C45	119.7(3)	C35	C34	C33	120.0(4)
C57	O5	Gd2	137.1(3)	C11	C88A	C12	100.4(5)
C9	C4	C5	119.7(4)	C11	C88B	C12	115.3(5)
C3	C4	C5	121.0(4)				

**Crystallographic Table 84** Hydrogen Atom Coordinates ( $\text{\AA}\times 10^4$ ) and Isotropic Displacement Parameters ( $\text{\AA}^2\times 10^3$ ) for  $\text{Gd}_2[\text{L}^{\text{VII}}]_3$ .

Atom	x	y	z	U(eq)
H71	8050(3)	13297(3)	-1964(3)	34.7(10)
H46	10642(3)	13616(2)	-3654(2)	21.9(8)
H39	11558(3)	12991(2)	-597(2)	22.9(8)
H67	10363(3)	10965(2)	-555(2)	26.0(8)
H58	13677(4)	8820(2)	-1460(2)	34.9(10)
H72	9085(3)	12590(2)	-3019(2)	27.8(9)
H82	12057(4)	9741(3)	-6114(2)	37.0(11)
H30	14671(3)	10778(2)	-1723(2)	26.8(9)
H7	15040(12)	10815(16)	-3370(30)	45.7(10)

H77	9321(3)	12028(3)	-4670(2)	31.2(9)
H74	9603(3)	11607(2)	-3645(2)	23.7(8)
H44	10119(3)	14636(2)	-3001(2)	32.2(10)
H54	13243(4)	11707(3)	-6070(2)	31.8(10)
H55	13723(3)	11442(2)	-4912(2)	26.3(8)
H41	11016(4)	14204(3)	-605(2)	34.1(10)
H70	8400(4)	13077(3)	-740(2)	36.1(10)
H78	8708(4)	12233(3)	-5792(3)	38.3(11)
H31	14840(4)	10525(2)	-477(2)	32.6(10)
H11	13596(3)	15171(2)	-1738(2)	24.0(8)
H18	14347(3)	14388(2)	-5107(2)	23.8(8)
H13	12497(4)	15826(2)	-2224(2)	30.9(9)
H49	10590(4)	14111(3)	-4753(3)	38.6(11)
H79	9439(5)	11444(3)	-6872(3)	49.2(14)
H69	9768(3)	12129(2)	-562(2)	30.6(9)
H83	12754(4)	9540(2)	-5039(2)	31.8(10)
H26	16847(4)	11551(3)	-6063(2)	33.1(10)
H51	10881(5)	13507(3)	-6983(3)	53.6(15)
H59	13500(4)	8508(2)	-178(3)	37.9(11)
H80	10813(5)	10473(3)	-6818(3)	46.8(13)
H16	12909(3)	15144(2)	-4807(2)	30.1(9)
H5	14677(4)	13891(3)	1117(2)	39.8(11)
H21	14140(4)	14071(3)	-6177(2)	37.4(11)
H61	12706(4)	8787(3)	1211(3)	42.5(12)
H15	11928(4)	16307(2)	-4346(3)	36.4(10)
H2	15998(3)	12647(2)	-1207(2)	29.8(9)
H27	16609(3)	11737(2)	-4763(2)	30.3(9)
H43	9197(4)	15383(3)	-1937(3)	42.1(12)
H64	10593(4)	10949(3)	537(2)	40.1(11)
H3	15737(4)	13072(2)	37(2)	33.6(10)
H24	16327(4)	11882(3)	-7298(2)	41.6(12)
H36	12118(4)	13021(3)	427(2)	40.2(11)
H50	10119(5)	14324(3)	-5940(3)	50.0(14)
H8	12735(4)	15231(3)	-537(2)	33.4(10)
H6	13341(4)	14881(3)	1596(2)	42.6(12)
H42	9656(4)	15175(3)	-748(3)	43.4(12)
H22	14328(5)	13811(3)	-7467(3)	49.1(14)
H14	11718(4)	16645(2)	-3056(3)	35.8(10)



H62	11509(5)	9516(3)	2173(3)	48.0(13)
H63	10480(5)	10619(3)	1825(3)	50.2(14)
H52	12149(4)	12495(3)	-6863(2)	44.7(13)
H33	14340(4)	10832(3)	925(3)	45.4(13)
H35	12336(5)	12745(3)	1668(3)	51.7(14)
H7a	12369(4)	15553(3)	758(3)	42.2(12)
H87a	16339(5)	14018(3)	-3812(3)	56.0(15)
H87b	16587(5)	13593(3)	-3048(3)	56.0(15)
H8a	15910(40)	11849(4)	-3470(20)	42.7(9)
H23	15387(5)	12705(3)	-8030(3)	51.2(14)
H34	13405(5)	11623(3)	1924(3)	54.4(15)
H85a	15130(70)	9670(50)	-3360(50)	60.9(17)
H85b	15630(60)	9760(40)	-3980(40)	60.9(17)
H85c	14330(60)	9490(40)	-3690(40)	60.9(17)
H86a	16760(60)	11010(40)	-2480(40)	60.9(17)
H86b	16490(50)	11890(40)	-2400(40)	60.9(17)
H86c	17480(60)	11590(40)	-2970(40)	60.9(17)
H88a	19395(12)	13424(6)	-9811(6)	66(4)
H88b	19000(12)	13940(6)	-9038(6)	66(4)
H88c	17984(7)	12451(6)	-8015(6)	43(2)
H88d	18329(7)	11892(6)	-8744(6)	43(2)

**Crystallographic Table 85** Atomic Occupancy for  $\text{Gd}_2[\text{L}^{\text{VII}}]_3$ .

<i>Atom</i>	<i>Occupancy</i>	<i>Atom</i>	<i>Occupancy</i>	<i>Atom</i>	<i>Occupancy</i>
C88A	0.500000	C88B	0.500000	H88a	0.500000
H88b	0.500000	H88c	0.500000	H88d	0.500000

Refinement model description

Number of restraints - 3, number of constraints - 126.

Details:

1. Others

Fixed Sof: C88A(0.5) C88B(0.5) H88a(0.5) H88b(0.5) H88c(0.5) H88d(0.5)

**Ho<sub>2</sub>[L<sup>VII</sup>]<sub>3</sub>****Crystallographic Table 86** Crystal data and structure refinement for **Ho<sub>2</sub>[L<sup>VII</sup>]<sub>3</sub>**

Empirical formula	C <sub>87</sub> H <sub>66</sub> Ho <sub>2</sub> N <sub>6</sub> O <sub>9</sub>
Formula weight	1669.39
Temperature/K	180.65
Crystal system	triclinic
Space group	P-1
a/Å	10.3525(1)
b/Å	17.6031(2)
c/Å	18.9169(2)
α/°	82.6930(6)
β/°	86.1741(6)
γ/°	82.4147(6)
Volume/Å <sup>3</sup>	3385.05(6)
Z	2
ρ <sub>calc</sub> /mg/mm <sup>3</sup>	1.6377
m/mm <sup>-1</sup>	2.390
F(000)	1672.6
Crystal size/mm <sup>3</sup>	0.22 × 0.21 × 0.2
Radiation	Mo Kα (λ = 0.71073)
2θ range for data collection	3 to 61.1°
Index ranges	-14 ≤ h ≤ 14, -25 ≤ k ≤ 25, -27 ≤ l ≤ 27
Reflections collected	127024
Independent reflections	20696 [R <sub>int</sub> = 0.0361, R <sub>sigma</sub> = 0.0277]
Data/restraints/parameters	20696/3/944
Goodness-of-fit on F <sup>2</sup>	1.154
Final R indexes [I >= 2σ (I)]	R <sub>1</sub> = 0.0271, wR <sub>2</sub> = 0.0561
Final R indexes [all data]	R <sub>1</sub> = 0.0427, wR <sub>2</sub> = 0.0675
Largest diff. peak/hole / e Å <sup>-3</sup>	3.23/-1.90

**Crystallographic Table 87** Fractional Atomic Coordinates (×10<sup>4</sup>) and Equivalent Isotropic Displacement Parameters (Å<sup>2</sup>×10<sup>3</sup>) for **Ho<sub>2</sub>[L<sup>VII</sup>]<sub>3</sub>**. U<sub>eq</sub> is defined as 1/3 of of the trace of the orthogonalised U<sub>ij</sub> tensor.

Atom	x	y	z	U(eq)
Ho1	2619.07(10)	7771.32(6)	2630.58(6)	14.39(3)
Ho2	6073.49(11)	7857.42(6)	1753.80(6)	15.40(3)
O4	4341.5(17)	8515.7(9)	2378.6(9)	16.3(3)
O3	4313.6(17)	7143.9(9)	1945.2(9)	15.6(3)

N4	3616(2)	7984.6(11)	3765.2(11)	15.8(4)
N5	7139(2)	6663.8(12)	2388.1(12)	18.3(4)
N3	3705(2)	6581.1(11)	3367.4(11)	16.6(4)
C47	4130(2)	9281.8(13)	3346.0(13)	15.6(5)
N6	7103(2)	8050.6(12)	2832.0(11)	17.2(4)
C56	4321(2)	9195.5(13)	2616.3(13)	15.6(4)
O2	1829.3(19)	8594.2(10)	1718.6(10)	22.8(4)
C38	4296(2)	5804.8(14)	2391.8(14)	17.3(5)
O1	1554.8(18)	6961.6(11)	2133.6(10)	20.5(4)
C29	4330(2)	6408.8(13)	1830.9(13)	16.2(5)
C55	4551(2)	9846.8(14)	2113.3(14)	19.5(5)
C46	4045(2)	8614.5(14)	3873.1(13)	16.8(5)
C40	3682(2)	6622.9(14)	4112.7(13)	17.7(5)
N2	1191(2)	8810.2(12)	3133.9(12)	17.9(4)
C81	7968(3)	10747.0(15)	2314.2(17)	25.0(6)
C75	7600(2)	9372.5(14)	2498.3(14)	18.9(5)
C45	3641(2)	7362.6(14)	4324.8(13)	16.8(5)
N1	922(2)	7316.7(12)	3509.3(11)	16.5(4)
O7	4913(2)	8513.5(12)	762.6(11)	28.8(4)
C68	7160(2)	6681.3(14)	3135.2(14)	17.8(5)
C84	7562(3)	9378.7(15)	1752.4(15)	20.7(5)
C30	4419(3)	6232.0(15)	1115.7(14)	21.8(5)
O5	7037(2)	7178.6(11)	933.4(10)	24.4(4)
C37	4374(3)	5015.3(14)	2236.6(15)	21.6(5)
C72	7049(3)	7470.2(16)	4104.2(14)	22.3(5)
C48	4127(2)	10037.3(14)	3571.8(15)	19.7(5)
C74	7536(2)	8675.5(14)	2973.8(14)	18.4(5)
C67	7604(3)	6022.3(15)	2131.0(15)	21.9(5)
C39	4221(2)	5949.0(14)	3129.7(14)	18.0(5)
C4	579(3)	4766.1(15)	2793.3(15)	24.4(6)
C66	7639(3)	5869.1(15)	1405.8(15)	21.6(5)
C53	4374(3)	10668.8(14)	3060.1(16)	21.8(5)
C54	4579(3)	10552.5(15)	2328.1(16)	23.3(5)
C18	989(3)	9529.3(15)	2852.0(15)	20.6(5)
C12	496(2)	7825.8(14)	4028.2(13)	16.7(5)
C1	1203(2)	6286.0(15)	2365.1(15)	20.3(5)
C17	662(2)	8605.3(14)	3833.5(13)	17.5(5)
C28	1667(3)	9338.2(15)	1600.1(14)	20.8(5)

O6	7275.6(19)	8798.7(11)	1456.6(10)	23.5(4)
C73	7119(2)	7412.4(14)	3373.6(13)	17.0(5)
C9	448(3)	5306.1(15)	3298.1(15)	21.7(5)
C32	4470(3)	4865.0(15)	1514.1(16)	24.7(6)
C10	746(2)	6085.0(14)	3074.2(14)	18.0(5)
C13	-8(3)	7593.8(16)	4714.0(14)	23.8(5)
C20	1372(3)	10656.1(15)	1977.8(15)	21.3(5)
C76	7757(2)	10076.4(15)	2788.7(15)	21.2(5)
C44	3579(3)	7448.2(16)	5052.2(14)	24.2(5)
C11	449(2)	6661.9(14)	3555.1(14)	17.9(5)
C65	7962(3)	5075.1(16)	1252.0(17)	27.1(6)
C69	7149(3)	6029.5(15)	3643.6(15)	24.1(5)
C31	4480(3)	5491.6(16)	964.5(16)	25.3(6)
C57	7432(3)	6465.2(16)	838.0(15)	22.9(5)
C71	7050(3)	6816.9(17)	4598.1(15)	26.8(6)
C83	7864(3)	10053.4(17)	1295.1(16)	27.4(6)
C41	3655(3)	5987.2(16)	4633.5(15)	27.1(6)
C43	3589(3)	6810.0(17)	5559.7(15)	29.8(6)
C36	4294(4)	4383.5(16)	2773.3(17)	35.4(7)
C6	-179(4)	3781.6(18)	3683.0(19)	46.8(10)
C16	335(3)	9123.8(16)	4338.9(16)	30.1(6)
C60	8208(3)	4923.2(18)	532.7(18)	33.8(7)
C82	8060(3)	10703.0(17)	1566.4(17)	28.8(6)
C19	1375(2)	9827.5(14)	2144.8(14)	19.7(5)
C77	7651(3)	10146.8(17)	3526.8(16)	27.4(6)
C70	7100(3)	6097.7(17)	4365.1(16)	28.9(6)
C42	3624(3)	6078.8(17)	5350.0(16)	32.8(7)
C78	7786(3)	10829.4(18)	3779.2(19)	34.3(7)
C21	1314(3)	11159.0(16)	2506.2(17)	27.9(6)
C52	4369(3)	11408.8(16)	3276.7(19)	31.8(7)
C22	1369(3)	11939.7(17)	2332.3(18)	33.7(7)
C2	1259(3)	5729.5(17)	1866.6(15)	26.0(6)
C58	7671(3)	6285.4(19)	121.3(17)	35.1(7)
C3	975(3)	5004.6(17)	2073.3(16)	28.4(6)
C8	22(3)	5043.6(17)	4001.6(16)	33.1(7)
C27	1728(3)	9700.3(17)	872.5(16)	27.4(6)
C26	1640(3)	10476.4(17)	713.7(16)	31.4(7)
C15	-189(4)	8884.8(18)	5006.5(17)	35.3(7)

C25	1512(3)	10979.4(16)	1258.7(16)	26.8(6)
C49	3841(3)	10182.5(17)	4288.5(16)	29.7(6)
C62	8650(4)	3555(2)	905(2)	51.9(11)
C5	280(4)	4005.7(17)	3004.5(18)	36.1(7)
C59	8055(4)	5548(2)	-16.3(18)	41.0(8)
C80	8085(3)	11440.8(17)	2592(2)	36.5(7)
C14	-365(3)	8120.8(17)	5195.3(15)	29.2(6)
C24	1556(3)	11781.6(18)	1095.5(18)	35.3(7)
C33	4505(4)	4095.1(17)	1356.2(18)	36.2(7)
C23	1485(3)	12253.4(17)	1617.6(19)	36.9(7)
C63	8352(4)	3694.0(19)	1606(2)	49.5(10)
C79	8004(3)	11485.6(19)	3312(2)	40.6(8)
C7	-318(4)	4310.9(19)	4184.9(18)	43.2(9)
C50	3838(4)	10913.5(18)	4478.4(19)	36.9(7)
C51	4110(3)	11528.8(17)	3975(2)	38.3(8)
C64	7999(4)	4435.7(17)	1779(2)	38.3(8)
C35	4332(5)	3642.5(18)	2597(2)	51.9(11)
C85	5477(5)	8943(3)	163(2)	57.6(12)
C61	8557(4)	4154(2)	381(2)	47.5(9)
O9	1309(2)	7347.0(14)	698.7(12)	38.3(5)
O8	3186(2)	8053.6(15)	3.0(13)	41.1(6)
C86	3838(4)	7628(2)	-532(2)	46.7(9)
C34	4442(4)	3497.9(18)	1887(2)	48.9(10)
C87	82(5)	7821(3)	659(3)	77.6(16)

**Crystallographic Table 88** Anisotropic Displacement Parameters ( $\text{\AA}^2 \times 10^3$ ) for  $\text{Ho}_2[\text{L}^{\text{VII}}]_3$ . The Anisotropic displacement factor exponent takes the form: -  $2\pi^2[h^2a^*{}^2U_{11}+2hka^*b^*U_{12}+\dots]$

Atom	$U_{11}$	$U_{22}$	$U_{33}$	$U_{12}$	$U_{13}$	$U_{23}$
Ho1	15.58(5)	11.24(5)	16.81(6)	-2.06(4)	-0.36(4)	-3.23(4)
Ho2	17.05(6)	13.05(5)	16.53(6)	-3.12(4)	0.53(4)	-2.83(4)
O4	18.6(8)	12.4(8)	19.2(9)	-4.0(6)	1.7(7)	-5.7(6)
O3	18.4(8)	10.3(7)	18.9(8)	-4.3(6)	2.3(7)	-4.0(6)
N4	17.7(10)	11.6(9)	18(1)	-1.0(7)	-0.7(8)	-2.2(7)
N5	18.1(10)	16(1)	21.4(11)	-1.5(8)	-2.6(8)	-5.0(8)
N3	18.8(10)	12.6(9)	18.9(10)	-3.6(8)	-0.3(8)	-2.7(8)
C47	16.8(11)	10.4(10)	20.3(12)	-1.3(8)	-1.9(9)	-5.1(9)
N6	19.1(10)	12.9(9)	19.2(10)	-1.4(8)	-1.3(8)	-1.6(8)
C56	13.9(11)	12.6(10)	21.1(12)	-3.2(8)	-1.0(9)	-3.8(9)

O2	29.8(10)	16.7(9)	21.4(9)	0.3(7)	-5.6(8)	-1.8(7)
C38	17.9(11)	11.4(10)	23.1(12)	-1.3(9)	1.0(9)	-4.9(9)
O1	20.2(9)	22.5(9)	20.9(9)	-8.8(7)	2.1(7)	-6.4(7)
C29	15.5(11)	12.1(10)	21.5(12)	-2.0(8)	1.7(9)	-5.2(9)
C55	19.3(12)	15.5(11)	22.8(13)	-2.9(9)	1.4(10)	0.1(9)
C46	18.1(11)	15.8(11)	17.5(11)	-2.8(9)	-0.9(9)	-5.3(9)
C40	20.5(12)	13.9(11)	18.6(12)	-2.9(9)	0.8(9)	-1.5(9)
N2	18.3(10)	14.8(9)	20.5(10)	-0.7(8)	-2.1(8)	-2.7(8)
C81	19.6(13)	16.9(12)	39.2(16)	-3.8(10)	-0.9(11)	-4.8(11)
C75	16.6(11)	15.6(11)	25.4(13)	-4.7(9)	-1.7(10)	-3.1(10)
C45	18.5(11)	14.3(11)	17.5(11)	-3.2(9)	-1.1(9)	-0.4(9)
N1	16.3(10)	13.8(9)	20.3(10)	-1.5(7)	-1.3(8)	-5.2(8)
O7	30.8(11)	32.0(11)	22.4(10)	-4.0(9)	-4.0(8)	2.8(8)
C68	16.8(11)	14.9(11)	21.3(12)	-0.9(9)	-2.0(9)	-1.5(9)
C84	18.1(12)	18.9(12)	26.0(13)	-6.7(9)	-0.4(10)	-2.3(10)
C30	25.1(13)	19.9(12)	20.8(13)	-3.9(10)	2.4(10)	-4.4(10)
O5	30.8(11)	19.9(9)	22.5(10)	-3.0(8)	5.7(8)	-5.5(7)
C37	25.1(13)	11.5(11)	28.7(14)	-1.1(9)	-0.1(11)	-6.2(10)
C72	22.5(13)	21.5(12)	22.7(13)	-0.6(10)	-0.4(10)	-4.9(10)
C48	18.8(12)	14.1(11)	27.8(13)	-2.7(9)	-1.2(10)	-7.9(10)
C74	16.7(11)	17.4(11)	21.5(12)	-0.2(9)	-2.7(9)	-4.5(9)
C67	21.1(13)	17.2(12)	27.5(14)	0.9(10)	-3.7(10)	-4.8(10)
C39	19.9(12)	11.5(10)	22.9(12)	-4.4(9)	-0.9(10)	-1.0(9)
C4	27.9(14)	19.0(12)	28.1(14)	-1.2(10)	-6.6(11)	-9.1(11)
C66	17.3(12)	20.1(12)	28.2(14)	0.7(9)	-0.4(10)	-9.2(10)
C53	19.9(12)	12.2(11)	34.5(15)	-2.6(9)	-0.5(11)	-6.5(10)
C54	23.5(13)	13.1(11)	32.2(15)	-3.2(10)	0.6(11)	0.8(10)
C18	18.2(12)	18.0(12)	25.2(13)	0.6(9)	-1.6(10)	-3.3(10)
C12	16.3(11)	16.0(11)	18.6(12)	-1.0(9)	-1.5(9)	-6.0(9)
C1	15.7(11)	21.4(12)	26.0(13)	-4.2(9)	-2(1)	-8.7(10)
C17	18.9(12)	14.4(11)	19.5(12)	-1.1(9)	-1.4(9)	-3.8(9)
C28	20.8(12)	19.0(12)	22.3(13)	-0.6(10)	-5.7(10)	-0.4(10)
O6	28.4(10)	21.8(9)	22.3(9)	-11.1(8)	1.1(8)	-3.9(7)
C73	15.9(11)	16.1(11)	18.7(12)	-1.9(9)	-1.2(9)	-0.8(9)
C9	25.8(13)	16.4(11)	23.6(13)	-1.2(10)	-5.7(10)	-4.6(10)
C32	27.9(14)	17.0(12)	31.2(15)	-2.7(10)	0.6(11)	-11.6(11)
C10	18.7(12)	14.7(11)	21.7(12)	-2.4(9)	-0.7(9)	-6.5(9)
C13	32.8(15)	19.2(12)	19.7(13)	-4.4(11)	2.0(11)	-3.8(10)

C20	18.2(12)	15.9(11)	28.9(14)	-0.8(9)	-2.7(10)	0.6(10)
C76	16.5(12)	16.4(11)	31.6(14)	-1.7(9)	-3.4(10)	-5.8(10)
C44	32.0(15)	21.0(13)	20.3(13)	-4.5(11)	0.4(11)	-4.4(10)
C11	18.0(11)	16.8(11)	19.2(12)	-2.8(9)	0.2(9)	-3.4(9)
C65	22.7(13)	22.2(13)	39.1(16)	1.3(10)	-9.3(12)	-14.2(12)
C69	26.4(14)	16.2(12)	29.2(14)	-3.8(10)	-0.9(11)	0.3(10)
C31	28.4(14)	22.8(13)	26.4(14)	-3.7(11)	1.7(11)	-11.1(11)
C57	21.2(13)	22.8(13)	26.1(14)	-4.8(10)	4.9(10)	-9.0(11)
C71	30.3(15)	30.8(15)	18.0(13)	-2.8(12)	-0.3(11)	0.3(11)
C83	32.5(15)	25.1(14)	25.2(14)	-11.0(12)	2.3(12)	0.1(11)
C41	38.6(16)	17.0(12)	25.5(14)	-7.7(11)	3.2(12)	-0.6(10)
C43	41.8(17)	30.5(15)	16.5(13)	-5.8(13)	1.4(12)	-0.7(11)
C36	62(2)	14.7(12)	29.9(16)	-4.5(13)	-2.9(15)	-3.6(11)
C6	89(3)	17.4(14)	36.8(19)	-13.4(16)	-13.7(19)	0.1(13)
C16	46.5(18)	15.6(12)	29.0(15)	-1.9(12)	-0.4(13)	-8.1(11)
C60	31.3(16)	30.9(15)	42.4(19)	2.4(12)	-4.1(14)	-21.7(14)
C82	30.1(15)	21.8(13)	34.9(16)	-9.8(11)	-0.9(12)	2.1(12)
C19	17.3(12)	16.6(11)	23.9(13)	1.7(9)	-4.2(10)	-0.1(10)
C77	28.0(14)	23.0(13)	32.7(15)	-3.2(11)	-3.1(12)	-8.1(11)
C70	32.4(15)	23.7(14)	28.8(15)	-4.7(12)	-0.9(12)	4.6(11)
C42	52(2)	23.7(14)	20.5(14)	-8.9(13)	4.0(13)	5.6(11)
C78	34.9(17)	32.7(16)	39.5(18)	-7.2(13)	-0.5(14)	-18.5(14)
C21	30.9(15)	19.9(13)	31.0(15)	1.0(11)	-0.2(12)	-0.5(11)
C52	34.5(16)	13.1(12)	49.2(19)	-4.7(11)	-2.1(14)	-7.4(12)
C22	41.0(18)	17.3(13)	41.8(18)	-0.5(12)	-2.1(14)	-3.0(12)
C2	27.0(14)	30.6(14)	24.0(14)	-11.1(11)	6.1(11)	-13.0(11)
C58	47.3(19)	32.5(16)	26.0(15)	-7.4(14)	9.5(14)	-8.6(13)
C3	30.6(15)	28.1(14)	30.4(15)	-7.0(12)	1.9(12)	-17.0(12)
C8	56(2)	19.3(13)	25.9(15)	-6.4(13)	-6.2(14)	-3.9(11)
C27	34.3(16)	23.4(13)	23.6(14)	-0.7(11)	-5.1(12)	-0.7(11)
C26	41.8(18)	26.6(14)	23.5(14)	-1.0(13)	-6.0(13)	5.2(11)
C15	56(2)	24.1(14)	26.4(15)	-1.0(14)	4.1(14)	-14.4(12)
C25	27.4(14)	20.0(13)	31.3(15)	-1.4(11)	-5.5(12)	3.6(11)
C49	39.3(17)	21.8(13)	30.2(15)	-6.6(12)	2.7(13)	-11.3(11)
C62	58(2)	28.4(17)	74(3)	11.8(16)	-26(2)	-31.4(18)
C5	58(2)	17.0(13)	35.9(17)	-2.8(13)	-11.5(15)	-8.2(12)
C59	53(2)	40.4(19)	31.3(17)	-3.1(16)	8.0(15)	-19.9(15)
C80	39.4(18)	18.9(13)	53(2)	-8.7(12)	0.0(15)	-8.1(13)

C14	40.9(17)	26.8(14)	20.1(13)	-2.0(12)	2.9(12)	-7.9(11)
C24	46.2(19)	23.0(14)	34.0(17)	-3.5(13)	-5.8(14)	8.1(12)
C33	53(2)	20.7(14)	37.5(18)	-4.3(13)	0.2(15)	-14.9(13)
C23	44.0(19)	16.0(13)	49(2)	-2.8(12)	-7.1(15)	3.4(13)
C63	65(3)	21.3(15)	66(3)	5.2(15)	-28(2)	-13.9(16)
C79	41.8(19)	26.6(15)	59(2)	-11.4(14)	0.9(16)	-20.4(15)
C7	78(3)	24.7(15)	28.3(16)	-13.8(16)	-7.0(17)	2.7(13)
C50	49(2)	27.6(15)	38.0(18)	-6.1(14)	3.1(15)	-19.4(13)
C51	47(2)	18.8(14)	53(2)	-4.8(13)	-3.0(16)	-20.0(14)
C64	51(2)	20.1(14)	47(2)	3.0(13)	-17.6(16)	-12.3(13)
C35	96(3)	12.9(14)	46(2)	-7.4(17)	-4(2)	-2.4(14)
C85	69(3)	67(3)	38(2)	-35(2)	-17.0(19)	20.1(19)
C61	50(2)	40(2)	56(2)	6.3(16)	-9.1(18)	-32.3(18)
O9	46.3(14)	44.9(14)	26.9(11)	-10.9(11)	-5.7(10)	-8.9(10)
O8	39.9(14)	47.9(14)	37.7(13)	-9.7(11)	-2.7(11)	-8.3(11)
C86	52(2)	52(2)	35.7(19)	1.1(18)	-4.8(16)	-9.7(17)
C34	85(3)	15.3(14)	49(2)	-6.9(16)	0(2)	-13.0(14)
C87	59(3)	103(4)	78(4)	-13(3)	-39(3)	-19(3)

**Crystallographic Table 89** Bond Lengths for  $\text{Ho}_2[\text{L}^{\text{VII}}]_3$ .

Atom	Atom	Length/Å	Atom	Atom	Length/Å
O4	C56	1.328(3)	C12	C17	1.405(3)
O3	C29	1.337(3)	C12	C13	1.397(4)
N4	C46	1.292(3)	C1	C10	1.410(4)
N4	C45	1.422(3)	C1	C2	1.437(4)
N5	C68	1.419(3)	C17	C16	1.400(4)
N5	C67	1.307(3)	C28	C19	1.418(4)
N3	C40	1.420(3)	C28	C27	1.442(4)
N3	C39	1.290(3)	C9	C10	1.450(4)
C47	C56	1.406(3)	C9	C8	1.414(4)
C47	C46	1.449(3)	C32	C31	1.417(4)
C47	C48	1.447(3)	C32	C33	1.420(4)
N6	C74	1.305(3)	C10	C11	1.438(3)
N6	C73	1.420(3)	C13	C14	1.381(4)
C56	C55	1.429(3)	C20	C19	1.452(3)
O2	C28	1.291(3)	C20	C21	1.410(4)
C38	C29	1.406(3)	C20	C25	1.412(4)
C38	C37	1.447(3)	C76	C77	1.413(4)



C38	C39	1.445(4)	C44	C43	1.381(4)
O1	C1	1.304(3)	C65	C60	1.420(4)
C29	C30	1.421(4)	C65	C64	1.404(5)
C55	C54	1.360(4)	C69	C70	1.382(4)
C40	C45	1.405(3)	C57	C58	1.429(4)
C40	C41	1.396(4)	C71	C70	1.386(4)
N2	C18	1.305(3)	C83	C82	1.355(4)
N2	C17	1.420(3)	C41	C42	1.383(4)
C81	C76	1.421(4)	C43	C42	1.390(4)
C81	C82	1.423(4)	C36	C35	1.381(4)
C81	C80	1.412(4)	C6	C5	1.367(5)
C75	C84	1.413(4)	C6	C7	1.401(5)
C75	C74	1.433(4)	C16	C15	1.378(4)
C75	C76	1.450(3)	C60	C59	1.413(5)
C45	C44	1.400(4)	C60	C61	1.415(4)
N1	C12	1.422(3)	C77	C78	1.375(4)
N1	C11	1.302(3)	C78	C79	1.396(5)
O7	C85	1.417(4)	C21	C22	1.380(4)
C68	C73	1.411(3)	C52	C51	1.368(5)
C68	C69	1.401(4)	C22	C23	1.398(5)
C84	O6	1.300(3)	C2	C3	1.351(4)
C84	C83	1.434(4)	C58	C59	1.360(4)
C30	C31	1.362(4)	C8	C7	1.377(4)
O5	C57	1.299(3)	C27	C26	1.353(4)
C37	C32	1.420(4)	C26	C25	1.431(4)
C37	C36	1.414(4)	C15	C14	1.380(4)
C72	C73	1.395(4)	C25	C24	1.413(4)
C72	C71	1.387(4)	C49	C50	1.379(4)
C48	C53	1.416(4)	C62	C63	1.386(6)
C48	C49	1.416(4)	C62	C61	1.351(6)
C67	C66	1.428(4)	C80	C79	1.371(5)
C4	C9	1.419(4)	C24	C23	1.361(5)
C4	C3	1.423(4)	C33	C34	1.363(5)
C4	C5	1.416(4)	C63	C64	1.383(4)
C66	C65	1.455(4)	C50	C51	1.393(5)
C66	C57	1.409(4)	C35	C34	1.394(5)
C53	C54	1.423(4)	O9	C87	1.426(5)
C53	C52	1.414(4)	O8	C86	1.417(4)

C18      C19      1.425(4)

**Crystallographic Table 90** Bond Angles for **Ho<sub>2</sub>[L<sup>VII</sup>]<sub>3</sub>**.

Atom	Atom	Atom	Angle/°	Atom	Atom	Atom	Angle/°
O3	Ho1	O4	68.85(6)	C5	C4	C3	120.8(3)
N4	Ho1	O4	68.89(6)	C65	C66	C67	118.5(3)
N4	Ho1	O3	106.11(6)	C57	C66	C67	122.0(2)
N3	Ho1	O4	101.82(6)	C57	C66	C65	119.4(3)
N3	Ho1	O3	69.95(6)	C54	C53	C48	119.2(2)
N3	Ho1	N4	63.32(6)	C52	C53	C48	119.9(3)
O2	Ho1	O4	79.99(7)	C52	C53	C54	120.9(3)
O2	Ho1	O3	95.14(7)	C53	C54	C55	121.2(2)
O2	Ho1	N4	131.80(6)	C19	C18	N2	126.3(2)
O2	Ho1	N3	162.62(7)	C17	C12	N1	116.3(2)
O1	Ho1	O4	140.73(6)	C13	C12	N1	124.4(2)
O1	Ho1	O3	78.58(6)	C13	C12	C17	119.2(2)
O1	Ho1	N4	144.05(7)	C10	C1	O1	123.1(2)
O1	Ho1	N3	86.41(7)	C2	C1	O1	118.1(2)
O1	Ho1	O2	81.74(7)	C2	C1	C10	118.8(2)
N2	Ho1	O4	93.12(6)	C12	C17	N2	117.1(2)
N2	Ho1	O3	160.09(6)	C16	C17	N2	124.2(2)
N2	Ho1	N4	73.30(7)	C16	C17	C12	118.7(2)
N2	Ho1	N3	124.13(7)	C19	C28	O2	123.7(2)
N2	Ho1	O2	72.65(7)	C27	C28	O2	118.8(2)
N2	Ho1	O1	114.00(7)	C27	C28	C19	117.4(2)
N1	Ho1	O4	147.55(6)	C68	C73	N6	115.9(2)
N1	Ho1	O3	133.90(6)	C72	C73	N6	124.6(2)
N1	Ho1	N4	80.99(7)	C72	C73	C68	119.5(2)
N1	Ho1	N3	73.71(7)	C10	C9	C4	119.4(2)
N1	Ho1	O2	113.98(7)	C8	C9	C4	117.0(2)
N1	Ho1	O1	71.70(7)	C8	C9	C10	123.6(2)
N1	Ho1	N2	66.00(7)	C31	C32	C37	119.1(2)
O3	Ho2	O4	69.20(6)	C33	C32	C37	119.5(3)
N5	Ho2	O4	116.15(7)	C33	C32	C31	121.3(3)
N5	Ho2	O3	80.13(7)	C9	C10	C1	119.5(2)
N6	Ho2	O4	78.21(6)	C11	C10	C1	120.7(2)
N6	Ho2	O3	115.16(6)	C11	C10	C9	119.6(2)
N6	Ho2	N5	66.30(7)	C14	C13	C12	121.0(3)

O7	Ho2	O4	81.27(7)	C21	C20	C19	123.0(3)
O7	Ho2	O3	84.50(7)	C25	C20	C19	119.5(2)
O7	Ho2	N5	150.11(7)	C25	C20	C21	117.4(2)
O7	Ho2	N6	143.52(7)	C75	C76	C81	119.2(3)
O5	Ho2	O4	157.23(7)	C77	C76	C81	117.3(2)
O5	Ho2	O3	93.96(7)	C77	C76	C75	123.4(2)
O5	Ho2	N5	73.77(7)	C43	C44	C45	120.4(3)
O5	Ho2	N6	123.92(7)	C10	C11	N1	126.5(2)
O5	Ho2	O7	81.95(7)	C60	C65	C66	119.3(3)
O6	Ho2	O4	99.48(6)	C64	C65	C66	123.4(3)
O6	Ho2	O3	162.94(7)	C64	C65	C60	117.2(3)
O6	Ho2	N5	116.80(7)	C70	C69	C68	120.9(3)
O6	Ho2	N6	73.03(7)	C32	C31	C30	121.4(3)
O6	Ho2	O7	81.08(7)	C66	C57	O5	123.0(2)
O6	Ho2	O5	93.00(7)	C58	C57	O5	117.9(3)
C45	N4	C46	119.1(2)	C58	C57	C66	119.1(3)
C67	N5	C68	118.1(2)	C70	C71	C72	119.7(3)
C39	N3	C40	118.5(2)	C82	C83	C84	121.2(3)
C46	C47	C56	120.6(2)	C42	C41	C40	120.6(3)
C48	C47	C56	119.2(2)	C42	C43	C44	120.0(3)
C48	C47	C46	120.0(2)	C35	C36	C37	120.8(3)
C73	N6	C74	118.4(2)	C7	C6	C5	119.1(3)
C47	C56	O4	121.9(2)	C15	C16	C17	121.0(3)
C55	C56	O4	118.4(2)	C59	C60	C65	118.7(3)
C55	C56	C47	119.7(2)	C61	C60	C65	119.6(3)
C37	C38	C29	120.0(2)	C61	C60	C59	121.7(3)
C39	C38	C29	121.5(2)	C83	C82	C81	121.6(3)
C39	C38	C37	118.5(2)	C28	C19	C18	121.2(2)
C38	C29	O3	122.4(2)	C20	C19	C18	118.5(2)
C30	C29	O3	118.6(2)	C20	C19	C28	120.2(2)
C30	C29	C38	119.0(2)	C78	C77	C76	121.5(3)
C54	C55	C56	121.0(2)	C71	C70	C69	120.3(3)
C47	C46	N4	125.3(2)	C43	C42	C41	120.2(3)
C45	C40	N3	116.5(2)	C79	C78	C77	121.0(3)
C41	C40	N3	124.3(2)	C22	C21	C20	121.7(3)
C41	C40	C45	119.2(2)	C51	C52	C53	120.9(3)
C17	N2	C18	118.7(2)	C23	C22	C21	120.2(3)
C82	C81	C76	119.1(2)	C3	C2	C1	121.6(3)

C80	C81	C76	119.6(3)	C59	C58	C57	120.9(3)
C80	C81	C82	121.3(3)	C2	C3	C4	121.2(3)
C74	C75	C84	121.2(2)	C7	C8	C9	121.9(3)
C76	C75	C84	119.6(2)	C26	C27	C28	121.7(3)
C76	C75	C74	119.1(2)	C25	C26	C27	121.8(3)
C40	C45	N4	116.0(2)	C14	C15	C16	120.3(3)
C44	C45	N4	124.5(2)	C26	C25	C20	118.6(3)
C44	C45	C40	119.5(2)	C24	C25	C20	119.7(3)
C11	N1	C12	118.8(2)	C24	C25	C26	121.7(3)
C73	C68	N5	117.0(2)	C50	C49	C48	120.5(3)
C69	C68	N5	124.2(2)	C61	C62	C63	119.3(3)
C69	C68	C73	118.7(2)	C6	C5	C4	121.5(3)
O6	C84	C75	123.2(2)	C58	C59	C60	122.2(3)
C83	C84	C75	118.7(2)	C79	C80	C81	121.6(3)
C83	C84	O6	118.0(2)	C15	C14	C13	119.7(3)
C31	C30	C29	121.4(3)	C23	C24	C25	121.5(3)
C32	C37	C38	119.1(2)	C34	C33	C32	121.1(3)
C36	C37	C38	123.0(3)	C24	C23	C22	119.5(3)
C36	C37	C32	117.9(2)	C64	C63	C62	121.1(4)
C71	C72	C73	120.8(3)	C80	C79	C78	118.9(3)
C53	C48	C47	119.6(2)	C8	C7	C6	120.6(3)
C49	C48	C47	122.5(2)	C51	C50	C49	121.3(3)
C49	C48	C53	117.8(2)	C50	C51	C52	119.4(3)
C75	C74	N6	126.4(2)	C63	C64	C65	121.1(3)
C66	C67	N5	127.4(3)	C34	C35	C36	120.9(3)
C38	C39	N3	125.5(2)	C62	C61	C60	121.5(3)
C3	C4	C9	119.3(2)	C35	C34	C33	119.7(3)
C5	C4	C9	119.9(3)				

**Crystallographic Table 91** Hydrogen Atom Coordinates ( $\text{\AA}\times 10^4$ ) and Isotropic Displacement Parameters ( $\text{\AA}^2\times 10^3$ ) for  $\text{Ho}_2[\text{L}^{\text{VII}}]_3$ .

Atom	x	y	z	U(eq)
H55	4685(2)	9786.0(14)	1620.9(14)	23.4(6)
H46	4328(2)	8642.6(14)	4335.6(13)	20.1(6)
H7	4250(20)	8341(16)	608(12)	43.2(7)
H30	4436(3)	6638.8(15)	734.9(14)	26.2(6)
H72	7001(3)	7963.3(16)	4265.2(14)	26.7(6)
H74	7838(2)	8667.1(14)	3438.4(14)	22.1(6)

H67	7959(3)	5610.7(15)	2464.5(15)	26.3(6)
H39	4583(2)	5544.3(14)	3467.9(14)	21.6(6)
H54	4739(3)	10975.7(15)	1983.3(16)	27.9(7)
H18	541(3)	9888.3(15)	3146.6(15)	24.7(6)
H13	-105(3)	7065.4(16)	4851.1(14)	28.6(7)
H44	3530(3)	7948.6(16)	5197.9(14)	29.1(7)
H11	-153(2)	6554.4(14)	3945.0(14)	21.4(6)
H69	7175(3)	5534.0(15)	3490.4(15)	29.0(7)
H31	4530(3)	5393.3(16)	480.5(16)	30.3(7)
H71	7016(3)	6862.0(17)	5094.3(15)	32.2(7)
H83	7927(3)	10044.8(17)	792.8(16)	32.8(7)
H41	3658(3)	5487.0(16)	4494.6(15)	32.5(7)
H43	3571(3)	6871.0(17)	6052.2(15)	35.8(8)
H36	4212(4)	4469.7(16)	3260.8(17)	42.5(9)
H6	-401(4)	3273.9(18)	3812.4(19)	56.2(12)
H16	476(3)	9648.3(16)	4220.1(16)	36.1(8)
H82	8263(3)	11139.5(17)	1249.7(17)	34.6(7)
H77	7484(3)	9712.5(17)	3856.2(16)	32.9(7)
H70	7101(3)	5649.5(17)	4702.9(16)	34.7(7)
H42	3627(3)	5640.6(17)	5699.7(16)	39.4(8)
H78	7729(3)	10854.9(18)	4279.1(19)	41.1(8)
H21	1234(3)	10954.8(16)	2994.5(17)	33.5(7)
H52	4549(3)	11828.5(16)	2932.4(19)	38.1(8)
H22	1328(3)	12264.9(17)	2699.4(18)	40.4(8)
H2	1503(3)	5874.7(17)	1380.0(15)	31.2(7)
H58	7561(3)	6686.8(19)	-264.0(17)	42.1(9)
H3	1039(3)	4647.8(17)	1731.8(16)	34.1(7)
H8	-31(3)	5382.2(17)	4358.3(16)	39.8(8)
H27	1833(3)	9385.8(17)	495.0(16)	32.8(7)
H26	1663(3)	10693.1(17)	227.4(16)	37.7(8)
H15	-429(4)	9247.6(18)	5338.1(17)	42.4(9)
H49	3649(3)	9772.8(17)	4641.3(16)	35.6(8)
H62	8916(4)	3045(2)	795(2)	62.2(13)
H5	401(4)	3643.1(17)	2667.1(18)	43.4(9)
H59	8227(4)	5448(2)	-497.8(18)	49.2(10)
H80	8223(3)	11887.5(17)	2272(2)	43.8(9)
H14	-731(3)	7958.1(17)	5654.8(15)	35.0(7)
H24	1638(3)	11996.7(18)	610.4(18)	42.4(9)

H33	4572(4)	3994.5(17)	872.6(18)	43.5(9)
H23	1513(3)	12791.7(17)	1497.0(19)	44.3(9)
H63	8390(4)	3272.0(19)	1974(2)	59.4(12)
H79	8096(3)	11955.5(19)	3490(2)	48.7(10)
H7a	-649(4)	4163.4(19)	4655.8(18)	51.9(11)
H50	3646(4)	10999.4(18)	4962.1(19)	44.3(9)
H51	4115(3)	12027.5(17)	4116(2)	46.0(9)
H64	7778(4)	4513.9(17)	2262(2)	46.0(9)
H35	4283(5)	3225.4(18)	2966(2)	62.3(13)
H85a	6090(20)	8595(4)	-103(10)	86.4(18)
H85b	4787(5)	9199(15)	-147(9)	86.4(18)
H85c	5950(30)	9333(12)	324(2)	86.4(18)
H61	8731(4)	4056(2)	-101(2)	57.0(11)
H86a	3810(20)	7951(6)	-994(3)	70.1(13)
H86b	4749(8)	7470(14)	-414(8)	70.1(13)
H86c	3409(17)	7169(9)	-557(10)	70.1(13)
H34	4474(4)	2985.3(18)	1773(2)	58.7(12)
H8a	2580(30)	7820(13)	202(16)	61.7(8)
H9	1500(20)	7230(20)	1127.9(17)	57.5(8)
H87a	78(14)	8180(15)	218(11)	116(2)
H87b	-616(6)	7495(4)	660(20)	116(2)
H87c	-59(18)	8113(17)	1071(11)	116(2)

#### Refinement model description

Number of restraints - 3, number of constraints - 125.

Details:

##### 1. Fixed Uiso

At 1.2 times of:

All C(H) groups

At 1.5 times of:

All C(H,H,H) groups, All O(H) groups

##### 2. Restrained distances

O7-H7

0.87 with sigma of 0.01

C85-H7

1.863295 with sigma of 0.02

Ho2-H7

2.957705 with sigma of 0.02

3.a Aromatic/amide H refined with riding coordinates:

C55(H55), C46(H46), C30(H30), C72(H72), C74(H74), C67(H67), C39(H39),  
C54(H54), C18(H18), C13(H13), C44(H44), C11(H11), C69(H69), C31(H31),  
C71(H71),

C83(H83), C41(H41), C43(H43), C36(H36), C6(H6), C16(H16), C82(H82), C77(H77),  
C70(H70), C42(H42), C78(H78), C21(H21), C52(H52), C22(H22), C2(H2), C58(H58),  
C3(H3), C8(H8), C27(H27), C26(H26), C15(H15), C49(H49), C62(H62), C5(H5),  
C59(H59), C80(H80), C14(H14), C24(H24), C33(H33), C23(H23), C63(H63),  
C79(H79),

C7(H7a), C50(H50), C51(H51), C64(H64), C35(H35), C61(H61), C34(H34)

3.b Idealised Me refined as rotating group:

C85(H85a,H85b,H85c), C86(H86a,H86b,H86c), C87(H87a,H87b,H87c)

3.c Idealised tetrahedral OH refined as rotating group:

O9(H9), O8(H8a)

**Yb<sub>2</sub>[L<sup>VII</sup>]<sub>3</sub>**

**Crystallographic Table 92** Crystal data and structure refinement for **Yb<sub>2</sub>[L<sup>VII</sup>]<sub>3</sub>**

Empirical formula	C <sub>87</sub> H <sub>62</sub> Cl <sub>4</sub> N <sub>6</sub> O <sub>7</sub> Yb <sub>2</sub>
Formula weight	1791.38
Temperature/K	180.45
Crystal system	monoclinic
Space group	P2 <sub>1</sub> /c
a/Å	17.4061(8)
b/Å	20.4222(10)
c/Å	20.6605(10)
α/°	90
β/°	96.2697(8)
γ/°	90
Volume/Å <sup>3</sup>	7300.3(6)
Z	4
ρ <sub>calc</sub> /mg/mm <sup>3</sup>	1.6298
m/mm <sup>-1</sup>	2.756
F(000)	3562.0
Crystal size/mm <sup>3</sup>	0.12 × 0.1 × 0.09
Radiation	Mo Kα (λ = 0.71073)
2θ range for data collection	2.82 to 52.74°
Index ranges	-21 ≤ h ≤ 21, -25 ≤ k ≤ 25, -25 ≤ l ≤ 25
Reflections collected	104807
Independent reflections	14938 [R <sub>int</sub> = 0.0586, R <sub>sigma</sub> = 0.0431]
Data/restraints/parameters	14938/3/958
Goodness-of-fit on F <sup>2</sup>	1.062
Final R indexes [I >= 2σ (I)]	R <sub>1</sub> = 0.0666, wR <sub>2</sub> = 0.1489
Final R indexes [all data]	R <sub>1</sub> = 0.0772, wR <sub>2</sub> = 0.1561
Largest diff. peak/hole / e Å <sup>-3</sup>	5.13/-1.84

**Crystallographic Table 93** Fractional Atomic Coordinates (×10<sup>4</sup>) and Equivalent Isotropic Displacement Parameters (Å<sup>2</sup>×10<sup>3</sup>) for **Yb<sub>2</sub>[L<sup>VII</sup>]<sub>3</sub>**. U<sub>eq</sub> is defined as 1/3 of of the trace of the orthogonalised U<sub>ij</sub> tensor.

Atom	x	y	z	U(eq)
Yb1	7266.79(18)	5570.08(17)	7475.85(16)	17.83(10)
Yb2	7078.7(2)	3998.24(18)	6506.85(17)	20.58(10)
C45	8344(5)	4876(4)	8744(4)	22.0(17)
O4	7843(3)	4893(3)	6779(3)	19.4(11)



O3	6458(3)	4703(3)	7125(3)	21.4(12)
O2	8083(3)	6270(3)	7111(3)	22.3(12)
C47	9185(5)	4947(4)	7175(4)	22.6(17)
O1	6479(3)	5980(3)	6649(3)	29.0(14)
N6	8201(4)	3461(3)	7054(3)	22.4(15)
O6	7719(3)	3662(3)	5729(3)	30.1(14)
C19	9007(5)	6516(4)	8022(4)	23.3(17)
N3	6983(4)	4878(3)	8408(3)	20.7(14)
N2	7754(4)	6277(3)	8386(3)	21.3(14)
N4	8409(4)	5005(3)	8072(3)	20.8(14)
O5	6094(4)	3415(3)	6125(3)	31.7(15)
C30	5094(5)	4642(4)	6844(5)	27.3(19)
C40	7587(5)	4805(4)	8919(4)	24.8(18)
C39	6305(5)	4631(4)	8474(4)	22.0(17)
C73	8152(5)	3302(4)	7720(4)	24.3(18)
C54	9501(5)	5100(5)	5879(5)	33(2)
C55	8747(5)	5055(4)	6020(4)	24.9(18)
C10	5272(5)	6234(4)	7048(4)	24.5(18)
C4	4129(5)	6375(5)	6242(5)	34(2)
N1	6265(4)	6134(3)	7980(3)	21.5(14)
C38	5649(4)	4665(4)	7984(4)	20.0(16)
C46	9032(4)	4845(4)	7836(4)	22.6(17)
C29	5748(4)	4678(4)	7327(4)	19.7(16)
C11	5591(4)	6316(4)	7717(4)	22.4(17)
C28	8785(5)	6439(4)	7350(4)	23.4(17)
C8	3930(5)	6340(5)	7377(5)	31(2)
C56	8583(5)	4968(4)	6669(4)	22.3(17)
C75	9021(5)	3436(4)	6158(4)	23.6(18)
C31	4372(5)	4608(4)	7026(5)	29(2)
C9	4453(5)	6328(4)	6899(4)	25.3(18)
C32	4243(5)	4614(4)	7696(5)	31(2)
C67	6119(5)	3072(4)	7481(4)	23.5(17)
C25	10363(5)	6700(5)	7801(5)	31(2)
C18	8438(5)	6532(4)	8477(4)	24.6(18)
C60	4020(5)	2912(4)	6810(5)	31(2)
C65	4686(5)	2967(4)	7267(4)	26.0(18)
C74	8849(5)	3333(4)	6809(4)	23.6(18)
C27	9355(5)	6557(5)	6912(5)	31(2)

C64	4593(5)	2916(5)	7934(5)	32(2)
C72	8787(5)	3240(5)	8186(4)	30(2)
C66	5426(5)	3102(4)	7034(4)	24.1(18)
C41	7487(6)	4692(5)	9574(4)	33(2)
C81	10007(6)	3392(5)	5386(5)	35(2)
O7	6560(4)	4824(3)	5763(3)	36.5(16)
C12	6451(5)	6265(4)	8652(4)	21.2(17)
N5	6786(4)	3320(4)	7396(3)	22.1(15)
C63	3878(6)	2799(5)	8132(6)	42(3)
C83	8653(6)	3556(6)	4988(5)	41(3)
C51	11511(6)	5129(6)	6712(7)	52(3)
C44	8971(6)	4856(5)	9222(5)	37(2)
C48	9978(5)	4998(4)	7030(5)	27.5(19)
C5	3323(5)	6475(5)	6085(5)	38(2)
C37	4878(5)	4656(4)	8180(5)	27.7(19)
C76	9819(5)	3380(4)	6033(5)	27.3(19)
C71	8685(5)	3109(5)	8824(5)	33(2)
C17	7238(5)	6348(4)	8868(4)	24.2(18)
C13	5916(6)	6295(5)	9106(5)	33(2)
C43	8856(6)	4735(6)	9858(5)	44(3)
C53	10127(5)	5072(4)	6368(5)	31(2)
C57	5467(5)	3225(4)	6362(4)	27.9(19)
C49	10615(5)	5020(5)	7520(6)	39(2)
C68	7407(5)	3239(4)	7897(4)	23.4(17)
C6	2846(5)	6504(5)	6564(6)	40(2)
C2	5389(5)	6181(5)	5888(5)	35(2)
C1	5740(5)	6124(4)	6545(4)	23.8(18)
C69	7315(5)	3120(4)	8549(4)	29(2)
C33	3464(6)	4600(5)	7873(6)	44(3)
C50	11361(6)	5081(6)	7347(7)	52(3)
C84	8441(5)	3558(5)	5648(4)	30(2)
C26	10107(5)	6680(5)	7127(5)	34(2)
C24	11154(5)	6774(5)	8028(6)	41(3)
C58	4779(5)	3136(5)	5926(5)	38(2)
C14	6151(7)	6404(6)	9758(5)	44(3)
C82	9392(6)	3471(6)	4872(5)	45(3)
C59	4091(5)	2983(5)	6137(5)	36(2)
C77	10442(6)	3332(5)	6527(5)	40(2)

C3	4632(6)	6303(6)	5742(5)	42(3)
C16	7477(6)	6442(5)	9526(4)	37(2)
C42	8116(7)	4646(6)	10043(5)	45(3)
C20	9814(5)	6618(4)	8257(5)	28.0(19)
C52	10915(6)	5128(5)	6229(6)	44(3)
C61	3291(5)	2779(5)	7045(6)	40(2)
C62	3223(6)	2714(5)	7688(6)	47(3)
C36	4725(6)	4709(5)	8834(5)	37(2)
C7	3147(5)	6429(5)	7212(5)	36(2)
C70	7945(6)	3052(5)	9008(5)	37(2)
C34	3354(6)	4644(6)	8516(7)	54(3)
Cl1	5733(2)	1928(2)	4641.8(19)	82.6(12)
Cl2	6420(3)	1397(3)	5860(2)	110.0(18)
Cl4	9367(3)	6302(3)	10625(3)	123(2)
Cl3	8650(6)	6574(6)	11752(4)	201(4)
C21	10091(5)	6624(5)	8926(5)	35(2)
C35	3971(7)	4702(6)	8990(6)	52(3)
C22	10869(6)	6712(5)	9124(6)	48(3)
C80	10785(7)	3343(7)	5258(6)	55(3)
C79	11372(6)	3296(7)	5745(6)	58(3)
C23	11407(6)	6781(6)	8681(6)	48(3)
C78	11194(6)	3295(6)	6386(6)	50(3)
C15	6938(7)	6473(6)	9971(5)	47(3)
C85	6647(10)	4978(7)	5109(6)	73(4)
C87	9001(10)	6904(9)	11056(11)	113(8)
C86	6386(10)	2070(8)	5338(8)	84(5)

**Crystallographic Table 94** Anisotropic Displacement Parameters ( $\text{\AA}^2 \times 10^3$ ) for  $\text{Yb}_2[\text{L}^{\text{VII}}]_3$ . The Anisotropic displacement factor exponent takes the form: -  $2\pi^2[h^2a^{*2}U_{11}+2hka^*b^*U_{12}+\dots]$

Atom	$U_{11}$	$U_{22}$	$U_{33}$	$U_{12}$	$U_{13}$	$U_{23}$
Yb1	13.51(16)	22.65(18)	17.51(17)	0.48(13)	2.49(12)	1.55(13)
Yb2	17.15(18)	25.62(19)	19.00(18)	-4.08(14)	2.16(13)	-0.78(14)
C45	20(4)	25(4)	19(4)	4(3)	-5(3)	2(3)
O4	12(3)	25(3)	21(3)	-4(2)	3(2)	-4(2)
O3	15(3)	29(3)	21(3)	-2(2)	7(2)	0(2)
O2	19(3)	27(3)	22(3)	-6(2)	4(2)	2(2)
C47	21(4)	18(4)	29(4)	-1(3)	6(3)	-7(3)
O1	20(3)	41(4)	27(3)	3(3)	8(2)	8(3)

N6	21(3)	23(4)	24(4)	-5(3)	5(3)	1(3)
O6	22(3)	48(4)	20(3)	-1(3)	2(2)	-7(3)
C19	19(4)	20(4)	30(4)	-2(3)	1(3)	2(3)
N3	17(3)	26(4)	19(3)	6(3)	4(3)	-1(3)
N2	23(4)	22(4)	19(3)	2(3)	4(3)	1(3)
N4	16(3)	26(4)	20(3)	2(3)	0(3)	1(3)
O5	30(3)	43(4)	22(3)	-17(3)	6(3)	-2(3)
C30	22(4)	25(4)	34(5)	-6(4)	3(4)	1(4)
C40	30(5)	18(4)	26(4)	7(3)	2(4)	-1(3)
C39	26(4)	19(4)	22(4)	3(3)	11(3)	1(3)
C73	23(4)	27(4)	23(4)	4(3)	2(3)	0(3)
C54	31(5)	40(5)	30(5)	-4(4)	16(4)	-4(4)
C55	22(4)	28(5)	26(4)	-6(3)	8(3)	-2(4)
C10	23(4)	18(4)	33(5)	2(3)	6(4)	6(3)
C4	27(5)	36(5)	39(5)	3(4)	4(4)	15(4)
N1	25(4)	18(3)	22(3)	1(3)	7(3)	3(3)
C38	15(4)	18(4)	27(4)	1(3)	7(3)	5(3)
C46	11(4)	23(4)	34(5)	-1(3)	-3(3)	-3(4)
C29	15(4)	12(4)	33(5)	-2(3)	8(3)	2(3)
C11	11(4)	21(4)	35(5)	-1(3)	5(3)	6(3)
C28	20(4)	23(4)	29(4)	-5(3)	7(3)	1(3)
C8	23(4)	31(5)	41(5)	7(4)	6(4)	-2(4)
C56	17(4)	15(4)	36(5)	-1(3)	9(3)	-7(3)
C75	24(4)	22(4)	26(4)	1(3)	8(3)	-5(3)
C31	11(4)	24(5)	52(6)	0(3)	4(4)	3(4)
C9	21(4)	18(4)	38(5)	4(3)	6(4)	6(4)
C32	23(5)	21(4)	50(6)	3(3)	16(4)	7(4)
C67	29(4)	15(4)	28(4)	1(3)	7(4)	2(3)
C25	21(4)	28(5)	43(5)	-2(4)	6(4)	5(4)
C18	22(4)	28(5)	23(4)	-1(3)	-3(3)	-1(3)
C60	23(4)	23(5)	49(6)	-3(4)	9(4)	-2(4)
C65	26(4)	17(4)	37(5)	-1(3)	9(4)	-1(4)
C74	19(4)	21(4)	32(5)	1(3)	7(3)	-2(3)
C27	35(5)	32(5)	28(5)	-3(4)	8(4)	3(4)
C64	27(5)	28(5)	43(6)	-4(4)	7(4)	3(4)
C72	27(5)	32(5)	32(5)	-1(4)	7(4)	3(4)
C66	22(4)	12(4)	38(5)	-3(3)	4(4)	-2(3)
C41	42(6)	36(5)	22(4)	5(4)	4(4)	6(4)

C81	32(5)	33(5)	41(6)	4(4)	17(4)	0(4)
O7	43(4)	41(4)	26(3)	4(3)	2(3)	5(3)
C12	16(4)	24(4)	25(4)	2(3)	9(3)	0(3)
N5	15(3)	29(4)	23(4)	-1(3)	4(3)	3(3)
C63	44(6)	41(6)	47(6)	4(5)	26(5)	7(5)
C83	37(6)	60(7)	27(5)	-1(5)	7(4)	-16(5)
C51	19(5)	55(7)	86(9)	-2(5)	20(5)	2(7)
C44	33(5)	46(6)	31(5)	5(4)	-2(4)	4(4)
C48	18(4)	20(4)	45(5)	3(3)	8(4)	-3(4)
C5	25(5)	43(6)	44(6)	7(4)	-7(4)	5(5)
C37	20(4)	24(4)	41(5)	2(3)	12(4)	7(4)
C76	23(4)	24(4)	38(5)	3(3)	15(4)	0(4)
C71	23(5)	43(6)	33(5)	3(4)	-2(4)	-1(4)
C17	32(5)	20(4)	22(4)	0(3)	8(3)	-4(3)
C13	31(5)	35(5)	36(5)	6(4)	13(4)	7(4)
C43	37(6)	60(7)	33(5)	7(5)	-11(4)	5(5)
C53	25(5)	25(5)	47(6)	-7(4)	14(4)	-3(4)
C57	24(4)	26(5)	34(5)	-7(4)	4(4)	-3(4)
C49	17(4)	46(6)	53(6)	-3(4)	9(4)	-6(5)
C68	23(4)	23(4)	25(4)	3(3)	4(3)	2(3)
C6	13(4)	41(6)	65(7)	5(4)	7(4)	3(5)
C2	25(5)	52(6)	29(5)	11(4)	6(4)	20(4)
C1	15(4)	28(5)	28(4)	4(3)	3(3)	11(4)
C69	26(5)	30(5)	31(5)	-6(4)	2(4)	8(4)
C33	19(5)	39(6)	75(8)	0(4)	14(5)	9(5)
C50	13(5)	60(8)	81(9)	-1(5)	-1(5)	1(6)
C84	29(5)	31(5)	31(5)	-3(4)	12(4)	-10(4)
C26	24(5)	29(5)	52(6)	-5(4)	17(4)	6(4)
C24	22(5)	27(5)	73(8)	-4(4)	8(5)	-1(5)
C58	29(5)	50(6)	33(5)	-14(4)	-1(4)	-4(5)
C14	49(6)	55(7)	32(5)	8(5)	19(5)	4(5)
C82	50(7)	54(7)	32(5)	3(5)	16(5)	-12(5)
C59	19(4)	43(6)	43(6)	-12(4)	-1(4)	-3(5)
C77	27(5)	51(6)	43(6)	9(5)	10(4)	7(5)
C3	37(6)	56(7)	34(5)	12(5)	3(4)	20(5)
C16	32(5)	55(7)	25(5)	-2(5)	4(4)	0(4)
C42	60(7)	49(7)	24(5)	9(5)	-2(5)	7(4)
C20	24(4)	22(4)	37(5)	2(3)	-1(4)	-2(4)

C52	27(5)	36(6)	75(8)	1(4)	30(5)	2(5)
C61	18(4)	33(5)	68(7)	-6(4)	7(5)	-5(5)
C62	31(6)	39(6)	75(8)	-1(5)	25(5)	0(6)
C36	31(5)	40(6)	45(6)	-4(4)	22(4)	6(5)
C7	23(5)	39(6)	48(6)	3(4)	9(4)	-1(5)
C70	51(6)	31(5)	29(5)	-6(4)	6(4)	8(4)
C34	26(6)	57(7)	83(9)	8(5)	26(6)	11(7)
Cl1	76(2)	116(3)	60(2)	-6(2)	27.6(19)	4(2)
Cl2	64(3)	177(5)	91(3)	2(3)	15(2)	49(3)
Cl4	91(3)	160(5)	115(4)	23(3)	-8(3)	-48(4)
Cl3	216(9)	295(12)	104(5)	40(8)	68(6)	23(6)
C21	27(5)	44(6)	33(5)	-1(4)	-5(4)	4(4)
C35	45(7)	52(7)	67(8)	11(5)	43(6)	8(6)
C22	42(6)	43(6)	53(7)	2(5)	-22(5)	3(5)
C80	48(7)	74(9)	50(7)	8(6)	33(6)	1(6)
C79	25(5)	92(10)	60(8)	17(6)	24(5)	18(7)
C23	22(5)	45(6)	75(8)	0(4)	-7(5)	3(6)
C78	23(5)	70(8)	59(7)	5(5)	12(5)	14(6)
C15	54(7)	68(8)	22(5)	4(6)	15(5)	-5(5)
C85	121(13)	55(8)	43(7)	11(8)	15(8)	5(6)
C87	76(12)	69(11)	180(20)	23(9)	-25(13)	-40(13)
C86	83(11)	73(10)	98(12)	-16(9)	24(9)	-30(9)

**Crystallographic Table 95 Bond Lengths for Yb<sub>2</sub>[L<sup>VII</sup>]<sub>3</sub>.**

Atom	Atom	Length/Å	Atom	Atom	Length/Å
Yb1	O4	2.303(5)	C32	C33	1.443(12)
Yb1	O3	2.328(6)	C67	C66	1.438(12)
Yb1	O2	2.206(5)	C67	N5	1.296(11)
Yb1	O1	2.234(6)	C25	C26	1.416(14)
Yb1	N3	2.481(7)	C25	C24	1.413(13)
Yb1	N2	2.447(7)	C25	C20	1.423(13)
Yb1	N4	2.504(6)	C60	C65	1.417(13)
Yb1	N1	2.419(7)	C60	C59	1.416(14)
Yb2	O4	2.294(5)	C60	C61	1.433(12)
Yb2	O3	2.274(6)	C65	C64	1.408(13)
Yb2	N6	2.413(7)	C65	C66	1.450(12)
Yb2	O6	2.165(6)	C27	C26	1.360(13)
Yb2	O5	2.165(6)	C64	C63	1.372(13)

Yb2	O7	2.392(7)	C72	C71	1.374(13)
Yb2	N5	2.400(7)	C66	C57	1.422(13)
C45	N4	1.430(10)	C41	C42	1.384(14)
C45	C40	1.410(12)	C81	C76	1.412(13)
C45	C44	1.390(12)	C81	C82	1.432(15)
O4	C56	1.340(9)	C81	C80	1.412(14)
O3	C29	1.347(9)	O7	C85	1.411(13)
O2	C28	1.313(10)	C12	C17	1.403(12)
C47	C46	1.434(12)	C12	C13	1.393(12)
C47	C56	1.398(12)	N5	C68	1.422(11)
C47	C48	1.449(11)	C63	C62	1.394(16)
O1	C1	1.315(10)	C83	C84	1.450(13)
N6	C73	1.424(11)	C83	C82	1.346(14)
N6	C74	1.312(10)	C51	C50	1.368(18)
O6	C84	1.302(11)	C51	C52	1.358(17)
C19	C28	1.409(12)	C44	C43	1.374(14)
C19	C18	1.439(12)	C48	C53	1.426(13)
C19	C20	1.450(12)	C48	C49	1.419(13)
N3	C40	1.415(10)	C5	C6	1.361(14)
N3	C39	1.304(11)	C37	C36	1.409(13)
N2	C18	1.294(11)	C76	C77	1.410(14)
N2	C17	1.419(10)	C71	C70	1.387(14)
N4	C46	1.278(10)	C17	C16	1.391(12)
O5	C57	1.302(10)	C13	C14	1.381(14)
C30	C29	1.432(12)	C43	C42	1.395(16)
C30	C31	1.352(12)	C53	C52	1.436(12)
C40	C41	1.402(12)	C57	C58	1.430(12)
C39	C38	1.444(11)	C49	C50	1.390(13)
C73	C72	1.391(12)	C68	C69	1.395(12)
C73	C68	1.392(12)	C6	C7	1.391(15)
C54	C55	1.378(12)	C2	C1	1.432(12)
C54	C53	1.404(14)	C2	C3	1.342(13)
C55	C56	1.413(12)	C69	C70	1.377(13)
C10	C11	1.442(12)	C33	C34	1.367(17)
C10	C9	1.438(12)	C24	C23	1.372(16)
C10	C1	1.408(12)	C58	C59	1.355(13)
C4	C9	1.416(13)	C14	C15	1.398(16)
C4	C5	1.419(13)	C77	C78	1.374(13)

C4	C3	1.432(14)	C16	C15	1.385(14)
N1	C11	1.291(10)	C20	C21	1.412(13)
N1	C12	1.416(11)	C61	C62	1.354(16)
C38	C29	1.387(12)	C36	C35	1.386(13)
C38	C37	1.442(11)	C34	C35	1.377(18)
C28	C27	1.435(12)	C11	C86	1.757(17)
C8	C9	1.414(12)	C12	C86	1.745(18)
C8	C7	1.381(13)	C14	C87	1.683(18)
C75	C74	1.425(12)	C13	C87	1.76(2)
C75	C76	1.444(11)	C21	C22	1.384(14)
C75	C84	1.401(13)	C22	C23	1.385(17)
C31	C32	1.427(14)	C80	C79	1.355(17)
C32	C37	1.411(13)	C79	C78	1.393(16)

**Crystallographic Table 96** Bond Angles for  $\text{Yb}_2[\text{L}^{\text{VII}}]_3$ .

Atom	Atom	Atom	Angle/°	Atom	Atom	Atom	Angle/°
O3	Yb1	O4	68.82(18)	C55	C56	O4	118.2(8)
O2	Yb1	O4	80.5(2)	C55	C56	C47	120.0(7)
O2	Yb1	O3	140.9(2)	C76	C75	C74	117.5(8)
O1	Yb1	O4	91.1(2)	C84	C75	C74	121.9(8)
O1	Yb1	O3	75.3(2)	C84	C75	C76	120.6(8)
O1	Yb1	O2	81.9(2)	C32	C31	C30	121.2(9)
N3	Yb1	O4	106.3(2)	C4	C9	C10	119.8(8)
N3	Yb1	O3	69.2(2)	C8	C9	C10	123.4(8)
N3	Yb1	O2	145.6(2)	C8	C9	C4	116.7(8)
N3	Yb1	O1	130.5(2)	C37	C32	C31	119.7(8)
N2	Yb1	O4	134.1(2)	C33	C32	C31	119.8(9)
N2	Yb1	O3	146.6(2)	C33	C32	C37	120.5(9)
N2	Yb1	O2	72.5(2)	N5	C67	C66	126.7(8)
N2	Yb1	O1	119.9(2)	C24	C25	C26	121.3(9)
N2	Yb1	N3	79.7(2)	C20	C25	C26	119.1(8)
N4	Yb1	O4	69.8(2)	C20	C25	C24	119.6(9)
N4	Yb1	O3	103.0(2)	N2	C18	C19	125.7(8)
N4	Yb1	O2	87.7(2)	C59	C60	C65	119.6(8)
N4	Yb1	O1	159.6(2)	C61	C60	C65	118.6(9)
N4	Yb1	N3	64.6(2)	C61	C60	C59	121.8(9)
N4	Yb1	N2	72.8(2)	C64	C65	C60	118.2(8)
N1	Yb1	O4	159.8(2)	C66	C65	C60	119.0(8)



N1	Yb1	O3	93.2(2)	C66	C65	C64	122.7(8)
N1	Yb1	O2	111.1(2)	C75	C74	N6	127.8(8)
N1	Yb1	O1	74.9(2)	C26	C27	C28	122.1(9)
N1	Yb1	N3	73.9(2)	C63	C64	C65	120.7(9)
N1	Yb1	N2	66.0(2)	C71	C72	C73	120.4(8)
N1	Yb1	N4	125.4(2)	C65	C66	C67	119.5(8)
O3	Yb2	O4	69.91(19)	C57	C66	C67	120.4(8)
N6	Yb2	O4	80.2(2)	C57	C66	C65	120.0(8)
N6	Yb2	O3	115.8(2)	C42	C41	C40	121.0(10)
O6	Yb2	O4	95.9(2)	C82	C81	C76	118.2(8)
O6	Yb2	O3	158.8(2)	C80	C81	C76	120.1(10)
O6	Yb2	N6	75.3(2)	C80	C81	C82	121.7(10)
O5	Yb2	O4	160.5(2)	C85	O7	Yb2	134.4(7)
O5	Yb2	O3	98.4(2)	C17	C12	N1	116.4(7)
O5	Yb2	N6	119.3(2)	C13	C12	N1	124.7(8)
O5	Yb2	O6	90.4(2)	C13	C12	C17	118.8(8)
O7	Yb2	O4	76.3(2)	C67	N5	Yb2	126.7(6)
O7	Yb2	O3	75.2(2)	C68	N5	Yb2	114.6(5)
O7	Yb2	N6	148.4(2)	C68	N5	C67	118.5(7)
O7	Yb2	O6	86.3(2)	C62	C63	C64	121.8(10)
O7	Yb2	O5	85.7(2)	C82	C83	C84	121.0(10)
N5	Yb2	O4	116.0(2)	C52	C51	C50	119.6(9)
N5	Yb2	O3	77.4(2)	C43	C44	C45	119.9(9)
N5	Yb2	N6	66.9(2)	C53	C48	C47	118.9(8)
N5	Yb2	O6	123.7(2)	C49	C48	C47	122.8(9)
N5	Yb2	O5	74.6(2)	C49	C48	C53	118.1(8)
N5	Yb2	O7	143.3(2)	C6	C5	C4	120.5(9)
C40	C45	N4	116.4(7)	C32	C37	C38	118.8(8)
C44	C45	N4	123.7(8)	C36	C37	C38	123.2(9)
C44	C45	C40	119.9(8)	C36	C37	C32	117.9(8)
Yb2	O4	Yb1	110.5(2)	C81	C76	C75	119.6(9)
C56	O4	Yb1	122.0(5)	C77	C76	C75	123.7(8)
C56	O4	Yb2	126.2(5)	C77	C76	C81	116.6(8)
Yb2	O3	Yb1	110.4(2)	C70	C71	C72	120.1(9)
C29	O3	Yb1	118.4(5)	C12	C17	N2	115.8(7)
C29	O3	Yb2	131.2(5)	C16	C17	N2	123.8(8)
C28	O2	Yb1	130.4(5)	C16	C17	C12	120.2(8)
C56	C47	C46	121.0(7)	C14	C13	C12	121.0(9)

C48	C47	C46	119.2(8)	C42	C43	C44	121.4(9)
C48	C47	C56	119.8(8)	C48	C53	C54	119.0(8)
C1	O1	Yb1	135.8(5)	C52	C53	C54	122.3(9)
C73	N6	Yb2	115.1(5)	C52	C53	C48	118.6(9)
C74	N6	Yb2	126.6(6)	C66	C57	O5	123.6(8)
C74	N6	C73	118.2(7)	C58	C57	O5	118.7(8)
C84	O6	Yb2	136.8(6)	C58	C57	C66	117.7(8)
C18	C19	C28	120.8(7)	C50	C49	C48	119.9(10)
C20	C19	C28	119.9(8)	N5	C68	C73	116.9(7)
C20	C19	C18	119.3(8)	C69	C68	C73	118.7(8)
C40	N3	Yb1	116.4(5)	C69	C68	N5	124.4(8)
C39	N3	Yb1	124.1(5)	C7	C6	C5	119.9(9)
C39	N3	C40	119.2(7)	C3	C2	C1	122.2(9)
C18	N2	Yb1	125.8(6)	C10	C1	O1	123.4(8)
C17	N2	Yb1	114.0(5)	C2	C1	O1	118.7(8)
C17	N2	C18	119.9(7)	C2	C1	C10	117.8(8)
C45	N4	Yb1	114.8(5)	C70	C69	C68	121.1(9)
C46	N4	Yb1	126.2(6)	C34	C33	C32	118.7(10)
C46	N4	C45	119.0(7)	C49	C50	C51	122.3(11)
C57	O5	Yb2	133.6(6)	C75	C84	O6	123.9(8)
C31	C30	C29	120.2(9)	C83	C84	O6	118.0(9)
N3	C40	C45	115.9(7)	C83	C84	C75	118.0(8)
C41	C40	C45	118.8(8)	C27	C26	C25	121.0(9)
C41	C40	N3	125.3(8)	C23	C24	C25	121.5(10)
C38	C39	N3	124.3(7)	C59	C58	C57	122.4(9)
C72	C73	N6	124.3(8)	C15	C14	C13	119.9(9)
C68	C73	N6	115.6(7)	C83	C82	C81	122.2(10)
C68	C73	C72	120.1(8)	C58	C59	C60	121.0(9)
C53	C54	C55	121.8(9)	C78	C77	C76	121.7(10)
C56	C55	C54	120.3(8)	C2	C3	C4	121.4(9)
C9	C10	C11	117.4(8)	C15	C16	C17	120.3(9)
C1	C10	C11	122.1(8)	C43	C42	C41	118.9(9)
C1	C10	C9	120.2(8)	C25	C20	C19	119.4(8)
C5	C4	C9	120.6(9)	C21	C20	C19	122.9(9)
C3	C4	C9	118.2(8)	C21	C20	C25	117.6(8)
C3	C4	C5	121.2(9)	C53	C52	C51	121.4(11)
C11	N1	Yb1	128.2(6)	C62	C61	C60	121.8(10)
C12	N1	Yb1	114.4(5)	C61	C62	C63	118.8(9)

C12	N1	C11	117.3(7)	C35	C36	C37	120.4(11)
C29	C38	C39	120.9(7)	C6	C7	C8	120.7(9)
C37	C38	C39	119.4(8)	C69	C70	C71	119.7(9)
C37	C38	C29	119.7(8)	C35	C34	C33	121.1(10)
N4	C46	C47	125.4(8)	C22	C21	C20	120.6(10)
C30	C29	O3	118.1(7)	C34	C35	C36	121.3(11)
C38	C29	O3	121.4(7)	C23	C22	C21	121.8(10)
C38	C29	C30	120.4(7)	C79	C80	C81	121.8(10)
N1	C11	C10	127.5(8)	C78	C79	C80	118.5(10)
C19	C28	O2	123.0(7)	C22	C23	C24	118.8(10)
C27	C28	O2	119.0(8)	C79	C78	C77	121.2(11)
C27	C28	C19	118.0(8)	C16	C15	C14	119.8(9)
C7	C8	C9	121.4(9)	C13	C87	C14	109.9(11)
C47	C56	O4	121.7(8)	C12	C86	C11	110.5(9)

**Crystallographic Table 97** Hydrogen Atom Coordinates ( $\text{\AA}\times 10^4$ ) and Isotropic Displacement Parameters ( $\text{\AA}^2\times 10^3$ ) for  $\text{Yb}_2[\text{L}^{\text{VII}}]_3$ .

Atom	x	y	z	U(eq)
H30	5167(5)	4642(4)	6395(5)	33(2)
H39	6240(5)	4414(4)	8871(4)	26(2)
H54	9601(5)	5150(5)	5439(5)	39(3)
H55	8336(5)	5083(4)	5679(4)	30(2)
H46	9426(4)	4642(4)	8122(4)	27(2)
H11	5270(4)	6528(4)	7996(4)	27(2)
H8	4123(5)	6286(5)	7822(5)	38(2)
H31	3942(5)	4579(4)	6701(5)	35(2)
H67	6085(5)	2846(4)	7879(4)	28(2)
H18	8576(5)	6748(4)	8880(4)	30(2)
H74	9253(5)	3150(4)	7100(4)	28(2)
H27	9201(5)	6549(5)	6456(5)	38(2)
H64	5029(5)	2962(5)	8249(5)	39(2)
H72	9295(5)	3288(5)	8064(4)	36(2)
H41	6980(6)	4647(5)	9698(4)	40(3)
H7	6440(50)	5188(16)	5950(10)	55(2)
H63	3828(6)	2775(5)	8585(6)	51(3)
H83	8264(6)	3615(6)	4633(5)	50(3)
H51	12028(6)	5163(6)	6610(7)	63(4)
H44	9479(6)	4926(5)	9108(5)	44(3)

H5	3116(5)	6523(5)	5643(5)	46(3)
H71	9121(5)	3057(5)	9138(5)	40(3)
H13	5382(6)	6239(5)	8966(5)	40(3)
H43	9290(6)	4711(6)	10179(5)	53(3)
H49	10531(5)	4992(5)	7966(6)	46(3)
H6	2308(5)	6576(5)	6456(6)	48(3)
H2	5703(5)	6131(5)	5542(5)	42(3)
H69	6809(5)	3085(4)	8678(4)	35(2)
H33	3036(6)	4562(5)	7548(6)	52(3)
H50	11782(6)	5089(6)	7681(7)	62(4)
H26	10467(5)	6754(5)	6820(5)	41(3)
H24	11519(5)	6821(5)	7722(6)	49(3)
H58	4805(5)	3185(5)	5471(5)	45(3)
H14	5779(7)	6433(6)	10060(5)	53(3)
H82	9510(6)	3464(6)	4434(5)	54(3)
H59	3650(5)	2923(5)	5830(5)	43(3)
H77	10339(6)	3325(5)	6970(5)	48(3)
H3	4426(6)	6342(6)	5299(5)	51(3)
H16	8011(6)	6484(5)	9671(4)	44(3)
H42	8045(7)	4556(6)	10483(5)	54(3)
H52	11022(6)	5166(5)	5789(6)	53(3)
H61	2844(5)	2735(5)	6741(6)	48(3)
H62	2738(6)	2613(5)	7834(6)	56(3)
H36	5141(6)	4750(5)	9170(5)	45(3)
H7a	2810(5)	6439(5)	7544(5)	43(3)
H70	7873(6)	2966(5)	9450(5)	44(3)
H34	2844(6)	4633(6)	8639(7)	65(4)
H21	9739(5)	6568(5)	9242(5)	42(3)
H35	3878(7)	4738(6)	9434(6)	62(4)
H22	11040(6)	6724(5)	9576(6)	58(3)
H80	10901(7)	3342(7)	4820(6)	66(4)
H79	11893(6)	3265(7)	5650(6)	69(4)
H23	11940(6)	6832(6)	8827(6)	58(3)
H78	11600(6)	3268(6)	6731(6)	60(4)
H15	7102(7)	6541(6)	10420(5)	57(3)
H85a	6136(10)	5030(50)	4864(13)	109(7)
H85b	6940(60)	5390(30)	5093(7)	109(7)
H85c	6930(60)	4620(30)	4917(17)	109(7)

H87a	9408(10)	7231(9)	11187(11)	135(9)
H87b	8576(10)	7126(9)	10783(11)	135(9)
H86a	6907(10)	2154(8)	5207(8)	100(6)
H86b	6223(10)	2463(8)	5568(8)	100(6)

## Refinement model description

Number of restraints - 3, number of constraints - 119.

### Details:

#### 1. Fixed Uiso

At 1.2 times of:

All C(H) groups, All C(H,H) groups

At 1.5 times of:

All C(H,H,H) groups, All O(H) groups

#### 2. Restrained distances

O7-H7

0.87 with sigma of 0.01

C85-H7

1.886919 with sigma of 0.02

Yb2-H7

2.888526 with sigma of 0.02

#### 3.a Secondary CH2 refined with riding coordinates:

C87(H87a,H87b), C86(H86a,H86b)

#### 3.b Aromatic/amide H refined with riding coordinates:

C30(H30), C39(H39), C54(H54), C55(H55), C46(H46), C11(H11), C8(H8), C31(H31),  
C67(H67), C18(H18), C74(H74), C27(H27), C64(H64), C72(H72), C41(H41),

C63(H63),

C83(H83), C51(H51), C44(H44), C5(H5), C71(H71), C13(H13), C43(H43), C49(H49),  
C6(H6), C2(H2), C69(H69), C33(H33), C50(H50), C26(H26), C24(H24), C58(H58),  
C14(H14), C82(H82), C59(H59), C77(H77), C3(H3), C16(H16), C42(H42), C52(H52),  
C61(H61), C62(H62), C36(H36), C7(H7a), C70(H70), C34(H34), C21(H21), C35(H35),  
C22(H22), C80(H80), C79(H79), C23(H23), C78(H78), C15(H15)

#### 3.c Idealised Me refined as rotating group:

C85(H85a,H85b,H85c)

**Eu<sub>2</sub>[L<sup>VII</sup>]<sub>3</sub>****Crystallographic Table 98** Crystal data and structure refinement for **Eu<sub>2</sub>[L<sup>VII</sup>]<sub>3</sub>**

Empirical formula	C <sub>87</sub> H <sub>62</sub> N <sub>6</sub> O <sub>7</sub> Eu <sub>2</sub> Cl <sub>4</sub>
Formula weight	1749.24
Temperature/K	180.45
Crystal system	monoclinic
Space group	P2 <sub>1</sub> /c
a/Å	17.512(7)
b/Å	20.500(8)
c/Å	20.517(8)
α/°	90
β/°	96.457(7)
γ/°	90
Volume/Å <sup>3</sup>	7319(5)
Z	4
ρ <sub>calc</sub> /mg/mm <sup>3</sup>	1.5873
m/mm <sup>-1</sup>	1.907
F(000)	3507.5
Crystal size/mm <sup>3</sup>	0.12 × 0.1 × 0.08
Radiation	Mo Kα (λ = 0.71073)
2θ range for data collection	2.82 to 29.5°
Index ranges	-12 ≤ h ≤ 12, -14 ≤ k ≤ 14, -14 ≤ l ≤ 14
Reflections collected	23881
Independent reflections	2833 [R <sub>int</sub> = 0.1459, R <sub>sigma</sub> = 0.0769]
Data/restraints/parameters	2833/3/438
Goodness-of-fit on F <sup>2</sup>	1.129
Final R indexes [I >= 2σ (I)]	R <sub>1</sub> = 0.0647, wR <sub>2</sub> = 0.1637
Final R indexes [all data]	R <sub>1</sub> = 0.0946, wR <sub>2</sub> = 0.1807
Largest diff. peak/hole / e Å <sup>-3</sup>	2.65/-0.83

**Crystallographic Table 99** Fractional Atomic Coordinates (×10<sup>4</sup>) and Equivalent Isotropic Displacement Parameters (Å<sup>2</sup>×10<sup>3</sup>) for **Eu<sub>2</sub>[L<sup>VII</sup>]<sub>3</sub>**. U<sub>eq</sub> is defined as 1/3 of the trace of the orthogonalised U<sub>ij</sub> tensor.

Atom	x	y	z	U(eq)
Eu1	2252.8(10)	574.8(9)	7422.2(8)	23.7(9)
Eu2	2103.5(10)	-1047.0(9)	6424.3(8)	26.2(9)
O4	2899(12)	-119(9)	6720(9)	23(6)
N6	3261(14)	-1590(11)	7010(11)	16(8)

O3	1443(12)	-336(9)	7066(9)	27(6)
N1	1227(14)	1146(11)	7963(12)	18(8)
C75	4100(20)	-1594(14)	6109(16)	26(10)
C64	-318(19)	-2095(14)	7964(15)	29(10)
N2	2728(16)	1303(12)	8360(12)	27(8)
C65	-251(17)	-2058(13)	7289(15)	11(10)
C84	3500(20)	-1493(15)	5596(17)	34(11)
C66	470(18)	-1961(14)	7029(15)	17(10)
N5	1827(16)	-1751(12)	7371(12)	26(8)
C76	4900(20)	-1652(14)	6049(17)	28(11)
C57	500(20)	-1837(16)	6340(17)	36(11)
C63	-994(19)	-2210(14)	8219(16)	34(11)
C62	-1661(19)	-2275(14)	7786(15)	32(10)
C74	3934(18)	-1713(14)	6769(15)	21(10)
C67	1173(18)	-1981(14)	7458(15)	15(10)
O1	1382(12)	970(9)	6587(9)	27(6)
O6	2795(12)	-1395(9)	5649(9)	30(7)
C31	-629(19)	-423(13)	6987(15)	23(10)
O2	3099(12)	1324(9)	7086(9)	26(7)
C37	-117(18)	-371(13)	8168(15)	15(10)
C30	88(18)	-399(13)	6820(15)	24(10)
O5	1109(12)	-1675(9)	6082(9)	28(7)
C38	648(18)	-364(13)	7938(15)	15(10)
O7	1545(12)	-160(10)	5680(10)	43(7)
C60	-930(20)	-2107(15)	6841(17)	33(11)
C61	-1649(19)	-2227(14)	7097(15)	29(10)
C59	-889(18)	-2047(13)	6179(15)	17(10)
C82	4520(20)	-1550(14)	4830(17)	36(11)
C81	5080(20)	-1605(16)	5378(18)	41(12)
C83	3770(20)	-1480(15)	4942(16)	37(11)
C29	760(18)	-360(13)	7290(15)	11(9)
C39	1288(18)	-411(14)	8446(15)	24(10)
C2	270(20)	1165(14)	5856(16)	34(11)
C73	3193(19)	-1733(14)	7693(15)	16(10)
C28	3800(20)	1457(14)	7352(16)	21(10)
C51	6520(20)	98(15)	6742(16)	39(11)
C17	2196(18)	1350(13)	8850(15)	9(9)
C72	3847(19)	-1787(14)	8168(15)	29(10)

C11	524(18)	1316(13)	7712(14)	16(10)
C25	5360(20)	1682(14)	7832(17)	26(10)
C32	-760(20)	-419(15)	7662(17)	39(11)
C10	203(19)	1209(14)	7045(15)	18(10)
C35	-1009(19)	-319(14)	8979(16)	33(11)
C49	5640(20)	-41(15)	7570(17)	41(11)
C19	4013(19)	1523(14)	8033(16)	23(10)
C36	-245(18)	-299(14)	8829(16)	28(10)
C47	4228(19)	-73(14)	7176(16)	18(10)
C26	5097(19)	1679(14)	7160(16)	31(11)
C77	5503(19)	-1679(14)	6546(16)	30(11)
C33	-1520(20)	-417(15)	7864(17)	46(12)
C52	5960(20)	112(15)	6258(17)	41(11)
C55	3792(19)	43(14)	5999(16)	33(11)
C1	650(20)	1119(15)	6507(17)	34(11)
C48	5026(19)	-28(14)	7038(16)	18(10)
C20	4820(20)	1625(14)	8295(16)	25(10)
C78	6260(19)	-1700(14)	6434(16)	28(10)
C18	3393(19)	1568(14)	8435(14)	19(10)
C53	5162(19)	69(15)	6387(16)	24(10)
C56	3660(20)	-53(15)	6659(17)	27(10)
Cl3	5682(9)	-1307(8)	9358(7)	157(6)
N4	3419(14)	-3(11)	8069(11)	14(8)
Cl4	6406(11)	-1628(9)	8283(9)	196(8)
N3	1983(14)	-143(11)	8387(11)	13(7)
C70	2995(19)	-1961(14)	8996(16)	28(10)
C80	5900(20)	-1645(15)	5284(18)	51(12)
C8	-1109(19)	1326(14)	7384(16)	28(10)
C5	-1770(20)	1449(15)	6105(17)	41(11)
C6	-2230(20)	1467(15)	6601(16)	36(11)
C69	2380(20)	-1929(14)	8551(16)	33(11)
C21	5040(20)	1638(15)	8975(17)	41(11)
C23	6375(19)	1740(14)	8762(16)	26(10)
C27	4346(19)	1561(14)	6913(16)	30(11)
C4	-940(20)	1357(15)	6221(16)	28(10)
C9	-620(20)	1295(15)	6898(17)	27(10)
C58	-227(19)	-1934(14)	5925(16)	34(11)
C12	1436(19)	1272(14)	8634(15)	15(10)



C15	1900(20)	1474(15)	9974(17)	45(12)
C3	-470(20)	1295(14)	5727(17)	35(11)
C14	1130(20)	1399(15)	9762(16)	44(11)
C50	6380(20)	48(17)	7387(19)	66(13)
C24	6120(20)	1730(15)	8127(17)	40(11)
C7	-1886(19)	1391(14)	7246(16)	34(11)
C54	4564(18)	83(13)	5872(15)	23(10)
C16	2450(19)	1476(14)	9517(15)	30(10)
C68	2450(20)	-1821(14)	7876(16)	25(10)
C34	-1570(20)	-384(16)	8507(18)	57(12)
Cl1	758(6)	-1891(5)	9618(5)	81(4)
Cl2	1441(7)	-1370(6)	10839(6)	109(5)
C41	2489(19)	-301(14)	9562(16)	31(10)
C71	3733(19)	-1917(14)	8814(15)	27(10)
C43	3830(20)	-260(15)	9859(17)	44(12)
C13	880(20)	1291(14)	9081(16)	39(11)
C46	4048(19)	-179(14)	7832(15)	23(10)
C44	3966(19)	-126(14)	9237(16)	31(11)
C22	5820(20)	1697(15)	9185(18)	52(12)
C42	3120(20)	-339(15)	10050(17)	43(11)
C45	3342(19)	-138(14)	8747(16)	15(10)
C86	1430(20)	-2035(18)	10307(17)	84(14)
C85	5990(30)	-1980(20)	8970(20)	121(18)
C79	6470(20)	-1692(16)	5777(18)	57(12)
C40	2610(20)	-218(15)	8910(17)	30(11)
C87	1720(20)	70(20)	5032(16)	104(16)

**Crystallographic Table 100** Anisotropic Displacement Parameters ( $\text{\AA}^2 \times 10^3$ ) for  $\text{Eu}_2[\text{L}^{\text{VII}}]_3$ . The Anisotropic displacement factor exponent takes the form: -  
 $2\pi^2[h^2a^{*2}U_{11}+2hka^*b^*U_{12}+\dots]$

Atom	$U_{11}$	$U_{22}$	$U_{33}$	$U_{12}$	$U_{13}$	$U_{23}$
Eu1	19.7(15)	32.3(16)	18.9(14)	0.6(12)	1.1(10)	0.8(12)
Eu2	24.0(16)	34.0(16)	20.4(14)	-2.5(12)	1.6(11)	-1.7(12)

**Crystallographic Table 101** Bond Lengths for  $\text{Eu}_2[\text{L}^{\text{VII}}]_3$ .

Atom	Atom	Length/ $\text{\AA}$	Atom	Atom	Length/ $\text{\AA}$
Eu1	O4	2.396(19)	C73	C68	1.40(4)
Eu1	O3	2.408(19)	C28	C19	1.41(4)
Eu1	N1	2.51(2)	C28	C27	1.40(4)

Eu1	N2	2.50(2)	C51	C52	1.32(3)
Eu1	O1	2.31(2)	C51	C50	1.37(4)
Eu1	O2	2.29(2)	C17	C12	1.37(3)
Eu1	C29	3.23(3)	C17	C16	1.41(3)
Eu1	N4	2.59(2)	C72	C71	1.39(3)
Eu1	N3	2.55(2)	C11	C10	1.44(3)
Eu2	O4	2.395(19)	C25	C26	1.40(3)
Eu2	N6	2.50(2)	C25	C20	1.42(4)
Eu2	O3	2.35(2)	C25	C24	1.41(4)
Eu2	N5	2.51(2)	C32	C33	1.45(4)
Eu2	C57	3.23(4)	C10	C1	1.44(4)
Eu2	O6	2.22(2)	C10	C9	1.45(4)
Eu2	O5	2.22(2)	C35	C36	1.41(4)
Eu2	O7	2.502(19)	C35	C34	1.31(4)
O4	C56	1.36(3)	C49	C48	1.44(3)
N6	C74	1.35(3)	C49	C50	1.41(4)
N6	C73	1.45(3)	C19	C20	1.46(4)
O3	C29	1.33(3)	C19	C18	1.44(4)
N1	C11	1.33(3)	C47	C48	1.46(4)
N1	C12	1.41(3)	C47	C56	1.37(3)
C75	C84	1.41(4)	C47	C46	1.43(3)
C75	C76	1.43(4)	C26	C27	1.38(4)
C75	C74	1.44(4)	C77	C78	1.37(4)
C64	C65	1.40(3)	C33	C34	1.34(4)
C64	C63	1.37(4)	C52	C53	1.45(4)
N2	C17	1.45(3)	C55	C56	1.41(4)
N2	C18	1.28(3)	C55	C54	1.41(4)
C65	C66	1.44(3)	C48	C53	1.40(3)
C65	C60	1.42(3)	C20	C21	1.41(4)
C84	O6	1.28(3)	C78	C79	1.43(4)
C84	C83	1.47(4)	C53	C54	1.40(3)
C66	C57	1.44(4)	C13	C85	1.72(4)
C66	C67	1.43(3)	N4	C46	1.30(3)
N5	C67	1.27(3)	N4	C45	1.44(3)
N5	C68	1.43(3)	C14	C85	1.81(4)
C76	C81	1.45(4)	N3	C40	1.45(3)
C76	C77	1.38(4)	C70	C69	1.34(3)
C57	O5	1.29(3)	C70	C71	1.39(4)

C57	C58	1.46(4)	C80	C79	1.34(4)
C63	C62	1.39(3)	C8	C9	1.39(4)
C62	C61	1.42(3)	C8	C7	1.37(4)
O1	C1	1.31(3)	C5	C6	1.36(4)
C31	C30	1.34(3)	C5	C4	1.46(4)
C31	C32	1.43(4)	C6	C7	1.40(4)
O2	C28	1.32(3)	C69	C68	1.42(4)
C37	C38	1.47(4)	C21	C22	1.39(4)
C37	C32	1.44(4)	C23	C24	1.33(3)
C37	C36	1.41(3)	C23	C22	1.38(4)
C30	C29	1.44(3)	C4	C9	1.44(4)
C38	C29	1.36(3)	C4	C3	1.38(4)
C38	C39	1.45(3)	C12	C13	1.41(4)
O7	C87	1.48(3)	C15	C14	1.38(4)
C60	C61	1.44(4)	C15	C16	1.42(4)
C60	C59	1.37(3)	C14	C13	1.43(4)
C59	C58	1.34(3)	C11	C86	1.76(3)
C82	C81	1.41(4)	C12	C86	1.75(4)
C82	C83	1.35(4)	C41	C42	1.40(4)
C81	C80	1.48(4)	C41	C40	1.39(4)
C39	N3	1.35(3)	C43	C44	1.35(4)
C2	C1	1.43(4)	C43	C42	1.36(4)
C2	C3	1.32(4)	C44	C45	1.40(3)
C73	C72	1.42(3)	C45	C40	1.38(4)

**Crystallographic Table 102 Bond Angles for  $\text{Eu}_2[\text{L}^{\text{VII}}]_3$ .**

Atom	Atom	Atom	Angle/°	Atom	Atom	Atom	Angle/°
O3	Eu1	O4	70.1(7)	C59	C60	C61	121(3)
N1	Eu1	O4	162.5(7)	C60	C61	C62	119(3)
N1	Eu1	O3	94.0(7)	C58	C59	C60	123(3)
N2	Eu1	O4	132.6(8)	C83	C82	C81	118(4)
N2	Eu1	O3	146.0(8)	C82	C81	C76	124(4)
N2	Eu1	N1	64.8(8)	C80	C81	C76	116(3)
O1	Eu1	O4	94.5(7)	C80	C81	C82	120(3)
O1	Eu1	O3	74.3(6)	C82	C83	C84	125(3)
O1	Eu1	N1	73.6(7)	O3	C29	Eu1	41.9(13)
O1	Eu1	N2	119.8(7)	C30	C29	Eu1	133(2)
O2	Eu1	O4	81.5(7)	C30	C29	O3	118(3)

O2	Eu1	O3	143.8(7)	C38	C29	Eu1	97(2)
O2	Eu1	N1	109.9(7)	C38	C29	O3	125(3)
O2	Eu1	N2	70.2(8)	C38	C29	C30	117(3)
O2	Eu1	O1	86.4(7)	N3	C39	C38	123(3)
C29	Eu1	O4	91.7(7)	C3	C2	C1	123(4)
C29	Eu1	O3	21.6(6)	C72	C73	N6	122(3)
C29	Eu1	N1	72.6(8)	C68	C73	N6	118(3)
C29	Eu1	N2	128.0(8)	C68	C73	C72	120(3)
C29	Eu1	O1	71.7(7)	C19	C28	O2	124(3)
C29	Eu1	O2	156.5(7)	C27	C28	O2	116(3)
N4	Eu1	O4	68.8(7)	C27	C28	C19	120(3)
N4	Eu1	O3	101.8(7)	C50	C51	C52	122(4)
N4	Eu1	N1	123.3(8)	C12	C17	N2	116(3)
N4	Eu1	N2	72.8(7)	C16	C17	N2	122(3)
N4	Eu1	O1	163.0(7)	C16	C17	C12	122(3)
N4	Eu1	O2	87.8(7)	C71	C72	C73	119(3)
N4	Eu1	C29	110.8(7)	C10	C11	N1	125(3)
N3	Eu1	O4	105.3(7)	C20	C25	C26	119(3)
N3	Eu1	O3	68.6(7)	C24	C25	C26	127(3)
N3	Eu1	N1	73.8(7)	C24	C25	C20	113(3)
N3	Eu1	N2	79.7(8)	C37	C32	C31	120(3)
N3	Eu1	O1	127.9(7)	C33	C32	C31	122(3)
N3	Eu1	O2	143.2(7)	C33	C32	C37	118(3)
N3	Eu1	C29	60.3(8)	C1	C10	C11	124(3)
N3	Eu1	N4	62.9(8)	C9	C10	C11	117(3)
N6	Eu2	O4	79.3(7)	C9	C10	C1	118(3)
O3	Eu2	O4	71.0(7)	C34	C35	C36	120(4)
O3	Eu2	N6	115.5(7)	C50	C49	C48	115(3)
N5	Eu2	O4	114.7(7)	C20	C19	C28	121(3)
N5	Eu2	N6	65.7(8)	C18	C19	C28	116(3)
N5	Eu2	O3	76.9(7)	C18	C19	C20	122(3)
C57	Eu2	O4	152.8(7)	C35	C36	C37	118(3)
C57	Eu2	N6	117.1(8)	C56	C47	C48	118(3)
C57	Eu2	O3	82.0(8)	C46	C47	C48	121(3)
C57	Eu2	N5	60.7(9)	C46	C47	C56	121(3)
O6	Eu2	O4	95.1(7)	C27	C26	C25	124(3)
O6	Eu2	N6	74.0(8)	C78	C77	C76	123(3)
O6	Eu2	O3	160.2(7)	C34	C33	C32	117(4)

O6	Eu2	N5	122.5(7)	C53	C52	C51	121(4)
O6	Eu2	C57	109.9(8)	C54	C55	C56	117(3)
O5	Eu2	O4	162.9(7)	C2	C1	O1	119(3)
O5	Eu2	N6	117.4(7)	C10	C1	O1	123(3)
O5	Eu2	O3	96.8(7)	C10	C1	C2	118(3)
O5	Eu2	N5	72.5(8)	C47	C48	C49	120(3)
O5	Eu2	C57	17.0(7)	C53	C48	C49	123(3)
O5	Eu2	O6	93.3(7)	C53	C48	C47	118(3)
O7	Eu2	O4	75.8(7)	C19	C20	C25	117(3)
O7	Eu2	N6	149.1(7)	C21	C20	C25	122(3)
O7	Eu2	O3	73.1(6)	C21	C20	C19	121(3)
O7	Eu2	N5	142.6(8)	C79	C78	C77	121(3)
O7	Eu2	C57	93.1(8)	C19	C18	N2	130(3)
O7	Eu2	O6	90.2(7)	C48	C53	C52	117(3)
O7	Eu2	O5	89.4(7)	C54	C53	C52	121(3)
Eu2	O4	Eu1	108.9(8)	C54	C53	C48	122(3)
C56	O4	Eu1	122.0(18)	C47	C56	O4	124(3)
C56	O4	Eu2	127.2(18)	C55	C56	O4	112(3)
C74	N6	Eu2	127(2)	C55	C56	C47	124(3)
C73	N6	Eu2	113.8(19)	C46	N4	Eu1	126(2)
C73	N6	C74	119(3)	C45	N4	Eu1	115.4(19)
Eu2	O3	Eu1	109.9(8)	C45	N4	C46	119(3)
C29	O3	Eu1	116.5(17)	C39	N3	Eu1	123(2)
C29	O3	Eu2	133.5(18)	C40	N3	Eu1	116.4(19)
C11	N1	Eu1	129(2)	C40	N3	C39	120(3)
C12	N1	Eu1	113.5(19)	C71	C70	C69	121(3)
C12	N1	C11	117(3)	C79	C80	C81	124(4)
C76	C75	C84	127(3)	C7	C8	C9	123(3)
C74	C75	C84	121(3)	C4	C5	C6	123(3)
C74	C75	C76	112(3)	C7	C6	C5	119(3)
C63	C64	C65	124(3)	C68	C69	C70	121(3)
C17	N2	Eu1	112.9(19)	C22	C21	C20	118(3)
C18	N2	Eu1	124(2)	C22	C23	C24	116(3)
C18	N2	C17	122(3)	C26	C27	C28	119(3)
C66	C65	C64	123(3)	C9	C4	C5	116(3)
C60	C65	C64	119(3)	C3	C4	C5	124(3)
C60	C65	C66	118(3)	C3	C4	C9	120(3)
O6	C84	C75	127(3)	C8	C9	C10	122(3)

C83	C84	C75	113(3)	C4	C9	C10	119(3)
C83	C84	O6	119(3)	C4	C9	C8	119(3)
C57	C66	C65	121(3)	C59	C58	C57	122(3)
C67	C66	C65	120(3)	C17	C12	N1	118(3)
C67	C66	C57	119(3)	C13	C12	N1	121(3)
C67	N5	Eu2	125(2)	C13	C12	C17	120(3)
C68	N5	Eu2	115(2)	C16	C15	C14	120(3)
C68	N5	C67	119(3)	C4	C3	C2	122(3)
C81	C76	C75	113(3)	C13	C14	C15	120(3)
C77	C76	C75	128(3)	C49	C50	C51	122(4)
C77	C76	C81	119(3)	C23	C24	C25	128(4)
C66	C57	Eu2	99(2)	C6	C7	C8	121(3)
O5	C57	Eu2	30.3(14)	C53	C54	C55	121(3)
O5	C57	C66	125(3)	C15	C16	C17	118(3)
C58	C57	Eu2	143(2)	C73	C68	N5	117(3)
C58	C57	C66	115(3)	C69	C68	N5	125(3)
C58	C57	O5	120(3)	C69	C68	C73	118(3)
C62	C63	C64	118(3)	C33	C34	C35	127(4)
C61	C62	C63	122(3)	C40	C41	C42	120(3)
C75	C74	N6	126(3)	C70	C71	C72	120(3)
N5	C67	C66	129(3)	C42	C43	C44	124(4)
C1	O1	Eu1	137(2)	C14	C13	C12	119(3)
C84	O6	Eu2	136(2)	N4	C46	C47	126(3)
C32	C31	C30	120(3)	C45	C44	C43	118(3)
C28	O2	Eu1	128.3(19)	C23	C22	C21	123(4)
C32	C37	C38	116(3)	C43	C42	C41	117(3)
C36	C37	C38	124(3)	C44	C45	N4	123(3)
C36	C37	C32	120(3)	C40	C45	N4	117(3)
C29	C30	C31	123(3)	C40	C45	C44	120(3)
C57	O5	Eu2	133(2)	C12	C86	C11	109(2)
C29	C38	C37	123(3)	C14	C85	C13	102(2)
C39	C38	C37	115(3)	C80	C79	C78	118(4)
C39	C38	C29	121(3)	C41	C40	N3	123(3)
C87	O7	Eu2	132.7(17)	C45	C40	N3	117(3)
C61	C60	C65	119(3)	C45	C40	C41	120(3)
C59	C60	C65	120(3)				

**Crystallographic Table 103** Hydrogen Atom Coordinates ( $\text{\AA}\times 10^4$ ) and Isotropic Displacement Parameters ( $\text{\AA}^2\times 10^3$ ) for  $\text{Eu}_2[\text{L}^{\text{VII}}]_3$ .

Atom	x	y	z	U(eq)
H64	134(19)	-2038(14)	8261(15)	34(13)
H63	-1009(19)	-2243(14)	8679(16)	41(13)
H62	-2135(19)	-2354(14)	7956(15)	38(12)
H74	4335(18)	-1896(14)	7063(15)	25(12)
H67	1146(18)	-2197(14)	7865(15)	18(12)
H31	-1053(19)	-444(13)	6655(15)	27(12)
H30	156(18)	-407(13)	6367(15)	29(12)
H7	1170(90)	60(80)	5820(50)	65(10)
H61	-2110(19)	-2274(14)	6808(15)	35(12)
H59	-1349(18)	-2087(13)	5889(15)	21(12)
H82	4660(20)	-1561(14)	4396(17)	43(13)
H83	3400(20)	-1419(15)	4574(16)	44(13)
H39	1217(18)	-639(14)	8838(15)	29(12)
H2	560(20)	1100(14)	5499(16)	41(13)
H51	7030(20)	123(15)	6643(16)	46(13)
H72	4351(19)	-1735(14)	8046(15)	35(12)
H11	208(18)	1526(13)	7995(14)	19(11)
H35	-1116(19)	-285(14)	9422(16)	40(13)
H49	5540(20)	-106(15)	8013(17)	49(13)
H36	171(18)	-239(14)	9163(16)	33(12)
H26	5460(19)	1763(14)	6859(16)	37(13)
H77	5386(19)	-1683(14)	6987(16)	37(13)
H33	-1960(20)	-439(15)	7553(17)	56(14)
H52	6080(20)	150(15)	5819(17)	50(13)
H55	3380(19)	78(14)	5657(16)	40(13)
H78	6651(19)	-1719(14)	6794(16)	34(13)
H18	3492(19)	1837(14)	8812(14)	22(12)
H70	2927(19)	-2014(14)	9446(16)	33(12)
H80	6030(20)	-1636(15)	4848(18)	61(14)
H8	-895(19)	1301(14)	7830(16)	33(12)
H5	-2000(20)	1497(15)	5666(17)	50(14)
H6	-2770(20)	1531(15)	6511(16)	43(13)
H69	1880(20)	-1979(14)	8687(16)	40(13)
H21	4670(20)	1608(15)	9279(17)	50(14)
H23	6906(19)	1774(14)	8916(16)	32(12)

H27	4200(19)	1549(14)	6453(16)	36(13)
H58	-230(19)	-1917(14)	5462(16)	41(13)
H15	2060(20)	1524(15)	10429(17)	54(14)
H3	-680(20)	1346(14)	5284(17)	42(13)
H14	760(20)	1420(15)	10068(16)	53(14)
H50	6800(20)	74(17)	7720(19)	79(16)
H24	6500(20)	1759(15)	7835(17)	48(14)
H7a	-2200(19)	1384(14)	7594(16)	40(13)
H54	4681(18)	119(13)	5433(15)	27(12)
H16	2977(19)	1560(14)	9656(15)	35(13)
H34	-2080(20)	-410(16)	8637(18)	68(15)
H41	1980(19)	-332(14)	9678(16)	37(13)
H71	4163(19)	-1977(14)	9134(15)	33(12)
H43	4260(20)	-301(15)	10183(17)	53(14)
H13	350(20)	1234(14)	8933(16)	46(13)
H46	4423(19)	-399(14)	8123(15)	27(12)
H44	4469(19)	-28(14)	9136(16)	37(13)
H22	5970(20)	1708(15)	9644(18)	63(15)
H42	3040(20)	-417(15)	10496(17)	51(14)
H86a	1280(20)	-2435(18)	10535(17)	101(17)
H86b	1940(20)	-2101(18)	10167(17)	101(17)
H85a	6390(30)	-2230(20)	9260(20)	150(20)
H85b	5560(30)	-2280(20)	8820(20)	150(20)
H79	6990(20)	-1720(16)	5694(18)	68(15)
H87a	1950(140)	-280(40)	4800(60)	160(20)
H87b	1240(30)	210(120)	4770(50)	160(20)
H87c	2070(120)	440(80)	5089(17)	160(20)

#### Refinement model description

Number of restraints - 3, number of constraints - 119.

Details:

##### 1. Fixed Uiso

At 1.2 times of:

All C(H) groups, All C(H,H) groups

At 1.5 times of:

All C(H,H,H) groups, All O(H) groups



2. Restrained distances

O7-H7

0.87 with sigma of 0.01

C87-H7

1.989295 with sigma of 0.02

Eu2-H7

2.994132 with sigma of 0.02

3.a Secondary CH2 refined with riding coordinates:

C86(H86a,H86b), C85(H85a,H85b)

3.b Aromatic/amide H refined with riding coordinates:

C64(H64), C63(H63), C62(H62), C74(H74), C67(H67), C31(H31), C30(H30),  
C61(H61), C59(H59), C82(H82), C83(H83), C39(H39), C2(H2), C51(H51), C72(H72),  
C11(H11), C35(H35), C49(H49), C36(H36), C26(H26), C77(H77), C33(H33),  
C52(H52),

C55(H55), C78(H78), C18(H18), C70(H70), C80(H80), C8(H8), C5(H5), C6(H6),  
C69(H69), C21(H21), C23(H23), C27(H27), C58(H58), C15(H15), C3(H3), C14(H14),  
C50(H50), C24(H24), C7(H7a), C54(H54), C16(H16), C34(H34), C41(H41), C71(H71),  
C43(H43), C13(H13), C46(H46), C44(H44), C22(H22), C42(H42), C79(H79)

3.c Idealised Me refined as rotating group:

C87(H87a,H87b,H87c)

**Tb<sub>2</sub>[L<sup>VII</sup>]<sub>3</sub>**

**Crystallographic Table 104** Crystal data and structure refinement for **Tb<sub>2</sub>[L<sup>VII</sup>]<sub>3</sub>**

Identification code	<b>Tb<sub>2</sub>[L<sup>VII</sup>]<sub>3</sub></b>
Empirical formula	C <sub>87</sub> Cl <sub>4</sub> N <sub>6</sub> O <sub>7</sub> Tb <sub>2</sub> H <sub>62</sub>
Formula weight	1760.13
Temperature/K	180.45
Crystal system	monoclinic
Space group	P2 <sub>1</sub> /c
a/Å	17.4955(6)
b/Å	20.5102(7)
c/Å	20.6076(8)
α/°	90
β/°	96.4934(10)
γ/°	90
Volume/Å <sup>3</sup>	7347.3(5)
Z	4
ρ <sub>calc</sub> /mg/mm <sup>3</sup>	1.5911
m/mm <sup>-1</sup>	2.118
F(000)	3511.0
Crystal size/mm <sup>3</sup>	0.3 × 0.28 × 0.15
Radiation	Mo Kα (λ = 0.71073)
2θ range for data collection	2.34 to 54.96°
Index ranges	-22 ≤ h ≤ 22, -26 ≤ k ≤ 26, -26 ≤ l ≤ 25
Reflections collected	111448
Independent reflections	16845 [R <sub>int</sub> = 0.0508, R <sub>sigma</sub> = 0.0403]
Data/restraints/parameters	16845/3/949
Goodness-of-fit on F <sup>2</sup>	1.084
Final R indexes [I ≥ 2σ (I)]	R <sub>1</sub> = 0.0610, wR <sub>2</sub> = 0.1273
Final R indexes [all data]	R <sub>1</sub> = 0.0756, wR <sub>2</sub> = 0.1418
Largest diff. peak/hole / e Å <sup>-3</sup>	3.29/-1.56

**Crystallographic Table 105** Fractional Atomic Coordinates (×10<sup>4</sup>) and Equivalent Isotropic Displacement Parameters (Å<sup>2</sup>×10<sup>3</sup>) for **Tb<sub>2</sub>[L<sup>VII</sup>]<sub>3</sub>**. U<sub>eq</sub> is defined as 1/3 of of the trace of the orthogonalised U<sub>ij</sub> tensor.

Atom	x	y	z	U(eq)
Tb1	2254.28(13)	4429.63(12)	2434.26(11)	20.82(6)
Tb2	2083.24(13)	6030.80(12)	1446.19(11)	22.83(7)
C40	3356(2)	5132(2)	3720(2)	17.3(9)

C68	3170(3)	6724(2)	2683(2)	23.5(10)
N3	3406(2)	5014(2)	3053.0(19)	22.6(9)
N5	3224(2)	6575(2)	2012(2)	22.4(8)
O1	3100.1(19)	3703.5(18)	2085.2(17)	26.5(8)
C29	3602(3)	5042(2)	1635(2)	21.8(10)
C38	4192(3)	5073(2)	2151(3)	25.4(11)
O2	1419(2)	4009(2)	1611.0(18)	35.2(9)
O4	1433.6(18)	5316.9(17)	2083.2(16)	22.7(7)
N2	1243(2)	3858(2)	2959(2)	23.5(9)
O3	2864.3(18)	5116.0(17)	1738.5(16)	23.1(7)
C45	2591(3)	5214(2)	3905(2)	26.3(11)
C56	740(3)	5341(2)	2296(3)	22.9(10)
C65	4865(3)	6636(3)	1023(3)	29.0(11)
C46	1310(3)	5386(2)	3447(2)	23.8(10)
C73	2428(3)	6791(2)	2874(2)	23.1(10)
C74	1138(3)	6958(3)	2460(3)	26.7(11)
O6	1069(2)	6635(2)	1090.6(18)	33.1(9)
N1	2738(2)	3718(2)	3368.5(19)	23.8(9)
C47	652(3)	5346(2)	2958(3)	24(1)
O5	2772(2)	6374(2)	677.6(17)	32.8(9)
C54	-637(3)	5412(3)	2012(3)	33.8(13)
C21	-1100(3)	3671(3)	2382(3)	33.0(12)
C37	4989(3)	5021(3)	2023(3)	31.3(12)
C77	-366(3)	7087(3)	2948(3)	35.9(13)
C18	556(3)	3689(2)	2704(3)	26.0(11)
C28	684(3)	3871(3)	1523(3)	28.6(11)
C41	3960(3)	5152(3)	4207(3)	37.8(14)
C19	238(3)	3768(2)	2040(3)	25.5(11)
C1	3800(3)	3558(2)	2347(3)	26.5(11)
C66	4058(3)	6585(3)	1137(3)	26.4(11)
C72	2339(3)	6901(3)	3532(3)	29.6(11)
C9	4793(3)	3380(3)	3271(3)	30.8(12)
C10	3998(3)	3483(2)	3019(3)	26.5(11)
C60	5061(3)	6618(3)	373(3)	37.5(13)
C17	1441(3)	3730(3)	3637(2)	25.7(10)
C20	-587(3)	3676(3)	1894(3)	26.9(11)
C44	2488(4)	5316(3)	4558(3)	35.5(13)
C76	-284(3)	7052(2)	2271(3)	28.6(11)

C30	3788(3)	4950(3)	994(3)	31.9(12)
C4	5357(3)	3325(3)	2832(3)	31.6(12)
C82	-915(3)	7047(3)	1155(3)	36.8(13)
C12	2230(3)	3652(2)	3857(2)	24.8(10)
C11	3422(3)	3453(3)	3466(3)	26.7(11)
C67	3877(3)	6698(2)	1786(3)	27.1(11)
C53	-763(3)	5398(3)	2679(3)	34.3(13)
C81	-968(3)	7104(3)	1833(3)	32.9(12)
C34	6514(3)	4889(3)	1733(4)	53.6(19)
C26	-438(3)	3678(3)	729(3)	42.7(15)
C16	913(3)	3719(3)	4096(3)	34.1(13)
C57	3490(3)	6475(3)	607(3)	31.0(12)
C69	3804(3)	6780(3)	3156(3)	31.3(12)
C48	-114(3)	5356(3)	3161(3)	31.8(12)
C36	5617(3)	5009(3)	2527(3)	42.1(15)
C31	4536(3)	4903(3)	867(3)	33.1(12)
C64	5475(3)	6678(3)	1531(3)	38.0(14)
C59	4467(4)	6540(4)	-146(3)	45.5(16)
C55	81(3)	5383(2)	1826(3)	28.0(11)
C78	-1063(4)	7199(3)	3170(4)	44.7(15)
C32	5148(3)	4944(3)	1372(3)	33.5(13)
C3	5123(3)	3342(3)	2154(3)	34.9(13)
C84	450(3)	6817(3)	1349(3)	29.8(12)
C13	2460(3)	3568(3)	4517(3)	35.5(13)
C42	3852(4)	5266(3)	4854(3)	45.9(16)
C58	3719(4)	6468(3)	-35(3)	39.7(14)
C83	-245(3)	6902(3)	922(3)	38.2(14)
C75	440(3)	6929(2)	2020(3)	27.3(11)
C15	1151(4)	3620(3)	4752(3)	43.6(15)
C2	4374(3)	3453(3)	1919(3)	30.8(12)
C25	-923(3)	3618(3)	1233(3)	33.1(12)
C24	-1726(3)	3527(3)	1093(3)	39.5(14)
C27	322(3)	3802(3)	867(3)	42.3(16)
C70	3711(3)	6908(3)	3804(3)	36.2(13)
C63	6223(4)	6718(4)	1407(4)	53.2(19)
C71	2974(3)	6964(3)	3988(3)	38.5(14)
C23	-2190(3)	3510(3)	1579(3)	40.8(14)
C5	6145(3)	3252(3)	3080(4)	43.5(16)

C8	5054(3)	3368(3)	3949(3)	39.1(14)
C14	1927(4)	3543(3)	4960(3)	46.0(16)
C7	5823(4)	3295(3)	4166(4)	50.9(18)
C43	3109(4)	5351(3)	5025(3)	46.0(16)
C35	6354(3)	4942(4)	2377(4)	55.6(19)
C33	5927(3)	4883(3)	1241(4)	47.5(17)
C62	6407(4)	6715(4)	762(4)	61(2)
C6	6377(3)	3242(3)	3734(4)	50.6(18)
C22	-1882(3)	3592(3)	2231(3)	40.1(14)
C61	5842(4)	6663(4)	263(4)	54.9(19)
O7	1538(3)	5174(2)	694(2)	46.6(11)
C80	-1680(3)	7225(3)	2079(4)	44.9(16)
C52	-1509(4)	5407(3)	2879(4)	52.9(19)
C79	-1729(4)	7280(3)	2735(4)	46.8(16)
C51	-1619(4)	5355(4)	3516(5)	64(2)
C49	-252(4)	5289(3)	3822(3)	41.7(15)
C50	-988(4)	5292(4)	3992(4)	57(2)
N4	1984(2)	5139(2)	3391(2)	23.4(9)
N6	1803(2)	6718(2)	2371(2)	23.1(9)
C39	4026(3)	5180(2)	2822(3)	27.0(11)
C85	1670(6)	4966(5)	55(5)	84(3)

**Crystallographic Table 106** Anisotropic Displacement Parameters ( $\text{\AA}^2 \times 10^3$ ) for  $\text{Tb}_2[\text{L}^{\text{VII}}]_3$ . The Anisotropic displacement factor exponent takes the form: -  $2\pi^2[h^2a^{*2}U_{11}+2hka^*b^*U_{12}+\dots]$

Atom	$U_{11}$	$U_{22}$	$U_{33}$	$U_{12}$	$U_{13}$	$U_{23}$
Tb1	15.23(11)	25.90(12)	21.42(12)	-0.63(9)	2.45(8)	-1.04(9)
Tb2	18.78(12)	27.82(13)	21.82(12)	2.67(9)	2.00(9)	0.54(9)
C40	12(2)	25(2)	13(2)	-4.0(17)	-5.8(16)	-1.1(17)
C68	22(2)	26(3)	22(2)	-3(2)	0.4(19)	0.5(19)
N3	19(2)	28(2)	20(2)	0.7(17)	0.2(16)	1.3(17)
N5	21(2)	22(2)	25(2)	1.2(16)	3.3(16)	0.8(16)
O1	21.3(17)	32(2)	26.0(18)	4.9(15)	1.3(14)	-4.6(15)
C29	15(2)	23(2)	28(3)	1.9(18)	6.1(19)	1.2(19)
C38	19(2)	21(2)	37(3)	-0.6(19)	7(2)	5(2)
O2	18.4(18)	59(3)	29(2)	-12.0(17)	5.2(15)	-16.8(18)
O4	17.6(16)	29.1(18)	22.1(17)	3.3(14)	5.1(13)	-1.1(14)
N2	22(2)	23(2)	26(2)	-2.7(17)	3.4(17)	-4.0(17)
O3	17.7(16)	30.5(19)	22.3(17)	2.2(14)	6.9(13)	3.5(14)

C45	32(3)	22(3)	24(3)	-4(2)	0(2)	1(2)
C56	15(2)	21(2)	32(3)	3.0(18)	1.5(19)	0(2)
C65	24(3)	24(3)	40(3)	-4(2)	8(2)	-2(2)
C46	23(2)	26(3)	24(2)	-3(2)	9.0(19)	-5(2)
C73	21(2)	18(2)	29(3)	1.2(18)	-1.4(19)	1.5(19)
C74	25(3)	27(3)	28(3)	4(2)	5(2)	-2(2)
O6	24.5(19)	48(2)	26.6(19)	14.8(17)	1.5(15)	3.4(17)
N1	28(2)	24(2)	19(2)	-5.4(17)	0.8(16)	2.9(16)
C47	19(2)	21(2)	33(3)	-0.8(19)	4(2)	-4(2)
O5	26.2(19)	48(2)	24.0(19)	0.7(17)	3.2(15)	6.3(17)
C54	18(2)	29(3)	53(4)	1(2)	-2(2)	-6(3)
C21	21(3)	39(3)	40(3)	-2(2)	4(2)	-2(2)
C37	14(2)	25(3)	54(4)	0(2)	2(2)	6(2)
C77	36(3)	32(3)	40(3)	3(2)	7(3)	0(2)
C18	22(2)	23(2)	33(3)	-4(2)	5(2)	-2(2)
C28	20(2)	32(3)	33(3)	-4(2)	2(2)	-9(2)
C41	32(3)	43(3)	36(3)	-7(3)	-8(2)	3(3)
C19	22(2)	19(2)	35(3)	-4.3(19)	3(2)	-4(2)
C1	27(3)	21(2)	33(3)	-2(2)	7(2)	-4(2)
C66	25(3)	28(3)	27(3)	-3(2)	5(2)	6(2)
C72	32(3)	32(3)	26(3)	4(2)	8(2)	-7(2)
C9	23(3)	26(3)	42(3)	0(2)	-2(2)	-1(2)
C10	29(3)	20(2)	31(3)	4(2)	5(2)	0(2)
C60	38(3)	37(3)	40(3)	-4(3)	15(3)	1(3)
C17	25(3)	28(3)	24(3)	-3(2)	5(2)	-2(2)
C20	20(2)	25(3)	35(3)	-2(2)	3(2)	-3(2)
C44	38(3)	41(3)	27(3)	-7(3)	4(2)	-2(2)
C76	24(3)	19(2)	42(3)	3(2)	4(2)	-2(2)
C30	28(3)	38(3)	31(3)	-1(2)	9(2)	-1(2)
C4	19(2)	27(3)	49(3)	2(2)	5(2)	1(2)
C82	27(3)	28(3)	54(4)	4(2)	-6(3)	3(3)
C12	31(3)	22(2)	23(2)	0(2)	7(2)	-0.7(19)
C11	24(3)	29(3)	26(3)	5(2)	-1(2)	1(2)
C67	26(3)	25(3)	30(3)	-4(2)	3(2)	-2(2)
C53	21(3)	24(3)	59(4)	0(2)	12(3)	-5(3)
C81	25(3)	25(3)	49(3)	4(2)	2(2)	3(2)
C34	18(3)	51(4)	95(6)	-1(3)	21(3)	-6(4)
C26	27(3)	65(4)	35(3)	-7(3)	0(2)	-22(3)

C16	28(3)	37(3)	39(3)	-9(2)	16(2)	-6(2)
C57	30(3)	38(3)	26(3)	1(2)	11(2)	5(2)
C69	24(3)	38(3)	31(3)	-1(2)	-1(2)	0(2)
C48	28(3)	24(3)	45(3)	-1(2)	15(2)	-4(2)
C36	15(3)	52(4)	59(4)	-1(2)	6(3)	10(3)
C31	30(3)	35(3)	37(3)	3(2)	16(2)	3(2)
C64	27(3)	46(4)	42(3)	-8(3)	9(2)	-8(3)
C59	46(4)	66(4)	28(3)	1(3)	18(3)	8(3)
C55	22(3)	25(3)	35(3)	0(2)	-3(2)	-3(2)
C78	38(3)	41(4)	58(4)	-1(3)	17(3)	-5(3)
C32	23(3)	25(3)	56(4)	1(2)	20(3)	-1(2)
C3	27(3)	34(3)	46(3)	8(2)	12(2)	2(3)
C84	25(3)	26(3)	38(3)	11(2)	0(2)	-2(2)
C13	33(3)	51(4)	24(3)	-1(3)	4(2)	1(2)
C42	46(4)	58(4)	28(3)	-7(3)	-20(3)	-1(3)
C58	37(3)	60(4)	22(3)	2(3)	5(2)	9(3)
C83	34(3)	44(3)	35(3)	11(3)	-2(2)	2(3)
C75	26(3)	20(2)	35(3)	6(2)	3(2)	2(2)
C15	46(4)	55(4)	33(3)	-9(3)	21(3)	-1(3)
C2	35(3)	27(3)	31(3)	5(2)	7(2)	1(2)
C25	22(3)	36(3)	41(3)	-2(2)	2(2)	-8(2)
C24	25(3)	46(4)	46(4)	-4(3)	-4(2)	-8(3)
C27	24(3)	70(5)	31(3)	-7(3)	1(2)	-20(3)
C70	24(3)	52(4)	30(3)	-3(3)	-7(2)	-4(3)
C63	24(3)	79(5)	57(4)	-17(3)	6(3)	-16(4)
C71	40(3)	48(4)	27(3)	5(3)	3(2)	-4(3)
C23	17(3)	49(4)	56(4)	-6(2)	-2(3)	-3(3)
C5	20(3)	35(3)	75(5)	2(2)	2(3)	5(3)
C8	34(3)	41(3)	41(3)	2(3)	-3(3)	4(3)
C14	51(4)	60(4)	28(3)	-3(3)	13(3)	7(3)
C7	34(3)	53(4)	61(4)	-3(3)	-17(3)	-3(3)
C43	63(4)	47(4)	27(3)	-10(3)	1(3)	-1(3)
C35	16(3)	65(5)	85(6)	-6(3)	2(3)	3(4)
C33	23(3)	47(4)	77(5)	5(3)	23(3)	-5(3)
C62	28(3)	94(6)	63(5)	-16(4)	23(3)	-10(4)
C6	19(3)	55(4)	72(5)	0(3)	-19(3)	1(4)
C22	28(3)	43(3)	51(4)	-1(3)	11(3)	2(3)
C61	40(4)	80(5)	49(4)	-7(4)	23(3)	-1(4)

O7	50(3)	57(3)	33(2)	-11(2)	2(2)	-14(2)
C80	26(3)	32(3)	76(5)	4(2)	7(3)	6(3)
C52	21(3)	51(4)	88(6)	0(3)	14(3)	-16(4)
C79	30(3)	46(4)	68(5)	3(3)	19(3)	-6(3)
C51	27(3)	63(5)	106(7)	-5(3)	32(4)	-15(5)
C49	37(3)	41(3)	51(4)	-2(3)	21(3)	-11(3)
C50	55(4)	54(4)	69(5)	-2(4)	40(4)	-12(4)
N4	27(2)	23(2)	21(2)	-4.5(17)	7.1(17)	-1.2(16)
N6	21(2)	24(2)	25(2)	2.9(16)	1.2(16)	-0.0(17)
C39	19(2)	24(3)	37(3)	-5(2)	-1(2)	4(2)

**Crystallographic Table 107 Bond Lengths for Tb<sub>2</sub>[L<sup>VII</sup>]<sub>3</sub>.**

Atom	Atom	Length/Å	Atom	Atom	Length/Å
Tb1	N3	2.558(4)	C41	C42	1.388(9)
Tb1	O1	2.273(3)	C19	C20	1.454(7)
Tb1	O2	2.279(3)	C1	C10	1.396(7)
Tb1	O4	2.379(3)	C1	C2	1.426(7)
Tb1	N2	2.472(4)	C66	C67	1.429(7)
Tb1	O3	2.350(3)	C66	C57	1.410(7)
Tb1	N1	2.487(4)	C72	C71	1.379(8)
Tb1	N4	2.538(4)	C9	C10	1.443(7)
Tb2	N5	2.462(4)	C9	C4	1.416(8)
Tb2	O4	2.344(3)	C9	C8	1.421(8)
Tb2	O3	2.359(3)	C10	C11	1.442(7)
Tb2	O6	2.220(3)	C60	C59	1.413(9)
Tb2	O5	2.211(4)	C60	C61	1.413(8)
Tb2	O7	2.464(4)	C17	C12	1.413(7)
Tb2	N6	2.463(4)	C17	C16	1.395(7)
C40	N3	1.407(6)	C20	C25	1.426(8)
C40	C45	1.443(7)	C44	C43	1.371(8)
C40	C41	1.374(7)	C76	C81	1.420(7)
C68	N5	1.429(6)	C76	C75	1.443(7)
C68	C73	1.406(7)	C30	C31	1.368(7)
C68	C69	1.398(7)	C4	C3	1.412(8)
N3	C39	1.279(6)	C4	C5	1.423(7)
N5	C67	1.306(6)	C82	C81	1.416(9)
O1	C1	1.316(6)	C82	C83	1.349(8)
C29	C38	1.398(7)	C12	C13	1.385(7)



C29	O3	1.340(5)	C53	C48	1.424(8)
C29	C30	1.407(7)	C53	C52	1.412(8)
C38	C37	1.453(7)	C81	C80	1.419(8)
C38	C39	1.462(7)	C34	C35	1.391(11)
O2	C28	1.310(6)	C34	C33	1.360(10)
O4	C56	1.337(6)	C26	C25	1.419(8)
N2	C18	1.302(6)	C26	C27	1.352(8)
N2	C17	1.425(6)	C16	C15	1.384(8)
C45	C44	1.394(7)	C57	C58	1.425(7)
C45	N4	1.421(6)	C69	C70	1.388(8)
C56	C47	1.391(7)	C48	C49	1.418(8)
C56	C55	1.422(7)	C36	C35	1.367(8)
C65	C66	1.460(7)	C31	C32	1.409(8)
C65	C60	1.420(8)	C64	C63	1.364(8)
C65	C64	1.410(8)	C59	C58	1.361(8)
C46	C47	1.444(7)	C78	C79	1.398(9)
C46	N4	1.300(6)	C32	C33	1.425(7)
C73	C72	1.399(7)	C3	C2	1.363(8)
C73	N6	1.427(6)	C84	C83	1.430(7)
C74	C75	1.438(7)	C84	C75	1.403(8)
C74	N6	1.296(6)	C13	C14	1.378(8)
O6	C84	1.313(6)	C42	C43	1.395(10)
N1	C12	1.422(6)	C15	C14	1.384(9)
N1	C11	1.310(6)	C25	C24	1.414(7)
C47	C48	1.447(7)	C24	C23	1.360(9)
O5	C57	1.297(6)	C70	C71	1.389(8)
C54	C53	1.417(9)	C63	C62	1.403(10)
C54	C55	1.355(7)	C23	C22	1.399(9)
C21	C20	1.423(7)	C5	C6	1.363(10)
C21	C22	1.378(8)	C8	C7	1.377(8)
C37	C36	1.424(8)	C7	C6	1.392(10)
C37	C32	1.408(8)	C62	C61	1.347(10)
C77	C76	1.420(8)	O7	C85	1.427(10)
C77	C78	1.370(8)	C80	C79	1.368(10)
C18	C19	1.428(7)	C52	C51	1.352(11)
C28	C19	1.407(7)	C51	C50	1.397(11)
C28	C27	1.433(7)	C49	C50	1.373(8)

**Crystallographic Table 108 Bond Angles for Tb<sub>2</sub>[L<sup>VII</sup>]<sub>3</sub>.**

Atom	Atom	Atom	Angle/°	Atom	Atom	Atom	Angle/°
O1	Tb1	N3	87.71(13)	C28	C19	C18	123.7(5)
O2	Tb1	N3	161.95(13)	C20	C19	C18	117.1(5)
O2	Tb1	O1	84.37(13)	C20	C19	C28	119.0(5)
O4	Tb1	N3	101.99(12)	C10	C1	O1	123.2(5)
O4	Tb1	O1	142.84(12)	C2	C1	O1	117.9(5)
O4	Tb1	O2	75.47(14)	C2	C1	C10	118.9(5)
N2	Tb1	N3	124.53(13)	C67	C66	C65	117.4(5)
N2	Tb1	O1	110.59(13)	C57	C66	C65	119.8(5)
N2	Tb1	O2	73.51(13)	C57	C66	C67	122.7(5)
N2	Tb1	O4	93.36(13)	C71	C72	C73	120.4(5)
O3	Tb1	N3	68.71(12)	C4	C9	C10	119.6(5)
O3	Tb1	O1	80.94(12)	C8	C9	C10	123.1(5)
O3	Tb1	O2	93.98(13)	C8	C9	C4	117.2(5)
O3	Tb1	O4	69.90(11)	C9	C10	C1	119.6(5)
O3	Tb1	N2	161.48(13)	C11	C10	C1	121.7(5)
N1	Tb1	N3	73.11(13)	C11	C10	C9	118.5(5)
N1	Tb1	O1	71.56(13)	C59	C60	C65	118.7(5)
N1	Tb1	O2	119.16(15)	C61	C60	C65	119.4(6)
N1	Tb1	O4	145.60(13)	C61	C60	C59	121.9(6)
N1	Tb1	N2	65.18(14)	C12	C17	N2	117.2(4)
N1	Tb1	O3	133.31(12)	C16	C17	N2	124.1(5)
N4	Tb1	N3	63.26(13)	C16	C17	C12	118.6(5)
N4	Tb1	O1	143.80(13)	C19	C20	C21	123.1(5)
N4	Tb1	O2	129.42(13)	C25	C20	C21	116.8(5)
N4	Tb1	O4	68.82(12)	C25	C20	C19	120.1(5)
N4	Tb1	N2	74.10(13)	C43	C44	C45	120.5(6)
N4	Tb1	O3	105.56(12)	C81	C76	C77	116.6(5)
N4	Tb1	N1	79.17(14)	C75	C76	C77	123.5(5)
O4	Tb2	N5	115.87(12)	C75	C76	C81	119.7(5)
O3	Tb2	N5	79.90(13)	C31	C30	C29	121.2(5)
O3	Tb2	O4	70.35(11)	C3	C4	C9	119.0(5)
O6	Tb2	N5	118.55(14)	C5	C4	C9	119.8(6)
O6	Tb2	O4	96.52(13)	C5	C4	C3	121.2(5)
O6	Tb2	O3	161.22(14)	C83	C82	C81	121.7(5)
O5	Tb2	N5	73.53(14)	C17	C12	N1	115.3(4)
O5	Tb2	O4	159.70(14)	C13	C12	N1	124.9(5)

O5	Tb2	O3	95.10(13)	C13	C12	C17	119.6(5)
O5	Tb2	O6	93.80(14)	C10	C11	N1	125.2(5)
O7	Tb2	N5	148.99(15)	C66	C67	N5	126.7(5)
O7	Tb2	O4	74.27(13)	C48	C53	C54	118.6(5)
O7	Tb2	O3	76.42(14)	C52	C53	C54	122.2(6)
O7	Tb2	O6	87.28(16)	C52	C53	C48	119.3(6)
O7	Tb2	O5	88.85(15)	C82	C81	C76	118.5(5)
N6	Tb2	N5	66.17(13)	C80	C81	C76	119.9(6)
N6	Tb2	O4	76.86(13)	C80	C81	C82	121.7(6)
N6	Tb2	O3	114.69(12)	C33	C34	C35	119.7(6)
N6	Tb2	O6	73.39(14)	C27	C26	C25	121.2(6)
N6	Tb2	O5	122.99(14)	C15	C16	C17	120.9(5)
N6	Tb2	O7	142.95(14)	C66	C57	O5	123.0(5)
C45	C40	N3	116.1(4)	C58	C57	O5	118.7(5)
C41	C40	N3	126.3(5)	C58	C57	C66	118.2(5)
C41	C40	C45	117.6(5)	C70	C69	C68	121.1(5)
C73	C68	N5	117.2(4)	C53	C48	C47	119.4(5)
C69	C68	N5	124.0(5)	C49	C48	C47	122.7(5)
C69	C68	C73	118.8(5)	C49	C48	C53	117.8(5)
C40	N3	Tb1	115.8(3)	C35	C36	C37	120.3(7)
C39	N3	Tb1	126.4(3)	C32	C31	C30	121.1(5)
C39	N3	C40	117.8(4)	C63	C64	C65	121.7(6)
C68	N5	Tb2	114.6(3)	C58	C59	C60	121.6(5)
C67	N5	Tb2	127.9(3)	C54	C55	C56	121.1(5)
C67	N5	C68	117.3(4)	C79	C78	C77	121.0(6)
C1	O1	Tb1	128.8(3)	C31	C32	C37	119.7(5)
O3	C29	C38	121.0(4)	C33	C32	C37	119.1(6)
C30	C29	C38	119.4(4)	C33	C32	C31	121.1(6)
C30	C29	O3	119.6(4)	C2	C3	C4	121.0(5)
C37	C38	C29	120.0(5)	C83	C84	O6	117.9(5)
C39	C38	C29	121.2(4)	C75	C84	O6	123.3(5)
C39	C38	C37	118.7(5)	C75	C84	C83	118.8(5)
C28	O2	Tb1	136.2(3)	C14	C13	C12	120.8(6)
Tb2	O4	Tb1	109.50(13)	C43	C42	C41	119.8(5)
C56	O4	Tb1	117.9(3)	C59	C58	C57	122.1(6)
C56	O4	Tb2	132.5(3)	C84	C83	C82	121.4(6)
C18	N2	Tb1	128.5(4)	C76	C75	C74	118.9(5)
C17	N2	Tb1	114.2(3)	C84	C75	C74	121.6(5)

C17	N2	C18	117.2(4)	C84	C75	C76	119.5(5)
Tb2	O3	Tb1	110.02(13)	C14	C15	C16	119.8(5)
C29	O3	Tb1	122.8(3)	C3	C2	C1	121.4(5)
C29	O3	Tb2	126.1(3)	C26	C25	C20	118.4(5)
C44	C45	C40	119.9(5)	C24	C25	C20	119.9(5)
N4	C45	C40	115.4(4)	C24	C25	C26	121.7(5)
N4	C45	C44	124.6(5)	C23	C24	C25	121.0(6)
C47	C56	O4	121.8(4)	C26	C27	C28	122.4(6)
C55	C56	O4	118.4(5)	C71	C70	C69	119.4(5)
C55	C56	C47	119.7(5)	C62	C63	C64	120.3(6)
C60	C65	C66	119.4(5)	C70	C71	C72	120.5(5)
C64	C65	C66	123.3(5)	C22	C23	C24	120.5(5)
C64	C65	C60	117.3(5)	C6	C5	C4	121.6(6)
N4	C46	C47	125.1(5)	C7	C8	C9	120.9(6)
C72	C73	C68	119.7(5)	C15	C14	C13	120.3(6)
N6	C73	C68	116.2(4)	C6	C7	C8	121.8(7)
N6	C73	C72	124.1(5)	C42	C43	C44	120.2(6)
N6	C74	C75	127.3(5)	C36	C35	C34	121.4(7)
C84	O6	Tb2	133.6(3)	C32	C33	C34	121.0(7)
C12	N1	Tb1	114.7(3)	C61	C62	C63	119.8(6)
C11	N1	Tb1	126.0(3)	C7	C6	C5	118.7(6)
C11	N1	C12	119.0(4)	C23	C22	C21	119.7(6)
C46	C47	C56	121.2(4)	C62	C61	C60	121.5(6)
C48	C47	C56	119.5(5)	C85	O7	Tb2	134.6(5)
C48	C47	C46	119.2(5)	C79	C80	C81	121.5(6)
C57	O5	Tb2	138.1(3)	C51	C52	C53	121.2(7)
C55	C54	C53	121.6(5)	C80	C79	C78	118.9(6)
C22	C21	C20	122.1(6)	C50	C51	C52	120.2(6)
C36	C37	C38	123.0(5)	C50	C49	C48	120.7(7)
C32	C37	C38	118.5(5)	C49	C50	C51	120.7(7)
C32	C37	C36	118.4(5)	C45	N4	Tb1	116.8(3)
C78	C77	C76	122.0(6)	C46	N4	Tb1	122.9(3)
C19	C18	N2	126.8(5)	C46	N4	C45	120.0(4)
C19	C28	O2	123.2(5)	C73	N6	Tb2	114.8(3)
C27	C28	O2	118.4(5)	C74	N6	Tb2	126.0(3)
C27	C28	C19	118.4(5)	C74	N6	C73	118.9(4)
C42	C41	C40	122.0(6)	C38	C39	N3	125.4(5)

**Crystallographic Table 109** Hydrogen Atom Coordinates ( $\text{\AA}\times 10^4$ ) and Isotropic Displacement Parameters ( $\text{\AA}^2\times 10^3$ ) for  $\text{Tb}_2[\text{L}^{\text{VII}}]_3$ .

Atom	x	y	z	U(eq)
H46	1245(3)	5610(2)	3841(2)	28.6(12)
H74	1108(3)	7178(3)	2862(3)	32.0(13)
H54	-1067(3)	5443(3)	1687(3)	40.6(15)
H21	-898(3)	3724(3)	2826(3)	39.6(15)
H77	76(3)	7030(3)	3256(3)	43.0(15)
H18	234(3)	3493(2)	2990(3)	31.2(13)
H41	4468(3)	5086(3)	4098(3)	45.4(16)
H72	1837(3)	6933(3)	3664(3)	35.5(14)
H44	1983(4)	5362(3)	4680(3)	42.6(15)
H30	3386(3)	4920(3)	644(3)	38.2(14)
H82	-1364(3)	7112(3)	856(3)	44.1(16)
H11	3550(3)	3223(3)	3864(3)	32.0(13)
H67	4273(3)	6882(2)	2085(3)	32.5(13)
H34	7031(3)	4857(3)	1637(4)	64(2)
H26	-651(3)	3631(3)	287(3)	51.2(19)
H16	381(3)	3782(3)	3956(3)	40.9(15)
H69	4308(3)	6730(3)	3033(3)	37.5(14)
H36	5522(3)	5047(3)	2971(3)	50.5(18)
H31	4646(3)	4842(3)	430(3)	39.7(15)
H64	5361(3)	6678(3)	1971(3)	45.6(16)
H59	4592(4)	6539(4)	-582(3)	54.6(19)
H55	144(3)	5391(2)	1374(3)	33.5(13)
H78	-1094(4)	7222(3)	3626(4)	53.6(18)
H3	5493(3)	3275(3)	1857(3)	41.9(15)
H13	2992(3)	3526(3)	4667(3)	42.6(16)
H42	4281(4)	5285(3)	5180(3)	55.0(19)
H58	3338(4)	6412(3)	-397(3)	47.7(17)
H83	-236(3)	6856(3)	464(3)	45.8(16)
H15	785(4)	3604(3)	5058(3)	52.3(18)
H2	4232(3)	3461(3)	1461(3)	37.0(14)
H24	-1945(3)	3478(3)	652(3)	47.5(17)
H27	627(3)	3845(3)	516(3)	50.7(19)
H70	4148(3)	6956(3)	4119(3)	43.5(16)
H63	6621(4)	6747(4)	1759(4)	64(2)
H71	2908(3)	7047(3)	4432(3)	46.2(16)

H23	-2727(3)	3441(3)	1476(3)	49.0(17)
H5	6519(3)	3209(3)	2782(4)	52.2(19)
H8	4693(3)	3411(3)	4258(3)	46.9(16)
H14	2091(4)	3474(3)	5410(3)	55.2(19)
H7	5980(4)	3280(3)	4622(4)	61(2)
H43	3034(4)	5434(3)	5467(3)	55.2(19)
H35	6766(3)	4931(4)	2719(4)	67(2)
H33	6038(3)	4837(3)	802(4)	57(2)
H62	6928(4)	6749(4)	677(4)	73(3)
H6	6906(3)	3200(3)	3892(4)	61(2)
H22	-2211(3)	3593(3)	2568(3)	48.1(17)
H61	5972(4)	6657(4)	-172(4)	66(2)
H7a	1390(30)	4821(12)	891(10)	69.9(17)
H80	-2133(3)	7270(3)	1782(4)	53.9(19)
H52	-1943(4)	5450(3)	2560(4)	63(2)
H79	-2208(4)	7371(3)	2892(4)	56.2(19)
H51	-2125(4)	5362(4)	3640(5)	76(3)
H49	170(4)	5241(3)	4152(3)	50.1(18)
H50	-1070(4)	5252(4)	4438(4)	68(2)
H39	4411(3)	5391(2)	3111(3)	32.5(13)
H85a	1187(10)	4990(30)	-236(9)	125(4)
H85b	2050(30)	5250(20)	-112(14)	125(4)
H85c	1860(40)	4517(13)	75(7)	125(4)

**Crystallographic Table 110** Solvent masks information for  $\text{Tb}_2[\text{L}^{\text{VII}}]_3$ .

Number	X	Y	Z	Volume	Electron count	Content
1	0.000	0.000	0.500	7.0	0.0	
2	0.152	0.204	0.032	346.2	109.5	2DCM/H2O
3	0.152	0.296	0.532	346.2	105.1	2DCM/H2O
4	0.000	0.500	0.000	7.0	0.0	
5	-0.152	0.704	0.468	346.2	112.3	2DCM/H2O
6	-0.152	0.796	0.968	346.2	107.9	2DCM/H2O

Refinement model description

Number of restraints - 3, number of constraints - 113.

**Dy<sub>2</sub>[L<sup>VII</sup>]<sub>3</sub>****Crystallographic Table 111** Crystal data and structure refinement for **Dy<sub>2</sub>[L<sup>VII</sup>]<sub>3</sub>**

Identification code	<b>Dy<sub>2</sub>[L<sup>VII</sup>]<sub>3</sub></b>
Empirical formula	C <sub>87</sub> H <sub>62</sub> N <sub>6</sub> O <sub>7</sub> Dy <sub>2</sub> Cl <sub>4</sub>
Formula weight	1770.30
Temperature/K	180.45
Crystal system	monoclinic
Space group	P2 <sub>1</sub> /c
a/Å	17.4752(9)
b/Å	20.4942(11)
c/Å	20.6008(10)
α/°	90
β/°	96.4456(10)
γ/°	90
Volume/Å <sup>3</sup>	7331.3(7)
Z	4
ρ <sub>calc</sub> /mg/mm <sup>3</sup>	1.6038
m/mm <sup>-1</sup>	2.231
F(000)	3530.8
Crystal size/mm <sup>3</sup>	0.2 × 0.18 × 0.09
Radiation	Mo Kα (λ = 0.71073)
2θ range for data collection	2.34 to 45.98°
Index ranges	-19 ≤ h ≤ 19, -22 ≤ k ≤ 22, -22 ≤ l ≤ 22
Reflections collected	94401
Independent reflections	10188 [R <sub>int</sub> = 0.0550, R <sub>sigma</sub> = 0.0357]
Data/restraints/parameters	10188/2/958
Goodness-of-fit on F <sup>2</sup>	1.107
Final R indexes [I ≥ 2σ (I)]	R <sub>1</sub> = 0.0489, wR <sub>2</sub> = 0.0911
Final R indexes [all data]	R <sub>1</sub> = 0.0618, wR <sub>2</sub> = 0.0967
Largest diff. peak/hole / e Å <sup>-3</sup>	2.12/-1.58

**Crystallographic Table 112** Fractional Atomic Coordinates (×10<sup>4</sup>) and Equivalent Isotropic Displacement Parameters (Å<sup>2</sup>×10<sup>3</sup>) for **Dy<sub>2</sub>[L<sup>VII</sup>]<sub>3</sub>**. U<sub>eq</sub> is defined as 1/3 of of the trace of the orthogonalised U<sub>ij</sub> tensor.

Atom	x	y	z	U(eq)
Dy1	2906.80(18)	6036.87(17)	3535.16(16)	19.23(10)
Dy2	2741.09(18)	4440.98(16)	2554.43(15)	16.03(10)
O1	1910(3)	3720(2)	2914(2)	21.5(11)

O6	3900(3)	6647(3)	3898(2)	30.4(13)
N6	3186(3)	6722(3)	2619(3)	18.7(13)
O5	2233(3)	6380(3)	4307(2)	30.7(13)
O2	3565(3)	4039(3)	3384(2)	28.7(13)
N1	2260(3)	3729(3)	1631(3)	19.8(13)
O3	2131(2)	5126(2)	3249(2)	20.1(11)
N4	3009(3)	5145(3)	1600(3)	16.9(13)
O4	3550(3)	5328(2)	2903(2)	20.5(11)
C85	3316(8)	4967(8)	4933(7)	109(5)
N5	1769(3)	6576(3)	2974(3)	20.0(13)
N2	3755(3)	3869(3)	2038(3)	19.3(13)
N3	1589(3)	5018(3)	1931(3)	21.7(14)
C40	1657(4)	5138(4)	1258(3)	23.1(17)
C45	2408(4)	5214(3)	1090(3)	22.3(17)
C84	4524(4)	6821(3)	3646(4)	24.9(18)
C83	5218(5)	6914(4)	4072(4)	36(2)
C82	5895(4)	7055(4)	3848(4)	34(2)
C81	5955(4)	7110(4)	3170(4)	29.9(19)
C80	6667(4)	7235(4)	2928(5)	36(2)
C79	6722(5)	7291(4)	2276(5)	46(2)
C78	6066(5)	7213(4)	1838(5)	41(2)
C77	5361(5)	7099(4)	2052(4)	34(2)
C76	5278(4)	7060(3)	2727(4)	23.9(17)
C75	4550(4)	6939(3)	2977(3)	22.2(17)
C74	3856(4)	6965(3)	2533(4)	22.8(17)
C73	2564(4)	6797(3)	2122(3)	19.6(16)
C68	1817(4)	6732(4)	2303(4)	26.0(18)
C67	1129(4)	6699(3)	3208(4)	23.4(17)
C66	937(4)	6582(3)	3859(3)	22.2(17)
C57	1513(4)	6473(4)	4380(4)	26.9(18)
C58	1281(5)	6464(4)	5026(4)	38(2)
C59	542(5)	6533(4)	5136(4)	41(2)
C60	-56(5)	6617(4)	4624(4)	34(2)
C65	135(4)	6640(4)	3973(4)	26.3(18)
C64	-478(4)	6684(4)	3475(4)	34(2)
C63	-1232(5)	6724(5)	3594(5)	49(3)
C62	-1406(5)	6719(5)	4236(5)	58(3)
C61	-836(5)	6654(5)	4733(5)	48(2)



C69	1186(4)	6785(4)	1826(4)	27.1(18)
C70	1283(5)	6911(4)	1185(4)	33(2)
C71	2022(5)	6971(4)	1003(4)	34(2)
C72	2644(4)	6906(4)	1463(4)	26.9(18)
C18	4432(4)	3701(3)	2300(4)	22.0(17)
C19	4760(4)	3779(3)	2964(3)	18.9(16)
C20	5582(4)	3691(3)	3112(4)	24.1(17)
C25	5912(4)	3643(4)	3770(4)	30.0(19)
C24	6715(4)	3549(4)	3913(4)	38(2)
C23	7182(4)	3523(4)	3433(4)	39(2)
C22	6868(4)	3595(4)	2782(4)	36(2)
C21	6091(4)	3679(4)	2631(4)	29.6(19)
C26	5429(5)	3706(5)	4274(4)	42(2)
C27	4659(4)	3838(4)	4131(4)	36(2)
C28	4303(4)	3893(4)	3472(4)	26.3(18)
C17	3554(4)	3739(3)	1362(3)	19.2(16)
C12	2775(4)	3660(3)	1150(3)	21.5(17)
C11	1579(4)	3466(3)	1536(3)	20.3(16)
C10	1007(4)	3492(3)	1982(4)	21.5(17)
C1	1213(4)	3568(3)	2658(3)	20.9(16)
C2	628(4)	3464(4)	3083(4)	26.5(18)
C3	-116(4)	3347(4)	2849(4)	29.7(19)
C4	-357(4)	3326(4)	2173(4)	26.7(18)
C9	204(4)	3391(4)	1734(4)	25.2(17)
C8	-53(5)	3377(4)	1060(4)	36(2)
C7	-824(5)	3299(4)	847(5)	45(2)
C6	-1370(5)	3246(4)	1289(5)	43(2)
C5	-1142(4)	3259(4)	1934(4)	37(2)
C13	2546(4)	3565(4)	485(4)	29.1(19)
C14	3077(5)	3543(5)	43(4)	42(2)
C15	3850(5)	3621(4)	252(4)	36(2)
C16	4090(5)	3722(4)	903(4)	28.9(19)
C39	968(4)	5182(3)	2166(4)	21.3(17)
C38	807(4)	5078(4)	2830(4)	22.6(17)
C29	1394(4)	5055(4)	3343(4)	22.3(17)
C30	1203(4)	4960(4)	3991(4)	27.5(18)
C31	464(4)	4911(4)	4117(4)	33(2)
C32	-153(4)	4947(4)	3615(4)	32(2)

C37	6(4)	5026(4)	2961(4)	27.1(18)
C36	-618(4)	5013(4)	2462(5)	38(2)
C35	-1361(5)	4942(5)	2613(5)	52(3)
C34	-1520(5)	4893(4)	3258(5)	48(3)
C33	-930(5)	4883(4)	3751(5)	46(2)
C46	3680(4)	5391(3)	1541(3)	21.5(17)
C47	4345(4)	5356(3)	2032(3)	18.5(16)
C56	4247(4)	5353(3)	2696(3)	18.3(16)
C55	4905(4)	5398(3)	3162(4)	22.8(17)
C54	5631(4)	5425(4)	2985(4)	30.7(19)
C53	5754(4)	5402(3)	2316(4)	29.5(19)
C52	6504(5)	5411(4)	2119(5)	43(2)
C51	6624(5)	5362(5)	1485(5)	54(3)
C50	5993(5)	5299(5)	1009(5)	51(3)
C49	5251(5)	5294(4)	1168(4)	33(2)
C48	5106(4)	5359(3)	1828(4)	23.7(18)
C44	2510(5)	5319(4)	432(4)	30.6(19)
C43	1886(5)	5352(4)	-38(4)	42(2)
C42	1151(5)	5262(5)	135(4)	46(2)
C41	1033(5)	5150(4)	777(4)	35(2)
O7	3453(3)	5195(3)	4282(2)	39.0(14)

**Crystallographic Table 113** Anisotropic Displacement Parameters ( $\text{\AA}^2 \times 10^3$ ) for  $\text{Dy}_2[\text{L}^{\text{VII}}]_3$ . The Anisotropic displacement factor exponent takes the form: -  $2\pi^2[h^2a^2U_{11}+2hka*b*U_{12}+...]$

Atom	$U_{11}$	$U_{22}$	$U_{33}$	$U_{12}$	$U_{13}$	$U_{23}$
Dy1	14.73(18)	26.6(2)	16.55(18)	-4.48(15)	2.64(13)	-2.37(15)
Dy2	10.01(17)	23.27(19)	14.92(17)	0.33(14)	1.88(12)	1.19(15)
O6	20(3)	47(4)	24(3)	-16(3)	5(2)	0(3)
N6	7(3)	21(3)	27(3)	-2(3)	0(3)	-4(3)
O5	24(3)	47(4)	22(3)	1(3)	6(2)	-7(3)
O2	12(3)	52(4)	22(3)	4(2)	3(2)	10(3)
N1	18(3)	22(3)	19(3)	1(3)	4(3)	3(3)
O3	13(3)	26(3)	22(3)	-4(2)	4(2)	-2(2)
N4	5(3)	22(3)	24(3)	1(3)	3(2)	0(3)
O4	14(3)	29(3)	19(3)	-2(2)	3(2)	-2(2)
N5	17(3)	23(3)	21(3)	-1(3)	8(3)	-1(3)
N2	16(3)	17(3)	25(3)	-3(3)	4(3)	5(3)

N3	17(3)	22(3)	26(3)	-1(3)	2(3)	-2(3)
C40	19(4)	31(5)	18(4)	4(3)	-4(3)	5(3)
C45	26(4)	14(4)	27(4)	5(3)	4(3)	4(3)
C84	24(4)	13(4)	36(5)	-9(3)	0(4)	-7(3)
C83	37(5)	40(5)	29(5)	-14(4)	0(4)	-2(4)
C82	20(4)	33(5)	45(5)	-7(4)	-7(4)	-2(4)
C81	25(4)	18(4)	47(5)	-8(3)	6(4)	-3(4)
C80	19(4)	24(5)	63(6)	-1(4)	3(4)	-2(4)
C79	31(5)	38(6)	74(7)	1(4)	25(5)	10(5)
C78	31(5)	42(5)	54(6)	2(4)	24(4)	9(5)
C77	32(5)	28(5)	42(5)	-2(4)	7(4)	-2(4)
C76	24(4)	14(4)	35(5)	-4(3)	10(3)	-1(3)
C75	22(4)	17(4)	27(4)	-6(3)	1(3)	-2(3)
C74	22(4)	22(4)	25(4)	2(3)	6(3)	-1(3)
C73	23(4)	16(4)	21(4)	0(3)	4(3)	1(3)
C68	24(4)	28(5)	28(4)	3(3)	8(3)	-3(3)
C67	25(4)	18(4)	27(4)	4(3)	-2(3)	0(3)
C66	22(4)	20(4)	26(4)	1(3)	10(3)	-7(3)
C57	28(5)	28(5)	26(4)	-3(4)	10(4)	-5(3)
C58	33(5)	55(6)	28(5)	-2(4)	10(4)	-11(4)
C59	44(6)	54(6)	27(5)	-1(5)	12(4)	-12(4)
C60	31(5)	37(5)	39(5)	2(4)	18(4)	-5(4)
C65	22(4)	22(4)	37(5)	2(3)	14(4)	1(4)
C64	24(4)	42(5)	37(5)	9(4)	10(4)	7(4)
C63	36(5)	64(7)	48(6)	10(5)	8(4)	17(5)
C62	27(5)	81(8)	70(7)	16(5)	26(5)	13(6)
C61	40(6)	64(7)	45(6)	1(5)	24(5)	-3(5)
C69	19(4)	34(5)	28(4)	0(3)	2(3)	0(4)
C70	30(5)	39(5)	27(5)	3(4)	-4(4)	7(4)
C71	36(5)	46(5)	22(4)	0(4)	8(4)	1(4)
C72	21(4)	32(5)	29(4)	-6(3)	4(3)	8(4)
C18	18(4)	14(4)	36(5)	2(3)	11(3)	2(3)
C19	17(4)	15(4)	24(4)	1(3)	1(3)	7(3)
C20	18(4)	17(4)	38(5)	0(3)	8(3)	11(3)
C25	22(4)	30(5)	39(5)	3(4)	4(4)	14(4)
C24	21(4)	46(6)	43(5)	0(4)	-7(4)	13(4)
C23	10(4)	44(6)	62(6)	1(4)	0(4)	5(5)
C22	20(4)	43(5)	46(5)	-2(4)	11(4)	1(4)

C21	19(4)	30(5)	39(5)	1(3)	3(4)	3(4)
C26	37(5)	61(6)	27(5)	6(5)	-3(4)	22(4)
C27	26(4)	60(6)	23(4)	14(4)	5(3)	17(4)
C28	22(4)	26(4)	31(4)	0(3)	4(3)	12(4)
C17	24(4)	15(4)	18(4)	-1(3)	2(3)	3(3)
C12	26(4)	18(4)	21(4)	6(3)	6(3)	4(3)
C11	21(4)	23(4)	17(4)	5(3)	0(3)	-1(3)
C10	16(4)	17(4)	31(4)	-1(3)	3(3)	2(3)
C2	32(5)	28(4)	21(4)	-1(4)	9(3)	5(3)
C3	18(4)	29(5)	46(5)	-2(3)	20(4)	2(4)
C4	18(4)	22(4)	40(5)	-1(3)	4(4)	0(4)
C9	25(4)	21(4)	28(4)	2(3)	-3(3)	0(3)
C8	26(5)	37(5)	42(5)	-4(4)	-9(4)	7(4)
C7	42(6)	42(6)	47(6)	2(4)	-12(5)	3(5)
C6	16(4)	42(6)	66(7)	0(4)	-19(4)	4(5)
C5	20(4)	34(5)	57(6)	-6(4)	7(4)	-1(4)
C13	27(4)	35(5)	25(4)	0(4)	1(4)	-3(4)
C14	46(6)	57(6)	22(5)	0(5)	7(4)	-2(4)
C15	43(5)	36(5)	33(5)	11(4)	21(4)	5(4)
C16	31(5)	29(5)	29(5)	10(4)	15(4)	7(4)
C39	8(4)	18(4)	36(5)	0(3)	-3(3)	-1(3)
C38	16(4)	23(4)	30(4)	4(3)	8(3)	-3(3)
C29	13(4)	25(4)	31(4)	-3(3)	9(3)	-8(3)
C30	21(4)	32(5)	31(5)	-4(4)	12(3)	-4(4)
C31	31(5)	33(5)	40(5)	-6(4)	20(4)	-4(4)
C32	22(4)	21(4)	55(6)	-1(3)	18(4)	-6(4)
C37	17(4)	21(4)	44(5)	2(3)	6(4)	-6(4)
C36	22(5)	37(5)	56(6)	0(4)	7(4)	-3(4)
C35	10(4)	61(7)	84(8)	1(4)	4(5)	-8(6)
C34	16(5)	44(6)	85(8)	1(4)	18(5)	1(5)
C33	33(5)	41(6)	69(7)	-4(4)	27(5)	4(5)
C46	33(5)	15(4)	19(4)	9(3)	11(3)	-1(3)
C47	15(4)	11(4)	32(4)	-2(3)	10(3)	2(3)
C56	10(4)	16(4)	29(4)	-2(3)	6(3)	3(3)
C55	15(4)	22(4)	32(4)	-2(3)	4(3)	5(3)
C54	16(4)	27(5)	48(5)	1(3)	-2(4)	0(4)
C53	19(4)	15(4)	56(6)	0(3)	12(4)	0(4)
C52	20(5)	36(5)	75(7)	6(4)	15(5)	9(5)

C51	27(5)	59(7)	83(8)	8(5)	34(5)	16(6)
C50	45(6)	56(6)	61(7)	10(5)	40(5)	13(5)
C49	35(5)	28(5)	39(5)	3(4)	16(4)	3(4)
C48	18(4)	12(4)	43(5)	2(3)	13(4)	6(3)
C44	30(5)	35(5)	27(4)	10(4)	4(4)	8(4)
C43	59(6)	50(6)	15(4)	11(5)	-1(4)	6(4)
C42	42(6)	52(6)	38(5)	10(5)	-16(4)	9(5)
C41	29(5)	41(5)	33(5)	4(4)	-1(4)	0(4)
O7	38(3)	54(4)	24(3)	4(3)	-2(3)	10(3)

**Crystallographic Table 114 Bond Lengths for Dy<sub>2</sub>[L<sup>VII</sup>]<sub>3</sub>.**

Atom	Atom	Length/Å	Atom	Atom	Length/Å
Dy1	O6	2.202(5)	C63	C62	1.389(13)
Dy1	N6	2.446(6)	C62	C61	1.353(13)
Dy1	O5	2.197(5)	C69	C70	1.375(10)
Dy1	O3	2.343(5)	C70	C71	1.389(11)
Dy1	O4	2.324(5)	C71	C72	1.366(10)
Dy1	N5	2.448(6)	C18	C19	1.431(10)
Dy1	O7	2.434(5)	C19	C20	1.445(10)
Dy2	O1	2.255(5)	C19	C28	1.405(10)
Dy2	O2	2.263(5)	C20	C25	1.417(11)
Dy2	N1	2.469(6)	C20	C21	1.405(10)
Dy2	O3	2.345(5)	C25	C24	1.415(10)
Dy2	N4	2.525(6)	C25	C26	1.415(11)
Dy2	O4	2.365(5)	C24	C23	1.353(12)
Dy2	N2	2.464(6)	C23	C22	1.398(12)
Dy2	N3	2.554(6)	C22	C21	1.370(10)
O1	C1	1.309(8)	C26	C27	1.371(11)
O6	C84	1.308(8)	C27	C28	1.433(10)
N6	C74	1.302(9)	C17	C12	1.391(10)
N6	C73	1.415(9)	C17	C16	1.404(10)
O5	C57	1.298(9)	C12	C13	1.398(10)
O2	C28	1.316(8)	C11	C10	1.432(10)
N1	C12	1.417(9)	C10	C1	1.409(10)
N1	C11	1.301(9)	C10	C9	1.453(10)
O3	C29	1.331(8)	C1	C2	1.433(10)
N4	C45	1.407(9)	C2	C3	1.356(10)
N4	C46	1.295(9)	C3	C4	1.409(11)

O4	C56	1.335(8)	C4	C9	1.414(10)
C85	O7	1.465(14)	C4	C5	1.412(10)
N5	C68	1.430(9)	C9	C8	1.410(11)
N5	C67	1.291(9)	C8	C7	1.378(11)
N2	C18	1.290(9)	C7	C6	1.396(13)
N2	C17	1.423(9)	C6	C5	1.344(12)
N3	C40	1.425(9)	C13	C14	1.371(11)
N3	C39	1.282(9)	C14	C15	1.381(12)
C40	C45	1.402(10)	C15	C16	1.375(11)
C40	C41	1.389(10)	C39	C38	1.442(10)
C45	C44	1.403(10)	C38	C29	1.389(10)
C84	C83	1.428(10)	C38	C37	1.459(10)
C84	C75	1.405(10)	C29	C30	1.426(10)
C83	C82	1.349(11)	C30	C31	1.350(10)
C82	C81	1.416(11)	C31	C32	1.411(11)
C81	C80	1.415(11)	C32	C37	1.415(11)
C81	C76	1.414(11)	C32	C33	1.423(11)
C80	C79	1.363(12)	C37	C36	1.412(11)
C79	C78	1.386(12)	C36	C35	1.376(11)
C78	C77	1.374(11)	C35	C34	1.392(13)
C77	C76	1.418(11)	C34	C33	1.365(13)
C76	C75	1.445(10)	C46	C47	1.454(10)
C75	C74	1.436(10)	C47	C56	1.398(10)
C73	C68	1.405(10)	C47	C48	1.439(9)
C73	C72	1.398(10)	C56	C55	1.416(10)
C68	C69	1.395(10)	C55	C54	1.360(10)
C67	C66	1.439(10)	C54	C53	1.418(11)
C66	C57	1.405(10)	C53	C52	1.415(11)
C66	C65	1.451(10)	C53	C48	1.429(11)
C57	C58	1.435(11)	C52	C51	1.349(13)
C58	C59	1.344(11)	C51	C50	1.398(14)
C59	C60	1.410(12)	C50	C49	1.372(11)
C60	C65	1.418(11)	C49	C48	1.417(11)
C60	C61	1.408(11)	C44	C43	1.376(11)
C65	C64	1.401(11)	C43	C42	1.383(12)
C64	C63	1.370(11)	C42	C41	1.380(12)

**Crystallographic Table 115** Bond Angles for  $\text{Dy}_2[\text{L}^{\text{VII}}]_3$ .

Atom	Atom	Atom	Angle/°	Atom	Atom	Atom	Angle/°
N6	Dy1	O6	73.62(18)	C65	C66	C57	120.7(6)
O5	Dy1	O6	92.19(19)	C66	C57	O5	123.8(6)
O5	Dy1	N6	122.98(19)	C58	C57	O5	119.0(7)
O3	Dy1	O6	161.84(18)	C58	C57	C66	117.2(7)
O3	Dy1	N6	115.03(17)	C59	C58	C57	122.2(8)
O3	Dy1	O5	95.45(17)	C60	C59	C58	122.2(8)
O4	Dy1	O6	97.64(17)	C65	C60	C59	118.5(7)
O4	Dy1	N6	77.02(17)	C61	C60	C59	122.5(8)
O4	Dy1	O5	159.69(18)	C61	C60	C65	119.0(8)
O4	Dy1	O3	70.37(15)	C60	C65	C66	119.1(7)
N5	Dy1	O6	118.2(2)	C64	C65	C66	124.0(7)
N5	Dy1	N6	66.32(18)	C64	C65	C60	116.9(7)
N5	Dy1	O5	74.02(18)	C63	C64	C65	123.0(8)
N5	Dy1	O3	79.85(17)	C62	C63	C64	119.2(9)
N5	Dy1	O4	115.84(17)	C61	C62	C63	120.0(8)
O7	Dy1	O6	87.10(19)	C62	C61	C60	121.9(8)
O7	Dy1	N6	142.81(18)	C70	C69	C68	121.2(7)
O7	Dy1	O5	88.50(19)	C71	C70	C69	119.7(7)
O7	Dy1	O3	76.67(18)	C72	C71	C70	119.7(7)
O7	Dy1	O4	74.37(17)	C71	C72	C73	122.0(7)
O7	Dy1	N5	149.14(18)	C19	C18	N2	128.4(7)
O2	Dy2	O1	83.80(17)	C20	C19	C18	118.0(6)
N1	Dy2	O1	71.95(17)	C28	C19	C18	122.0(6)
N1	Dy2	O2	119.95(19)	C28	C19	C20	119.9(6)
O3	Dy2	O1	80.65(16)	C25	C20	C19	119.9(7)
O3	Dy2	O2	92.98(17)	C21	C20	C19	123.2(7)
O3	Dy2	N1	133.25(17)	C21	C20	C25	116.9(7)
N4	Dy2	O1	144.41(17)	C24	C25	C20	119.8(7)
N4	Dy2	O2	129.67(17)	C26	C25	C20	118.9(7)
N4	Dy2	N1	79.32(18)	C26	C25	C24	121.3(7)
N4	Dy2	O3	105.63(17)	C23	C24	C25	121.2(8)
O4	Dy2	O1	142.11(16)	C22	C23	C24	119.6(7)
O4	Dy2	O2	75.08(18)	C21	C22	C23	120.2(8)
O4	Dy2	N1	145.94(17)	C22	C21	C20	122.2(8)
O4	Dy2	O3	69.64(15)	C27	C26	C25	120.8(7)
O4	Dy2	N4	68.91(16)	C28	C27	C26	122.1(7)
N2	Dy2	O1	110.59(17)	C19	C28	O2	124.4(7)

N2	Dy2	O2	74.05(18)	C27	C28	O2	117.6(7)
N2	Dy2	N1	65.48(18)	C27	C28	C19	118.0(7)
N2	Dy2	O3	161.25(17)	C12	C17	N2	117.0(6)
N2	Dy2	N4	74.36(17)	C16	C17	N2	123.5(6)
N2	Dy2	O4	93.56(17)	C16	C17	C12	119.4(7)
N3	Dy2	O1	88.18(17)	C17	C12	N1	116.4(6)
N3	Dy2	O2	161.36(18)	C13	C12	N1	124.4(7)
N3	Dy2	N1	72.86(18)	C13	C12	C17	119.0(6)
N3	Dy2	O3	69.06(17)	C10	C11	N1	125.6(6)
N3	Dy2	N4	63.13(17)	C1	C10	C11	121.2(6)
N3	Dy2	O4	101.98(17)	C9	C10	C11	119.1(6)
N3	Dy2	N2	124.58(18)	C9	C10	C1	119.6(6)
C1	O1	Dy2	128.9(4)	C10	C1	O1	123.2(6)
C84	O6	Dy1	132.8(4)	C2	C1	O1	118.9(6)
C74	N6	Dy1	125.7(5)	C2	C1	C10	117.8(6)
C73	N6	Dy1	114.6(4)	C3	C2	C1	122.0(7)
C73	N6	C74	119.3(6)	C4	C3	C2	121.7(7)
C57	O5	Dy1	137.4(5)	C9	C4	C3	118.5(7)
C28	O2	Dy2	135.8(4)	C5	C4	C3	121.3(7)
C12	N1	Dy2	114.2(4)	C5	C4	C9	120.1(7)
C11	N1	Dy2	125.9(5)	C4	C9	C10	120.0(7)
C11	N1	C12	119.7(6)	C8	C9	C10	122.5(7)
Dy2	O3	Dy1	109.89(17)	C8	C9	C4	117.5(7)
C29	O3	Dy1	126.3(4)	C7	C8	C9	120.6(8)
C29	O3	Dy2	122.5(4)	C6	C7	C8	121.1(8)
C45	N4	Dy2	116.8(4)	C5	C6	C7	119.7(8)
C46	N4	Dy2	123.0(5)	C6	C5	C4	121.1(8)
C46	N4	C45	119.9(6)	C14	C13	C12	120.9(7)
Dy2	O4	Dy1	109.88(18)	C15	C14	C13	120.1(8)
C56	O4	Dy1	132.1(4)	C16	C15	C14	120.1(7)
C56	O4	Dy2	117.9(4)	C15	C16	C17	120.4(7)
C68	N5	Dy1	115.2(4)	C38	C39	N3	125.7(7)
C67	N5	Dy1	127.1(5)	C29	C38	C39	121.3(6)
C67	N5	C68	117.6(6)	C37	C38	C39	118.7(6)
C18	N2	Dy2	128.0(5)	C37	C38	C29	120.0(7)
C17	N2	Dy2	113.6(4)	C38	C29	O3	122.0(6)
C17	N2	C18	118.4(6)	C30	C29	O3	118.9(6)
C40	N3	Dy2	114.9(4)	C30	C29	C38	119.1(6)



C39	N3	Dy2	125.7(5)	C31	C30	C29	121.3(7)
C39	N3	C40	119.3(6)	C32	C31	C30	121.6(7)
C45	C40	N3	116.3(6)	C37	C32	C31	119.3(7)
C41	C40	N3	123.5(7)	C33	C32	C31	121.2(8)
C41	C40	C45	120.2(7)	C33	C32	C37	119.5(8)
C40	C45	N4	116.4(6)	C32	C37	C38	118.6(7)
C44	C45	N4	124.8(6)	C36	C37	C38	123.1(7)
C44	C45	C40	118.7(7)	C36	C37	C32	118.3(7)
C83	C84	O6	118.7(7)	C35	C36	C37	120.5(9)
C75	C84	O6	123.9(6)	C34	C35	C36	121.2(9)
C75	C84	C83	117.4(7)	C33	C34	C35	119.8(8)
C82	C83	C84	122.4(8)	C34	C33	C32	120.6(9)
C81	C82	C83	121.3(7)	C47	C46	N4	125.2(6)
C80	C81	C82	121.8(7)	C56	C47	C46	120.3(6)
C76	C81	C82	118.7(7)	C48	C47	C46	119.3(6)
C76	C81	C80	119.4(8)	C48	C47	C56	120.3(6)
C79	C80	C81	121.6(8)	C47	C56	O4	121.9(6)
C78	C79	C80	119.2(8)	C55	C56	O4	119.1(6)
C77	C78	C79	121.1(8)	C55	C56	C47	119.0(6)
C76	C77	C78	121.3(8)	C54	C55	C56	122.1(7)
C77	C76	C81	117.3(7)	C53	C54	C55	120.5(7)
C75	C76	C81	119.3(7)	C52	C53	C54	121.6(8)
C75	C76	C77	123.4(7)	C48	C53	C54	119.3(7)
C76	C75	C84	120.4(6)	C48	C53	C52	119.0(8)
C74	C75	C84	120.8(6)	C51	C52	C53	121.7(9)
C74	C75	C76	118.8(7)	C50	C51	C52	119.3(8)
C75	C74	N6	127.4(7)	C49	C50	C51	121.7(9)
C68	C73	N6	117.3(6)	C48	C49	C50	120.2(8)
C72	C73	N6	124.6(6)	C53	C48	C47	118.7(7)
C72	C73	C68	118.0(7)	C49	C48	C47	123.3(7)
C73	C68	N5	115.8(6)	C49	C48	C53	117.9(7)
C69	C68	N5	124.8(6)	C43	C44	C45	120.8(8)
C69	C68	C73	119.3(7)	C42	C43	C44	119.7(8)
C66	C67	N5	128.2(7)	C41	C42	C43	120.8(8)
C57	C66	C67	121.1(6)	C42	C41	C40	119.8(8)
C65	C66	C67	118.0(7)				

**Crystallographic Table 116** Hydrogen Atom Coordinates ( $\text{\AA} \times 10^4$ ) and Isotropic

Displacement Parameters ( $\text{\AA}^2 \times 10^3$ ) for  $\text{Dy}_2[\text{L}^{\text{VII}}]_3$ .

Atom	x	y	z	U(eq)
H85a	2890(40)	5220(40)	5080(20)	163(7)
H85b	3180(60)	4503(15)	4912(12)	163(7)
H85c	3780(20)	5030(50)	5237(13)	163(7)
H83	5202(5)	6875(4)	4530(4)	43(2)
H82	6340(4)	7119(4)	4150(4)	41(2)
H80	7118(4)	7282(4)	3228(5)	43(3)
H79	7204(5)	7381(4)	2123(5)	55(3)
H78	6104(5)	7240(4)	1382(5)	49(3)
H77	4922(5)	7044(4)	1741(4)	41(2)
H74	3889(4)	7184(3)	2131(4)	27(2)
H67	736(4)	6891(3)	2913(4)	28(2)
H58	1663(5)	6407(4)	5388(4)	46(3)
H59	418(5)	6524(4)	5573(4)	49(3)
H64	-365(4)	6686(4)	3034(4)	41(2)
H63	-1631(5)	6756(5)	3243(5)	59(3)
H62	-1925(5)	6761(5)	4325(5)	70(3)
H61	-966(5)	6632(5)	5168(5)	58(3)
H69	681(4)	6732(4)	1947(4)	33(2)
H70	848(5)	6958(4)	869(4)	39(2)
H71	2094(5)	7057(4)	561(4)	41(2)
H72	3146(4)	6935(4)	1331(4)	32(2)
H18	4753(4)	3499(3)	2016(4)	26(2)
H24	6931(4)	3503(4)	4355(4)	45(3)
H23	7720(4)	3457(4)	3537(4)	47(3)
H22	7195(4)	3585(4)	2443(4)	43(2)
H21	5890(4)	3731(4)	2186(4)	35(2)
H26	5640(5)	3657(5)	4717(4)	50(3)
H27	4353(4)	3894(4)	4479(4)	43(3)
H11	1451(4)	3237(3)	1138(3)	24(2)
H2	766(4)	3478(4)	3542(4)	32(2)
H3	-483(4)	3278(4)	3149(4)	36(2)
H8	308(5)	3421(4)	751(4)	43(3)
H7	-986(5)	3282(4)	391(5)	54(3)
H6	-1901(5)	3201(4)	1135(5)	52(3)
H5	-1516(4)	3222(4)	2234(4)	44(3)
H13	2014(4)	3515(4)	336(4)	35(2)

H14	2913(5)	3475(5)	-407(4)	50(3)
H15	4217(5)	3604(4)	-54(4)	43(3)
H16	4622(5)	3781(4)	1044(4)	35(2)
H39	581(4)	5390(3)	1879(4)	26(2)
H30	1605(4)	4930(4)	4342(4)	33(2)
H31	357(4)	4850(4)	4555(4)	40(2)
H36	-524(4)	5055(4)	2018(5)	46(3)
H35	-1772(5)	4925(5)	2270(5)	62(3)
H34	-2038(5)	4868(4)	3354(5)	57(3)
H33	-1039(5)	4833(4)	4190(5)	55(3)
H46	3743(4)	5611(3)	1144(3)	26(2)
H55	4837(4)	5410(3)	3613(4)	27(2)
H54	6058(4)	5459(4)	3311(4)	37(2)
H52	6934(5)	5453(4)	2441(5)	52(3)
H51	7132(5)	5370(5)	1364(5)	65(3)
H50	6079(5)	5258(5)	564(5)	62(3)
H49	4833(5)	5247(4)	834(4)	40(2)
H44	3015(5)	5367(4)	310(4)	37(2)
H43	1960(5)	5435(4)	-480(4)	50(3)
H42	723(5)	5279(5)	-191(4)	55(3)
H41	527(5)	5080(4)	889(4)	41(2)
H7a	3501(3)	4835(3)	4067(2)	59(2)

**Crystallographic Table 117** Solvent masks information for  $\text{Dy}_2[\text{L}^{\text{VII}}]_3$ .

Number	X	Y	Z	Volume	Electron count	Content
1	0.347	0.204	0.465	322.5	105.0	2DCM/1H2O
2	0.347	0.296	0.965	322.5	101.1	2DCM/1H2O
3	-0.347	0.704	0.035	322.5	102.0	2DCM/1H2O
4	-0.347	0.796	0.535	322.5	98.2	2DCM/1H2O

Refinement model description

Number of restraints - 0, number of constraints - 114.

$\text{Er}_2[\text{L}^{\text{VII}}]_3$ **Crystallographic Table 118** Crystal data and structure refinement for  $\text{Er}_2[\text{L}^{\text{VII}}]_3$ 

Empirical formula	$\text{C}_{87}\text{H}_{66}\text{Er}_2\text{N}_6\text{O}_9$
Formula weight	1674.04
Temperature/K	180.65
Crystal system	triclinic
Space group	P-1
$a/\text{\AA}$	10.309(2)
$b/\text{\AA}$	17.582(4)
$c/\text{\AA}$	18.939(4)
$\alpha/^\circ$	82.655(4)
$\beta/^\circ$	86.443(4)
$\gamma/^\circ$	82.386(4)
Volume/ $\text{\AA}^3$	3371.2(12)
Z	2
$\rho_{\text{calc}}/\text{mg}/\text{mm}^3$	1.6490
$m/\text{mm}^{-1}$	2.542
F(000)	1676.2
Crystal size/ $\text{mm}^3$	$0.11 \times 0.09 \times 0.06$
Radiation	Mo K $\alpha$ ( $\lambda = 0.71073$ )
$2\Theta$ range for data collection	2.18 to $44.92^\circ$
Index ranges	$-11 \leq h \leq 11, -18 \leq k \leq 18, -20 \leq l \leq 20$
Reflections collected	26445
Independent reflections	8754 [ $R_{\text{int}} = 0.1455, R_{\text{sigma}} = 0.1934$ ]
Data/restraints/parameters	8754/3/435
Goodness-of-fit on $F^2$	0.941
Final R indexes [ $I \geq 2\sigma(I)$ ]	$R_1 = 0.0608, wR_2 = 0.1208$
Final R indexes [all data]	$R_1 = 0.1226, wR_2 = 0.1462$
Largest diff. peak/hole / $e \text{\AA}^{-3}$	2.74/-2.53

**Crystallographic Table 119** Fractional Atomic Coordinates ( $\times 10^4$ ) and Equivalent Isotropic Displacement Parameters ( $\text{\AA}^2 \times 10^3$ ) for  $\text{Er}_2[\text{L}^{\text{VII}}]_3$ .  $U_{\text{eq}}$  is defined as 1/3 of the trace of the orthogonalised  $U_{ij}$  tensor.

Atom	x	y	z	U(eq)
Er1	-1088.2(5)	2144.3(3)	3232.8(3)	19.31(19)
Er2	2357.3(5)	2229.5(3)	2366.5(3)	18.54(19)
O1	-2279(7)	1207(5)	3534(4)	32(2)
N2	-2165(8)	3332(5)	2603(4)	16(2)

O3	-2039(7)	2807(5)	4055(4)	28(2)
O4	669(6)	2839(4)	3055(3)	21.1(19)
O5	3138(7)	1424(4)	3275(4)	27(2)
O6	3446(6)	3023(4)	2867(4)	22(2)
O7	638(6)	1510(4)	2606(3)	18.6(19)
O8	93(7)	1487(5)	4214(4)	29(2)
O9	1789(8)	1951(5)	4990(5)	48(3)
O10	3662(8)	2654(5)	4305(4)	45(2)
N1	-2113(8)	1949(6)	2166(5)	24(2)
C0aa	-2617(10)	3987(7)	2875(6)	27(3)
N3	3768(8)	1199(5)	1875(4)	20(2)
N4	4029(8)	2686(5)	1496(4)	19(2)
N5	1375(8)	2031(5)	1235(4)	18(2)
N6	1275(8)	3426(5)	1633(4)	19(2)
C1	-2560(10)	1343(7)	2021(6)	21(3)
C2	-2622(10)	635(7)	2497(6)	18(3)
C3	-2550(10)	621(7)	3240(6)	22(3)
C4	-2863(10)	-70(7)	3688(6)	28(3)
C5	-3068(10)	-709(8)	3419(6)	33(3)
C6	-2976(10)	-745(7)	2684(6)	25(3)
C7	-2765(10)	-64(7)	2197(6)	22(3)
C8	-2657(10)	-144(7)	1472(6)	30(3)
C9	-2760(11)	-838(7)	1218(6)	32(3)
C10	-2990(11)	-1488(8)	1703(7)	43(4)
C11	-3067(11)	-1448(8)	2407(6)	38(3)
C12	-2145(10)	2598(7)	1628(6)	21(3)
C13	-2072(10)	2561(7)	885(6)	28(3)
C14	-2099(10)	3204(7)	388(6)	24(3)
C15	-2143(10)	3913(7)	631(6)	29(3)
C16	-2199(10)	3983(7)	1341(6)	24(3)
C17	-2165(10)	3330(7)	1861(6)	23(3)
C18	-2651(10)	4127(7)	3593(6)	20(3)
C19	-2427(10)	3530(7)	4142(6)	27(3)
C20	-2656(11)	3709(8)	4863(6)	36(3)
C21	-3034(12)	4427(8)	5022(7)	48(4)
C22	-3187(11)	5047(7)	4466(6)	31(3)
C23	-3553(11)	5819(8)	4621(7)	43(4)
C24	-3667(12)	6435(8)	4118(7)	46(4)

C25	-3352(12)	6297(8)	3407(7)	48(4)
C26	-3009(11)	5560(8)	3222(6)	36(3)
C27	-2970(10)	4912(7)	3748(6)	22(3)
C28	3321(11)	667(7)	3408(6)	28(3)
C29	3606(10)	179(7)	2870(6)	21(3)
C30	3980(10)	486(7)	2170(6)	24(3)
C31	4315(10)	1403(7)	1184(6)	22(3)
C32	4480(10)	2177(7)	974(6)	17(3)
C33	4502(10)	3349(7)	1455(6)	20(3)
C34	4217(10)	3920(7)	1930(6)	17(3)
C35	3771(10)	3708(7)	2635(6)	21(3)
C36	3748(10)	4272(7)	3134(6)	30(3)
C37	4026(10)	4984(7)	2920(6)	33(3)
C38	4372(11)	5231(7)	2215(6)	27(3)
C39	4495(10)	4699(7)	1700(6)	27(3)
C40	4869(12)	4969(8)	1016(7)	46(4)
C41	5241(14)	5691(9)	829(8)	64(5)
C42	5120(13)	6199(9)	1343(7)	61(4)
C43	4653(12)	5977(8)	2006(7)	48(4)
C44	4967(10)	2398(7)	295(6)	25(3)
C45	5337(10)	1879(7)	-191(6)	31(3)
C46	5139(11)	1136(8)	13(6)	35(3)
C47	4632(11)	889(8)	684(6)	38(4)
C48	3630(10)	-658(7)	3036(6)	25(3)
C49	3490(10)	-960(7)	3747(6)	28(3)
C50	3350(11)	-468(8)	4294(7)	37(4)
C51	3247(11)	320(7)	4130(6)	32(3)
C52	3418(11)	-1790(8)	3924(7)	45(4)
C53	3539(11)	-2258(8)	3397(6)	39(4)
C54	3632(11)	-1946(8)	2692(7)	41(4)
C55	3694(10)	-1169(7)	2516(6)	29(3)
C56	1353(9)	2650(6)	674(5)	15(3)
C57	1298(10)	3378(7)	898(6)	21(3)
C58	753(9)	4049(7)	1880(5)	19(3)
C59	686(10)	4198(7)	2608(6)	19(3)
C60	602(10)	4982(7)	2768(6)	21(3)
C61	678(11)	5607(7)	2238(7)	36(3)
C62	658(12)	6344(9)	2410(7)	52(4)

C63	518(12)	6486(9)	3125(7)	48(4)
C64	480(11)	5899(8)	3653(7)	44(4)
C65	519(11)	5121(7)	3472(6)	28(3)
C66	504(10)	4511(7)	4030(6)	29(3)
C67	572(10)	3767(7)	3870(6)	24(3)
C68	675(10)	3604(7)	3153(6)	17(3)
C69	1332(10)	4024(7)	366(6)	24(3)
C70	1341(10)	3929(7)	-336(6)	29(3)
C71	1396(10)	3205(7)	-551(6)	32(3)
C72	1399(10)	2568(7)	-52(6)	28(3)
C73	943(10)	1402(7)	1135(6)	24(3)
C74	871(9)	721(6)	1647(5)	18(3)
C75	671(9)	817(7)	2377(6)	16(3)
C76	456(9)	165(6)	2872(6)	20(3)
C77	431(10)	-543(7)	2665(6)	25(3)
C78	637(10)	-678(7)	1942(6)	24(3)
C79	889(10)	-41(7)	1421(6)	20(3)
C80	1171(11)	-193(8)	719(6)	35(3)
C81	1191(11)	-924(8)	533(7)	41(4)
C82	932(11)	-1539(8)	1034(7)	42(4)
C83	657(10)	-1417(7)	1728(6)	34(3)
C84	1152(12)	2378(8)	5521(6)	50(4)
C85	4879(14)	2213(9)	4315(8)	79(5)
C1aa	-479(13)	1080(9)	4810(7)	73(5)

**Crystallographic Table 120** Anisotropic Displacement Parameters ( $\text{\AA}^2 \times 10^3$ ) for  $\text{Er}_2[\text{L}^{\text{VII}}]_3$ . The Anisotropic displacement factor exponent takes the form: -  $2\pi^2[h^2a^*2U_{11}+2hka*b*U_{12}+\dots]$

Atom	$U_{11}$	$U_{22}$	$U_{33}$	$U_{12}$	$U_{13}$	$U_{23}$
Er1	25.1(3)	12.0(4)	20.6(4)	-0.6(3)	-2.5(3)	-2.0(3)
Er2	23.7(3)	10.5(4)	21.1(4)	0.8(3)	-4.0(3)	-2.5(3)

**Crystallographic Table 121** Bond Lengths for  $\text{Er}_2[\text{L}^{\text{VII}}]_3$ .

Atom	Atom	Length/ $\text{\AA}$	Atom	Atom	Length/ $\text{\AA}$
Er1	O1	2.182(8)	C24	C25	1.408(15)
Er1	N2	2.436(8)	C25	C26	1.380(16)
Er1	O3	2.172(7)	C26	C27	1.413(15)
Er1	O4	2.301(7)	C28	C29	1.408(15)
Er1	O7	2.318(7)	C28	C51	1.427(14)

Er1	O8	2.373(7)	C29	C30	1.416(14)
Er1	N1	2.420(9)	C29	C48	1.461(15)
Er2	O4	2.337(7)	C31	C32	1.397(15)
Er2	O5	2.205(7)	C31	C47	1.386(15)
Er2	O6	2.233(7)	C32	C44	1.378(13)
Er2	O7	2.301(7)	C33	C34	1.421(14)
Er2	N3	2.414(9)	C34	C35	1.406(13)
Er2	N4	2.451(8)	C34	C39	1.445(15)
Er2	N5	2.508(8)	C35	C36	1.452(15)
Er2	N6	2.535(9)	C36	C37	1.329(15)
O1	C3	1.301(12)	C37	C38	1.390(14)
N2	C0aa	1.337(13)	C38	C39	1.423(15)
N2	C17	1.406(12)	C38	C43	1.384(16)
O3	C19	1.309(13)	C39	C40	1.373(15)
O4	C68	1.381(12)	C40	C41	1.371(18)
O5	C28	1.313(13)	C41	C42	1.392(18)
O6	C35	1.307(12)	C42	C43	1.347(16)
O7	C75	1.340(12)	C44	C45	1.380(15)
O8	C1aa	1.399(13)	C45	C46	1.353(16)
O9	C84	1.409(13)	C46	C47	1.382(14)
O10	C85	1.385(15)	C48	C49	1.389(14)
N1	C1	1.283(12)	C48	C55	1.410(15)
N1	C12	1.428(13)	C49	C50	1.421(15)
C0aa	C18	1.409(14)	C49	C52	1.465(16)
N3	C30	1.302(13)	C50	C51	1.372(16)
N3	C31	1.415(12)	C52	C53	1.363(15)
N4	C32	1.434(13)	C53	C54	1.379(15)
N4	C33	1.313(12)	C54	C55	1.372(16)
N5	C56	1.420(13)	C56	C57	1.391(14)
N5	C73	1.285(12)	C56	C72	1.398(13)
N6	C57	1.404(12)	C57	C69	1.422(14)
N6	C58	1.285(12)	C58	C59	1.432(13)
C1	C2	1.447(14)	C59	C60	1.441(15)
C2	C3	1.411(13)	C59	C68	1.372(14)
C2	C7	1.446(15)	C60	C61	1.398(15)
C3	C4	1.451(15)	C60	C65	1.381(14)
C4	C5	1.337(15)	C61	C62	1.372(16)
C5	C6	1.399(14)	C62	C63	1.405(16)



C6	C7	1.448(15)	C63	C64	1.344(16)
C6	C11	1.419(15)	C64	C65	1.446(16)
C7	C8	1.394(14)	C65	C66	1.408(15)
C8	C9	1.385(15)	C66	C67	1.372(15)
C9	C10	1.408(16)	C67	C68	1.418(13)
C10	C11	1.342(15)	C69	C70	1.360(13)
C12	C13	1.413(14)	C70	C71	1.378(15)
C12	C17	1.409(15)	C71	C72	1.369(15)
C13	C14	1.375(14)	C73	C74	1.449(14)
C14	C15	1.378(15)	C74	C75	1.413(13)
C15	C16	1.364(13)	C74	C79	1.456(14)
C16	C17	1.412(15)	C75	C76	1.417(14)
C18	C19	1.387(15)	C76	C77	1.355(14)
C18	C27	1.440(15)	C77	C78	1.418(14)
C19	C20	1.437(14)	C78	C79	1.434(15)
C20	C21	1.338(16)	C78	C83	1.408(15)
C21	C22	1.415(16)	C79	C80	1.396(14)
C22	C23	1.423(16)	C80	C81	1.373(16)
C22	C27	1.408(14)	C81	C82	1.387(16)
C23	C24	1.346(16)	C82	C83	1.366(14)

**Crystallographic Table 122 Bond Angles for Er<sub>2</sub>[L<sup>VII</sup>]<sub>3</sub>.**

Atom	Atom	Atom	Angle/°	Atom	Atom	Atom	Angle/°
N2	Er1	O1	116.9(3)	C18	C19	O3	124.7(11)
O3	Er1	O1	92.4(3)	C20	C19	O3	117.1(11)
O3	Er1	N2	74.3(3)	C20	C19	C18	118.2(12)
O4	Er1	O1	162.1(3)	C21	C20	C19	122.7(13)
O4	Er1	N2	81.0(3)	C22	C21	C20	119.5(13)
O4	Er1	O3	94.2(3)	C23	C22	C21	120.7(12)
O7	Er1	O1	100.3(3)	C27	C22	C21	120.6(12)
O7	Er1	N2	115.5(3)	C27	C22	C23	118.7(12)
O7	Er1	O3	156.9(2)	C24	C23	C22	123.4(13)
O7	Er1	O4	68.3(2)	C25	C24	C23	117.2(14)
O8	Er1	O1	80.9(3)	C26	C25	C24	122.0(13)
O8	Er1	N2	150.3(3)	C27	C26	C25	120.4(12)
O8	Er1	O3	81.7(3)	C22	C27	C18	118.5(11)
O8	Er1	O4	83.6(2)	C26	C27	C18	123.5(11)
O8	Er1	O7	81.4(2)	C26	C27	C22	117.9(12)

N1	Er1	O1	73.3(3)	C29	C28	O5	123.0(11)
N1	Er1	N2	66.5(3)	C51	C28	O5	118.8(10)
N1	Er1	O3	124.5(3)	C51	C28	C29	118.2(11)
N1	Er1	O4	115.7(3)	C30	C29	C28	120.2(11)
N1	Er1	O7	78.0(3)	C48	C29	C28	120.7(10)
N1	Er1	O8	143.2(3)	C48	C29	C30	118.9(10)
O5	Er2	O4	94.0(2)	C29	C30	N3	128.0(11)
O6	Er2	O4	79.3(2)	C32	C31	N3	118.4(10)
O6	Er2	O5	80.7(3)	C47	C31	N3	124.0(11)
O7	Er2	O4	68.0(2)	C47	C31	C32	117.5(11)
O7	Er2	O5	80.7(2)	C31	C32	N4	114.5(9)
O7	Er2	O6	140.8(2)	C44	C32	N4	125.6(10)
N3	Er2	O4	159.2(3)	C44	C32	C31	119.8(10)
N3	Er2	O5	73.1(3)	C34	C33	N4	127.2(10)
N3	Er2	O6	113.4(3)	C35	C34	C33	119.8(10)
N3	Er2	O7	93.5(3)	C39	C34	C33	119.5(10)
N4	Er2	O4	134.3(3)	C39	C34	C35	120.5(10)
N4	Er2	O5	114.6(3)	C34	C35	O6	123.4(10)
N4	Er2	O6	71.7(3)	C36	C35	O6	119.1(10)
N4	Er2	O7	147.4(3)	C36	C35	C34	117.5(10)
N4	Er2	N3	66.4(3)	C37	C36	C35	121.2(11)
N5	Er2	O4	106.6(2)	C38	C37	C36	122.6(12)
N5	Er2	O5	132.8(3)	C39	C38	C37	119.6(11)
N5	Er2	O6	143.9(3)	C43	C38	C37	121.3(12)
N5	Er2	O7	69.2(2)	C43	C38	C39	119.0(11)
N5	Er2	N3	73.4(3)	C38	C39	C34	118.2(10)
N5	Er2	N4	80.2(3)	C40	C39	C34	124.6(11)
N6	Er2	O4	70.6(3)	C40	C39	C38	117.2(12)
N6	Er2	O5	161.8(3)	C41	C40	C39	123.0(13)
N6	Er2	O6	86.8(3)	C42	C41	C40	118.5(15)
N6	Er2	O7	101.4(3)	C43	C42	C41	120.0(15)
N6	Er2	N3	124.4(3)	C42	C43	C38	121.8(13)
N6	Er2	N4	73.2(3)	C45	C44	C32	122.5(12)
N6	Er2	N5	63.2(3)	C46	C45	C44	117.0(12)
C3	O1	Er1	135.6(7)	C47	C46	C45	122.5(12)
C0aa	N2	Er1	127.2(7)	C46	C47	C31	120.6(12)
C17	N2	Er1	113.9(7)	C49	C48	C29	118.0(10)
C17	N2	C0aa	118.5(9)	C55	C48	C29	123.8(11)

C19	O3	Er1	138.7(7)	C55	C48	C49	118.0(11)
Er2	O4	Er1	111.4(3)	C50	C49	C48	120.7(12)
C68	O4	Er1	126.9(6)	C52	C49	C48	119.0(11)
C68	O4	Er2	119.6(6)	C52	C49	C50	120.2(11)
C28	O5	Er2	133.3(7)	C51	C50	C49	120.8(12)
C35	O6	Er2	131.6(6)	C50	C51	C28	121.0(12)
Er2	O7	Er1	112.1(3)	C53	C52	C49	120.0(12)
C75	O7	Er1	126.3(6)	C54	C53	C52	120.2(13)
C75	O7	Er2	121.5(6)	C55	C54	C53	120.5(12)
C1aa	O8	Er1	124.1(7)	C54	C55	C48	122.1(12)
C1	N1	Er1	128.7(8)	C57	C56	N5	114.5(9)
C12	N1	Er1	113.3(7)	C72	C56	N5	125.0(11)
C12	N1	C1	117.9(9)	C72	C56	C57	120.5(11)
C18	C0aa	N2	127.8(11)	C56	C57	N6	118.2(10)
C30	N3	Er2	125.7(8)	C69	C57	N6	123.9(11)
C31	N3	Er2	114.8(7)	C69	C57	C56	117.8(10)
C31	N3	C30	119.4(9)	C59	C58	N6	126.7(10)
C32	N4	Er2	115.1(7)	C60	C59	C58	119.4(10)
C33	N4	Er2	126.4(7)	C68	C59	C58	120.8(11)
C33	N4	C32	118.5(9)	C68	C59	C60	119.7(10)
C56	N5	Er2	116.6(7)	C61	C60	C59	122.4(11)
C73	N5	Er2	123.9(7)	C65	C60	C59	119.1(11)
C73	N5	C56	119.5(9)	C65	C60	C61	118.4(12)
C57	N6	Er2	114.6(7)	C62	C61	C60	121.0(12)
C58	N6	Er2	125.4(7)	C63	C62	C61	120.3(14)
C58	N6	C57	119.9(9)	C64	C63	C62	120.6(15)
C2	C1	N1	125.9(11)	C65	C64	C63	119.0(13)
C3	C2	C1	121.1(11)	C64	C65	C60	120.6(11)
C7	C2	C1	118.6(10)	C66	C65	C60	121.1(12)
C7	C2	C3	120.2(10)	C66	C65	C64	118.4(11)
C2	C3	O1	123.0(11)	C67	C66	C65	119.2(11)
C4	C3	O1	119.5(10)	C68	C67	C66	121.1(11)
C4	C3	C2	117.4(11)	C59	C68	O4	124.1(10)
C5	C4	C3	122.3(12)	C67	C68	O4	116.0(10)
C6	C5	C4	121.2(12)	C67	C68	C59	119.8(11)
C7	C6	C5	120.0(11)	C70	C69	C57	120.2(12)
C11	C6	C5	120.8(11)	C71	C70	C69	121.3(12)
C11	C6	C7	119.3(11)	C72	C71	C70	119.9(12)

C6	C7	C2	117.9(10)	C71	C72	C56	120.2(12)
C8	C7	C2	125.0(11)	C74	C73	N5	127.0(11)
C8	C7	C6	117.0(11)	C75	C74	C73	118.5(11)
C9	C8	C7	122.3(12)	C79	C74	C73	121.5(10)
C10	C9	C8	119.6(12)	C79	C74	C75	119.8(10)
C11	C10	C9	120.6(13)	C74	C75	O7	121.7(10)
C10	C11	C6	121.2(13)	C76	C75	O7	119.7(10)
C13	C12	N1	125.4(11)	C76	C75	C74	118.7(11)
C17	C12	N1	116.8(10)	C77	C76	C75	122.0(11)
C17	C12	C13	117.7(11)	C78	C77	C76	122.0(11)
C14	C13	C12	123.2(12)	C79	C78	C77	118.2(11)
C15	C14	C13	117.8(11)	C83	C78	C77	122.2(11)
C16	C15	C14	121.5(12)	C83	C78	C79	119.5(11)
C17	C16	C15	121.5(12)	C78	C79	C74	119.2(10)
C12	C17	N2	115.6(10)	C80	C79	C74	123.2(11)
C16	C17	N2	126.2(11)	C80	C79	C78	117.6(11)
C16	C17	C12	118.2(11)	C81	C80	C79	121.1(13)
C19	C18	C0aa	121.8(11)	C82	C81	C80	121.4(13)
C27	C18	C0aa	118.0(10)	C83	C82	C81	119.4(14)
C27	C18	C19	120.1(10)	C82	C83	C78	121.0(12)

**Crystallographic Table 123** Hydrogen Atom Coordinates ( $\text{\AA}\times 10^4$ ) and Isotropic Displacement Parameters ( $\text{\AA}^2\times 10^3$ ) for  $\text{Er}_2[\text{L}^{\text{VII}}]_3$ .

Atom	x	y	z	U(eq)
H1	-2880(10)	1360(7)	1558(6)	26(4)
H4	-2925(10)	-69(7)	4191(6)	34(4)
H5	-3281(10)	-1146(8)	3733(6)	40(4)
H8a	-2508(10)	292(7)	1140(6)	36(4)
H9	-2675(11)	-874(7)	721(6)	39(4)
H10	-3092(11)	-1959(8)	1529(7)	52(5)
H11	-3185(11)	-1899(8)	2727(6)	46(4)
H13	-2000(10)	2067(7)	722(6)	34(4)
H14	-2088(10)	3161(7)	-108(6)	29(4)
H15	-2135(10)	4364(7)	296(6)	35(4)
H16	-2261(10)	4483(7)	1490(6)	29(4)
H20	-2535(11)	3300(8)	5242(6)	43(4)
H21	-3198(12)	4521(8)	5504(7)	57(5)
H23	-3727(11)	5905(8)	5105(7)	51(4)

H24	-3947(12)	6942(8)	4236(7)	55(5)
H25	-3376(12)	6724(8)	3044(7)	58(5)
H26	-2799(11)	5489(8)	2738(6)	43(4)
H30	4442(10)	127(7)	1880(6)	28(4)
H33	5100(10)	3460(7)	1065(6)	25(4)
H36	3529(10)	4129(7)	3624(6)	36(4)
H37	3987(10)	5338(7)	3262(6)	39(4)
H40	4871(12)	4641(8)	654(7)	56(5)
H41	5574(14)	5841(9)	360(8)	77(6)
H42	5368(13)	6703(9)	1225(7)	73(5)
H43	4512(12)	6342(8)	2340(7)	57(5)
H44	5052(10)	2929(7)	156(6)	30(4)
H45	5714(10)	2036(7)	-648(6)	38(4)
H46	5357(11)	769(8)	-317(6)	43(4)
H47	4500(11)	363(8)	803(6)	46(4)
H50	3327(11)	-688(8)	4779(7)	45(4)
H51	3124(11)	639(7)	4504(6)	39(4)
H52	3288(11)	-2001(8)	4406(7)	55(5)
H53	3560(11)	-2801(8)	3515(6)	46(4)
H54	3653(11)	-2271(8)	2326(7)	49(4)
H55	3783(10)	-970(7)	2027(6)	35(4)
H58	372(9)	4453(7)	1545(5)	23(3)
H61	744(11)	5521(7)	1751(7)	43(4)
H62	740(12)	6760(9)	2043(7)	63(5)
H63	450(12)	7001(9)	3238(7)	58(5)
H64	428(11)	5993(8)	4137(7)	53(5)
H66	446(10)	4613(7)	4513(6)	34(4)
H67	550(10)	3355(7)	4245(6)	29(4)
H69	1348(10)	4525(7)	501(6)	28(4)
H70	1308(10)	4369(7)	-685(6)	35(4)
H71	1432(10)	3148(7)	-1044(6)	38(4)
H72	1433(10)	2069(7)	-200(6)	33(4)
H73	638(10)	1382(7)	675(6)	29(4)
H76	327(9)	225(6)	3363(6)	23(4)
H77	269(10)	-961(7)	3015(6)	30(4)
H80	1352(11)	217(8)	363(6)	42(4)
H81	1387(11)	-1011(8)	50(7)	50(4)
H82	945(11)	-2041(8)	895(7)	50(4)

H83	476(10)	-1838(7)	2071(6)	40(4)
H84a	1130(70)	2045(14)	5977(11)	76(6)
H84b	1630(40)	2820(30)	5570(30)	76(6)
H84c	250(30)	2570(40)	5390(20)	76(6)
H85a	5540(20)	2520(19)	4440(50)	119(8)
H85b	4850(30)	1750(30)	4670(40)	119(8)
H85c	5110(40)	2050(50)	3842(15)	119(8)
H10a	3530(50)	2880(50)	3891(14)	67(4)
H8	890(30)	1530(50)	4320(30)	44(3)
H1aa	-990(80)	700(40)	4654(8)	110(7)
H1ab	208(14)	810(40)	5120(30)	110(7)
H1ac	-1060(70)	1442(11)	5070(30)	110(7)
H0aa	-2957(10)	4409(7)	2545(6)	32(4)
H9a	2470(60)	2140(40)	4840(40)	72(4)

#### Refinement model description

Number of restraints - 3, number of constraints - 125.

Details:

N/A

**Lu<sub>2</sub>[L<sup>VII</sup>]<sub>3</sub>**

**Crystallographic Table 124** Crystal data and structure refinement for **Lu<sub>2</sub>[L<sup>VII</sup>]<sub>3</sub>**

Empirical formula	C <sub>88</sub> H <sub>63</sub> Cl <sub>4</sub> Lu <sub>2</sub> N <sub>6</sub> O <sub>8</sub>
Formula weight	1824.26
Temperature/K	180.65
Crystal system	monoclinic
Space group	P2 <sub>1</sub> /c
a/Å	17.3991(17)
b/Å	20.433(2)
c/Å	20.680(2)
α/°	90
β/°	96.1761(13)
γ/°	90
Volume/Å <sup>3</sup>	7309.6(12)
Z	4
ρ <sub>calc</sub> /mg/mm <sup>3</sup>	1.6576
m/mm <sup>-1</sup>	2.897
F(000)	3629.3
Crystal size/mm <sup>3</sup>	0.19 × 0.16 × 0.15
Radiation	Mo Kα (λ = 0.71073)
2θ range for data collection	2.36 to 52.74°
Index ranges	-21 ≤ h ≤ 21, -25 ≤ k ≤ 25, -25 ≤ l ≤ 25
Reflections collected	76877
Independent reflections	14911 [R <sub>int</sub> = 0.0553, R <sub>sigma</sub> = 0.0387]
Data/restraints/parameters	14911/3/977
Goodness-of-fit on F <sup>2</sup>	2.488
Final R indexes [I ≥ 2σ (I)]	R <sub>1</sub> = 0.1865, wR <sub>2</sub> = 0.4959
Final R indexes [all data]	R <sub>1</sub> = 0.1983, wR <sub>2</sub> = 0.5228
Largest diff. peak/hole / e Å <sup>-3</sup>	5.69/-11.33

**Crystallographic Table 125** Fractional Atomic Coordinates (×10<sup>4</sup>) and Equivalent Isotropic Displacement Parameters (Å<sup>2</sup>×10<sup>3</sup>) for **Lu<sub>2</sub>[L<sup>VII</sup>]<sub>3</sub>**. U<sub>eq</sub> is defined as 1/3 of the trace of the orthogonalised U<sub>ij</sub> tensor.

Atom	x	y	z	U(eq)
Lu1	2271.0(3)	4440.2(3)	2482.5(2)	55.9(3)
Lu2	2082.3(3)	6010.9(3)	1524.0(2)	59.9(3)
O4	1448(5)	5289(5)	2130(4)	53.4(18)
O1	3093(5)	3751(5)	2093(4)	61(2)

O5	2723(5)	6371(6)	737(4)	72(3)
O3	2839(5)	5120(4)	1781(4)	58(2)
N3	3385(6)	5010(5)	3086(5)	54(2)
O2	1497(5)	4048(5)	1650(4)	67(2)
N1	2725(7)	3757(5)	3371(5)	56(2)
C40	3363(8)	5117(6)	3747(7)	62(3)
N4	1987(6)	5128(5)	3402(5)	57(2)
C39	4035(7)	5158(7)	2828(6)	58(3)
C38	4188(8)	5050(7)	2163(6)	61(3)
N5	3181(6)	6558(5)	2069(5)	55(2)
C45	2591(8)	5205(6)	3904(6)	57(3)
C68	3177(9)	6684(7)	2748(7)	66(3)
C32	5116(9)	4920(8)	1363(8)	71(4)
C29	3589(7)	5033(6)	1660(6)	57(3)
N2	1289(6)	3873(5)	2965(5)	55(2)
C47	635(6)	5350(6)	2996(7)	54(3)
C53	-763(8)	5373(7)	2714(7)	62(3)
C10	4010(7)	3487(7)	3013(6)	60(3)
C30	3750(8)	4943(7)	1024(6)	65(3)
C1	3784(7)	3574(7)	2347(7)	62(3)
O7	1549(6)	5207(5)	776(4)	66(2)
C11	3428(7)	3482(7)	3456(6)	60(3)
C4	5350(7)	3303(7)	2786(7)	64(3)
C54	-628(7)	5413(8)	2061(8)	70(4)
C60	5024(10)	6598(10)	401(8)	84(4)
C55	90(7)	5365(6)	1872(7)	58(3)
C34	6522(10)	4838(9)	1695(10)	93(6)
C73	2374(8)	6765(5)	2909(5)	53(3)
C65	4825(8)	6634(6)	1038(8)	68(3)
O6	1107(6)	6610(6)	1132(5)	79(3)
C41	3984(11)	5137(9)	4218(7)	82(5)
C19	291(8)	3787(7)	2058(7)	64(3)
C7	5842(9)	3305(8)	4105(8)	74(4)
C77	-406(10)	7067(7)	2947(9)	76(4)
C81	-977(9)	7085(8)	1834(7)	71(3)
C44	2503(10)	5309(7)	4580(7)	69(3)
C69	3796(9)	6738(7)	3192(7)	67(3)
C78	-1114(12)	7228(7)	3141(9)	84(5)



C37	4996(7)	5018(6)	2040(7)	59(3)
N6	1788(6)	6676(5)	2407(5)	56(2)
C74	1125(7)	6932(7)	2474(6)	61(3)
C57	3418(7)	6443(7)	653(6)	60(3)
C31	4518(9)	4907(9)	889(8)	77(4)
C25	-861(8)	3624(8)	1219(7)	67(3)
C36	5642(7)	4999(8)	2521(9)	74(4)
C46	1328(8)	5363(7)	3483(5)	59(3)
C76	-306(9)	7037(8)	2290(9)	78(4)
C17	1435(8)	3733(7)	3645(6)	63(3)
C70	3700(9)	6897(7)	3830(8)	72(4)
C21	-1072(10)	3669(7)	2351(7)	74(4)
C66	4030(10)	6568(8)	1181(7)	72(4)
C72	2313(10)	6880(6)	3574(8)	71(4)
C24	-1665(9)	3571(9)	1050(6)	77(4)
C67	3843(8)	6673(7)	1830(6)	63(3)
C56	776(7)	5346(6)	2364(7)	58(3)
C9	4792(9)	3367(8)	3256(7)	71(4)
C20	-540(9)	3666(7)	1875(8)	70(3)
C75	424(7)	6906(8)	2039(7)	64(3)
C13	2468(7)	3538(8)	4520(7)	72(4)
C48	-115(8)	5353(6)	3182(7)	64(3)
C82	-888(8)	7037(7)	1170(8)	67(3)
C3	5104(9)	3325(7)	2129(8)	73(4)
C83	-224(10)	6892(9)	948(8)	81(4)
C12	2236(9)	3667(7)	3849(7)	67(3)
C18	611(8)	3700(7)	2712(6)	62(3)
C5	6161(9)	3232(7)	3009(9)	77(4)
C26	-340(11)	3664(9)	756(9)	86(5)
C16	891(9)	3733(8)	4080(8)	71(4)
C43	3095(12)	5337(10)	5039(7)	87(5)
C35	6379(10)	4903(9)	2355(9)	86(5)
C2	4361(8)	3463(7)	1903(7)	67(3)
C84	477(8)	6805(7)	1398(7)	70(4)
C27	425(8)	3812(9)	875(7)	78(4)
C59	4380(11)	6535(11)	-128(9)	94(6)
C33	5901(9)	4876(9)	1233(8)	80(4)
C42	3868(10)	5231(9)	4882(7)	77(4)

C71	2910(11)	6924(9)	4018(7)	80(4)
C28	753(8)	3896(7)	1557(6)	61(3)
C58	3645(9)	6444(9)	7(8)	78(4)
C64	5438(9)	6667(9)	1533(8)	78(4)
C80	-1730(9)	7196(11)	2062(10)	95(6)
C6	6375(9)	3269(10)	3650(8)	89(5)
C15	1131(10)	3615(8)	4739(8)	78(4)
C61	5770(14)	6660(9)	271(9)	100(6)
C63	6190(10)	6645(12)	1364(10)	101(6)
C23	-2163(9)	3498(8)	1537(9)	79(4)
C22	-1846(9)	3568(8)	2177(8)	78(4)
C14	1916(11)	3536(10)	4942(8)	88(5)
C8	5074(10)	3355(9)	3919(7)	80(4)
C52	-1496(10)	5424(8)	2935(10)	82(4)
C49	-267(9)	5275(8)	3848(7)	71(4)
C50	-1019(10)	5303(9)	4036(9)	83(4)
C79	-1808(11)	7289(8)	2690(8)	82(5)
C51	-1655(9)	5352(10)	3561(11)	100(6)
C62	6357(12)	6689(12)	741(10)	106(7)
C85	1614(8)	5060(6)	105(6)	60

**Crystallographic Table 126** Anisotropic Displacement Parameters ( $\text{\AA}^2 \times 10^3$ ) for  $\text{Lu}_2[\text{L}^{\text{VII}}]_3$ . The Anisotropic displacement factor exponent takes the form: -  
 $2\pi^2[h^2a^*{}^2U_{11}+2hka^*b^*U_{12}+\dots]$

Atom	$U_{11}$	$U_{22}$	$U_{33}$	$U_{12}$	$U_{13}$	$U_{23}$
Lu1	48.1(4)	66.0(4)	54.5(4)	0.51(19)	9.3(2)	-1.78(19)
Lu2	53.7(4)	69.9(4)	56.9(4)	7.4(2)	9.8(2)	2.6(2)
O4	44(4)	74(5)	44(4)	6(4)	14(3)	1(3)
O1	50(4)	75(5)	61(5)	11(4)	18(4)	-18(4)
O5	55(5)	108(8)	56(5)	-8(5)	18(4)	17(5)
O3	59(5)	49(4)	72(5)	10(3)	34(4)	17(4)
N3	43(5)	71(6)	51(5)	-6(4)	17(4)	1(4)
O2	40(4)	101(7)	60(5)	-19(4)	1(4)	-29(5)
N1	63(6)	59(5)	46(4)	-4(5)	5(4)	0(4)
C40	59(7)	54(6)	74(8)	-3(5)	7(6)	10(5)
N4	55(6)	57(5)	60(5)	-14(4)	12(4)	-5(4)
C39	37(5)	71(7)	66(7)	1(5)	6(5)	12(6)
C38	58(7)	68(7)	59(6)	4(6)	20(5)	6(5)
N5	52(5)	52(5)	63(5)	1(4)	9(4)	-4(4)

C45	63(7)	64(7)	46(5)	-11(5)	11(5)	4(5)
C68	70(8)	59(7)	71(8)	1(6)	16(6)	-14(6)
C32	60(8)	79(9)	76(9)	15(7)	21(6)	4(7)
C29	39(5)	70(7)	65(7)	3(5)	21(5)	13(5)
N2	60(6)	49(5)	58(5)	-1(4)	20(4)	3(4)
C47	26(4)	58(6)	79(8)	-3(4)	10(4)	-7(5)
C53	56(7)	61(7)	69(7)	3(5)	8(6)	5(6)
C10	48(6)	66(7)	67(7)	0(5)	17(5)	-6(5)
C30	63(8)	86(9)	50(6)	1(6)	29(5)	-5(6)
C1	45(6)	75(8)	67(7)	5(5)	13(5)	2(6)
O7	77(6)	70(5)	49(4)	12(5)	4(4)	-5(4)
C11	48(6)	67(7)	63(7)	-11(5)	-3(5)	6(5)
C4	45(6)	79(8)	70(7)	-8(6)	17(5)	-8(6)
C54	30(5)	81(9)	98(10)	1(5)	-1(6)	-7(7)
C60	74(10)	109(13)	73(9)	3(9)	24(7)	12(8)
C55	45(6)	60(6)	67(7)	-2(5)	5(5)	-1(5)
C34	62(9)	94(11)	129(15)	20(8)	35(9)	38(11)
C73	83(8)	36(4)	39(4)	2(5)	5(5)	11(4)
C65	62(8)	51(6)	92(10)	7(5)	19(7)	-4(6)
O6	61(6)	106(8)	69(6)	43(6)	6(4)	21(5)
C41	86(11)	92(11)	64(8)	-40(9)	-5(7)	3(7)
C19	59(7)	64(7)	69(7)	0(6)	10(6)	-12(6)
C7	61(8)	74(8)	83(9)	12(6)	-7(7)	-21(7)
C77	73(9)	65(8)	94(11)	-6(7)	28(8)	-9(7)
C81	70(9)	76(9)	70(8)	8(7)	18(7)	8(6)
C44	82(10)	60(7)	64(7)	-1(7)	2(6)	-9(6)
C69	61(8)	57(7)	81(8)	3(6)	3(6)	8(6)
C78	110(13)	46(6)	99(11)	-10(7)	23(10)	-7(7)
C37	43(6)	56(6)	80(8)	10(5)	15(5)	14(5)
N6	50(5)	60(5)	60(5)	8(4)	15(4)	4(4)
C74	49(6)	70(7)	65(7)	4(5)	9(5)	-2(6)
C57	51(6)	76(8)	55(6)	8(5)	20(5)	2(5)
C31	54(8)	105(12)	78(9)	-6(7)	29(7)	10(8)
C25	51(7)	87(9)	62(7)	6(6)	3(5)	-17(6)
C36	40(6)	75(8)	107(12)	-9(6)	9(6)	4(7)
C46	61(7)	75(7)	42(5)	7(6)	5(5)	4(5)
C76	61(8)	68(8)	108(12)	14(6)	22(8)	8(8)
C17	59(7)	74(8)	55(6)	14(6)	12(5)	8(5)

C70	66(8)	65(7)	83(9)	-4(6)	1(7)	-22(7)
C21	88(10)	68(8)	72(8)	19(7)	28(7)	16(6)
C66	82(10)	73(8)	63(7)	6(7)	16(7)	17(6)
C72	87(10)	45(6)	87(9)	13(6)	37(8)	-4(6)
C24	71(9)	109(12)	48(6)	-12(8)	-1(6)	-4(7)
C67	59(7)	73(8)	58(6)	3(6)	12(5)	-15(6)
C56	47(6)	54(6)	72(7)	1(5)	6(5)	-16(5)
C9	66(8)	75(8)	70(8)	20(7)	-3(6)	6(6)
C20	59(8)	60(7)	93(10)	2(6)	16(7)	-9(6)
C75	41(6)	80(8)	74(8)	1(5)	15(5)	6(6)
C13	41(6)	110(11)	65(7)	26(7)	7(5)	-17(7)
C48	53(7)	58(6)	85(9)	2(5)	30(6)	2(6)
C82	50(6)	59(7)	88(9)	12(5)	-10(6)	-2(6)
C3	72(9)	55(7)	98(10)	14(6)	38(8)	4(6)
C83	69(9)	89(10)	82(10)	12(8)	1(7)	14(8)
C12	72(8)	65(7)	68(7)	-1(6)	26(6)	-12(6)
C18	66(8)	64(7)	57(6)	-3(6)	8(5)	0(5)
C5	60(8)	59(7)	110(12)	18(6)	0(7)	3(7)
C26	86(11)	94(11)	80(10)	8(9)	21(8)	-19(8)
C16	58(8)	75(8)	84(9)	-9(6)	24(7)	-11(7)
C43	96(12)	106(12)	55(7)	-2(10)	-12(7)	3(8)
C35	65(9)	92(11)	103(12)	-20(8)	10(8)	-6(9)
C2	62(8)	69(7)	70(7)	3(6)	15(6)	-9(6)
C84	63(8)	68(8)	80(9)	25(6)	22(7)	7(6)
C27	45(6)	128(13)	59(7)	-4(7)	-10(5)	-25(8)
C59	73(10)	128(16)	88(11)	-2(10)	33(9)	-8(11)
C33	55(8)	112(12)	81(9)	1(8)	36(7)	5(8)
C42	79(10)	89(10)	64(8)	-14(8)	7(7)	-19(7)
C71	85(11)	94(11)	60(7)	-1(9)	-2(7)	15(7)
C28	54(7)	74(8)	56(6)	11(6)	4(5)	-7(5)
C58	66(9)	97(11)	77(9)	4(8)	30(7)	21(8)
C64	56(8)	99(11)	83(9)	-22(7)	23(7)	-24(8)
C80	47(7)	120(15)	116(14)	-4(8)	4(8)	23(11)
C6	51(7)	134(15)	81(10)	-35(9)	1(7)	6(9)
C15	75(9)	85(10)	79(9)	7(8)	35(7)	15(7)
C61	140(18)	86(11)	81(11)	-30(12)	49(12)	-2(9)
C63	53(9)	139(17)	113(14)	6(10)	12(9)	13(13)
C23	62(8)	76(9)	98(11)	-6(7)	10(7)	8(8)

C22	66(9)	87(10)	82(9)	-3(7)	20(7)	-17(8)
C14	84(11)	118(14)	66(8)	-11(10)	23(8)	14(8)
C8	81(10)	95(11)	62(8)	15(9)	1(7)	-10(7)
C52	63(9)	78(9)	108(13)	0(7)	26(8)	1(8)
C49	73(9)	76(8)	69(8)	-4(7)	31(7)	2(6)
C50	78(10)	94(11)	85(10)	4(8)	41(8)	-4(8)
C79	100(12)	68(8)	85(10)	20(8)	48(9)	2(7)
C51	46(8)	112(14)	146(18)	-2(8)	31(9)	-33(12)
C62	93(13)	145(19)	90(12)	-22(13)	53(11)	-9(12)

**Crystallographic Table 127 Bond Lengths for Lu<sub>2</sub>[L<sup>VII</sup>]<sub>3</sub>.**

Atom	Atom	Length/Å	Atom	Atom	Length/Å
Lu1	O4	2.316(9)	C34	C35	1.42(2)
Lu1	O1	2.219(8)	C34	C33	1.36(2)
Lu1	O3	2.307(7)	C73	N6	1.387(15)
Lu1	N3	2.480(10)	C73	C72	1.410(17)
Lu1	O2	2.218(8)	C65	C66	1.45(2)
Lu1	N1	2.374(10)	C65	C64	1.40(2)
Lu1	N4	2.457(10)	O6	C84	1.338(15)
Lu1	N2	2.371(10)	C41	C42	1.42(2)
Lu2	O4	2.295(8)	C19	C20	1.48(2)
Lu2	O5	2.196(8)	C19	C18	1.417(19)
Lu2	O3	2.276(8)	C19	C28	1.397(19)
Lu2	N5	2.390(10)	C7	C6	1.39(2)
Lu2	O7	2.375(9)	C7	C8	1.35(2)
Lu2	O6	2.177(8)	C77	C78	1.38(2)
Lu2	N6	2.375(10)	C77	C76	1.39(2)
O4	C56	1.317(14)	C81	C76	1.42(2)
O1	C1	1.311(15)	C81	C82	1.40(2)
O5	C57	1.250(15)	C81	C80	1.46(2)
O3	C29	1.366(13)	C44	C43	1.33(2)
N3	C40	1.390(17)	C69	C70	1.39(2)
N3	C39	1.336(14)	C78	C79	1.45(3)
O2	C28	1.325(16)	C37	C36	1.42(2)
N1	C11	1.339(16)	N6	C74	1.288(15)
N1	C12	1.384(16)	C74	C75	1.436(18)
C40	C45	1.427(18)	C57	C66	1.46(2)
C40	C41	1.37(2)	C57	C58	1.433(17)

N4	C45	1.405(16)	C25	C24	1.410(19)
N4	C46	1.270(16)	C25	C20	1.41(2)
C39	C38	1.444(17)	C25	C26	1.39(2)
C38	C29	1.392(18)	C36	C35	1.38(2)
C38	C37	1.457(16)	C76	C75	1.447(18)
N5	C68	1.427(17)	C17	C12	1.42(2)
N5	C67	1.322(16)	C17	C16	1.375(18)
C45	C44	1.438(17)	C70	C71	1.47(2)
C68	C73	1.481(19)	C21	C20	1.42(2)
C68	C69	1.34(2)	C21	C22	1.37(2)
C32	C37	1.453(19)	C66	C67	1.430(18)
C32	C31	1.35(2)	C72	C71	1.31(2)
C32	C33	1.422(18)	C24	C23	1.41(2)
C29	C30	1.385(16)	C9	C8	1.406(19)
N2	C17	1.431(15)	C75	C84	1.36(2)
N2	C18	1.288(17)	C13	C12	1.43(2)
C47	C46	1.485(16)	C13	C14	1.37(2)
C47	C56	1.356(18)	C48	C49	1.438(18)
C47	C48	1.401(15)	C82	C83	1.32(2)
C53	C54	1.40(2)	C3	C2	1.36(2)
C53	C48	1.41(2)	C83	C84	1.46(2)
C53	C52	1.40(2)	C5	C6	1.34(2)
C10	C1	1.403(18)	C26	C27	1.36(2)
C10	C11	1.439(17)	C16	C15	1.40(2)
C10	C9	1.420(18)	C43	C42	1.43(3)
C30	C31	1.396(18)	C27	C28	1.473(17)
C1	C2	1.449(17)	C59	C58	1.35(2)
O7	C85	1.437(14)	C64	C63	1.39(2)
C4	C9	1.451(19)	C80	C79	1.33(2)
C4	C3	1.38(2)	C15	C14	1.39(2)
C4	C5	1.443(19)	C61	C62	1.33(3)
C54	C55	1.352(17)	C63	C62	1.35(3)
C60	C65	1.40(2)	C23	C22	1.38(2)
C60	C59	1.49(3)	C52	C51	1.36(3)
C60	C61	1.36(3)	C49	C50	1.406(19)
C55	C56	1.483(17)	C50	C51	1.40(3)

**Crystallographic Table 128 Bond Angles for Lu<sub>2</sub>[L<sup>VII</sup>]<sub>3</sub>.**

Atom	Atom	Atom	Angle/°	Atom	Atom	Atom	Angle/°
O1	Lu1	O4	139.6(3)	C59	C60	C65	117.0(15)
O3	Lu1	O4	69.1(3)	C61	C60	C65	121.2(18)
O3	Lu1	O1	79.5(3)	C61	C60	C59	121.6(16)
N3	Lu1	O4	103.3(3)	C56	C55	C54	120.3(13)
N3	Lu1	O1	89.0(3)	C33	C34	C35	117.3(15)
N3	Lu1	O3	70.7(3)	N6	C73	C68	116.9(10)
O2	Lu1	O4	73.9(4)	C72	C73	C68	114.2(12)
O2	Lu1	O1	81.4(3)	C72	C73	N6	128.8(13)
O2	Lu1	O3	89.7(4)	C66	C65	C60	121.6(15)
O2	Lu1	N3	159.5(3)	C64	C65	C60	116.5(14)
N1	Lu1	O4	145.7(3)	C64	C65	C66	121.6(14)
N1	Lu1	O1	74.6(4)	C84	O6	Lu2	130.8(9)
N1	Lu1	O3	135.4(4)	C42	C41	C40	120.4(17)
N1	Lu1	N3	73.1(4)	C18	C19	C20	119.9(13)
N1	Lu1	O2	120.8(4)	C28	C19	C20	117.5(13)
N4	Lu1	O4	69.3(3)	C28	C19	C18	122.0(13)
N4	Lu1	O1	146.6(4)	C8	C7	C6	121.4(15)
N4	Lu1	O3	106.2(3)	C76	C77	C78	120.4(18)
N4	Lu1	N3	63.5(3)	C82	C81	C76	118.4(14)
N4	Lu1	O2	130.6(4)	C80	C81	C76	119.9(15)
N4	Lu1	N1	79.3(4)	C80	C81	C82	121.7(15)
N2	Lu1	O4	92.8(3)	C43	C44	C45	123.2(16)
N2	Lu1	O1	111.3(4)	C70	C69	C68	120.1(14)
N2	Lu1	O3	159.4(4)	C79	C78	C77	122.9(17)
N2	Lu1	N3	125.3(3)	C32	C37	C38	114.6(12)
N2	Lu1	O2	75.2(4)	C36	C37	C38	125.9(13)
N2	Lu1	N1	65.3(4)	C36	C37	C32	119.1(12)
N2	Lu1	N4	74.9(3)	C73	N6	Lu2	116.7(7)
O5	Lu2	O4	158.9(4)	C74	N6	Lu2	125.8(9)
O3	Lu2	O4	70.0(3)	C74	N6	C73	117.4(11)
O3	Lu2	O5	96.6(3)	C75	C74	N6	128.8(13)
N5	Lu2	O4	116.8(3)	C66	C57	O5	123.7(11)
N5	Lu2	O5	75.5(4)	C58	C57	O5	119.7(13)
N5	Lu2	O3	81.4(3)	C58	C57	C66	116.4(12)
O7	Lu2	O4	74.6(3)	C30	C31	C32	122.3(14)
O7	Lu2	O5	86.7(4)	C20	C25	C24	121.5(13)

O7	Lu2	O3	77.0(3)	C26	C25	C24	122.4(14)
O7	Lu2	N5	150.1(3)	C26	C25	C20	116.0(14)
O6	Lu2	O4	99.4(4)	C35	C36	C37	121.2(16)
O6	Lu2	O5	88.4(4)	C47	C46	N4	125.6(11)
O6	Lu2	O3	160.9(4)	C81	C76	C77	117.7(14)
O6	Lu2	N5	117.7(4)	C75	C76	C77	124.4(16)
O6	Lu2	O7	85.0(4)	C75	C76	C81	117.7(15)
N6	Lu2	O4	78.0(3)	C12	C17	N2	112.1(11)
N6	Lu2	O5	123.1(4)	C16	C17	N2	125.5(13)
N6	Lu2	O3	116.5(3)	C16	C17	C12	122.0(13)
N6	Lu2	N5	66.3(4)	C71	C70	C69	118.1(14)
N6	Lu2	O7	142.6(4)	C22	C21	C20	120.7(15)
N6	Lu2	O6	75.0(4)	C57	C66	C65	119.8(12)
Lu2	O4	Lu1	109.6(3)	C67	C66	C65	119.7(14)
C56	O4	Lu1	119.6(8)	C67	C66	C57	120.4(13)
C56	O4	Lu2	129.9(8)	C71	C72	C73	123.9(15)
C1	O1	Lu1	129.0(8)	C23	C24	C25	120.1(13)
C57	O5	Lu2	135.9(9)	C66	C67	N5	128.3(13)
Lu2	O3	Lu1	110.6(3)	C47	C56	O4	127.9(11)
C29	O3	Lu1	121.3(7)	C55	C56	O4	115.5(11)
C29	O3	Lu2	127.0(7)	C55	C56	C47	116.5(11)
C40	N3	Lu1	117.8(7)	C4	C9	C10	117.6(13)
C39	N3	Lu1	123.7(8)	C8	C9	C10	124.7(15)
C39	N3	C40	118.2(11)	C8	C9	C4	117.6(14)
C28	O2	Lu1	134.4(8)	C25	C20	C19	122.2(13)
C11	N1	Lu1	124.8(8)	C21	C20	C19	120.9(15)
C12	N1	Lu1	116.9(9)	C21	C20	C25	116.5(14)
C12	N1	C11	118.2(11)	C76	C75	C74	119.2(14)
C45	C40	N3	111.6(11)	C84	C75	C74	118.5(12)
C41	C40	N3	126.8(14)	C84	C75	C76	122.2(14)
C41	C40	C45	121.5(14)	C14	C13	C12	118.5(13)
C45	N4	Lu1	116.0(8)	C53	C48	C47	120.9(13)
C46	N4	Lu1	125.3(9)	C49	C48	C47	122.3(14)
C46	N4	C45	118.3(11)	C49	C48	C53	116.6(12)
C38	C39	N3	126.6(12)	C83	C82	C81	123.3(14)
C29	C38	C39	121.1(11)	C2	C3	C4	122.0(13)
C37	C38	C39	116.9(13)	C84	C83	C82	120.5(15)
C37	C38	C29	121.8(11)	C17	C12	N1	115.7(13)



C68	N5	Lu2	117.4(8)	C13	C12	N1	126.0(14)
C67	N5	Lu2	126.2(8)	C13	C12	C17	118.2(12)
C67	N5	C68	115.6(11)	C19	C18	N2	127.0(13)
N4	C45	C40	117.8(11)	C6	C5	C4	118.0(15)
C44	C45	C40	116.1(13)	C27	C26	C25	125.9(16)
C44	C45	N4	125.8(12)	C15	C16	C17	118.8(14)
C73	C68	N5	110.3(12)	C42	C43	C44	120.4(16)
C69	C68	N5	126.8(13)	C36	C35	C34	121.2(17)
C69	C68	C73	122.9(13)	C3	C2	C1	120.9(14)
C31	C32	C37	121.5(13)	C75	C84	O6	126.3(14)
C33	C32	C37	115.6(14)	C83	C84	O6	116.0(14)
C33	C32	C31	122.9(14)	C83	C84	C75	117.6(13)
C38	C29	O3	120.8(11)	C28	C27	C26	118.0(15)
C30	C29	O3	119.1(12)	C58	C59	C60	121.0(16)
C30	C29	C38	120.1(11)	C34	C33	C32	125.1(15)
C17	N2	Lu1	116.8(8)	C43	C42	C41	118.2(15)
C18	N2	Lu1	129.3(9)	C72	C71	C70	120.3(15)
C18	N2	C17	113.8(11)	C19	C28	O2	124.1(12)
C56	C47	C46	115.9(10)	C27	C28	O2	116.0(12)
C48	C47	C46	121.8(12)	C27	C28	C19	119.8(13)
C48	C47	C56	122.4(12)	C59	C58	C57	123.7(17)
C48	C53	C54	117.5(12)	C63	C64	C65	118.6(16)
C52	C53	C54	124.3(14)	C79	C80	C81	121.8(17)
C52	C53	C48	117.8(14)	C5	C6	C7	122.4(15)
C11	C10	C1	119.0(12)	C14	C15	C16	119.5(13)
C9	C10	C1	121.7(12)	C62	C61	C60	122.2(17)
C9	C10	C11	119.2(12)	C62	C63	C64	122.7(19)
C31	C30	C29	119.5(14)	C22	C23	C24	117.4(15)
C10	C1	O1	125.2(11)	C23	C22	C21	123.1(15)
C2	C1	O1	117.3(12)	C15	C14	C13	122.7(15)
C2	C1	C10	117.6(12)	C9	C8	C7	120.6(16)
C85	O7	Lu2	135.0(8)	C51	C52	C53	126.0(17)
C10	C11	N1	127.5(12)	C50	C49	C48	122.2(16)
C3	C4	C9	119.7(13)	C51	C50	C49	119.8(15)
C5	C4	C9	119.8(14)	C80	C79	C78	116.7(15)
C5	C4	C3	120.5(13)	C50	C51	C52	116.6(15)
C55	C54	C53	122.1(13)	C63	C62	C61	117.8(18)

**Crystallographic Table 129** Hydrogen Atom Coordinates ( $\text{\AA}\times 10^4$ ) and Isotropic Displacement Parameters ( $\text{\AA}^2\times 10^3$ ) for  $\text{Lu}_2[\text{L}^{\text{VII}}]_3$ .

Atom	x	y	z	U(eq)
H39	4437(7)	5354(7)	3110(6)	70(3)
H30	3341(8)	4906(7)	683(6)	78(4)
H7	1370(70)	4840(30)	928(13)	98(3)
H11	3556(7)	3258(7)	3856(6)	72(3)
H54	-1054(7)	5476(8)	1739(8)	84(4)
H55	156(7)	5344(6)	1423(7)	69(3)
H34	7030(10)	4771(9)	1579(10)	112(7)
H41	4493(11)	5089(9)	4099(7)	98(6)
H7a	6021(9)	3295(8)	4555(8)	88(5)
H77	17(10)	6976(7)	3264(9)	91(5)
H44	1996(10)	5359(7)	4703(7)	83(4)
H69	4300(9)	6668(7)	3069(7)	80(4)
H78	-1149(12)	7303(7)	3590(9)	101(6)
H74	1095(7)	7171(7)	2865(6)	73(3)
H31	4624(9)	4872(9)	449(8)	93(5)
H36	5565(7)	5053(8)	2966(9)	89(5)
H46	1274(8)	5564(7)	3890(5)	71(3)
H70	4134(9)	6985(7)	4138(8)	86(4)
H21	-889(10)	3742(7)	2795(7)	89(5)
H72	1811(10)	6929(6)	3708(8)	85(4)
H24	-1871(9)	3586(9)	605(6)	92(5)
H67	4246(8)	6848(7)	2126(6)	76(4)
H13	2995(7)	3455(8)	4669(7)	86(5)
H82	-1327(8)	7112(7)	865(8)	80(4)
H3	5466(9)	3242(7)	1826(8)	87(5)
H83	-202(10)	6845(9)	494(8)	97(5)
H18	291(8)	3492(7)	2994(6)	75(3)
H5	6531(9)	3161(7)	2710(9)	92(5)
H26	-536(11)	3580(9)	317(9)	103(5)
H16	361(9)	3810(8)	3937(8)	85(4)
H43	3007(12)	5429(10)	5475(7)	105(6)
H35	6799(10)	4881(9)	2688(9)	104(6)
H2	4217(8)	3487(7)	1447(7)	80(4)
H27	737(8)	3860(9)	528(7)	94(5)
H59	4486(11)	6559(11)	-569(9)	113(7)

H33	6001(9)	4874(9)	790(8)	97(5)
H42	4292(10)	5223(9)	5213(7)	93(5)
H71	2830(11)	6975(9)	4463(7)	96(5)
H58	3256(9)	6376(9)	-345(8)	94(5)
H64	5343(9)	6704(9)	1975(8)	94(5)
H80	-2178(9)	7202(11)	1755(10)	114(7)
H6	6911(9)	3270(10)	3799(8)	107(6)
H15	762(10)	3590(8)	5045(8)	94(5)
H61	5877(14)	6684(9)	-169(9)	120(8)
H63	6604(10)	6597(12)	1700(10)	122(7)
H23	-2697(9)	3404(8)	1432(9)	94(5)
H22	-2180(9)	3545(8)	2510(8)	93(5)
H14	2073(11)	3479(10)	5393(8)	106(6)
H8	4723(10)	3381(9)	4239(7)	96(5)
H52	-1919(10)	5516(8)	2618(10)	98(5)
H49	155(9)	5202(8)	4171(7)	85(4)
H50	-1097(10)	5289(9)	4484(9)	100(5)
H79	-2294(11)	7389(8)	2835(8)	98(5)
H51	-2172(9)	5337(10)	3670(11)	120(7)
H62	6874(12)	6739(12)	643(10)	128(8)
H85a	1293(8)	4679(6)	-27(6)	90
H85b	1439(8)	5437(6)	-164(6)	90
H85c	2155(8)	4964(6)	49(6)	90

**Crystallographic Table 130** Solvent masks information for  $\text{Lu}_2[\text{L}^{\text{VII}}]_3$ .

Number	X	Y	Z	Volume	Electron count	Content
1	0.155	0.209	0.033	327.6	127.0	3DCM
2	0.155	0.291	0.533	327.6	121.2	3DCM
3	-0.155	0.709	0.467	327.6	131.6	3DCM
4	-0.155	0.791	0.967	327.6	125.9	3DCM

Refinement model description

Number of restraints - 3, number of constraints - 113.

Details:

1. Others

Fixed Uiso: C85(0.06) H85a(0.09) H85b(0.09) H85c(0.09)

**UO<sub>2</sub>[L<sup>VII</sup>]**

**Crystallographic Table 131** Crystal data and structure refinement for **UO<sub>2</sub>[L<sup>VII</sup>]**

Empirical formula	C <sub>60</sub> H <sub>48</sub> Cl <sub>8</sub> N <sub>4</sub> O <sub>10</sub> U <sub>2</sub>
Formula weight	1744.75
Temperature/K	180.0
Crystal system	monoclinic
Space group	P2 <sub>1</sub> /n
a/Å	15.4659(12)
b/Å	19.3294(14)
c/Å	22.2346(16)
α/°	90
β/°	106.655(1)
γ/°	90
Volume/Å <sup>3</sup>	6368.1(8)
Z	4
ρ <sub>calc</sub> /mg/mm <sup>3</sup>	1.8197
m/mm <sup>-1</sup>	5.476
F(000)	3269.1
Crystal size/mm <sup>3</sup>	0.18 × 0.12 × 0.1
Radiation	Mo Kα (λ = 0.71073)
2θ range for data collection	2.84 to 51.52°
Index ranges	-18 ≤ h ≤ 18, -23 ≤ k ≤ 23, -27 ≤ l ≤ 27
Reflections collected	74217
Independent reflections	12168 [R <sub>int</sub> = 0.0706, R <sub>sigma</sub> = 0.0463]
Data/restraints/parameters	12168/0/759
Goodness-of-fit on F <sup>2</sup>	1.094
Final R indexes [I >= 2σ (I)]	R <sub>1</sub> = 0.0440, wR <sub>2</sub> = 0.0935
Final R indexes [all data]	R <sub>1</sub> = 0.0628, wR <sub>2</sub> = 0.1031
Largest diff. peak/hole / e Å <sup>-3</sup>	3.33/-1.96

**Crystallographic Table 132** Fractional Atomic Coordinates (×10<sup>4</sup>) and Equivalent Isotropic Displacement Parameters (Å<sup>2</sup>×10<sup>3</sup>) for **UO<sub>2</sub>[L<sup>VII</sup>]**. U<sub>eq</sub> is defined as 1/3 of the trace of the orthogonalised U<sub>ij</sub> tensor.

Atom	x	y	z	U(eq)
U1	-802.24(16)	10935.58(14)	554.71(13)	17.87(8)
U2	-2483.41(17)	9914.97(14)	-1991.78(13)	19.85(8)
O1	225(3)	10825(3)	343(2)	23.9(11)
O2	-326(3)	10031(3)	1230(2)	23.5(11)

O3	-1824(3)	11064(3)	749(2)	23.4(11)
O4	-1513(3)	9961(3)	-83(2)	24.0(11)
O5	-1643(3)	10049(3)	-2663(3)	30.9(13)
O6	-1256(3)	10646(3)	-1350(2)	23.5(11)
O8	-3149(3)	10648(3)	-2297(2)	28.1(12)
N1	-53(4)	11368(3)	1634(3)	22.2(14)
N2	-549(4)	12221(3)	667(3)	23.1(14)
N3	-3892(4)	9209(3)	-2061(3)	24.2(14)
N4	-3194(4)	9318(3)	-3020(3)	24.6(14)
C1	-595(4)	9919(4)	1739(4)	25.0(17)
C2	-627(5)	10446(4)	2162(4)	25.7(17)
C3	-182(5)	11103(4)	2133(4)	26.9(18)
C4	485(5)	11975(4)	1665(4)	25.5(17)
C5	234(5)	12422(4)	1155(4)	27.0(17)
C6	-1082(6)	12710(4)	365(4)	28.8(18)
C7	-1882(5)	12597(4)	-146(4)	25.9(17)
C8	-1992(5)	11999(4)	-516(3)	23.5(16)
C9	-2736(5)	11942(4)	-1059(4)	27.3(17)
C10	-3366(6)	12453(5)	-1205(4)	33.1(19)
C11	-3300(6)	13061(4)	-848(4)	33.8(19)
C12	-2553(6)	13145(4)	-312(4)	33(2)
C13	-2519(8)	13759(5)	31(4)	49(3)
C14	-3185(9)	14251(5)	-152(5)	63(3)
C15	-3925(8)	14162(6)	-668(5)	60(3)
C16	-3973(7)	13576(5)	-1002(5)	48(3)
C18	752(6)	13007(5)	1136(4)	39(2)
C19	1505(6)	13145(5)	1641(5)	44(2)
C20	1741(5)	12707(5)	2148(4)	37(2)
C21	1249(5)	12111(4)	2176(4)	28.8(18)
C22	-1007(5)	10309(5)	2667(4)	35(2)
C23	-1199(6)	10840(6)	3044(5)	50(3)
C24	-1625(9)	10693(7)	3502(6)	73(4)
C25	-1895(10)	10017(8)	3579(6)	81(4)
C26	-1719(9)	9489(7)	3222(6)	73(4)
C27	-1287(6)	9629(5)	2754(4)	43(2)
C28	-1162(6)	9100(5)	2345(4)	42(2)
C29	-849(5)	9233(4)	1846(4)	31.3(19)
C31	-3699(5)	10179(4)	-992(4)	22.8(16)

C32	-4516(5)	9862(4)	-1345(4)	24.5(17)
C33	-5342(5)	10030(4)	-1198(4)	26.6(17)
C34	-5328(5)	10493(4)	-707(4)	29.4(18)
C35	-4487(5)	10799(4)	-370(4)	30.9(19)
C36	-3715(5)	10646(4)	-503(4)	28.3(18)
C37	-6132(5)	10647(5)	-551(4)	34(2)
C38	-6927(5)	10349(5)	-871(4)	37(2)
C39	-6958(5)	9908(5)	-1363(4)	37(2)
C40	-6194(5)	9754(5)	-1533(4)	32(2)
C41	-4508(5)	9334(4)	-1794(4)	27.1(18)
C42	-3998(5)	8625(4)	-2468(4)	27.8(18)
C43	-3655(5)	8689(4)	-2986(4)	28.7(18)
C44	-3206(5)	9561(5)	-3565(4)	31.8(19)
C45	-2687(5)	10127(5)	-3681(4)	31.3(19)
C46	-1880(5)	10315(4)	-3232(4)	28.9(18)
C47	-1277(6)	10788(5)	-3396(4)	39(2)
C48	-1508(7)	11086(5)	-3978(5)	47(2)
C49	-2327(7)	10933(5)	-4437(5)	45(2)
C50	-2932(6)	10458(5)	-4293(4)	40(2)
C51	-3749(7)	10335(6)	-4752(5)	56(3)
C52	-3943(8)	10660(7)	-5323(5)	65(3)
C53	-3349(9)	11123(6)	-5467(6)	69(3)
C54	-2569(8)	11266(6)	-5030(5)	60(3)
C55	-3752(6)	8141(5)	-3405(4)	37(2)
C56	-4192(6)	7540(5)	-3330(5)	45(2)
C57	-4510(7)	7474(5)	-2807(5)	50(3)
C58	-4416(6)	8010(5)	-2377(4)	39(2)
O0aa	-2919(3)	10028(3)	-1085(2)	26.2(12)
O1aa	-1408(3)	11481(3)	-385(2)	23.6(11)
Cl7	-7846(4)	12606(3)	-1649(3)	160(2)
Cl8	-5953(4)	12463(3)	-1023(4)	182(3)
Cl9	-5981(4)	11775(3)	-2822(4)	182(3)
Cl10	-5554(4)	10499(4)	-3289(3)	163(2)
C0aa	-5254(10)	11112(9)	-2679(8)	107(6)
Cl1aa	-6978(16)	12067(10)	-1402(14)	240(17)
O3aa	-1847(3)	9173(3)	-1669(3)	28.7(12)
Cl1	-1475(4)	8048(3)	197(2)	126.9(18)
Cl2	-3313(4)	8092(2)	-611(2)	115.1(16)

Cl6	-3014(7)	12149(4)	1825(3)	224(4)
Cl0a	-4357(5)	12405(4)	754(4)	252(5)
C2aa	-3113(19)	12262(13)	1074(11)	249(17)
C3aa	-2137(12)	8081(8)	-540(8)	114(6)

**Crystallographic Table 133** Anisotropic Displacement Parameters ( $\text{\AA}^2 \times 10^3$ ) for  $\text{UO}_2[\text{L}^{\text{VII}}]$ . The Anisotropic displacement factor exponent takes the form: -  $2\pi^2[h^2a^2U_{11}+2hka*b*U_{12}+\dots]$

Atom	$U_{11}$	$U_{22}$	$U_{33}$	$U_{12}$	$U_{13}$	$U_{23}$
U1	13.80(12)	19.81(15)	19.73(14)	-0.97(10)	4.36(10)	-3.72(11)
U2	14.37(13)	21.43(15)	22.28(15)	-0.88(10)	2.92(10)	-3.19(12)
O1	20(2)	30(3)	24(3)	-2(2)	10(2)	-4(2)
O2	21(2)	24(3)	24(3)	-1(2)	6(2)	-3(2)
O3	19(2)	29(3)	24(3)	-2(2)	8(2)	-7(2)
O4	17(2)	24(3)	28(3)	1(2)	2(2)	-2(2)
O5	22(3)	47(4)	26(3)	-4(2)	9(2)	-4(3)
O6	16(2)	25(3)	28(3)	-1(2)	5(2)	-5(2)
O8	22(3)	32(3)	28(3)	-1(2)	3(2)	-3(2)
N1	20(3)	22(3)	24(3)	-4(2)	6(3)	-6(3)
N2	30(3)	19(3)	22(3)	-9(3)	10(3)	-6(3)
N3	22(3)	25(4)	26(3)	-7(3)	6(3)	-5(3)
N4	21(3)	26(4)	25(4)	-2(3)	3(3)	-8(3)
C1	11(3)	33(5)	28(4)	0(3)	1(3)	-2(4)
C2	16(3)	33(5)	25(4)	2(3)	1(3)	2(4)
C3	18(4)	37(5)	23(4)	-3(3)	3(3)	-10(4)
C4	21(4)	26(4)	32(4)	-9(3)	12(3)	-17(4)
C5	33(4)	24(4)	27(4)	-1(3)	13(3)	-4(3)
C6	44(5)	19(4)	22(4)	3(4)	8(4)	2(3)
C7	36(4)	22(4)	23(4)	-1(3)	13(3)	4(3)
C8	31(4)	22(4)	20(4)	1(3)	13(3)	2(3)
C9	31(4)	23(4)	28(4)	-2(3)	8(3)	0(3)
C10	36(4)	39(5)	23(4)	8(4)	7(4)	7(4)
C11	48(5)	28(5)	26(4)	10(4)	11(4)	8(4)
C12	56(5)	19(4)	28(5)	0(4)	16(4)	5(4)
C13	83(8)	30(5)	31(5)	12(5)	13(5)	-2(4)
C14	102(9)	28(6)	54(7)	26(6)	15(7)	-3(5)
C15	94(9)	52(7)	33(6)	42(6)	16(6)	11(5)
C16	68(7)	41(6)	34(5)	23(5)	13(5)	8(4)
C18	41(5)	36(5)	38(5)	-16(4)	9(4)	-10(4)

C19	48(5)	35(5)	50(6)	-23(4)	17(5)	-9(5)
C20	26(4)	40(5)	43(5)	-13(4)	5(4)	-22(4)
C21	24(4)	32(5)	29(4)	-1(3)	6(3)	-11(4)
C22	26(4)	48(6)	31(5)	-8(4)	9(4)	-2(4)
C23	47(6)	67(7)	42(6)	-12(5)	22(5)	-9(5)
C24	92(9)	86(10)	57(7)	-21(8)	48(7)	-21(7)
C25	104(10)	98(11)	55(8)	-33(9)	48(7)	6(8)
C26	98(10)	75(9)	55(7)	-29(7)	36(7)	10(7)
C27	41(5)	54(6)	34(5)	-6(4)	12(4)	9(5)
C28	46(5)	36(5)	42(5)	-6(4)	8(4)	14(4)
C29	23(4)	29(5)	40(5)	-1(3)	4(3)	7(4)
C31	16(3)	28(4)	26(4)	1(3)	8(3)	-1(3)
C32	22(4)	27(4)	23(4)	-4(3)	4(3)	-1(3)
C33	24(4)	31(5)	26(4)	-1(3)	10(3)	3(4)
C34	22(4)	37(5)	30(4)	1(3)	7(3)	4(4)
C35	27(4)	34(5)	32(5)	-2(3)	9(3)	-13(4)
C36	15(3)	41(5)	26(4)	-9(3)	0(3)	-6(4)
C37	28(4)	40(5)	35(5)	6(4)	12(4)	0(4)
C38	23(4)	53(6)	39(5)	7(4)	16(4)	8(5)
C39	18(4)	47(6)	42(5)	-7(4)	4(3)	4(4)
C40	19(4)	46(5)	32(5)	-6(3)	6(3)	-5(4)
C41	19(4)	25(4)	38(5)	-5(3)	9(3)	-3(4)
C42	23(4)	28(4)	31(5)	-3(3)	4(3)	-7(4)
C43	18(4)	32(5)	35(5)	-4(3)	7(3)	-10(4)
C44	27(4)	39(5)	26(5)	-1(4)	1(3)	-8(4)
C45	31(4)	41(5)	24(4)	-3(4)	10(3)	-2(4)
C46	24(4)	35(5)	33(5)	0(3)	14(3)	-3(4)
C47	33(5)	40(5)	43(5)	-8(4)	11(4)	-3(4)
C48	56(6)	43(6)	50(6)	-13(5)	29(5)	0(5)
C49	55(6)	35(5)	42(6)	0(4)	12(5)	3(5)
C50	46(5)	38(5)	35(5)	1(4)	10(4)	4(4)
C51	48(6)	75(8)	41(6)	-6(5)	5(5)	19(6)
C52	64(7)	77(8)	42(6)	-6(6)	-3(5)	18(6)
C53	90(9)	65(8)	47(7)	-1(7)	13(6)	23(6)
C54	79(8)	52(7)	53(7)	-9(6)	26(6)	12(6)
C55	33(4)	45(6)	36(5)	-5(4)	13(4)	-15(4)
C56	45(5)	41(6)	52(6)	-16(4)	19(5)	-26(5)
C57	58(6)	37(6)	58(7)	-25(5)	22(5)	-19(5)



C58	40(5)	37(5)	44(5)	-18(4)	18(4)	-12(4)
O0aa	13(2)	36(3)	29(3)	-4(2)	5(2)	-8(3)
O1aa	29(3)	19(3)	22(3)	3(2)	7(2)	-1(2)
Cl7	160(5)	115(4)	191(6)	1(4)	29(5)	-40(4)
Cl8	145(5)	124(4)	234(7)	-30(4)	-13(5)	72(5)
Cl9	100(4)	132(5)	334(10)	27(3)	96(5)	76(5)
Cl10	109(4)	170(6)	178(6)	-26(4)	-12(4)	1(5)
C0aa	79(10)	131(15)	106(13)	24(10)	18(9)	44(11)
C1aa	180(20)	79(14)	340(40)	-38(14)	-130(20)	64(18)
O3aa	23(3)	26(3)	35(3)	1(2)	5(2)	-7(3)
Cl1	163(4)	117(4)	106(3)	-72(3)	46(3)	5(3)
Cl2	163(4)	108(3)	88(3)	65(3)	59(3)	20(2)
Cl6	319(11)	169(6)	137(5)	-71(7)	-10(6)	-49(5)
Cl0a	152(6)	239(8)	303(10)	96(6)	-36(6)	-151(8)
C2aa	370(30)	250(30)	260(20)	250(30)	290(30)	190(20)
C3aa	168(16)	87(11)	135(15)	-18(11)	119(14)	8(11)

**Crystallographic Table 134** Bond Lengths for  $\text{UO}_2[\text{L}^{\text{VII}}]$ .

Atom	Atom	Length/Å	Atom	Atom	Length/Å
U1	O1	1.795(5)	C22	C23	1.408(13)
U1	O2	2.285(5)	C22	C27	1.414(13)
U1	O3	1.771(5)	C23	C24	1.393(14)
U1	O4	2.424(5)	C24	C25	1.396(17)
U1	N1	2.491(6)	C25	C26	1.368(18)
U1	N2	2.516(6)	C26	C27	1.415(14)
U1	O1aa	2.288(5)	C27	C28	1.418(14)
U2	O5	2.259(5)	C28	C29	1.357(12)
U2	O6	2.466(5)	C31	C32	1.420(10)
U2	O8	1.769(5)	C31	C36	1.419(11)
U2	N3	2.538(6)	C31	O0aa	1.315(8)
U2	N4	2.515(6)	C32	C33	1.445(10)
U2	O0aa	2.311(5)	C32	C41	1.431(11)
U2	O3aa	1.771(5)	C33	C34	1.407(11)
O2	C1	1.330(9)	C33	C40	1.418(10)
O5	C46	1.315(10)	C34	C35	1.430(11)
N1	C3	1.290(10)	C34	C37	1.415(11)
N1	C4	1.428(9)	C35	C36	1.344(11)
N2	C5	1.428(10)	C37	C38	1.360(12)

N2	C6	1.307(10)	C38	C39	1.377(13)
N3	C41	1.282(9)	C39	C40	1.373(11)
N3	C42	1.425(10)	C42	C43	1.404(11)
N4	C43	1.424(10)	C42	C58	1.396(11)
N4	C44	1.294(10)	C43	C55	1.390(11)
C1	C2	1.397(11)	C44	C45	1.424(12)
C1	C29	1.422(11)	C45	C46	1.403(11)
C2	C3	1.454(11)	C45	C50	1.452(12)
C2	C22	1.433(11)	C46	C47	1.428(11)
C4	C5	1.390(11)	C47	C48	1.366(13)
C4	C21	1.409(10)	C48	C49	1.411(14)
C5	C18	1.396(11)	C49	C50	1.412(13)
C6	C7	1.437(11)	C49	C54	1.418(14)
C7	C8	1.400(11)	C50	C51	1.399(13)
C7	C12	1.455(11)	C51	C52	1.370(14)
C8	C9	1.412(10)	C52	C53	1.384(16)
C8	O1aa	1.324(9)	C53	C54	1.342(16)
C9	C10	1.360(11)	C55	C56	1.380(13)
C10	C11	1.404(12)	C56	C57	1.392(13)
C11	C12	1.411(12)	C57	C58	1.389(12)
C11	C16	1.410(12)	C17	C1aa	1.66(2)
C12	C13	1.404(12)	C18	C1aa	1.74(2)
C13	C14	1.376(14)	C19	C0aa	1.675(16)
C14	C15	1.379(15)	C110	C0aa	1.760(19)
C15	C16	1.346(14)	C11	C3aa	1.665(19)
C18	C19	1.393(12)	C12	C3aa	1.781(17)
C19	C20	1.373(13)	C16	C2aa	1.65(2)
C20	C21	1.392(12)	C10a	C2aa	1.87(3)

**Crystallographic Table 135 Bond Angles for  $\text{UO}_2[\text{L}^{\text{VII}}]$ .**

Atom	Atom	Atom	Angle/°	Atom	Atom	Atom	Angle/°
O2	U1	O1	86.4(2)	C16	C11	C10	121.7(8)
O3	U1	O1	178.5(2)	C16	C11	C12	119.5(8)
O3	U1	O2	95.1(2)	C11	C12	C7	118.8(7)
O4	U1	O1	92.4(2)	C13	C12	C7	124.4(8)
O4	U1	O2	78.29(17)	C13	C12	C11	116.8(8)
O4	U1	O3	88.0(2)	C14	C13	C12	121.0(10)
N1	U1	O1	95.2(2)	C15	C14	C13	122.2(10)

N1	U1	O2	69.53(19)	C16	C15	C14	117.8(9)
N1	U1	O3	85.3(2)	C15	C16	C11	122.7(10)
N1	U1	O4	146.34(19)	C19	C18	C5	119.0(9)
N2	U1	O1	91.1(2)	C20	C19	C18	120.6(8)
N2	U1	O2	132.69(19)	C21	C20	C19	121.8(8)
N2	U1	O3	87.8(2)	C20	C21	C4	117.5(8)
N2	U1	O4	148.99(19)	C23	C22	C2	122.4(8)
N2	U1	N1	63.7(2)	C27	C22	C2	119.2(8)
O1aa	U1	O1	88.7(2)	C27	C22	C23	118.1(8)
O1aa	U1	O2	157.47(18)	C24	C23	C22	120.7(11)
O1aa	U1	O3	89.9(2)	C25	C24	C23	120.1(11)
O1aa	U1	O4	79.95(17)	C26	C25	C24	120.7(11)
O1aa	U1	N1	132.88(19)	C27	C26	C25	119.9(11)
O1aa	U1	N2	69.34(19)	C26	C27	C22	120.4(10)
O6	U2	O5	79.84(18)	C28	C27	C22	118.7(8)
O8	U2	O5	92.0(2)	C28	C27	C26	120.8(10)
O8	U2	O6	91.7(2)	C29	C28	C27	122.2(8)
N3	U2	O5	131.93(19)	C28	C29	C1	119.6(8)
N3	U2	O6	148.02(18)	C36	C31	C32	119.4(6)
N3	U2	O8	90.7(2)	O0aa	C31	C32	121.9(7)
N4	U2	O5	68.63(19)	O0aa	C31	C36	118.7(6)
N4	U2	O6	148.43(19)	C33	C32	C31	118.8(7)
N4	U2	O8	87.9(2)	C41	C32	C31	120.7(7)
N4	U2	N3	63.5(2)	C41	C32	C33	120.2(7)
O0aa	U2	O5	158.85(18)	C34	C33	C32	120.1(7)
O0aa	U2	O6	79.01(17)	C40	C33	C32	123.1(7)
O0aa	U2	O8	88.7(2)	C40	C33	C34	116.9(7)
O0aa	U2	N3	69.17(18)	C35	C34	C33	118.6(7)
O0aa	U2	N4	132.51(18)	C37	C34	C33	120.3(7)
O3aa	U2	O5	90.1(2)	C37	C34	C35	121.0(8)
O3aa	U2	O6	89.0(2)	C36	C35	C34	121.8(7)
O3aa	U2	O8	177.8(2)	C35	C36	C31	121.3(7)
O3aa	U2	N3	87.5(2)	C38	C37	C34	120.6(8)
O3aa	U2	N4	92.5(2)	C39	C38	C37	119.9(8)
O3aa	U2	O0aa	89.5(2)	C40	C39	C38	121.1(8)
C1	O2	U1	124.3(4)	C39	C40	C33	121.2(8)
C46	O5	U2	128.7(5)	C32	C41	N3	127.9(7)
C3	N1	U1	123.5(5)	C43	C42	N3	116.7(7)

C4	N1	U1	115.3(5)	C58	C42	N3	123.8(7)
C4	N1	C3	121.1(6)	C58	C42	C43	119.5(7)
C5	N2	U1	114.7(5)	C42	C43	N4	115.6(7)
C6	N2	U1	127.3(5)	C55	C43	N4	125.0(7)
C6	N2	C5	117.8(6)	C55	C43	C42	119.4(8)
C41	N3	U2	127.5(5)	C45	C44	N4	126.2(7)
C42	N3	U2	113.9(4)	C46	C45	C44	120.1(8)
C42	N3	C41	118.5(6)	C50	C45	C44	119.9(7)
C43	N4	U2	115.9(5)	C50	C45	C46	119.5(8)
C44	N4	U2	124.8(5)	C45	C46	O5	122.0(7)
C44	N4	C43	119.2(7)	C47	C46	O5	118.2(7)
C2	C1	O2	122.2(7)	C47	C46	C45	119.7(8)
C29	C1	O2	117.6(7)	C48	C47	C46	120.0(8)
C29	C1	C2	120.1(7)	C49	C48	C47	122.3(9)
C3	C2	C1	119.9(7)	C50	C49	C48	119.1(9)
C22	C2	C1	119.7(7)	C54	C49	C48	121.4(9)
C22	C2	C3	120.0(7)	C54	C49	C50	119.4(9)
C2	C3	N1	125.2(7)	C49	C50	C45	119.2(8)
C5	C4	N1	116.5(7)	C51	C50	C45	123.2(9)
C21	C4	N1	122.4(7)	C51	C50	C49	117.6(9)
C21	C4	C5	121.1(7)	C52	C51	C50	120.7(10)
C4	C5	N2	115.4(7)	C53	C52	C51	121.8(11)
C18	C5	N2	124.5(7)	C54	C53	C52	119.0(11)
C18	C5	C4	120.0(7)	C53	C54	C49	121.5(10)
C7	C6	N2	124.8(7)	C56	C55	C43	121.4(8)
C8	C7	C6	121.5(7)	C57	C56	C55	118.9(8)
C12	C7	C6	118.7(7)	C58	C57	C56	121.0(9)
C12	C7	C8	119.6(7)	C57	C58	C42	119.8(8)
C9	C8	C7	119.9(7)	C31	O0aa	U2	132.0(5)
O1aa	C8	C7	122.3(7)	C8	O1aa	U1	128.6(4)
O1aa	C8	C9	117.8(7)	C110	C0aa	C19	110.8(9)
C10	C9	C8	120.0(8)	C18	C1aa	C17	114.9(12)
C11	C10	C9	122.8(8)	C10a	C2aa	C16	101.1(9)
C12	C11	C10	118.8(7)	C12	C3aa	C11	114.3(8)

**Crystallographic Table 136** Hydrogen Atom Coordinates ( $\text{\AA}\times 10^4$ ) and Isotropic Displacement Parameters ( $\text{\AA}^2\times 10^3$ ) for  $\text{UO}_2[\text{L}^{\text{VII}}]$ .

Atom	x	y	z	U(eq)
H29	-800(5)	8870(4)	1569(4)	38(2)
H28	-1301(6)	8636(5)	2424(4)	50(3)
H21	1421(5)	11808(4)	2526(4)	35(2)
H20	2255(5)	12813(5)	2489(4)	45(3)
H19	1858(6)	13546(5)	1635(5)	52(3)
H18	594(6)	13308(5)	783(4)	47(3)
H9	-2797(5)	11547(4)	-1321(4)	33(2)
H10	-3871(6)	12397(5)	-1564(4)	40(2)
H23	-1035(6)	11303(6)	2985(5)	60(3)
H24	-1733(9)	11052(7)	3763(6)	87(4)
H25	-2204(10)	9923(8)	3883(6)	97(5)
H26	-1886(9)	9028(7)	3288(6)	87(4)
H13	-2029(8)	13835(5)	396(4)	58(3)
H14	-3133(9)	14667(5)	83(5)	75(4)
H15	-4386(8)	14503(6)	-782(5)	72(4)
H16	-4481(7)	13506(5)	-1357(5)	58(3)
H47	-715(6)	10896(5)	-3102(4)	46(3)
H48	-1104(7)	11407(5)	-4077(5)	56(3)
H58	-4636(6)	7958(5)	-2022(4)	47(3)
H57	-4795(7)	7056(5)	-2744(5)	60(3)
H56	-4276(6)	7178(5)	-3630(5)	54(3)
H55	-3509(6)	8181(5)	-3750(4)	45(3)
H36	-3167(5)	10854(4)	-264(4)	34(2)
H35	-4475(5)	11119(4)	-43(4)	37(2)
H51	-4174(7)	10023(6)	-4668(5)	68(3)
H52	-4500(8)	10565(7)	-5629(5)	78(4)
H53	-3491(9)	11337(6)	-5868(6)	83(4)
H54	-2170(8)	11597(6)	-5121(5)	71(4)
H40	-6236(5)	9457(5)	-1880(4)	39(2)
H39	-7518(5)	9708(5)	-1589(4)	44(3)
H38	-7461(5)	10445(5)	-756(4)	44(3)
H37	-6116(5)	10962(5)	-220(4)	40(2)
H4a	-2096(4)	10015(16)	-190(20)	36.0(17)
H4b	-1370(30)	9583(4)	135(10)	36.0(17)
H6a	-1436(14)	10850(20)	-1059(18)	35.3(17)

H6b	-791(14)	10387(5)	-1180(20)	35.3(17)
H3	30(5)	11357(4)	2513(4)	32(2)
H6	-930(6)	13174(4)	492(4)	35(2)
H41	-5022(5)	9040(4)	-1908(4)	32(2)
H44	-3598(5)	9340(5)	-3921(4)	38(2)
H0aa	-4637(10)	11286(9)	-2639(8)	129(7)
H0ab	-5251(10)	10889(9)	-2278(8)	129(7)
H1aa	-7122(16)	11728(10)	-1111(14)	290(20)
H1ab	-6905(16)	11808(10)	-1768(14)	290(20)
H2aa	-2766(19)	12669(13)	1004(11)	300(20)
H2ab	-2916(19)	11847(13)	888(11)	300(20)
H3aa	-1984(12)	8501(8)	-743(8)	137(7)
H3ab	-2005(12)	7675(8)	-771(8)	137(7)

#### Refinement model description

Number of restraints - 0, number of constraints - 90.

Details:

N/A

## References

1. Bruker Bruker AXS Inc.: Madison, Wisconsin, USA, 2001.
2. Sheldrick, G. M., *Acta Crystallogr., Sect. A: Found. Crystallogr.* **2008**, *A64*, 112.
3. Bourhis, L. J.; Dolomanov, O. V.; Gildea, R. J.; Howard, J. A. K.; Puschmann, H., The anatomy of a comprehensive constrained, restrained refinement program for the modern computing environment - Olex2 dissected. *Acta Crystallogr.* **2015**, *A71* (1), 59-75.
4. Dolomanov, O. V.; Bourhis, L. J.; Gildea, R. J.; Howard, J. A. K.; Puschmann, H., OLEX2: A complete structure solution, refinement and analysis program. *J. Appl. Cryst.* **2009**, *42*, 339-341.